

Legacy and Emerging Per- and Polyfluoroalkyl Substances in the Aquatic Environment – Sources, Sinks and Long-Range Transport to the Arctic

Dissertation zur Erlangung des Grades
Doktorin der Naturwissenschaften (Dr. rer. nat.)
im Fachbereich Chemie der Universität Hamburg

vorgelegt von
Hanna Katharina Joerss
aus Köln

Juni 2020

Die Arbeiten zur vorliegenden Dissertation wurden in der Zeit von Juli 2016 bis Juni 2020 in der Abteilung Umweltchemie des Instituts für Küstenforschung am Helmholtz-Zentrum Geesthacht angefertigt.

1. Gutachter

Prof. Dr. Michael Steiger

Universität Hamburg, Institut für Anorganische und Angewandte Chemie

2. Gutachter

Prof. Dr. Ralf Ebinghaus

Helmholtz-Zentrum Geesthacht, Institut für Küstenforschung, Abteilung Umweltchemie

Tag der Disputation: 18.09.2020

Druckfreigabe: 18.09.2020

Abstract

Per- and polyfluoroalkyl substances (PFASs) are a group of more than 4,700 anthropogenic chemicals that have been produced for over 70 years and used in a broad range of industrial applications and consumer products. Due to their adverse effects on human health and the environment, attention has been drawn to so-called “long-chain” PFASs as global contaminants since the late 1990s. Along with regulatory actions and voluntary industry initiatives to restrict the production, use and release of these chemicals, an industrial transition has taken place. This includes a geographical shift of production from countries in Europe and North America to countries in Asia and a transition to replacement chemicals, of which many are still PFASs. While regulated long-chain PFASs have been well investigated (“legacy PFASs”), potential adverse properties, environmental occurrence and fate of other PFASs are largely unknown (“emerging PFASs”). In addition, only a small amount of PFASs on the global market is monitored using conventional compound-specific analytical methods. This raises the question if the commonly analysed PFASs are representative or if they make up only a small fraction of anthropogenic PFAS releases.

This thesis aimed at identifying which emerging PFASs are of relevance in the European coastal environment and at investigating their potential long-range transport to the Arctic. A comparison to legacy PFASs was to be made and knowledge gaps regarding the ultimate sinks of PFASs in the aquatic environment were intended to be filled. Moreover, it was the aim to characterize the unknown fraction of PFASs in German and Chinese river water impacted by industrial point sources.

To achieve these aims, analytical methods for the selective and sensitive determination of 29 legacy and emerging PFASs in seawater, river water and sediment were developed and validated. The instrumental analysis was performed by means of liquid chromatography coupled to tandem mass spectrometry (LC-MS/MS). Method detection limits were in the pg/L range for aqueous matrices and in the pg/g range for sediment. Hence, they were suitable for the analysis of samples from the marine environment. Samples were collected in coastal areas of the North and Baltic Seas, along a sampling transect from Europe to the Arctic and within Fram Strait, situated between Greenland and Svalbard. Additional samples were taken from German and Chinese rivers, up- and downstream of suspected point sources.

Hexafluoropropylene oxide-dimer acid (HFPO-DA), an ether-based replacement compound for the legacy compound perfluorooctanoic acid (PFOA), was detected in 191 of the 202 analysed surface water samples. This finding adds to a growing body of literature indicating the ubiquitous presence of HFPO-DA. In addition, HFPO-DA was detected in Arctic surface water for the first time, providing evidence that the compound undergoes long-range transport to remote areas, similar to PFOA.

In contrast to HFPO-DA, the occurrence of the other investigated emerging PFASs was limited to particular study areas, country-specific or source-specific. This included the cyclic compound perfluoro-4-ethylcyclohexanesulfonic acid (PFECHS), two perfluoroalkyl phosphinic acids (6:6

and 6:8 PFPiA), as well as the ether-based compounds 4,8-dioxa-3*H*-perfluorononanoic acid (DONA) and 6:2 chlorinated polyfluoroalkyl ether sulfonic acid (6:2 Cl-PFESA).

In coastal waters of the North Sea, a downward trend of legacy long-chain PFASs in combination with a shift to HFPO-DA as most prevalent compound was observed. This can be attributed to the phase-out and regulation of long-chain PFASs in Europe. In contrast, the analysis of Chinese river water indicated ongoing high emissions of the legacy compound PFOA in China from point sources in the Xiaoqing River Basin and along the Yangtze River, reflecting the geographical shift of production. Moreover, legacy long-chain compounds still played a major role in surface water from the European Baltic Sea and in sediments from both North and Baltic Seas. This points to ongoing emissions from diffuse sources and underlines the relevance of sediments as sink of legacy long-chain PFASs in the marine environment.

Based on seven vertical PFAS profiles in Fram Strait (down to 3,117 m depth), PFAS mass flows entering the Arctic Ocean from the North Atlantic and exiting the Arctic in the opposite direction were estimated. The results indicate a net inflow of long-chain PFASs with ≥ 8 perfluorinated carbons and a net outflow of shorter-chain homologues. The PFAS composition profile provides a possible explanation for this, suggesting a higher contribution of atmospheric sources to outflowing water compared to inflowing water, in which oceanic transport plays a more important role. The higher retention of the long-chain compounds in melting snow and ice may serve as an additional explanation.

In German and Chinese river water, 24 of 29 analysed PFASs were detected, with a sum ranging from 2.7 ng/L to 420,000 ng/L. As an upcoming analytical approach, the Total Oxidizable Precursor (TOP) assay was applied to estimate the sum of PFAS precursors in the samples that oxidize to targeted PFASs. Upon oxidative conversion, the sum of targeted PFASs significantly increased, indicating the presence of unknown precursors. To elucidate the composition of the unknown fraction, a high-resolution mass spectrometry (HRMS)-based approach was applied. Screening the river water samples for the more than 4,700 known PFASs as “suspects”, 83 PFASs from 13 homologous series were identified. Of these, 13 have not been reported in the environment before.

The results from the TOP assay and the suspect screening show that commonly analysed PFASs only represent a fraction of the PFASs present in the investigated German and Chinese river water. This indicates that environmental and human exposure to PFASs may be considerably underestimated. In addition, it underlines that further actions on PFASs require a grouping approach. If implemented on a regulatory level, this will also help to avoid regrettable substitution. Beyond the prioritization and assessment of replacements in use and the development of safe alternatives, the systematic differentiation between essential and non-essential uses of PFAS can be a way forward. In many consumer products, PFASs are not essential and raising public awareness of this issue can contribute to eliminate such applications as a starting point.

Zusammenfassung

Per- und polyfluorierte Alkylsubstanzen (PFASs) stellen eine Gruppe von mehr als 4.700 anthropogenen Chemikalien dar, die seit mehr als 70 Jahren produziert werden und in vielen industriellen Anwendungen und Konsumgütern ihren Einsatz finden. Sogenannte „langkettige“ PFASs stehen aufgrund ihrer nachteiligen Auswirkungen auf Mensch und Umwelt seit Ende der 1990er-Jahre als globale Umweltkontaminanten im Fokus. Einhergehend mit regulatorischen Maßnahmen und freiwilligen Herstellerinitiativen zur Einschränkung der Produktion, Verwendung und Freisetzung dieser Substanzen fand ein industrieller Wandel statt. Einerseits wurde ein Teil der Produktion von europäischen und nordamerikanischen Ländern nach Asien verlagert und andererseits wird auf nicht regulierte Ersatzstoffe ausgewichen, die meist auch zur Stoffgruppe der PFASs gehören. Während regulierte langkettige PFASs gut untersucht sind („klassische PFASs“), sind potentiell schädliche Eigenschaften, das Umweltvorkommen und der Verbleib anderer PFASs größtenteils unbekannt („neuartige PFASs“). Darüber hinaus decken konventionelle analytische Methoden nur eine geringe Anzahl der PFASs auf dem Weltmarkt ab. Daher stellt sich die Frage, ob die üblicherweise analysierten Substanzen repräsentativ sind oder nur einen geringen Anteil der freigesetzten PFASs ausmachen.

Ziel dieser Doktorarbeit war es, die Relevanz von neuartigen PFASs in europäischen Küstengewässern und ihren möglichen Langstreckentransport in die Arktis zu untersuchen. Es sollte ein Vergleich zu Vorkommen, Verteilung und Verbleib klassischer PFASs gezogen werden und Wissenslücken in Hinblick auf Senken der Substanzen in der aquatischen Umwelt geschlossen werden. Darüber hinaus sollte anhand von deutschen und chinesischen Flusswasserproben, die durch potentielle Punktquellen beeinflusst waren, der unbekannte Anteil an PFASs näher charakterisiert werden.

Hierzu wurde zunächst eine analytische Methode für die selektive und sensitive Bestimmung von 29 PFASs in Meerwasser, Flusswasser und Sedimenten entwickelt und validiert. Die Messung erfolgte mittels Flüssigchromatographie mit Tandem-Massenspektrometrie-Kopplung (LC-MS/MS). Die Nachweisgrenzen der Methode lagen im pg/L-Bereich für Wasser und im pg/g-Bereich für Sedimente und waren somit für die Analytik von Proben aus der marinen Umwelt geeignet. Proben wurden in küstennahen Gebieten der Nord- und Ostsee, entlang einer Transekte von der Nordsee in den Arktischen Ozean sowie in der Framstraße zwischen Grönland und Spitzbergen gesammelt. Darüber hinaus erfolgten Probenahmen flussauf- und flussabwärts von potentiellen Punktquellen in Deutschland und China.

Hexafluorpropylenoxid-Dimersäure (HFPO-DA), ein Ersatzstoff für die regulierte Substanz Perfluorooctansäure (PFOA), wurde in 191 der 202 untersuchten Oberflächenwasserproben nachgewiesen. Dieses Ergebnis untermauert eine zunehmende Anzahl an Veröffentlichungen, die auf ein ubiquitäres Vorkommen von HFPO-DA hinweisen. Darüber hinaus wurde die Substanz in

dieser Arbeit erstmals in arktischem Oberflächenwasser nachgewiesen. Das liefert einen empirischen Beweis dafür, dass HFPO-DA wie seine Vorgängersubstanz PFOA über weite Strecken in entlegene Gebiete transportiert werden kann.

Im Gegensatz zu HFPO-DA war das Vorkommen anderer untersuchter neuartiger PFASs auf bestimmte Untersuchungsgebiete beschränkt, länder- oder quellenspezifisch. Dies schloss die cyclische Substanz Perfluor-4-ethylcyclohexansulfonsäure (PFECHS), zwei perfluorierte Phosphinsäuren (6:6 und 6:8 PFPiA), die Polyfluoralkylethercarbonsäure 4,8-Dioxa-3H-Perfluornonansäure (DONA) und eine chlorierte Polyfluoralkylethersulfonsäure (6:2 Cl-PFESA) ein.

In Küstengewässern der Nordsee stellte HFPO-DA die dominierende PFAS-Komponente dar, wohingegen die Konzentrationen der klassischen PFASs im Vergleich zu früheren Messungen zurückgingen. Das spiegelt den industriellen Trend von den klassischen PFASs hin zu Ersatzstoffen wider. Im Gegensatz dazu zeigten die Analysenergebnisse der chinesischen Flusswasserproben, dass die Emissionen der klassischen Substanz PFOA in China durch Punktquellen im Einzugsgebiet der Flüsse Xiaoqing und Yangtze anhaltend hoch sind. Es ist davon auszugehen, dass das im Zusammenhang mit der Produktionsverlagerung nach China steht. Darüber hinaus waren klassische PFASs dominierende Substanzen in Oberflächenwasserproben der Ostsee und in Sedimenten der Nord- und Ostsee. Das deutet auf anhaltende Emissionen aus diffusen Quellen hin und stellt die Rolle mariner Sedimente als Senke für langkettige PFASs heraus.

Auf Basis von sieben Tiefenprofilen in der Framstraße, bis in eine Tiefe von 3.117 m, wurde die Menge an PFASs abgeschätzt, die jährlich über Wassermassen vom Nordatlantik in den Arktischen Ozean hineintransportiert wird und entgegengesetzt die Arktis verlässt. Die Ergebnisse deuten darauf hin, dass langkettige PFASs mit ≥ 8 perfluorierten Kohlenstoffatomen in der Summe in die Arktis hineintransportiert werden, wohingegen kürzerkettige Substanzen die Arktis verlassen. Das Verteilungsmuster der PFASs lässt darauf schließen, dass im austretenden Wasser ein größerer Anteil der PFASs aus atmosphärischen Quellen stammt als im eintretenden Wasser, in dem der Transport mit den Meeresströmungen eine größere Rolle spielt. Darüber hinaus kann die höhere Anreicherung langkettiger Verbindungen in Schnee und Eis einen Einfluss haben.

In deutschen und chinesischen Flusswasserproben wurden 24 der 29 untersuchten PFASs nachgewiesen, wobei die Summe der PFASs zwischen 2,7 ng/L und 420,000 ng/L lag. Als neuer summarischer Ansatz wurde der *Total Oxidizable Precursor*-Assay (TOP)-Assay angewandt, um auf die Menge an unbekanntem Vorläuferverbindungen in den Proben zu schließen, die zu den in der Messmethode enthaltenden stabilen Endprodukten oxidiert werden können. In den oxidierten Proben war die Summe der analysierten PFASs signifikant höher als in den nicht oxidierten Proben, was auf unbekanntem Vorläufersubstanzen hindeutet. Um die Zusammensetzung des unbekanntem Anteils näher zu charakterisieren, wurde hochauflösende Massenspektrometrie (HRMS) eingesetzt. Durch ein Screening der Flusswasserproben auf mehr als 4.700 bekannte PFASs als sogenannte „Suspects“ wurden 83 PFASs aus 13 homologen Serien identifiziert. Davon wurden 13 Substanzen vorher noch nicht in der Umwelt beschrieben.

Die Ergebnisse des TOP-Assays und des Suspect-Screenings zeigen, dass die üblicherweise analysierten PFASs nur einen Teil der PFASs in den untersuchten deutschen und chinesischen Flüssen abdecken. Das deutet darauf hin, dass die Exposition von Mensch und Umwelt mit PFASs deutlich unterschätzt wird. Zudem zeigt es die Wichtigkeit, PFASs nicht einzeln, sondern als Substanzgruppe zu betrachten. Ein solcher Ansatz auf regulatorischer Ebene könnte dazu beitragen, bedauerliche Substitutionsentscheidungen zu vermeiden. Darüber hinaus könnte neben der Priorisierung und der Beurteilung von bereits verwendeten Ersatzstoffen und der Entwicklung von sicheren Alternativstoffen vor allem eine systematische Unterscheidung von essentiellen und nicht-essentiellen Anwendungen von PFASs einen Weg nach vorne bedeuten. In vielen Konsumgütern sind PFASs nicht unerlässlich und die öffentliche Sensibilisierung hierfür könnte dazu beitragen, in einem ersten Schritt solche Anwendungen zu unterbinden.

Acknowledgement

This thesis would not have been possible without the support, help and guidance of many people.

First of all, I would like to thank Prof. Dr. Ralf Ebinghaus for entrusting me with the PFAS topic and for sharing your network, which made it possible to get a global perspective and collaborate with scientists from different fields and countries.

I would also like to thank Prof. Dr. Michael Steiger for the possibility to do the doctorate at Universität Hamburg and for your uncomplicated and reliable way of giving support.

To my advisory panel PFAS experts Ass. Prof. Lutz Ahrens from SLU Uppsala and Dr. Zhanyun Wang from ETH Zürich, thank you for your valuable advice, for your ideas, encouragement and enthusiasm.

In addition, I would like to thank Ass. Prof. Jianhui Tang and Ass. Prof. Lutz Ahrens for making research stays in China and Sweden possible, for welcoming me in your working groups and for sharing not only scientific knowledge, but also part of the countries' culture and traditions.

To the PhD students Frank Menger, Jack Garnett and Charlotte Wagner from Uppsala, Lancaster and Boston, thank you for the great collaboration on PFAS-related issues. And to Thekla-Regine Schramm and Julian Schaaf, thank you for the great work during your Master thesis.

To all current and former colleagues at HZG, thank you for creating such a good working atmosphere: Christina for so many shared experiences and moments in the lab, in the office, on conference trips and campaigns, Jürgen for your positivity, your pragmatic answers to all kind of questions and for proofreading, Célia and Andreas for the time in Yantai and thoughts about life and work, Franzi for introducing me into the secrets of PFAS analysis, Jing for the time in Grenoble and Chinese delicacies and music, Danijela, Freya, Danilo, Hendrik, Zhiyong, Christiane, Volker, Ina, Gesa, Renate, Pu, Rui, Lijie, Bianca, Tanja and Jonathan.

Moreover, I would like to thank my parents, brothers, grandparents and friends for your continuous support, for your interest in my work and for encouraging me to find my own way. Finally, to Patrick, thank you for going through the ups and downs of this PhD journey with me and for making sure that life beyond work is enjoyable, adventurous and fulfilling.

Table of Contents

Abstract.....	III
Zusammenfassung.....	V
Acknowledgement.....	IX
Table of Contents.....	XI
List of Abbreviations	XVII
List of Tables	XIX
List of Figures	XXV
1. Introduction	1
2. Background.....	3
2.1 Terminology and classification of PFASs	3
2.2 Physical and chemical properties.....	5
2.3 Production and use.....	6
2.4 Environmental concerns about long-chain PFASs.....	9
2.4.1 Persistence	9
2.4.2 Bioaccumulation	9
2.4.3 Toxicity	10
2.4.4 Occurrence and long-range transport	12
2.5 Regulatory actions and voluntary industry initiatives	14
2.6 Shift of production	15
2.7 Environmental concerns about emerging and novel PFASs	21
2.8 Trends in analytical methods.....	23
2.8.1 Target analysis.....	23
2.8.2 Sum parameters	24
2.8.3 Suspect and non-target analysis.....	25
3. Point of Departure and Research Objectives.....	29
4. Development and Validation of Targeted Analytical Methods.....	33
4.1 Definition of the analytical scope.....	33
4.2 Development of the instrumental method.....	38
4.2.1 Determination of precursor and product ions.....	38
4.2.2 Optimization of transition-specific mass spectrometric parameters	40
4.2.3 Optimization of the chromatographic method.....	41
4.2.4 Optimization of a scheduled MRM method	51
4.2.5 Optimization of ion source-dependent parameters	52

4.3	Validation of the instrumental method	54
4.3.1	Instrumental blank	54
4.3.2	Measurement precision.....	55
4.3.3	Linear range.....	56
4.3.4	Instrumental detection limit (IDL)	58
4.4	Optimization of the sample preparation for aqueous matrices	60
4.4.1	Optimization of the solid phase extraction procedure	63
4.4.2	Optimization of the volume reduction step.....	64
4.4.3	Final method	67
4.5	Validation of the overall method for aqueous matrices.....	67
4.5.1	Matrix spike recovery tests.....	67
4.5.2	Blanks, method detection limits and method quantification limits	70
4.5.3	Method precision.....	74
4.5.4	Analysis of a certified reference material (CRM).....	75
4.6	Optimization of the sample preparation for sediments	78
4.6.1	Optimization of the volume reduction step.....	78
4.6.2	Extraction efficiency	81
4.6.3	Final method	82
4.7	Validation of the overall method for sediments.....	83
4.7.1	Matrix spike recovery tests.....	83
4.7.2	Blanks, method detection limits and method quantification limits	84
4.7.3	Method precision.....	86
4.8	Summary and conclusion.....	87
5.	Emerging Per- and Polyfluoroalkyl Substances in Surface Water and Sediment of the North and Baltic Seas	89
5.1	Sample collection	89
5.2	Materials and methods	91
5.2.1	Sample preparation and instrumental analysis	91
5.2.2	Quality assurance and quality control.....	91
5.2.3	Data analysis.....	92
5.3	Results and discussion.....	92
5.3.1	PFAS concentrations and composition patterns in surface water	92
5.3.2	Spatial distribution of PFASs in surface water and potential sources	93
5.3.3	PFAS concentrations and composition patterns in sediments.....	95
5.3.4	Spatial distribution of PFASs in sediments and potential sources.....	96
5.3.5	Partitioning of PFASs between sediment and water.....	98
5.3.6	Temporal trends	102
5.4	Summary and conclusion.....	103

6. Transport of Legacy Perfluoroalkyl Substances and the Replacement Compound HFPO-DA through the Atlantic Gateway to the Arctic Ocean – Is the Arctic a Sink or a Source?	105
6.1 Sample collection	106
6.2 Materials and methods	106
6.2.1 Sample preparation and instrumental analysis	106
6.2.2 Quality assurance and quality control.....	106
6.2.3 Data analysis.....	107
6.3 Results and discussion.....	109
6.3.1 PFAS concentrations and composition patterns in surface water	109
6.3.2 Transport and sources of PFASs along a latitudinal transect from Europe to the Arctic	109
6.3.3 Potential long-range transport of the replacement compound HFPO-DA	111
6.3.4 Sources of PFASs to surface water entering and exiting the Arctic Ocean.....	112
6.3.5 Depth profiles of PFASs in Fram Strait	114
6.3.6 PFAS mass transport estimates through Fram Strait.....	116
6.4 Summary and conclusion.....	118
7. Per- and Polyfluoroalkyl Substances in Chinese and German River Water – Point Source- and Country-Specific Fingerprints including Unknown Precursors	121
7.1 Selection of the study sites	122
7.2 Sample collection	126
7.3 Materials and methods	129
7.3.1 Sample preparation and instrumental analysis	129
7.3.2 Quality assurance and quality control for target analysis.....	129
7.3.3 Quality assurance and quality control for TOP assay analysis.....	130
7.3.4 Data analysis.....	131
7.4 Results and discussion.....	132
7.4.1 PFAS concentrations and composition patterns	132
7.4.2 Source characterization by principal component analysis	134
7.4.3 Source characterization by isomer profiling.....	135
7.4.4 Contributions of unknown precursors.....	137
7.4.5 PFAS mass flow estimates	138
7.5 Summary and conclusion.....	139
8. Discovery of Emerging and Novel Per- and Polyfluoroalkyl Substances in Chinese and German River Water Using a Suspect Screening Approach.....	141
8.1 Materials and methods	141

8.1.1	Sample preparation and instrumental analysis	141
8.1.2	Quality assurance and quality control.....	142
8.2	Development of a workflow for post-acquisition data treatment.....	142
8.2.1	Data pre-processing	143
8.2.2	Creation of a PFAS suspect list.....	145
8.2.3	Suspect screening and reduction of components	147
8.2.4	Evaluation of the candidate components	148
8.2.5	Back-mapping to the original database	150
8.3	Results and Discussion	151
8.3.1	Peak picking and componentization.....	151
8.3.2	PFAS suspect screening and filtering of candidates.....	153
8.3.3	Discovery of PFAS homologous series	154
8.3.4	Source-specific fingerprints	161
8.4	Summary and conclusion.....	164
9.	Overall Conclusions and Future Perspectives	167
10.	Experimental.....	175
10.1	Chemicals	175
10.1.1	Solvents and other chemicals	175
10.1.2	Analytical standards	175
10.2	Instrumental methods	179
10.2.1	LC-MS/MS.....	179
10.2.2	LC-QToF-MS ^E	183
10.3	Sampling.....	184
10.4	Analysis of physicochemical parameters	187
10.4.1	Water temperature, pH value and salinity.....	187
10.4.2	Total organic carbon.....	187
10.5	Sample preparation of aqueous samples	187
10.5.1	Target analysis.....	187
10.5.2	TOP assay.....	189
10.5.3	Suspect screening	189
10.6	Sample preparation of sediment samples	190
10.7	Quantification of PFASs.....	192
10.7.1	Calculation of PFAS concentrations	192
10.7.2	Calculation of recovery rates	194
10.8	Data analysis	194
11.	List of Publications	197
12.	References	201

A. Appendix A	227
A.1 Supplementary to Chapter 5.....	227
A.2 Supplementary to Chapter 6.....	248
A.3 Supplementary to Chapter 7.....	275
A.4 Supplementary to Chapter 8.....	297
A.5 Safety data information.....	302
Eidesstattliche Versicherung	309

List of Abbreviations

AFFF	aqueous film forming foam
AMOC	Atlantic Meridional Overturning Circulation
AOF	adsorbable organic fluorine
AW	Atlantic Water
BfR	<i>Bundesinstitut für Risikobewertung</i> (German Federal Institute for Risk Assessment)
bw	body weight
CAS	Chemical Abstracts Service
CE	collision energy
CIC	combustion ion chromatography
CTD	conductivity, temperature, depth
CXP	collision cell exit potential
DDT	dichlorodiphenyltrichloroethane
DP	declustering potential
dw	dry weight
ECF	electrochemical fluorination
ECHA	European Chemicals Agency
EFSA	European Food Safety Authority
EGC	East Greenland Current
EOF	extractable organic fluorine
EP	entrance potential
ESI	electrospray ionization
FTIs	fluorotelomer iodides
FTOHs	fluorotelomer alcohols
HRMS	high resolution mass spectrometry
HZG	Helmholtz-Zentrum Geesthacht
IARC	International Agency for Research on Cancer
IDL	instrumental detection limit
IRMM	Institute for Reference Materials and Measurements
IUPAC	International Union of Pure and Applied Chemistry
JRC	European Commission Joint Research Center
LC	liquid chromatography
MDL	method detection limit
MQL	method quantification limit
MRM	multiple reaction monitoring
MS	mass spectrometry
MS/MS	tandem mass spectrometry
NCC	Norwegian Coastal Current
NMR	nuclear magnetic resonance spectroscopy

NOAEL	no observed adverse effect level
NwAC	Norwegian Atlantic Current
OECD	Organisation for Economic Co-operation and Development
PBDEs	polybrominated diphenylethers
PASF	perfluoroalkane sulfonyl fluoride
PCA	principal component analysis
PCBs	polychlorinated biphenyls
PEEK	polyether ether ketone
PFAAs	perfluoroalkyl acids
PFASs	per- and polyfluoroalkyl substances
PFCAs	perfluoroalkyl carboxylic acids
PFECAs	per- and polyfluoroalkyl ether carboxylic acids
PFESAs	per- and polyfluoroalkyl ether sulfonic acids
PFPiAs	bis(perfluoroalkyl)phosphinic acids
PFSAAs	perfluoroalkane sulfonic acids
PIGE	particle-induced gamma ray emission spectroscopy
POPs	persistent organic pollutants
POSF	perfluorooctane sulfonyl fluoride
PPAR α	peroxisome proliferator-activated receptor α
PSW	Polar Surface Water
PTFE	polytetrafluoroethylene
PVDF	polyvinylidene fluoride
QqQ	triple quadrupole
QToF	quadrupole time-of-flight
REACH	registration, evaluation, authorization and restriction of chemicals
SD	standard deviation
SMILES	simplified molecular-input line-entry system
SPE	solid phase extraction
TDI	tolerable daily intake
TFE	tetrafluoroethylene
TOC	total organic carbon
TOP assay	total oxidizable precursor assay
TWI	tolerable weekly intake
US EPA	United States Environmental Protection Agency
WAX	weak anion exchange
WFD	Water Framework Directive
WSC	West Spitsbergen Current

Note: Single PFASs are not included in this list of abbreviations. An overview of their acronyms linked to their chemical structures is provided in Table 4.1-1 and Table 4.1-2.

List of Tables

Background

Table 2.2-1:	Characteristics of carbon-halogen and the carbon-carbon bonds.	5
Table 2.6-1:	Known fluorinated alternatives to long-chain PFCAs and PFSA and their precursors used in fluoropolymer manufacture and metal plating.	18
Table 2.6-2:	Known fluorinated alternatives to long-chain PFCAs and PFSA and their precursors used in different industrial branches.	19

Method Development and Validation

Table 4.1-1:	Chemical structures of replacement compounds and/or overlooked PFASs chosen as target analytes.	35
Table 4.1-2:	Chemical structures of perfluoroalkyl carboxylic and sulfonic acids as well as precursors chosen as target analytes.	36
Table 4.1-3:	Isotopically labelled internal standards used for quantification of the target analytes.	37
Table 4.2-1:	Chromatographic method for the analysis of PFASs and changes made in course of the optimization.	50
Table 4.2-2:	Optimization of ion-source dependent parameters.	53
Table 4.3-1:	Performance of the LC-MS/MS method.	59
Table 4.4-1:	Overview of solid phase extraction methods in literature for the determination of PFASs in aqueous matrices.	61
Table 4.5-1:	Campaign-specific method detection limits (MDLs) and method quantification limits (MQLs) for the determination of PFASs in aqueous matrices.	72
Table 4.5-2:	Verification of the method's trueness by analysis of the reference material IRMM-428.	76
Table 4.7-1:	Method detection limits (MDLs) and method quantification limits (MQLs) for the determination of PFASs in sediments.	85

North and Baltic Seas

Table 5.3-1:	Sediment-water partitioning coefficients $\log K_D$ and $\log K_{OC}$ in this study (mean \pm SD) compared to values reported in previous field studies.	100
Table 5.3-2:	Comparison of PFBS, L-PFOS and PFOA concentrations in this study to previous studies in the same investigation areas.	102

Suspect Screening

Table 8.2-1:	Compilation of US EPA PFAS Master List.	146
Table 8.3-1:	Discovered homologous series of perfluoroalkyl carbonyl compounds.	157
Table 8.3-2:	Discovered homologous series of perfluoroalkyl sulfonyl compounds.	158

Table 8.3-3:	Discovered homologous series of per- and polyfluoroalkyl ether-based compounds.	159
Table 8.3-4:	Discovered homologous series of fluorotelomer-related compounds and other PFASs.	160

Experimental

Table 10.1-1:	Solvents, other chemicals and gases used for sample preparation (P), measurement (M) and cleaning (C).	175
Table 10.1-2:	Overview of analytical standards for PFCAs and PFSAs, their CAS registry number and IUPAC names.	176
Table 10.1-3:	Overview of analytical standards for replacement compounds and/or overlooked PFASs, as well as precursors to PFAAs, their CAS number and IUPAC names.	177
Table 10.1-4:	Overview of isotopically-labelled internal standards, their IUPAC names and the standards' suppliers.	178
Table 10.2-1:	Overview of hardware components and parameter settings for the chromatographic separation of the target analytes.	179
Table 10.2-2:	Overview of hardware components and parameter settings for the mass-spectrometric detection of the target analytes.	179
Table 10.2-3:	Compound-specific parameter settings for the LC-MS/MS analysis of PFCAs and PFSAs.	180
Table 10.2-4:	Compound-specific parameter settings for the LC-MS/MS analysis of replacement compounds, overlooked PFASs and precursors.	181
Table 10.2-5:	Compound-specific parameter settings for the LC-MS/MS analysis of the internal standards used for quantification of PFASs.	182
Table 10.2-6:	Overview of hardware components and parameter settings for the chromatographic separation as first step of the LC-QToF-MS ^E analysis.	183
Table 10.2-7:	Overview of hardware components and parameter settings for the mass spectrometric measurement as the second step of the LC-QToF-MS ^E analysis.	183
Table 10.3-1:	Overview of samples collected and analysed for this thesis.	186

Appendix North and Baltic Seas

Table A.1-1:	Sampling locations of water and sediment samples analysed in this study and physicochemical parameters measured in the water phase.	227
Table A.1-2:	Total organic carbon (TOC) content of the sediment samples analysed in this study.	229
Table A.1-3:	Mean concentrations of PFASs in procedural blanks \pm standard deviation (SD), method detection limits (MDLs) and method quantification limits (MQLs).	230
Table A.1-4:	Percentage absolute recoveries of internal standards in analysed surface water samples ($n = 92$) and sediment samples ($n = 24$).	232

Table A.1-5: Coefficients of variation [%] for quantified PFASs, calculated from triplicate analysis of water samples ($n = 7$) and duplicate analysis of sediment samples ($n = 3$).....	233
Table A.1-6: Detection frequencies, concentration ranges [ng/L], mean concentrations [ng/L] and median values [ng/L] of detected PFASs in surface water from the German Bight, the Elbe River, the German Baltic Sea and the Oder Lagoon.	234
Table A.1-7: Detection frequencies, concentration ranges [ng/g dw], mean concentrations [ng/g dw] and median values [ng/g dw] of detected PFASs in surface sediment from the entire study area, the German Bight, and the Elbe estuary. ...	235
Table A.1-8: Detection frequencies, concentration ranges [ng/g dw], mean concentrations [ng/g dw] and median values [ng/g dw] of detected PFASs in surface sediment from the Kattegat/Skagerrak, the Baltic Sea and the Oder Lagoon.....	236
Table A.1-9: Concentrations [ng/L] of detected PFASs in surface seawater samples from the German Bight (GB1-GB14).....	237
Table A.1-10: Concentrations [ng/L] of detected PFASs in surface seawater samples from the German Bight (GB15-GB29).....	238
Table A.1-11: Concentrations [ng/L] of detected PFASs in surface seawater samples from the Elbe River (E1-E18).....	239
Table A.1-12: Concentrations [ng/L] of detected PFASs in surface seawater samples from the Baltic Sea (BS2-BS17).....	240
Table A.1-13: Concentrations [ng/L] of detected PFASs in surface seawater samples from the Baltic Sea (BS18-BS33).....	241
Table A.1-14: Concentrations [ng/L] of detected PFASs in surface seawater samples from the Baltic Sea (BS34-BS43), the Oder Lagoon (OL1-OL3) and the Peene and Warnow Rivers (P1 and W1).....	241
Table A.1-15: Concentrations [ng/g dw] of detected PFASs in sediment samples from the German Bight and the Elbe River.	242
Table A.1-16: Concentrations [ng/g dw] of detected PFASs in surface sediment samples from the Kattegat/Skagerrak, the Baltic Sea and the Oder Lagoon.	243
Table A.1-17: Pearson correlation coefficients r between salinity and PFASs as well as among individual PFASs in surface water samples from the Elbe River.	244
Table A.1-18: Pearson correlation coefficients r and Spearman correlation coefficients r_{SP} (values in bold) between salinity and PFASs as well as among individual PFASs in surface water samples from the Baltic Sea.	245
Table A.1-19: Pearson correlation coefficients r between salinity and PFASs as well as among individual PFASs in surface water samples from the German Bight.	246
Table A.1-20: Pearson correlation coefficients r between TOC and PFASs as well as among individual PFASs in sediment samples over the entire study area.	247

Appendix Atlantic Gateway to the Arctic Ocean

Table A.2-1: Sampling locations of surface seawater samples analysed in this study and physicochemical parameters measured in the water phase.	248
--	-----

Table A.2-2: Sampling information for depth profiles analysed in this study and physico-chemical parameters measured in samples from the respective sampling depths.	250
Table A.2-3: Mean concentrations of PFASs in procedural blanks \pm standard deviation (SD), method detection limits (MDLs) and method quantification limits (MQLs).....	253
Table A.2-4: Coefficients of variation [%] for quantified PFASs, calculated from triplicate analysis of surface water samples taken by seawater intake system ($n = 2$) and samples taken by CTD/rosette sampler and seawater intake system at the same time ($n = 7$).....	254
Table A.2-5: Percent absolute recoveries of internal standards in analysed seawater samples ($n = 109$).	255
Table A.2-6: Detection frequencies [%], concentration ranges [pg/L], mean concentrations [pg/L] and median values [pg/L] of detected PFASs in surface water samples of the entire study area and along a latitudinal transect from the European continent to the Arctic.....	257
Table A.2-7: Detection frequencies [%], concentration ranges [pg/L], mean concentrations [pg/L] and median values [pg/L] of detected PFASs in surface water samples along a longitudinal and a latitudinal sampling transect in Fram Strait.....	258
Table A.2-8: Concentrations [pg/L] of detected PFASs in surface seawater samples taken along a latitudinal transect from the European continent to the Arctic.	259
Table A.2-9: Concentrations [pg/L] of detected PFASs in surface seawater samples taken along a longitudinal transect across Fram Strait... ..	260
Table A.2-10: Concentrations [pg/L] of detected PFASs in surface seawater samples taken along a latitudinal transect along the prime meridian.....	260
Table A.2-11: Pearson correlation coefficients r between physicochemical parameters and PFASs as well as among individual PFASs in surface water samples taken along a longitudinal transect across Fram Strait.	264
Table A.2-12: Detection frequencies [%], concentration ranges [pg/L], mean concentrations [pg/L] and median values [pg/L] of detected PFASs in all samples and in different water masses of the seven depth profiles taken in Fram Strait.....	265
Table A.2-13: Detection frequencies [%], concentration ranges [pg/L], mean concentrations [pg/L] and median values [pg/L] of detected PFASs in different water masses (Recirculating Atlantic Water/Arctic Atlantic Water (RAW/AAW), Intermediate Waters (IW) and Deep Waters (DW)) of the seven depth profiles taken in Fram Strait.	266
Table A.2-14: Concentrations [pg/L] of detected PFASs in depth profiles. Values in brackets are between MDL and MQL.	268
Table A.2-15: Water mass definitions used for classification of water samples taken for this study, adapted from Rudels <i>et al.</i> [287]......	270
Table A.2-16: PFAS mass transport estimates through Fram Strait via the boundary currents, based on water transport data derived from MITgcm model.	272
Table A.2-17: PFAS mass transport estimates through Fram Strait via the boundary currents, based on water transport data derived from observations.	273

Appendix Chinese and German Point Sources

Table A.3-1: Sampling locations and results of physicochemical parameters for surface water samples collected from German rivers.....	275
Table A.3-2: Sampling locations and results of physicochemical parameters for surface water samples collected from Chinese rivers.	276
Table A.3-3: Categorization of samples for target analysis.	277
Table A.3-4: Percentage absolute recoveries of internal standards in river water samples analysed by target analysis ($n = 58$) and TOP assay ($n = 31$).....	278
Table A.3-5: Method detection limits (MDLs) [ng/L] and method quantification limits (MQLs) [ng/L] for target analysis.....	279
Table A.3-6: Conversion yields of model precursors derived from oxidation tests in this study compared to data from literature.....	280
Table A.3-7: Method detection limits (MDLs) [ng/L] and method quantification limits (MQLs) [ng/L] for unoxidized and oxidized aliquots from the total oxidizable precursor (TOP) assay.	281
Table A.3-8: Annual flow rates for the investigated rivers.....	282
Table A.3-9: Concentrations [ng/L] of detected PFCAs and PFSA in surface water samples taken from German rivers.....	283
Table A.3-10: Concentrations [ng/L] of detected PFCAs and PFSA in surface water samples taken from Chinese rivers.	284
Table A.3-11: Concentrations [ng/L] of detected PFASs other than PFCAs and PFSA in surface water samples taken from German rivers.	285
Table A.3-12: Concentrations [ng/L] of detected PFASs other than PFCAs and PFSA in surface water samples taken from Chinese rivers.....	286
Table A.3-13: Percent contribution of the sum of branched isomers to total PFHpA, PFOA, PFHxS, PFOS and FOSA.....	288
Table A.3-14: Difference in PFAS concentrations between unoxidized and oxidized aliquots of samples taken from German rivers.....	290
Table A.3-15: Difference in PFAS concentrations between unoxidized and oxidized aliquots of samples taken from Chinese rivers.	292
Table A.3-16: Theoretical conversion of the precursor 6:2 FTSA, detected in German and Chinese river samples.	293
Table A.3-17: Percentage of measured difference in concentration of C ₄ to C ₇ -PFCAs attributed and unattributed to oxidation of 6:2 FTSA.....	294
Table A.3-18: Average PFAS mass flows estimates in river water downstream of point sources investigated in this study.	296

Appendix Suspect Screening

Table A.4-1: Back-mapping of observed structures to the original US EPA PFAS Master List.....	297
--	-----

Appendix Safety Data Information

Table A.5-1: Safety data information for used chemicals other than PFASs according to the Globally Harmonized System of Classification and Labelling of Chemicals (GHS).....	302
Table A.5-2: Safety data information on PFCAs according to the Globally Harmonized System of Classification and Labelling of Chemicals (GHS).....	304
Table A.5-3: Safety data information on PFASs and precursors according to the Globally Harmonized System of Classification and Labelling of Chemicals (GHS).....	305
Table A.5-4: Safety data information on PFAS standards other than PFCAs, PFASs and precursors according to the Globally Harmonized System of Classification and Labelling of Chemicals (GHS).....	306

List of Figures

Background

- Figure 2.1-1:** Exemplary chemical structure of A) perfluorooctanoic acid (PFOA) as a perfluoroalkyl substance and B) 8:2 fluorotelomer alcohol (8:2 FTOH) as a polyfluoroalkyl substance.3
- Figure 2.1-2:** General classification of per- and polyfluoroalkyl substances (PFASs).4
- Figure 2.4-1:** Comparison of the surface seawater concentration ranges of PFOA (red) and PFOS (blue) in coastal areas and different oceanic regions, reported in previous studies.13
- Figure 2.6-1:** Estimated annual releases of C₄ to C₁₄ PFCAs from fluoropolymer production sites between 1950 and 2015, comparing Japan, Western Europe and the US (blue) to India, Poland, China and Russia (red).16
- Figure 2.8-1:** Scheme of HRMS-based analytical approaches addressing targets, suspects and non-targets.26
- Figure 2.8-2:** Selectivity and inclusivity associated with targeted methods, sum parameters and HRMS-based approaches related to PFAS analysis.27

Method Development and Validation

- Figure 4.2-1:** Product ion spectrum of m/z 377.0, [M-H]⁻ of the replacement compound DONA.39
- Figure 4.2-2:** Ion path of API4000 triple quadrupole mass spectrometer.40
- Figure 4.2-3:** Optimization of transition-specific mass spectrometric parameters for HFPO-DA (329>169).41
- Figure 4.2-4:** LC-MS/MS chromatogram of a 100 pg/μL standard in methanol, using the initial LC method and the optimized mass spectrometric parameters.42
- Figure 4.2-5:** Boxplots showing the effects of different concentrations of ammonium acetate and acetic acid as modifier of the mobile phases on peak areas of target analytes (quantifiers and qualifiers) and internal standards.43
- Figure 4.2-6:** Peak shape of PFBA using different mobile phase additives and injection volumes.44
- Figure 4.2-7:** Peak shape of PFBA and the internal standard ¹³C₄-PFBA using a sample solvent composition of methanol:water 80:20 (v/v) for A) a calibration standard (15 pg/μL), B) a sediment sample, and C) a seawater sample.45
- Figure 4.2-8:** LC-MS/MS chromatogram of a 15 pg/μL calibration standard using the final chromatographic method.46
- Figure 4.2-9:** LC-MS/MS chromatograms of detected target analytes in a seawater sample using the final chromatographic method.47
- Figure 4.2-10:** LC-MS/MS chromatograms of the detected target analytes in a sediment sample using the final chromatographic method.48
- Figure 4.2-11:** LC-MS/MS chromatograms of PFOS and ¹³C₄-PFOS for A, B) a calibration standard, and C), D) a river water sample.49

Figure 4.2-12: A) MRM scheduling during the run with a maximum of 29 concurrent mass transitions. B) Effect of different target scan times on the number of data points acquired across the HFPO-DA peak.	52
Figure 4.2-13: Optimization of the heater (or turbo) gas pressure (gas 2).	53
Figure 4.3-1: LC-MS/MS chromatogram of an instrumental blank sample (methanol) showing MRMs of all target analytes and internal standards.	54
Figure 4.3-2: Boxplots showing coefficients of variation [%] of peak areas obtained for mass transitions used as A) quantifiers and B) qualifiers, resulting from tenfold measurements of standard mixes containing the native PFASs in concentrations of 1 pg/ μ L and 100 pg/ μ L (injection volume: 10 μ L).	55
Figure 4.3-3: A) Calibration curve of 6:2 Cl-PFESA in the linear range (0–100 pg/ μ L) using unweighted linear regression and 1/x weighted linear regression. B) Residuals [%] between the measured data points and the unweighted and 1/x weighted linear regression line versus the concentration of 6:2 Cl-PFESA [pg/ μ L] on a logarithmic scale.	57
Figure 4.4-1: Comparison of absolute recoveries of internal standards in river water and seawater applying the ISO standard 25101:2009.	63
Figure 4.4-2: Absolute recoveries of internal standards in seawater using different washing volumes during SPE.	64
Figure 4.4-3: Absolute IS recoveries in seawater using different approaches for the volume reduction step.	65
Figure 4.4-4: Overall method for the analysis of PFASs in aqueous samples and changes made in course of the optimization.	66
Figure 4.5-1: Relative recoveries resulting from matrix spike recovery tests for aqueous matrices for A) target analytes with isotopically-labelled analogues used as internal standards B) target analytes for which isotopically-labelled analogues are not available and which were assigned to structurally similar IS.	69
Figure 4.5-2: Coefficient of variation for PFASs > MQL, determined by sixfold analysis of a North Sea sample.	74
Figure 4.5-3: Comparison of own measured values (marked in green) for PFBA, PFOA and PFDA with laboratory intercomparison results (laboratories L1–L12), provided in the CRM certification report.	77
Figure 4.5-4: Comparison of own measured values (marked in green) for PFUnDA and PFDoDA with laboratory intercomparison results (laboratories L1–L12) provided in the CRM certification report.	77
Figure 4.6-1: Absolute matrix spike recoveries for A) PFCAs and PFSA, and B) other target analytes in marine sediment using different approaches for the volume reduction step.	80
Figure 4.6-2: Sequential extraction profile of a Baltic Sea sediment sample.	81
Figure 4.6-3: Final method for the analysis of PFASs in sediments and steps added in course of the method optimization.	82
Figure 4.7-1: Relative recoveries (mean \pm SD) for A) target analytes with corresponding internal standard and B) target analytes without corresponding internal standard, resulting from matrix spike recovery tests for marine sediments ($n = 3$, spiking level 0.6 ng/g dw).	83

Figure 4.7-2: Method precision for sediment analysis.....86

North and Baltic Seas

Figure 5.1-1: Sampling locations A) over the entire study area, including Skagerrak and Kattegat (SK1–SK4) and open water regions of the North Sea (31–33), B) in coastal areas of the German Bight (1–30) including the Elbe River (E1–E18), C) in coastal areas of the German Baltic Sea (1–43) including the Oder Lagoon (OL1–OL3) and the Peene and Warnow Rivers (P1 and W1).90

Figure 5.3-1: Concentrations [ng/L] and composition profiles of individual PFASs over the entire study area.92

Figure 5.3-2: Concentrations [ng/g dw] and composition profiles of individual PFASs in surface sediment samples over the entire study area.....96

Figure 5.3-3: Sediment/water partitioning coefficients $\log K_{OC}$ for individual PFCAs in this study in comparison to a laboratory study by Higgins and Luthy [259].....99

Figure 5.3-4: LC-MS/MS chromatograms of the replacement compound HFPO-DA and its predecessor PFOA and pie charts illustrating the ratio of the peak areas. Data resulted from the reanalysis of sample extracts taken in the area of the East Frisian Islands in the German Bight in 2007, 2011 and 2014, which were compared to a sample from this study, collected in 2017 in the same area.....103

Atlantic Gateway to the Arctic Ocean

Figure 6.2-1: A) Surface water sampling locations (red dots; samples taken at 11 m depth) along a latitudinal transect from the European continent to the Arctic Ocean (N1–N21), and a longitudinal (F1–F15) and latitudinal (P1–P5) transect within Fram Strait.....108

Figure 6.3-1: Sea ice concentration in the Arctic during the cruise.....112

Figure 6.3-2: PFHpA/PFNA ratio and sum of PFASs with a detection frequency > 50 % (C6 to C9 PFCAs, PFBS and HFPO-DA) versus salinity [psu] and temperature [°C] in samples taken along a longitudinal transect across Fram Strait.....113

Figure 6.3-3: Distribution of A) water masses, B) sum of PFASs with a detection frequency > 50 % (C6, C7, C9, C11 PFCAs and PFBS), C) temperature, D) salinity from bottom to surface and E) PFHpA and F) PFNA from 600 m depth to surface along the east-west cross section at ~79 °N (depth profiles V1 to V6, cruise stations PS114_12, 9, 25, 43, 46 and 49).116

Figure 6.3-4: PFAS mass transport estimates through Fram Strait via the boundary currents, calculated by combining measured PFAS concentrations (mean±SD) in Atlantic Water (AW), Polar Surface Water (PSW) and Recirculating/Arctic Atlantic Water (RAW/AAW) from this study with the average water volume transport [m^3/s] for the respective water mass over the years 2010–2015, derived from the MITgcm ECCO v4 model.....117

Chinese and German Point Sources

Figure 7.1-1: Pre-study to identify potential point sources along the River Rhine.124

Figure 7.1-2: Overview of selected study sites A) in Germany and B) in China.126

Figure 7.2-1:	Sampling site maps of the Chinese sites.....	127
Figure 7.2-2:	Sampling site maps of the German sites.	128
Figure 7.3-1:	Fate of ether-based PFASs in the TOP assay, compared to ¹³ C ₂ -PFOA.....	131
Figure 7.4-1:	PFAS concentrations and composition profiles up- and downstream of the point sources at site XQ (Xiaoqing River Basin, Dong Zhulong tributary, Huantai, China) and at site AZ (Alz River, Burgkirchen, Germany).....	133
Figure 7.4-2:	Contributions of individual PFASs to ΣPFASs in selected samples, downstream of the suspected point sources in the investigated rivers.	134
Figure 7.4-3:	Results from principal component analysis (PCA) on PFASs measured up- and downstream of the suspected point sources.....	135
Figure 7.4-4:	Percent contribution of the sum of branched isomers A) to total PFHxS and PFOS, and B) to total PFHpA and PFOA in the investigated rivers.....	136
Figure 7.4-5:	Percent increase of C ₄ to C ₇ PFCAs upon oxidative conversion by application of the TOP assay in A) German river water samples and B) Chinese river water samples.....	137
Suspect Screening		
Figure 8.2-1:	Developed PFAS suspect screening workflow using the Unifi software.....	143
Figure 8.2-2:	Peak picking in three-dimensional full-scan continuous data (low-energy function) of a river water sample (Fuxin River, FX_009).	144
Figure 8.2-3:	Workflow to create an “MS-ready” suspect list based on the “PFAS Master List” from the US EPA chemical database.....	147
Figure 8.3-1:	Number of components listed by Unifi after peak picking and componentization in analysed samples.	151
Figure 8.3-2:	Three-dimensional plots of full-scan continuous data (low-energy function) of Alz river water samples taken A) up- and B) downstream of the point source, and Dong Zhulong river water samples collected C) up- and D) downstream of the point source.	152
Figure 8.3-3:	Filtering of the componentized LC-QTOF-MS ^E data in the analysed samples from A) German rivers and B) Chinese rivers.....	153
Figure 8.3-4:	Overview of PFASs (tentatively) identified in this study, grouped according to their classification in the OECD PFAS database.....	154
Figure 8.3-5:	A) CF ₂ -adjusted Kendrick mass defect plots and B) retention time versus number of perfluorinated carbon atoms of PFASs (tentatively) identified in this study.....	155
Figure 8.3-6:	Peak areas of detected PFCAs and H-PFCAs downstream of the fluorochemical plants located at the Dong Zhulong River and the Alz River....	161
Figure 8.3-7:	Source-specific fingerprints of detected PFASs in selected samples.....	162
Figure 8.3-8:	Contribution of individual PFECAs to the total peak area of PFECAs downstream of the fluorochemical plants located at the German Alz River (AZ_003) and the Chinese Dong Zhulong River (XQ_005) and Xi River (FX_005).....	163
Figure 8.3-9:	PFBS/H-PFBS peak area ratio in the investigated rivers.....	164

Experimental

- Figure 10.3-1:** Different techniques for the collection of water samples, including A) a stainless steel frame with a mounted PP bottle, B) the ship's seawater intake system (stainless steel pipe), and C) a CTD/rosette sampler.....184
- Figure 10.3-2:** Sample collection of sediment samples using a stainless steel box corer.....185
- Figure 10.5-1:** Schematic overview of the sample preparation of aqueous samples.....188
- Figure 10.5-2:** Scheme of in-house prepared solid-phase extraction cartridges.....189
- Figure 10.6-1:** Schematic overview of the sample preparation of sediment samples.....191

Appendix Atlantic Gateway to the Arctic Ocean

- Figure A.2-1:** A) Salinity data and B) water temperature data from *Polarstern* cruise PS114, measured by sensor TSG1 (SBE21-3189, SBE38-118).249
- Figure A.2-2:** LC-MS/MS chromatograms of PFOA showing differences in contamination between cartridges of the same manufacturer and part number, packed with different WAX resin sorbent batches, 0035 (A) and 0038 (B).252
- Figure A.2-3:** Preparation and analysis of blank samples.....252
- Figure A.2-4:** Boxplots showing PFAS concentrations in surface water samples from the North Sea continental shelf (samples N1–N5, red), the continental slope (N6 to N11, blue) and deep water regions of the Norwegian Sea and Greenland Sea (N12 to N21, yellow).261
- Figure A.2-5:** Sampling locations of reanalysed samples, taken in the Rhine-Meuse delta in 2008 by Möller *et al.* [161].....263
- Figure A.2-6:** LC-MS/MS chromatograms of the replacement compound HFPO-DA in sample extracts from 2008, reanalysed using the current instrumental method.263
- Figure A.2-7:** Potential temperature θ [°C] versus salinity [psu] plots for A) CTD/rosette casts taken west of the surface front between inflowing Atlantic Water (AW) and outflowing Polar Surface Water (PSW) (~79 °N) and B) CTD/rosette casts taken east of it.271
- Figure A.2-8:** Comparison of estimated net transport of PFASs through Fram Strait via the boundary columns.....274

Appendix Chinese and German Point Sources

- Figure A.3-1:** Loadings for each principal component with dominant loadings shaded.287
- Figure A.3-2:** Molar percentage of C₄ to C₇ PFCAs pre-TOP and post-TOP, attributed and unattributed to conversion of the detected precursor 6:2 FTSA.295

1. Introduction

Per- and polyfluoroalkyl substances (PFASs) form a group of thousands of man-made chemicals that have been produced and used since the 1940s. The substances are chemically and thermally stable as well as repellent to water and oil. This explains their use in fire fighting foams and protective clothing, as well as in consumer products such as non-stick cookware, grease-proof fast food wrappers and outdoor gear.

Since the late 1990s, attention has been drawn to the role of long-chain PFASs as global contaminants of high concern because of their adverse effects on human health and the environment. Due to their extraordinary persistence, the compounds are expected to remain in the environment for hundreds of years. They have been detected globally in humans and wildlife and undergo long-range transport to remote regions, such as the Arctic and Antarctic. In several species, toxic effects on the liver are an indicative response to PFAS-exposure. The adverse effects also include a compromised immune response and effects on lipid metabolism.

Some PFASs, such as the well-known compounds perfluorooctanoic acid (PFOA) and perfluorooctane sulfonic acid (PFOS), have been extensively investigated and regulated. Along with regulatory actions to restrict their production, use and release, an industrial transition has taken place. This includes a geographical shift of production to countries with less stringent environmental law on the one hand and a transition to replacement chemicals and technologies on the other hand. For PFASs other than the well-studied long-chain compounds, information on the properties, environmental fate and transport, exposure and toxic effects is limited or completely missing. Similar molecular structures indicate that at least some of the replacement compounds are “regrettable substitutes”. Moreover, only a small fraction of the PFASs on the global market can be determined using conventional analytical methods. This raises the question whether currently monitored PFASs are representative or only make up a small fraction of anthropogenic PFAS releases.

This thesis aimed at developing analytical methods for the simultaneous determination of well-studied, regulated PFASs as well as replacement and “overlooked” PFASs in aqueous matrices and sediment. It was the aim to collect environmental samples in the North and Baltic Seas and along a sampling transect to the Arctic to investigate if replacement and “overlooked” PFASs are of relevance in the European coastal environment and if they are transported over long distances. For the long-chain PFASs, this thesis aimed at filling knowledge gaps on their ultimate sinks, including the deep ocean and marine sediments. In addition, Chinese and German river water samples impacted by industrial point sources were intended to be collected for application of new analytical approaches to characterize the unknown fraction of PFASs.

2. Background

2.1 Terminology and classification of PFASs

Per- and polyfluoroalkyl substances (PFASs) are a group of anthropogenic chemicals containing at least one perfluoroalkyl moiety, i.e. $-C_nF_{2n+1}$ [1]. Compounds in which all hydrogen substituents on all carbon atoms in the alkyl chain are replaced by fluorine are defined as perfluoroalkyl substances, whereas polyfluoroalkyl substances contain an alkyl chain in which not all carbon atoms (but at least one) are fully fluorinated (Figure 2.1-1) [1].

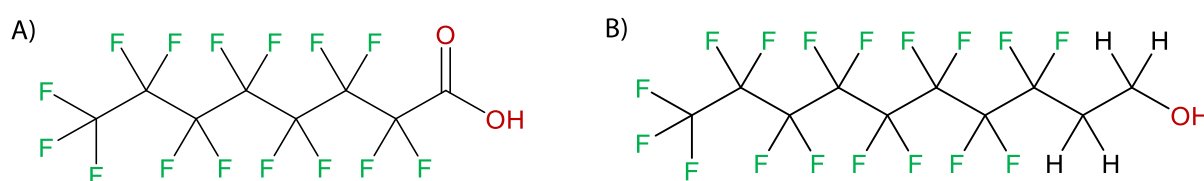


Figure 2.1-1: Exemplary chemical structure of A) perfluorooctanoic acid (PFOA) as a perfluoroalkyl substance and B) 8:2 fluorotelomer alcohol (8:2 FTOH) as a polyfluoroalkyl substance.

The well-established terminology of Buck *et al.* differentiates between non-polymeric and polymeric PFASs. The group of non-polymeric PFASs includes three major subgroups: (i) perfluoroalkyl acids (PFAAs) that are differentiated by their functional groups, such as perfluoroalkyl carboxylic acids (PFCAs) and perfluoroalkane sulfonic acids (PFSAs); (ii) precursors to PFAAs, including perfluoroalkane sulfonyl fluoride (PASF)-based precursors and fluorotelomer-based precursors, and (iii) per- and polyfluoroalkyl ether-based substances [1]. An overview of the general classification of PFASs is provided in Figure 2.1-2.

Moreover, a distinction is made between “long-chain” and “short-chain” PFASs. Adopting the definition provided by the Organisation for Economic Co-operation and Development (OECD), “long-chain” applies to PFCAs with seven or more perfluoroalkyl carbons ($C_nF_{2n+1}COOH$, $n \geq 7$), PFSAs with six or more perfluoroalkyl carbons ($C_nF_{2n+1}SO_3H$, $n \geq 6$), and their precursors. For PFASs other than that, a common terminology to differentiate between “long-chain” and “short-chain” homologues has not been agreed on [2].

The group of polymeric PFASs can be divided into fluoropolymers, side-chain fluorinated polymers and perfluoropolyethers. Fluoropolymers consist of a carbon-only backbone with fluorine atoms directly attached to the backbone (for example polytetrafluoroethylene (PTFE), also known as Teflon), whereas side-chain fluorinated polymers have a non-fluorinated polymer backbone with fluorinated side chains. Perfluoropolyethers consist of an ether backbone with fluorine atoms directly attached to it [1].

PFAS inventories are growing and increasingly diverse. In a recent study, 4,730 PFAS-related CAS registry numbers have been identified on the global market and were manually categorized [3]. The authors underline that this global PFAS database is comprehensive but not exhaustive, indicating that the list of PFASs will continue to expand. In addition to the commonly recognized groups of PFASs with an established terminology as in Buck *et al.*, new groups of PFASs have been identified, for example perfluorinated alkanes or perfluoroalkyl alcohols. They fulfil the well-established definition of PFASs but have not yet been commonly regarded as PFASs [3].



Figure 2.1-2: General classification of per-and polyfluoroalkyl substances (PFASs), adapted from Wang and co-authors [4].

In the past, PFASs were often referred to as “PFCs” (per- and polyfluorinated chemicals). However, the acronym “PFCs” has also been used to specifically designate perfluorocarbons (for example under the Kyoto Protocol), which contain only carbon and fluorine and no functional group. Containing a C_nF_{2n+1} moiety, perfluorocarbons are, by definition, PFASs, but the group of PFASs includes a much broader range of substances than just perfluorocarbons, as shown in Figure 2.1-2. Consequently, not the acronym “PFC” but the acronym “PFASs” and associated terminology as proposed by Buck *et al.* [1] is used in this thesis. For the newly identified PFAS classes, this thesis follows the terminology and categorization proposed for the OECD global PFAS database [3].

2.2 Physical and chemical properties

The unique properties of fluorine as a substituent in organic chemistry are key for the broad range of PFAS applications and their environmental behaviour [5].

Fluorine is the most electronegative element ($\chi = 3.98$ on the Pauling scale [6]), resulting in highly polarized carbon-fluorine bonds with significant electrostatic character ($C^{\delta+}-F^{\delta-}$). The attraction between the partial charges contributes to the strength of the carbon-fluorine bond, the strongest single bond between a carbon atom and any element [7]. Increasing fluorine substitution at the carbon increases the C-F mean bond enthalpy (CH_3F 448 kJ/mol < CH_2F_2 459 kJ/mol < CHF_3 480 kJ/mol < CF_4 486 kJ/mol) [5]. The main reason for this stabilization is the nearly optimum overlap between the 2s and 2p orbitals of fluorine and the corresponding orbitals of carbon [8].

In addition to the strength of the carbon-fluorine bond, the moderate size of fluorine is an important factor for the thermal stability of PFASs. The van der Waals radius of fluorine is 147 pm, which is smaller than that of the other halogens (Table 2.2-1) and close to that of hydrogen (120 pm) [9]. In combination with the comparatively short C-F bond length (Table 2.2-1), this leads to shielding of the carbon skeleton by fluorine atoms without steric stress [5]. Moreover, the three tightly bound non-bonding electron pairs per fluorine atom and the negative partial charge shield the central carbon atoms against nucleophilic attacks, explaining the high chemical stability of PFASs [8].

Table 2.2-1: Characteristics of carbon-halogen and the carbon-carbon bonds, redrawn from Kirsch [8].

X	H	F	Cl	Br	I	C
bond length C-X [pm]	109	138	177	194	213	-
binding energy C-X [kcal/mol]	98.0	115.7	77.2	64.3	50.7	~83
electronegativity χ (Pauling scale)	2.20	3.98	3.16	2.96	2.66	2.55
dipole moment μ , C-X	(0.4)	1.41	1.46	1.38	1.19	-
van der Waals radius [pm]	120	147	175	185	198	-
atom polarizability a [$10^{-24}/cm$]	0.667	0.557	2.18	3.05	4.7	-

In addition to their high stability, PFASs are characterized by their low surface tension along with their high surface activity. Although the carbon-fluorine bond is highly polarized, perfluorocarbons are among the most non-polar solvents. This can be explained by the fact that the local dipole moments within the same molecule cancel one another. Due to weak intermolecular interactions, the surface tension γ of perfluoroalkanes is lower than that of the non-fluorinated analogues. As an example, γ is 11.4 dyn/cm for perfluorohexane compared to 17.9 dyn/cm for the non-fluorinated analogue *n*-hexane [8]. In addition to the hydrophobic fluorinated alkyl chain, PFASs typically contain a hydrophilic headgroup. This amphiphilicity contrasts the properties of other halogenated compounds, which are mainly lipophilic, and results in compounds with a high surface activity, which are water- and oil-repellent at the same time. The longer the perfluorinated alkyl chain, the higher the surface activity, i.e. the surface tension reduction. At relatively low concentrations, PFASs, also referred to as “fluorosurfactants”, lower surface tension more than other surfactants. For example, fluorosurfactants (for example $n\text{-C}_n\text{F}_{2n+1}\text{COOLi}$, with $n \geq 6$) can commonly reduce the surface tension of water ($\gamma = 72$ dyn/cm) to 15–20 dyn/cm compared to 25–35 dyn/cm for analogous hydrocarbon surfactants [10].

Due to the strong electron-withdrawing effects of fluorine, the acidity of acids, alcohols, and amides is increased by fluorination. For instance, the acid dissociation constant (pK_a) of trifluoroacetic acid (0.52) is four orders of magnitude lower than that of the non-fluorinated acetic acid (4.76) [8]. pK_a values are only available for a limited number of PFASs and of great uncertainty. For perfluorooctanoic acid (PFOA) as one of the best-studied PFASs, available model-predicted and experimental pK_a values range from -0.5 to 3.8 and the scientific debate on what is the environmentally relevant pK_a is still ongoing [11]. Challenges in experimental pK_a determination for PFASs, as well as in the measurement of other physicochemical and environmental partitioning properties, such as the $\log K_{ow}$, result from the surfactant properties of the compounds, their enrichment at surfaces and the self-aggregation in solution [11]. However, as strong acids, PFOA and other PFAAs are expected to be present in the dissociated anionic form at most environmentally relevant pH values ($\text{pH} \geq 5$) and are characterized by a high water solubility and a negligible vapour pressure. In contrast, fluorotelomer alcohols and other precursors to PFAAs, are non-ionic at neutral pH. They have a low water-solubility and sufficient vapour pressure to partition out of water to air [5].

2.3 Production and use

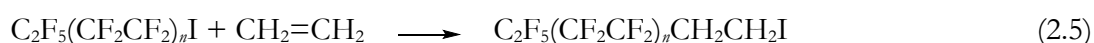
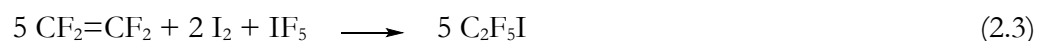
PFASs have been produced since the mid-20th century, using three major synthesis routes: electrochemical fluorination (ECF), telomerization and oligomerization [1, 5, 10].

The ECF process was developed by J.H. Simons and co-workers and patented by 3M in the 1940s [12, 13]. An organic raw material undergoes electrolysis in anhydrous hydrogen fluoride (HF), resulting in the substitution of hydrogen atoms in the feedstock with fluorine. Thereby, perfluoroalkane sulfonyl or carbonyl fluorides (PASFs/PACFs) can be produced using alkane sulfonyl or carbonyl fluorides as a starting material (2.1 and (2.2). The PASFs/PACFs can be hydrolysed to yield the corresponding acids (i.e. PFSA/PFCA) or their salts, or be further reacted to related derivatives, for example to perfluoroalkyl sulfonamides.



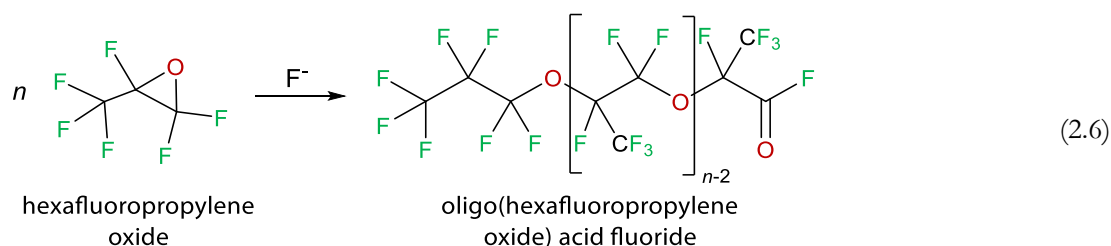
During the ECF process, fragmentation and rearrangement of the carbon skeleton occurs, resulting in a complex mixture of the target compounds and homologues of varying chain lengths (even- and odd-carbon-numbered), linear and branched isomers, as well as different by-products [14]. In the case of the most discussed and reported PFASs, perfluorooctane sulfonic acid (PFOS) and PFOA, ECF yields approximately 70 % to 80 % linear and 20 % to 30 % branched isomers [1].

As second major synthesis route, the commercial telomerization of tetrafluoroethylene (TFE) with pentafluoroethyl iodide was developed by the DuPont company (now Chemours) in the 1970s. By reacting iodine pentafluoride and iodine with TFE, pentafluoroethyl iodide is prepared as a “telogen” (2.3). The subsequent radical reaction with TFE as an unsaturated “taxogen” molecule results in a mixture of even-carbon-numbered perfluoroalkyl iodides (PFAIs) with varying chain lengths (2.4) [5]. While PFAIs can be directly hydrolysed to PFCAs, the free-radical ethenylation to fluorotelomer iodides (FTIs) gives a more versatile synthesis intermediate (2.5). By various reactions, FTIs can be transformed to fluorotelomer-based derivatives, for example to fluorotelomer alcohols, thiols or (meth)acrylates [14].



If linear telogen and taxogen are used as starting material, the resulting PFAIs have exclusively linear perfluoroalkyl chains. Although their formation mechanism is unknown, PFCAs were detected as by-products using the telomerization synthesis route [1].

Using the oligomerization approach as a third synthesis route, already fluorinated compounds are combined in a building block manner [15]. The process is typically used for the production of per- and polyfluoroether-based substances. For example, the fluoride-catalysed oligomerization of hexafluoropropylene oxide (HFPO; 2,2,3-trifluoro-3-trifluoromethyloxirane), an epoxide, yields perfluoroalkyl ether acid fluorides (2.6) [16]. These can be further converted into an acid, into an acid salt, such as the ammonium salt of the HFPO dimer acid (HFPO-DA), and other related derivatives as esters and amides, analogous to the derivatives from the ECF synthesis [17].



Due to their high chemical and thermal stability and amphiphilic nature, PFASs are used in a wide range of industrial applications and consumer products. This includes their use as emulsifiers in the polymerization of certain fluoropolymers, such as PTFE and PVDF, as film formers in fire-fighting foams and as wetting and mist-suppressing agents in metal (chromium) plating. Moreover, PFASs are used as surface treatment agents in a range of products to impart both water and oil/stain repellency, for instance to textiles, outdoor equipment, shoes, upholstery and carpets, as well as to food contact materials like non-stick kitchenware, fast food wrappers, pizza boxes and coffee-to-go cups. Additionally, ski waxes for competitive skiers often contain PFASs because their high water repellency results in a better glide compared to hydrocarbon-based waxes [5, 18]. PFASs are also used as active ingredients in pesticides, for example in ant baits or plant growth regulators [19]. Due to the similar van der Waals radius (see Chapter 2.2), fluorine can be used to replace hydrogen in active ingredients without changing the chemical structure significantly in geometry and shape. At the same time, fluorination changes the properties of the compound, which is used in design of pharmaceuticals and agrochemicals to improve effectiveness and/or to achieve inertness [8, 20].

Release of PFASs to the environment occurs during the production of PFASs and during the life-cycle of products, including manufacture, use and disposal. Products can contain PFASs as ingredients, unreacted raw materials (residuals) or unintended by-products (impurities). These sources are considered as “direct” sources, whereas “indirect” sources refer to formation of particular PFASs by degradation of precursors [19]. PFASs may enter the environment via different routes. Point sources include manufacturing sites, fire training and fire response sites, wastewater

treatment plants and landfills, whereas diffuse sources include surface runoff and wet/dry deposition [21].

2.4 Environmental concerns about long-chain PFASs

Since the late 1990s, attention has been drawn to the role of long-chain PFCAs and PFSA and their precursors as global contaminants of high concern because of their adverse effects on human health and the environment.

2.4.1 Persistence

PFCAs and PFSA are resistant to abiotic and biotic degradation and thus persistent in the environment [19]. In contrast to the fully fluorinated acids, many partially fluorinated PASF- and fluorotelomer-based derivatives, such as fluorotelomer alcohols (FTOHs) and perfluorooctane sulfonamido ethanols (FOSEs) can undergo degradation, abiotically or biotically. During this process, PFCAs and/or PFSA are formed as persistent end products. For example, biotransformation or atmospheric degradation of 8:2 FTOH results in formation of PFOA [22-24].

In degradation studies conducted in systems similar to the natural environment, the atmospheric lifetimes of PFCAs with three or more carbons were estimated to be approximately 130 days. However, the major atmospheric removal mechanism is supposed to be wet and dry deposition, which probably occurs on a time scale of the order of 10 days [25]. In other environmental media, degradation is assumed to be negligible [26-28]. The photolytic half-life of PFOA was estimated to be at least 256 years at a water depth of 0 m, > 5,000 years in the mixing layer of the open ocean and > 25,000 years in the coastal ocean [28]. This is much longer than most of the competing environmental processes, such as sediment burial and transport to deep ocean water, which are assumed to determine the long-term fate of PFCAs and PFSA [29].

2.4.2 Bioaccumulation

Long-chain PFCAs and PFSA are bioaccumulative [30, 31] and have the potential to biomagnify along food chains [32-34]. Laboratory and field studies show a substantial interspecies variability in bioaccumulation of long-chain PFCAs and PFSA. Serum elimination half-lives of PFOS are on the order of one to two months in rats and mice and approximately four months in monkeys [35]. In human serum, estimated half-lives are much longer with 5.4 years reported for retired fluorochemical production workers [36].

Unlike lipophilic persistent organic pollutants, such as polychlorinated biphenyls (PCBs) and polybrominated diphenylethers (PBDEs), long-chain PFASs are typically enriched in protein-rich tissues like blood, liver and kidneys and they are not predominantly present in adipose tissue [37-39]. The interaction of PFASs with proteins has been identified as important factor for this

distribution. Long-chain PFCAs and PFSAAs have a high binding affinity to plasma albumin, explaining their accumulation in blood [40, 41]. Moreover, human renal membrane transport proteins, namely organic anion transporter 4 (OAT 4) and urate transporter 1 (URAT1), were shown to facilitate the reabsorption of PFOA from urine back to blood and may contribute to the long half-life of particular PFAAs in humans [42]. In addition, PFAAs bind to cytosolic fatty acid binding proteins (FABPs), which facilitate the transfer of fatty acids between extra- and intracellular membranes in different tissues [43-45].

During pregnancy, PFAAs can cross the placental barrier in both laboratory animals and humans, exposing neonates through their mother's blood. Maternal transfer also occurs postnatally through breastfeeding [46, 47].

For a given chain length, bioaccumulation is dependent on the functional group. It is more effective for PFSAs than for PFCAs, probably due to a higher binding affinity to proteins [48]. For example, bioaccumulation factor means of perfluorononanoic acid (PFNA) and PFOS, both having eight perfluorinated carbon atoms, were 900 and 1800 L/kg, respectively [30]. Moreover, bioaccumulation is directly related to the carbon chain length of PFCAs and PFSAs, with a higher bioaccumulation factor the longer the chain is [30].

2.4.3 Toxicity

Most of the toxicity studies have focused on PFOS and PFOA. While the acute toxicity of PFOS and PFOA is considered to be moderate after oral administration, continuous or repeated exposure causes adverse effects in animals and humans [49, 50].

In laboratory animal toxicity studies, the liver has been identified as the major target organ of PFOS and PFOA in rodents, as indicated by increased liver weight and induction of peroxisomal β -oxidation, which affects the fatty acid metabolism [49]. Exposure of rodents to high doses of PFOS or PFOA resulted in increased neonatal mortality, while growth deficits and developmental delays were reported for offspring exposed to lower doses [51-53]. The most sensitive endpoints for PFOS were the impact on maternal liver weight, placental physiology and aspects of glucose metabolism, at doses of 0.3, 0.5 and 0.3 mg/kg body weight (bw) per day [49, 54]. Following PFOA exposure, increased liver-weight was noted at doses of 0.1 mg/kg bw/day in mice pups and of 0.6 mg/kg bw/day in mothers, respectively [55]. Due to the developmental toxicity potential of PFOS and PFOA, both compounds are classified as toxic for reproduction category 1B according to Regulation (EC) No 1272/2008 on classification, labelling and packaging of substances and mixtures (CLP Regulation) [56].

Affecting structural and functional parameters in rodents' immune systems, PFOS and PFOA are also considered potential immunotoxins [49]. Laboratory studies indicate that the compounds suppress both acquired and innate immunity in mice and compromise their cell-mediated and

humoral immune responses [50]. The no observed adverse effect level (NOAEL) in mice was 1.66 µg/kg bw per day for PFOS [57] and 1 mg/kg bw per day for PFOA [58], respectively.

In carcinogenicity studies, PFOS was shown to induce liver tumours in rats [59]. In rats treated with PFOA chronically, increased incidences of testicular (Leydig cell) tumours were found [49, 60]. The International Agency for Research on Cancer (IARC) classified PFOA as “possibly carcinogenic to humans” (group 2B) [61], whereas no evaluation is available for PFOS.

Additional adverse effects attributed to PFAAs include the endocrine-disrupting, neurotoxic and obesogenic potential of PFOS and PFOA. However, these effects require substantial additional elucidation as they are only discussed in a few studies that are partly contradictory [50].

For many of the observed effects, activation of the peroxisome proliferator-activated receptor α (PPAR α) has been described as the major mechanism of action [62, 63]. PPAR α is a ligand-activated transcription factor regulating expression of genes involved in lipid and glucose metabolism, cell proliferation and differentiation, and inflammatory responses [64]. It was shown that PFCAs are stronger activators of mouse and human PPAR α than PFSA. Moreover, activity increased with increasing chain length of the PFAA up to PFNA [65, 66]. Due to the differences in peroxisome proliferation expression, results from experimental studies in rodents cannot be translated directly to human health impacts [65-67].

Prompted by the findings in laboratory animal toxicity studies, human epidemiological studies were conducted to assess links between PFAS exposure and human health.

The most comprehensive epidemiological study involved 69,000 individuals and was conducted by the C8 Science Panel, formed as part of the settlement of a class action lawsuit between communities in the Mid-Ohio Valley in the United States and the chemical company DuPont. The population had been potentially affected by the releases of PFOA, emitted since the 1950s from DuPont’s Washington Works Plant [68]. Probable links between PFOA exposure and six diseases have been identified in this study: high cholesterol, ulcerative colitis, thyroid diseases, testicular and kidney cancer, and pregnancy-induced hypertension [69-72]. Moreover, a birth cohort study of 656 children from the Faroe Islands revealed that elevated exposures to PFOS, PFOA and PFHxS in children aged 5 and 7 years were associated with reduced humoral immune response to routine childhood immunizations for tetanus and diphtheria [73].

Based on human epidemiological studies, the European Food Safety Authority (EFSA) identified the increase in serum cholesterol in adults as the critical effect for PFOS and PFOA [49], i.e. that adverse effect which is likely to occur at the lowest dose under the expected conditions of exposure [74]. For PFOS in children, the decrease in antibody response at vaccination was identified as critical effect. EFSA estimated that consumption of fish and other seafood make the most important contribution to chronic exposure to PFOS (up to 86 % in adults). For PFOA, the most

important sources were milk and dairy products for toddlers (up to 86 %), drinking water (up to 60 % in infants) and fish and other seafood (up to 56 % in elderly). A tolerable weekly intake (TWI) of 13 ng/kg bw per week for PFOS and 6 ng/kg bw per week for PFOA was proposed by EFSA in 2018. These values are considerably lower than the tolerable daily intakes (TDIs) defined by EFSA in its original assessment in 2008 (150 ng/kg bw per day for PFOS and 1,500 ng/kg bw per day for PFOA). Based on different dietary scenarios, EFSA concluded that exposure of a considerable proportion of the European population exceeds the proposed TWIs. EFSA pointed out that due to high scientific uncertainties, specifically regarding the exposure assessment, the conclusions shall be considered provisional. They will be reviewed while the second part of the assessment, which is on PFASs other than PFOS and PFOA, is completed [49]. However, commenting on the EFSA reassessment, the German Federal Institute for Risk Assessment (Bundesinstitut für Risikobewertung, BfR) stated that “BfR cannot fully uphold its 2008 statement that a health risk to consumers is unlikely due to current exposure to PFOS and PFOA through food” [75]. This underlines that exposure of the European population to PFOS and PFOA is of concern.

2.4.4 Occurrence and long-range transport

The global occurrence of PFOS in wildlife was first reported in 2001 [76]. Since then, PFCAs, PFASs and their precursors have been detected in environmental matrices [21, 77, 78], aquatic and arctic wildlife [79, 80] and humans [81-84] worldwide. This includes areas remote from the sources of their release, such as the Arctic [85-88] and Antarctic [89-91].

Data that has been collected on PFOS and PFOA in coastal and open-ocean surface water since the 2000s is summarized in Figure 2.4-1. The occurrence of the compounds in all major divisions of the global ocean underlines their ubiquitous presence. Depending on the location and the compound, concentrations are typically several tens to hundreds of pg/L in open-ocean seawater. In coastal areas, concentrations are up to three orders of magnitude higher. PFOS and PFOA were typically in the same concentration range in open-ocean seawater, whereas in coastal seawater, significantly higher concentrations of PFOA than of PFOS are reported in recent studies, particularly from Asian countries (Figure 2.4-1, f and g) [92, 93]. This is possibly related to the global phase-out of PFOS in the 2000s (see Chapter 2.5), having a faster effect on coastal areas influenced by point sources than on open-ocean seawater. Along latitudinal transects in the Atlantic Ocean, concentrations in the northern hemisphere, influenced by major source areas in North America and Europe, were generally higher than in the southern hemisphere (Figure 2.4-1, i and j) [87, 94]. An exception was the Southwest Atlantic, where comparatively high concentrations of PFOS and PFOA were observed along the South American coast (Figure 2.4-1, l and k) [95, 96]. This is possibly attributable to the use of the pesticide Sulfluramid (*N*-ethyl perfluorooctane

sulfonamide, *N*-EtFOSA) in South America. *N*-EtFOSA is applied to control leaf-cutting ants and known to degrade to PFOS and/or PFOA [95, 96].

Based on these data, it is undisputed in the scientific community that long-chain PFCAs and PFSA s undergo long-range transport. As potential transport mechanisms, transport by ocean currents [97] and atmospheric transport of volatile precursors, which are degraded to PFCAs and PFSA s [98], were identified. Discussions on the proportion to which each process contributes to the long-range transport of PFCAs and PFSA s are still ongoing [23, 86].

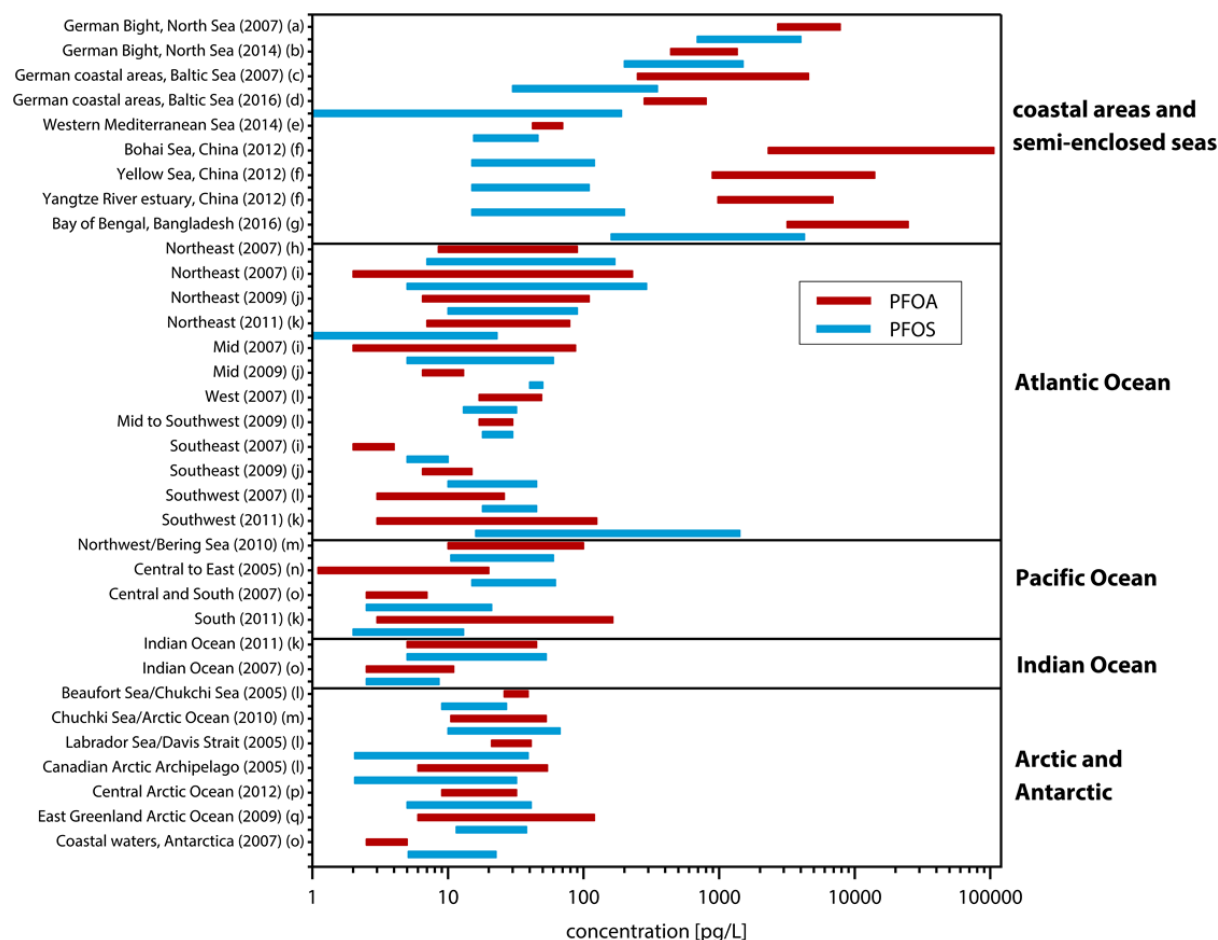


Figure 2.4-1: Comparison of the surface seawater concentration ranges of PFOA (red) and PFOS (blue) in coastal areas and different oceanic regions, reported in previous studies. The major oceanic division investigated in the respective study is given on the right and the subdivision on the left. The sampling year is given in brackets. The bars extend from the minimum to the maximum of the reported values on a logarithmic scale. Concentrations below the method detection (MDL) limit are given as one-half the MDL. (a) Ahrens *et al.* [99], (b) Heydebreck *et al.* [100], (c) Ahrens *et al.* [101], (d) Heydebreck *et al.* [102], (e) Brumowský *et al.* [103], (f) Zhao *et al.* [92], (g) Habibullah *et al.* [93], (h) Theobald *et al.* [104], (i) Ahrens *et al.* [94], (j) Zhao *et al.* [87], (k) González-Gaya *et al.* [96], (l) Benskin *et al.* [95], (m) Cai *et al.* [105], (n) Yamashita *et al.* [106], (o) Wei *et al.* [107], (p) Yeung *et al.* [108], (q) Busch *et al.* [109].

While data on PFOS and PFOA in surface water cover all major divisions of the global ocean, data on deeper ocean water is very limited. Strong differences between the available vertical profiles indicate that intrusion of PFASs into deep waters is influenced by stratification, mixing and deep water formation in the respective sampling area [110]. In the Labrador Sea, a region with young

deep water (< 10 years [111]), PFASs were detected down to 3,500 m depth [112]. In contrast, PFASs were only detectable above 150 m depth in the central Arctic [108], where deep water is much older (up to 450 years [113]) and does not reflect a period of substantial PFAS production. More information on the vertical distribution of PFASs in the oceans is essential to reduce uncertainties in global PFAS mass balances and assess the role of the oceans as a sink of PFASs.

In addition to deep ocean water, marine sediments are a potential ultimate sink for PFASs. The distribution of PFASs in coastal sediments was investigated in a few studies [114-118], albeit to a smaller extent than the distribution of PFASs in surface seawater. In comparison to studies focusing on quantities of PFASs entering into the aquatic environment, there is only limited information on the partitioning behaviour of the compounds between water and sediment, which is crucial for understanding the transport and fate of PFASs in the marine environment [93, 117-119]. Findings have been inconsistent and show that the partitioning of PFASs is a complex process, depending not only on the physicochemical characteristics of the compounds but also on the sediment nature such as the organic carbon fraction and environmental parameters that vary regionally [93, 117].

2.5 Regulatory actions and voluntary industry initiatives

The increased understanding of the adverse effects of long-chain PFCAs and PFASs, i.e. of the fact that they are persistent, bioaccumulative, toxic and undergo long-range transport, has led to a number of initiatives by regulatory authorities and industry.

In 2000, the major manufacturer 3M announced a global phase-out plan to be carried out by 2002 for products derived from perfluorooctane sulfonyl fluoride (POSF), including the C₆ and C₁₀ homologues (3M, 2000). Industrial initiatives were continued in 2006 when eight major producers, namely Arkema, Asahi, Ciba (now BASF), Clariant (now Archroma), Daikin, DuPont (now Chemours), 3M, and Solvay Solexis, joined in a global stewardship program implemented by the United States Environmental Protection Agency (US EPA). Thereby, they committed to working toward eliminating perfluorooctanoic acid (PFOA), its precursors and related higher-homologue chemicals by 2015 [120].

At an international regulatory level, PFOS, its salts and POSF were added to Annex B of the Stockholm Convention on Persistent Organic Pollutants in 2009, implementing restrictions on their production and use [121]. In 2019, the Parties to the Stockholm Convention also adopted the listing of PFOA, its salts and PFOA-related compounds in Annex A and thereby committed to eliminating the production and use of the compounds [122]. The evaluation of perfluorohexane sulfonic acid (PFHxS) is currently ongoing [123]. The Stockholm Convention was implemented in

the European Union by Regulation (EC) No 850/2004, which is directly applicable law in all Member States.

Under the European regulation for Registration, Evaluation, Authorization and Restriction of Chemicals (REACH), PFOA, PFHxS as well as C₉ to C₁₄-PFCAs, their salts and precursors were added to the Candidate List of Substances of Very High Concern from 2012 to 2017 (ECHA, 2019). To restrict PFOA, its salts and precursors under REACH, the Commission Regulation (EU) No 2017/1000 came into force in 2017 and will be implemented beginning in 2020.

The regulations discussed above, which aim at restricting production and use of the compounds, are accompanied by regulations to minimize emissions to the environment and human exposure. On European level, PFOS and its derivatives are classified as priority hazardous substances under the Water Framework Directive (WFD) 2000/60/EC. The WFD is complemented by the Directive on Environmental Quality Standards (2008/105/EC, amended by 2013/39/EC), setting the annual average environmental quality standard (AA-EQS) of PFOS at 0.65 ng/L in inland surface waters and 0.13 ng/L in seawater. The maximum allowable concentration (MAQ-EQS) is 36 µg/L in inland surface waters and 7.2 µg/L in seawater, respectively [124]. On a national level, a drinking water guidance value of 0.1 µg/L for PFOS and PFOA was set in Germany [125]. For sewage sludge used as fertilizer, the limit value for the sum of PFOS and PFOA is 100 µg/kg dw (dry weight) according to the German Fertilizer Ordinance [126].

2.6 Shift of production

Along with the regulatory actions to restrict the production, use and release of long-chain PFCAs and PFSA, an industrial transition has taken place – a geographical shift on the one hand and a transition to replacement chemicals and technologies on the other hand.

Production has been shifted from countries in North America, Europe and Japan to countries with less stringent regulations, especially to China and other Asian countries. Thus, the stepwise phase-out of the production of long-chain PFCAs, PFSA and their major precursors in Europe, North America, and Japan is contrasted with only a limited phase-out and sometimes even increasing production in Asian countries [127, 128]. For example, Chinese companies began large-scale production of PFOS and related products in 2003 – after the American company 3M announced the phase-out of the compound in 2002. In addition, Western companies built production sites in Asia and ramped up production. Consequently, the estimated annual production of POSF in China increased from 50 t in 2003 to 250 t in 2006, of which approximately 100 t was exported to other countries, including Brazil and member states of the European Union [129]. Likewise, global emission estimates for C₄ to C₁₄ PFCAs decreased for Europe, North America,

and Japan after 2002, while strongly increasing for emerging economies in continental Asia [130]. This is exemplified for releases from fluoropolymer production sites in Figure 2.6-1.

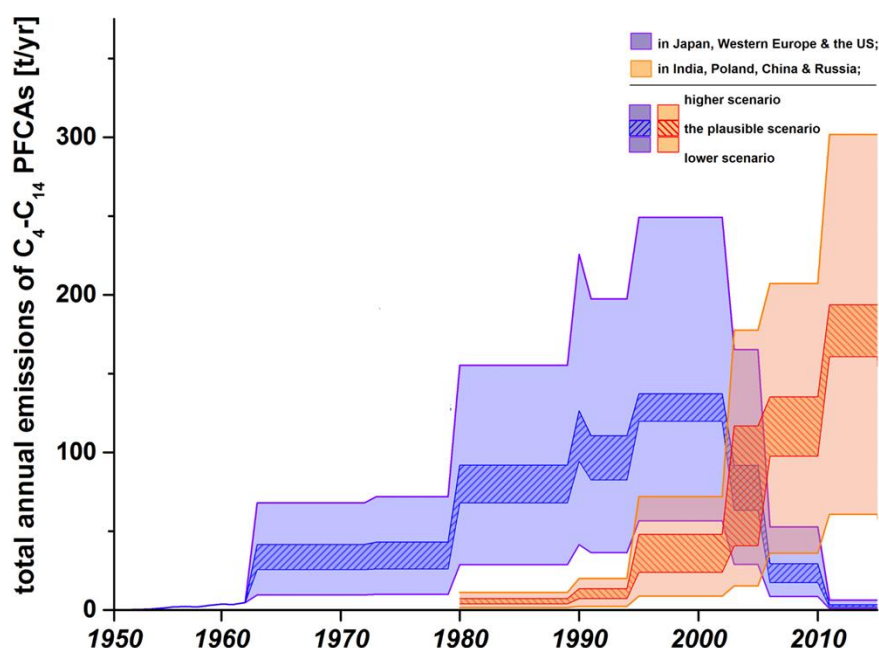


Figure 2.6-1: Estimated annual releases of C₄ to C₁₄ PFCAs from fluoropolymer production sites between 1950 and 2015, comparing Japan, Western Europe and the US (blue) to India, Poland, China and Russia (red). Reproduced from Wang *et al.* [128].

In the meantime, production and use of both PFOS and PFOA and related compounds have been restricted on an international level in 2009 and 2019, respectively. Consequently, major producers in continental Asia have also announced reduction actions regarding long-chain PFASs and PFCAs, requiring substantial resources [4]. For example, the project “Reduction and Phase-out of PFOS in Priority Sectors in China”, supported by the Global Environment Facility (GEF) and planned for five years (2015-2020), will cost 177 million USD [131]. Although no clear timeline is given, it is expected that emissions of PFOS, PFOA and their precursors are being reduced and their production and use will be globally eliminated in the foreseeable future [4].

Along with the phase-out of long-chain PFASs and their precursors, an industrial transition to replacement compounds has been taking place since the 2000s. Many of the substitutes are still PFASs. They include short-chain homologues and their precursors, such as perfluorobutane sulfonic acid (PFBS) and 6:2 fluorotelomer-based compounds, but also PFASs with different functionalities, such as per- and polyfluoroalkyl ether carboxylic and sulfonic acids (PFECAs and PFESAs) [132].

To replace salts of PFOA as processing aid in fluoropolymer manufacturing, the single largest direct use of PFASs, the major manufacturers have developed different PFECAs. Chemours makes use of the dimer acid of hexafluoropropylene oxide (HFPO-DA, 2,3,3,3-tetrafluoro-2-

(1,1,2,2,3,3,3-heptafluoropropoxy)propanoic acid), introduced into the market as its ammonium salt GenX. In contrast, 3M applies 2,2,3-trifluoro-3-[1,1,2,2,3,3-hexafluoro-3-(trifluoromethoxy)propoxy]propanoic acid, marketed as its ammonium salt ADONA, and Asahi uses 2,2-difluoro-2-[1,1,2,2-tetrafluoro-2-(1,1,2,2,2-pentafluoroethoxy)ethoxy]acetic acid, sold as its ammonium salt EEA-NH₄ [132, 133]. The substitution of salts of PFOA by multiple other compounds increases the variety of PFASs on the global market. This also applies to the replacements of PFOS salts used as wetting and mist-suppressing agents in metal plating. In China, 6:2 chlorinated polyfluoroalkyl ether sulfonic acid (6:2 Cl-PFESA), a PFESA marketed as its potassium salt F-53B, has been used as alternative since the 1970s [134]. In addition, salts of 6:2 fluorotelomer sulfonic acid (6:2 FTSA) are applied as PFOS substitutes in metal plating in both Europe and China [129]. An overview of known replacements and their predecessors in different industrial branches is given in Table 2.6-1.

In some cases, a lower efficacy and higher costs have been reported as drawbacks of replacements. For example, 6:2 FTSA has been mentioned to be less efficient and less durable under the harsh conditions of metal plating, due to its higher surface tension compared to PFOS. Consequently, larger quantities of the substitute are needed to provide the same performance [135]. In China, the cost of F53-B is claimed to be approximately 10–15 % higher than the price of the PFOS-containing product [129].

Table 2.6-1: Known fluorinated alternatives to long-chain PFCAs and PFSA's and their precursors used in fluoropolymer manufacture and metal plating.

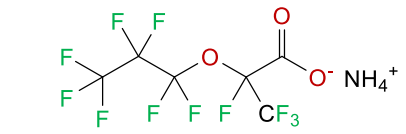
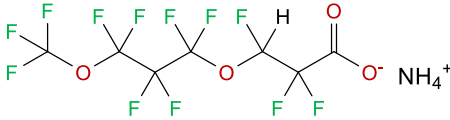
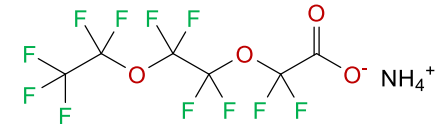
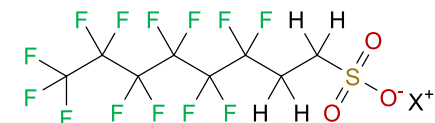
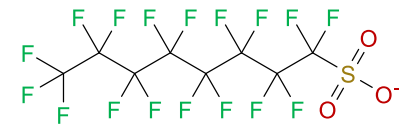
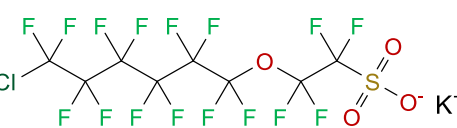
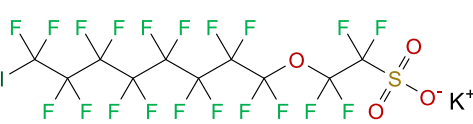
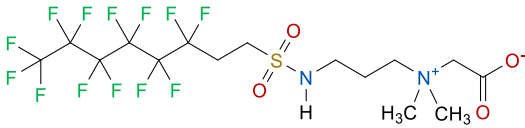
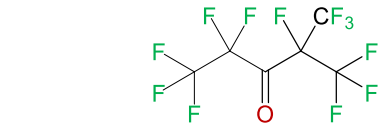
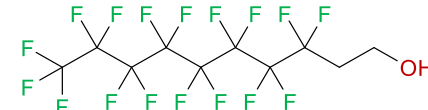
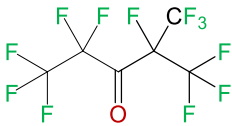

industrial branch, purpose and legacy PFAS	known fluorinated replacements		
	common names (acronyms)	trade name	chemical structure
fluoropolymer manufacture purpose: processing aids in the polymerization of e.g. PTFE legacy PFAS: salts of PFOA	salts of perfluoroether carboxylic acids (PFECAs) [133]		
	<ul style="list-style-type: none"> • ammonium 2,3,3,3-tetrafluoro-2-(1,1,2,2,3,3,3-heptafluoropropoxy)propionate (IUPAC) • ammonium salt of hexafluoropropylene oxide dimer acid (HFPO-DA/HFPO2/C3 dimer acid) • ammonium perfluoro-2-propoxypropionate (PFPrOPrA) [136] 	GenX (DuPont, now Chemours) CAS: 62037-80-3	
	<ul style="list-style-type: none"> • ammonium 2,2,3-trifluoro-3-[1,1,2,2,3,3-hexafluoro-3-(trifluoromethoxy)propoxy]propionate (IUPAC) • ammonium 4,8-dioxa-3H-perfluorononanoate (ADONA) [137] 	ADONA (3M) CAS: 958445-44-8	
	<ul style="list-style-type: none"> • ammonium 2,2-difluoro-2-[1,1,2,2-tetrafluoro-2-(1,1,2,2,2-pentafluoroethoxy)ethoxy]acetate (IUPAC) • perfluoro[(2-ethoxy-ethoxy)acetic acid] [138] 	EEA-NH4 (Asahi) CAS: 908020-52-0	
metal (chromium) plating purpose: wetting agents and mist-suppressing agents legacy PFAS: salts of PFOA	salts of 6:2 fluorotelomer sulfonic acid (6:2 FTSA) [139, 140]		
	<ul style="list-style-type: none"> • 3,3,4,4,5,5,6,6,7,7,8,8-tridecafluorooctane-1-sulfonic acid (IUPAC) • 6:2 fluorotelomer sulfonic acid (6:2 FTSA) [1, 139] • 1H,1H,2H,2H-perfluorooctane sulfonic acid (H4PFOS) • 1,1,2,2-tetrahydroperfluorooctane sulfonic acid (THPFOS) 	Fumetrol 21 (Atotech) CAS: 27619-97-2	
	salts of perfluoroether sulfonic acids (PFESAs) – mainly used in China [139, 140]		
	<ul style="list-style-type: none"> • potassium 2-(6-chloro-1,1,2,2,3,3,4,4,5,5,6,6-dodecafluorohexyloxy)-1,1,2,2-tetrafluoroethane sulfonate (IUPAC) (6:2 Cl-PFESA, 6:2 PFAES) • potassium 9-chlorohexadecafluoro-3-oxanone-1-sulfonate (9Cl-PF3ONS) 	F-53B – major component (e.g. Hangzhou Dayangchem Co. Ltd.) CAS: 73606-19-6	
	<ul style="list-style-type: none"> • potassium 2-(8-chloro-1,1,2,2,3,3,4,4,5,5,6,6,7,7,8,8-hexadecafluorooctoxy)-1,1,2,2-tetrafluoroethanesulfonate (IUPAC) (8:2 Cl-PFESA, 8:2 PFAES) • potassium 11-chloroeicosafluoro-3-oxaundecane-1-sulfonate (11Cl-PF3OUDS) 	F-53B – minor component CAS: 83329-89-9	

Table 2.6-2: Known fluorinated alternatives to long-chain PFCAs and PFSA and their precursors used in different industrial branches.

industrial branch, purpose and legacy PFAS	known fluorinated replacements		
	common names (acronyms)	trade name	chemical structure
fire-fighting foams purpose: film formers, fuel repellents, foam stabilizers legacy PFAS: various long-chain PFSA-, PFC- and fluorotelomer-based derivatives, e.g. PFOS and 8:2 FTOH	fluorotelomers based on a perfluorohexane (C ₆) chain [139]	Forafac 1157 (DuPont) CAS: 13875-90-8	
exemplary structure: 8:2 FTOH	<ul style="list-style-type: none"> N-(carboxymethyl)-N,N-dimethyl-3-[[[(3,3,4,4,5,5,6,6,7,7,8,8,8-tridecafluorooctyl)sulfonyl]amino]propan-1-aminium hydroxide (IUPAC) carboxymethyldimethyl-3-[[[(3,3,4,4,5,5,6,6,7,7,8,8,8-tridecafluorooctyl)sulphonyl]amino]propylammonium hydroxide [141] 6:2 fluorotelomer sulfonamide alkylbetaine (6:2 FTAB) 	Forafac 1183 (DuPont) CAS: 80475-32-7	
	<ul style="list-style-type: none"> N-[3-(dimethylamino)propyl]-3,3,4,4,5,5,6,6,7,7,8,8,8-tridecafluoro-1-octanesulfonamide (IUPAC) 6:2 fluorotelomer sulfonamide aminoxide A) perfluoroalkyl keton [139]	Novac 1230 (3M) CAS: 756-13-8	
food contact materials purpose: surface treatment legacy PFAS: POSF or long-chain fluorotelomer-based phosphate monoesters and diesters, side-chain fluorinated polymers	<ul style="list-style-type: none"> 1,1,1,2,2,4,5,5,5-nonafluoro-4-(trifluoromethyl)pentan-3-one (IUPAC) perfluoro-2-methyl-3-pentanone [3] dodecafluoro-2-methylpentan-3-one [139] 	<ul style="list-style-type: none"> 6:2 fluorotelomer-based phosphate diesters (6:2 diPAPs) 6:2 fluorotelomer-based side-chain fluorinated polymers perfluoropolyethers (e.g. Solvera from Solvay) [132, 142] 	
carpets, leather and textiles purpose: surface treatment legacy PFAS: POSF or long-chain fluorotelomer-based side-chain fluorinated polymers	<ul style="list-style-type: none"> PFHxSF- and PBSF-based side-chain fluorinated polymers (e.g. Scotchgard PM-3622 from 3M) 6:2 fluorotelomer-based side-chain fluorinated polymers (e.g. Unidyne TG-5521 from Daikin/Dow Corning) 3:1/5:1 fluorotelomer-based side-chain fluorinated polymers (e.g. RM610 from Miteni) perfluoropolyethers (e.g. Fluorolink from Solvay) [132] 		

Chemical substitutes for long-chain PFCAs, PFSAAs and their precursors also include non-fluorinated chemicals, for example alkyl sulfonates in decorative chrome plating [135] and paraffin waxes, silicones, dendrimers and inorganic nanoparticles in the textile sector [143]. Due to the unique properties of PFASs, the non-fluorinated substitutes often do not replace the functions of PFASs in all aspects. For example, the non-fluorinated replacements used in the textile sector provide comparable high water repellency to that of PFASs, but do not deliver the oil/stain repellency that PFASs provide additionally [143, 144]. Thus, the non-fluorinated replacements can be considered as suitable substitutes for example for consumer outdoor gear, while not meeting the requirements for certain occupational settings. These include the fire fighting and oil and gas sector, where protective clothing has to withstand the penetration of harmful liquids [18].

In addition to substitution with fluorinated or non-fluorinated chemicals, the development of non-chemical alternatives or alternative processes has been promoted. For example, new technology using chromium (III) instead of the toxic chromium (VI) has made the use of POSF-based mist suppressants in decorative metal plating obsolete. However, this technology cannot be applied to hard chrome plating. Here, “closed loop systems” have been developed to minimize the use of POSF-based compounds [129, 145]. In paper and board for food contact, the use of material with an extra-dense cellulose structure can impart grease resistance without using chemicals [142].

The discussed PFASs account for only a small part of the 4,730 PFAS-related CAS numbers, which have been identified on the global market [3]. In addition to replacement compounds for long-chain PFCAs, PFSAAs and their precursors, more and more classes of “overlooked” PFASs have been identified over the last years. Some of these compounds have already been in use for several decades but have not yet been in focus. Among them are perfluoroalkyl phosphinic acids (PFPIAs), which are used as defoamers in pesticide formulations and wetting agents in consumer products [146], and cyclic PFASs such as perfluoro-4-ethylcyclohexanesulfonate (PFECCHS), which is added to aircraft hydraulic fluids as an erosion inhibitor [147]. Both PFPIAs and PFECCHS have also been suggested as potential replacements for PFOS [139].

Irrespective of overlooked substances, the number and structural diversity of PFASs has increased over the last years, amongst others due to the common practice to replace one phased-out compound by multiple others [4]. In a study analyzing human plasma samples from the German cities Münster and Halle, an increasing amount and proportion of unidentified organofluorine was observed in Münster samples after 2000, suggesting that humans are exposed to new and unidentified organofluorine compounds [148].

Replacements to long-chain PFCAs, PFSA and their precursors, as well as overlooked groups of PFASs are often referred to as “emerging” or “novel” PFASs. Using the terminology that has been previously applied to brominated flame retardants, the term “emerging” refers to compounds which have been detected in the environment and/or wildlife, humans or other biological matrices [149], but which are not regulated and whose fate and impacts are poorly understood [150]. “Novel” compounds are known to be present in manufacturing processes, materials and products but have not yet been identified in the environment and/or wildlife, humans or other biological matrices [149]. Emerging and novel pollutants are contrasted by well-studied, internationally regulated “legacy” pollutants [150]. Originally used for pollutants initially included in the Stockholm Convention, such as polychlorinated biphenyls (PCBs), the term “legacy” is used more and more in scientific literature to refer to long-chain PFCAs, PFSA and their major precursors [136, 151, 152]. This terminology is also used in this thesis, differentiating between the well-studied, internationally regulated long-chain PFCAs, PFSA and their major precursors as “legacy PFASs” and replacements and overlooked PFASs as “emerging”, or respectively “novel” PFASs.

2.7 Environmental concerns about emerging and novel PFASs

While long-chain PFCAs, PFSA and their major precursors have been well studied and are subject of regulations, only limited information on the properties, environmental fate and transport, exposure and toxic effects is available for most of the other PFASs [4, 153]. This gets obvious when comparing the bare number of peer-reviewed articles available for legacy and emerging PFASs in 2016 (the beginning of this doctoral work). 4,066 articles had been published on PFOA since 2002, whereas for its replacement compounds HFPO-DA and DONA, only 26 and 4 studies were available, related to all aspects of research. Similarly, 3,507 studies related to PFOS had been published, but only 14 dealing with its substitute 6:2 Cl-PFESA [4].

Most of the known replacements possess a structure similar to the chemicals they replace (Table 2.6-1). In addition, they are potentially used in larger quantities because of a lower performance and it is likely that stable perfluorinated degradation products in the environment will increase due to the expanding use of fluorinated replacements. Consequently, it has to be questioned whether the applied fluorinated alternatives are a substantial improvement and pose smaller environmental and human health risks than their predecessors. Scientists and other professionals have raised their concerns about the transition to replacements in the Helsingør, Madrid and Zürich Statements [153-155].

Recent research indicates that at least some of the emerging and novel PFASs can also be considered contaminants of global concern. This includes short-chain PFCAs and PFSA as well as PFECAs and PFESAs. Long- and short-chain PFCAs and PFSA were originally distinguished

because short-chain homologues have been shown to be less bioaccumulative than long-chain homologues [1, 156, 157]. In fact, according to the current knowledge, short-chain PFCAs and PFSAAs do not meet regulatory bioaccumulation or toxicity criteria [31, 158]. However, they are as persistent as long-chain PFASs and they are stable transformation products into which several precursors ultimately degrade [132, 158, 159]. Due to their higher aqueous solubility and lower adsorption potential compared to long-chain PFASs, short-chain PFASs are very mobile [160]. This is underlined by their widespread occurrence in abiotic [21, 161, 162] and biotic [163, 164] compartments, including remote areas [165-167].

PFECAs and PFESAs are characterized by an ether linkage, which had been inserted as a “weak point” in the perfluorinated alkyl chain to increase degradability. However, the ether oxygens are sterically sheltered and electron-depleted by the electron withdrawing perfluorinated alkyl chain [168]. An *in silico* study indicated that the insertion of the ether linkage does not significantly change the physicochemical properties of the molecule [169]. Most of the alternatives were estimated to be similarly persistent in the environment compared to their common predecessors. As an example, the same overall persistence P_{ov} of ≈ 1038 days was modelled for HFPO-DA and its predecessor PFOA [169]. Laboratory studies confirmed that perfluoroether chains are similarly resistant to abiotic (photolysis, hydrolysis and reactions with hydroxyl radicals) and biotic degradation as perfluoroalkyl chains under environmentally relevant conditions [170].

Data on bioaccumulation potential and toxicity of PFECAs and PFESAs is still rare. However, based on their structural similarity, it is assumed that known PFECAs and PFESAs have likely the same or a similar mode-of-action as PFOS and PFOA [170]. A recent study indicates that HFPO-DA has higher toxicity to modelled serum and liver than PFOA [171].

Due to their comparable physicochemical properties (high water solubility and low pK_a), known PFECAs and PFESA are assumed to be similarly mobile as their predecessors [169, 170]. This is supported by the first findings of particular PFECAs and PFESAs in the abiotic and biotic environment. DONA has been identified mainly in river water from Germany thus far [100, 172, 173], whereas the occurrence of HFPO-DA has already been reported in different countries, especially in river water downstream of fluoropolymer manufacturing plants or industries applying fluorochemicals in Europe [100, 174], the United States [136] and China [100]. In a large-scale study, the compound was detected in 153 of 160 surface water samples taken in China, Europe, the United States and Korea with a median concentration of 0.95 ng/L in 2016. This study also showed that in addition to HFPO-DA, which is the dimer acid of HFPO, the trimer acid (HFPO-TrA) is widely present in river water [173].

Although F-53B has been already used in China since the 1970s, the first report on the occurrence of its major component, 6:2 Cl-PFESA, in the environment dates from 2013 [175]. Additionally,

6:2 Cl-PFESA was detected in sewage sludge [176], biota [177] and human serum samples [178] from China. Together with the first report on 6:2 Cl-PFESA in Arctic biota [179], these data indicate that PFECAs and PFESAs can be globally distributed and reach remote areas. However, data on their occurrence in the marine environment and their potential long-range transport is still rare.

For most of the other emerging and novel PFASs, public information on properties, environmental transport and fate, exposure and toxicity is even scarcer. Thus, they remain largely unassessed and unregulated in the public domain [153].

2.8 Trends in analytical methods

The increasingly large and diverse number of PFASs has resulted in analytical challenges. While the recently released database of PFASs on the worldwide market lists 4,730 PFAS-related CAS registry numbers [3], the most comprehensive conventional targeted analytical methods include up to approximately 70 PFASs [180]. Generally, 10–20 PFASs are considered in environmental monitoring programs and 20–40 compounds are analysed by research institutions with a focus on PFASs. The large discrepancy between the number of manufactured and analysed PFASs indicates that environmental and human exposure to PFASs may be significantly underestimated. To address this concern, targeted analytical methods with an extended spectrum of compounds have been complemented with upcoming analytical approaches to characterize the unknown pool of PFASs. These include sum parameters to estimate the proportion of the unknown fraction of PFASs [181] and high-resolution mass spectrometry (HRMS)-based approaches to elucidate the composition of the latter [182].

2.8.1 Target analysis

Conventionally, analytical methods for determination of PFASs in environmental matrices comprise extraction with polar solvents, clean-up steps and measurement by liquid chromatography coupled to tandem mass spectrometry (LC-MS/MS). Mostly, triple quadrupole mass spectrometers equipped with an ion source operating in negative electrospray ionization mode are used [183]. Gas chromatography coupled to mass spectrometry (GC-MS) is used for the detection of volatile PFASs, of particular relevance when analysing air samples [184]. These techniques provide high selectivity and sensitivity, allowing quantification of targeted PFASs at ppq to ppt levels in a broad range of environmental and human matrices [185].

While starting with a small number of PFASs in the beginning of the 2000s (often only PFOS and PFOA), most laboratories have tackled the increasingly large number of known PFASs by implementing emerging PFASs into the existing targeted analytical methods over the last years.

However, a major limitation of these compound-specific approaches is that even with the most comprehensive methods only a small proportion of the PFASs on the worldwide market can be covered. Moreover, only compounds which are known and selected by the respective laboratory are considered and the analysis does not reveal any information on the share and identity of unknown PFASs [153]. An additional limitation is that analytical reference standards have to be available for the unambiguous identification and quantification by LC-MS/MS and GC-MS. Such standards can be currently purchased for less than 100 PFASs [181]. Isotopically labelled internal standards, which are used to correct for compound losses and matrix effects, can be obtained for less than 50 compounds. Often, several years pass from the first notice about new compounds until an analytical standard is commercially available. As an example, industry has started using ADONA as a replacement compound for salts of PFOA in the 2000s, a discussion on the compound has arisen around 2011 [137] and a certified analytical reference standard became available only in 2016 [186]. To bridge this time gap, cooperation with industry and research laboratories of organic synthesis is an option, though often costly in terms of time and labour.

2.8.2 Sum parameters

To study the proportion of the unknown PFAS fraction, a number of techniques have been developed in recent years, varying in their selectivity and their inclusivity.

Particle-induced gamma ray emission spectroscopy (PIGE), a commonly-used ion beam analysis technique, has been recently applied for total fluorine determination in paper and textiles [187]. However, this method does not differentiate between organic and inorganic fluorine. While the inorganic fluorine contribution is assumed negligible in paper and textiles, it is high in natural waters. Consequently, separation of inorganic and organic fluorine, for example by solid-phase extraction, would have to be included as sample preparation step for aqueous matrices. Research on this is still ongoing [188].

To directly measure total organic fluorine related to PFASs in aqueous samples, Fluorine-19 nuclear magnetic resonance spectroscopy (^{19}F -NMR) has been applied. By monitoring the chemical shift associated with the terminal CF_3 peak, Moody and co-authors developed ^{19}F -NMR into a more selective method for PFAS-related compounds [189]. However, detection limits of this method are in the $\mu\text{g/L}$ range and, consequently, too high to be suitable for most environmental samples [189]. A sufficient sensitivity can be reached by extracting a certain fraction of the total fluorine of a solid sample using organic solvents and using combustion ion chromatography (CIC) for measuring “extractable organic fluorine” (EOF) [190]. Similarly, aqueous samples can be extracted using a sorbent, which is then subjected to combustion ion chromatography (“adsorbable organic fluorine” (AOF), detection limits $\leq 1\mu\text{g F/L}$) [191]. Selectivity of this method can be modified by using different sample preparation strategies [181].

The most selective and sensitive sum parameter is the Total Oxidizable Precursor (TOP) assay. One aliquot of the sample is exposed to hydroxyl radicals generated by thermolysis of persulfate under alkaline conditions. By this means, PFAS precursors are oxidized and for example transformed into a PFCA of a related chain length, whereas PFCAs as endpoint compounds remain intact. The oxidized aliquot and a second untreated aliquot are processed using the routine target analysis method and analysed by LC-MS/MS. The difference in concentration of targeted PFASs with and without TOP assay gives an estimate of the sum of PFAS precursors in the sample that oxidize to targeted PFASs [192]. Due to the use of the targeted analysis method for sample preparation and measurement, the TOP assay results in low method detection limits (ng/L range for aqueous samples). Compared to sum parameters other than that, it provides the best assurance that the fraction of unidentified organofluorine is associated with PFAS contamination. However, the high selectivity also has its drawbacks. Because the sum is based on the compounds targeted by LC-MS/MS, it does not include not oxidizable not targeted PFASs and not targeted oxidation products, which may also contribute to the unknown fraction [181].

2.8.3 Suspect and non-target analysis

High-resolution mass spectrometry (HRMS) provides the high resolving power (ratio of mass to mass difference $\geq 20,000$) and the high mass accuracy (< 5 ppm) necessary for discovery of novel compounds [193]. In the field of PFASs, HRMS is mostly coupled to liquid chromatography for sample separation [182]. A scheme of HRMS-based analytical approaches is provided in Figure 2.8-1. In suspect screening, full scan mass chromatograms are searched for accurate masses of molecular ions of compounds of interest (“suspects”) without using an analytical reference standard. Additional mass spectral and chromatographic information, such as the fragmentation pattern, isotope pattern and retention time are used to tentatively identify suspect hits. As for target analysis, reference standards are needed for unequivocal confirmation and quantification of the candidates [194]. In non-target screening, full scan mass chromatograms are screened for masses of interest, so-called features, without *a priori* hypothesis. Criteria for feature selection often include signal intensity, mass accuracy and study-specific criteria, in case of PFASs based on the mass defect of fluorine and series of chain-length homologues. Subsequently, tentative identification and confirmation of candidates is performed as in suspect screening [182].

Suspect and non-target screening allow the sensitive and untargeted detection of hundreds of compounds in a sample, assuming that the substances are compatible with sampling, extraction, separation and ionization [194]. In addition to the discovery of novel PFASs (including precursors, intermediates and degradation products), full scan HRMS analyses and HRMS/MS spectra can serve as “digital archive”. Typically, a single HRMS measurement of a complex environmental sample results in several thousands of signals. Even with the best instruments and data evaluation

workflows, a significant proportion of signals remains unannotated and unknown. If new concerns or new knowledge arise, the data can be exploited retrospectively without the need for a new measurement [195, 196].

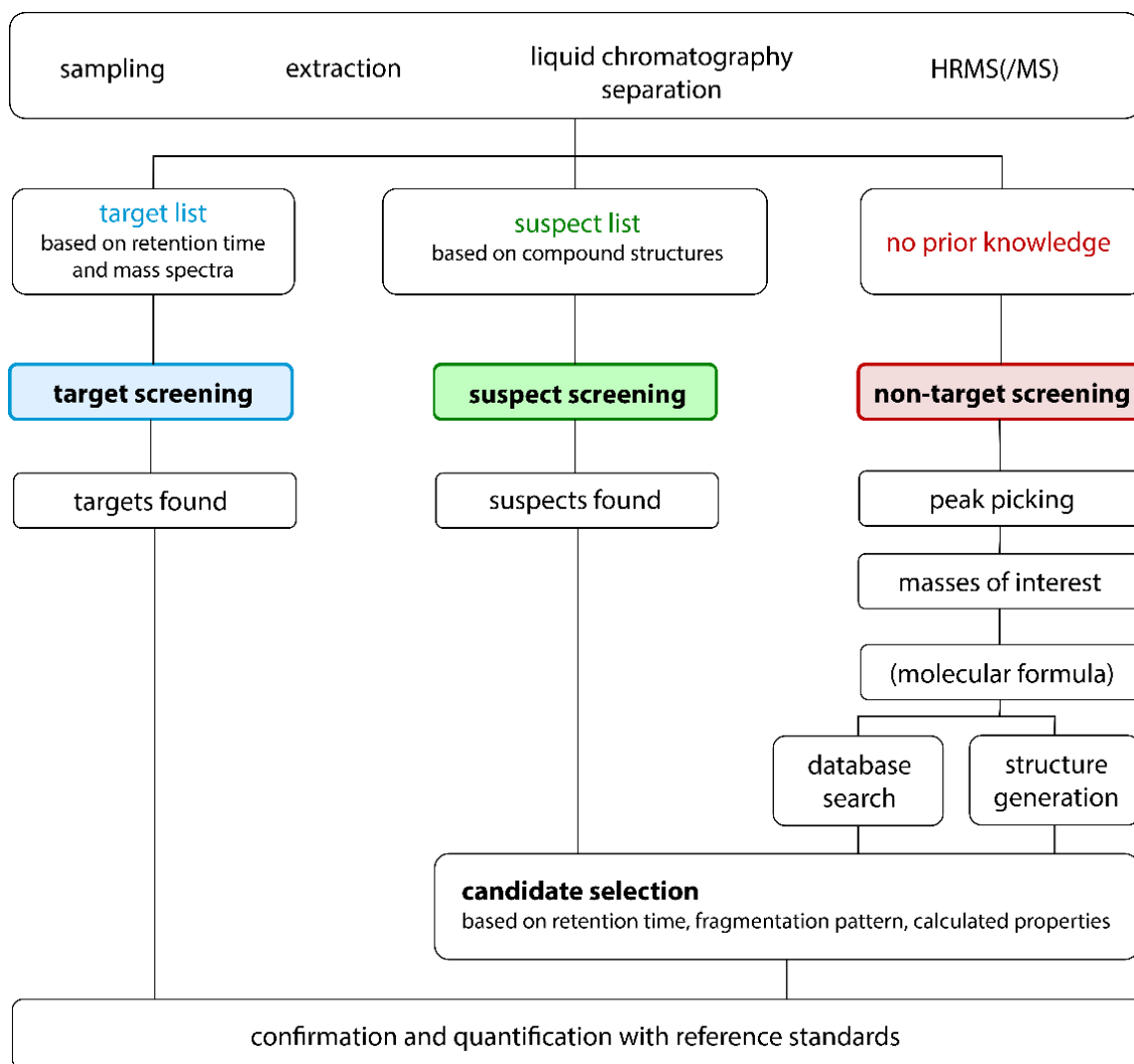


Figure 2.8-1: Scheme of HRMS-based analytical approaches addressing targets, suspects and non-targets. Modified after Brack *et al.* [197].

The application of sum parameters and the use of suspect and non-target analysis in the field of PFASs is still in its beginning stages and standardized methods are not available. However, the difference in selectivity and inclusivity associated with the various approaches can be used to obtain a more holistic view on PFASs in environmental samples (Figure 2.8-2). The combination of target analysis with one or more sum parameters and an HRMS-based approach opens up new opportunities for a more comprehensive understanding of PFAS composition, sources and health risks [181].

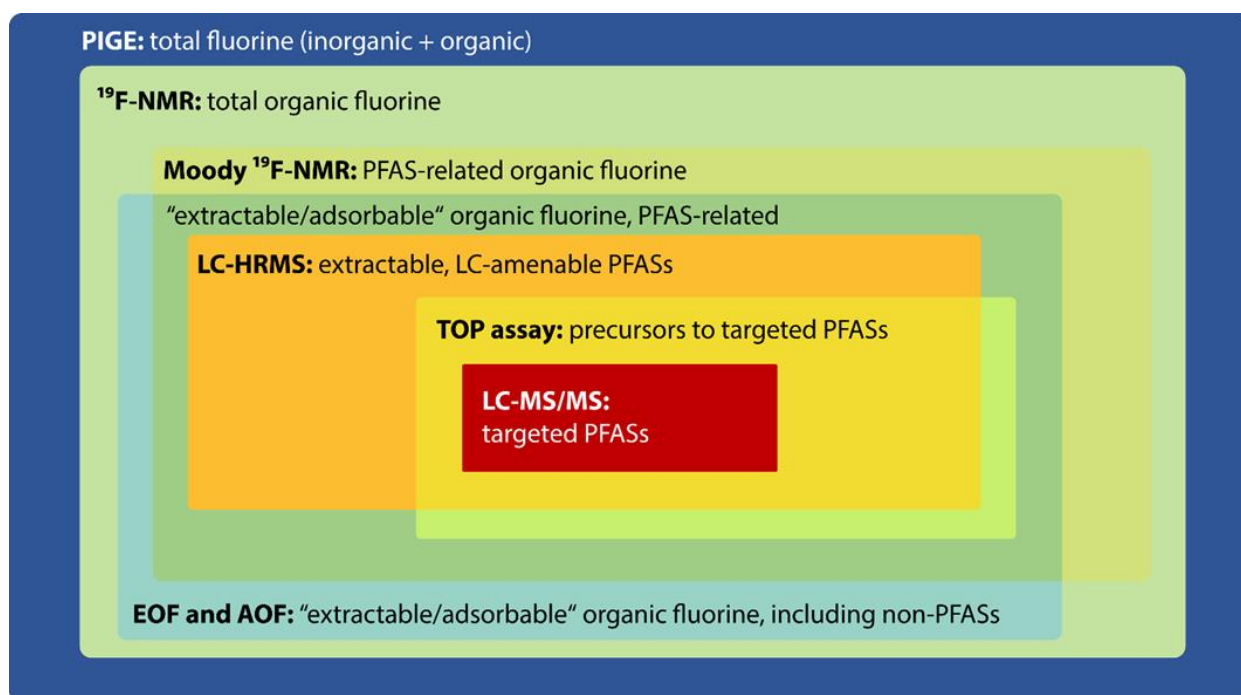


Figure 2.8-2: Selectivity and inclusivity associated with targeted methods, sum parameters and HRMS-based approaches related to PFAS analysis. The sizes of the boxes are meant to differentiate between more specific and more general fractions, but do not represent the actual relative size of the fractions. Redrawn from McDonough *et al.* [181]

3. Point of Departure and Research Objectives

When starting this doctoral research, legacy long-chain PFCAs and PFSAAs were recognized as global contaminants of high concern and had been banned or voluntarily phased out on an international and/or European level. An industrial shift was taking place, moving away from long-chain PFCAs and PFSAAs toward replacement compounds that are still PFASs, such as the ether-based PFECAs and PFESAs. First studies on the environmental occurrence of PFECAs and PFESAs, predominantly close to point sources, had been published. However, data on their occurrence and distribution in the marine environment and their potential long-range transport to remote areas was still rare. In the Helsingør and Madrid Statements, scientists and other professionals had raised their concerns about the shift to replacements. They had pointed out that at least some of the replacements may be “regrettable substitutes” and their use may result in similar adverse effects to those of long-chain PFCAs and PFSAAs. The initiators had called for action on different levels; on the part of science, this included developing analytical methods for replacements and investigating environmental exposure to the compounds.

Even though emissions of long-chain PFCAs and PFSAAs had been reduced, their high persistence had led to irreversible environmental exposure and the compounds were predicted to remain in the environment for hundreds of years. Thus, understanding the global dynamics and ultimate sinks of the compounds was identified as essential to assess their environmental impact and fate in the upcoming decades. While it was undisputed that the compounds undergo long-range transport, there were ongoing discussions on the contribution of oceanic versus atmospheric long-range transport. Moreover, there was a knowledge gap with regard to the occurrence and distribution of PFASs in the deep ocean and the related vertical transport mechanisms. Little information was available on the compounds’ partitioning behaviour between water and sediment in the marine environment.

In addition to replacement compounds for long-chain PFCAs and PFSAAs, more and more classes of “overlooked” PFASs had been identified on the global market. Using conventional compound-specific analytical methods, only a small number of the manufactured PFASs had been determined. This had raised the question if the conventionally monitored PFASs were representative or if environmental and human exposure to PFASs was significantly underestimated.

Based on this point of departure, the overarching aims of this PhD project were

- (i) To develop targeted analytical methods for the simultaneous determination of legacy and emerging PFASs in aqueous matrices and sediment,
- (ii) To identify which emerging PFASs are of relevance in the European coastal environment and investigate their potential long-range transport to the Arctic,

- (iii) To fill knowledge gaps regarding the ultimate sinks of legacy long-chain PFCAs and PFSAAs, including the deep ocean and marine sediments,
- (iv) To characterize the unknown fraction of PFASs in German and Chinese river water impacted by industrial point sources, which is not accounted for by target analysis.

These aims were addressed by five studies, included as Chapters 4 to Chapter 8 in this thesis. The specific objectives of the different studies were as follows:

Study 1 aimed at developing quantitative multi-methods for the analysis of legacy and emerging PFASs, including replacement compounds and overlooked PFASs, in fresh water, seawater and sediment by means of LC-MS/MS. After a review on literature and on available analytical standards, the scope of target analytes was defined. The existing instrumental method was transferred to a newly acquired mass spectrometer and new compounds were implemented. The instrumental method as well as the overall methods for aqueous samples and sediments were optimized and validated, focusing on the broad spectrum of compounds and the chosen marine environmental matrices, characterized by inorganic salts and expected PFAS concentrations in the pg/L, or respectively pg/g range.

Study 2 aimed at investigating whether particular emerging PFASs are of relevance in the coastal environment of the North and Baltic Seas and if there has been a transition from legacy long-chain PFCAs and PFSAAs to replacement compounds. More specifically, surface water and sediment samples were taken along the German coastlines to investigate the compounds' occurrence and composition profiles as well as their spatial distribution and potential sources. To examine the partitioning behaviour of PFASs between sediment and water, field-based partitioning coefficients were calculated. In addition, water sample extracts from the last decade were reanalysed to elucidate as to whether there has been a shift to emerging PFASs over time.

Study 3 aimed at investigating occurrence and distribution of legacy and emerging PFASs along the oceanic transport pathway from the North Sea to the Arctic. In addition to surface water samples, water samples were collected from bottom to surface at different depths to provide knowledge on the deep ocean as ultimate sink of PFASs. The PFAS composition pattern was examined for indications on transport and sources of PFASs in water masses entering and exiting the Arctic Ocean through Fram Strait, the Atlantic gateway to the Arctic Ocean. Moreover, the study aimed at estimating mass flows of PFASs through Fram Strait by combining the measured PFAS concentrations with water volume transport data from an ocean circulation model.

The aim of **study 4** was to compare source-specific PFAS fingerprints in German and Chinese river water. Potential point sources were chosen to cover major areas of PFAS production and application, such as fluoropolymer production and plating industry. They were selected based on a pre-study along the German Rhine River, by literature research and expert knowledge. Source-

specific fingerprints in Germany as a country where long-chain PFCAs and PFSAAs had been phased out were compared to those in China as a country to which part of the production had been shifted. Target analysis by LC-MS/MS was complemented with the Total Oxidizable Precursor (TOP) assay as a sum parameter to estimate whether a significant fraction of unknown PFAS precursors is present in the samples. To elucidate the composition of the latter and identify novel PFASs of potential environmental relevance, a HRMS-based suspect screening approach was developed and applied in **study 5**.

4. Development and Validation of Targeted Analytical Methods

The analysis of PFASs in the marine environment is challenging due to the low concentration of the compounds (ppq to ppt range) combined with a high risk of cross-contamination during sampling, storage and sample analysis due to the compounds' presence in laboratory and personal equipment [183]. Moreover, seawater and marine sediment are complex matrices, mainly because of the high amount of inorganic salts present, which interfere with the analysis [198, 199].

Numerous publications, reviewed by Trojanowicz *et al.* [200] and Nakayama *et al.* [201], as well as international [202] and national standards [203, 204] are available for the analysis of PFASs in environmental samples, especially for aqueous matrices. However, most of the methods include only a selected number of well-known legacy PFASs and have been mostly developed and validated for ultrapure and fresh water [198]. Generally, the MDLs and MQLs they provide are in the ppb or high ppt range and thus too high to be suitable for the marine environment. In addition, methods developed for a selected number of legacy PFASs often have to be adapted when PFASs of a different chain length or different structural category with different properties are added [1].

This study aimed at developing analytical methods for the simultaneous determination of legacy and emerging PFASs in aqueous matrices, with a focus on seawater, and marine sediments. It was the aim to develop an LC-MS/MS method that could be used for all matrices. In contrast, the sample extraction and cleanup had to be optimized for aqueous matrices and sediments individually. Method detection limits were intended to be in the low pg/L range for seawater samples and in the low pg/g range for sediment samples. To verify the suitability of the analytical procedures for the intended use, the study aimed at validating the instrumental method as well as the overall method for aqueous matrices and sediments.

4.1 Definition of the analytical scope

To define the scope of target analytes, peer-reviewed literature, publicly available reports, the research database SciFinder and the regulatory database of REACH were screened for the identity of PFASs replacing long-chain PFCAs and PFSAAs as well as “overlooked” PFAS classes (Chapter 2.6). Considering availability of analytical standards and applicability of LC-MS/MS, nine replacement compounds and/or overlooked PFASs from four different structural classes were included in the spectrum of target analytes. Among them were four PFECAs and two PFESAs as replacements for PFOA and PFOS as well as two PFPiAs and one cyclic PFSA as “overlooked” PFASs (Table 4.1-1). Of the well-known PFASs, 11 PFCAs, five PFSAAs and four precursors were analysed (Table 4.1-2).

To correct for substance losses during analysis and matrix effects during the measurement, the study aimed at using isotopically labelled internal standards for quantification. These were available for seven PFCAs, three PFSA and two precursors, but for emerging PFASs from other groups of PFASs, only $^{13}\text{C}_3$ -HFPO-DA could be obtained (Table 4.1-3). Substances without isotopically labelled analogues were assigned to structurally similar internal standards in the course of the method development (see Chapter 4.5.1). As injection standard for the calculation of the internal standards' recovery rates, $^{13}\text{C}_8$ -PFOA was used.

In total, the analytical scope included 29 target analytes, 13 internal standards and one injection standard from eight structural classes. The CAS registry numbers and IUPAC names of the target analytes and mass-labelled standards as well as the analytical standards' suppliers, purity and concentration are provided in Table 10.1-2 to Table 10.1-4.

Table 4.1-1: Chemical structures of replacement compounds and/or overlooked PFASs chosen as target analytes. The name and the structure of the free acid are given, whereas the measured form is the anion.

common name	acronym	structure
per- and polyfluoroalkyl ether carboxylic acids (PFECAs)		
4,8-dioxa-3H-perfluorononanoic acid	DONA	
hexafluoropropylene oxide dimer acid	HFPO-DA	
hexafluoropropylene oxide trimer acid	HFPO-TrA	
hexafluoropropylene oxide tetramer acid	HFPO-TeA	
per- and polyfluoroalkyl ether sulfonic acids (PFESAs)		
6:2 chlorinated polyfluoroalkyl ether sulfonic acid	6:2 Cl-PFESA	
8:2 chlorinated polyfluoroalkyl ether sulfonic acid	8:2 Cl-PFESA	
perfluoroalkyl phosphinic acids (PFPIAs)		
bis(perfluorohexyl) phosphinic acid	6:6 PFPIA	
perfluorohexylperfluorooctyl phosphinic acid	6:8 PFPIA	
cyclic perfluoroalkane sulfonic acids (cyclic PFSA)		
perfluoro-4-ethylcyclohexane sulfonic acid	PFECHS	

Table 4.1-2: Chemical structures of perfluoroalkyl carboxylic and sulfonic acids as well as precursors chosen as target analytes.

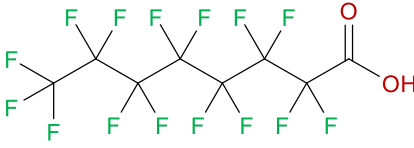
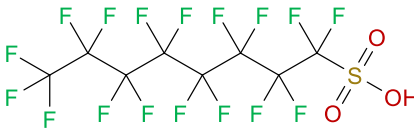
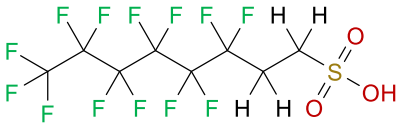
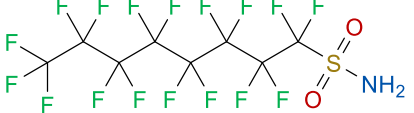
analyte	acronym	<i>n</i>	structure
perfluoroalkyl carboxylic acids (PFCAs)			
perfluorobutanoic acid	PFBA	3	
perfluoropentanoic acid	PFPeA	4	
perfluorohexanoic acid	PFHxA	5	
perfluoroheptanoic acid	PFHpA	6	
perfluorooctanoic acid	PFOA	7	general structure: C _{<i>n</i>} F _{2<i>n</i>+1} COOH <i>n</i> < 7: short-chain <i>n</i> ≥ 7: long-chain
perfluorononanoic acid	PFNA	8	exemplary structure: PFOA
perfluorodecanoic acid	PFDA	9	
perfluoroundecanoic acid	PFUnDA	10	
perfluorododecanoic acid	PFDoDA	11	
perfluorotridecanoic acid	PFTTrDA	12	
perfluorotetradecanoic acid	PFTeDA	13	
perfluoroalkane sulfonic acids (PFSAs)			
perfluorobutane sulfonic acid	PFBS	4	general structure: C _{<i>n</i>} F _{2<i>n</i>+1} SO ₃ H <i>n</i> < 6: short-chain <i>n</i> ≥ 6: long-chain
perfluorohexane sulfonic acid	PFHxS	6	
perfluoroheptane sulfonic acid	PFHpS	7	exemplary structure: PFOS
perfluorooctane sulfonic acid	PFOS	8	
perfluorodecane sulfonic acid	PFDS	10	
precursors to PFCAs and PFSAs			
4:2 fluorotelomer sulfonic acid	4:2 FTSA	4	general structure: C _{<i>n</i>} F _{2<i>n</i>+1} CH ₂ CH ₂ SO ₃ H
6:2 fluorotelomer sulfonic acid	6:2 FTSA	6	exemplary structure: 6:2 FTSA
8:2 fluorotelomer sulfonic acid	8:2 FTSA	8	
perfluorooctane sulfonamide	FOSA	-	

Table 4.1-3: Isotopically labelled internal standards used for quantification of the target analytes.

analyte	acronym	structure
hexafluoropropylene oxide- [¹³ C ₃]-dimer acid	¹³ C ₃ -HFPO-DA	
perfluoro-[¹³ C ₄]- butanoic acid	¹³ C ₄ -PFBA	
perfluoro-[1,2- ¹³ C ₂]- hexanoic acid	¹³ C ₂ -PFHxA	
perfluoro-[1,2,3,4- ¹³ C ₄]- octanoic acid	¹³ C ₄ -PFOA	
perfluoro-[1,2,3,4,5- ¹³ C ₅]- nonanoic acid	¹³ C ₅ -PFNA	
perfluoro-[1,2- ¹³ C ₂]- decanoic acid	¹³ C ₂ -PFDA	
perfluoro-[1,2- ¹³ C ₂]- undecanoic acid	¹³ C ₂ -PFUnDA	
perfluoro-[1,2- ¹³ C ₂]- dodecanoic acid	¹³ C ₂ -PFDoDA	
perfluoro-[2,3,4- ¹³ C ₃]- butane sulfonic acid	¹³ C ₃ -PFBS	
perfluorohexane- [¹⁸ O ₂]-sulfonic acid	¹⁸ O ₂ -PFHxS	
perfluoro-[1,2,3,4- ¹³ C ₄]- octane sulfonic acid	¹³ C ₄ -PFOS	
perfluoro-[¹³ C ₈]- octanesulfonamide	¹³ C ₈ -FOSA	
1H,1H,2H,2H-perfluoro- [1,2- ¹³ C ₂]-octane sulfonic acid	¹³ C ₂ -6:2 FTSA	

4.2 Development of the instrumental method

Instrumental analysis was performed by LC-MS/MS, using an HP 1100 LC system (Agilent, USA) coupled to an API 4000 triple quadrupole (QqQ) mass spectrometer (AB Sciex, USA). For ionization, a Turbo V ion source (AB Sciex, USA) was used, operating in negative electrospray ionization mode.

In contrast to the LC system, the API 4000 mass spectrometer had not been used for PFAS analysis before. Consequently, after coupling the LC system to the API 4000 mass spectrometer, the existing method [102] had to be transferred to the newly combined LC-MS/MS system, the instrument-specific mass spectrometric parameters had to be optimized and new compounds implemented. Firstly, precursor and product ions were determined for all target analytes and internal standards. In a next step, the transition-specific mass spectrometric parameters were adjusted. Afterwards, the LC method was optimized with regard to the chosen scope of target analytes. Based on the adapted LC method, the acquisition method was amended using the scheduled multiple reaction monitoring algorithm to ensure a sufficient high number of data point across the LC peaks. Lastly, the ion source-dependent parameters were optimized.

4.2.1 Determination of precursor and product ions

For quantification, QqQ mass spectrometers are typically operated in multiple reaction monitoring (MRM) mode. The first quadrupole Q_1 is set to select a precursor ion, which is fragmented in q_2 (collision cell) by collision with neutral gas molecules. The product ions are passed into Q_3 , where a particular product ion is selected and detected by a channel electron multiplier. Such precursor/product ion pairs (transitions) of the target analytes are monitored over time, resulting in a set of chromatographic traces with the retention time and the signal intensity of a specific product ion as coordinates. By ignoring all other ions present, the experiment gains sensitivity, while being highly selective [205]. For unambiguous identification, it is recommended to monitor at least two mass transitions per compound [206].

The precursor ions and product ions of the target analytes were determined by using flow injection analysis and two different MS scan experiments. 1 ng absolute of the single standards (10 μ L of a 100 pg/ μ L solution) was injected into the flowing LC solvent (0.2 mL/min). By operating Q_1 in full scan mode, the presence of a stable precursor ion of the compound of interest was confirmed in a first MS experiment. Afterwards, a product ion scan experiment was conducted to determine product ions of the respective compound. For this, Q_1 was set to select the precursor ion which had been confirmed in the first experiment. For fragmentation in q_2 , the collision energy applied by the analytical standard supplier to obtain the mass spectra in the certificate of analysis was used as a starting point. Q_3 was set to scan for product ions. The most abundant product ion

was chosen for the quantification of the target compound (“quantifier”), whereas the second-most intense product ion was selected for the confirmation of the substances (“qualifier”). If these settings did not reveal two product ions, different collision energies between -10 and -90 eV were tested in increments of 10 eV.

The full scan Q1 spectra of the target analytes were all dominated by their respective $[M-H]^-$ ions. For example, in the full scan Q1 spectrum of the replacement compound DONA with a neutral mass of 378.0 Da, the presence of m/z 377.0 $[M-H]^-$ as a precursor ion was confirmed. The product ion scan of m/z 377.0 revealed m/z 251.0 as the product ion with the highest intensity, corresponding to the neutral loss of CO_2 and CF_2CHF $[M-44-82-H]^-$ and indicating the cleavage of the first ether bond (Figure 4.2-1). The m/z 85.0 fragment (CF_3O^-) can be explained by the cleavage of the second ether bond. Consequently, the mass transitions m/z 377.0 $>$ 251.0 and m/z 377.0 $>$ 85.0 were selected to be monitored for the quantification and qualification of DONA. The results for the other target analytes are provided in Table 10.2-3 to Table 10.2-5. For PFBA, PFPeA and FOSA, only one product ion with high enough intensity could be identified. This has also been reported by other authors [207, 208].

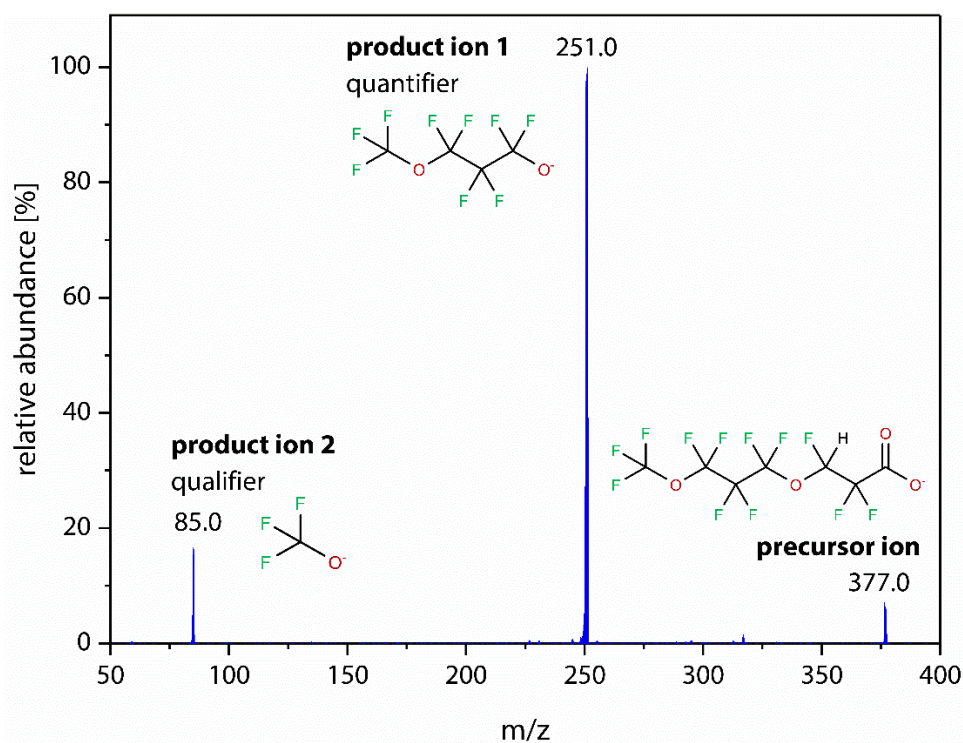


Figure 4.2-1: Product ion spectrum of m/z 377.0, $[M-H]^-$ of the replacement compound DONA (ESI $^-$, collision energy -20 eV, mass range m/z 50 to 400, scan time 2 s). The spectrum is annotated with proposed structures of the fragments.

4.2.2 Optimization of transition-specific mass spectrometric parameters

To increase sensitivity, transition-specific mass spectrometric parameters were optimized for each of the selected mass transitions. The declustering potential (DP) is a voltage applied to the orifice to decluster aggregated ions before entering the mass spectrometer, whereas the entrance potential (EP) guides and focuses ions through the Q0 region. The collision energy (CE) corresponds to the amount of energy the precursor ions receive as they are accelerated into the collision cell. An additional parameter to optimize is the collision cell exit potential (CXP), focusing and transmitting the product ions from q2 to Q3 (Figure 4.2-2) [209].

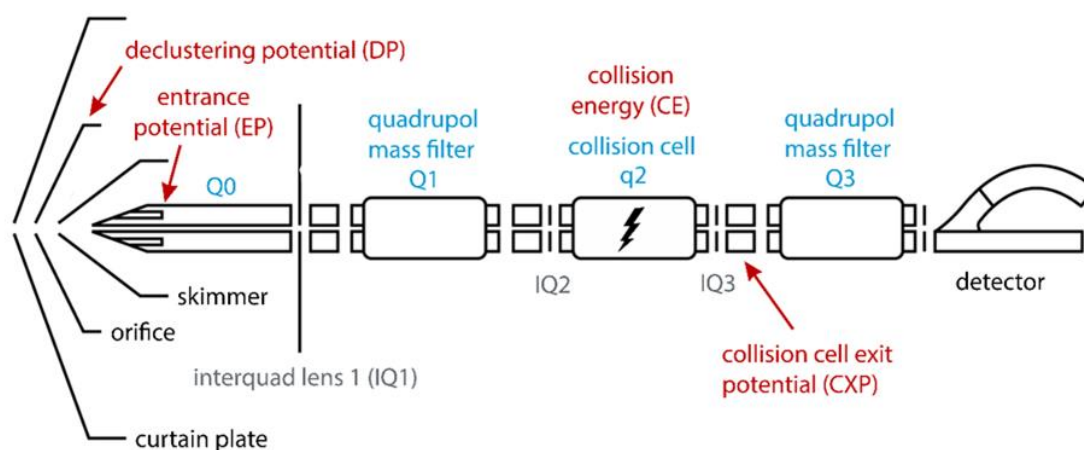


Figure 4.2-2: Ion path of API4000 triple quadrupole mass spectrometer with mass-spectrometric parameters optimizable for each mass transition labelled in red, adapted from AB Sciex (2010).

For each parameter, nine values within the working range given by the MS vendor [209] were tested for each mass transition using flow injection analysis. 1 ng absolute of each standard was injected into an LC flow of 0.2 mL/min and as MS scan type, MRM was selected. The voltages resulting in the most abundant signals were chosen as optimal values. The parameters were optimized in the order DP, EP, CE and CXP, starting with default values and then updating the method one by one with the optimal values. Having the highest effect on signal intensity [209], DP and CE were fine-tuned in a second optimization step, using a narrower range of tested voltages around the best value from the first step.

As an example, the results for HFPO-DA (m/z 329>169) are shown in Figure 4.2-3. Starting with default values of -10 , -10 , -10 and -5 eV for DP, EP, CE and CXP, the values resulting in the highest signal intensity were -20 , -4 , -20 and -8 eV. Covering one order of magnitude, the differences in signal intensity within the tested range were highest for DP and CE. This underlines that DP and CE have a major effect on the method's sensitivity. The fine-tuning for DP and CE resulted in values of -22 and -18 eV for HFPO-DA. The optimized transition-specific parameters for all target analytes are given in Table 10.2-3 to Table 10.2-5.

Using mass spectrometers of other vendors, several authors have reported significantly lower sensitivity for HFPO-DA than for the conventional PFASs [134, 210, 211]. Thus, it was a positive finding and a requirement for low MDLs that the signal intensity of HFPO-DA was in the same range as that of the conventional PFASs using the AB Sciex instrument. Probably, this difference results from the vendor-specific construction of the ion source, preventing in-source fragmentation of the compound.

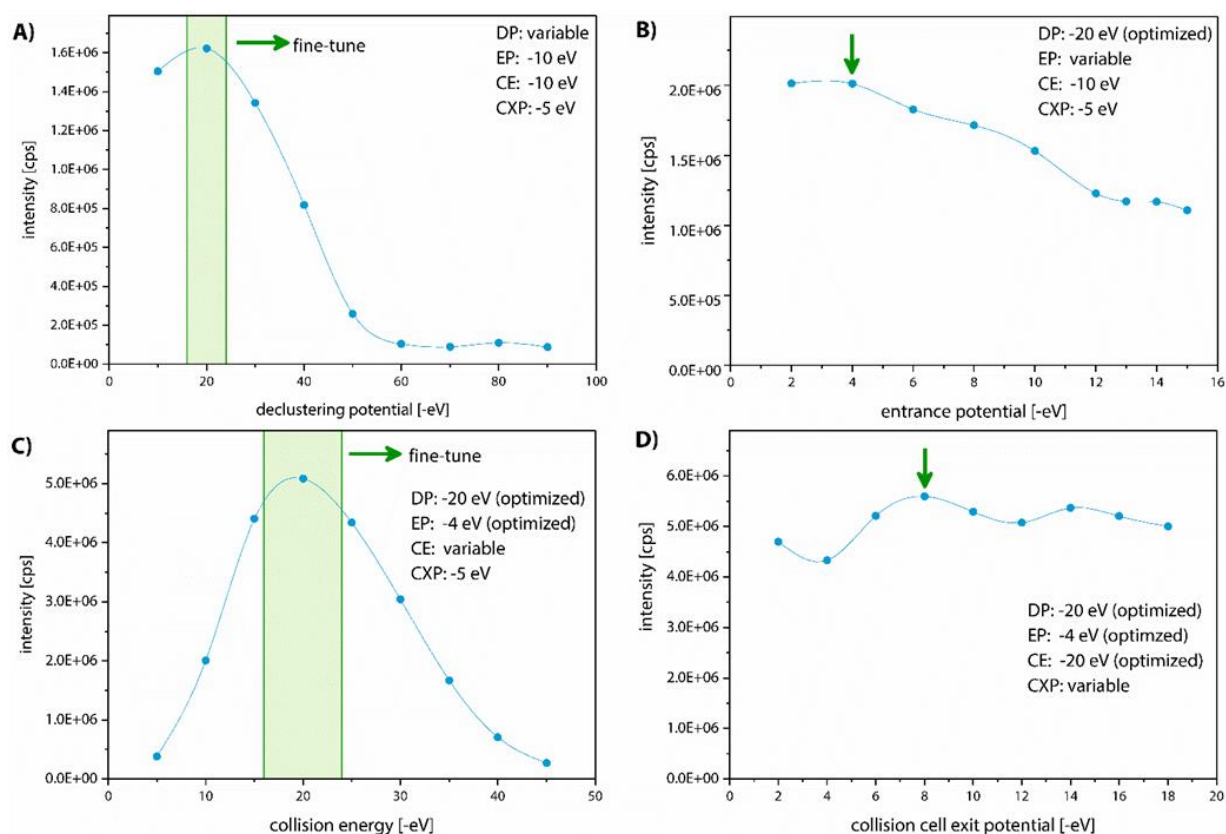


Figure 4.2-3: Optimization of transition-specific mass spectrometric parameters for HFPO-DA (329>169), including A) declustering potential (DP), B) entrance potential (EP), C) collision energy (CE) and D) collision cell exit potential (CXP). For EP and CXP, green arrows mark voltages resulting in the highest signal intensity. DP and CE were fine-tuned in a second step of optimization, testing values between -16 and -24 eV in increments of 1. This resulted in optimal values of -22 eV and -18 eV for these parameters.

4.2.3 Optimization of the chromatographic method

For chromatographic separation, a polar embedded reversed phase C_{18} column (Synergi Fusion-RP C_{18} , 150 mm x 2 mm, particle size 4 μm , pore size 80 \AA , Phenomenex, USA) was used in combination with a guard column containing the same phase (4 mm x 2 mm, Phenomenex, USA). This study aimed at verifying if the gradient method previously used by Heydebreck *et al.* [102] was suitable for the newly implemented compounds. Moreover, different mobile phase compositions were tested, aiming at increasing the method's sensitivity and improving peak shapes, in particular of the early eluting compound PFBA.

As a starting point, the optimized mass-spectrometric parameters were used in combination with the existing chromatographic method, summarized in Table 4.2-1 [102]. The chromatogram in Figure 4.2-4 shows that the newly implemented compounds elute within the range of the conventional PFASs and their peak shape and intensity is comparable. Consequently, one single LC-MS/MS method could be used for the chosen scope of target analytes.

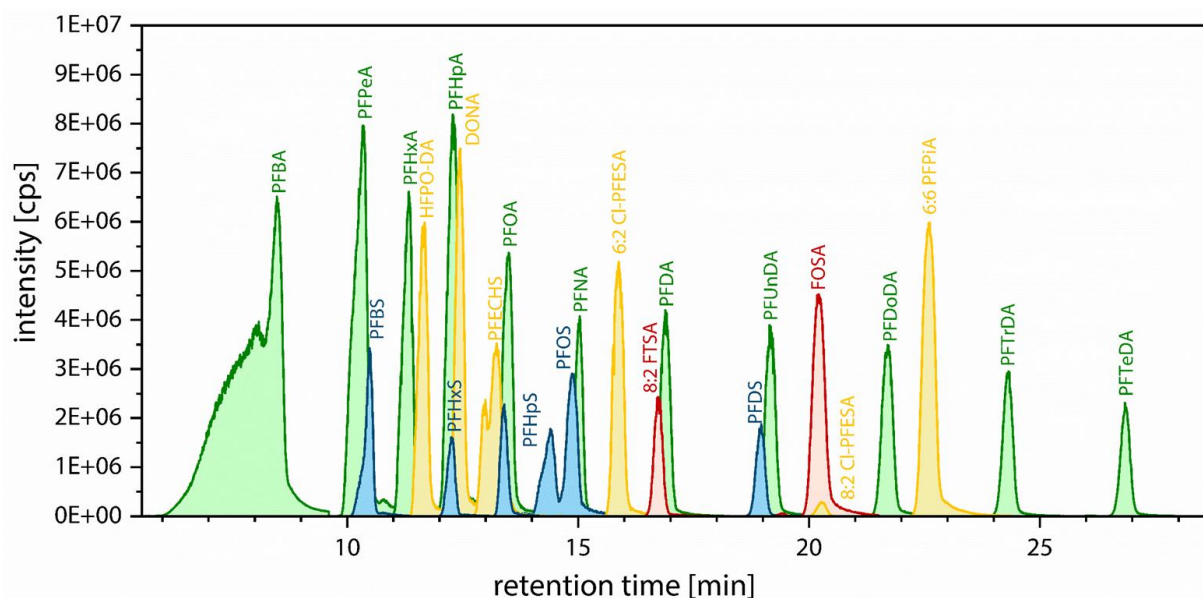


Figure 4.2-4: LC-MS/MS chromatogram of a 100 pg/ μ L standard in methanol (injection volume 10 μ L), using the initial LC method and the optimized mass spectrometric parameters. Only 24 of the 29 target analytes are included because the analytical standards for the other compounds had not been available yet. PFCAs are marked in green, PFSA in blue, replacement compounds and overlooked PFASs in yellow and precursors in red.

As shown in Figure 4.2-4, the peak for PFBA was distorted. The other peaks had a better shape, though most of them were tailing. Poor chromatography of PFBA is a common issue, which often results in non-reporting of PFBA as it impairs the quantification of the compound [102, 161, 207]. However, the compound is of increasing interest due to the industrial transition from long-chain PFASs to short-chain homologues (Chapter 2.6).

In the initial LC method, 10 mM ammonium acetate (NH_4OAc) was added to both eluents, A) water and B) methanol [102, 212]. NH_4OAc is commonly used as buffer in LC-MS/MS and for PFAS analysis [201], as it is sufficiently volatile not to precipitate in the ion source after solvent evaporation [213]. Although the suggestion has not been taken up in literature, the validation document for the German DIN norm 38407-42 mentions that a lower concentration of ammonium acetate in the aqueous eluent in combination with addition of acetic acid (0.05 %) to the organic eluent can result in higher responses and a later elution of the peaks [214]. As a later peak elution may have positive effects on the peak shape of PFBA, this approach was tested using

different concentrations of NH_4OAc (10 mM, 5 mM and 2 mM) in both eluents and replacing NH_4OAc in the organic eluent with 0.05 % acetic acid (Figure 4.2-5).

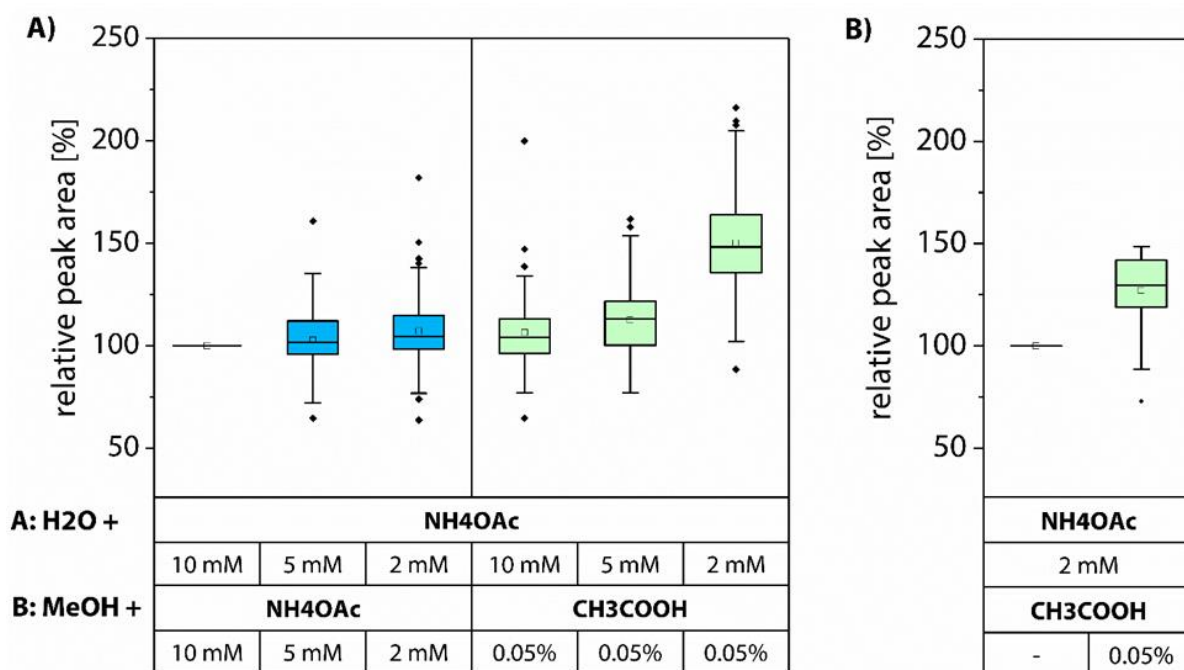


Figure 4.2-5: Boxplots showing the effects of different concentrations of ammonium acetate and acetic acid as modifier of the mobile phases on peak areas of target analytes (quantifiers and qualifiers) and internal standards. A 100 $\mu\text{g}/\mu\text{L}$ standard in methanol was measured for all solvent compositions (injection volume 10 μL). The peak areas were normalized to the initial solvent composition. The box represents the 25 % to 75 % quartile, the median is plotted by the band inside the box and the mean by the blank square. The ends of the whiskers display the lowest and the highest concentration still within 1.5 interquartile range (IQR) of the lower and higher quartile. Outliers are plotted with a black diamond.

Figure 4.2-5A shows that the combination of 2 mM NH_4OAc and 0.05 % CH_3COOH resulted in significantly higher relative peak areas than the other tested mobile phase compositions (mean (150 ± 24) % versus (103 ± 15) % to (113 ± 15) %). To test if the difference was related to the presence of acetic acid or to the non-presence of 2 mM NH_4OAc in the organic eluent, methanol with 0.05 % acetic acid was compared to pure methanol as organic eluent (Figure 4.2-5B). In relation to pure methanol, mean peak areas increased to (131 ± 21) % when using acidic methanol, underlining that the increase in peak areas is due to the addition of acetic acid.

At first sight, this is surprising because weak organic acids, such as formic or acetic acid, are often added to facilitate protonation of analytes when positive ESI is performed, whereas basic modifiers, such as ammonium hydroxide, are added to facilitate deprotonation when negative ESI is performed. However, reports of so-called “wrong-way-round” ionization have shown that acidic mobile phases can also promote strong ionization in negative ESI analysing amino acids [215] and lipids [216]. Investigating the effects of weak acids on the ionization efficiency of four selective androgen receptor modulators, Wu *et al.* [217] showed that acetic acid enhanced the negative ion ESI response, whereas formic acid resulted in signal suppression. The authors hypothesized that

this is caused by the high gas-phase proton affinity of the acetate anion, the reducibility of H^+ , which facilitates droplet charging, and the small molecular volume, which is important not to suppress the analytes' ionization. They pointed out that negative ESI response is a dynamic interplay between the mobile-phase modifier and the properties of the respective target analytes [217].

For PFASs, no systematic investigation on the choice of mobile phase additives is available. The results from this study in Figure 4.2-5 show that for the chosen analytical scope, the combination of 2 mM NH_4OAc in water as eluent A and 0.05 % CH_3COOH in methanol as eluent B results in enhanced signals compared to the commonly used additives, whereas other studies report that formic acid leads to PFAS signal suppression [199, 218]. This indicates that the differences in effects of acetic and formic acid observed by Wu and co-workers [217] also apply to PFAS analysis. However, further studies testing additional concentrations and additives in different compositions are necessary to better understand the underlying cause of the effects and find the optimal eluent composition for PFAS analysis. For this PhD work, the combination of 2 mM NH_4OAc in water as eluent A and 0.05 % CH_3COOH in methanol as eluent B was taken, as it resulted in the highest peak areas within the tested range.

An additional effect of the adapted solvent composition was an increased retention time of all target analytes. A possible explanation is the protonation of free silanol groups of the reversed phase column material, thereby preventing repulsion of the acidic functional groups of the target analytes [199]. In addition to a later retention time, a peak splitting was observed for PFBA (Figure 4.2-6B). As one of the possible reasons, the difference in solvent strength of the eluent's starting gradient (70 % A and 30 % B) and the standard/samples itself (100 % methanol) was identified. An injection solvent stronger than the mobile phase can interfere with the adsorption of the samples at the column head. Generally, this issue can be overcome with a lower injection volume or a weaker standard/sample solvent [213, 219].

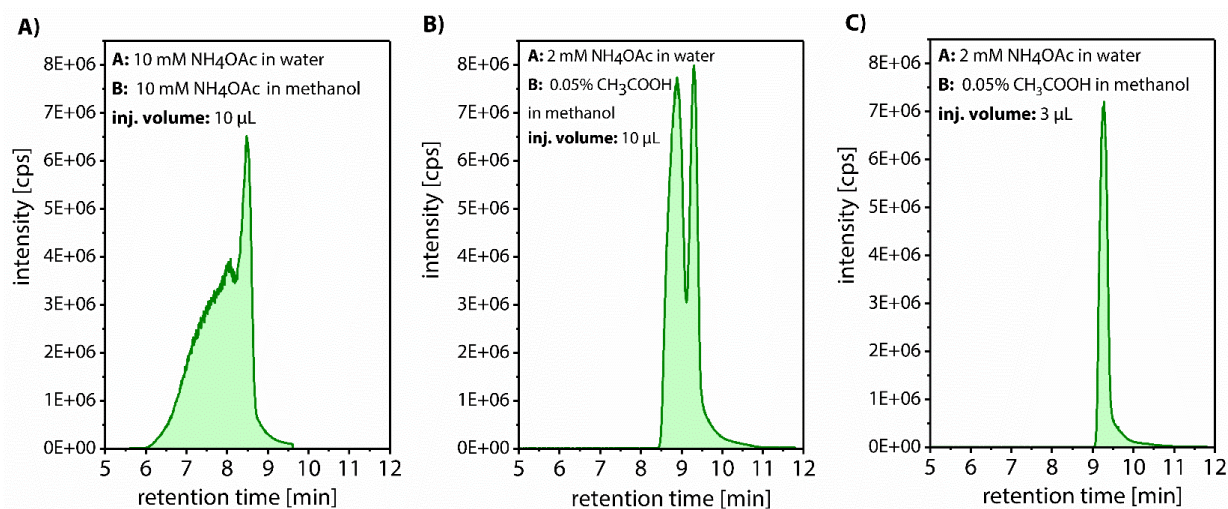


Figure 4.2-6: Peak shape of PFBA using different mobile phase additives and injection volumes. A solution of 100 pg/ μL PFBA in methanol was injected and analysed based on the conditions given in A) to C).

Moreover, the use of this sample solvent reduced the tailing of the other target analytes and resulted in symmetric peaks for most of the compounds. Figure 4.2-8, Figure 4.2-9 and Figure 4.2-10 show exemplary chromatograms of a calibration standard, a seawater sample and a sediment sample using the final chromatographic method.

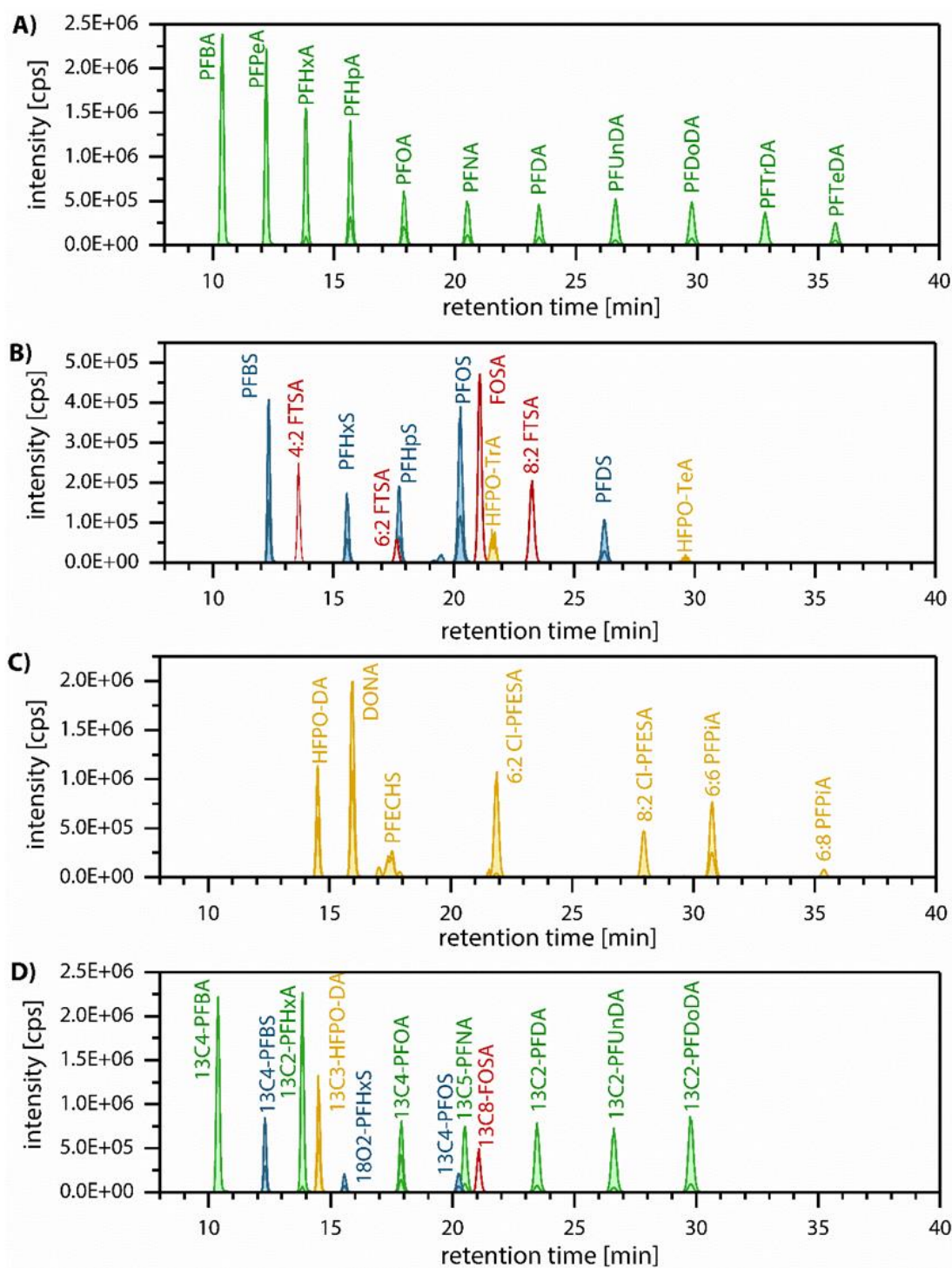


Figure 4.2-8: LC-MS/MS chromatogram of a 15 pg/ μ L calibration standard using the final chromatographic method with A) PFCAs (green), B) PFSA (blue), precursors (red) and the two replacement compounds HFPO-TrA and HFPO-TeA (yellow), C) replacement/overlooked PFASs (yellow) and D) the internal standards.

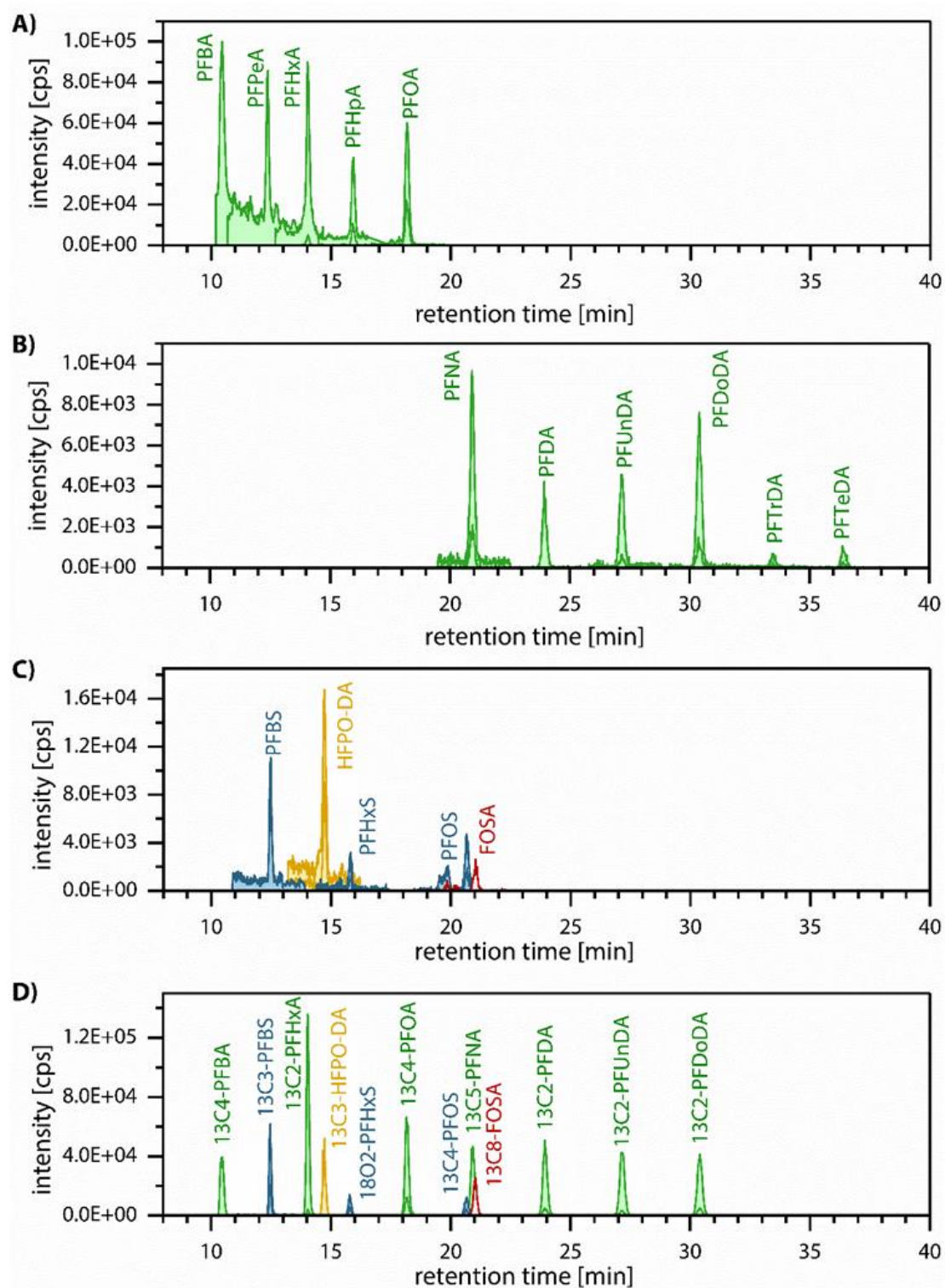


Figure 4.2-9: LC-MS/MS chromatograms of detected target analytes in a seawater sample using the final chromatographic method with A) C₄ to C₈ PFCAs (green), B) C₉ to C₁₄ PFCAs (green), C) PFSA (blue), a precursor (red) and a replacement compound (yellow), and D) internal standards.

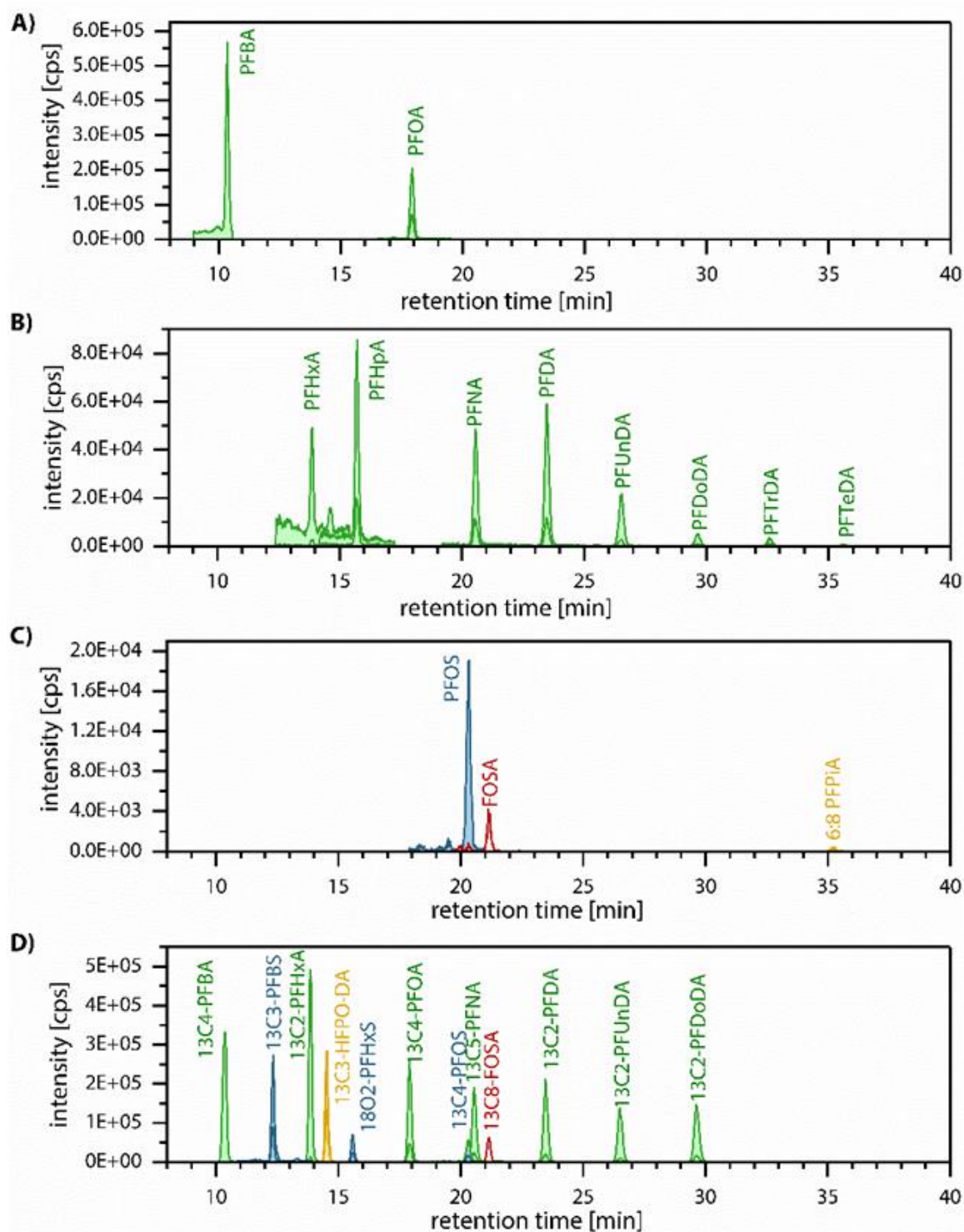


Figure 4.2-10: LC-MS/MS chromatograms of the detected target analytes in a sediment sample using the final chromatographic method with A) C₄ and C₈ PFCAs (green), B) C₆, C₇ and C₉ to C₁₄ PFCAs (green), C) PFOS (blue), FOSA (red) and 6:8 PFPiA (yellow), and D) internal standards.

The used analytical standard solutions contained the linear isomers of the target analytes. However, the production of PFOS and other PFASs using electrochemical fluorination yields approximately 20 % to 30 % branched isomers in addition to the linear isomers (Chapter 2.3). Consequently, environmental samples also contain a mixture of different isomers. Isomer patterns can provide useful information when comparing enrichment in different matrices (Chapter 5.3.5) or PFAS patterns of point sources with different production processes (Chapter 7.4.3).

Figure 4.2-11 exemplarily shows chromatograms for linear PFOS and its linear internal standard $^{13}\text{C}_4$ -PFOS in a calibration standard in contrast to a river sample with a mixture of linear and branched isomers of PFOS (L-PFOS and Br-PFOS). As the peaks of the linear and branched isomers of PFOS were baseline-separated in environmental samples, they were quantified individually against the linear calibration standard (mass transition m/z 498.9>80.0). This was done in a similar way for the precursor compound FOSA and for PFHpA and PFOA in samples impacted by point sources (Chapter 7.4.3). Due to differences in ionization and fragmentation efficiencies of the various isomers, the quantification of the sum of the branched isomers against the linear calibration standard leads to a systematic analytical bias. In case of PFOS, the use of the mass transition 498.9>80.0 may overestimate the sum of branched isomers [220, 221]. Consequently, the results for the branched isomers have to be considered as semiquantitative.

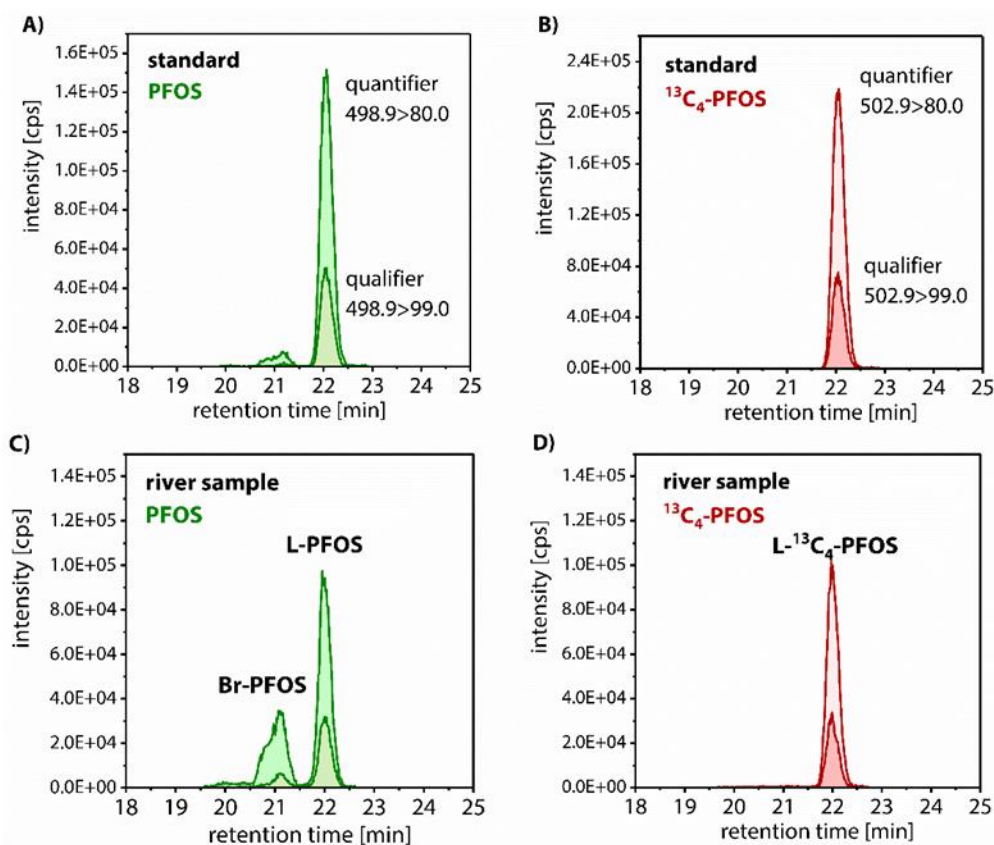


Figure 4.2-11: LC-MS/MS chromatograms of PFOS and $^{13}\text{C}_4$ -PFOS for A, B) a calibration standard, and C), D) a river water sample.

To sum up, the final chromatographic method was suitable for the analysis of the 29 target analytes, 13 internal standards and the injection standard. The optimization of the mobile phase composition in combination with a different sample solvent resulted in higher peak intensities and an acceptable peak shape for the early eluting compound PFBA. The linear isomer and the sum of branched isomers could be chromatographically separated and quantified individually for PFOS, FOSA, PFOA and PFHpA in environmental samples. An overview of the chromatographic method and the changes made in comparison to the initial method is given in Table 4.2-1.

Table 4.2-1: Chromatographic method for the analysis of PFASs and changes made in course of the optimization.

hardware	type			
binary pump	HP 1100 LC binary pump G1312 (Agilent, USA)			
autosampler	HP 1100 LC autosampler G1313 (Agilent, USA)			
analytical column	Synergi Fusion-RP: polar embedded C ₁₈ phase with trimethylsilyl endcapping, 150 mm x 2 mm, particle size 4 µm, pore size 80 Å (Phenomenex, USA)			
guard column	SecurityGuard cartridge for Fusion-RP HPLC columns, 4 mm x 2 mm (Phenomenex, USA)			
software	Analyst 1.5 (AB Sciex, USA)			
parameter	settings			
injection volume	10 µL (needle rinsed twice with methanol before injection)			
column temperature	30 °C			
flow rate	0.2 mL/min			
mobile phases	initial method		final method	
	A: 10 mM NH ₄ OAc in water B: 10 mM NH ₄ OAc in methanol		A: 2 mM NH ₄ OAc in water B: 0.05 % acetic acid in methanol	
sample/standard solvent	100 % methanol		methanol:water 80:20 (v/v)	
gradient	Time [min]	A [%]	B [%]	note
	-8	70	30	equilibration
	0	70	30	
	3	30	70	
	29	10	90	
	31	0	100	purging
45	0	100		

4.2.4 Optimization of a scheduled MRM method

Including all target analytes and internal standards, 79 mass transitions had to be monitored in a single run. In MRM mode, the instrument cycles through a list of transitions spending a defined time, the dwell time, on each transition. On the one hand, the dwell time has to be high enough to accumulate enough counts and achieve high sensitivity, but on the other hand, a peak cannot be properly reconstructed if too few data points are recorded over the chromatographic elution of a target analyte [205]. For precise quantification, more than 12 data points should be acquired across a chromatographic peak [203]. A strategy to monitor a large number of transitions without a decrease in dwell time and in the number of data points across peaks is to monitor each transition only around the elution time of the compound. This decreases the number of mass transitions that have to be monitored in parallel. Using the scheduled MRM algorithm provided with the instrument's software, the "retention time window" and the "target scan time" have to be settled, referring to the number of seconds each transition is monitored, or respectively the amount of time the instrument takes to cycle through a list of transitions. For both parameters, only one value can be chosen for all target analytes.

The retention time window was defined based on chromatographic considerations. PFOS was identified as the compound that has to be monitored the longest because the elution of the branched and linear isomer peaks in environmental samples takes approximately 120 s in total (Figure 4.2-11C). Thus, the retention time window was set to 180 s to ensure that the PFOS peaks are also in the retention time window if shifts occur. Based on this setting and the retention time of all target analytes, a maximum of 29 parallel transitions had to be monitored during the run (Figure 4.2-12A). Considering a typical peak width of 30 s and 29 scanned mass transitions, a target scan time of 1, 2 or 3 s would theoretically result in 30, 15 or 10 data points per peak. This was verified by extracting the number of data points acquired by the instrument for HFPO-DA in the course of the measurement of a calibration standard. With 31, 16 and 11 actual data points across the peak, the calculation was confirmed (Figure 4.2-12B). As more than 12 data points should be acquired per peak for a precise quantification [203], a target scan time of 2 s was chosen for the final method. Using a non-scheduled simple MRM method (dwell time 500 ms), the software reconstructed the HFPO-DA based on only one data point (Figure 4.2-12B). Although the accuracy of this data point is excellent at 500 ms dwell time, the peak area cannot be estimated correctly. This underlines the importance of the scheduled MRM algorithm when monitoring a large number of mass transitions.

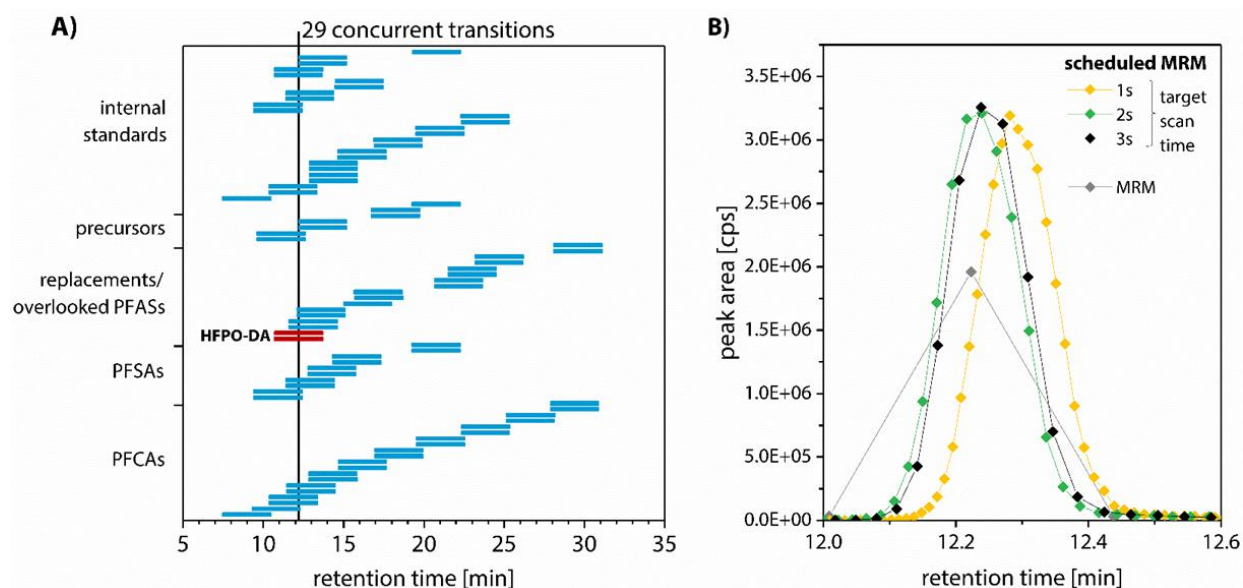


Figure 4.2-12: A) MRM scheduling during the run with a maximum of 29 concurrent mass transitions. B) Effect of different target scan times on the number of data points acquired across the HFPO-DA peak.

4.2.5 Optimization of ion source-dependent parameters

The optimization of ion source-dependent parameters ensures that the target analytes are optimally ionized and transferred into the gas phase. The parameters depend on the flow rate and on the solvent composition of the mobile phase entering the ion source. Consequently, they were optimized as a last step, using the optimized LC method and transitions-specific mass spectrometric settings.

Five parameters had to be tested: nebulizer gas pressure (gas 1), ion spray voltage, heater gas pressure (gas 2), heater gas temperature and curtain gas pressure. The gas 1 parameter controls the pressure of the nebulizer gas, helping to spray the LC effluent. A mist of small droplets is generated, having the same polarity as the voltage applied to the needle that ionizes the sample. The ion spray voltage itself can also be adapted. The gas 2 parameter controls the pressure of the heater (or turbo) gas, which affects the solvent evaporation and helps to increase the ionization of the target analytes. In addition, its temperature can be adjusted to optimize the evaporation of the spray droplets. The curtain gas interface is located between the curtain plate and the orifice, preventing ambient air and solvent droplets from entering and contaminating the ion optics [222].

Only one value per parameter can be set for the whole method. Thus, the chosen value has to be a compromise for all target analytes. In the hardware manual, a typical operational range of the parameters is given, dependent on the LC flow [222]. The range given for the used LC flow of 0.2 mL/min was tested for each parameter, aiming at a high sensitivity and high signal stability. As an example, for the heater gas pressure a typical range of 30 to 50 psig is given by the manufacturer

[222]. Within this range, different pressures were tested in increments of 5. Normalized peak areas are compared in Figure 4.2-13.

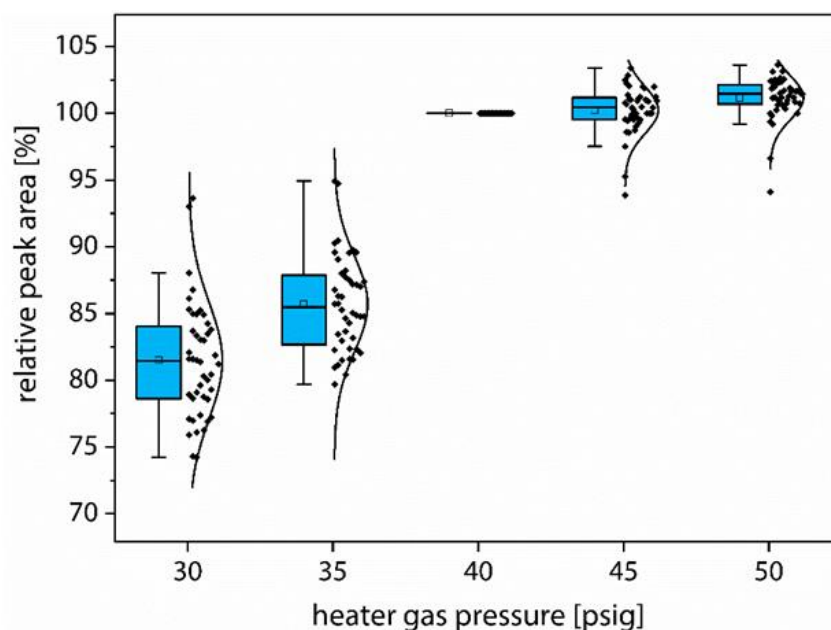


Figure 4.2-13: Optimization of the heater (or turbo) gas pressure (gas 2). Measuring a 100 pg/ μ L standard, the heater gas pressure was varied and the peak areas of the target analytes were determined ($n = 2$). The mean peak areas of the target analytes were normalized to the mean peak areas resulting from a pressure of 40 psig. The box represents the 25 % to 75 % quartile, the median is plotted by the band inside the box and the mean by the blank square. The ends of the whiskers display the lowest and the highest value still within 1.5 interquartile range (IQR) of the lower and higher quartile. The individual data points are plotted with black diamonds.

A heater gas pressure of 40, 45 and 50 psig resulted in a higher relative mean peak area than a pressure of 30 or 35 psig (99 to 100 % versus 83 and 86 %) (Figure 4.2-13). As 40, 45 and 50 psig gave comparable results and a too high gas flow can produce a noisy or unstable signal, 40 psig was chosen for gas 2. For the other ion-source dependent parameters, the tested ranges and chosen values are given in Table 4.2-2.

Table 4.2-2: Optimization of ion-source dependent parameters.

parameter	test range	increments	optimized value
gas 1 (nebulizer gas)	40 to 60 psig	5 psig	60 psig
gas 2 (turbo gas)	30 to 50 psig	5 psig	40 psig
curtain gas	10 to 30 psig	5 psig	15 psig
ion spray voltage	(-3000) to (-5000) V	500 V	-4500 V
temperature	250 to 450 °C	50 °C	400 °C

An overview of the final LC-MS/MS method is given in Table 10.2-1 and Table 10.2-2 for the compound-independent settings and in Table 10.2-3 to Table 10.2-5 for the compound-specific parameters.

4.3 Validation of the instrumental method

To validate the developed instrumental method, instrumental blanks, measurement precision, linear range and instrumental detection limit were determined for all target analytes. This part of the method validation aimed at characterizing the performance of the LC-MS/MS method itself. Thus, sample preparation steps were not considered and only standards without matrix were analysed. The results of the overall method validation for water and sediment are discussed in Chapters 4.5 and 4.7.

4.3.1 Instrumental blank

Having been used for PFAS analysis for several years already, the LC system had been modified to avoid instrumental blank contamination [223]. All PTFE-containing tubing had been replaced with polypropylene tubing or polyether ether ketone (PEEK) tubing and the degasser unit, containing fine porous PTFE-membranes, had been disconnected from the system [223]. Instead, the mobile phases were degassed in an ultrasonic bath for 30 min before the measurement. The solvents used to prepare the mobile phases, listed in Table 10.1-1 were regularly tested for PFAS contamination. Only stainless steel inlet filters without PTFE parts were used on the lines that draw solvent into the pump head. Glass autosampler vials, which typically contain septa made of PTFE-lined silicone, were replaced by PP vials with caps having a PP membrane.

Taking these measures, the target analytes were usually not detected in instrumental blank samples and noise levels were low (Figure 4.3-1). This was verified in every measurement sequence, injecting instrumental blank samples before and after the calibration and after every sixth sample. If target analytes were detected in the instrumental blank samples, for example after the measurement of a highly concentrated standard or sample, the LC column was rinsed and other cleaning measures were taken, if necessary. The efficiency of the measures was verified by measuring an additional blank sample before injecting further samples.

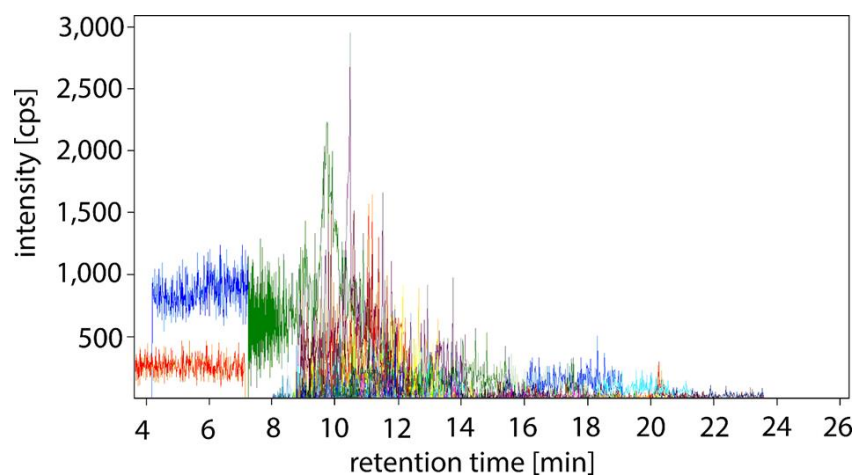


Figure 4.3-1: LC-MS/MS chromatogram of an instrumental blank sample (methanol) showing MRMs of all target analytes and internal standards.

4.3.2 Measurement precision

The measurement precision (instrument precision, system precision) refers to the closeness of agreement among a set of replicate measurements of the same sample [224]. It was determined using a low (1 pg/ μ L) and a high (100 pg/ μ L) calibration standard. The standards were injected ten times within a single sequence, using the optimized LC-MS/MS method. Based on the obtained peak areas, the coefficient of variation was calculated for each mass transition. The results were tested for outliers using the Grubb's test (two-sided test, $P = 98\%$). If present, outliers were eliminated and the Grubb's test was applied again before the coefficient of variation was recalculated. Boxplots comparing the coefficient of variation for the low and high calibration standard as well as quantifiers and qualifiers are shown in Figure 4.3-2, whereas individual results are provided in Table 4.3-1.

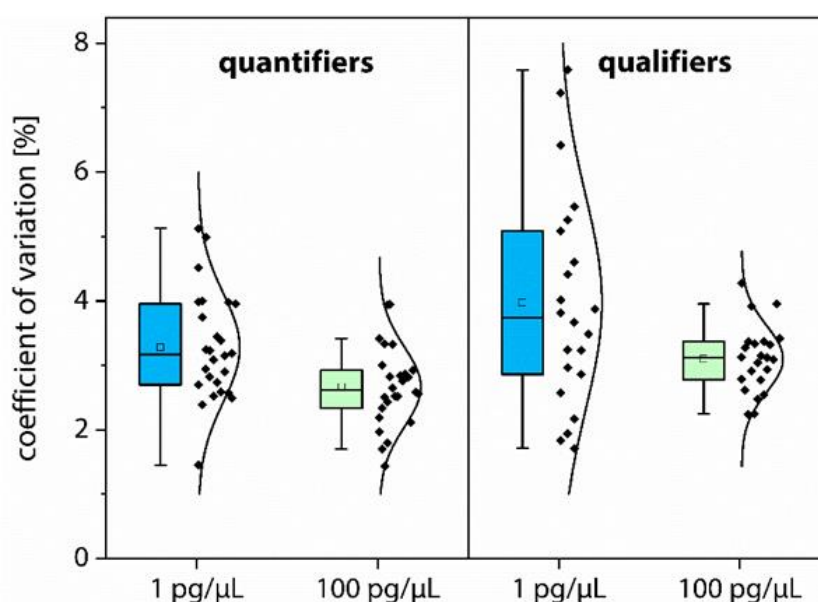


Figure 4.3-2: Boxplots showing coefficients of variation [%] of peak areas obtained for mass transitions used as A) quantifiers and B) qualifiers, resulting from tenfold measurements of standard mixes containing the native PFASs in concentrations of 1 pg/ μ L and 100 pg/ μ L (injection volume: 10 μ L). Peak areas were not normalized to internal standards. The box represents the 25 % to 75 % quartile, the median is plotted by the band inside the box and the mean by the blank square. The ends of the whiskers display the lowest and the highest value still within 1.5 interquartile range (IQR) of the lower and higher quartile. Black data points represent the individual data points.

The coefficients of variation obtained for mass transitions used as quantifiers ranged from 1.4 % to 5.1 % (Figure 4.3-2A). As all values were below 15 %, the precision is acceptable according to guidelines for method validation by the United States Food and Drug administration and other authorities, reviewed by Krueve *et al.* [225]. For the low concentration standard with a concentration of 1 pg/ μ L, the dispersion and the median was higher than for the high concentration standard of 100 pg/ μ L (median 3.2 % versus 2.6 %). This concentration-dependence of the measurement precision is generally observed in LC-MS/MS, with a lower precision at low concentrations that

are closer to the limit of detection [225]. Additionally, the measurement precision for the qualifiers (Figure 4.3-2B) was lower than that for the quantifiers (Figure 4.3-2B) at the same concentration, in particular at 1 pg/ μ L. This is coherent as the product ions selected as qualifiers had a lower signal abundance than the quantifiers (see Chapter 4.2) and are thus closer to their limit of detection at the same concentration.

4.3.3 Linear range

The unknown concentration of an analyte in a sample is calculated based on the correlation between the quotient of the instrument's response of the target analyte and its internal standard and the quotient of the concentration of the target analyte and its internal standard in calibration standards (Chapter 10.7.1). Typically, the instrument's response is directly proportional to the concentration in a certain range. This is the linear range of an instrumental method, which can be characterized by a linear regression model [226]. As the linear range is limited and compound-dependent, the linearity of the calibration curve has to be verified and the linear range has to be determined for each compound [224].

For this, a 13-point calibration ranging from 0 to 250 pg/ μ L was measured twice. The calibration levels of the native PFASs were 0, 0.01, 0.05, 0.1, 1, 5, 10, 25, 50, 100, 150, 200 and 250 pg/ μ L, whereas the internal standards had a concentration of 25 pg/ μ L in all calibration samples. The injection volume was 10 μ L. The large concentration range of native PFASs, spanning five orders of magnitude, was chosen as the samples collected for this PhD project were expected to cover a broad range of concentrations, from the pg/L range in Arctic seawater samples to μ g/L range in river water samples impacted by industrial point sources.

The most commonly used calibration model is the unweighted linear regression, where the instrument's response is plotted against the corresponding concentration. However, a requirement for the use of unweighted regression models is that the errors of the instrument's response are independent from each other, uncorrelated with the concentration and have equal variance across different concentration levels (homoscedasticity) [225]. Homoscedasticity was tested by means of an *F*-test, whereby the ratio of variance of the response obtained at a low and a high concentration is compared to a tabulated value (Equation (4.1)).

$$F = \frac{s_1^2}{s_2^2} \text{ with } s_1 > s_2 \quad (4.1)$$

with	F	test value
	s_1^2	variance of the first test series
	s_2^2	variance of a second test series

As an example, the variance of responses resulting from a tenfold-measurement of the replacement compound 6:2 Cl-PFESA at a concentration of 100 pg/ μ L was $s_{100}^2 = 2.2 \cdot 10^{-1}$, whereas s_1^2 was $1.3 \cdot 10^{-4}$ at a concentration of 1 pg/ μ L, resulting in an F-value of $1.8 \cdot 10^3$. With $N-1 = 9$ degrees of freedom, the tabulated value is 3.2 for $P = 95 \%$, 5.4 for $P = 99 \%$ and 10.1 for $P = 99.9 \%$. Comparing the calculated F value of $1.8 \cdot 10^3$ to these values, the null hypothesis of equality of variances is not true. This was not only observed for the compound 6:2 Cl-PFESA, but variance generally increased with concentration and the homoscedasticity assumption was not met. This is often observed for LC-MS/MS calibration curves spanning several orders of magnitude, leading to precision loss in the low concentration region [227]. Consequently, calibration curves were weighted to improve fit for the low concentration levels, applying a factor of $1/x$. The linear range was determined by visual inspection of the plot of the signal-concentration relationship. In addition, the percentage deviation of actual data points from the regression line was calculated (residuals) and plotted against the concentration on a logarithmic scale. A random pattern of residuals without a systematic structure confirms linearity [225].

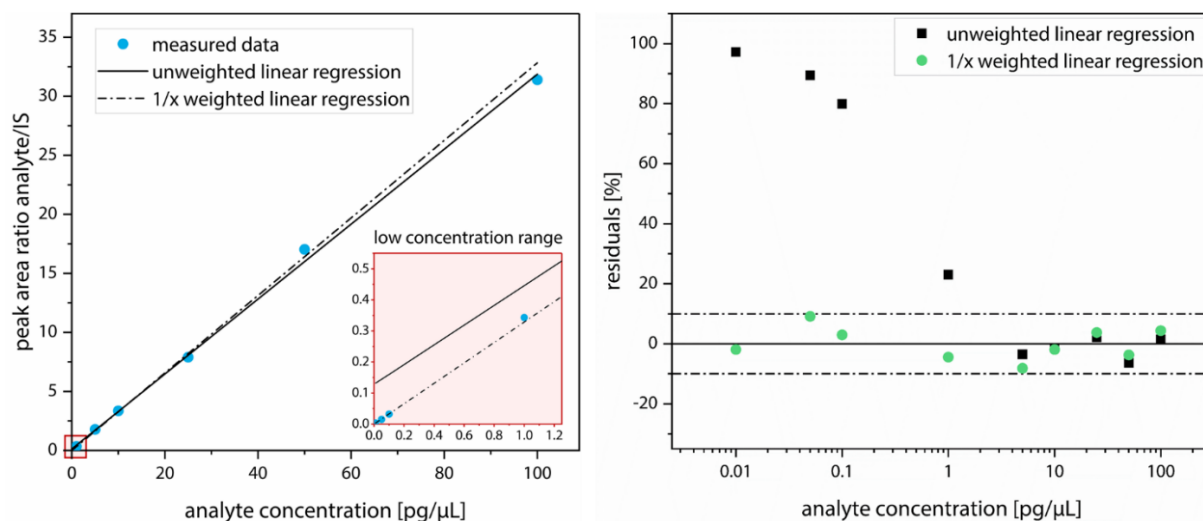


Figure 4.3-3: A) Calibration curve of 6:2 Cl-PFESA in the linear range (0–100 pg/ μ L) using unweighted linear regression and $1/x$ weighted linear regression. 10 μ L of the respective calibration solution were injected and analysed using the optimized LC-MS/MS method. The measured values represent the mean of a double determination. B) Residuals [%] between the measured data points and the unweighted and $1/x$ weighted linear regression line versus the concentration of 6:2 Cl-PFESA [pg/ μ L] on a logarithmic scale.

The effect of the weighting is exemplarily shown for the compound 6:2 Cl-PFESA in Figure 4.3-3. Even though both the unweighted calibration function and the $1/x$ weighted function have high coefficients of determination ($R^2 > 0.99$), only the weighted function gives a good fit to the low concentration experimental data (Figure 4.3-3A). This becomes particularly obvious in the residual plot (Figure 4.3-3B). In the low concentration range (< 0.1 pg/ μ L), residuals are 80 % to 100 % using the unweighted calibration function, whereas they are below 10 % using the $1/x$ weighted calibration function. Relative residuals below $\pm 20 \%$ are considered acceptable according

to the Directorate-General for Health and Food Safety of the European Commission [225]. The random pattern of the relative residuals for the weighted calibration function in Figure 4.3-3B confirms linearity.

Table 4.3-1 lists the linear range of all target analytes, underlining its compound-dependency. The linear range of several of the long-chain PFASs (PFTeDA, 8:2 Cl-PFESA, 6:6 PFPiA and 8:8 PFPiA and 8:2 FTSA) spans all the tested range (0.1–2,500 pg absolute) and thus five orders of magnitude. In contrast, short-chain PFCAs (PFBA and PFPeA) and the replacement chemicals DONA and HFPO-DA are linear within a smaller range (0.1–250 pg absolute, or respectively 0.1–500 pg absolute). This has to be considered when preparing calibration curves and analysing samples. The calculated coefficients of determination R^2 are > 0.99 (Table 4.3-1).

4.3.4 Instrumental detection limit (IDL)

The limit of detection is the lowest amount of an analyte that can be reliably detected and identified [228]. Determined by analysis of a standard without sample matrix, the instrumental detection limit (IDL) is solely a measure of instrument performance. In contrast, the method detection limit (MDL) refers to the overall method, i.e. considers the respective matrix and all sample preparation steps (Chapters 5 and 4.7).

In the past, the IDL has been typically determined by using the signal-to-noise method. A signal-to-noise ratio of three was generally accepted for estimating IDL. However, evolution in MS instrumentation has led to low noise systems. In particular, baselines in MS/MS mode often do not exhibit noise anymore. This also applies to the baselines of some of the PFAS product ions using the instrumentation at hand. Consequently, the signal-to-noise method was not applicable for the determination of the IDL. Instead, a multi-injection statistical methodology proposed by Wells *et al.* was used [229]. For this, a standard with a concentration of 0.05 pg/ μ L, close to the expected limit of detection, was injected ten times. The IDL is considered as the smallest amount of analyte required to produce a signal that is statistically distinguishable from the background within a specified confidence level. Consequently, the IDL is related to the relative standard deviation of the measured peak area of the replicate injections and a statistical confidence factor (4.2) [229].

$$IDL = \frac{s_{peak\ area}}{peak\ area_{mean}} \cdot t_{\alpha} \cdot m \quad (4.2)$$

with	IDL	instrumental detection limit [pg absolute]
	$s_{peak\ area}$	standard deviation of the analyte's peak area [cps]
	$peak\ area_{mean}$	analyte's mean peak area, resulting from tenfold injection [cps]
	t_{α}	Student's t -value (one-sided, 95 % confidence interval, 9 degrees of freedom), here 1.833
	m	injected amount of analyte, here 0.5 pg absolute

The determined IDLs for all target analytes ranged between 0.1 and 0.4 pg absolute (Table 4.3-1). Thus, without considering matrix interferences and sample preparation steps, the developed instrumental method is generally capable of detecting the target analytes in the sub pg range, which is a requirement for the analysis of the compounds in the marine environment.

Table 4.3-1: Performance of the LC-MS/MS method, including precision (coefficient of variation), linear range, regression coefficients and instrument detection limits (IDLs) of the target analytes.

acronym analyte	coefficient of variation [%]		linear range [pg abs]	R^2	IDL [pg abs]
	10 pg abs	100 pg abs			
PFCAs					
PFBA	2.7	3.4	0.2–250	0.996	0.2
PFPeA	2.4	2.2	0.2–250	0.998	0.2
PFHxA	2.9	2.0	0.1–750	0.998	0.1
PFHpA	2.8	1.7	0.1–750	0.990	0.1
PFOA	2.5	2.3	0.1–1,000	0.996	0.1
PFNA	4.0	2.5	0.2–1,000	0.998	0.2
PFDA	3.7	3.0	0.1–1,000	0.998	0.1
PFUnDA	3.2	2.4	0.2–1,500	0.990	0.2
PFDoDA	2.7	2.8	0.1–1,500	0.998	0.1
PFTrDA	3.2	2.6	0.2–1,500	0.990	0.2
PFTeDA	4.5	2.5	0.1–2,500	0.992	0.1
PFSA s					
PFBS	2.6	2.5	0.2–1,000	0.998	0.2
PFHxS	4.0	2.8	0.2–1,000	0.998	0.2
PFHpS	2.9	2.8	0.3–1,000	0.998	0.3
PFOS	1.5	2.9	0.2–1,000	0.998	0.2
PFDS	3.1	2.8	0.2–1,500	0.996	0.2
PFECHS	3.2	3.9	0.2–1,000	0.990	0.2
PFECAs and PFESAs					
DONA	3.4	2.1	0.2–500	0.996	0.2
HFPO-DA	3.4	1.4	0.2–500	0.991	0.2
HFPO-TrA	2.6	1.8	0.5–1,000	0.996	0.5
HFPO-TeA	3.5	2.6	0.5–1,000	0.994	0.5
6:2 Cl-PFESA	3.2	2.9	0.4–1,000	0.996	0.4
8:2 Cl-PFESA	4.0	3.3	0.3–2,500	0.998	0.3
PFPIAs					
6:6 PFPiA	4.0	3.3	0.2–2,500	0.998	0.2
6:8 PFPiA	5.0	2.6	0.2–2,500	0.994	0.2
precursors					
FOSA	2.5	2.6	0.2–1,000	0.998	0.2
4:2 FTSA	3.2	2.4	0.2–1,000	0.998	0.2
6:2 FTSA	3.7	2.9	0.4–1,000	0.998	0.4
8:2 FTSA	5.1	3.9	0.3–2,500	0.995	0.3

4.4 Optimization of the sample preparation for aqueous matrices

Analysing environmental samples, low PFAS concentrations and the presence of matrix components require enrichment of the target analytes and sample cleanup before the LC-MS/MS measurement. For aqueous samples, solid phase extraction (SPE) is the most commonly applied method, combining enrichment and cleanup in one sample preparation technique [183, 201]. This is also the method of choice in the German DIN 38407-42:2011-03 [203] and the international ISO standards 25101:2009-03 [202] for PFAS analysis.

Using the “bind and elute” approach, SPE typically involves five basic steps. Firstly, the stationary phase for extraction is conditioned by an appropriate solvent, which wets and activates the bonded phase. Then, the sorbent is equilibrated using a solvent with similar characteristics to the sample. When the sample is loaded, the target analytes interact with the sorbent and are retained. Simultaneously, water and non-interacting matrix components pass through. The sample loading is followed by a washing step to remove further matrix interferences, before the target analytes are eluted using an appropriate solvent [230].

Most conventionally analysed PFASs are strong acids and occur in their anionic form over a broad pH range (Chapter 2.2). Consequently, mixed-mode weak anion exchange/reversed phase (WAX) sorbents are most commonly applied as stationary phase in SPE for PFASs [183]. Typically, they consist of a polymeric sorbent which is functionalized with weak base moieties. During sample loading at neutral pH, the weak base on the sorbent’s surface is protonated, i.e. positively charged, and interacts with the negatively charged target analytes. The polymer itself retains target compounds by reversed-phase interactions. To elute the compounds of interest, a solution with basic pH, which neutralizes the weak base and cancels the interactions with the target analytes, is used [231]. The available SPE methods for PFAS analysis differ mainly in the kind and amount of solvent used for the washing and elution step (Table 4.4-1). Most of them were developed and validated for freshwater and only for a small scope of analytes.

Table 4.4-1: Overview of solid phase extraction methods in literature for the determination of PFASs in aqueous matrices.

	ISO 25101:2009-03 [202]	DIN 38407-42:2011-03 [203]	Gremmel <i>et al.</i> [207]	Ahrens <i>et al.</i> [94]	Heydebreck <i>et al.</i> [100]	Villaverde <i>et al.</i> [198]
conditioning ¹	4 mL 0.1 % NH ₄ OH in MeOH 4 mL methanol 4 mL water	4 mL 0.1 % NH ₄ OH in MeOH 4 mL methanol 4 mL water	2 mL 0.1 % NH ₄ OH in MeOH 2 x 2 mL MeOH 3 x 2 mL water	5 mL methanol 5 mL water	10 mL acetone 10 mL methanol 10 mL 0.25 % NH ₄ OH in MeOH	5 mL methanol 5 mL water
sample load	500 mL	50 mL	200 mL	2 L	1 L	1 L
washing	4 mL 25 mM NH ₄ OAc in water	4 mL water 4 mL acetone/ACN /HCOOH 50:50:1 4 mL methanol	3 mL water/MeOH 80:20 (v/v)	5 mL 0.1 % HCOOH in water	5 mL water	5 mL water/MeOH 90:10 (v/v)
elution	4 mL methanol 4 mL 0.1 % NH ₄ OH in MeOH	2 x 4 mL 0.1 % NH ₄ OH in MeOH	2 mL MeOH 4 mL 0.1 % NH ₄ OH in MeOH	14 mL ACN 5 mL 0.1 % NH ₄ OH in MeOH	10 mL 0.25 % NH ₄ OH in MeOH	10 mL MeOH
matrices	drinking, ground, surface water	drinking, ground, surface, treated waste water	aqueous samples, e.g. wastewater treatment plant effluents	seawater	river water, seawater	seawater
target analytes	PFOS, PFOA	C ₄ –C ₁₀ PFCAs; C ₄ , C ₆ , C ₈ PFESAs	52 PFASs of 14 different substance classes ²	33 PFASs of 8 structural classes ²	C ₄ –C ₁₂ PFCAs, C ₄ , C ₆ , C ₈ PFESAs, FOSA, HFPO-DA	C ₆ –C ₁₂ PFCAs; PFOS
applicability/ MDLs	concentration range: 2.0 to 10,000 ng/L for PFOS; 10 to 10,000 ng/L for PFOA	lower limit of applicability: 10 ng/L (treated waste water: 25 ng/L)	0.3 to 199 ng/L	pg/L range	MDLs: 0.03 to 0.63 ng/L	MDLs: 0.01 to 0.21 ng/L

¹ Oasis WAX (150 mg, 6cc, 30 µm) or other weak anion exchange (WAX) resins are recommended in the ISO and DIN standards and typically used as sorbents.

² These extensive methods did not include PFECAs/PFESAs, PFPiAs and PFECHS.

As a starting point for this study, the ISO standard 25101:2009-03 [202] was applied to river and seawater samples. Water:methanol 80:20 (v/v) was used as washing solution, according to a method developed for a diverse spectrum of 52 PFASs [207]. Due to the expected low concentrations, a comparatively large sample volume of 1 L was taken, as used in other studies dealing with seawater (Table 4.4-1). The method performance for river water and seawater was compared in terms of “absolute recoveries” of internal standards that were added before the sample preparation, calculated based on peak area ratio of the internal standard and the injection standard (4.4).

$$RF = \frac{\text{area (InjS cal)}}{\text{area (IS cal)}} \cdot \frac{c (IS cal)}{c (InjS cal)} \quad (4.3)$$

RF	response factor
<i>area (InjS cal)</i>	peak area of the injection standard ¹³ C ₈ -PFOA in the calibration standard [cps]
<i>area (IS cal)</i>	peak area of the internal standard in the calibration standard [cps]
<i>c (IS cal)</i>	concentration of the internal standard in the calibration standard [cps]
<i>c (InjS cal)</i>	concentration of the injection standard ¹³ C ₈ -PFOA in the calibration standard [cps]

$$\text{absolute IS recovery rate [\%]} = RF (mean) \cdot \frac{\text{area (IS sample)}}{\text{area (InjS sample)}} \cdot \frac{c (InjS sample)}{c (IS sample)} \cdot 100 \% \quad (4.4)$$

RF (mean)	mean response factor of all calibration standards
<i>area (IS sample)</i>	peak area of the internal standard in the sample [cps]
<i>area (InjS sample)</i>	peak area of the injection standard ¹³ C ₈ -PFOA in the sample [cps]
<i>c (InjS sample)</i>	concentration of the injection standard ¹³ C ₈ -PFOA in the sample [cps]
<i>c (IS sample)</i>	concentration of the internal standard in the sample [cps]

The injection standard, added directly before the measurement, corrects for differences in injection volume. In addition, it corrects for matrix-related losses of analyte signal during the measurement, e.g. due to ion suppression, as long as these are comparable for the injection standard and the internal standards. Thus, the absolute IS recoveries are a measure to quantify the losses of the compounds during sample preparation, excluding the measurement. The results of this preliminary test are shown in Figure 4.4-1.

Absolute IS recoveries generally ranged between (20±9) % and (88±9) % in river water and (6±2) % and (74±7) % in seawater (Figure 4.4-1). An exception was the compound ¹³C₂-6:2 FTSA, having an absolute recovery of (150±21) %, or respectively (170±27) %. Absolute recoveries of > 130 % for FTSA have also been reported in other studies [180, 207] and may be attributed to less ion suppression for FTSA than for other PFASs (and the injection standard) when measuring matrix-containing samples. As the internal standard ¹³C₂-6:2 FTSA is available for this group of PFASs, final results are corrected for these differences (Chapter 4.5.1).

Absolute IS recoveries for PFCAs with ≥ 9 perfluoroalkyl moieties (¹³C₂-PFDA, ¹³C₂-PFUnDA and ¹³C₂-PFDoDA) and other long-chain PFASs (¹³C₄-PFOS, ¹³C₈-FOSA), as well as PFBA, were

generally 20 % to 30 % lower in seawater compared to river water. This underlines that methods developed and validated for freshwater cannot be directly transferred to seawater. Thus, it was the aim of this study to optimize the solid phase extraction procedure with regard to the seawater matrix, in particular for the long-chain homologues.

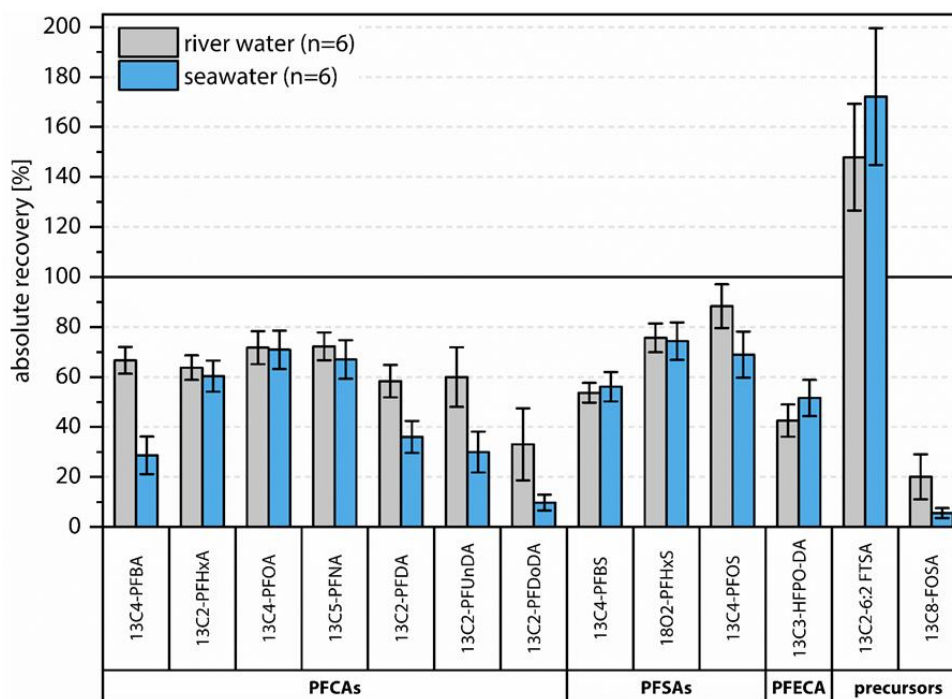


Figure 4.4-1: Comparison of absolute recoveries of internal standards in river water and seawater applying the ISO standard 25101:2009, which is for determination of PFOS and PFOA [202]. 1 L filtered sample was spiked with 3 ng of each internal standard. As washing solution in the SPE procedure, 4 mL water:methanol 80:20 (v/v) were taken [207]. Before the measurement, 1 ng of the injection standard $^{13}\text{C}_8$ -PFOA was added. The results represent the mean \pm standard deviation (SD) of sixfold determinations.

4.4.1 Optimization of the solid phase extraction procedure

The major difference between river water and seawater is the salt content. One litre of seawater from the open ocean contains on average 35 g of dissolved salts, predominantly chloride (55 %), sodium (31 %) and sulfate (8 %) ions. In contrast, the salt content of river water is typically < 0.5 g/L [232]. As the concentration of the dissolved salts in open seawater is approximately 10^{12} -fold higher than the typical PFAS concentration, the chloride and sulfate ions may compete with the anionic target analytes for ion-exchange sites of the SPE sorbent. To characterize this competition, Janda *et al.* [199] spiked a natural spring water sample to a total concentration of 250 mg Cl^-/L and determined the chloride concentration in the flow-through and in the eluate after application of the SPE procedure. They showed that 92 % of the chloride ions can be found in the flow-through and thus are not retained by the WAX resin. However, if co-retained species survive the SPE washing step, they are present in the eluate and can interfere with further steps of

analysis. Consequently, it was tested if larger washing volumes favourably affect the recovery rates in seawater (Figure 4.4-2).

The results show that a washing volume of 10 mL or 15 mL instead of 4 mL water:methanol 80:20 (v/v) increases the absolute recoveries, in particular of PFCAs with ≥ 9 perfluoroalkyl moieties ($^{13}\text{C}_2$ -PFDA, $^{13}\text{C}_2$ -PFUnDA and $^{13}\text{C}_2$ -PFDoDA) and other long-chain PFASs ($^{13}\text{C}_4$ -PFOS, $^{13}\text{C}_8$ -FOSA). The largest increase was observed for $^{13}\text{C}_2$ -PFDoDA, by 41 % for a washing volume of 10 mL instead of 4 mL, and by 50 % for a washing volume of 15 mL instead of 4 mL. Consequently, a washing volume of 15 mL was chosen for the final method. The favourable effect of a larger washing volume on the absolute recoveries of long-chain PFASs may be attributed to the fact that a higher amount of anions naturally present in seawater is washed away that would interfere with further steps of sample analysis.

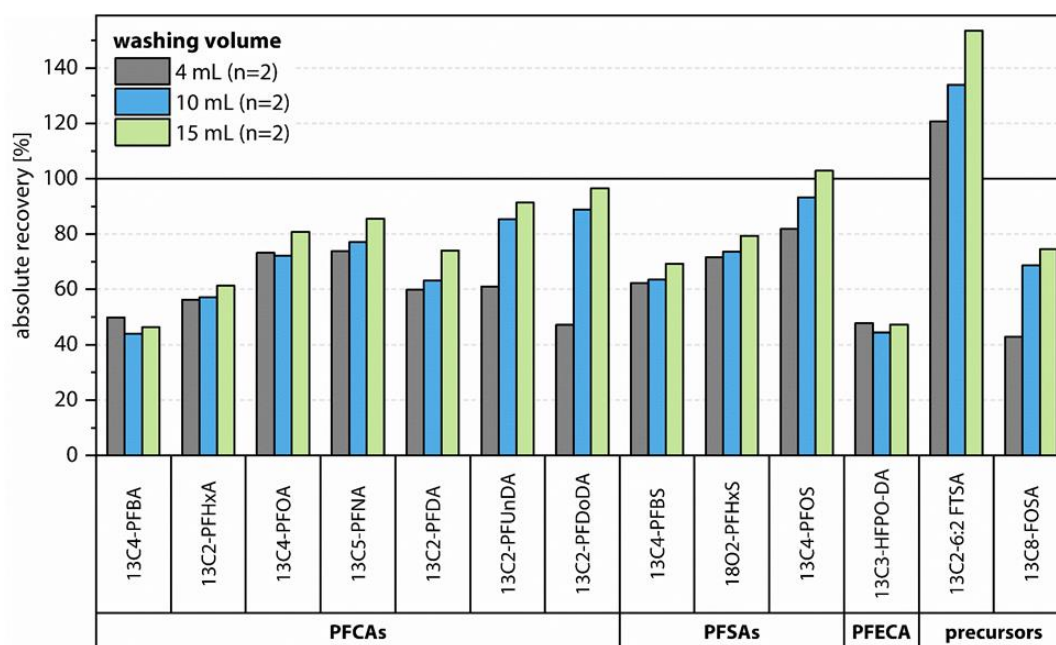


Figure 4.4-2: Absolute recoveries of internal standards in seawater using different washing volumes during SPE. 1 L filtered sample was spiked with 3 ng of each internal standard before analysis and water:methanol 80:20 (v/v) was used as washing solution. The results represent the mean of double determinations.

4.4.2 Optimization of the volume reduction step

The SPE eluate (12 mL) had to be further reduced to the μL range for analysis by LC-MS/MS. For this, a nitrogen flow evaporator, heated at 60 °C, was used (Flowtherm Optocontrol, Barkey, Germany). An advantage of this device to other nitrogen evaporators is the integration of an optical sensor, stopping the nitrogen flow at a specific sample volume to avoid evaporation to dryness. However, the customized vessels needed for the device are made of glass, to which long-chain PFASs are known to adsorb. According to the manufacturer, plastic vials are not available and the

glass vessels cannot be replaced due to the optical sensing mechanism (communication with Barkey, October 2016).

Generally, the walls of the glass vials were rinsed twice with 1 mL methanol during the sample volume reduction to 150 μ L. Afterwards, the sample was transferred from the glass sample vessels to polypropylene LC vials. It was assumed that due to their adsorption to glass walls, PFASs could not be transferred quantitatively in this step.

To test this, the glass vessel walls were rinsed once more with methanol after the sample transfer. The methanol used for rinsing was evaporated to 150 μ L and analysed as a second sample. The results confirmed that the transfer from the glass vessel to the LC vial was not quantitative and caused losses of all analytes (10–20 %) (Figure 4.4-3). Rinsing the vessels after sample transfer as described before and pooling the sample and the rinse before the measurement, could overcome the losses in this step. However, this resulted in higher MDLs and MQLs, as the sample was factor two less concentrated. Further tests showed that ultrasonication could also overcome the PFAS losses (Figure 4.4-3). For this, the glass vessels were put into an ultrasonic bath for 20 min before sample transfer (Sonorex Digiplus DL510H, Bandelin, Germany; nominal power 24 W/L, ultrasonic frequency 35 kHz). The ultrasound approach was chosen for the final method, as it could overcome the PFAS losses while keeping the end sample volume of 150 μ L and being less labour-intensive than the other approaches.

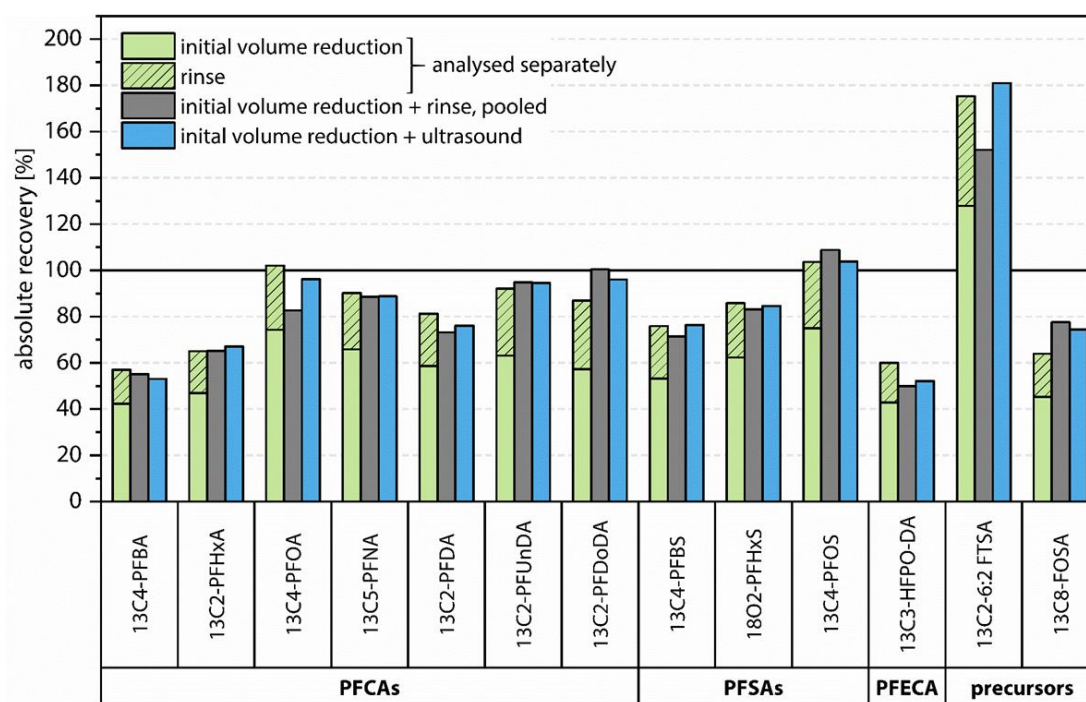


Figure 4.4-3: Absolute IS recoveries in seawater using different approaches for the volume reduction step. 1 L filtered sample was spiked with 3 ng of each internal standard before analysis. Before the measurement, 1 ng of the injection standard $^{13}\text{C}_8$ -PFOA was added. The results represent the mean of double determinations.

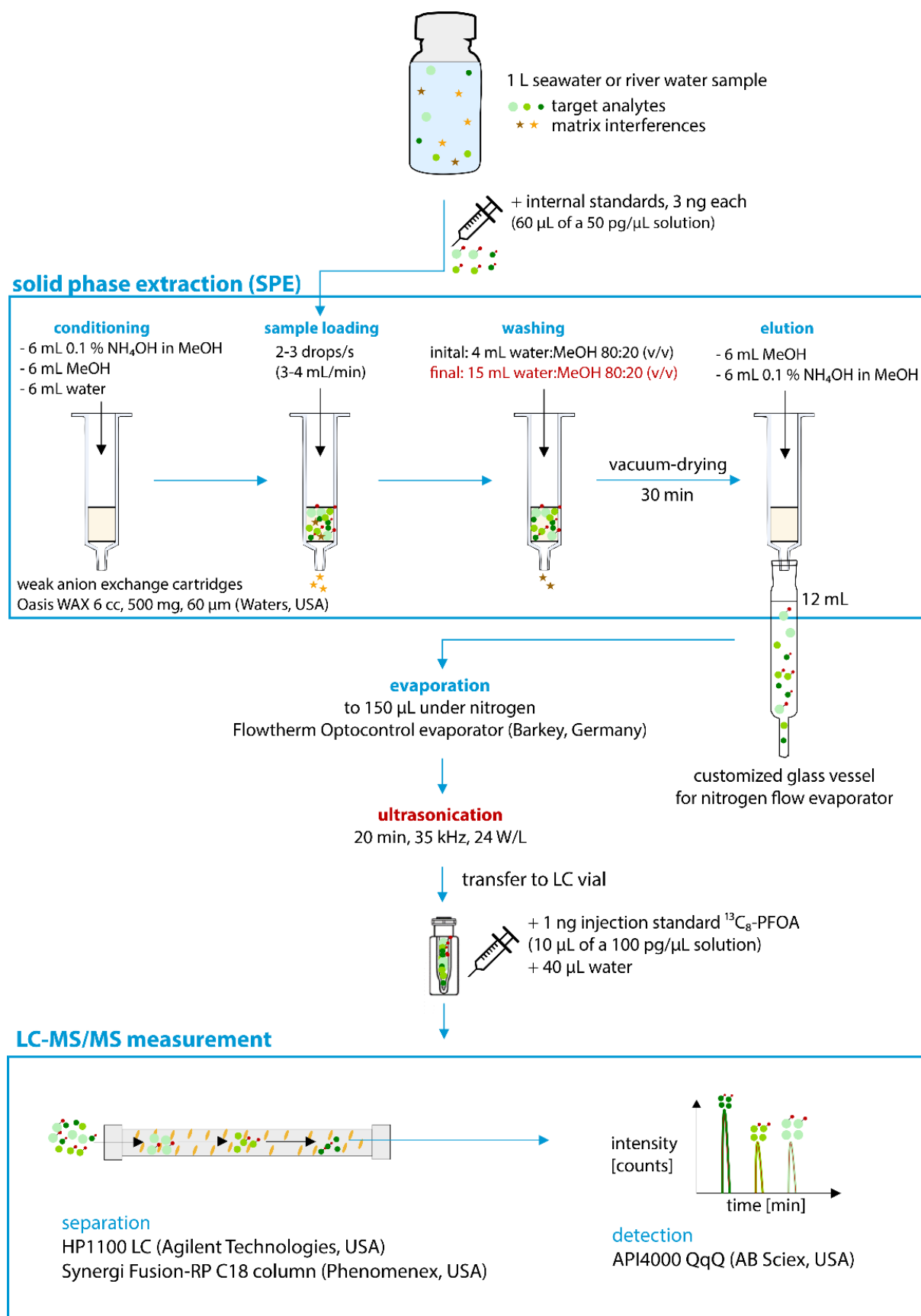


Figure 4.4-4: Overall method for the analysis of PFASs in aqueous samples and changes made in course of the optimization (red).

4.4.3 Final method

Compared to the initial sample preparation method, a volume of 15 mL instead of 4 mL water:methanol 80:20 (v/v) was used as washing solution during SPE in the final method. After the volume reduction, glass sample vessels were put into an ultrasonic bath before sample transfer (Figure 4.4-4). Details on the overall method for analysis of aqueous samples including the sampling procedure are provided in Chapters 10.3 and 10.5.1.

4.5 Validation of the overall method for aqueous matrices

To characterize the performance of the overall method for aqueous matrices, matrix spike recovery tests were performed, method blanks were evaluated to determine MDLs and MQLs and the method precision was investigated. In addition, a certified reference material was analysed.

4.5.1 Matrix spike recovery tests

In matrix spike recovery experiments, known amounts of the analytes and the internal standards are added to a real sample, before all sample preparation steps and the LC-MS/MS measurement are performed. The recovery of the spiked analyte is determined by comparing the amount of the analyte in the spiked sample to that in the unspiked sample (Equation 4.5).

$$\text{matrix spike recovery [\%]} = \frac{m_{\text{spiked sample}} - m_{\text{sample}}}{m_{\text{spike}}} \cdot 100 \% \quad (4.5)$$

with $m_{\text{spiked sample}}$ amount of the analyte in the spiked sample [ng]
 m_{sample} amount of analyte in the unspiked sample [ng]
 m_{spike} amount of the analyte spiked into the sample [ng]

The quantification of the compounds is based on the peak area ratio of the analyte and the assigned internal standard (Chapter 10.7.1). Consequently, the reported recoveries are “relative recoveries” that are corrected for analyte losses during sample preparation as well as matrix effects in LC-MS/MS analysis (ionization suppression/enhancement).

Based on matrix spike recovery tests, the performance of the overall method can be judged. Matrix spike recoveries close to 100 % show selectivity, trueness and robustness of the method for the tested matrix and concentration [233]. As recoveries are concentration-dependent, samples should be spiked at concentrations close to the environmental level [183]. Based on PFAS concentrations determined in previous studies in European coastal areas [101], in the North Atlantic [87] and in German rivers [100], 1 L seawater samples were spiked with an amount of 3 ng absolute, or respectively 400 pg absolute of each target analyte. 1 L river water samples were spiked with 3 ng absolute of the target analytes. In addition, recovery tests were performed for ultrapure water (supplied by a Milli-Q Integral 5 system, Merck, Germany), as it was planned to use it as

blank sample. The internal standards were added in the same amount as the native compounds. Triplicate samples were analysed using the optimized sample preparation method and relative recoveries of the target analytes were determined. During the development of the instrumental method, isotopically-labelled standards of the same structural group and the closest retention time were assigned to target analytes for which no isotopically-labelled analogues were available. However, only standards were analysed in this step and matrix effects were not considered. Consequently, during evaluation of the matrix spike recovery tests it was checked if other isotopically-labelled standards were better suited in the presence of matrix for the respective target analyte and result in higher recoveries. As this was not the case, the original assignment was also used for matrix-containing samples.

Figure 4.5-1A shows that for target analytes, for which isotopically-labelled analogues are available as internal standards, relative recoveries ranged between 90 and 110 %. An exception was PFOS, having a relative recovery of (84 ± 4) % and (85 ± 2) % in river and seawater spiked with 3 ng absolute, and HFPO-DA with a relative recovery of (117 ± 7) % in seawater. In general, the high recoveries show the suitability of the developed method for the aqueous matrices that were to be analysed for this PhD work at expected environmental concentrations.

As expected and depicted in Figure 4.5-1B, the relative recoveries of the target analytes for which no isotopically-labelled analogues were available as internal standards were not as good. Only for PFPeA, relative recoveries were in the range of 90 % to 110 % for all tested matrices. However, the majority of the compounds showed relative recoveries between 70 % and 115 %, which are still acceptable values in the field of ultratrace analysis [104]. An exception were the long-chain PFCAs PFTrDA with a relative recovery of (64 ± 3) % in seawater at a spiking level of 400 pg/L and PFTeDA, having recoveries of (64 ± 8) %, (72 ± 1) %, (54 ± 4) % and (63 ± 5) % in the different matrices. In addition, 6:8 PFPiA as well as 4:2 FTSA had relative recoveries below 70 %. The results for these compounds must be considered semiquantitative as they are most likely underestimated. This underlines the importance of the availability of matching isotopically labelled standards for quantification of target analytes. At a later point in the PhD project, the isotopically labelled analogues for 4:2 FTSA and 8:2 FTSA could be purchased and were used as internal standards for these compounds in the last study (Chapter 7).

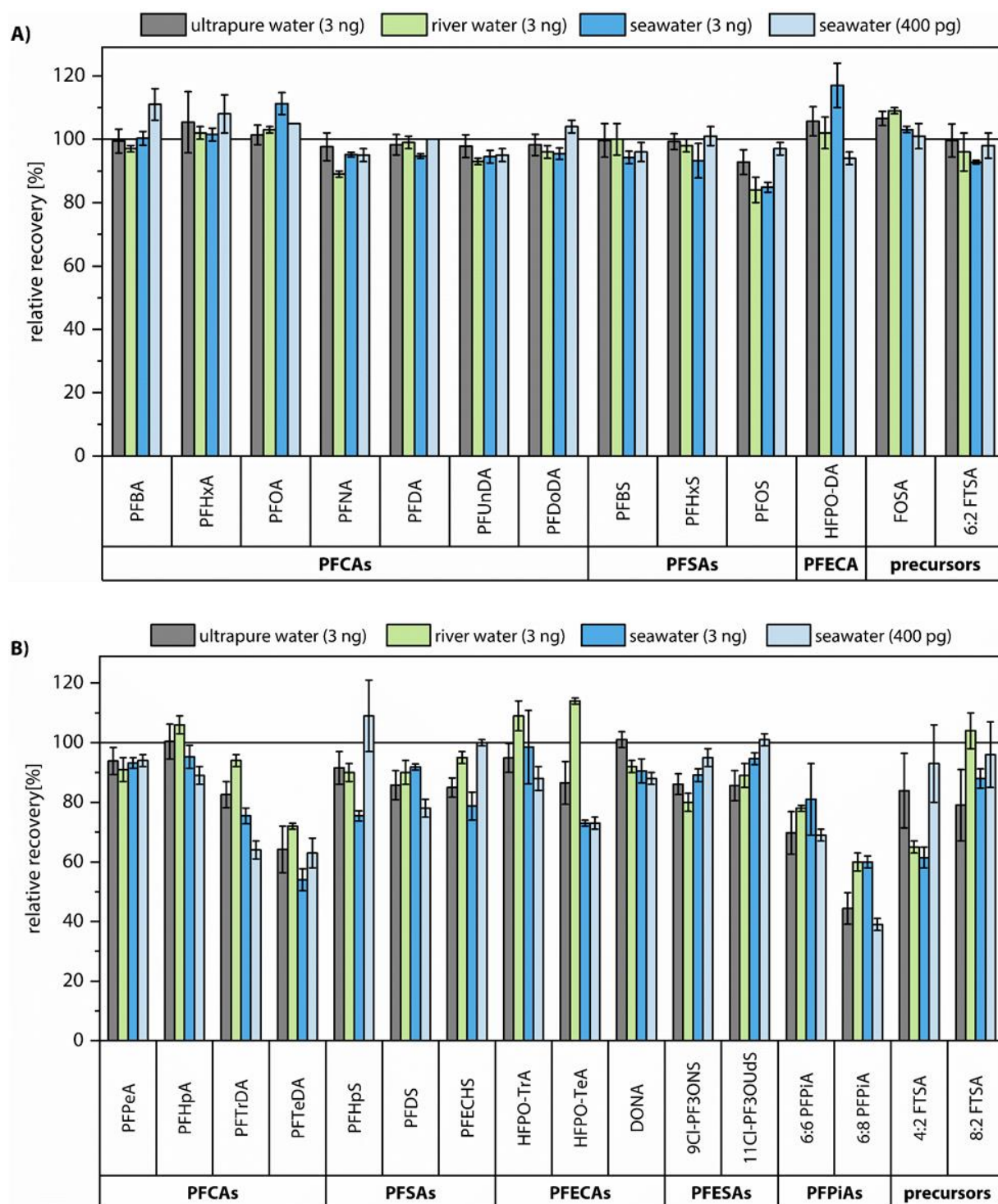


Figure 4.5-1: Relative recoveries resulting from matrix spike recovery tests for aqueous matrices for A) target analytes with isotopically-labelled analogues used as internal standards B) target analytes for which isotopically-labelled analogues are not available and which were assigned to structurally similar IS. 3 ng of each target analyte and internal standard were spiked to ultrapure water and river water. 3 ng or 400 pg of each target analyte and internal standard were spiked to seawater. The results are given as mean \pm standard deviation (SD) of a threefold determination.

4.5.2 Blanks, method detection limits and method quantification limits

Fluoropolymers, such as Teflon, and fluoroelastomer-based products, such as Viton, are widely used in laboratory supplies (caps, tape, vials), sampling devices and instruments (O-rings, tubing, surface coating, pump oil), and personal equipment (gloves, working clothes) [18]. Containing PFASs as impurities, these materials can cause sample contamination. Potential sources of contamination were identified and eliminated wherever possible. For example, bottle caps containing PTFE seals were replaced by polypropylene-only caps, stainless steel needles were used for sample elution during SPE and the fluoroelastomer-based tubing in the nitrogen concentrator had been substituted with a fluorine-free polymer. To avoid cross-contamination, standards were handled in a different laboratory than low-concentrated samples. Throughout the analysis, all containers and equipment were rinsed three times with methanol before and after usage. Reusable equipment was washed in a laboratory dishwasher. Afterwards, glass containers were heated at 250 °C for 10 h. Single use glass vials and glass fibre filters were baked in a Muffle furnace at 450 °C before usage.

The analysis of blanks was essential to monitor background contamination and to trace back contamination sources. In addition to the instrumental blanks (Chapter 4.3), a laboratory blank was analysed with every SPE batch of seven or eight samples. To prepare a laboratory blank, the internal standard mix was added to a preconditioned cartridge, which was left on the vacuum manifold during the extraction and treated as if it was a sample from the washing step on. Thus, the following components and processes can contribute to this blank: the SPE cartridge, the internal standard solution, the solvents used for the different SPE steps, the drying of the cartridges (air), and the concentration of the samples (nitrogen). During sampling campaigns, field blanks were prepared on different sampling days by filling sampling bottles with ultrapure water and analysing them like samples. In addition to the components listed for the laboratory blank, the sampling environment, the sampling bottles, the connection of the sampling bottles to the SPE cartridges (silicone tubes) and the ultrapure water itself can contribute to the field blanks.

All results were corrected by subtracting the average concentration of the respective compound in the laboratory blanks from the concentration in the sample. If field blanks showed higher concentrations of PFASs than laboratory blanks, field blank concentrations were subtracted. For PFASs present in the blanks, method detection limits (MDLs) and method quantification limits (MQLs) were calculated as mean blank concentration plus 3 or 10 times the standard deviation (SD), respectively. For PFASs not present in the blank samples, MDLs and MQLs were derived from a signal-to-noise ratio of 3 or 10, observed in low-level samples or spiked matrix samples.

The PhD project aimed at taking water samples not only in Germany, but also in China and the Arctic. Water samples have to be processed quickly after sampling [183] and customs regulations make it difficult to ship them from countries outside Europe to Germany. Consequently, samples

taken abroad were extracted in the laboratory of the Yantai Institute of Coastal Zone Research in China and on board the research vessel *Polarstern*, respectively. After loading the samples on the SPE cartridges, the sorbent was dried using vacuum and the cartridges could be easily shipped to HZG, where further steps of analysis were processed. The background contamination in the laboratories in China and on board *Polarstern* was unknown before starting the work. To reduce possible contamination sources, all needed materials and chemicals were tested for the presence of target PFASs at HZG before the campaigns and shipped to the respective location of sample preparation.

Due to the different places and times of sample preparation, campaign-specific MDLs and MQLs were calculated (Table 4.5-1). In contrast to the instrumental blanks, in which no PFASs could be detected, particular compounds were quantified in the laboratory and field blanks in the pg/L range (C₄-C₁₁ PFCAs, PFOS, 6:2 FTSA). This is further discussed for the specific studies in chapters 5 to 7. For most of the compounds, MDLs were still below 0.050 ng/L (Table 4.5-1). For the samples from the Arctic campaign, low MDLs had the highest relevance due to the expected low concentrations in the samples. Here, MDLs were below 20 pg/L for 18 compounds (C₆ to C₁₄ PFCAs, PFBS, PFHxS, HFPO-DA, DONA, 6:2 and 8:2 Cl-PFESA and 6:6 and 6:8 PFPiAs and FOSA) and between 20 and 50 pg/L for eight compounds (PFPeA; PFHpS, PFOS, PFDS; PFECBS, HFPO-TrA; 4:2 FTSA, 8:2 FTSA) (Table 4.5-1). This shows that the method is generally capable of detecting PFASs in the marine environment with expected concentrations in the pg/L range. However, the MDLs and expected concentrations are close to each other. Particularly in samples from remote areas, non-detects can be method-related. This is especially important when comparing results from different studies and working groups. MDLs and background contamination vary between methods and laboratories. In addition, the way of calculating and considering them differs between working groups. Consequently, these aspects have to be compared between studies in addition to mere numbers.

Higher MDLs in all campaigns were observed for 6:2 FTSA (up to 0.28 ng/L) due to comparatively high blanks and for HFPO-TeA (0.075 ng/L) due to a high instrumental noise. Moreover, comparatively high concentrations of PFBA were present in blank samples from the *Polarstern* cruise, strongly varying between different SPE batches (mean±SD (0.35±0.46) ng/L). Thus, no results were reported for PFBA in these samples (Chapter 6). Probably, the contamination was shipborne because significantly lower concentrations of PFBA were observed in blanks processed at HZG and in China, resulting in acceptable MDLs and MQLs (Table 4.5-1). In contrast, high concentrations of PFOA were present in blank samples processed in China, albeit still considerably below its concentration in the environmental samples. These differences underline the importance of campaign-specific blank samples and the calculation of campaign-specific MDLs and MQLs.

Table 4.5-1: Campaign-specific method detection limits (MDLs) and method quantification limits (MQLs) for the determination of PFASs in aqueous matrices.¹

sampling campaign code study area location (time) of sample extraction analyte ²	study 2 (chapter 5) research vessel <i>Ludwig Prandtl</i>				study 3 (chapter 6) research vessel <i>Polarstern</i>		study 4 (chapters 7 and 8) land-based			
	LP20170606		LP20170904		PS114 (ARK-XXXII/1)		RHINEALZ20180910		CHINESERIVERS2018	
	North Sea		Baltic Sea		Fram Strait		German rivers		Chinese rivers	
	HZG (06/2017)		HZG (09/2017)		<i>Polarstern</i> (07/2018)		HZG (09/2018)		YIC ⁴ (11/2018)	
	MDL	MQL	MDL	MQL	MDL	MQL	MDL	MQL	MDL ⁵	MQL ⁵
PFBA	0.16	0.35	0.077	0.19	- ³	- ³	0.14	0.33	0.20	0.52
PFPeA	0.042	0.12	0.051	0.14	0.023	0.053	0.032	0.085	0.25	0.70
PFHxA	0.055	0.095	0.043	0.14	0.012	0.027	0.083	0.28	0.19	0.63
PFHpA	0.024	0.079	0.039	0.13	0.012	0.021	0.015	0.050	0.043	0.11
PFOA	0.11	0.22	0.048	0.095	0.016	0.029	0.050	0.17	4.7	13
PFNA	0.063	0.14	0.033	0.063	0.0063	0.021	0.033	0.084	0.13	0.40
PFDA	0.041	0.087	0.024	0.046	0.0064	0.021	0.033	0.087	0.12	0.33
PFUnDA	0.028	0.063	0.024	0.050	0.0037	0.012	0.023	0.051	0.077	0.21
PFDoDA	0.017	0.057	0.017	0.057	0.0033	0.011	0.029	0.073	0.051	0.12
PFTTrDA	0.0046	0.015	0.0046	0.015	0.0046	0.015	0.048	0.16	0.10	0.32
PFTeDA	0.0088	0.029	0.0088	0.029	0.0088	0.029	0.0082	0.027	0.016	0.054
PFBS	0.045	0.15	0.052	0.17	0.013	0.045	0.037	0.12	0.12	0.39
PFHxS	0.073	0.24	0.10	0.34	0.018	0.061	0.087	0.29	0.17	0.58
PFHpS	0.027	0.090	0.027	0.090	0.027	0.090	0.049	0.16	0.060	0.20
PFOS	0.0057	0.019	0.015	0.036	0.021	0.044	0.074	0.25	0.15	0.49
PFDS	0.032	0.093	0.032	0.093	0.032	0.093	0.032	0.11	0.065	0.22
PFECHS	0.043	0.14	0.038	0.13	0.043	0.14	0.029	0.098	0.059	0.20
HFPO-DA	0.044	0.15	0.018	0.059	0.006	0.02	0.010	0.034	0.031	0.10
HFPO-TrA	0.044	0.15	0.044	0.15	0.044	0.15	0.044	0.15	0.088	0.30
HFPO-TeA	0.075	0.25	0.075	0.25	0.075	0.25	0.075	0.25	0.15	0.50
DONA	0.0075	0.025	0.0075	0.025	0.0075	0.025	0.013	0.035	0.019	0.061

6:2 Cl-PFESA	0.0069	0.023	0.0069	0.023	0.0069	0.023	0.0070	0.023	0.014	0.047
8:2 Cl-PFESA	0.0068	0.023	0.0068	0.023	0.0068	0.023	0.011	0.033	0.015	0.050
6:6 PFPiA	0.0049	0.016	0.0049	0.016	0.0049	0.016	0.0068	0.023	0.014	0.045
6:8 PFPiA	0.0087	0.029	0.0087	0.029	0.0087	0.029	0.013	0.042	0.026	0.084
FOSA	0.0036	0.012	0.0022	0.0074	0.008	0.027	0.012	0.017	0.012	0.017
4:2 FTSA	0.030	0.10	0.030	0.10	0.030	0.10	0.030	0.10	0.060	0.20
6:2 FTSA	0.061	0.15	0.28	0.48	0.070	0.21	0.063	0.21	0.11	0.35
8:2 FTSA	0.036	0.12	0.036	0.12	0.036	0.12	0.072	0.24	0.14	0.48

¹ For compounds present in blanks, MDLs and MQLs were calculated as the average blank value plus 3 or 10 times the standard deviation, respectively (blue). For PFASs other than these, the MDLs and MQLs were derived from a signal-to-noise ratio of 3 or 10, respectively, observed in low-level samples (green) or spiked matrix samples (yellow).

² The MDLs and MQLs for the linear isomers of all compounds are given in this table.

³ In blank samples processed on board, comparatively high concentrations of PFBA were found, strongly varying between the different SPE batches (red). Consequently, no results are reported for PFBA.

⁴ YIC: Yantai Institute of Coastal Zone Research

⁵ Due to expected higher concentrations, only 500 mL (instead of 1 L) of the Chinese river water samples was extracted, resulting in correspondingly higher MDLs and MQLs.

4.5.3 Method precision

To determine the overall method's precision (repeatability), six samples were collected at the same sampling site in the North Sea and analysed using the optimized analytical method. For target analytes > MQL, the coefficient of variation was calculated.

The results in Figure 4.5-2 show that coefficients of variation for the overall method ranged between 2.4 % (PFHpA) and 18 % (PFUnDA), covering a broader range than observed for the instrumental measurement (1.4 % to 5.1 %, see Chapter 4.3). This was expected because the method precision considers all steps of the method (sampling, sample preparation and measurement) and not only the measurement. For most of the quantified target analytes, the coefficient of variation was < 10 %, which is a good value for analyte concentrations in the ppq to ppt range determined in a complex matrix [233]. An exception was L-PFOS, having a coefficient of variation 15 %. In addition, the coefficients of variation increased to 11–19 % for compounds present in concentrations closer to the MQL (PFNA, PFDA, PFUnDA). This concentration-dependence of the measurement precision was also observed when determining the measurement precision (Chapter 4.3). However, coefficients of variation < 20 % can still be considered acceptable for ultratrace analysis in complex matrices [233].

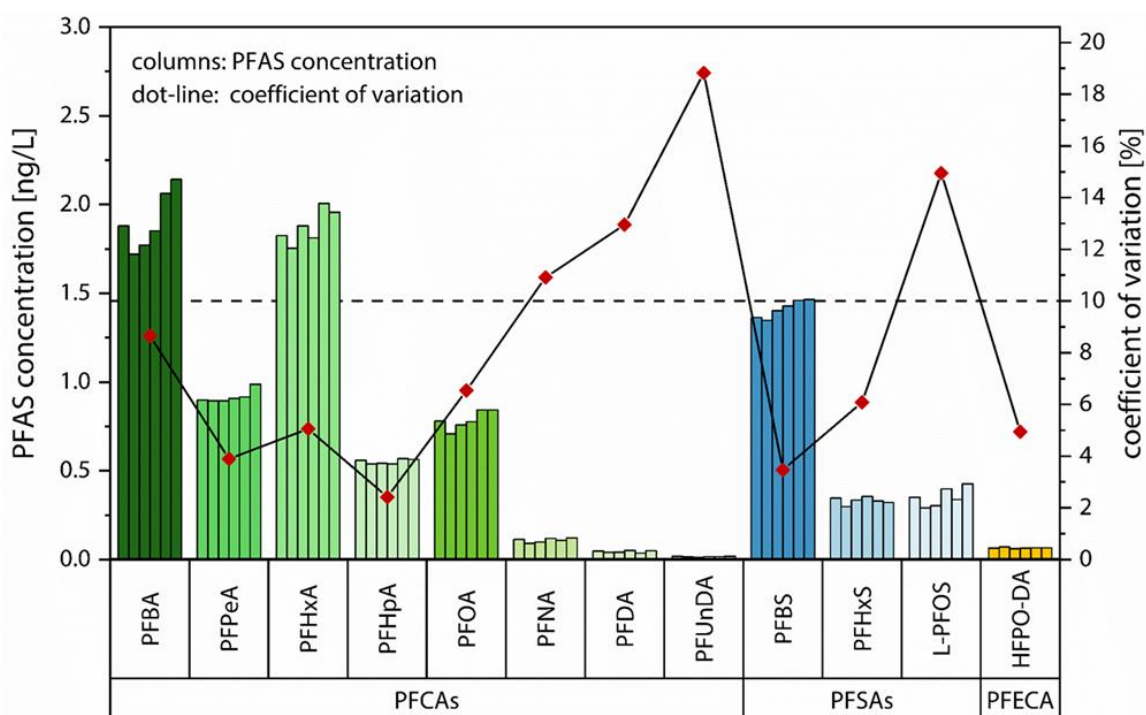


Figure 4.5-2: Coefficient of variation for PFASs > MQL, determined by sixfold analysis of a North Sea sample.

4.5.4 Analysis of a certified reference material (CRM)

While there is a variety of CRMs for trace metals, there is a lack of CRMs for organic pollutants in water. Several attempts by producers to prepare water CRMs for organics possessing the necessary homogeneity and stability have been unsuccessful [234, 235]. In 2016, the first CRM for organic pollutants became available, produced by the European Commission Joint Research Center (JRC), Institute for Reference Materials and Measurements (IRMM). Tap drinking water from the Netherlands was spiked with a mixture of 14 PFASs (PFCAs and PFASAs). Based on an intercomparison study among 12 laboratories, the JRC assigned six certified values and one indicative value to the CRM. Certified values are values fulfilling the highest standards of accuracy and represent the unweighted mean value of the means of accepted datasets, whereas indicative values are values where either the uncertainty is too large or too few independent datasets are available to allow certification and are therefore less reliable than certified values [236].

To verify the trueness of the developed analytical method, the CRM was analysed ($n = 3$) and the measured results were compared to the values given in the certification report. In addition to the recoveries, the \bar{x} -score was used as a statistical criterion to evaluate the results, indicating how many standard deviations a result is away from the reference value (4.6) [237, 238]. $|\bar{x}\text{-score}| < 2$ are considered acceptable, whereas a result of $2 < |\bar{x}\text{-score}| \leq 3$ is questionable and a $|\bar{x}\text{-score}| > 3$ is unacceptable [238].

$$|\bar{x}\text{-score}| = \frac{(c_{\text{measured}} - c_{\text{certified}})}{\sqrt{\left(\frac{U_{\text{ref}}}{2}\right)^2 + \left(\frac{SD}{\sqrt{3}}\right)^2}} \quad (4.6)$$

with	U_{Ref}	expanded uncertainty reference sample (confidence level 95 %, $k = 2$)
	SD	standard deviation of the measurement series ($n = 3$)
	c_{measured}	mean measured value [ng/L]
	$c_{\text{certified}}$	certified value [ng/L]

Resulting from the analysis of the CRM, calculated $|\bar{z}\text{-scores}|$ for PFASs with certified or indicative values were < 2 and thus acceptable (Table 4.5-2). Recoveries were also acceptable, ranging from 84 % (PFHpA) to 115 % (PFBS).

Table 4.5-2: Verification of the method's trueness by analysis of the reference material IRMM-428.

	certified value $\pm U_{\text{Ref}}^1$ [ng/L]	measured value $\pm SD^2$ [ng/L]	recovery [%]	z-score
PFPeA	4.0 \pm 1.0	3.7 \pm 0.1	93	-0.57
PFHxA	7.4 \pm 1.0	7.5 \pm 0.2	101	0.15
PFHpA	3.7 \pm 0.7	3.1 \pm 0.1	84	-1.6
PFNA	3.9 \pm 1.4*	3.4 \pm 0.4	87	-0.68
PFBS	5.5 \pm 1.4	6.3 \pm 0.1	115	1.1
PFHxS	3.6 \pm 1.0	3.6 \pm 0.1	101	0.050
L-PFOS	9.6 \pm 1.7	8.8 \pm 1.1	92	-0.71

¹ expanded uncertainty reference sample (confidence level 95 %, $k = 2$)

² standard deviation of the measurement series in our laboratory ($n = 3$); * indicative value

The JRC did not assign values to substances for which the interlaboratory comparison results disagreed significantly without a technical reason (PFBA, PFOA, PFDA) and to substances which were not included in homogeneity and stability studies (PFUnDA and PFDoDA). However, the measured values could be compared with the interlaboratory comparison results given in the CRM report [236]. Although no statistical evaluation could be performed due to the issues raised by JRC, Figure 4.5-3 and Figure 4.5-4 show that the results derived from the developed analytical method are generally in line with the results of the other labs from the intercomparison study.

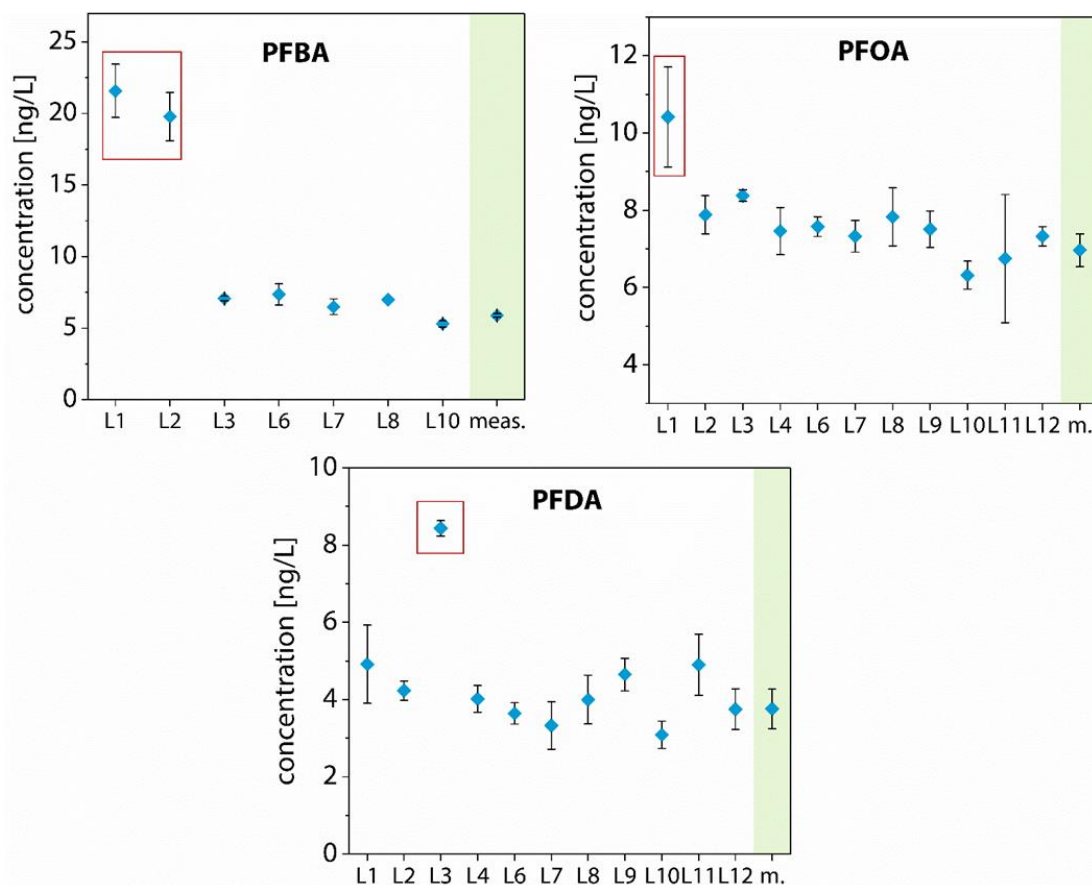


Figure 4.5-3: Comparison of own measured values (marked in green) for PFBA, PFOA and PFDA with laboratory intercomparison results (laboratories L1–L12), provided in the CRM certification report. The number of interlaboratory comparison results is different from compound to compound because the number of analytes differed between laboratories. Results identified as outliers by JRC [236] are marked in red.

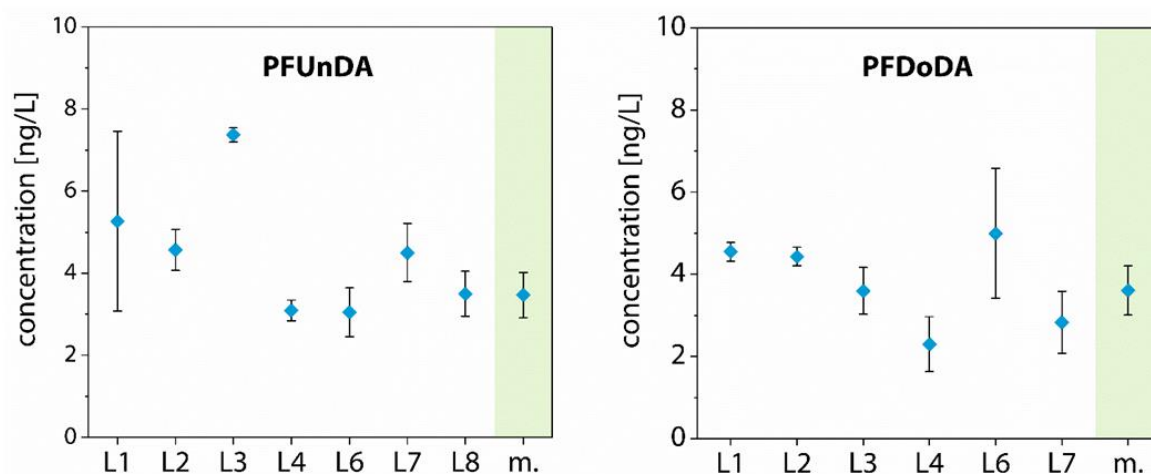


Figure 4.5-4: Comparison of own measured values (marked in green) for PFUnDA and PFDoDA with laboratory intercomparison results (laboratories L1–L12) provided in the CRM certification report. The number of interlaboratory comparison results is different from compound to compound because the number of analytes differed between laboratories.

4.6 Optimization of the sample preparation for sediments

For sediments, a larger variety of sample preparation methods than for aqueous matrices has been described in scientific literature. Common extraction procedures are based on solid-liquid extraction, using extraction solvents such as methanol [239], acidic methanol [240], alkaline methanol [241] and methyl *tert*-butyl ether (MTBE) with tetrabutylammonium hydrogen sulfate (ion pair extraction) [242]. In addition to these conventional extraction methods, automated pressurized fluid extraction systems have been applied [243, 244]. Typically, a clean-up of the extract is performed after all types of sample extraction, based on SPE using weak anion exchange sorbents (as for water samples) or graphitized carbon black.

The ultrasound-assisted methanol- and acetic acid-based extraction method by Higgins *et al.* [240] had proved to be a robust method with a high repeatability and good recoveries [93, 244-246]. This manual method is labour-intensive, but its use did not require new equipment. Sources for background contamination were expected to be similar to those for aqueous matrices. In contrast, automated systems often contain parts made of fluoropolymers or -elastomers, which can cause contamination of the samples and are difficult to replace. Consequently, it was decided to take the method developed by Higgins *et al.* [240] as a starting point for this PhD project.

MDLs determined by Higgins and co-workers ranged from 0.041 to 0.246 ng/g dw, using 1 g air-dried sediment sample [240]. As PFAS concentrations in North Sea coastal sediments were expected to be in the low pg/g range [114], the method was adapted to a larger sample amount as described by Yan *et al.* [246]. Instead of 1 g air-dried sediment sample, 5 g freeze-dried sediment samples were weighed in for analysis. Due to the larger sample amount, the volume of the extraction solvents was tripled. To clean and concentrate the sample extracts, an SPE extraction was performed for the sample extracts in the same way as for the water samples (Chapter 4.4). The eluent was reduced in volume and after addition of the injection standard $^{13}\text{C}_8$ -PFOA and water, the sample was measured using the optimized LC-MS/MS method (Chapter 4.2).

This study aimed at testing if this method can be applied to the broad spectrum of target analytes and if it is capable of detecting PFASs in the low pg/g range in marine sediments. The extraction efficiency had to be verified, as the amount of sample and extraction solvent had been changed in comparison to the validated method by Higgins and co-workers [240]. Moreover, it was an aim to optimize the volume reduction step.

4.6.1 Optimization of the volume reduction step

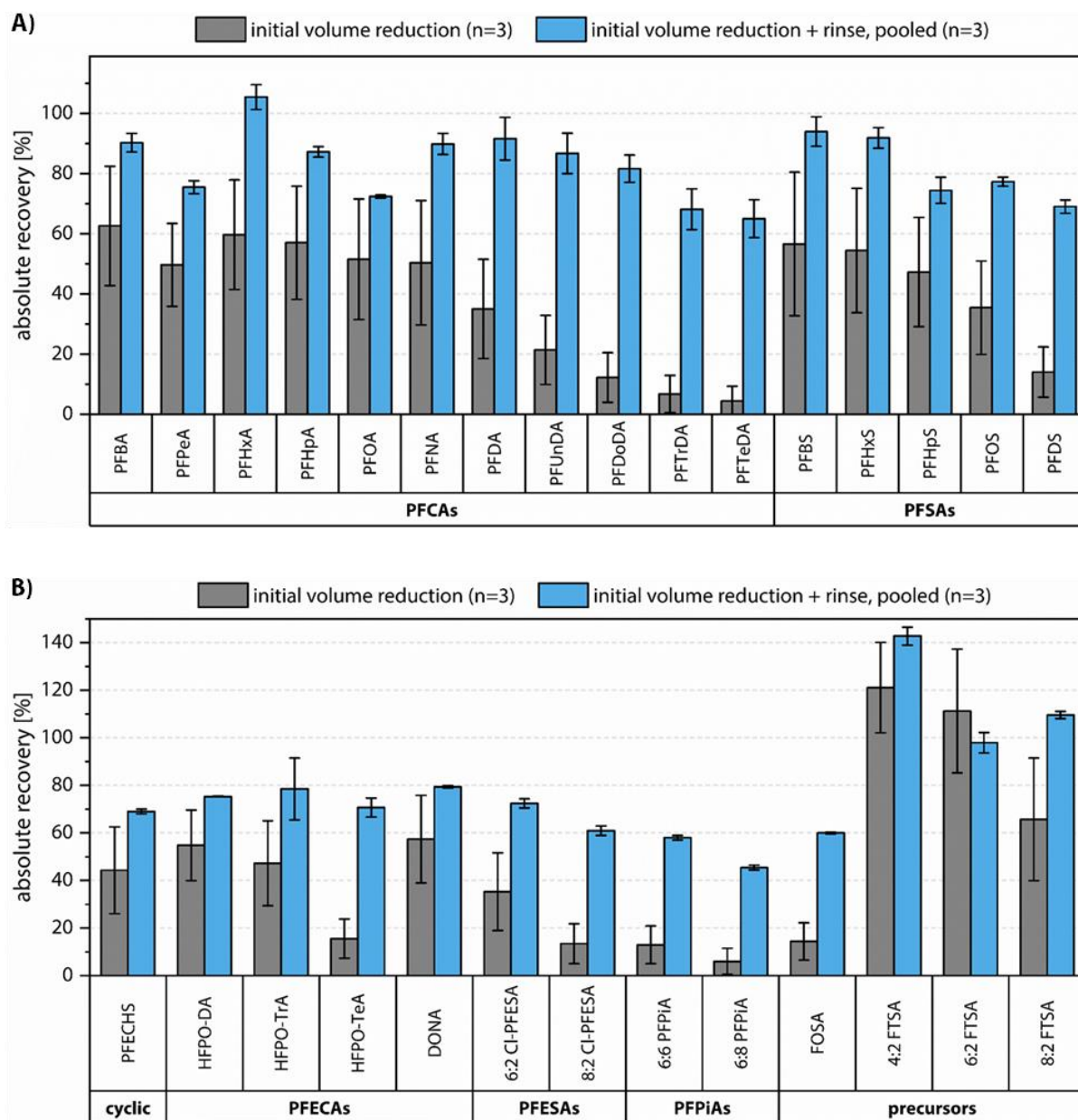
During the optimization of the sample preparation for aqueous matrices, it was shown that the transfer of the sample from the glass vessel used in the nitrogen evaporator to the LC vial was not quantitative and caused losses of all analytes (10–20 %) (Chapter 4.4.2). A possible explanation was

the adsorption of matrix components and target analytes to the glass vessels when evaporating the solvent. As seawater, marine sediment is a complex matrix, containing sea salt and organic matter that can interfere with the analysis. Consequently, the volume reduction step and the subsequent sample transfer had to be tested for sediments as well.

Although a sample clean-up using SPE had been performed after sample extraction, matrix precipitation was observed for most of the sediment samples during volume reduction when doing the first tests. As precipitate can block components of the LC-MS/MS system, a microfiltration step was included. After reducing the sample in volume to 1 mL under nitrogen, it was passed through a syringe filter (Spartan Whatman, pore size 0.2 μm , diameter 13 mm, GE Healthcare, USA) before the sample was further concentrated.

As for the water samples, different ways of volume reduction and sample transfer were tested, based on a North Sea sediment sample spiked with 3 ng of each target analyte. Firstly, the sample volume was reduced to 150 μL using the nitrogen evaporator in glass vessels, transferred to the polypropylene measurement vial and 10 μL injection standard $^{13}\text{C}_8$ -PFOA (100 $\text{pg}/\mu\text{L}$ solution) and 40 μL water were added. As a second option, the glass vessels were rinsed with 3 mL methanol after the sample transfer, the rinse was reduced to 150 μL and pooled with the sample before 20 μL injection standard $^{13}\text{C}_8$ -PFOA (100 $\text{pg}/\mu\text{L}$ solution) and 80 μL water were added. The absolute recoveries of the target analytes resulting from the two ways of volume reduction are given in Figure 4.6-1.

The results show that the rinsing step improved absolute recoveries of all target analytes by 21 % to 69 %, in particular of the long-chain PFASs. In addition, the repeatability of the method improved, with a mean standard deviation of (3 ± 3) % with rinsing in contrast to (16 ± 8) % without rinsing. As for the water samples, a possible explanation is that matrix components and target analytes adsorb to the glass vessels and can be removed by the rinsing step. Moreover, the dilution of the sample because of the rinse had a positive effect on matrix precipitate in the sample. Consequently, the rinsing step was included in the final method.



4.6.2 Extraction efficiency

To test the extraction efficiency of the method, an aliquot of 5 g of a freeze-dried Baltic Sea sediment sample was sequentially extracted four times. Each ultrasound-assisted extraction step consisted of an acetic acid wash (30 mL of a 1 % acetic acid in water solution) and an acetic methanol extraction (7.5 mL of a mixture of methanol and 1 % acetic acid in water (90:10, v/v)) (Figure 4.6-3). The four extracts of approximately 37.5 mL each were analysed separately. Figure 4.6-2 shows the percentage to which each extraction contributes to the total peak area of detected target analytes.

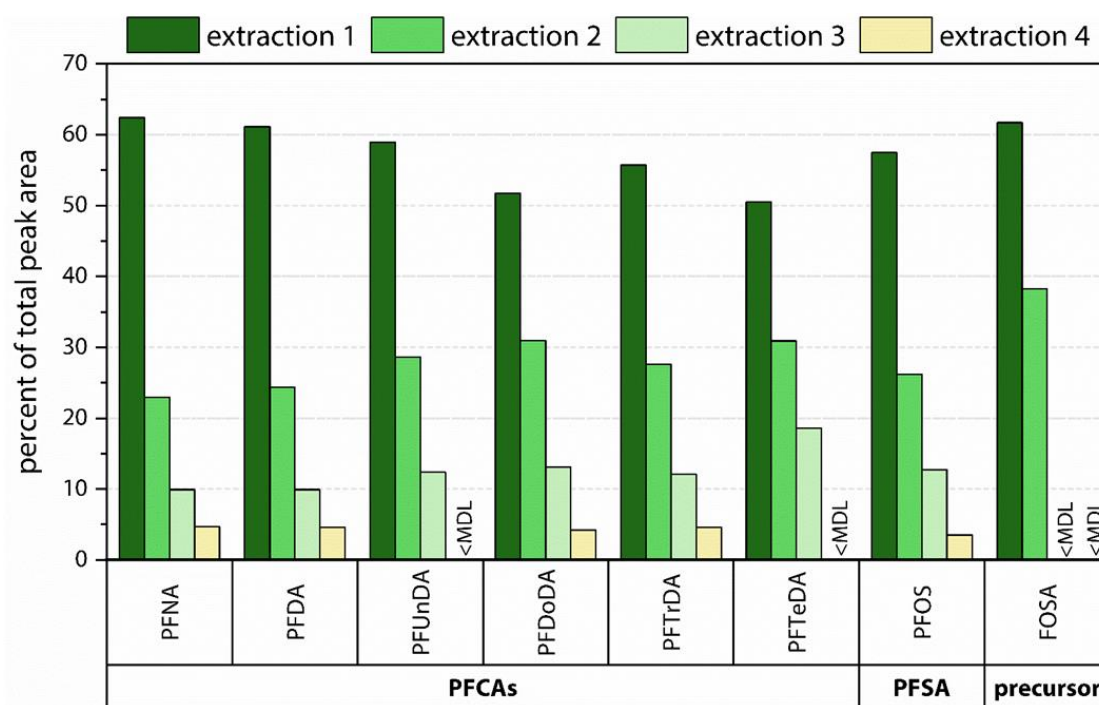


Figure 4.6-2: Sequential extraction profile of a Baltic Sea sediment sample. For detected target analytes, the percentage of the total peak area is given for each extraction. No recovery-correction was applied. The sample contained approximately 0.010 ng/g dw (PFTeDA) to 0.080 ng/g dw (L-PFOS) of the target analytes.

The sequential extraction experiment indicated that three extractions were necessary to extract the major part of the compounds. This is also the number of extractions performed by Yan *et al.* [246]. The fourth extract contributed to the total peak area of detected target analytes by < 5 %. Consequently, three extractions per sample were included in the final method.

4.6.3 Final method

An overview of the final method for the analysis of PFASs in sediment samples is given in Figure 4.6-3. Details on the individual steps including the sampling procedure are provided in Chapters 10.3 and 10.6.

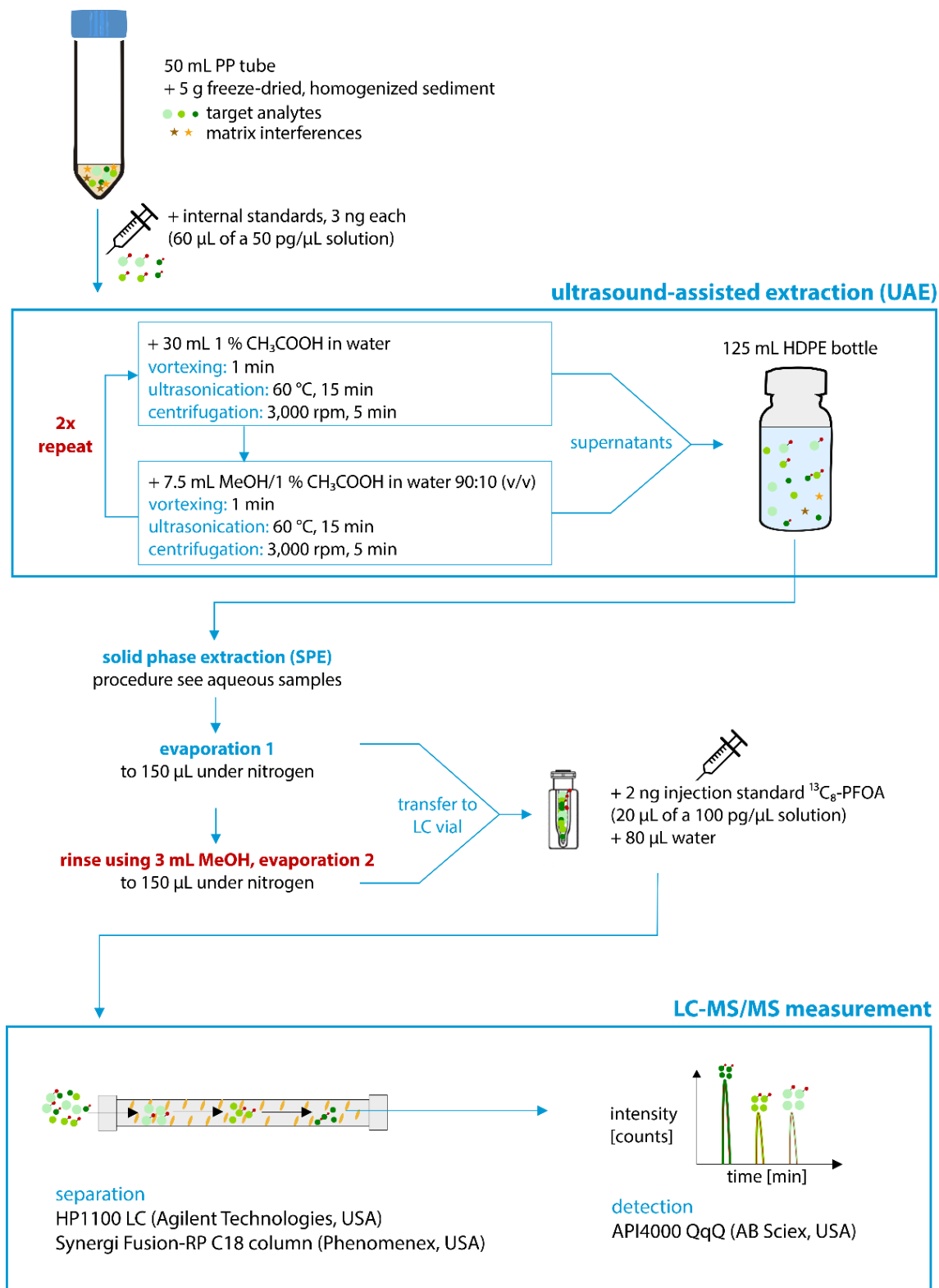


Figure 4.6-3: Final method for the analysis of PFASs in sediments and steps added in course of the method optimization (red). The initial method was based on the methanol- and acetic acid-based extraction method by [240] and adapted to a larger sample amount as described by [246].

4.7 Validation of the overall method for sediments

4.7.1 Matrix spike recovery tests

As for the aqueous matrices, matrix recovery tests were performed for marine sediments. 5 g of a freeze-dried North Sea sample was spiked with an amount of 3 ng absolute of each target analyte and internal standard. Triplicate samples were analysed using the optimized sample preparation method and relative recoveries were determined.

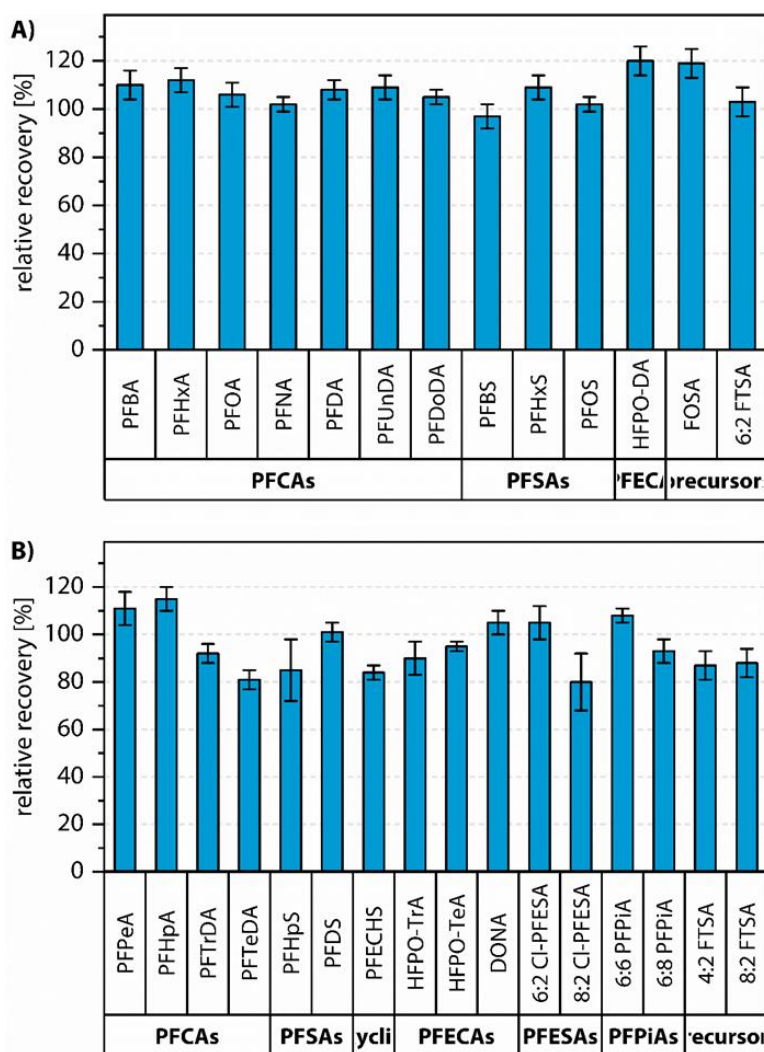


Figure 4.7-1: Relative recoveries (mean±SD) for A) target analytes with corresponding internal standard and B) target analytes without corresponding internal standard, resulting from matrix spike recovery tests for marine sediments ($n = 3$, spiking level 0.6 ng/g dw).

As shown in Figure 4.7-1A, relative recoveries for target analytes corrected by isotopically-labelled analogues varied between $(97 \pm 5) \%$ for PFBS and $(120 \pm 6) \%$ for HFPO-DA at a spiking level of 0.6 ng/g dw. For target analytes without corresponding isotopically labelled standards, relative recoveries were between $(80 \pm 12) \%$ for 8:2 Cl-PFESA and $(115 \pm 6) \%$ for 8:2 FTSA. As discussed for aqueous matrices in Chapter 4.5.1, these are acceptable values for ultratrace analysis. This underlines the suitability of the developed method for the chosen purpose.

4.7.2 Blanks, method detection limits and method quantification limits

Purified sea sand (Merck, Germany), baked at 450 °C, was used as laboratory blank for sediment analysis and analysed with every batch of seven samples. As for the water samples, particular compounds were quantified in the blanks in the low pg/g dw range (PFBA, C₆ to C₉ PFCAs and 6:2 FTSA; Table 4.7-1). All results were blank-corrected by subtracting the average PFAS concentration in the blanks from the concentrations in the samples. For compounds present in the blanks, method detection limits (MDLs) and method quantification limits (MQLs) were calculated as the mean blank values plus 3 or 10 times the standard deviation, respectively. For PFASs other than that, the MDLs and MQLs were derived from a signal-to-noise ratio of 3 or 10, observed in low-level samples or spiked matrices. All sediment samples were stored at -20 °C after the different sampling campaigns and processed in the same laboratory at HZG. Consequently, in contrast to the water samples, no campaign-specific MDLs and MQLs were calculated. For most of the target analytes, MDLs ranged from 0.0019 ng/g dw (6:2 Cl-PFESA) to 0.067 ng/g dw (PFOA) (Table 4.7-1). This shows that the method is generally capable of detecting PFASs in the marine environment with expected concentrations in the pg/g dw range. Higher MDLs were observed for HFPO-TrA (0.10 ng/g dw), HFPO-TeA (0.15 ng/g dw) and 6:2 FTSA (0.13 ng/g dw).

Table 4.7-1: Mean concentration of PFASs in laboratory blanks \pm standard deviation (SD) and method detection limits (MDLs) and method quantification limits (MQLs) for the determination of PFASs in sediments.¹

	mean concentration in laboratory blank \pm SD ($n = 6$) [ng/g dw]	MDL [ng/g dw]	MQL [ng/g dw]
PFBA	0.019 \pm 0.004	0.029	0.054
PFPeA	nd	0.0064	0.021
PFHxA	0.014 \pm 0.008	0.037	0.090
PFHpA	0.0065 \pm 0.0015	0.011	0.022
PFOA	0.055 \pm 0.004	0.067	0.095
PFNA	0.012 \pm 0.001	0.015	0.023
PFDA	nd	0.0033	0.011
PFUnDA	nd	0.0028	0.0094
PFDoDA	nd	0.0033	0.011
PFTrDA	nd	0.0028	0.0094
PFTeDA	nd	0.0032	0.011
PFBS	nd	0.011	0.037
PFHxS	nd	0.036	0.12
PFHpS	nd	0.064	0.21
L-PFOS	nd	0.012	0.040
Br-PFOS	nd	0.0093	0.031
PFDS	nd	0.056	0.19
PFECBS	nd	0.042	0.14
HFPO-DA	nd	0.0049	0.016
HFPO-TrA	nd	0.10	0.34
HFPO-TeA	nd	0.15	0.49
DONA	nd	0.0046	0.015
6:2 Cl-PFESA	nd	0.0019	0.0065
8:2 Cl-PFESA	nd	0.0075	0.025
6:6 PFPiA	nd	0.0031	0.010
6:8 PFPiA	nd	0.0039	0.013
L-FOSA	nd	0.0027	0.0091
Br-FOSA	nd	0.0026	0.0086
4:2 FTSA	nd	0.066	0.22
6:2 FTSA	0.053 \pm 0.024	0.13	0.30
8:2 FTSA	nd	0.054	0.18

¹ For compounds present in blanks, MDLs and MQLs were calculated as the average blank value plus 3 or 10 times the standard deviation, respectively (blue). For PFASs other than these, the MDLs and MQLs were derived from a signal-to-noise ratio of 3 or 10, respectively, observed in low-level samples (green) or spiked matrix samples (yellow).

4.7.3 Method precision

To determine the overall method's precision, six aliquots of a freeze-dried Baltic Sea sediment sample were analysed using the optimized analytical method. For target analytes > MQL, the coefficient of variation was calculated (Figure 4.7-2).

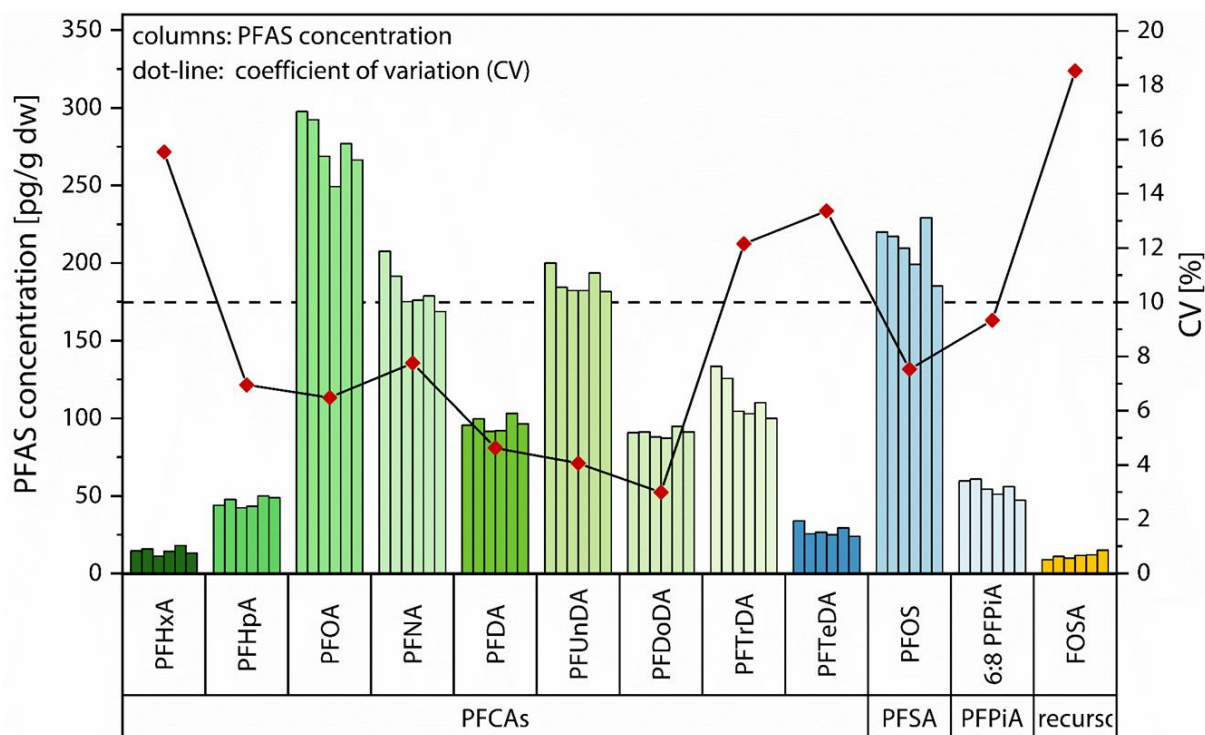


Figure 4.7-2: Method precision for sediment analysis. Concentrations of PFASs > MQL determined in a six-fold analysis and the coefficient of variation (CV) are given. The PFAS concentrations are not blank-corrected.

The results in Figure 4.7-2 show that coefficients of variation for the overall method ranged between 3.0 % (PFDoDA) and 19 % (FOSA), covering a similar range to that observed for the seawater (2.4 % to 18 %, Chapter 4.5.3). For most of the quantified target analytes, the coefficient of variation was < 10 %, which is a good value for analyte concentrations in the ppq to ppt range determined in a complex matrix [233]. An exception was PFTTrDA, having a coefficient of variation of 12 %. In addition, the coefficients of variation increased to 12–19 % for compounds present in concentrations which were close to the MQL (PFHxA, PFTeDA, FOSA). However, coefficients of variation < 20 % are still acceptable for ultratrace analysis in complex matrices [233].

4.8 Summary and conclusion

A quantitative multi-method for the determination of 29 PFASs from eight structural classes in aqueous matrices and sediment was developed and validated. It included eleven PFCAs, five PFSAAs and four precursors as well as nine emerging PFASs from different classes, among them six ether-based PFASs, two PFPiAs and the cyclic compound PFECHS.

During development of the instrumental method, a major improvement was achieved by using a mobile phase composition of 2 mM NH₄OAc in water as eluent A and 0.05 % CH₃COOH in methanol as eluent B. Compared to the tested commonly used eluents, this composition resulted in a signal enhancement by a factor of approximately 1.5 for all target analytes. In combination with an adjustment of the injection solvent to the eluents' starting gradient by using methanol:water 80:20 (v/v) instead of pure methanol, this also resulted in an acceptable peak shape for the early eluting compound PFBA, which had been distorted before.

When starting the optimization of the sample preparation for aqueous matrices, absolute recoveries of long-chain PFASs were generally 20 % to 30 % lower for seawater samples than for river water samples. Probably related to the high amount of dissolved salts in seawater samples, recoveries were considerably increased by using a washing volume of 15 mL water:methanol 80:20 (v/v) instead of 4 mL during the SPE procedure. For both the aqueous matrices and sediment, the sample transfer from the glass vessel used for volume reduction after SPE to the LC vial was identified as critical step, as it caused losses of all analytes. This may be attributed to adsorption of the analytes to the walls of the glass vessel because losses were reduced by the use of ultrasound before the sample transfer, or respectively a rinsing step, which was added to the final method.

Matrix spike recovery tests revealed acceptable relative recovery rates between 70 % and 115 % for most target analytes in all matrices. An exception were the long-chain PFCAs PFTrDA and PFTeDA, as well as 6:8 PFPiA and 4:2 FTSA, having relative recoveries below 70 % in aqueous matrices. The results for these compounds must be considered semiquantitative in seawater and river water samples as they are most likely underestimated.

MDLs for most of the target analytes ranged from 0.0019 ng/g dw to 0.067 ng/g dw in sediment samples and 0.0022 ng/L to 0.050 ng/L in 1 L aqueous samples. For 18 compounds, the MDL was below 0.020 ng/L for seawater samples from the *Polarstern* cruise. This shows that the method is generally capable of detecting PFASs in the marine environment with expected concentrations in the pg/g range, or respectively pg/L range. Higher MDLs for all kind of samples were observed for 6:2 FTSA due to a comparatively high concentration in the blank samples and for HFPO-TeA due to a high instrumental noise. Probably due to a shipborne contamination, high concentrations of PFBA were present in blank samples from the *Polarstern* cruise, strongly varying between different SPE batches. This underlines the importance of campaign- and batch-specific blank

samples in addition to the measures which have to be taken to avoid PFAS contamination throughout the process.

The linear range of the instrumental method was compound-dependent, spanning five orders of magnitude for several long-chain PFASs and one order of magnitude less for short-chain PFCAs and the ether-based replacements HFPO-DA and DONA. This has to be considered when preparing calibration curves and analysing environmental samples. The precision of the instrumental measurement and the overall method were acceptable with coefficients of variation ranging from 1.4 % to 5.1 % for the instrumental measurement and 2.4 % to 19 % for the overall method. To verify the trueness of the method for aqueous matrices, the certified reference material IRMM-428 was analysed. $|\bar{z}\text{-scores}|$ were satisfactory with values < 2 .

In consideration of the discussed drawbacks for individual substances, the developed method is suitable for a selective, precise, accurate and robust measurement of PFASs in river water, seawater and sediment samples within the environmental concentration range.

5. Emerging Per- and Polyfluoroalkyl Substances in Surface Water and Sediment of the North and Baltic Seas

The first field study of the PhD project aimed at investigating whether emerging PFASs are of relevance as pollutants in European coastal environments and if there has been a transition from legacy long-chain PFCAs and PFSAAs to replacement compounds. For this, 92 surface water and 24 surface sediment samples were collected in the North and Baltic Seas. Using the institute's research vessel *Ludwig Prandtl*, the North Sea sampling campaign was organized and performed within the scope of this PhD, whereas Christina Apel took the lead for the Baltic Sea campaign. Additional samples were collected by Tristan Zimmermann from the department of marine bioanalytical chemistry during a *Maria S. Merian* cruise (Chapter 5.1).

The North Sea is a North Atlantic shelf sea that connects to the Baltic Sea via the Skagerrak, the Kattegat and the Danish Straits. It is characterized by a constant exchange of water from and to the open sea [247]. In contrast, the semi-enclosed brackish Baltic Sea only has a limited exchange with open water and water residence times of approximately 30 years [248]. The catchment areas of the North and Baltic Seas are inhabited by approximately 184 [247] and 85 million people [248], respectively. Both seas are surrounded by highly industrialized countries, which include large river catchments, such as the Oder and Elbe Rivers in the study area [248].

By means of the developed analytical methods (Chapter 4), the samples were analysed for 29 PFASs. More specifically, the objectives of the study were i) to investigate the compounds' occurrence and composition profiles as well as their spatial distribution and potential sources, ii) to examine the partitioning behaviour of PFASs between sediment and water based on field-based partitioning coefficients, and iii) to reanalyse water sample extracts from the last decade to elucidate as to whether there has been a shift to emerging PFASs over time.

The study was published in the peer-reviewed journal *Science of the Total Environment* in 2019 (volume 686, pages 360–369). Details on the publication and presentations on conferences are given in Chapter 11.

5.1 Sample collection

Surface water and sediment samples in coastal areas of the German Bight and the German Baltic Sea were collected during two sampling campaigns with the research vessel *Ludwig Prandtl* in June and September 2017. Additional sediment samples were taken during the *Maria S. Merian* cruise MSM50 in January 2016, covering not only coastal areas, but also open water regions of the North Sea, the Skagerrak and Kattegat as well as the Baltic Sea (Figure 5.1-1).

Water samples were collected in 1 L polypropylene bottles 0.5 m below the surface, stored at 4 °C and processed in the lab within four weeks after sampling. Before sampling, the PP bottles were rinsed with methanol and water from the respective sampling site. Sediment samples were taken by a stainless-steel box corer or van Veen grabs. More information on the sampling procedure is given in Chapter 10.3.

After homogenization and removal of large pieces, such as sea shells and stones, sediment samples were transferred to aluminium shells and stored at –20 °C until sample preparation. Aluminium shells were cleaned with acetone and baked at 250 °C before usage. Water temperature, salinity and pH were measured continuously by the *in situ* FerryBox system during the cruises [249]. The coordinates of the sampling locations and the physicochemical parameters are provided in Table A.1-1.

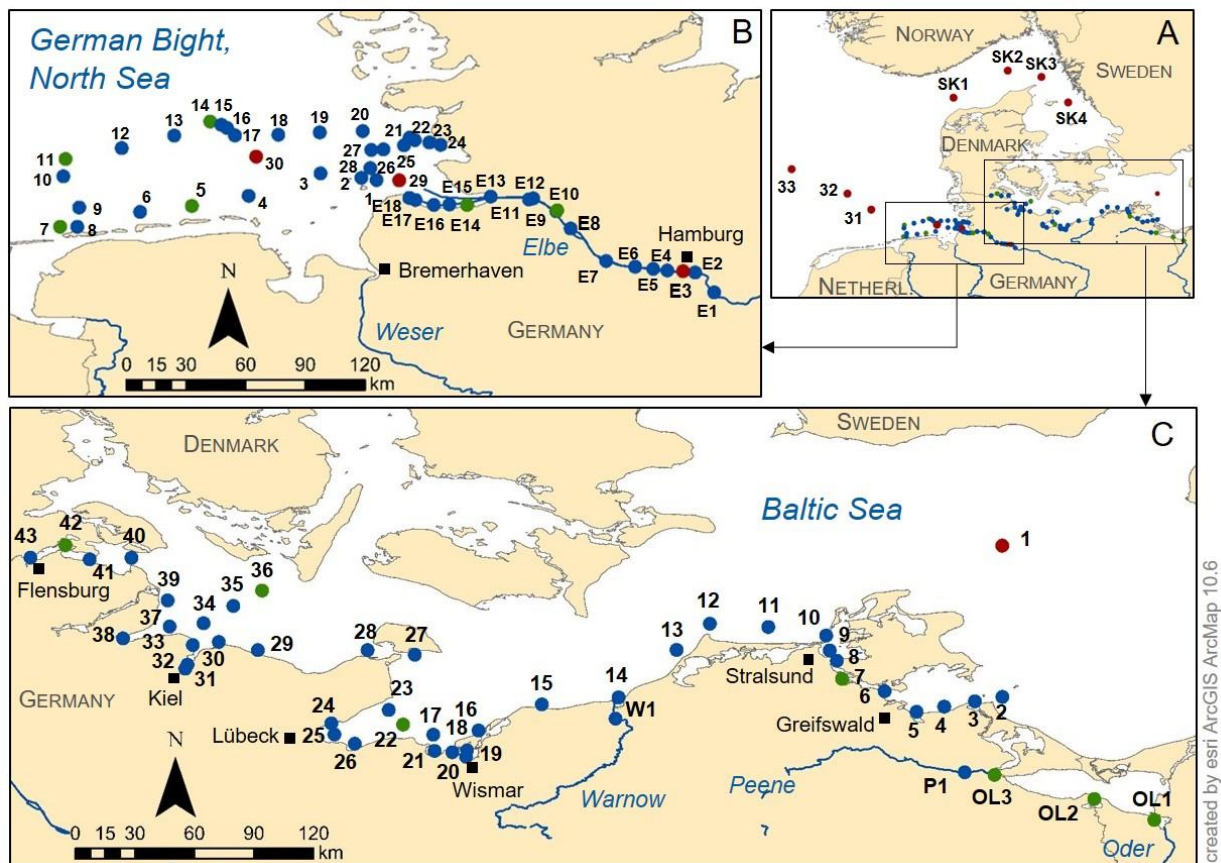


Figure 5.1-1: Sampling locations A) over the entire study area, including Skagerrak and Kattegat (SK1–SK4) and open water regions of the North Sea (31–33), B) in coastal areas of the German Bight (1–30) including the Elbe River (E1–E18), C) in coastal areas of the German Baltic Sea (1–43) including the Oder Lagoon (OL1–OL3) and the Peene and Warnow Rivers (P1 and W1). Water was collected at blue stations; water and sediment at green stations; and sediment only at red stations.

5.2 Materials and methods

5.2.1 Sample preparation and instrumental analysis

Water samples were filtered through glass microfiber filters (Whatman, grade GF/F, pore size 0.7 μm , diameter 47 mm, GE Healthcare, USA), which had been heated at 450 °C over night. Wet sediment was freeze-dried prior to sample extraction (Gamma 1-16 LSCplus, Christ, Germany). Afterwards, small stones and sticks were removed with forceps and the samples were homogenized using an agate mortar and pestle. To determine the total organic carbon (TOC) content, separate sub-samples were dried to constant weight at 40 °C and analysed using a RC612 multiphase carbon/hydrogen/moisture determinator (LECO, USA) (Chapter 10.4.2). The TOC content of the analysed samples ranged between 0.01 % and 6.13 % (Table A.1-2).

Based on the methods developed in Chapter 4, the water and sediment samples were analysed for 29 PFASs. A brief overview of the procedure is given in Chapters 10.5 and 10.6, whereas details on the instrumental method are provided in Chapter 10.2.

In addition to the samples taken for this study in 2017, water sample extracts and blanks from 2007, 2011 and 2014 were reanalysed using the current instrumental method. The extracts had been stored in vials at -20 °C, beginning from the first analysis onward. Before instrumental analysis, the vials were put into an ultrasonic bath for 30 min and vortexed for 5 min.

5.2.2 Quality assurance and quality control

As discussed in conjunction with the method validation (Chapters 4.5.2 and 4.7.2), different blank samples were processed. For samples from this study, no PFASs were detected in the instrumental blanks, whereas particular compounds were quantified in the laboratory blanks in the pg/L and pg/g dw range, respectively (Table A.1-3). In the field blanks, the same PFASs as in the laboratory blanks were quantified at comparable levels. This indicates that PFASs were not introduced into the blank samples during the sampling process and transportation, but by sample preparation in the laboratory. All results were blank-corrected by subtracting the average PFAS concentration in the laboratory blanks from the concentrations in the samples. MQLs were in a range of 0.0069 to 0.48 ng/L for seawater and 0.0065 to 0.49 ng/g dw for sediment. Average absolute recoveries of the internal standards in the samples are provided in Table A.1-4. Replicate samples showed standard deviations of < 20 % for the single compounds in seawater triplicates ($n = 7$) and sediment duplicates ($n = 3$) (Table A.1-5).

The results of the reanalysed sample extracts cannot be determined quantitatively, because it is not known how the long storage period affects the target analytes and internal standards. However, peak area ratios were used for indications of trends.

5.2.3 Data analysis

Sediment-water partitioning coefficients (K_D) [L/kg dw] were calculated by dividing the concentration of a compound in sediment [ng/kg dw] by the concentration of this compound in water [ng/L], given that the substance was detected in both the sediment and water phase of a sampling location. Organic carbon normalized sediment-water partitioning coefficients were derived from the equation $K_{OC} = K_D \cdot 100 / \text{TOC}$ where TOC is the content of total organic carbon [%]. Statistical methods that were applied to data from all studies are explained in Chapter 10.8.

5.3 Results and discussion

5.3.1 PFAS concentrations and composition patterns in surface water

Of the 29 analysed PFASs, 15 were detected in surface water from coastal areas of the German Bight and the Baltic Sea: the replacement compound HFPO-DA, the cyclic substance PFECHS, C_4 to C_{11} PFCAs, PFBS, PFHxS, L-PFOS/Br-PFOS as well as the precursors 6:2 FTSA and L-FOSA/Br-FOSA (Figure 5.3-1). Detection frequency, concentration range, mean and median of these compounds in the different sampling areas are shown in Table A.1-6. Concentrations of individual PFASs at all sampling sites are given in Table A.1-9 to Table A.1-14.

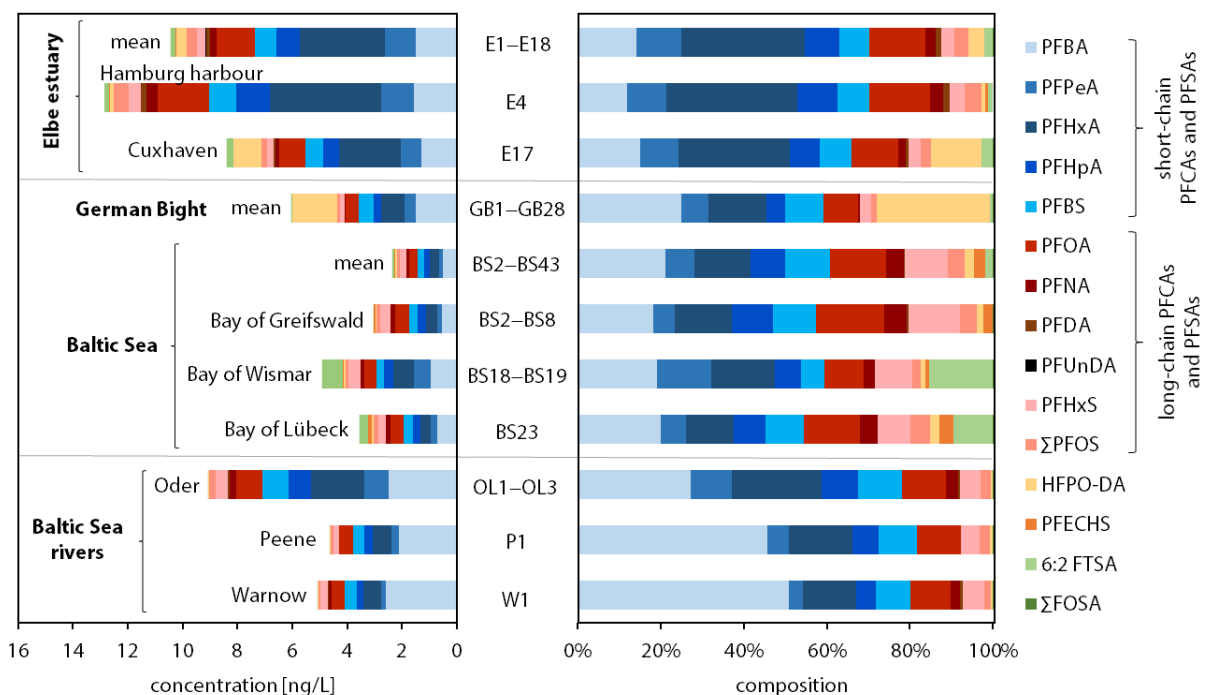


Figure 5.3-1: Concentrations [ng/L] and composition profiles of individual PFASs over the entire study area. Short-chain PFCAs and PFASs are shown in blue; long-chain PFCAs and PFASs in red; emerging PFASs in yellow; and precursors in green.

The sum of PFASs ranged from 4.7 to 7.4 ng/L in the German Bight (mean 6.0 ng/L), whereas in the Baltic Sea, concentrations were two to three times lower, ranging from 1.6 to 5.2 ng/L (mean

2.3 ng/L). The replacement compound HFPO-DA was detected in all seawater samples along the German coastline. With a mean concentration of (1.6 ± 0.3) ng/L, it contributed to the total PFAS concentration (Σ PFASs) by (27 ± 5) % in the German Bight and was the compound with the highest proportion. In contrast, the proportion of HFPO-DA was negligible in the Baltic Sea. In addition to HFPO-DA, the emerging cyclic compound PFECHS was detected in 86 % of the seawater samples from the Baltic Sea, whereas it was below the detection limit in all samples from the North Sea. The short-chain compounds PFBA, PFPeA, PFHxA, PFHpA and PFBS accounted for the sum of PFASs with about 60 % and had comparable proportions in both seas. On the contrary, the long-chain compounds PFOA, PFNA, PFHxS and Σ PFOS had a significantly higher proportion in the Baltic Sea than in the German Bight ((32 ± 4) % versus (13 ± 2) %). In both water bodies, L-PFOS and Br-PFOS contributed approximately equally to Σ PFOS. For the precursors 6:2 FTSA and L-FOSA/Br-FOSA, detection frequencies were below 30 %.

5.3.2 Spatial distribution of PFASs in surface water and potential sources

To explain the differences between the two seas and to find indications of sources, samples from river mouths were analysed and a correlation analysis was conducted to study relationships between individual PFASs and between PFASs and physicochemical parameters.

Concentrations of the replacement compound HFPO-DA in the Elbe estuary increased towards the German Bight and showed a statistically significant positive correlation with the salt content ($r = 0.99$, $p < 0.0001$; see Table A.1-17). Because fresh water from the Elbe River mixes with seawater moving in from the North Sea, salinity in the Elbe water samples increased towards the sea (0.5 to 17.8 psu). Consequently, the positive correlation between HFPO-DA and salinity in the Elbe estuary indicates that HFPO-DA enters the estuary with seawater from the North Sea and that the Elbe River is not a relevant source for HFPO-DA in the North Sea. In the investigated area of the German Bight itself, HFPO-DA was distributed homogeneously. Previous studies identified a fluoropolymer production plant as a point source in the Rhine-Meuse delta, in which PFOA has been replaced by HFPO-DA in fluoropolymer production since 2012 [100, 250]. River samples taken downstream from the chemical park showed HFPO-DA concentrations up to 812 ng/L in 2016 [174], which is about 2,000 times higher than the mean concentration in the Elbe estuary in this study (0.40 ng/L). It can be hypothesized that HFPO-DA is transported from the Rhine River to the Dutch North Sea water and from there to the German Bight by the easterly coastal current.

A positive correlation between HFPO-DA and salinity was also observed in the Baltic Sea ($r = 0.57$, $p < 0.0001$). In its westernmost region, the semi-enclosed Baltic Sea is connected to the North Sea via the Danish Straits, Kattegat and Skagerrak. Reflecting the growing influence of water inflow from the North Sea with a salinity of 35 psu in the Kattegat, salinity in the analysed samples from the brackish Baltic Sea increased from east (7.5 psu) to west (18.0 psu). Thus, the positive

correlation between HFPO-DA and salinity indicates that the water inflow from the North Sea can be a relevant source for HFPO-DA in the Baltic Sea. Interestingly, HFPO-DA was the only compound positively correlated with salinity in the Baltic Sea (Table A.1-18).

The occurrence of PFECHS in the European coastal environment has not yet been reported. The compound has already been identified in the North American Great Lakes [147], in Canadian water bodies close to Ontario airport [251], in environmental samples from the area around Beijing airport in China [252], and in Chinese coastal areas [253]. Additionally, it was detected in the Devon ice cap in the High Arctic [254]. The authors mainly explained the occurrence of PFECHS with its usage as an erosion inhibitor in aircraft hydraulic fluids, but it was also pointed out that PFECHS can be present as an impurity in POSF-based products such as aqueous film forming foams (AFFFs) for fire fighting [254]. In this study, PFECHS was detected in one sample from the Elbe River (E4). It was taken in direct proximity to the Finkenwerder Airport and near the industrialized port of Hamburg, both considered potential sources. In addition, PFECHS was primarily detected in the eastern part of the coastline investigated (Baltic Sea samples BS2-BS32). In samples from the Oder Lagoon, as well as the Warnow and Peene Rivers, which are potential sources in this coastal area, PFECHS could not be identified. PFECHS showed a weak significant positive correlation to Br-PFOS ($r = 0.35, p = 0.022$) and L-PFOS ($r = 0.49, p = 0.0011$). A positive relationship could result from emissions of PFECHS present as an impurity in POSF-based products. However, PFECHS concentrations were in the same range as those of Σ PFOS, indicating that distinct emissions, for example from hydraulic fluids, can play a role as well.

In general, the semi-enclosed Baltic Sea is susceptible to accumulation of pollutants because of its limited water exchange with open waters, its shallowness and its large catchment area. As the residence time of water in the Baltic Sea is approximately 30 years, the system reacts more slowly to changes in source patterns than other water bodies [248]. This may explain the significantly higher proportion of long-chain PFCAs and PFSA in the investigated coastal areas of the Baltic Sea in comparison to the German Bight as well as in comparison to the inflowing Oder, Peene and Warnow Rivers. A higher proportion of long-chain compounds was also found in Baltic Sea water collected along the Scandinavian coastline in comparison to Swedish rivers [255]. In addition to river inflow, atmospheric deposition can be a relevant source of long-chain PFASs to the Baltic Sea [256]. Despite the long water residence times in the Baltic Sea, the sum of PFASs is two to three times lower than in coastal areas of the North Sea. This has also been described for samples taken in 2007 and 2016 [101, 102] and may be attributed to the continuous input of PFASs from the Rhine-Meuse delta to the North Sea related to point sources, whereas diffuse sources are dominant in the Baltic Sea region.

The riverine influences on PFCA and PFSA concentrations can be clearly seen in both study areas. In the Baltic Sea, the sum of PFASs and the proportion of short-chain compounds was significantly higher in the Bay of Greifswald (BS2-BS8), which is close to the Oder Lagoon, than in the western portion of the study area. In the other samples from the Baltic Sea (BS9-BS43), PFASs were homogeneously distributed, with exception of the three samples BS18, BS19 and BS23, taken in the Bay of Wismar and the Bay of Lübeck. In these samples, the precursor compound 6:2 FTSA was comparatively high in proportion (17 %, 12 % and 9 %, respectively). This observation suggests a local source in this area, such as the effluents of a wastewater treatment plant or the use of AFFFs, which typically contain 6:2 FTSA and related compounds as substitutes for PFOS.

In the German Bight, concentrations of PFCAs and PFSA generally decreased with increasing distance to the Elbe estuary and the coast, with exception of the short-chain compounds PFBS and PFBA as well as the replacement compound HFPO-DA. These differences were also reflected in Pearson correlations as all compounds showed significant positive correlations to each other ($r > 0.67$, $p < 0.05$) and significant negative relationships with salinity ($r < -0.74$, $p < 0.05$), with exception of PFBS, PFBA and HFPO-DA (Table A.1-19). This points to different sources, such as the Rhine River, or to a different environmental behaviour, such as the higher mobility of short-chain homologues, of these three compounds.

5.3.3 PFAS concentrations and composition patterns in sediments

In surface sediment from coastal areas of the German Bight and the Baltic Sea as well as from the Kattegat and Skagerrak, 16 PFASs were detected: 6:6 and 6:8 PFPiAs, PFBA and C₆₋₁₄ PFCAs, PFHxS, L-PFOS/Br-PFOS, and the precursors 6:2 FTSA and L-FOSA/Br-FOSA (Figure 5.3-2). Detection frequency, concentration range, mean and median are shown in Table A.1-7 and Table A.1-8. Additionally, concentrations of individual PFASs at all sampling sites are given in Table A.1-15 and Table A.1-16.

The spatial variation of PFASs in sediment was more variable than for water samples with regard to concentration levels and composition. Over the entire study area, the sum of PFASs ranged from 0.018 ng/g dw to 2.6 ng/g dw (mean: 0.64 ng/g dw, median: 0.36 ng/g dw). As mean values were skewed by single samples with high concentrations, median values are used to describe central tendencies for sediment samples in the following. The median concentration of Σ PFASs in the German Bight was significantly lower than in the Skagerrak/Kattegat area and the Baltic Sea (0.12 ng/g dw versus 1.0 ng/g dw and 0.72 ng/g dw, respectively). However, the highest concentrations were determined for sample GB7 from the North Sea, taken close to the East Frisian island of Norderney, and sample E3, taken in the Elbe estuary at Hamburg Harbour.

Of the emerging PFASs, 6:6 and 6:8 PFPiAs were identified in coastal sediment for the first time. They were detected in 8 % and 25 % of the sediment samples, respectively. Concentrations of 6:6 PFPiA were between MDL and MQL, whereas 6:8 PFPiA was quantified in a range of 0.013 ng/g dw to 0.052 ng/g dw, contributing to the sum of PFASs with 1 % to 8 %.

Regarding PFCAs and PFSAs, L-PFOS was the dominant compound over the entire study area with a median concentration of 0.085 ng/g dw and a proportion of (20 ± 12) % of Σ PFASs. In contrast to L-PFOS, with a high detection frequency of 83 %, Br-PFOS was detected in only 17 % of the samples. In addition to L-PFOS, the long-chain C_9 to C_{14} PFCAs (67 % to 100 %) as well as the short-chain compound PFBA (67 %) were frequently detected. Due to comparatively high MDLs resulting from blanks, PFOA had a detection frequency of only 42 %. C_9 to C_{11} PFCAs and PFBA contributed to the sum of PFASs with 10 % to 17 % each. Of the precursors, L-FOSA and Br-FOSA were detected in 75 % and 63 % of the samples, accounting for the sum of PFASs with an average proportion of (6 ± 4) %. 6:2 FTSA was detected only in sample E3 from the Port of Hamburg with a concentration of 0.40 ng/g dw and a proportion of 18 %.

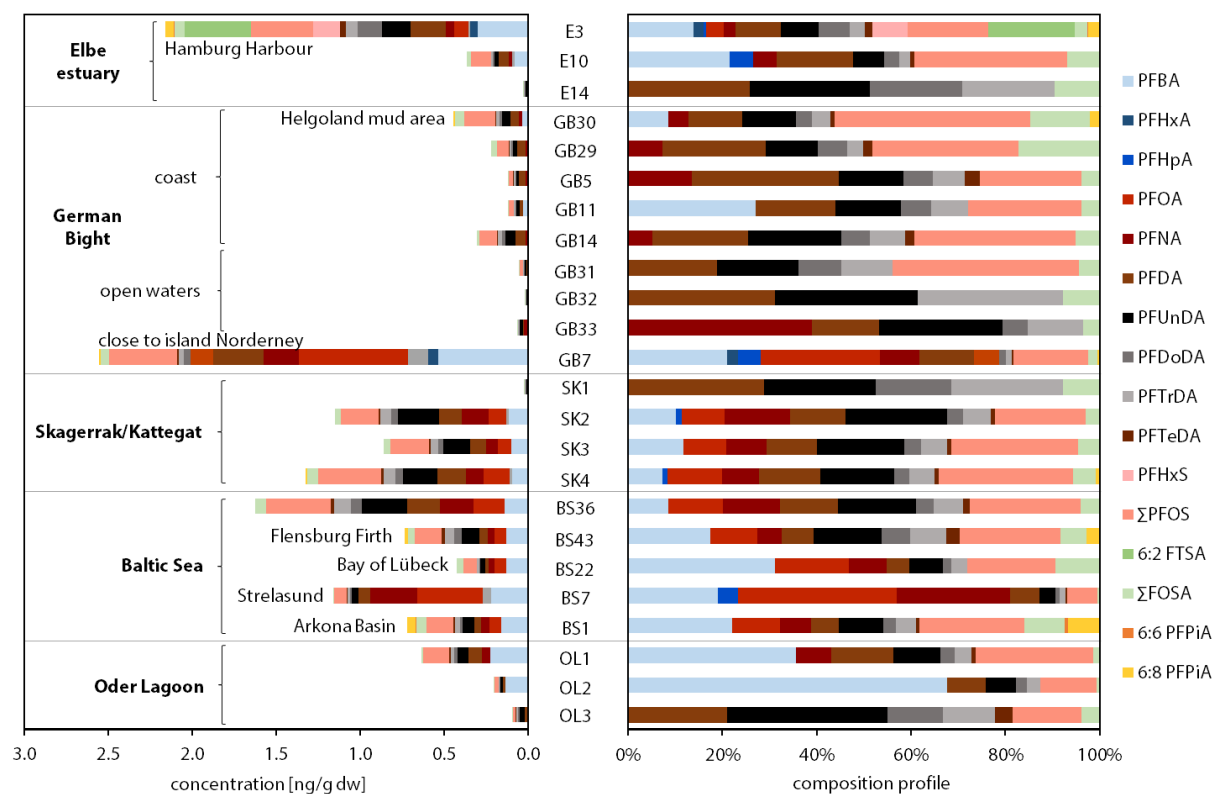


Figure 5.3-2: Concentrations [ng/g dw] and composition profiles of individual PFASs in surface sediment samples over the entire study area.

5.3.4 Spatial distribution of PFASs in sediments and potential sources

The emerging compounds 6:6 PFPiA and 6:8 PFPiA were identified mainly in areas with potential inputs from industrial sources, such as Hamburg Harbour (E3) and Flensburg Firth (BS43), as well

as in known sedimentation areas, such as the Skagerrak (SK4), the Helgoland mud area in the North Sea (GB30) and the Arkona Basin in the Baltic Sea (BS1). Although there has been an increasing interest in PFPiAs in recent years, PFPiAs have not yet been reported in the coastal or marine environment. In Germany, the use of pesticide formulations containing PFPiAs and perfluoroalkyl phosphonic acids (PFPA) as antifoaming agents, such as Fluowet PL80-B and Masurf FS-780, is still permitted in contrast to the United States [257, 258]. The use of these products on the German mainland might explain the occurrence of PFPiAs in different areas of the investigated coastlines. However, concentrations of PFPiAs were generally about an order of magnitude lower than those of L-PFOS. These lower concentrations might be explained by lower production volumes and releases, as well as degradation or biotransformation of PFPiAs, yielding to perfluoroalkyl phosphonic acids (PFPA) [146].

In addition to source-specific contributions, sediment characteristics can play an important role for the sorption of PFASs [259, 260]. This is reflected in the spatial distribution of PFCAs and PFSA in this study. Over the entire study area, correlation analysis showed no significant relationship between the TOC content and concentrations of individual PFASs with the exception of PFNA ($r = 0.70, p < 0.001$). Disregarding the four samples with the highest TOC contents (BS22, BS7, BS1 and E10; TOC 4.57 % to 6.13 %), concentrations of all PFCAs and PFSA showed a significant positive relationship to the TOC content ($r > 0.5, p < 0.05$). In particular, the long-chain compounds PFNA, PFUnDA, PFTrDA, L-PFOS and Σ PFASs were strongly correlated with TOC ($r > 0.7, p < 0.001$) (Table A.1-20). This is in accordance with the results from previous field studies in the coastal environment [114, 115]. In addition to TOC, sediment characteristics that were not considered in this study may play a role for PFAS sorption, especially for short-chain compounds and the four samples with the highest TOC contents. Potential factors include the black carbon content of the sediment, grain size, density, pH and metal ion concentrations [259-261].

Sediment samples from the German Bight were mostly sandy and their TOC contents were generally lower than those of the more muddy samples from the Baltic Sea and the Skagerrak-/Kattegat area. In addition, sediment processes in the North Sea are strongly influenced by tides and waves and there is a continuous redistribution with only a few depositional areas, such as the Helgoland mud area and the Skagerrak/Kattegat [262]. These differences in sediment characteristics and processes can serve as an explanation for the significantly lower Σ PFASs in sediment from the German Bight in comparison to samples from the Baltic Sea and Skagerrak/Kattegat. Showing the highest concentrations in this study, sample GB7, which was taken close to the East Frisian island of Norderney in the German Bight, was an exception (Σ PFASs: 2.6 ng/g dw). In contrast to other samples from the North Sea, PFHxA, PFHpA and PFOA were detected in this sample, pointing to a local source. Comparatively high concentrations (Σ PFASs: 2.2 ng/g dw) were also

found in sample E3 from the Elbe estuary, taken close to the Port of Hamburg in the Elbe River. It was the only sampling location where PFHxS and the precursor 6:2 FTSA were identified. Together with the presence of the precursors L-FOSA and Br-FOSA, this points to local inputs.

5.3.5 Partitioning of PFASs between sediment and water

The emerging PFASs identified in this study were detected either in the sediment phase or in the water phase. HFPO-DA was identified only in water samples while its predecessor PFOA occurred in both matrices. Lower sorption to sediment of HFPO-DA than of PFOA is supported by laboratory experiments showing that HFPO-DA is less adsorbable to powdered activated carbon than PFOA [136]. Additionally, modelling results by Gomis *et al.* [169] predicted a more hydrophilic behaviour of HFPO-DA than of PFOA, resulting from the smaller molecule size, which requires less energy for cavity formation among the strongly-bonded water molecules.

The cyclic compound PFECHS was also detected only in the water phase although having eight perfluorinated moieties like L-PFOS, which was one of the dominant compounds in sediment over the entire study area. In an airport-impacted ecosystem, in which concentrations of PFECHS in surface water were two to four orders of magnitude higher than in this study, PFECHS had a lower detection frequency in sediment samples as well [252]. The field-based sediment-water partitioning coefficients calculated by the authors of that study indicated a lower sorption affinity for solid environmental matrices of cyclic PFASs compared to linear and branched PFASs [252]. The lower hydrophobicity of cyclic PFASs in comparison to linear PFASs is underlined by the retention times on C₁₈ columns, which is lower for PFECHS (11.7 min in this study) than for L-PFOS (12.8 min).

The presence of 6:6 PFPiA and 6:8 PFPiA in sediment is consistent with laboratory sorption experiments, which indicated that PFPiAs would preferentially be retained by environmental solid phases, as their laboratory-derived partitioning coefficients are comparable to those of the long-chain compounds PFUnDA and PFDS [263].

For PFCAs, PFSA and FOSA, which were detected in both the sediment and water phase, sediment-water partitioning coefficients were calculated and compared to values from previous field studies (Table 5.3-1). To reduce the influence of sediment characteristics, the partitioning coefficients $\log K_D$ were normalized to organic carbon ($\log K_{OC}$).

For PFCAs, an increase of the $\log K_{OC}$ values with increasing number of perfluoroalkyl moieties could be observed from PFHpA to PFDA ($R^2 = 0.86$). This trend is consistent with previous field studies conducted in different areas [93, 117, 118] and a laboratory study by Higgins and Luthy [259] (Table 5.3-1). It can be explained by the increase of hydrophobicity with an increasing number of CF₂ units and underlines the importance of van der Waals interactions in PFAS sorption.

Despite its small number of perfluoroalkyl moieties, PFBA had a comparatively high $\log K_{OC}$ value (Figure 5.3-3). That the short-chain compounds PFBA and PFPeA do not follow the chain-length

dependent trend observed for PFCAs with a larger chain length was initially found in batch sorption experiments with soils [264] and was also reported in prior field studies [93, 118]. These findings indicate that mechanisms other than van der Waals interactions may play an important role for the water-sediment partitioning of short-chain compounds: for instance, ion exchange or the interaction with sorptive sites that are not available to larger molecules due to steric effects [264].

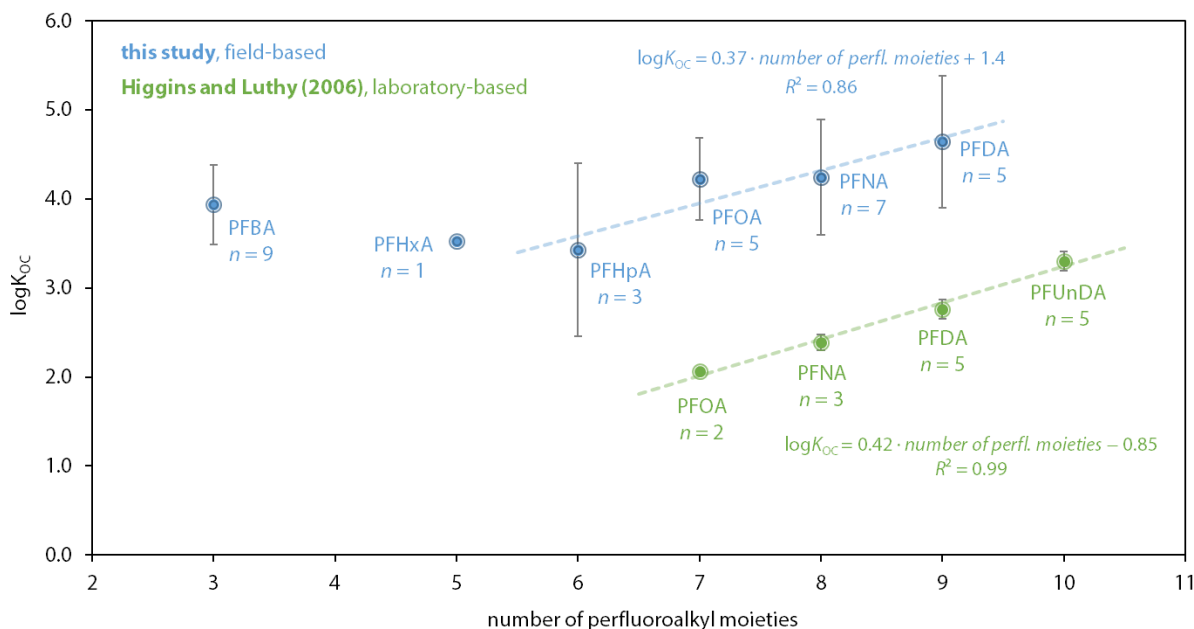


Figure 5.3-3: Sediment/water partitioning coefficients $\log K_{OC}$ for individual PFCAs in this study in comparison to a laboratory study by Higgins and Luthy [259]. Linear regression lines were calculated for PFCAs from PFHpA to PFDA (this study) and from PFOA to PFUnDA [259], respectively. n gives the number of sampling locations at which the compound was detected in both the sediment and water phase and for which partitioning coefficients were calculated.

For PFCAs, an increase of the $\log K_{OC}$ values with increasing number of perfluoroalkyl moieties was observed from PFHpA to PFDA ($R^2 = 0.86$, Figure 5.3-3). This trend is consistent with previous field studies conducted in different areas [93, 117, 118] and a laboratory study by Higgins and Luthy [259]. It can be explained by the increase of hydrophobicity with an increasing number of CF_2 units and underlines the importance of van der Waals interactions in PFAS sorption.

Despite its small number of perfluoroalkyl moieties, PFBA had a comparatively high $\log K_{OC}$ value (Figure 5.3-3). That the short-chain compounds PFBA and PFPeA do not follow the chain-length dependent trend observed for PFCAs with a larger chain length was initially found in batch sorption experiments with soils [264] and was also reported in prior field studies [93, 118]. These findings indicate that mechanisms other than van der Waals interactions may play an important role for the water-sediment partitioning of short-chain compounds: for instance, ion exchange or the interaction with sorptive sites that are not available to larger molecules due to steric effects [264].

Table 5.3-1: Sediment-water partitioning coefficients $\log K_D$ and $\log K_{OC}$ in this study (mean \pm SD) compared to values reported in previous field studies.

compound	n	this study		Baltic Proper (a)			coastal watersheds, China (b)		coastal area, Bangladesh (c)		Tokyo Bay, Japan (d)	
		$\log K_D$	$\log K_{OC}$	$\log K_D$	$\log K_D$	$\log K_{OC}$	$\log K_D$	$\log K_{OC}$	$\log K_D$	$\log K_{OC}$		
PFBA	9	2.2 \pm 0.5	3.9 \pm 0.4	-	1	3.2	2.63 \pm 0.39	4.68 \pm 0.52	-	-		
PFHxA	1	1.8	3.5	-	0.59	2.55	2.24 \pm 0.19	4.29 \pm 0.43	-	-		
PFHpA	3	2.0 \pm 0.7	3.4 \pm 1.0	2.63 \pm 0.01	0.45	2.33	2.25 \pm 0.51	4.32 \pm 0.58	-	-		
PFOA	5	2.8 \pm 0.3	4.2 \pm 0.5	2.49 \pm 0.01	0.63	2.68	1.63 \pm 0.44	4.02 \pm 0.54	0.04 \pm 0.3	1.9 \pm 0.1		
PFNA	7	2.6 \pm 0.6	4.2 \pm 0.6	3.25 \pm 0.01	1.03	3.07	2.01 \pm 0.35	4.35 \pm 0.34	0.6 \pm 0.1	2.4 \pm 0.1		
PFDA	5	2.6 \pm 0.6	4.6 \pm 0.7	3.95 \pm 0.01	1.6	3.59	2.03 \pm 0.49	4.36 \pm 0.55	1.8 \pm 0.1	3.6 \pm 0.1		
L-PFOS	13	3.1 \pm 0.6	5.2 \pm 0.7	2.94 \pm 0.03	1.7	3.75	2.87 \pm 0.47	5.11 \pm 0.60	2.1 \pm 0.1	3.8 \pm 0.1		
Br-PFOS	2	2.5	3.9	1.45 \pm 0.07	-	-	-	-	-	-		
L-FOSA	4	3.0 \pm 0.5	5.5 \pm 0.3	2.39 \pm 0.08	-	-	-	-	2.5 \pm 0.2	4.8 \pm 0.2		
Br-FOSA	2	2.9	4.4	2.33 \pm 0.01	-	-	--	-	-	-		

(a) Gebbink *et al.*, 2016 [163], $\log K_{OC}$ was not given; (b) Zhu *et al.*, 2014 [118]; (c) Habibullah-Al-Mamun *et al.*, 2016 [93]; (d) Ahrens *et al.*, 2010 [117].

Additionally, differences in the partitioning of isomers could be observed. Linear and branched PFOS were approximately equal in proportion in the water phase, whereas L-PFOS was the predominant isomer in sediment. This is reflected in the $\log K_{OC}$ value, which is approximately one log unit higher for L-PFOS (5.2) than for Br-PFOS (3.9). A similar trend was observed for L-FOSA and Br-FOSA (5.5 vs. 4.4). Higher sediment-water partitioning coefficients for the linear than for the branched isomers of PFOS and FOSA have also been reported for the Liao River Basin and Taihu Lake in China [265]. A possible explanation is the higher hydrophobicity of the linear isomers, reflected in the higher retention times using a reversed phase C_{18} column. Moreover, isomer-specific biotransformation of precursors might play a role in the differences between linear and branched isomers [266].

$\log K_{OC}$ values in the field studies discussed were generally higher than in laboratory studies. In this study, they were approximately two log units higher than in the laboratory study by Higgins and Luthy [259] (Figure 5.3-3). This variation can be attributed to the different experimental conditions. In contrast to laboratory experiments, an equilibrium between sediment and the overlying water column is rarely achieved in the dynamic coastal ecosystem. The water phase reacts faster to changes in source patterns, which include decreasing trends of long-chain PFASs over the last decade (discussed in the next section). The slower reaction of the sediment phase might explain higher $\log K_{OC}$ values of the long-chain PFCAs and PFSA in current field studies than in laboratory studies. Moreover, additional environmental factors and sediment characteristics that were not considered in this field study can influence the sediment-water partitioning process.

5.3.6 Temporal trends

In surface water from coastal areas of the German Bight, decreasing concentrations of the long-chain compound L-PFOS were observed, from a median concentration of 1.3 ng/L in 2007 [99] to 0.043 ng/L in 2017 (this study). For PFOA and the short-chain compound PFBS, a downward trend was observed as well (Table 5.3-2). It can be assumed that these decreasing trends in the German Bight are effects of the industrial transition that has been taking place in Europe since the 2000s, including the phase-out of long-chain PFCAs and PFSAs and the shift to replacement compounds such as HFPO-DA.

Table 5.3-2: Comparison of PFBS, L-PFOS and PFOA concentrations in this study to previous studies in the same investigation areas.

location	reference	year	PFBS	L-PFOS	PFOA
surface water			range (median) [ng/L]		
Ger. Bight	(a)	2007	3.4–18 (5.4)	0.69–4.0 (1.3)	2.7–7.8 (3.7)
	this study	2017	0.44–0.72 (0.53)	0.020–0.077 (0.043)	0.27–0.71 (0.51)
Baltic Sea	(b)	2007	0.26–0.88 (0.57)	<MDL–0.35 (0.23)	0.25–4.55 (1.30)
	this study	2017	0.15–0.43 (0.24)	<MQL–0.082 (0.040)	0.20–0.70 (0.27)
surface sediment			range (median) [ng/g dw]		
Ger. Bight	(c)	2004	<MQL	0.032–2.1 (0.14)*	0.079–1.6 (0.14)
	this study	2017	<MDL	<MDL–0.39 (0.029)	<MDL–0.65 (<MDL)
Baltic Sea	(c)	2004	<MQL	0.021–0.56 (0.27)*	0.061–0.68 (0.12)
	this study	2017	<MDL	0.074–0.38 (0.15)	<MQL–0.39 (0.073)

(a) Ahrens *et al.*, 2009 [99] - (b) Ahrens *et al.*, 2010 [101]- (c) Theobald *et al.*, 2012 [115]

* PFOS values that were reported in Theobald *et al.* [115] generally include a portion of 18 % branched isomers [104]. This was subtracted to obtain the values for L-PFOS given in the table.

When analytical standards became available, HFPO-DA was analysed for the first time in German Bight samples collected in 2014. In those samples, HFPO-DA had already been one of the dominant PFASs [100]. To investigate whether there has been a shift to HFPO-DA over time, stored sample extracts and blanks from 2007, 2011 and 2014 were reanalysed using the current instrumental method. All samples were taken in the German Bight, within the area of the East Frisian Islands, close to the coastline. The blanks and the sample extract from 2007 showed no peak for HFPO-DA, but the compound was detected in the sample extract from 2011. At that time, replacement compounds for long-chain PFCAs and PFSAs had not yet been in focus and analytical standards were not available. From 2011 to 2014, the peak area of HFPO-DA strongly increased in relation to the peak area of its predecessor PFOA, changing the peak area ratio from 0.1:1.0 in 2011 to 0.8:1.0 in 2014 and further to 1.1:1.0 in 2017 (this study) (Figure 5.3-4). This is consistent with the information that the fluoropolymer manufacturing plant in the Rhine-Meuse delta, which is assumed to be the major source of HFPO-DA in the German Bight, has replaced PFOA with HFPO-DA from 2012 onward [250].

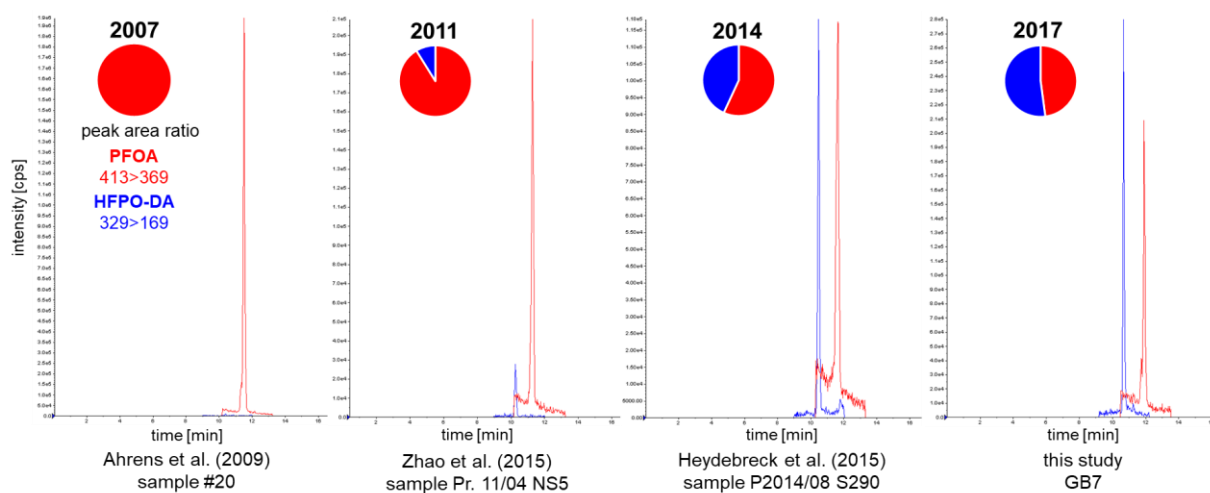


Figure 5.3-4: LC-MS/MS chromatograms of the replacement compound HFPO-DA and its predecessor PFOA and pie charts illustrating the ratio of the peak areas. Data resulted from the reanalysis of sample extracts taken in the area of the East Frisian Islands in the German Bight in 2007, 2011 and 2014, which were compared to a sample from this study, collected in 2017 in the same area.

In the investigated coastal areas of the Baltic Sea, the concentrations of L-PFOS, PFOA and PFBS in seawater also showed downward trends, but these were not as clear as in the German Bight (Table 5.3-2). A slower reaction of the Baltic Sea in comparison to the North Sea can be explained by the long residence times of water in the Baltic Sea and the dominance of diffuse sources with ongoing emissions. This is underlined by the results for the sediment samples. In the German Bight, median concentrations of L-PFOS decreased from 0.14 ng/g dw in 2004 [115] to 0.029 ng/g dw in 2017 (this study). As for the water samples, the trend was not as clear in the western Baltic Sea with a median value of 0.27 ng/g dw in 2004 and 0.15 ng/g dw in 2017.

5.4 Summary and conclusion

The spatial distribution and the partitioning of 29 PFASs was analysed in surface water and sediment from coastal areas of the North and Baltic Seas sampled in 2017. In North Sea surface water, concentrations of the ether-based replacement compound HFPO-DA were approximately three times higher than those of its predecessor PFOA. With a mean concentration of (1.6 ± 0.3) ng/L, it contributed to Σ PFASs by (27 ± 5) % and was the compound with the highest proportion in the North Sea, which is characterized by the influence of point sources and constant exchange with open water. Reanalysis of sample extracts from the last decade showed that HFPO-DA had already been present in 2011, when it had not yet been in focus. In the Baltic Sea with a limited water exchange and dominance of diffuse sources, the proportion of HFPO-DA was negligible, whereas long-chain PFCAs and PFASs still contributed to Σ PFASs with about 30 %. The emerging cyclic compound perfluoro-4-ethylcyclohexanesulfonate (PFECHS), which has not yet been reported in European coastal environments, was detected in 86 % of the Baltic Sea

samples. Influenced by sediment characteristics in addition to source-specific contributions, the spatial distribution of PFASs in surface sediments was more variable than for water samples. The linear isomer of the long-chain legacy substance PFOS was the predominant compound found over the entire study area. Of the emerging PFASs, 6:6 and 6:8 perfluoroalkyl phosphinic acids (PFPIAs) were identified close to potential industrial inputs and in sedimentation areas.

The occurrence of HFPO-DA in samples from times when fluorinated alternatives had not yet been under discussion shows the limitations of target analysis focussing on a predefined scope of well-known PFASs. Moreover, the detection of PFECHS and PFPIAs as “overlooked” PFASs that have already been in use for decades underlines the importance of new analytical approaches aimed at addressing the unknown pool of PFASs. These are further discussed and applied in Chapters 7 and 8.

The results of this study show that particular emerging PFASs play a relevant role in the investigated coastal environments and that a shift to replacements is dependent on sources and geographical conditions. The shift to the emerging substance HFPO-DA as one of the dominant PFASs in North Sea coastal water shows changes in pollution levels as a consequence of action taken by regulatory authorities and industry aiming to restrict long-chain PFASs. This demonstrates the necessity to further investigate this compound to provide a scientific basis for evaluation and potential future regulation. As one criterion for regulation under the Stockholm Convention, a potential long-range transport of the compound was investigated in the following study.

6. Transport of Legacy Perfluoroalkyl Substances and the Replacement Compound HFPO-DA through the Atlantic Gateway to the Arctic Ocean – Is the Arctic a Sink or a Source?

The shift to the replacement compound HFPO-DA as one of the dominant PFASs in North Sea coastal water (Chapter 5), raised the question if the substance is further transported to open seawater and remote areas such as the Arctic. Although modelling assessments indicated that HFPO-DA has a similar long-range transport potential compared to legacy PFASs such as PFOA [169], empirical evidence was still missing. It was undisputed in the scientific community that legacy long-chain PFCAs and PFSAAs undergo long-range transport. However, discussions on the proportion to which oceanic and atmospheric transport contribute to the long-range transport of PFCAs and PFSAAs were still ongoing [23, 86]. Moreover, there was a knowledge gap with regard to the occurrence and distribution of PFASs in deep ocean water, resulting in uncertainties in global PFAS mass balances and in discussions on the role of the deep ocean as ultimate PFAS sink (Chapter 2.4.4).

To acquire samples for the investigation of these topics, a proposal for supplemental use of the research icebreaker *Polarstern* was prepared in collaboration with Dr. Zhiyong Xie (N-2016-N-53). The proposal was approved for summer expedition PS114 in 2018, from Bremerhaven to Fram Strait, located between Svalbard and Greenland, and back to Tromsø in Norway.

As the Atlantic gateway to the Arctic Ocean, Fram Strait is an important region to investigate oceanic long-range transport of organic pollutants to the Arctic. In eastern Fram Strait, warm, saline Atlantic water enters the Arctic Ocean in the West Spitsbergen Current (WSC), whereas in western Fram Strait, cold, low-saline water and sea ice, as well as Atlantic Water that has spent significant time in the Arctic, exit the Arctic Ocean via the East Greenland Current (EGC). Fram Strait is the only deep connection between the Arctic Ocean and the remainder of global oceans and has the highest water volume fluxes both pole- and equatorward [267].

Surface water samples were taken along a transect from Europe to the Arctic and along two transects within Fram Strait. Additionally, water was collected from different depths of the water column at seven stations in Fram Strait. The aims of the study were (i) to investigate the occurrence and distribution of 29 PFASs, especially HFPO-DA and other emerging PFASs, along the oceanic transport pathway from Europe to the Arctic; ii) to provide knowledge on the transport and sources of PFASs in water masses entering and exiting the Arctic Ocean at different depths, and iii) to estimate mass flows of PFASs through the deep water passage of Fram Strait.

To estimate PFAS mass flows, the measured PFAS concentrations had to be combined with water volume transport data. For this, it was collaborated with Charlotte Wagner and Prof. Elsie Sunderland from Harvard University regarding an ocean general circulation model. With regard to physical oceanography in Fram Strait and observational water transport data from a mooring array, it was cooperated with Dr. Wilken-Jon von Appen from the Alfred Wegener Institute, Helmholtz Centre for Polar and Marine Research.

The manuscript presenting the results of this study has been accepted for publication in the peer-reviewed journal *Environmental Science and Technology*. Details are given in Chapter 11.

6.1 Sample collection

Samples were collected between 10 July and 3 August 2018 during the *Polarstern* expedition PS114 [268]. Forty surface water samples were taken at approximately 11 m depth using the ship's seawater intake system (stainless steel pipe). Sampling locations included a latitudinal transect from the European continent to the Arctic (57 °N to 79 °N at ~5 °E, $n = 21$) and a longitudinal and latitudinal transect within Fram Strait (9°E to 18 °W at ~79 °N, $n = 14$, and 78 °N to 80 °N at ~0°EW, $n = 5$). Additionally, a CTD/rosette sampler was used at seven stations in Fram Strait to collect water samples ($n = 58$) at five to twelve depths from bottom (up to 3,117 m) to surface (5 or 10 m). More information on the sampling procedures are given in Chapter 10.3. The samples were stored at 5 °C in 1 L polypropylene bottles and extracted on board within one week after sampling. A map showing the sampling locations is provided in Figure 6.2-1A. An overview of the sampling coordinates, sampling depths and physicochemical parameters is given in Table A.2-1, Table A.2-2 and Figure A.2-1.

6.2 Materials and methods

6.2.1 Sample preparation and instrumental analysis

Solid phase extraction (SPE) for one litre of the samples was performed on board as described previously (Chapter 10.5). Briefly, an IS mix was added to the samples (400 pg of each standard) before they were loaded onto preconditioned SPE cartridges. The cartridges were dried under vacuum and stored at -20 °C. Further processing of the samples was performed after the cruise at HZG before PFASs were analysed by LC-MS/MS (Chapter 10.2). The quantification procedure is explained in Chapter 10.7.

6.2.2 Quality assurance and quality control

Before the cruise, all reagents and materials were tested for the presence of target PFASs. Only SPE cartridges packed with sorbent lots for which tests showed no detectable levels of PFOA and

other target PFASs were taken on board (Figure A.2-2). Different types of blanks were analysed to be able to trace back possible contamination sources (Figure A.2-3). In the instrumental blanks, no PFASs were detected, whereas particular PFASs were detected in the laboratory blanks ($n = 10$) and field blanks ($n = 6$) in the low pg/L range (C_5 to C_8 PFCAs, L-PFOS and Br-PFOS, 6:2 FTSA) (Table A.2-3).

As concentrations in the field blanks were marginally higher than in the laboratory blanks, all results were corrected by subtracting the average concentration of the respective compound in the field blanks from the concentration in the sample. MDLs ranged from 3.3 pg/L (PFDoDA) to 75 pg/L (HFPO-TeA) (Table A.2-3). PFBA was an exception as comparatively high concentrations of the compound were determined in both the laboratory and the field blanks, strongly varying between different SPE batches (mean \pm SD (350 \pm 460) pg/L). Consequently, no results are reported for PFBA. In addition, PFPeA could not be evaluated because of matrix interferences.

To compare the two different sampling techniques, a sample was taken with the stainless steel pipe (seawater intake at 11 m depth) when surface water samples were taken with the CTD/rosette sampler (10 or 5 m depth) ($n = 7$). The results showed no significant differences between sampling techniques (two-sample t-test, $\alpha = 0.05$; Table A.2-4). For the CTD/rosette sampler, the three deep water samples V1/1, V3/1 and V7/1 served as additional field blanks because all target analytes were below the method detection limit. Recoveries of the internal standards are given in Table A.2-5.

6.2.3 Data analysis

Statistical methods that were applied to data from all studies are explained in Chapter 10.8.

To calculate PFAS mass transport estimates through Fram Strait (79 °N), reported in [kg/year], the mean PFAS concentration of different water masses, measured in summer 2018 [pg/L], was multiplied by the average water volume transport [m^3/s] from the MIT general circulation model (MITgcm) ECCO v4 [110]. The MITgcm has a horizontal resolution of $1^\circ \times 1^\circ$ in most regions and higher resolution in the Arctic (40 km \times 40 km). Advection fields are from Estimating the Circulation & Climate of the Ocean (ECCO-v4) climatology, optimized in ECCO-v4 to produce a best fit to *in situ* and satellite observations of the physical ocean state [269-271]. Boundary currents used to calculate PFAS mass flows were defined based on prior work [272]. A detailed explanation is provided in Section A.2-1. PFAS mass transport estimates based on water transport data derived from MITgcm were compared to observational data derived from a mooring array [272].

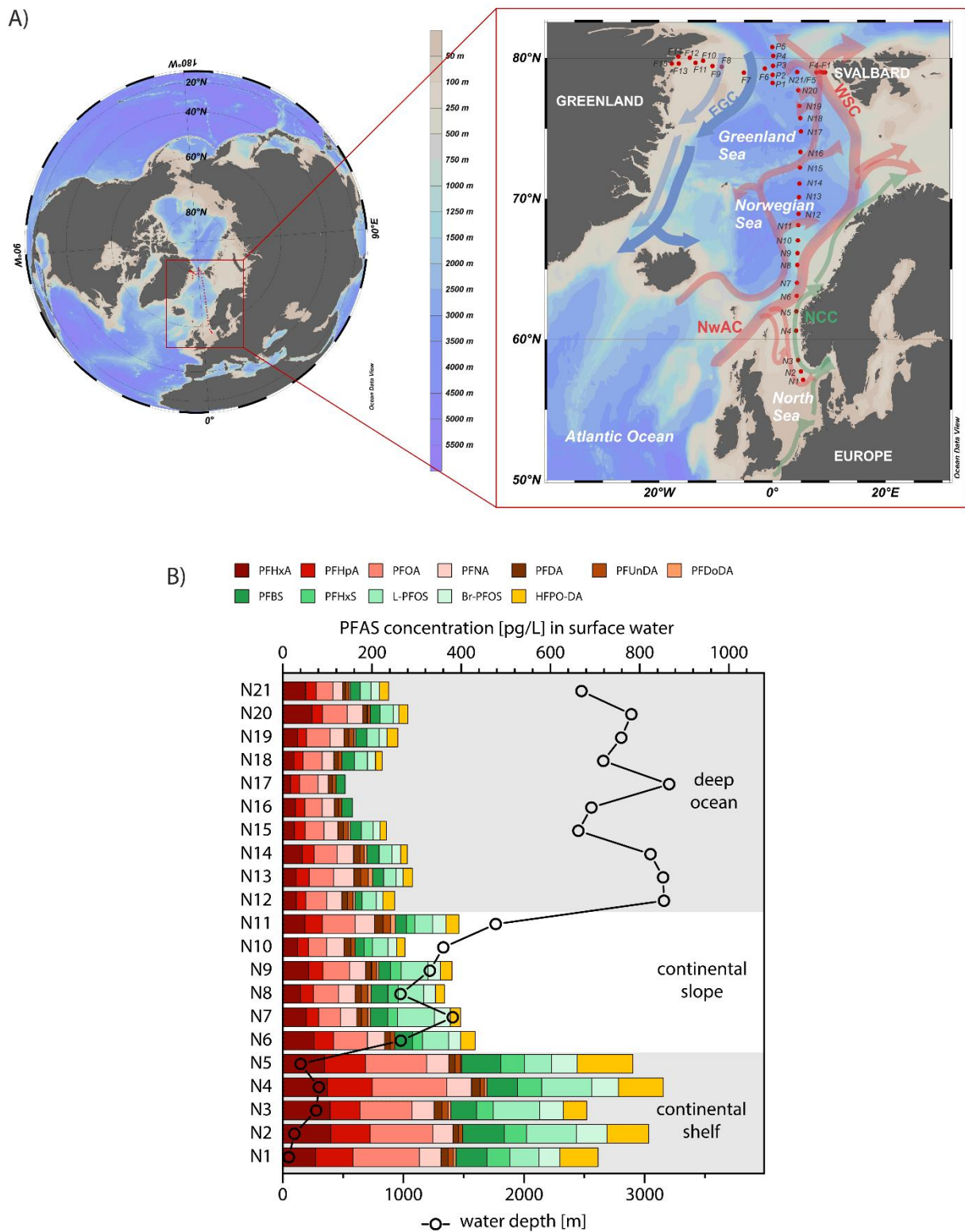


Figure 6.2-1: A) Surface water sampling locations (red dots; samples taken at 11 m depth) along a latitudinal transect from the European continent to the Arctic Ocean (N1–N21), and a longitudinal (F1–F15) and latitudinal (P1–P5) transect within Fram Strait. Arrows represent ocean currents (NCC: Norwegian Coastal Current; NwAC: Norwegian Atlantic Current; WSC: West Spitsbergen Current; EGC: East Greenland Current) [267], [273] B) Surface water concentrations [pg/L] of detected PFASs along the sampling transect from Europe to the Arctic in connection with water depth [m] at the respective sampling sites.

6.3 Results and discussion

6.3.1 PFAS concentrations and composition patterns in surface water

Eleven PFASs were detected in surface water samples from the cruise: HFPO-DA, C₆ to C₁₂ PFCAs and three PFASs (PFBS, PFHxS and L-PFOS/Br-PFOS) (Table A.2-6 and Table A.2-7).

The sum of the detected PFASs ranged from 140 pg/L in surface water from the Greenland Sea to 850 pg/L in the North Sea (mean 340 pg/L). The replacement compound HFPO-DA was detected in 90 % of the samples with a mean concentration of 30 pg/L. The substance with the highest mean concentration was the legacy compound PFOA (66 pg/L), having a detection frequency of 100 %. HFPO-DA and PFOA contributed on average (8±4) %, or respectively (20±3) % to the total PFAS concentration (ΣPFASs). In addition, the short-chain perfluoroalkyl acids (PFAAs) PFHxA, PFHpA and PFBS and the long-chain homologues PFNA and L-/Br-PFOS had high detection frequencies (93–100 %), contributing to ΣPFASs with 11 % to 17 % per compound. Individual results for all samples are provided in Table A.2-8 to Table A.2-10.

6.3.2 Transport and sources of PFASs along a latitudinal transect from Europe to the Arctic

ΣPFASs in surface water samples decreased from the North Sea continental shelf, to the continental slope, to deep ocean regions of the Norwegian Sea and Greenland Sea (Figure 6.2-1, Table A.2-8). This underlines the influence of ocean currents and fronts on PFAS concentrations in surface water. The Norwegian Coastal Current (NCC) affects sampling locations N1 to N5 in the northeastern part of the North Sea. In this region, PFAS concentrations (mean±SD (770±73) pg/L, this study) were about a factor eight lower than in coastal areas ((6,000±790) pg/L) [274], reflecting mixing and dilution effects with increasing distance from continental sources. From N5, still in the North Sea on the continental shelf (water depth: 148 m), to N6, in the Norwegian Sea on the continental slope (water depth: 900 m), ΣPFASs dropped from 780 pg/L to 430 pg/L. Here, the NCC continues in northeast direction on the continental shelf, whereas samples N6 to N11 were collected on the continental slope, along which the Norwegian Atlantic Current (NwAC) flows, extending the Gulf Stream and the North Atlantic Current in northeast direction [275]. The change in water masses between N5 and N6 is demonstrated by a salinity increase (32.59 psu to 34.69 psu), reflecting less freshwater influences in the Norwegian Sea compared to the North Sea. Both North and Baltic Sea are known to be influenced by PFAS sources on the European continent [101], explaining the significantly higher ΣPFASs in the samples from the continental shelf than those from the continental slope which are mainly influenced by Atlantic waters.

The main branch of the NwAC continues along the Norwegian shelf edge in northeast direction [275], whereas further surface water samples of the transect were taken in deep ocean regions in a northward direction (N12 to N23, water depth 2,450 m to 3,200 m). Consequently, these samples were less influenced by currents carrying water from the North Atlantic and Europe, explaining the significantly lower Σ PFASs in surface water samples taken north of 68 °N ((230±51) pg/L) than in samples from the continental slope and shelf ((370±54) pg/L and (770±73) pg/L).

Looking at individual PFASs, the compounds differed in the extent of the concentration decrease crossing the European continental shelf front. HFPO-DA showed the highest decrease from the NCC to the NwAC (70 %, (91±26) pg/L to (25±5) pg/L). Concentrations of C₆ to C₈ PFCAs, PFHxS and L-PFOS dropped between 40 % and 60 %, whereas C₉ to C₁₂ PFCAs showed a smaller (PFNA and PFDA, 20 % and 10 %) or no decrease (PFUnDA and PFDoDA) (Figure A.2-4).

These differences reflect combined effects of differing primary releases in source regions in the past, transport lag times, and mixing of water masses of different origin. Transit times derived from anthropogenic radionuclide tracers are one to two years from North Sea coastal waters to 60 °N in the NCC and another year to eastern Fram Strait [276]. In addition to North Sea coastal waters, the NCC carries waters from the Baltic Sea, which has a water turnover time of about 30 years [248], and recirculating Atlantic waters [273]. The NwAC carries waters from the North Atlantic that can be affected by multiple PFAS sources, among them the fluoropolymer production sites at the North American east coast. A time lag on the scale of decades is modelled between PFAS release into North American coastal waters and input to the Arctic because of slow oceanic transport and mixing processes [110]. Consequently, it can be assumed that historic emissions are still of relevance in the NwAC, whereas the NCC is influenced by both, recent PFAS emissions in North Sea coastal areas and historic emissions in the Baltic Sea and NwAC source regions.

The comparatively strong decrease of HFPO-DA from the NCC to the NwAC underlines that European coastal waters are currently a more important source for oceanic inputs of this compound into the Arctic than North Atlantic waters (Section A.2-2). In contrast, the negligible drop of C₉ to C₁₂ PFCAs suggests that these compounds are predominantly the products of semivolatile precursor oxidation, in which case one would not expect to see the gradient from NCC to NwAC waters, and/or play a minor role in recent European emissions. The latter is consistent with the phase-out of long-chain PFCAs in Western Europe and the transition to the production and use of replacement compounds such as HFPO-DA [128]. However, historic emissions of C₉ to C₁₂ PFCAs still play a relevant role with regard to Arctic inflow, having a proportion of approximately 25 % of Σ PFASs in waters from the NwAC.

6.3.3 Potential long-range transport of the replacement compound HFPO-DA

Although the concentration of HFPO-DA decreased stepwise along the latitudinal transect from the European continent to Fram Strait, the compound was detected in 19 of 21 samples. In deep ocean regions of the Norwegian Sea and Greenland Sea (69 °N to 79 °N), its surface water concentration ranged from < MDL to 26 pg/L (mean±SD (16±9) pg/L), approximately a factor three lower than that of PFOA (range 38–56 pg/L, mean (47±7) pg/L) (Table A.2-6).

These are the first findings of HFPO-DA in seawater from a remote region without known local sources, indicating that the compound undergoes long-range transport. This is consistent with a modelling study predicting similar overall persistence P_{OV} (≈ 1039 days) and characteristic travel distance CTD in water (≈ 1745 km) of HFPO-DA and PFOA [169].

According to Annex D of the Stockholm Convention, field data are accepted as evidence for the long-range transport of a chemical if 1) measured levels are available in locations distant from the sources of its release that are of potential concern; 2) monitoring data show that long-range environmental transport of the chemical may have occurred via air, water, or migratory species [277]. The mere detection of a chemical in a remote region cannot necessarily be understood as evidence of long-range transport, as the potential influence of local sources has to be considered [278]. In the investigated region, this includes potential sources on Svalbard [166], in northern Scandinavia and Greenland. The most distant sampling point from land where HFPO-DA was detected in this study is N15, approximately 600 km away from Svalbard and northern Scandinavia and approximately 800 km away from Greenland. This provides a minimum estimate for long-range transport of HFPO-DA.

Samples N16 and N17 in the southern Greenland Sea, the only samples along the latitudinal transect in which HFPO-DA was not detected, also had a lower Σ PFASs (160 pg/L and 140 pg/L) than the other samples taken in deep water regions ((260±25) pg/L). This coincided with a temperature decrease from 8.2 °C (N15) to 5.5 °C (N17), indicating that the sampling transect crossed the Arctic Front in this area, which separates waters in the Norwegian Sea, mainly directly originating from the North Atlantic, from apparently less HFPO-DA-contaminated waters in the Greenland Sea, also containing water that had spent significant time in the Arctic [279]. The influence of the WSC carrying waters from the south is an explanation for the detection of HFPO-DA in samples N18 to N21, taken north of N16 and N17.

6.3.4 Sources of PFASs to surface water entering and exiting the Arctic Ocean

The longitudinal sampling transect within Fram Strait ($\sim 79^\circ\text{N}$) cuts across the ice edge near the prime meridian (0°EW) (Figure 6.3-1). East of it, warm, saline Atlantic Water (AW) enters the Arctic Ocean, whereas west of it, low-saline Polar Surface Water (PSW) and sea ice is transported out of the Arctic.

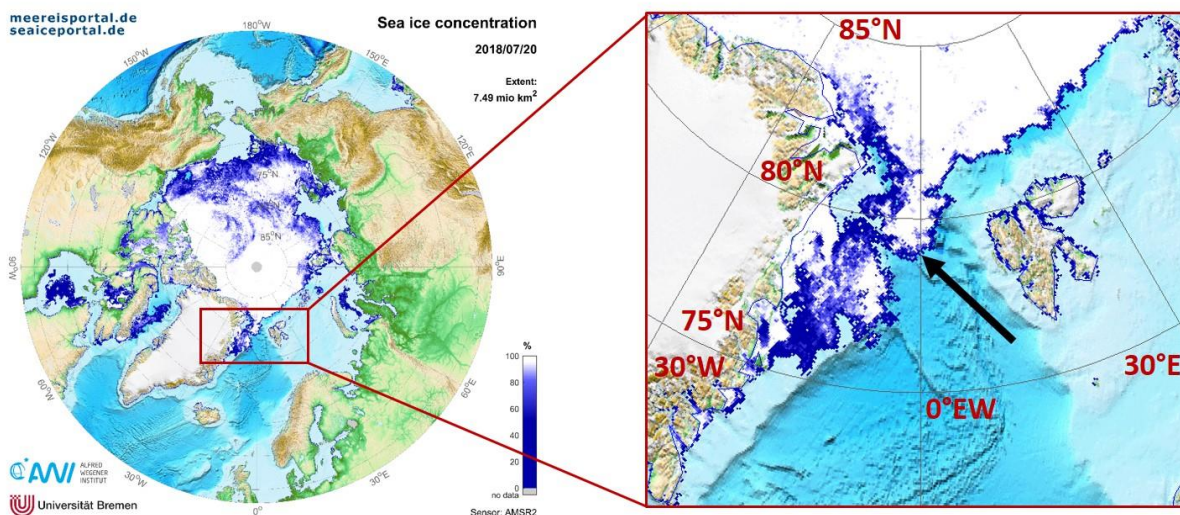


Figure 6.3-1: Sea ice concentration in the Arctic during the cruise [280]. The black arrow marks the location at which the longitudinal sampling transect in Fram Strait ($\sim 79^\circ\text{N}$) cuts across the ice edge near the prime meridian (0°EW).

The sum of PFASs with a detection frequency $> 50\%$ (C_6 to C_9 PFCAs, PFBS and HFPO-DA) was significantly higher in the samples taken west of 0°EW (F6 to F15, ice-covered, (260 ± 20) pg/L) than east of it (F1 to F5, ice-free, (190 ± 10) pg/L) (two-sample t-test, $\alpha = 0.05$, $p < 0.001$) (Figure 6.3-2). Additionally, ΣPFASs was higher in samples taken north of the ice edge (P3, 300 pg/L, ice-covered) than south of it (P1, 190 pg/L, ice-free) along the latitudinal transect within Fram Strait ($\sim 0^\circ\text{EW}$) (Table A.2-10).

For individual PFASs, the relative difference was highest for PFHpA ((46 ± 7) pg/L west of 0°EW versus (24 ± 3) pg/L east of 0°EW) and lowest for PFNA ((33 ± 2) pg/L versus (25 ± 2) pg/L). An exception was HFPO-DA, having a higher mean concentration in eastern Fram Strait (Table A.2-7). Moreover, HFPO-DA was the only compound not showing a significant negative correlation with temperature and salinity (Table A.2-11). Part of the AW entering the Arctic Ocean via the WSC in eastern Fram Strait spends significant time in the Arctic before exiting the Arctic Ocean via the EGC in western Fram Strait. Consequently, tracers transported by ocean currents reach western Fram Strait after longer lag times than eastern Fram Strait [276, 281]. Thus, the later start of HFPO-DA production compared to other PFASs may be an explanation for its lower mean

concentration west of 0 °EW than east of it and the non-negative correlation with salinity and temperature.

In addition to oceanic transport times, the Arctic in- and outflow differs in the amount of freshwater. Reflected in the lower salinity and temperature, freshwater inputs, such as sea ice and glacier melt water, precipitation and river runoff, are of higher relevance in the outflowing EGC than in the inflowing WSC [282]. Atmospheric long-range transport and degradation of volatile precursors can be expected to be the most important PFAS source to Arctic freshwater [108, 283-285]. The relative importance of atmospheric sources is influenced by the amount of direct emissions of a compound in relation to those of its precursors [23]. For example, global emission estimates of individual PFCAs from 1951–2030 show that > 74 % of PFHpA was released to the environment as degradation products of precursors, whereas > 75 % of PFNA was emitted from direct sources [128]. Consequently, a higher PFHpA/PFNA ratio can be indicative of atmospheric sources. In our study, the PFHpA/PFNA ratio increased from 0.95 ± 0.12 east of 0 °EW to 1.40 ± 0.22 west of it and showed a significant negative correlation with salinity ($r = -0.79$, $p < 0.001$) (Figure 6.3-2). This indicates that the contribution of atmospheric PFAS sources is higher to Arctic outflow than to Arctic inflow and may account for the higher Σ PFASs west of 0 °EW than east of it.

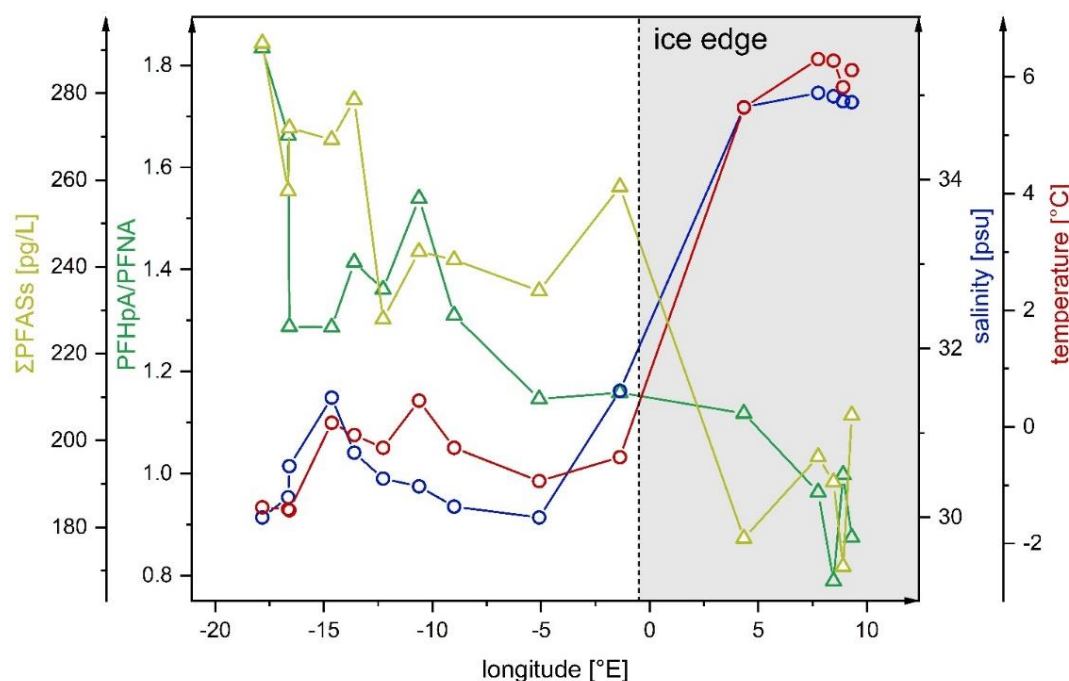


Figure 6.3-2: PFHpA/PFNA ratio and sum of PFASs with a detection frequency > 50 % (C6 to C9 PFCAs, PFBS and HFPO-DA) versus salinity [psu] and temperature [°C] in samples taken along a longitudinal transect across Fram Strait (~79 °N; surface water samples F1 to F15). Temperature and salinity data was taken from von Appen and Rohardt [286].

However, PFHpA/PFNA ratios in both Arctic in- and outflow were still considerably lower than in recent samples from North Sea coastal areas with a PFHpA/PFNA ratio of 5.4 ± 1.1 [274]. Influenced by recent emissions from point sources, the latter value reflects global emission estimates with a predicted PFHpA/PFNA ratio of 5.8 from 2016 to 2030 (higher scenario), which is higher than 1951-2002 (range 0.2–1.5) and 2003-2015 (range 0.5–1.7) [128]. Consequently, the PFHpA/PFNA ratio in both Arctic in- and outflow can be expected to increase within the next years, with a rate that depends on the relative contributions from slow oceanic transport and fast atmospheric transport.

6.3.5 Depth profiles of PFASs in Fram Strait

PFAS concentrations in different water depths varied among water masses. In general, the sum of PFASs with a detection frequency $> 50\%$ (C_6 , C_7 , C_9 , C_{11} PFCAs and PFBS) was higher in the surface water layer, including PSW ((170 ± 30) pg/L, $n = 16$) and AW ((120 ± 20) pg/L, $n = 18$), than in Recirculating Atlantic Water/Arctic Atlantic Water (RAW/AAW) ((90 ± 35) pg/L, $n = 10$) and in Intermediate Water (IW) ((73 ± 30) pg/L, $n = 6$). In Deep Water (DW) ($n = 8$), most of the results were $< MDL$, except for PFHxA, PFHpA, PFNA and PFUnDA, which were detected in one to three samples each (Table A.2-12 to Table A.2-14). To show PFAS concentrations in relation to the properties of the respective water masses, temperature versus salinity plots are given in Figure A.2-7.

The distribution of PFASs along the zonal section across Fram Strait is provided in Figure 6.3-3. Depth profiles V1 to V3 were taken in the eastern part of Fram Strait, where the warm, high-saline WSC enters the Arctic Ocean. In this area, the AW layer extends down to approximately 600 m, characterized by a potential temperature Θ of > 0 °C and a potential density isopycnal, referenced to 0 dbar, of $\sigma_0 \leq 27.97$ kg/m³. During winter, this is the depth to which the water column tends to be mixed, diluting tracers such as PFASs. This is reflected by comparatively stable PFAS concentrations from the surface to the sampling point at 500 m depth and significantly lower concentrations in IW and DW ($> 1,000$ m) Figure 6.3-3B. Depth profiles V4 and V5 were taken in the western part of Fram Strait, where the surface layer is dominated by cold, low-density PSW from the Arctic ($\Theta \leq 0$ °C, $\sigma_0 \leq 27.70$ kg/m³) which reaches down to about 100 m. Below PSW is RAW/AAW ($\Theta > 0$ °C, $\sigma_0 > 27.70$ kg/m³), flowing southwards as well. This water mass comprises recirculating Atlantic Water (a part of the WSC that does not enter the Arctic Ocean but flows westward in Fram Strait before joining the EGC), and Arctic Atlantic Water (transported into the Arctic Ocean by the WSC and flowing around the Arctic Ocean in a cyclonic boundary current before exiting via the EGC) [287]. Passing the water mass boundary from PSW to RAW/AAW corresponded with a decrease of Σ PFASs from 120 pg/L to 77 pg/L in V4 and 150 pg/L to

74 pg/L in V5, respectively (Figure 6.3-3B). As discussed for the surface water samples before, concentrations of specific PFASs were higher in PSW than in AW, especially of PFHpA ((42±9) pg/L versus (25±5) pg/L). In contrast, the long-chain compound PFNA showed comparable concentrations in PSW and AW ((31±6) pg/L versus (31±9) pg/L). Consequently, the gradient between PSW and RAW/AAW was also higher for PFHpA ((42±9) pg/L to (21±12) pg/L) than for PFNA ((31±9) pg/L to (22±6) pg/L (Figure 6.3-3B)). These observations suggest that atmospheric sources playing an important role for the outflowing surface water (PSW) are less relevant for RAW/AAW outflowing below.

AW and PSW in Fram Strait have an apparent mean age of approximately a decade, whereas intermediate waters have an apparent age of approximately 50 to 70 years, respectively [272]. Concentrations of HFPO-DA were below detection limit in older intermediate waters, reflecting production and use that began after 2000.

Depth profiles of PFASs in this study were different from those of more hydrophobic legacy POPs such as polychlorinated biphenyls (PCBs) and dichlorodiphenyltrichloroethanes (DDTs), for which highest concentrations in Fram Strait were not found in the upper water layers, but in intermediate or deep waters [288]. This was expected because for hydrophobic POPs, which partition readily to organic carbon and suspended particles, particle settling is suggested to be a dominant transport pathway to deeper water layers (“biological pump”). On the contrary, lateral and vertical transport due to physical mixing is thought to play a more important role for less hydrophobic compounds such as PFASs (“physical pump”) [108, 110, 289]. In agreement with this, the differences in PFAS concentrations and composition patterns between the upper and the deeper water layers, as well as the negligible intrusion of PFASs into DW indicate that physical mixing processes are more relevant for vertical PFAS transport in Fram Strait than sorption to sinking particles.

In a previous study, PFAS detection was generally limited to the upper water layers (< 150 m) in four vertical water column profiles from the central Arctic [108]. The authors attributed this to subsequent dilution and mixing of AW after entering the Arctic Ocean. This is consistent if looking at the water mass transport. Starting from V2 and V3 with comparatively constant PFAS concentrations down to 500 m (this study), water masses are further transported northwards and reach the sampling location PS80/227 of the previous study [108], at which PFASs could still be detected down to 250 m, before arriving at the three other sampling locations in the central Arctic, in which PFASs were non-detectable in the AW layer below 150 m.

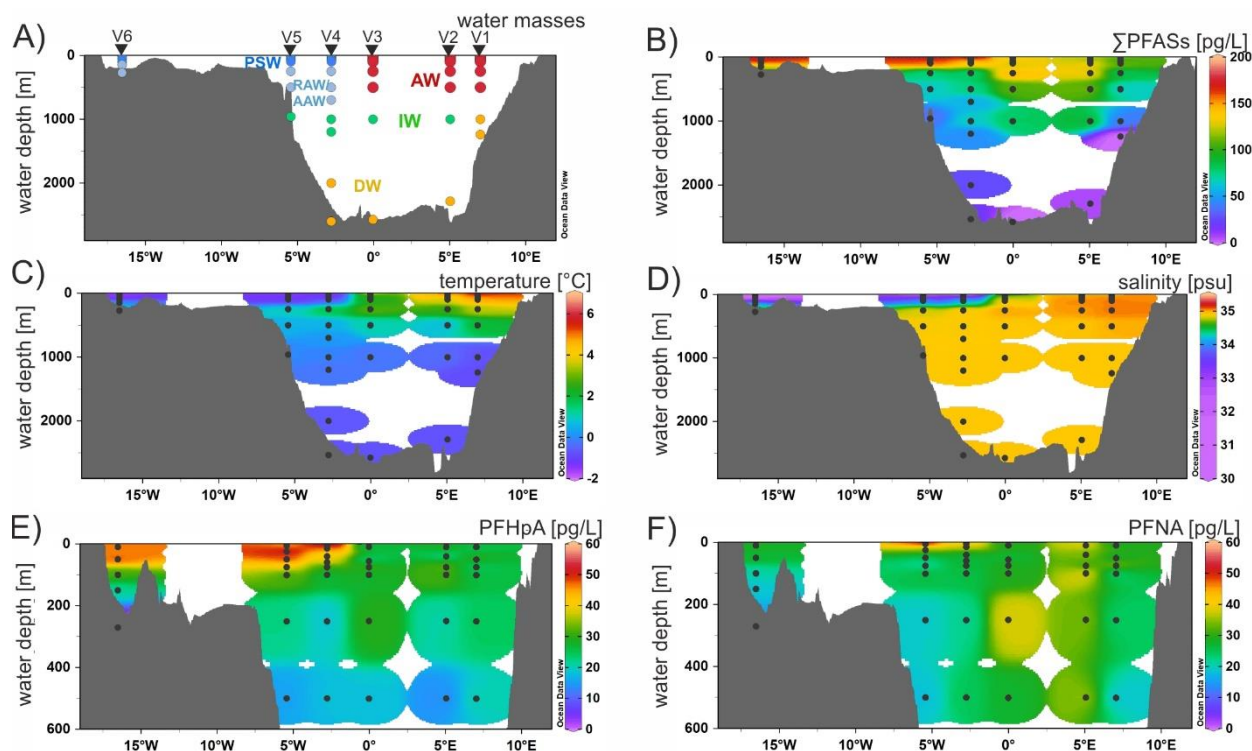


Figure 6.3-3: Distribution of A) water masses, B) sum of PFASs with a detection frequency > 50 % (C6, C7, C9, C11 PFCAs and PFBS), C) temperature, D) salinity from bottom to surface, E) PFHpA and F) PFNA from 600 m depth to surface along the east-west cross section at ~79°N. Black dots represent samples analysed for PFASs. Temperature and salinity data was taken from von Appen *et al.* [290]. For bottom bathymetry, GEBCO_2014 gridded data was used. Data were plotted using Ocean Data View [291].

6.3.6 PFAS mass transport estimates through Fram Strait

For compounds with ≥ 8 perfluorinated carbon atoms (C_9 to C_{11} PFCAs and L-/Br-PFOS) and HFPO-DA, summing mass flow estimates for the different water masses resulted in a net transport into the Arctic Ocean, whereas C_6 to C_8 PFCAs as well as C_4 and C_6 PFASs showed a net transport out of the Arctic Ocean (Figure 6.3-4). A comparable net transport pattern was observed when the calculation was based on water transport data derived from a mooring array instead of the MITgcm (Figure A.2-8 and Table A.2-17). Different statistical treatments of values below the MDL (zero, $\sqrt{2}/2 \cdot \text{MDL}$ and MDL) did not change the observation of a chain-length dependent net transport (Table A.2-16).

Estimated PFAS mass flows through Fram Strait in 2018 corresponded to approximately 2 % (PFOA) to 13 % (PFHxA) of the annual average of the higher value of estimated global cumulative emissions from 2003 to 2015 [128]. In modelling studies, PFOA mass flows into the Arctic through direct emissions and oceanic transport were estimated to be 8–23 t/year (1991–2004) [292], 9–20 t/year (2000–2005) [293] and 8–22 t/year (2005) [294]. The result of our study, combining measured PFOA concentrations and modeled water volume transport, is in the same order of

magnitude ((6.4 ± 1.0) t/year) for oceanic input through Fram Strait, the major gateway to the Arctic Ocean.

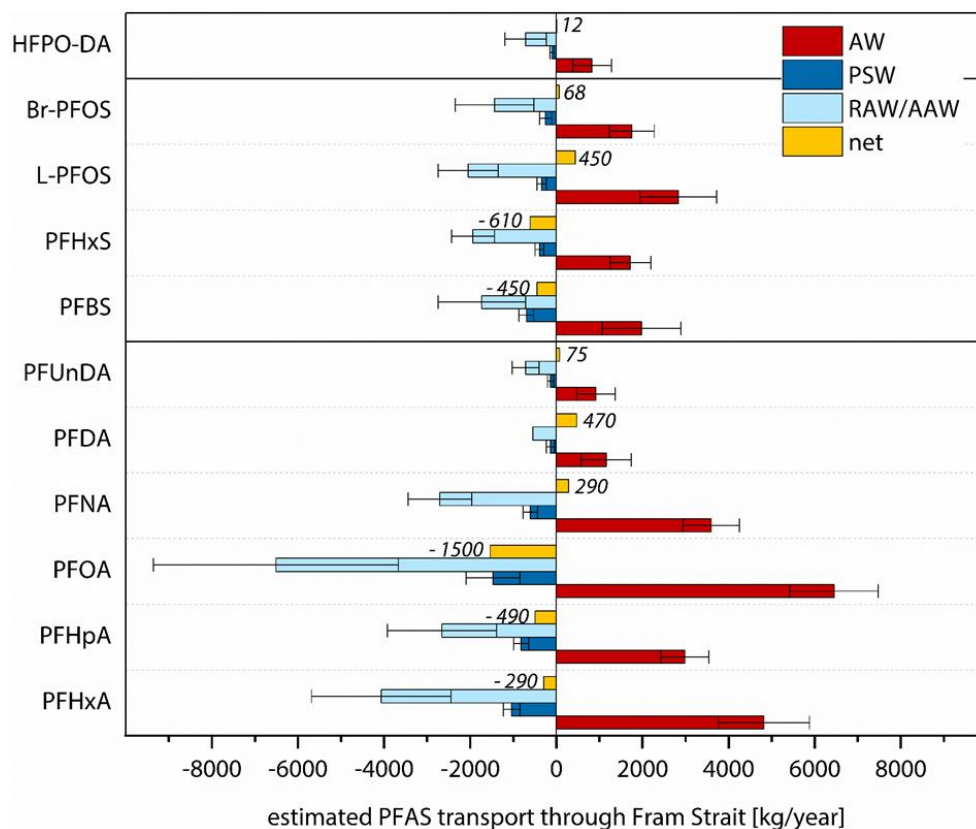


Figure 6.3-4: PFAS mass transport estimates through Fram Strait via the boundary currents, calculated by combining measured PFAS concentrations ($\text{mean} \pm \text{SD}$) in Atlantic Water (AW), Polar Surface Water (PSW) and Recirculating/Arctic Atlantic Water (RAW/AAW) from this study with the average water volume transport [m^3/s] for the respective water mass over the years 2010–2015, derived from the MITgcm ECCO v4 model (Section A.2-1). Positive values describe northward fluxes into the Arctic Ocean, whereas negative values describe southward fluxes to the Nordic Seas. The modeled average water volume transport was $3.7 \cdot 10^6 \text{ m}^3/\text{s}$ for AW, $-0.6 \cdot 10^6 \text{ m}^3/\text{s}$ for PSW and $-3.8 \cdot 10^6 \text{ m}^3/\text{s}$ for RAW/AAW. To calculate the mean value of each water mass in this figure, all values $< \text{MDL}$ were replaced by $\sqrt{2}/2$ times the MDL.

A possible explanation for the chain-length dependent net transport through Fram Strait is the different contribution of atmospheric sources to each homologue in the Arctic. Atmospheric transport to remote regions is fast (days to weeks) in comparison to oceanic transport (years to decades) [23]. This suggests a rapid response of atmospheric inputs to changes in production, i.e. the industrial shift from long-chain PFASs, PFCAs and their precursors to shorter-chain homologues. In snow pits from High Arctic ice caps, which receive inputs solely from atmospheric sources, concentrations of PFOS and its precursor perfluorooctane sulfonamide (FOSA) decreased in the early 2000s [254, 295]. Rapid declines in FOSA observed in North Atlantic pilot whales were also attributed to fast changes in atmospheric inputs, reflected in seawater concentrations [296]. In contrast, the oceanic response is slower, which is demonstrated by a higher contribution of long-chain homologues to ΣPFASs in the Arctic inflow than in water from regions close to emission

areas, such as the North Sea. As our study indicates that atmospheric inputs are of higher relevance for outflowing Arctic surface waters, the higher share of short-chain homologues and their precursors in recent emissions is a possible explanation for their higher concentrations in outflowing waters, resulting in a net southward transport.

In addition, fractionation of the compounds in the melting snowpack and sea ice due to different physicochemical properties of PFASs with varying chain length may be important. In a laboratory study, short-chain PFCAs and PFSAAs were released early during a snowmelt period, whereas the more hydrophobic long-chain PFAAs were enriched in the late meltwater and particle fractions [297]. PFCAs showed a similar behaviour to PFSAs with one perfluoroalkyl moiety less, indicating a higher affinity of the sulfonic group to the snow grain surface than the carboxylate group, as also observed for sediment [298]. Consequently, the higher retention of the long-chain compounds in snow, sea ice and terrestrial environments may serve as an additional explanation for the observation that for compounds with ≥ 8 perfluorinated carbons, the Arctic output is lower than the input.

6.4 Summary and conclusion

The spatial distribution of 29 PFASs in seawater was investigated along a sampling transect from Europe to the Arctic and two transects within Fram Strait, located between Greenland and Svalbard, in the summer of 2018. The replacement compound HFPO-DA was detected in 90 % of the samples with a mean concentration of 30 pg/L. This adds empirical evidence to modelling assessments [169] indicating that HFPO-DA, similar to PFOA, does undergo long-range transport. Consequently, it is a compound of global environmental concern and it should be evaluated with regard to future regulations. The recent detection of another ether-based PFAS (6:2 Cl-PFESA) in East Greenland marine mammals [179] highlights the potential role of long-range oceanic transport for delivering emerging PFASs to the Arctic food web.

The total PFAS concentration was significantly enriched in the cold, low-salinity surface water exiting the Arctic compared to warmer, higher-salinity water from the North Atlantic entering the Arctic. The higher ratio of PFHpA to PFNA in outflowing water from the Arctic suggests a higher contribution of atmospheric sources compared to ocean circulation. An east-west cross section of the Fram Strait, which included seven depth profiles, revealed higher PFAS concentrations in the surface water layer than in intermediate waters and a negligible intrusion into deep waters ($> 1,000$ m). Mass transport estimates indicated a net inflow of PFASs with ≥ 8 perfluorinated carbons via the boundary currents and a net outflow of shorter-chain homologues. It can be hypothesized that this reflects higher contributions from atmospheric sources to the Arctic outflow and a higher retention of the long-chain compounds in melting snow and ice.

The differences in Arctic in- and outflow highlight that the interplay of changes in source patterns, oceanic and atmospheric long-range transport as well as ice and snow as links between the atmosphere and the ocean has to be considered to assess the fate of PFASs in the Arctic. The results of this study indicate that atmospheric inputs are an important factor when assessing if the Arctic is a sink or source of PFASs. Future research on the relative importance of direct and indirect sources in remote areas can improve the understanding on the ultimate fate of PFASs.

The PFAS depth profiles in Fram Strait demonstrate that knowledge of the ocean circulation, vertical and lateral stratification as well as physical mixing processes is crucial for understanding the large-scale distribution and fate of PFASs. Using PFOS as an example, prior modelling results showed that weakened Atlantic Meridional Overturning Circulation (AMOC) due to climate change is likely to increase the magnitude of POPs entering the Arctic Ocean [110]. Additionally, the loss of perennial glacial mass and snow due to climate change could release long-chain PFASs deposited during earlier periods of high use, reinforcing the role of the Arctic as a secondary source [285, 299, 300]. Consequently, future PFAS depth profiles in Fram Strait and other key regions of the global oceanic circulation, as well as mechanistic studies on the post-deposition characteristics of PFASs in snow and ice interacting with ocean surface water, can help to elucidate how PFAS cycling is linked to climate change.

7. Per- and Polyfluoroalkyl Substances in Chinese and German River Water – Point Source- and Country-Specific Fingerprints including Unknown Precursors

By means of conventional compound-specific analytical methods, only a small fraction of the PFASs on the global market can be determined. With a number of 29 substances, the targeted analytical method developed in this PhD project includes less than 1 % of the more than 4,700 PFASs on the worldwide market [3]. This raises the question if the analysed PFASs are representative or if environmental and human health risks are considerably underestimated. Moreover, earlier identification of emerging pollutants in source regions is of concern to trigger mitigation measures before the substances become ubiquitously distributed [194, 301]. As an example, the detection of HFPO-DA in Arctic seawater (Chapter 6) and its addition to Candidate List of Substances of Very High Concern under REACH in 2019 [302] come at a time where emissions of the compound have been ongoing for more than 10 years [250], resulting in irreversible environmental exposure. As emerging compounds have to be known and considered by the scientist and analytical standards have to be available, conventional target analysis typically does not contribute to shorten the large time difference between the introduction of a compound by industry, its detection in the environment, studies on potential adverse effects, risk assessment, evaluation and possible regulation.

To address these concerns from an analytical perspective and obtain a more holistic view on PFAS contamination, targeted analytical methods can be complemented with analytical approaches to characterize the unknown pool of PFASs. These include the Total Oxidizable Precursor (TOP) assay, giving an estimate of the sum of precursors in a sample that oxidize to targeted PFASs [192]. Application of the TOP assay to river water samples from Japan [303] and France [304] has revealed that a significant proportion of unidentified PFCA precursors is present, albeit varying in amount. The mentioned studies have not considered replacement compounds, such as PFECAs and PFESAs, as terminal products or precursors in the TOP assay. A recent study highlighted that this can result in missing a fraction of the total PFAS amount [305]. Using HRMS-based approaches to elucidate the composition of the unknown fraction, more than 750 PFASs of more than 130 diverse classes have been identified in strategically selected environmental samples, biofluids or commercial products in recent years [153]. For example, over 240 individual PFASs of 57 classes were discovered in fire-fighting foams and impacted groundwater [168], underlining the potential of non-target analysis.

Studies investigating the impact of industrial point sources on the environment typically focus on one study site, one geographical region and one type of source [306-308]. Due to differing

analytical scopes in target analysis, especially regarding emerging PFASs, and non-standardized suspect and non-target workflows [309], it is often difficult to compare results from different studies. Consequently, a comparison of point sources from regions with a different history of PFAS production using one set of analytical methods can give a more comprehensive picture.

This study aimed at comparing source-specific fingerprints in river water from Germany as a country where long-chain PFCAs and PFASs has been phased out and China as a country to which part of the production has been shifted. More specifically, this study had the objectives i) to select study sites covering major areas of PFAS production and application in both countries, ii) to collect samples up- and downstream of the suspected point sources, iii) to investigate occurrence and composition profiles of 29 legacy and emerging PFASs by means of target analysis, iv) to further characterize source fingerprints based on isomer profiling and principal component analysis (PCA), v) to evaluate the significance of unknown precursors to targeted PFASs by applying the TOP assay with an expanded list of target analytes, including replacement compounds, and vi) to estimate riverine PFAS mass flows. Moreover, a PFAS suspect screening was to be performed in a follow-up study (Chapter 8).

For the establishment and validation of the TOP assay, a Master thesis was supervised (Thekla-Regine Schramm, 01 April 2018 to 31 January 2019). It is clearly indicated in the following chapter, where data was taken from her work. The German sampling campaign was organized and performed together with Thekla-Regine Schramm, whereas the sampling in China was conducted in collaboration with Ass. Prof. Jianhui Tang at the Yantai Institute of Coastal Zone Research, China. It took place during a one-month research stay in China, which was also used to extract the Chinese samples (28 October 2018 to 25 November 2018).

A manuscript presenting the results of this study is under review for publication in the peer-reviewed journal *Environmental Pollution*. More information is provided in Chapter 12.

7.1 Selection of the study sites

Industrial point sources covering major areas of PFAS production and application in both countries were selected based on a pre-study along the German Rhine River, literature research and expert knowledge.

With a catchment population of 49.0 million and an average discharge of 86 km³/year, the Rhine River belongs to the major European river catchments. Along the river course and its tributaries, several industrial regions are located [310]. In previous studies, the Rhine River has been identified as a major contributor to discharges of legacy long-chain PFASs from the European continent [77, 310]. Additionally, North Sea samples indicated that the Rhine River is the main source for emerging PFAS to the German Bight, such as PFBS [99, 161] and HFPO-DA [100]. The last study

reporting PFAS results for the whole river course dates from 2008 [161]. A broad spectrum of 40 PFASs was analysed at this time, but ether-based replacement compounds and other emerging PFASs, such as PFPiAs and PFECHS, had not been included yet. Consequently, a pre-study was conducted to decide on which sites along the River Rhine to focus in the main study. 12 water and 9 sediment samples were collected along the river course, up- and downstream of possible industrial point sources and inflow of tributary rivers known to be impacted by industrial areas (Figure 7.1-1). The samples were analysed using the targeted method developed in study 1.

Based on the results shown in Figure 7.1-1, the Lower Main, mouching into the Rhine River, was selected as first site of interest for the main study. Here, 6:6 and 6:8 PFPiA were quantified in comparatively high concentrations in sediment (S_043). In addition, the Main River sampling location (S_044) was the only one, at which 6:6 PFPiA was detected in the water phase. This may be attributed to a chemical park with more than 90 companies located at the Main River, just before discharging into the Rhine River. Amongst others, pesticide formulations containing PFPiAs and perfluoroalkyl phosphonic acids (PFPA) are produced by a large agricultural chemical company operating here [146]. In the further course of the Rhine River, a considerable increase of the short-chain compound PFBS after sampling location S_019 was observed (Figure 7.1-1B). This was also reported in previous studies, attributing PFBS emissions to the largest chemical park in Germany, which is located at the Rhine River close to Cologne and mainly dedicated to production of pharmaceuticals and pesticides [161]. Consequently, this area was chosen as the second German site for the main study. In addition, it was decided to focus on the Ruhr River and its mouth into the Rhine River. Historically characterized by coal mining, iron and steel production since the 19th century [311], the Ruhr Area is still a centre of metal plating. In this industrial branch, 6:2 FTSA is used as a replacement for PFOS [132], which was reflected in its comparatively high contribution to total PFASs in the Ruhr River samples (S_014). As reference site, the River Rhine tributary Lahn was selected because it had been previously described as river with little industrial influence and background PFAS concentrations [161, 312].

As a fourth German site, the Bavarian Alz River was chosen, mouching into the Inn River. Here, major manufacturers operate a chemical park for production of fluoropolymers and fluoromonomers. There were no peer-reviewed publications on PFAS concentrations in the Alz River available when starting this study, but it was known that PFOA salts have been used as processing aid until 2008 in the chemical park before being replaced by the ether-based compound ADONA [313].

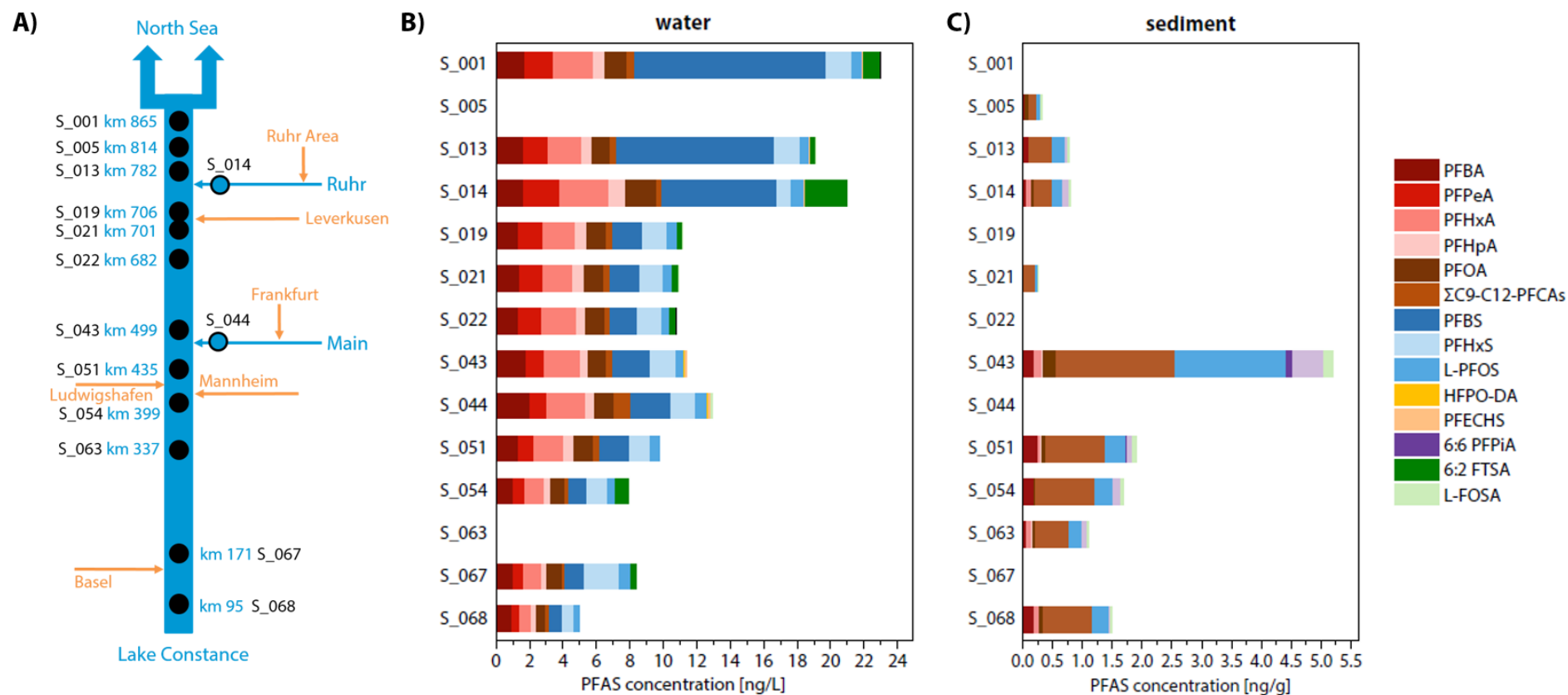


Figure 7.1-1: Pre-study to identify potential point sources along the River Rhine. A) Schematic overview of the River Rhine sampling locations (black) including the “Rhine-kilometres” (km), a scale running from Lake Constance (0 km) to the river mouth in the Netherlands (1,036 km). Industrial regions with possible point sources are marked in orange. PFAS concentrations are shown for B) analysed surface water samples and C) sediment samples. At sampling stations where no concentration is given, no water, or respectively sediment sample was taken. The samples were collected by the department for Marine Bioanalytical Chemistry (Table 10.3-1).

In China, sites were chosen based on discussions with Ass. Prof. Jianhui Tang from Yantai Institute of Coastal Zone Research and Dr. Zhanyun Wang from ETH Zürich, Switzerland. In addition to sites operated by Chinese companies, the study aimed at including sites operated by overseas companies, which built production plants and ramped up production in Asia after the phase-out of long-chain PFASs in Europe, North America and Japan [127]. The first selected site is located in the Xiaoqing River Basin (Huantai, Shandong Province), receiving discharge of one of the largest Asian fluoropolymer production sites, operated by a Chinese manufacturer. The chemical park's annual PTFE production capacity was rapidly expanded from 3 kt in 2002 to 30 kt in 2009 [127]. In 2015, its capacity was 44.3 kt of polytetrafluoroethylene (PTFE) and 10 to 13 kt of vinylidene fluoride (VDF), hexafluoropropylene oxide (HFPO) and fluoroelastomers (FKM) [314]. The second Chinese site is situated at the Xi River (Fuxin, Liaoning Province, Daling River Basin), where two fluorochemical industrial parks have been built due to the local abundance of fluorite [315]. Main products include short-chain PFAAs and other fluorine-containing pharmaceutical and pesticide intermediates, as well as fluorotelomers [308]. The third selected site in China is located at the Yangtze River in Changshu, Jiangsu Province, and in close proximity to the "Advanced Materials Industrial Park (AMIP)" with more than 15 overseas and domestic fluorochemical companies [306]. Various plants for different operations have been built since 1999, for example for production of PTFE, PVDF and fluoroelastomers, and several manufacturers from the United States and Europe have built up their Asian headquarter here [306].

An overview of the four sites in Germany and the three sites in China that were further investigated in the main study is given in Figure 7.1-2.

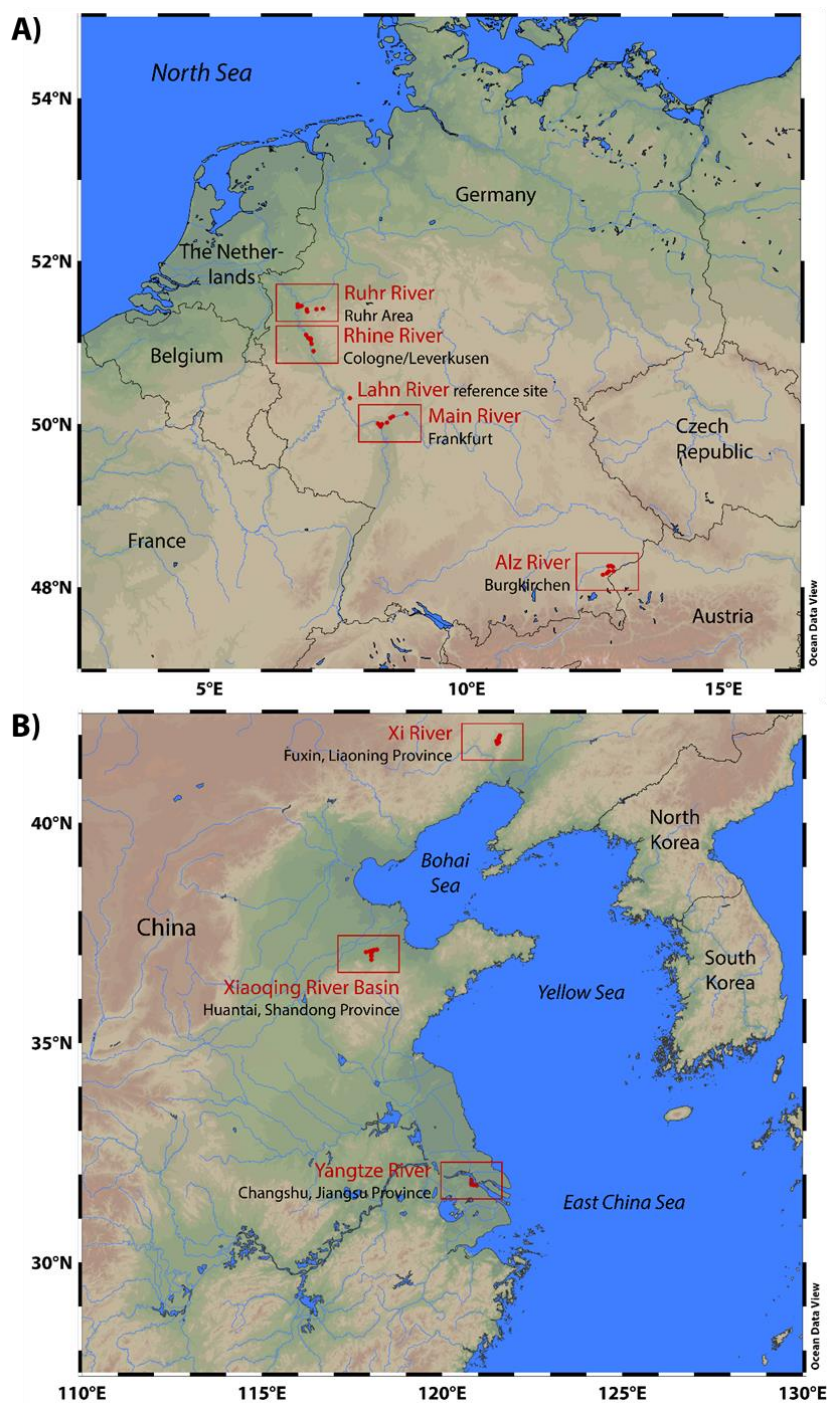


Figure 7.1-2: Overview of selected study sites A) in Germany and B) in China. Maps were plotted using Ocean Data View [291].

7.2 Sample collection

Sampling was performed from pontoons, bridges, moles or the riverside in September 2018 (Germany) and November 2018 (China). River water was collected 0.5 m below the surface at six to ten sampling locations per site, up- and downstream of the potential source. More information on the sampling procedure is given in Chapter 10.3. In total, samples for target analysis were taken at 58 stations in 1 L polypropylene bottles. At 31 of the stations, two aliquots of each sample were

filled into 125 mL high density polyethylene bottles for application of the TOP assay. At 22 of the stations, 500 mL triplicate samples were filled into polypropylene bottles for application of the suspect screening (Chapter 8). Samples were stored at 4 °C and processed in the laboratory within four weeks after sampling. Water temperature, salinity and pH were measured onsite using a portable measuring device (Chapter 10.4.1). The sampling coordinates and the results for the physicochemical parameters are given in Table A.3-1 and Table A.3-2. Schematic maps of the sampling sites are provided in Figure 7.2-1 and Figure 7.2-2.

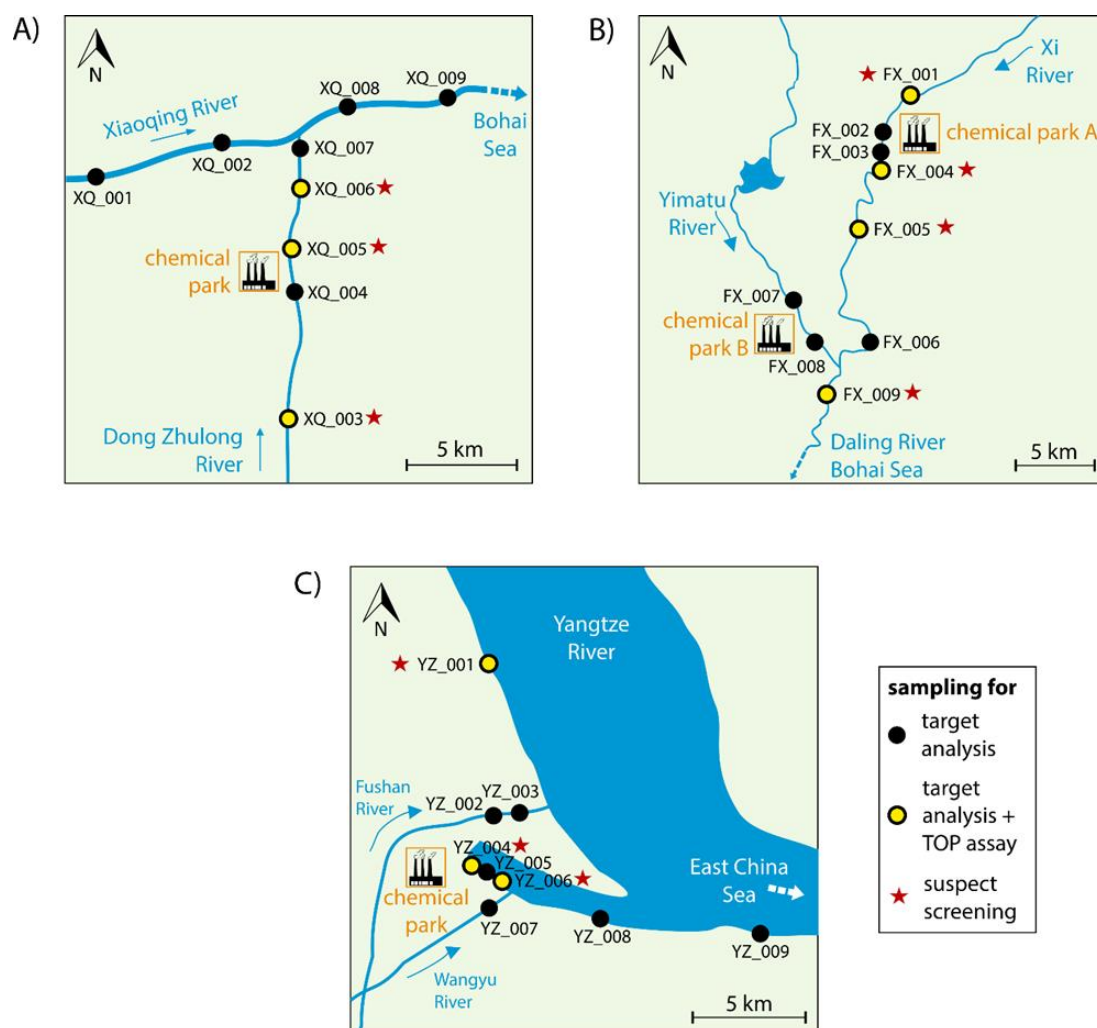


Figure 7.2-1: Sampling site maps of the Chinese sites. A) Site XQ (Xiaoqing River Basin, Huantai, Shandong Province), B) Site FX (Daling River Basin, Fuxin, Liaoning Province), C) site YZ (Yangtze River, Changshu, Jiangsu Province).

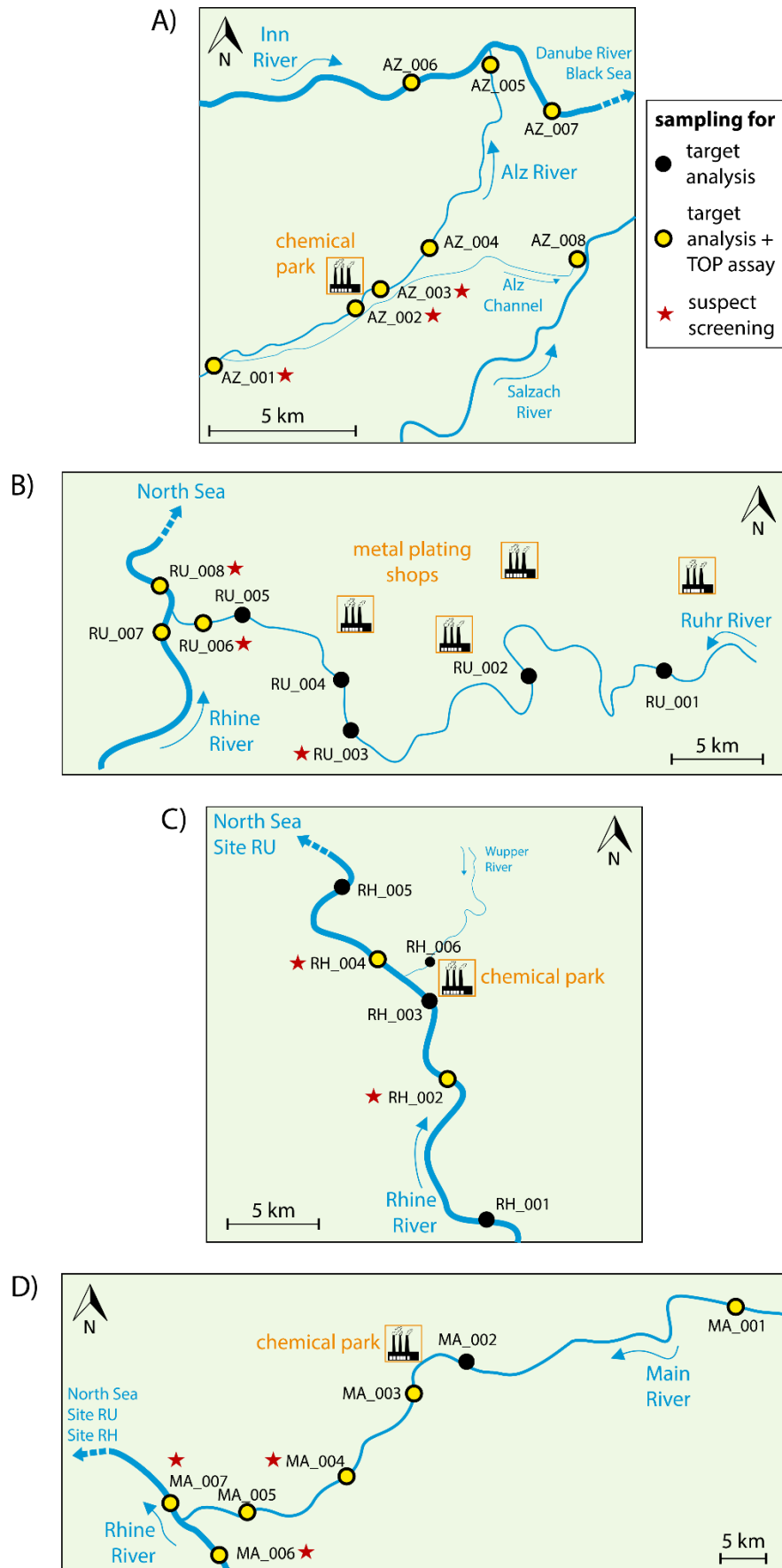


Figure 7.2-2: Sampling site maps of the German sites. A) Site AZ (Alz River, Burgkirchen), B) Site RU (Ruhr River, Ruhr Area), C) Site RH (Rhine River, Cologne/Leverkusen), D) Site MA (Main River, Frankfurt).

7.3 Materials and methods

7.3.1 Sample preparation and instrumental analysis

Based on concentrations reported in previous studies (low ng/L to high µg/L range) [100, 306, 308] and the linear range of the instrument (Chapter 4.3), samples from the different sites were categorized in four categories (Table A.3-3). Accordingly, 1 L river water, 500 mL, 100 mL or 1 mL diluted in 250 mL ultrapure water were used for target analysis. Solid phase extraction (SPE) was performed as described previously (Chapter 10.5.1). Briefly, samples were spiked with internal standards (5 ng each) and loaded onto preconditioned SPE cartridges. The cartridges were dried under vacuum and stored at -20 °C. Up to here, extraction of the German samples took place at HZG, whereas Chinese samples were processed at the Yantai Institute of Coastal Zone Research. The dried cartridges were shipped from China to Germany and all further steps of analysis were performed at HZG. PFASs were analysed by means of LC-MS/MS (Chapter 10.2). The quantification procedure is explained in Chapter 10.7.

The TOP assay was performed according to Houtz and Sedlak [192]. One of the two 125 mL sample aliquots was amended with 2 g potassium persulfate (60 mM) and 1.9 mL of 10 N sodium hydroxide solution (150 mM). The samples were placed in a temperature-controlled water bath at 85 °C for 6 h (20 L Circulation Bath, PolyScience, USA). After cooling them down in an ice bath, the pH of the samples was adjusted to a value between 6 and 8. The oxidized aliquot and a second untreated aliquot were spiked with internal standards (1.5 ng each) and processed using the target analysis method. The difference in concentration of targeted PFASs between the two aliquots gives an estimate of the sum of PFAS precursors in the sample that oxidize to targeted PFASs. The TOP assay for the German river samples was conducted by Thekla-Regine Schramm.

7.3.2 Quality assurance and quality control for target analysis

Due to prior categorization of the samples and extraction of different sample volumes, measured concentrations were mostly within the linear calibration range. If the calibration range was exceeded, the extract was diluted with the sample solvent and measured again. In a few cases, in which concentrations were still above the calibration range, results have to be considered as semiquantitative (marked in Table A.3-10 and Table A.3-11). Absolute recoveries of internal standards are provided in Table A.3-4. As samples from German and Chinese rivers were processed in different laboratories, campaign-specific MDLs and MQLs were calculated. MQLs ranged from 0.017 ng/L (L-FOSA) to 0.33 ng/L (PFBA) in 1 L water samples. Lower sample volumes resulted in correspondingly higher MQLs (Table A.3-5). Relative standard deviations of quantifiable compounds in triplicate samples were below 20 % ($n = 3$).

7.3.3 Quality assurance and quality control for TOP assay analysis

To validate the TOP assay, oxidation tests with model substances were performed, including *n*:2 fluorotelomer precursors (4:2 FTSA and 6:2 FTSA), sulfonamide-containing precursors (*N*-EtFOSAA, *N*-EtFOSE) and ether-based replacement compounds (DONA; HFPO-DA and 6:2 Cl-PFESA). The single compounds were added to ultrapure water at a spiking level of 15 ng/L ($n = 3$) and the TOP assay was performed as described in Chapter 7.3.1. The oxidation tests for the fluorotelomer and sulfonamide-containing precursors were conducted by Thekla-Regine Schramm after implementing three additional precursors in the instrumental method (*N*-EtFOSA, *N*-EtFOSAA, *N*-EtFOSE; Section A.3-1).

Molar conversion yields for the precursors were in good agreement with literature data [192, 199, 316] (Table A.3-6). Upon oxidation of *n*:2 fluorotelomer precursors, a mix of PFCAs was built, whereas PFOA was the prevailing product upon oxidation of sulfonamide-containing precursors. In contrast to the results of Houtz and Sedlak [192], the sulfonamide-containing precursors showed reproducible formation of 3–4 % PFHpA in addition to the major product PFOA. This has also been reported by Martin and co-authors [316].

Interestingly, the fate of the investigated replacement compounds differed from each other. As its predecessor PFOA, the perfluoroalkyl ether carboxylic acid HFPO-DA was stable under TOP assay conditions (Figure 7.3-1). This indicates that the introduction of an ether bond does not improve degradability and the compound represents an additional terminal end product [305]. In contrast, the polyfluoroalkyl ether carboxylic acid DONA and the polyfluoroalkyl ether sulfonic acid 6:2 Cl-PFESA were degraded partially by (78±4) % and (26±7) %. Based on the targeted PFASs in this study, the oxidation products could not be identified. Zhang *et al.* [305] observed perfluoro-3-methoxypropanoic acid (PFMOPrA) as oxidation product of DONA, suggesting that the -O-CHF- moiety is the site of hydroxyl radical attack. In contrast to our observations, 6:2 Cl-PFESA was reported not degradable under TOP assay conditions by Zhang and co-workers [305]. Possible explanations for the different observations are different spiking levels and concentrations of added persulfate. However, in a mechanochemical destruction study by milling with KOH, 6:2 Cl-PFESA also showed better degradability compared to the perfluorinated compound PFOS [317]. Based on observations for additional compounds in their study, the authors concluded that the replacement of one fluorine atom by chlorine rather than the introduction of the ether bond improves the degradability of the molecule [317]. The results from the oxidation tests underline that the TOP assay gives only a minimum estimate of the sum of unknown precursors in a sample because it does not consider not targeted oxidation products and not oxidizable not targeted PFASs.

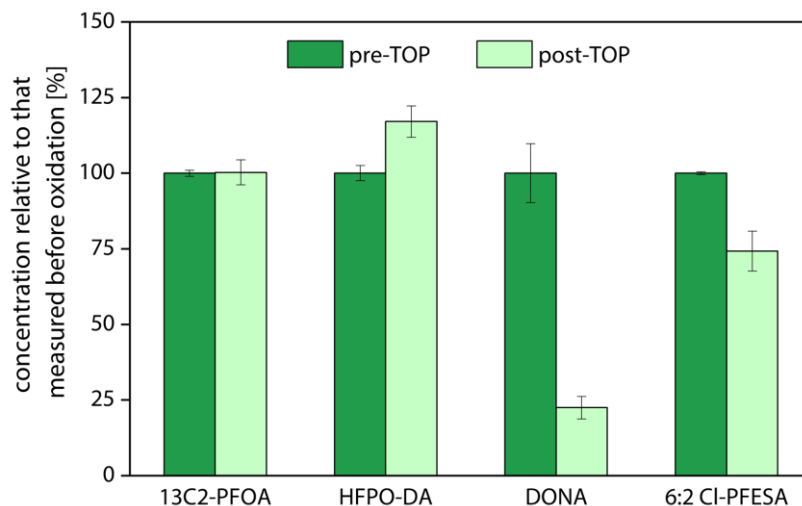


Figure 7.3-1: Fate of ether-based PFASs in the TOP assay, compared to ¹³C₂-PFOA.

Absolute recoveries of internal standards were lower in oxidized sample aliquots compared to unoxidized aliquots (Table A.3-4). This difference has also been reported by Janda [199]. A possible explanation are the sulfate anions in the oxidized aliquots, generated upon oxidation of persulfate, which may compete with the anionic target analytes for ion-exchange sites of the SPE sorbent. In addition, concentrations of particular target analytes (C₄ to C₈ PFCAs, L-PFOS) were higher in oxidized procedural blanks than in unoxidized procedural blanks. Consequently, MDLs and MQLs were calculated separately for oxidized and unoxidized samples. For the German sampling campaign, MQLs were in the range of 0.50 ng/L (PFUnDA) to 2.5 ng/L (L-PFOS) for unoxidized samples and of 0.50 ng/L (PFUnDA) to 7.9 ng/L (PFOA) for oxidized samples (Table A.3-7). Relative standard deviations of quantifiable compounds in both aliquots of triplicate samples were below 20 % for both aliquots ($n = 4$).

7.3.4 Data analysis

PCA was performed with OriginPro 2018 (version 9.5) on the proportions of single PFAS concentrations to the sum of PFASs for comparison of the different source patterns. Eigenvalue decomposition was performed on the correlation matrix of the dataset. Only PFASs with a detection frequency > 40 % were included. Measured values between MDL and MQL were used unaltered for the calculations and results < MDL were considered as $\sqrt{2}/2 \cdot \text{MDL}$.

PFAS mass flow estimates in the respective rivers [t/year] were calculated by multiplying the measured concentration [ng/L] with the mean annual water flow of the river [L/year] and 10^{-15} as conversion factor from ng to t. Water flow data was compiled from public sources for the gauging stations closest to the respective sampling sites (Table A.3-8).

7.4 Results and discussion

7.4.1 PFAS concentrations and composition patterns

24 of the 29 target analytes were detected in the Chinese and/or German river water samples: three ether-based compounds (DONA, HFPO-DA; 6:2 Cl-PFESA), the phosphinic acid 6:6 PFPiA, the cyclic PFAS PFECHS, ten PFCAs (C₄ to C₁₃ PFCAs, including L-/Br-PFHpA and L-/Br-PFOA), four PFSA_s (PFBS, L-/Br-PFHxS, PFHpS and L-/Br-PFOS) and five precursors (4:2, 6:2 and 8:2 FTSA, L-/Br-FOSA and N-EtFOSAA). The sum of these compounds ranged from 2.7 ng/L in the German Alz River upstream of the point source (sample AZ_002) to 420,000 ng/L in the Chinese Xiaoqing River Basin downstream of the point source (sample XQ_007). Results for individual samples are provided in Table A.3-9 to Table A.3-12.

HFPO-DA, used to substitute PFOA in fluoropolymer manufacture [132], was detected in 98 % of all samples. This underlines the widespread use and ubiquitous presence of this compound. In contrast, the occurrence of 6:2 Cl-PFESA was country-specific. While not detected in German river water samples, the compound had a detection frequency of 82 % in Chinese samples. Presumably, this is related to the production and use of F-53B, which contains the potassium salt of 6:2 Cl-PFESA as a major compound and has been applied by Chinese manufacturers as alternative to PFOS salts in metal plating since the 1970s [175]. The compounds DONA, PFECHS and 6:6 PFPiA were predominantly detected in German samples. However, lower detection frequencies in the Chinese samples can result from higher MDLs (Table A.3-5). Of the PFCAs, PFSA_s and their precursors, detection frequencies of ≥ 90 % in samples from both countries were observed for C₄ to C₉ PFCAs, PFBS, L-PFHxS and L-PFOS.

The comparison of PFAS concentrations and patterns before and after the suspected point sources clearly indicated an impact of the source at five of the seven sites, exemplarily shown for sites XQ and AZ in Figure 7.4-1. An exception were the sites at the Yangtze River (site YZ) and the Ruhr River (site RU), where no significant changes in the PFAS concentration and pattern were observed. For site YZ, a strong dilution due to the large river size (mean annual discharge 27,400 m³/s) in combination with an already high PFAS load due to upstream sources [173] may be an explanation. For site RU, the results indicate that major sources are further upstream than suspected.

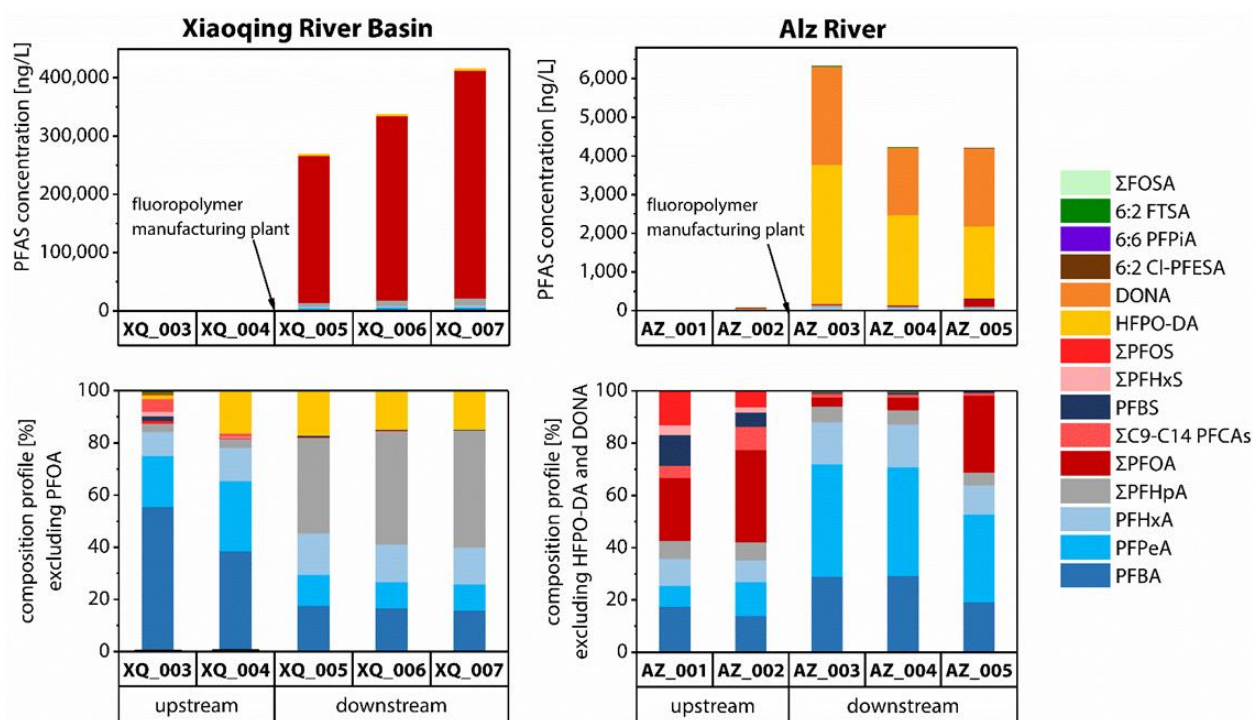


Figure 7.4-1: PFAS concentrations and composition profiles up- and downstream of the point sources at site XQ (Xiaoqing River Basin, Dong Zhulong tributary, Huantai, China) and at site AZ (Alz River, Burgkirchen, Germany). The composition profiles do not include the most dominant compounds (PFOA at site XQ and HFPO-DA and DONA at site AZ).

PFAS composition patterns of the different point sources are compared in Figure 7.4-2. The well-known legacy compound PFOA was the most prevalent substance at the Chinese fluoropolymer manufacturing site XQ, contributing to Σ PFASs with about 90 %. In contrast, its replacement compounds HFPO-DA and DONA were the predominant PFASs close to the German fluoropolymer production facility at site AZ, contributing to Σ PFASs with approximately 50 % and 40 %. This difference between Chinese and German fluoropolymer production sites reflects the geographical shift of production with a phase-out of long-chain PFCAs in Europe and a limited phase-out in Asian countries, such as China [128]. Downstream of the point sources at the Xi River in China (site FX) and the Rhine River in Germany (site RH), the short-chain compound PFBS was the predominant substance with a share of (70 ± 6) %, or respectively (66 ± 8) %. At these sites, pharmaceutical and pesticide intermediates are produced or applied, indicating the importance of short-chain PFASs or their precursors in this industrial branch. This is reinforced by a global market report, according to which the second largest application of PFBS was the use as intermediate in the pharmaceutical industry and the third largest application was the use as insecticides or their manufacture [318]. In comparison to the Lahn River as a River Rhine tributary with little industrial influence (site REF), the Ruhr River was characterized by a higher proportion of 6:2 FTSA (1.1 % of total PFASs versus (14 ± 3) %). This can be related to the hard chrome plating shops located in the highly industrialized Ruhr catchment, where salts of 6:2 FTSA

are typically used to replace PFOS salts as mist suppressants [132]. The Main River (site MA) showed a similar profile compared to site REF, albeit with a marginally higher proportion of PFHxS, PFECCHS, HFPO-DA and 6:6 PFPIA. This may be attributed to the close airport or the chemical park located here. The Yangtze River (site YZ) was characterized by a large contribution of PFOA and PFHxA, with $(40\pm 11)\%$ and $(39\pm 12)\%$.

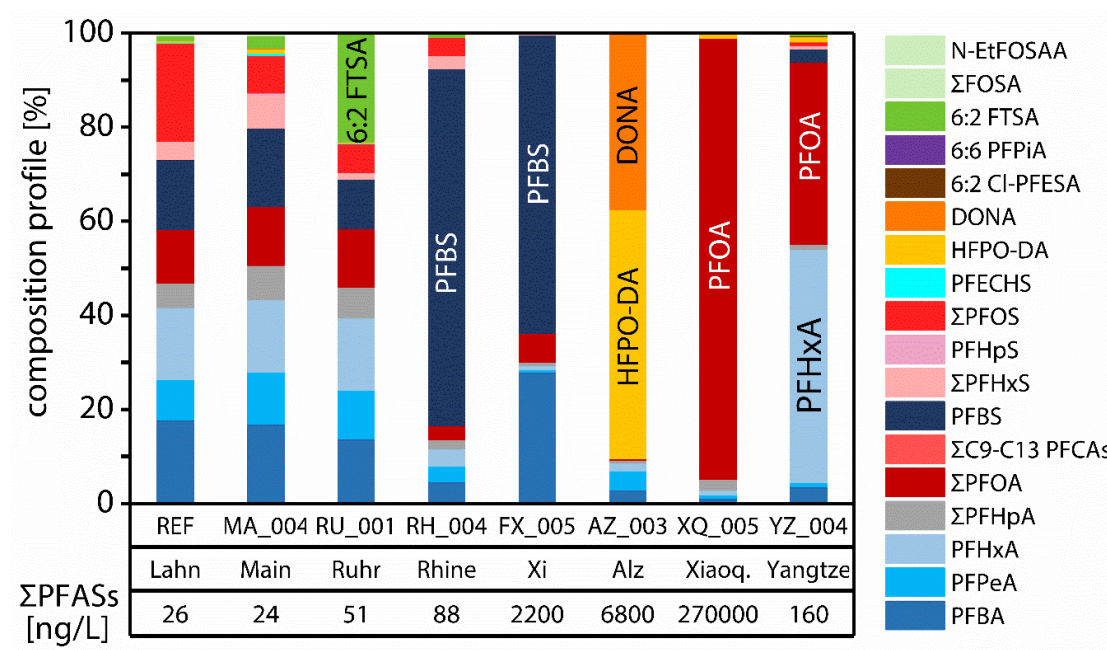


Figure 7.4-2: Contributions of individual PFASs to Σ PFASs in selected samples, downstream of the suspected point sources in the investigated rivers.

7.4.2 Source characterization by principal component analysis

Principal component analysis revealed three distinct groupings of PFASs, explaining 72 % of the variability in river water concentrations. Detailed loadings are provided in Figure A.3-1.

The first component explained 41 % of the variability and included legacy long-chain PFASs other than PFOA (PFNA, PFDA, Σ PFOS, Σ PFHxS and Σ FOSA), as well as the short-chain PFCAs PFPeA and Σ PFHpA. This component separated the German sites at the Rhine River and its tributaries from the Chinese sites and the German site at the Alz River. The second component explained 16 % of the variability and was dominated by the short-chain homologues PFBS and PFBA (with loadings of -0.52 and -0.48) and the ether-based replacements HFPO-DA and DONA (0.47 each). It had high negative scores at the site in the Xi River and high positive scores in the Alz River samples. The third component explained 14 % of the variability and had high negative loadings of PFCAs (PFOA and PFHxA) and the PFOS alternative 6:2 Cl-PFESA. Based on this component, the Xiaoqing River Basin and Yangtze River sites were distinguishable from the other rivers.

The PCA plot (Figure 7.4-3) shows a clear distinction between the samples taken before and after the respective point source for sites AZ, XQ and RH. The closer the upstream samples were taken to the source, the smaller was the variability in PFAS profiles in comparison to the samples taken after the source, shown for site XQ and site AZ in Figure 7.4-3. Upstream samples taken close to the source might be influenced by atmospheric inputs or other ways of PFAS discharge.

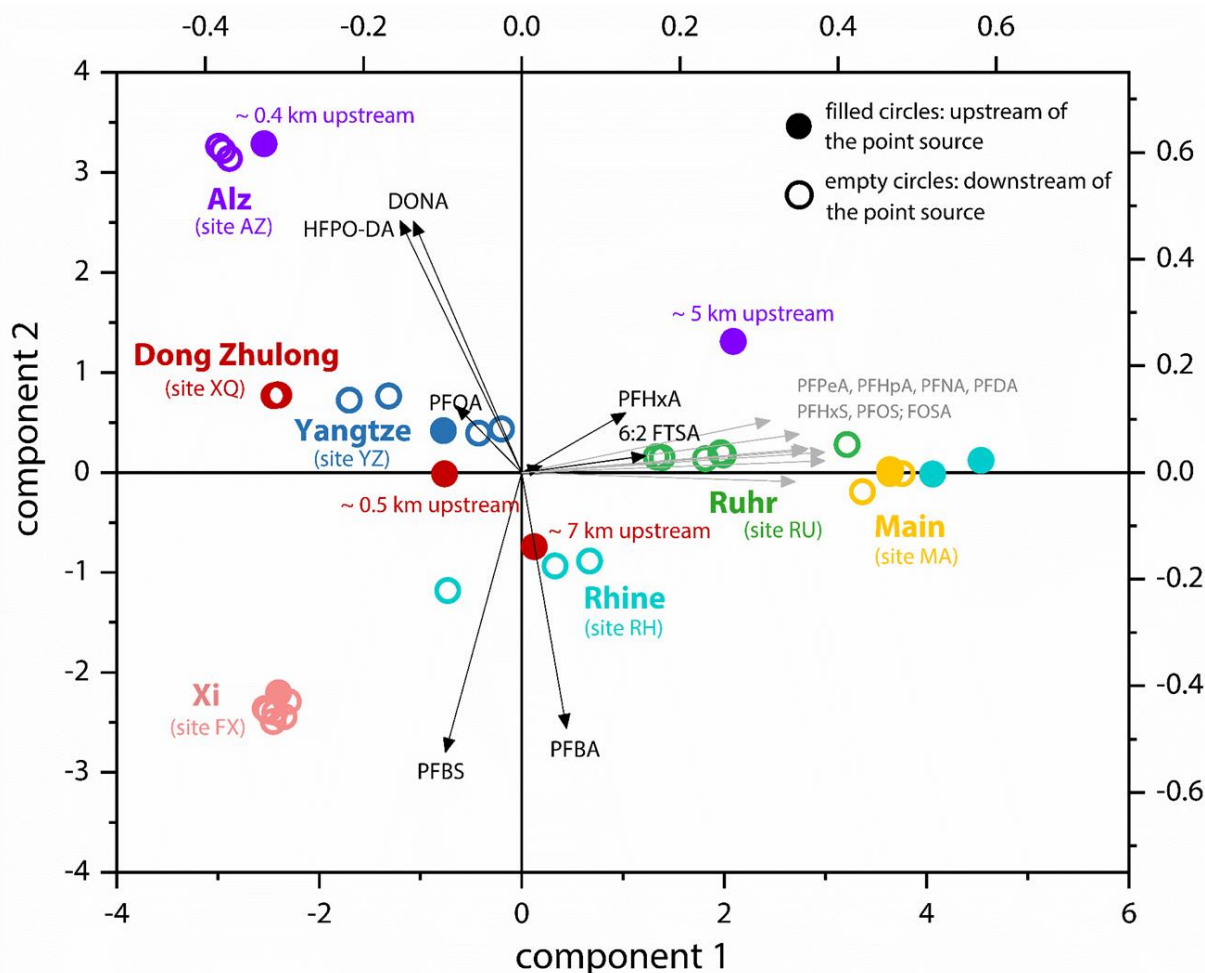


Figure 7.4-3: Results from principal component analysis (PCA) on PFASs measured up- and downstream of the suspected point sources. The figure depicts only samples taken from the rivers at which the point sources were located, not including tributaries. First and second components were plotted against each other and coloured by point source. Dominant compounds for each component are shown as vectors.

7.4.3 Source characterization by isomer profiling

The contribution of branched isomers to the sum of the respective compounds revealed differences between rivers and countries (Table A.3-13). In the German samples, the percentage of the sum of branched PFOS isomers (Br-PFOS) was $(19 \pm 7) \%$ (Figure 7.4-4A). This is in accordance with previous studies in Europe and North America, for example reporting a contribution of 20 % Br-PFOS in Swedish surface waters ($n = 285$) [319]. Although slightly enriched in linear PFOS, this pattern indicates a major contribution from the historical electrochemical fluorination (ECF) manufacturing process by the 3M company, typically yielding

30 % branched isomers [320]. ECF PFOS from major Chinese producers has been reported to contain a similar percentage of branched PFOS (28 to 34 %) [321]. Consequently, a higher proportion of Br-PFOS in the Chinese Yangtze River ((44 ± 12) %) and Xi River ((77 ± 8) %) points to a higher contribution from a different synthesis route, such as telomerization that yields relatively pure isopropyl (branched) or linear isomers [320]. For PFHxS, a similar difference between German rivers and the Xi River was observed. However, the contribution of (21 ± 5) % Br-PFHxS in the Yangtze River was more similar to the German samples (Figure 7.4-4A). This indicates that PFHxS and PFOS in the Yangtze River result from different types of production.

For PFHpA and PFOA, the percentage of branched isomers was higher in the Xiaoqing River Basin and in the Xi River Basin than in the German rivers and the Yangtze River (Figure 7.4-4B). As for PFOS, the percentage of branched isomers in commercial ECF PFOA products from Chinese manufacturers (20–26 %) has been reported to be similar to that of 3M ECF PFOA (22 %) [307, 321]. The contribution of Br-PFOA in the Xiaoqing River Basin ((19 ± 3) %) and Xi River Basin ((20 ± 2) %) was comparable to that of the commercial ECF products, indicating that ECF is the dominant source. The lower percentage of Br-PFOA in the other rivers (9–15 %) can probably be attributed to production of PFOA or fluorotelomer-based precursors by telomerization, yielding linear PFOA and diluting the ECF signature.

A higher proportion of branched isomers in the Chinese environment compared to earlier studies focusing on Europe and North America [320] has also been reported by other authors. This includes PFOA close to fluoropolymer manufacturing plants in the Xiaoqing River Basin (23 % branched) [307] and in the upper Yangtze River (26 % branched) [322] in contrast to the lower Yangtze River (12 % branched) [323]. These findings underline that environmental and human health risks can be underestimated when not considering branched isomers.

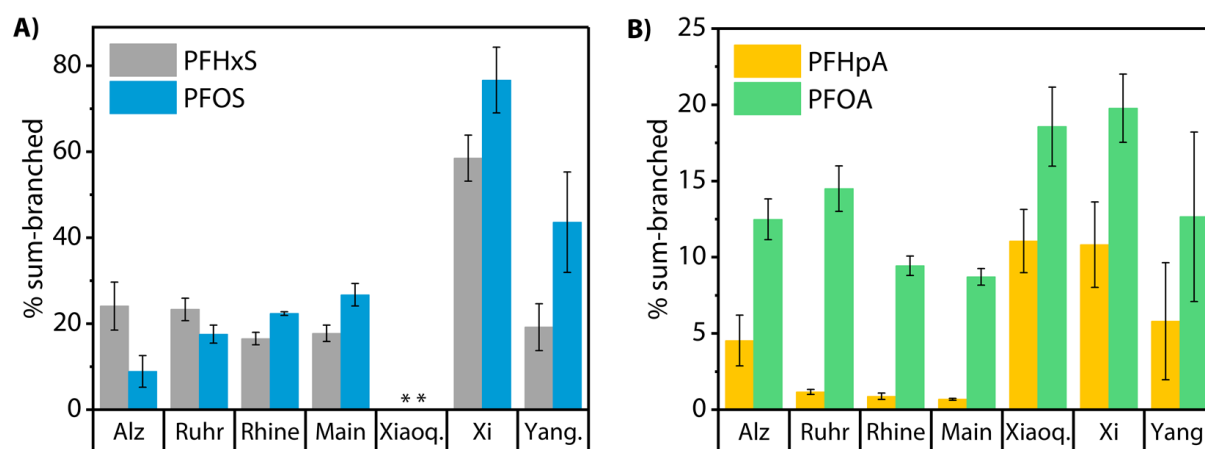


Figure 7.4-4: Percent contribution of the sum of branched isomers A) to total PFHxS and PFOS, and B) to total PFHpA and PFOA in the investigated rivers (mean \pm standard deviation (SD)). **As results of both linear and branched isomers were below MDL in more than 50 % of the samples, no mean values for the Xiaoqing River were calculated for the Xiaoqing River Basin (Xiaoq.) in A).

7.4.4 Contributions of unknown precursors

Upon oxidative conversion, ΣC_4-C_7 PFCAs increased by 18 % to 82 % in German samples (mean \pm SD (59 \pm 19) %) and up to 32 % in Chinese samples ((15 \pm 10) %), varying between countries, sources and individual samples (Figure 7.4-5). In general, a higher increase of the short-chain compound PFBA was observed in German samples with (88 \pm 30) % than in Chinese samples with (12 \pm 14) %. In contrast, PFHpA showed a larger increase in Chinese samples with (21 \pm 15) % compared to German samples with (2 \pm 9) %. This indicates the presence of a higher proportion of precursors to short-chain PFCAs in German rivers and precursors to longer-chain PFCAs in Chinese rivers, reflecting the geographical shift of production.

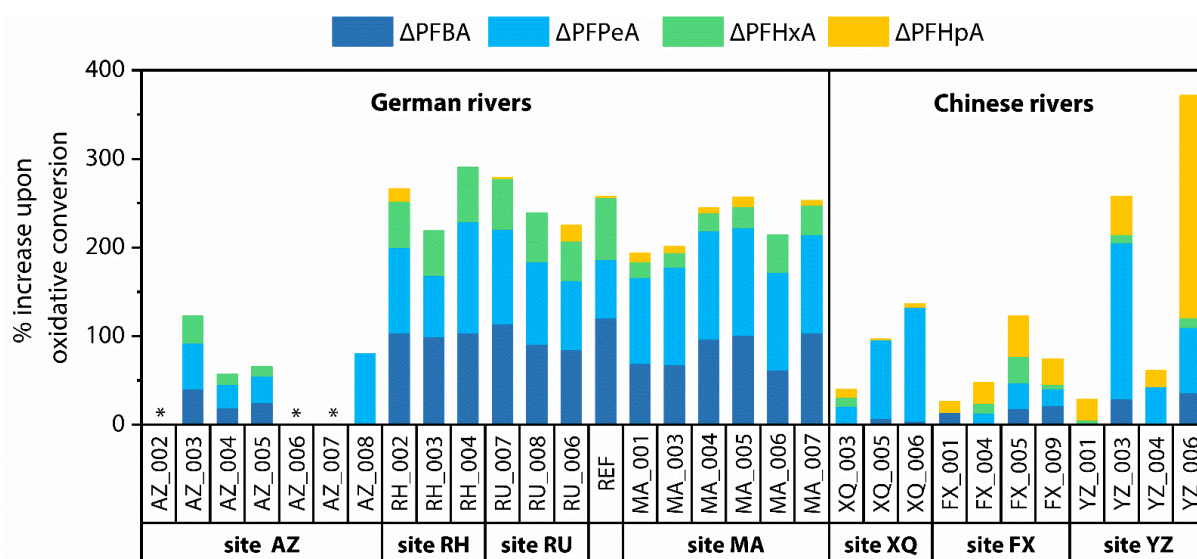


Figure 7.4-5: Percent increase of C_4 to C_7 PFCAs upon oxidative conversion by application of the TOP assay in A) German river water samples and B) Chinese river water samples. * Due to values < MDL, the % increase was not calculated for three samples from the Alz River.

The increase of PFOA was < 25 % in Chinese samples, except for sample YZ_006 with a PFOA increase of 460 % (Table A.3-15). This sample was not taken from flowing river water, but from stagnant, shallow water at the riverside. Possibly, the large difference between the oxidized and unoxidized aliquot of this sample is related to a higher impact of atmospheric sources, including precursors to long-chain PFCAs. Due to the differences between MQLs of oxidized and unoxidized samples (see Chapter 7.3.3 and Table A.3-7), C_8 to C_{10} PFCAs were below MQL in at least one of the sample aliquots in more than 80 % of the German samples. Consequently, this data was not considered for further evaluation. Results for individual samples are provided in Table A.3-14 and Table A.3-15.

In addition to PFCAs, the replacement compound HFPO-DA showed an increase upon oxidation at particular sites. An increase of (23 \pm 9) % was observed in the three Alz River samples

after the point source, in which HFPO-DA was a major compound and occurred in high concentrations ((1100±180) ng/L pre-TOP and (1400±300) ng/L post-TOP in samples AZ_003, AZ_004 and AZ_005). This indicates the presence of unknown ether-based precursors to this compound at one of its manufacturing sites and underlines the significance of HFPO-DA as terminal product.

Of the precursors, 6:2 FTSA was detected in 30 % of the unoxidized samples. It was fully degraded upon oxidation. Based on the molar conversion yields of 6:2 FTSA, determined during validation of the TOP assay (Table A.3-6), the percentage of the increase of C₄ to C₇ PFCA that can be attributed to oxidation of 6:2 FTSA was calculated (Table A.3-16 and Table A.3-17). In the 11 German samples, in which 6:2 FTSA was detected, 97–99 % of the molar increase of C₄ to C₇ PFCA remained unexplained (Figure A.3-2). In the two Yangtze River samples YZ_003 and YZ_004, a comparatively high proportion of 83 % and 29 % of the molar increase of C₄ to C₇ PFCA could be attributed to 6:2 FTSA, pointing to direct emissions of this precursor at the manufacturing site.

As observed in the oxidation tests with model substances, 6:2 Cl-PFESA was degraded partially in the samples by (12±16) %. In contrast, DONA was nearly fully oxidized. As an example, the DONA concentration in the Alz River samples decreased from (740±43) ng/L pre-TOP to (1.8±1.0) ng/L post-TOP. As discussed in Chapter 7.3.3, the oxidation products of 6:2 Cl-PFESA and DONA are not targeted. Consequently, the results of this study underline that the TOP assay gives a minimum estimate for oxidizable precursors and depends on targeted PFASs. The inclusion of oxidation products other than PFCA and of newly identified terminal products such as HFPO-DA can help to capture a larger amount of total PFASs at a specific site.

7.4.5 PFAS mass flow estimates

The mean mass flow estimates for the sum of PFASs varied between 0.03 t/year for the Lahn River as a small River Rhine tributary and 100 t/year for the Yangtze River (mean annual discharge 41 m³/s versus 27,400 m³/s). Estimates for the individual PFASs in the investigated rivers are provided in Table A.3-18. It has to be noted that this calculation is based on a small number samples for each river, taken close to point sources in different distance to the river mouths at one point in time. Mass flows may vary due to discontinuous emissions of PFASs by the industrial plants, variations in water discharge or seasonal trends. Consequently, the provided PFAS mass flows have to be considered as rough estimates.

The sum of the mass flows was highest for PFOA, with major contributions from the Chinese Xiaoqing River (mean 20 t/year) and Yangtze River (43 t/year). This is approximately a factor 250

higher than in the German Rhine River, a major contributor to PFOA discharges from the European continent [77, 310], underlining the significance of Chinese point sources for global PFOA emissions. PFOA mass flows were in the same order of magnitude as calculated in earlier studies for the Xiaoqing River (23–67 t/year) [307] and for the Yangtze River (6.7–26 t/year) [323]. However, the mass flow of PFHxA estimated for the Yangtze River in this study (41 t/year), based on samples from 2018, was considerably higher than estimated total PFHxA discharges from 19 Chinese rivers in 2013, including the Yangtze River (2.2–4.0 t/year) [323]. This finding suggests an increasing relevance of short-chain PFCAs in China.

Compared to PFOA and PFHxA, the mass flows of the short-chain compound PFBS in the German Rhine River had a higher share of total PFBS transported by the investigated rivers. Although the mean annual discharge of the Rhine River is only about 6 % of that of the Yangtze River, the PFBS mass flow in the Rhine River (2.3 t/year) was approximately half of that in the Yangtze River (4.3 t/year) [323]. Möller and co-authors [161] estimated a PFBS mass flow of 5.1 t/year for the Rhine River based on samples taken at similar sampling locations in 2008. This indicates ongoing emissions from the point source at site RH for more than ten years.

With respect to the ether-based PFASs, mass flows of HFPO-DA were in the same range in the Yangtze River, Xiaoqing River and the small German Alz River (0.9, 0.3 and 0.4 t/year), whereas the Alz River was the dominant contributor for DONA (0.4 t/year) and the Yangtze River for 6:2 Cl-PFESA (0.2 t/year).

The increase of C₄–C₇ PFCAs upon oxidative conversion in the TOP assay (Figure 7.4-5) indicates that riverine discharge derived from conventional target analysis reveals only part of the PFASs present in a sample which can ultimately be transformed to endpoint PFASs of concern during the compounds' transport from the rivers to the seas and further to remote areas.

7.5 Summary and conclusion

In this study, river water samples from China and Germany as countries with different histories of PFAS production were compared. Samples were collected up- and downstream of seven suspected point sources in autumn 2018. The analysis of 29 legacy and emerging PFASs revealed source- and country-specific PFAS fingerprints. 24 PFASs were detected, with a sum ranging from 2.7 ng/L (Alz River) to 420,000 ng/L (Xiaoqing River). While mass flow estimates for the Xiaoqing River and Yangtze River (mean 20 and 43 t/yr) indicate ongoing high emissions of the legacy compound PFOA in China, its ether-based replacements HFPO-DA and DONA showed the highest contribution downstream of a German fluoropolymer manufacturing site (50 % and 40 % of Σ PFASs).

HFPO-DA as one of the replacement compounds for PFOA in fluoropolymer production was detected in 98 % of the samples in this study, with highest concentrations close to a German fluoropolymer manufacturing site. As PFOA has been recently added to the Stockholm Convention [122], it can be expected that major producers in continental Asia will reduce emissions of PFOA and its precursors in the foreseeable future [4]. Although HFPO-DA is not as well-studied as PFOA, several studies indicate that it has similar properties and can be considered as a “regrettable substitute” to PFOA [169-171]. In order not to repeat the industrial transition from PFOA to HFPO-DA, which has been taking place in Europe and North America since the 2000s, in continental Asia, the evaluation and regulation of HFPO-DA and other replacements on an international level is essential.

In river water impacted by manufacturing sites for pharmaceutical and pesticide intermediates, the short-chain compound PFBS was the most prevalent substance in both countries. Receiving discharges from electroplating industry, the German Ruhr River was characterized by the PFOS replacement 6:2 FTSA.

Isomer profiling revealed a higher proportion of branched isomers in the Chinese Xi River and Xiaoqing River than in other rivers. This points to different synthesis routes and underlines the importance to include branched isomers in risks assessments. Upon oxidative conversion in the total oxidizable precursor (TOP) assay, the increase of the short-chain compound PFBA was higher in German samples than in Chinese samples ((88±30) % versus (12±14) %), suggesting the presence of a higher proportion of unknown precursors to short-chain compounds in the German environment. Of the ether-based replacements, HFPO-DA showed an increase upon oxidation at particular sites, whereas DONA and 6:2 Cl-PFESA were fully or partially degraded to not targeted oxidation products. This indicates that the inclusion of ether-based PFASs and their oxidation products in the TOP assay can help to capture a larger amount of the unknown PFAS fraction.

Both the higher percentage of branched isomers at Chinese sites compared to German rivers and the increase of target analytes upon oxidative conversion in the TOP assay underline the limitations of conventional target analysis. Dependent on the type of point source and the spectrum of target analytes, human and environmental health risks may be considerably underestimated, when analysing only a small proportion of the PFASs on the worldwide market. Although the TOP assay is a more inclusive method, it still depends on targeted PFASs and only gives a minimum estimate of the unknown oxidizable precursors present in an environmental sample. To obtain a more comprehensive view, target analysis and TOP assay can be complemented with a more inclusive sum parameter, such as the extractable organic fluorine (EOF) assay [181], and HRMS-based approaches to elucidate the composition of the unknown fraction.

8. Discovery of Emerging and Novel Per- and Polyfluoroalkyl Substances in Chinese and German River Water Using a Suspect Screening Approach

The concentration increase of target analytes upon oxidative conversion in the TOP assay (chapter 7) indicated the presence of a fraction of unknown precursors in the samples. To elucidate the composition of the latter and identify novel PFASs of potential environmental relevance, this study aimed at performing an HRMS-based suspect screening of PFASs, which are on the global market and listed in public databases. Based on the Chinese and German river water samples impacted by point sources, the objectives of the study were i) to develop a workflow for post-acquisition data treatment, including the creation of a PFAS suspect list, ii) to perform a PFAS suspect screening, to evaluate the tentative candidates and to assign them to confidence levels, and iii) to compare source fingerprints of the tentatively identified emerging and novel PFASs.

The study was conducted during a two-month research stay at the Swedish University of Agricultural Sciences (SLU), Department of Aquatic Sciences and Assessment, Uppsala, Sweden under supervision of Ass. Prof. Lutz Ahrens and Frank Menger (01/04/2019 to 26/05/2019).

A manuscript on the study is in preparation for submission to the peer-reviewed journal *Environmental Science and Technology*.

8.1 Materials and methods

8.1.1 Sample preparation and instrumental analysis

The suspect screening was performed in river water samples from 22 of the 59 sampling stations selected for target analysis. These included samples from all seven study sites, take up- and downstream of the suspected point sources. Study sites and sample collection are described in Chapters 7.1 and 7.2. Triplicates of 500 mL filtered samples were adjusted to pH 6.5 with formic acid and spiked with a mixture of internal standards (2.5 ng each). Sample extraction and measurement were conducted according to an established method at the Swedish University of Agricultural Sciences [324]. To achieve enrichment for a broad range of PFASs, mixed-bed SPE cartridges were prepared in-house, containing four sorbents with different properties. The sample extracts were analysed by means of an ultraperformance liquid chromatography (UPLC) system (Acquity H-Class with FTN injector, Waters, USA) coupled to a quadrupole time-of-flight (QToF) mass spectrometer (Xevo G2-S, Waters, UK). Negative electrospray ionization was used as ionization technique. The mass spectrometer was operated in MS^E mode, a data-independent acquisition mode that alternates between low and high collision energy scans throughout the acquisition period. Full-scan MS and MS/MS data was acquired in a single run and without the preselection of precursor ions. For the

first scan function, the collision energy was set to a low value of 4 eV, enabling collection of mass spectrometric data on the precursor ions in the sample. For the second scan function, the collision energy was ramped from 10 eV to 40 eV, allowing the collection of mass chromatograms with fragment ion information [325]. A detailed description of sample preparation and instrumental analysis is provided in Chapters 10.5.3 and 10.2.2.

8.1.2 Quality assurance and quality control

Extraction of the river water samples from German rivers took place at HZG, whereas Chinese samples were processed at the Yantai Institute of Coastal Zone Research. Consequently, triplicates of 500 mL ultrapure water were processed as blank samples in both laboratories.

Calibration of the mass axis from m/z 50 to 1200 was conducted before the measurement with a 0.5 mM sodium formate solution prepared in 90:10 (v/v) isopropanol/water. In addition to the sample eluent from the LC, a reference solution containing leucine enkephalin (m/z 236.1041 and 554.262) was constantly infused into the ion source via a second sprayer. Separated from the sample spray by an oscillating baffle, this “lockspray” was introduced into the mass spectrometer every 10 s. The software uses the lockspray data to calculate a correction factor for the mass-scale calibration, which is then applied to the sample data, providing accurate mass information [326]. Settings for the lock spray infusion are provided in Table 10.2-7.

8.2 Development of a workflow for post-acquisition data treatment

While the untargeted data acquisition by LC-QToF-MS^E and comparable HRMS-based techniques offers various advantages, sophisticated data processing workflows have to be developed to handle the wealth of data and to extract the significant information. For this, the instrument manufacturer’s software or open-source software can be used. To use open-source algorithms, having the advantages of free availability and comparability across different instrument platforms, the vendor-specific binary raw data files have to be converted to open-format files, such as mzML [327].

The vendor’s software Unifi Scientific Information System, version 1.9.4 (Waters, USA) was used for acquisition, processing and evaluation of the data. Post-acquisition data treatment was based on the generic workflow published by Krauss *et al.* [193] and adapted in regard to the possibilities and limitations of the Unifi software as well as the characteristics of PFASs. A schematic overview of the workflow is given in Figure 8.2-1. The individual steps are explained in the following.

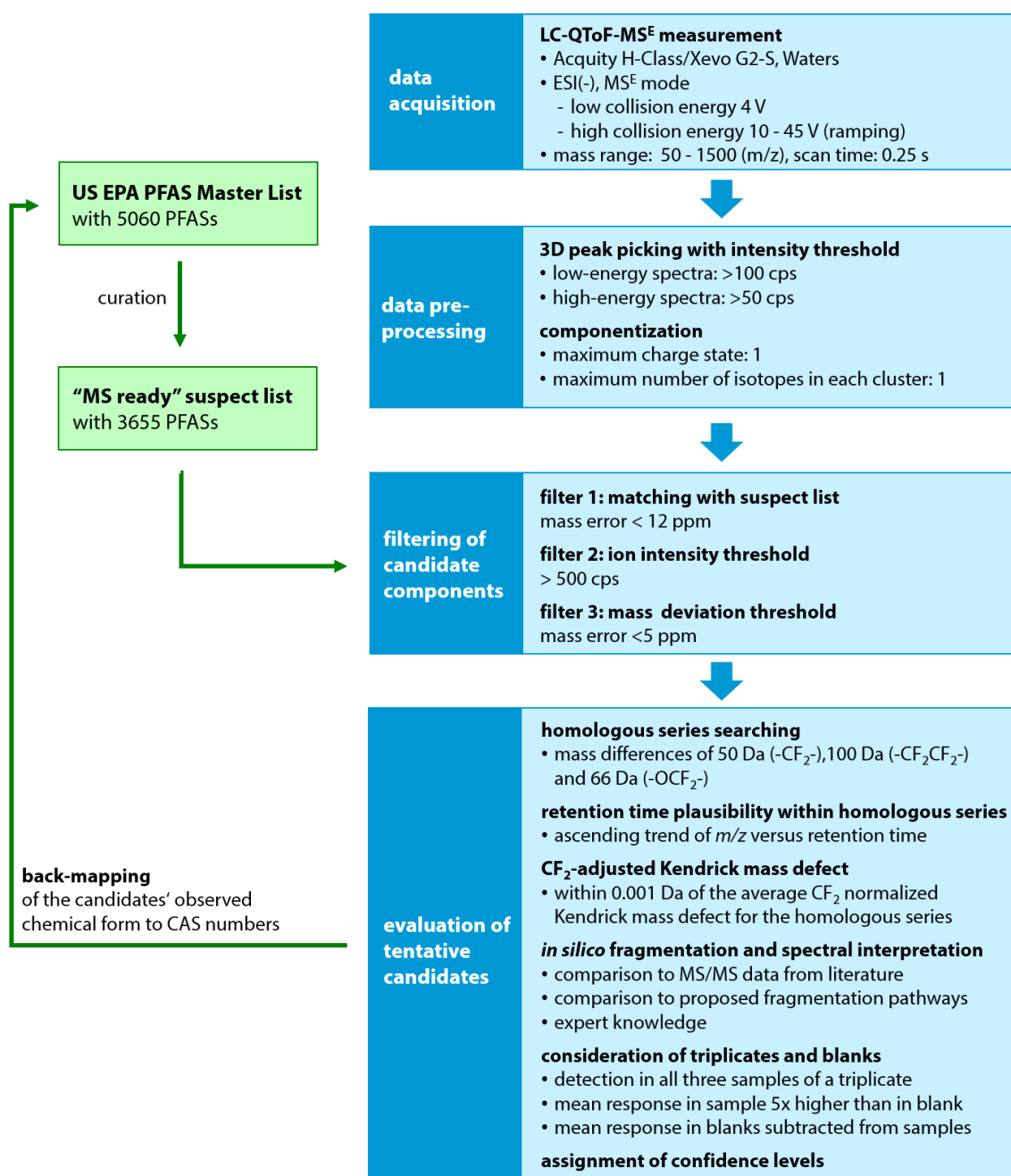


Figure 8.2-1: Developed PFAS suspect screening workflow using the Unifi software.

8.2.1 Data pre-processing

Peak picking. To convert the raw data into a list of detected peaks, Unifi uses the *Apex* peak picking algorithm, detecting the peak apexes of all the ion responses based on their three-dimensional peak shape. As an example, the full-scan continuous data of a river water sample is shown in three dimensions in Figure 8.2-2A and B. The peak apexes correspond to the dots overlaid on the data in Figure 8.2-2C. Each dot represents a single ion, which is characterized by a unique m/z -retention time pair, together with a measure of intensity, derived from the peak height [328]. In this study, the minimum intensity for peak picking was set to 100 counts for low-energy spectra and 50 counts for high-energy spectra.

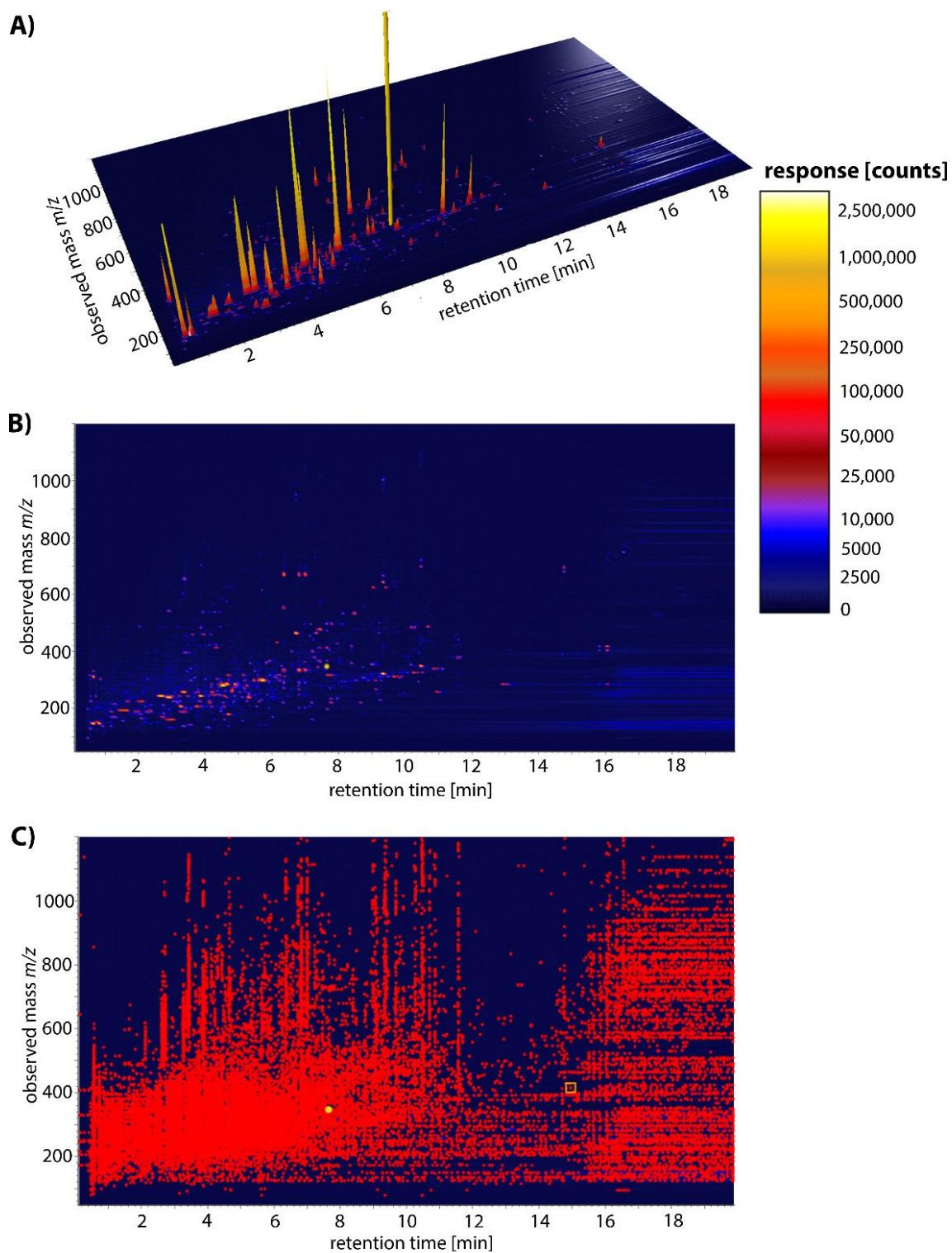


Figure 8.2-2: Peak picking in three-dimensional full-scan continuous data (low-energy function) of a river water sample (Fuxin River, FX_009). The red dots overlaid on the data in C) correspond to the peak apexes of the data shown in A) and B).

Componentization. In a next step, Unifi automatically organizes the single ions into “candidate components”. All ions detected in the low-energy data can be candidate components, with exception of those that are classified as isotopes of other ions. Associated with each candidate component is a low-energy spectrum and high-energy spectrum, containing ions with a peak apex at the same retention time as the candidate. In this study, the maximum charge state to consider for componentization was set to 1 and the maximum number of isotopes allowed in each cluster was limited to 2.

After data pre-processing including peak picking and componentization, Unifi provides a table with the candidate components and the associated spectra in a pane that allows review and filtering of the generated metadata.

8.2.2 Creation of a PFAS suspect list

To find the proverbial needle in a haystack, this study aimed at performing a PFAS suspect screening, i.e. screen the thousands of candidate components revealed by raw data processing against a database of known PFASs. Over the last years, several public lists of PFASs on the global market have become available. In 2015, a PFAS list with 2,396 compounds was published in a report by the Swedish Chemical Agency KEMI [329] and an international community-compiled list including 592 substances was made publicly available by Xenia Trier and colleagues [330]. In 2018, the OECD released a New Comprehensive Global Database of Per- and Polyfluoroalkyl Substances (PFASs), listing 4,730 PFAS-related CAS registry numbers [3]. A major effort was undertaken by researchers of the US EPA to curate and structure-annotate the various PFAS lists and compile a consolidated “PFAS Master List”, publicly accessible via the US EPA CompTox Chemicals Dashboard since August 2018 [331]. In addition to the three international lists, the researchers took four US EPA PFAS lists as a basis, as shown in Table 8.2-1.

The PFAS Master List is undergoing further curation and updated regularly by the US EPA researchers. When downloaded for this study in April 2019, it included 5060 entries. In addition to the chemical name of the substances, the downloaded Excel file contained the CAS number, the molecular formula and the chemical structure in the form of a line notation according to the simplified molecular-input line-entry system (SMILES), if available.

To use it as a suspect screening list for HRMS data, the downloaded list had to be further curated. List entries without CAS number and without a defined chemical structure (SMILES string) were removed because a defined chemical structure is needed to identify a compound by suspect screening. Only six list entries did not have a CAS number, but 1070 entries with CAS numbers did not have a defined chemical structure. These included polymers, such as PTFE (CAS number: 9002-84-0), and ill-defined reaction products, such as the “reaction product of potassium acrylate with 1-perfluoro[*n*-alkyl(C6,8,10,12,14,16,18)]-2-iodoethane” (CAS number: 509086-57-1).

Table 8.2-1: Compilation of US EPA PFAS Master List as it was made accessible in 2018. International lists that were taken as a basis are marked in blue, whereas US EPA lists are marked in green. The numbers given in red refer to the number of PFASs in the respective list, whereas the numbers below indicate how many of these PFASs are also included in the other lists. Redrawn from Sams et al. [332].

PFAS Master List with 5060 total unique substances <i>compiled from</i>	PFAS_OECD	PFAS_KEMI	PFAS_TRIER	EPAPFAS_RL	EPAPFAS_INV	EPAPFAS_INSOL	EPAPFA_S75S1
PFAS_OECD ¹	4,730						
PFAS_KEMI ²	2206	2,396					
PFAS_TRIER ³	493	578	592				
EPAPFAS_RL ⁴	132	116	71	199			
EPAPFAS_INV ⁵	309	324	226	61	430		
EPAPFAS_INSOL ⁶	43	42	24	12	0	43	
EPAPFAS_75S1 ⁷	51	47	38	25	74	0	74

¹OECD New comprehensive global database of PFASs [3]

²Swedish Chemical Agency KEMI report [329]

³community effort [330]

⁴EPAPFAS_RL: EPA research list compiled from various sources [332]

⁵EPAPFAS_INV: DMSO-solubilized PFASs in US EPA's ToxCast inventory [332]

⁶EPAPFAS_S75S1: prioritized subset of the PFASs in the ToxCast inventory [332]

⁷EPAPFAS_INSOL: PFASs procured, but found to be insoluble in DMSO by EPA [332]

For additional curation, it had to be considered that the PFAS form in the database does not match the form observed by the analyst. In databases, PFASs are typically represented in their neutral forms, as a part of a chemical mixture, and as multicomponent salts [333]. As an example, perfluoroheptane sulfonic acid (PFHpS, C₇HF₁₅O₃S) was also listed as its potassium, ammonium, bis(2-hydroxyethyl)ammonium and lithium salt in the US EPA PFAS Master List. Via HRMS, the compound is generally observed as a negatively charged *m/z* feature (C₇F₁₅O₃S) and based on this, the software automatically calculates the neutral monoisotopic mass. To create an “MS ready” list, non-PFAS counterions of the salts included in the PFAS Master List were removed and the remaining charged structures were neutralized. Of mixtures, the non-PFAS component was excluded. If mixtures contained more than one PFAS component, they were separated into individual components. Based on the resulting SMILES strings, duplicates were removed. To stay with the example of PFHpS, only one entry was included for the compound in the final list, because removal of counterions and neutralization of the structure resulted in the same SMILES string for the multiple salts. After this curation, the “MS-ready” Excel list included 3655 substances.

As a last step, .mol files of each compound of interest were generated using the software Marvin (ChemAxon). This chemical structure file format was required to import the compound structures into a scientific library in the Unifi software, which was used as a suspect list to screen the candidate

components for PFASs. The workflow for creation of the PFAS suspect list is summarized in Figure 8.2-3.

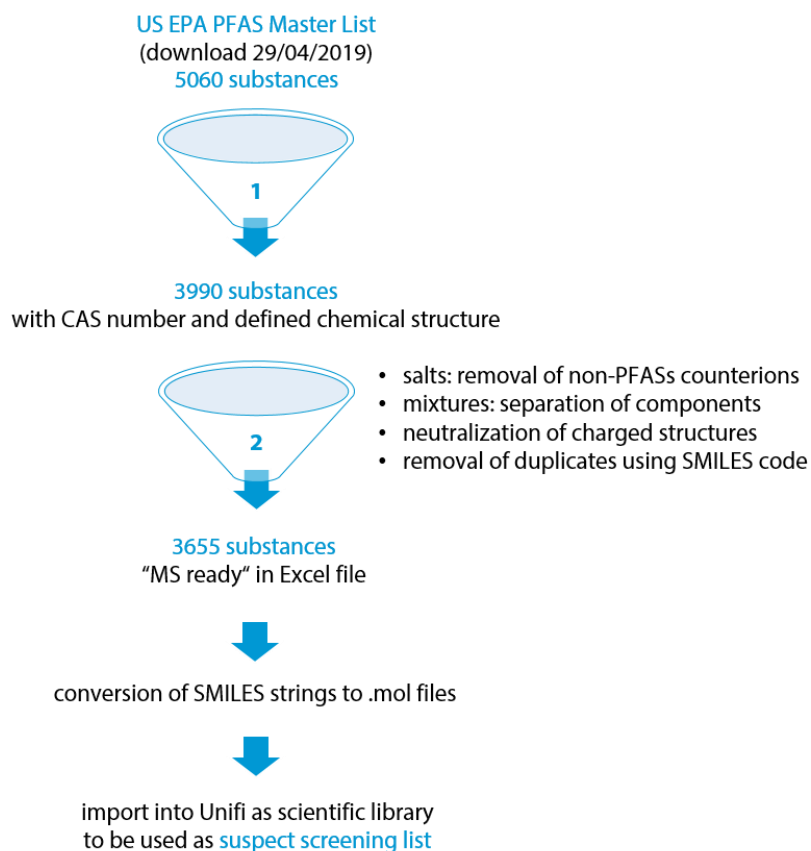


Figure 8.2-3: Workflow to create an “MS-ready” suspect list based on the “PFAS Master List” from the US EPA chemical database.

8.2.3 Suspect screening and reduction of components

The componentized LC-QTOF-MS^E data can be interrogated using filters within the Unifi review pane. Filters are flexible, automatic criteria that are user-defined and applied on top of the componentized data. As a combination of filter steps creates the workflow, no data is completely removed, but it is simply filtered out. The data can be reviewed with modified filters at a later point in time, for instance in regard to a new research objective [334].

The first filter was set to display only the components that match substances from the PFAS suspect screening list. For this, default screen settings for targeting candidate components by mass were used, including a precursor ion mass match tolerance of 12 ppm. To further refine these criteria, a second filter was applied to review only the candidate components with a peak intensity > 500 counts and a third filter to narrow the components down to those with a precursor ion mass error < 5 ppm.

8.2.4 Evaluation of the candidate components

Following the first reduction of components, the resulting candidate components were further evaluated to reject or confirm a compound's tentative identity. For this, data was analysed based on the distinct characteristics of PFASs.

Homologous series searching. PFASs were and are still manufactured as mixtures containing series of compounds which possess the same polar headgroup (or other shared structural features), but have a different carbon chain length. These homologous series of PFASs are classified by repeating units of 49.9997 Da ($-\text{CF}_2-$) for ECF-based PFASs, by 99.9936 Da ($-\text{CF}_2\text{CF}_2-$) for fluorotelomer-based PFASs or by 65.9917 ($-\text{OCF}_2-$) for polyether-based compounds [335]. The list of candidate components was searched manually for these mass differences to identify potential PFAS homologue series. The tentatively identified PFAS series were classified and named according to the OECD global PFAS database [3].

Retention time plausibility. On a reversed-phase chromatographic column, the retention time typically increases with increasing chain length in a homologue series. Consequently, it was evaluated if the elution order and retention time increase was consistent within a tentatively identified homologous series.

CF_2 normalized Kendrick mass defect. The mass defect is the difference between the nominal and exact mass of an atom or molecule. While the commonly used mass scale of the International Union of Pure and Applied Chemistry (IUPAC) is based on carbon (^{12}C) having an exact mass of 12.00000 Da, Edward Kendrick suggested a mass scale based on $^{12}\text{CH}_2 = 14.00000$ Da (instead of 14.01565 Da on the IUPAC scale) in 1963 [336]. As homologues differing by CH_2 have the same mass defect on the Kendrick scale, homologous series can be easily identified in high resolution mass spectrometric data using the Kendrick mass scale. This approach has been transferred to PFAS analysis by Myers *et al.* [337], using a mass scale based on $^{12}\text{CF}_2 = 50.00000$ Da to identify homologous series of fluoropolymer thermal decomposition products. The CF_2 normalized Kendrick mass defect of the observed masses in our study was calculated accordingly (Equations 8.1 and 8.2).

$$\text{mass}(\text{CF}_2 \text{ scale}) = \text{mass}(\text{IUPAC}) \cdot \frac{\text{nominal mass}(\text{CF}_2)}{\text{exact mass}(\text{CF}_2)} = \text{mass}(\text{IUPAC}) \cdot \frac{50.00000}{49.99681} \quad (8.1)$$

$$\text{mass defect}(\text{CF}_2 \text{ scale}) = \text{mass}(\text{CF}_2 \text{ scale}) - \text{nominal mass}(\text{rounded down}, \text{CF}_2 \text{ scale}) \quad (8.2)$$

Not to split homologous series with mass defects close to 1 by rounding, 1 was added if the mass defect (CF_2 scale) was below 0.1 [338].

To use the characteristic mass defect as an additional identification criterion, it was verified if the CF₂ normalized Kendrick mass defect of a compound within a homologous series fell within 0.001 Da of the average CF₂ normalized Kendrick mass defect for the given homologous series.

***In silico* fragmentation and spectral interpretation.** The fragmentation pattern of the candidate components was evaluated and compared within the homologous series. Unifi automatically applies an *in silico* “chopping” bond disconnection algorithm (MassFragment) to the molecular structures uploaded as suspect screening list. In contrast to rule-based fragmentation spectrum prediction, the bond disconnection algorithm is based on combinatorial fragmentation [339]. Using this approach, Unifi takes the structure of a molecule, “chops” the chemical bonds and calculates the exact mass of the resulting substructures. The m/z values of the substructures are then compared to the m/z values of ions in the high-energy data to verify if there are ions corresponding to the *in silico* postulated fragments.

This bond disconnection approach was shown to give a smaller number of false negatives than rule-based approaches in a previous study [339], as rule-based algorithms only propose fragmentation reactions that have been programmed into the system. However, the number of false positives is typically higher using bond disconnection algorithms compared to rule-based algorithms [339]. To minimize the number of false positives, Unifi requires that apexes of any fragment have to have the same retention time as the apex of the precursor ion, as is the case with spectra associated to components [328]. The mass deviation from measured and theoretical fragment mass was limited to 4.0 mDa.

Fragmentation mechanisms using negative electrospray ionization are generally not as well understood as those occurring by positive electrosprays ionization. For this reason, rule-based algorithms have been reported not to be useful for interpretation of PFAS fragments measured in negative electrospray ionization mode [335]. Thus, fragments proposed by Unifi’s *in silico* fragmentation, were manually interpreted based on comparison to MS/MS data from literature, proposed fragmentation pathways for PFASs and classical mass fragmentation theory. Fragmentation patterns of the different homologues in a series were compared to identify characteristic fragments.

Consideration of triplicates and blanks. The list with the remaining candidate components was exported from Unifi as an Excel file. Using an R script, only the candidate components that had been detected in all three samples of a triplicate were kept. Moreover, the mean response in a sample triplicate had to be at least 5-fold higher than the mean response in a blank to consider the compound as identified in the sample. The peak areas in the samples were blank-corrected by subtracting the mean response of a candidate component in the blank triplicate from the mean response in the sample triplicate.

Assignment of identification confidence levels. Based on the collected evidences, the compounds' identity was classified at different identification confidence levels based on the scheme proposed by Schymanski *et al.* [340]. Confidence levels range from 1 to 5, where 1 is the highest level of confidence and 5 is the lowest level of confidence. Level 1 represents structures which have been confirmed via reference standards (“certain identification”), level 2 represents probable structures with matching literature or library spectra or diagnostic evidence (“probable identification”) and level 3 represents tentative candidates for which a possible structure can be proposed, but there is insufficient information to assign one exact structure (“tentative identification”). Levels 4 and 5 are assigned if only an unambiguous molecular formula or an exact mass of interest exists, respectively [340].

In this study, subcategories of the levels were defined based on the characteristic properties of PFASs. At level 1, the structure of the compound was confirmed by internal standards or target analysis. At level 2, retention time increased with increasing chain length within the homologous series, a common CF₂ normalized Kendrick mass defect was observed and characteristic fragments matched literature spectra. If at least one of the homologues within the series was confirmed at level 1, other members of the series which fulfilled the named criteria were assigned level 2a. If at least one of the homologues within the series was confirmed by an authentic standard in an earlier study, members of the series were assigned level 2b. At level 3 the criteria listed for level 2 were fulfilled, but insufficient information for one structure only was available (for example for positional isomers). If there was a matching library spectrum, level 3a was assigned, and if no reference spectrum was available in literature, level 3b was assigned.

8.2.5 Back-mapping to the original database

As a last step of data evaluation, the observed chemical form of the tentatively identified PFASs was linked back to its entries within the original US EPA PFAS Master List, such as salts and mixtures with different CAS numbers. This back-mapping is essential to not only report the substances observed by HRMS in environmental samples, but to also identify potential sources based on the chemical forms of the substances available in commerce and used in consumer products.

8.3 Results and Discussion

8.3.1 Peak picking and componentization

Using the Unifi algorithms, peak picking and componentization revealed 14,676 to 40,880 components per sample before application of the PFAS suspect list (Figure 8.3-1).

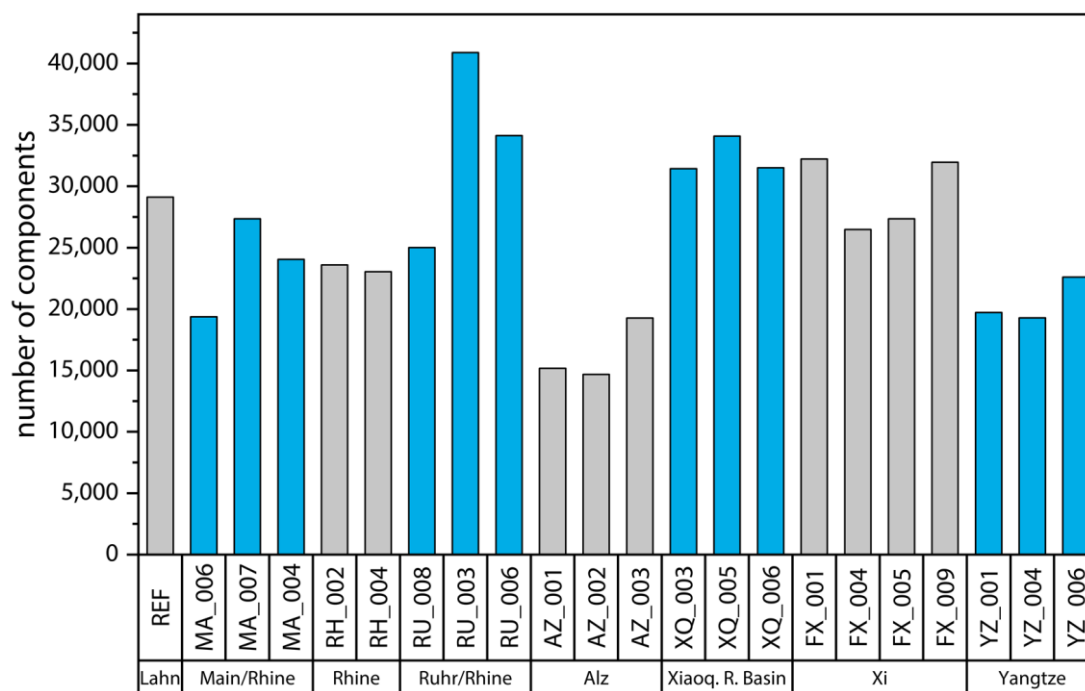


Figure 8.3-1: Number of components listed by Unifi after peak picking and componentization in analysed samples. Only the results for the first sample of each triplicate are shown. The grey and blue colour is used to visually distinguish the samples from different sites.

Even without filtering the components to focus on PFASs, a comparison of the three-dimensional peak overview showed obvious differences between samples taken up- and downstream of point sources and between samples from different rivers. This is exemplified in Figure 8.3-2 for samples taken up- and downstream of the fluorochemical parks at the rivers Alz and Dong Zhulong (Xiaoqing River Basin). The three-dimensional plots of the full-scan continuous data in the downstream samples (B and D) show series of masses differing by the same mass and increasing in retention time with increasing mass, pointing to homologous series.

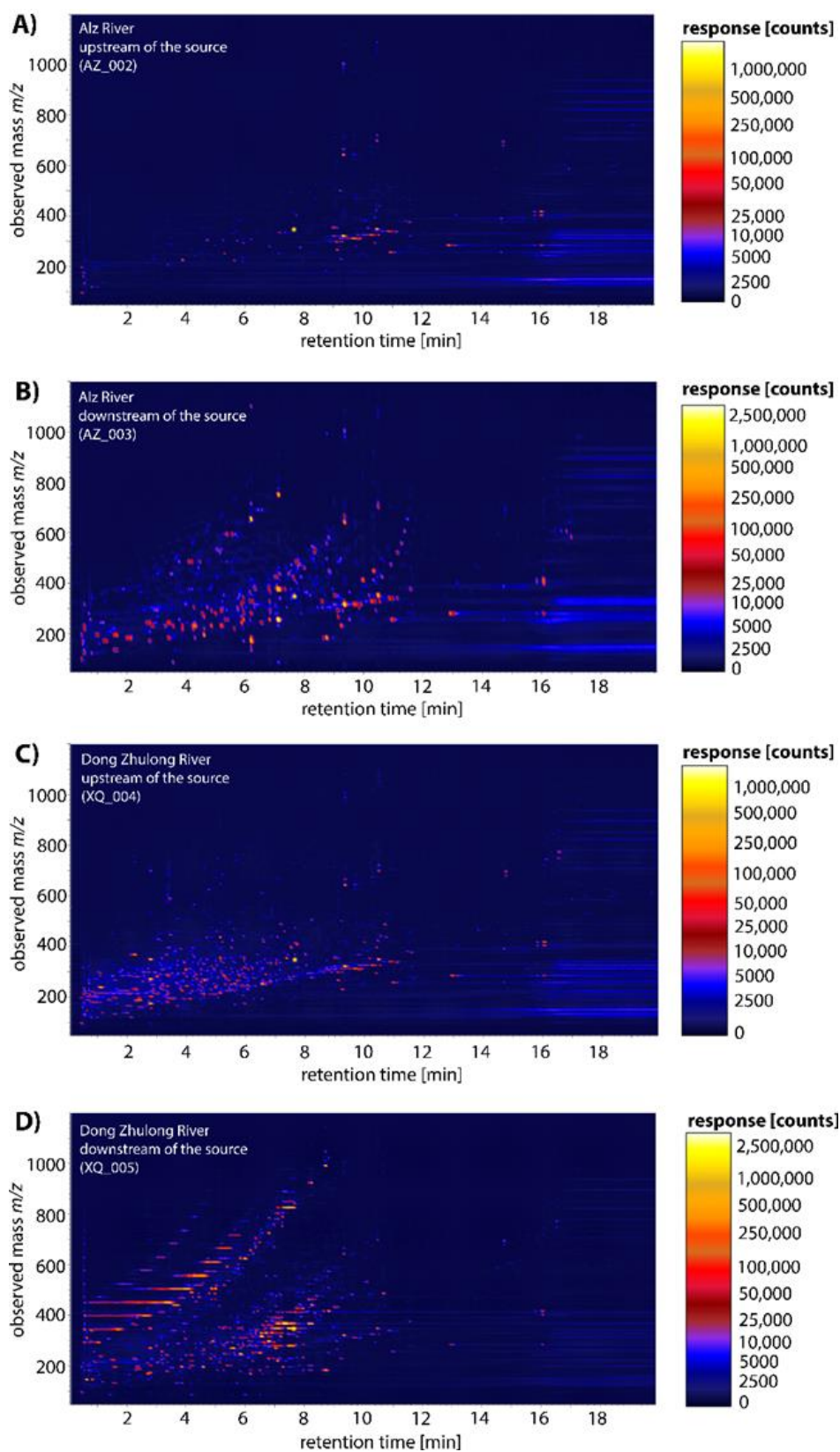


Figure 8.3-2: Three-dimensional plots of full-scan continuous data (low-energy function) of Alz river water samples taken A) up- and B) downstream of the point source, and Dong Zhulong river water samples collected C) up- and D) downstream of the point source.

8.3.2 PFAS suspect screening and filtering of candidates

Application of the PFAS suspect list and the peak area and mass error filter reduced the number of components from several thousands to 54 to 954 per sample (Figure 8.3-3). The number of remaining candidate components after filtering was highest in the samples taken after the point source in rivers with a small water flow rate, such as the Dong Zhulong River (XQ_005 and XQ_006 with 954 and 899 components) and the Alz River (AZ_003 with 498 components). In addition, a comparatively large difference in the number of candidate components before and after the point source could be observed in these two rivers, with an increase of 312 to 954 candidate components in the Dong Zhulong River (XQ_003 to XQ_005) and 71 to 498 candidate components in the Alz River (AZ_002 to AZ_003). Based on the bare number of candidate components after filtering, this clearly indicated an impact of the point sources. In contrast, in the large Yangtze and Rhine Rivers, the number of candidate components was comparatively small (mean 125) and no significant changes in the number of candidate components before and after the suspected point source could be observed. Strong dilution due to the large river size and an already high PFAS load due to upstream sources may be an explanation.

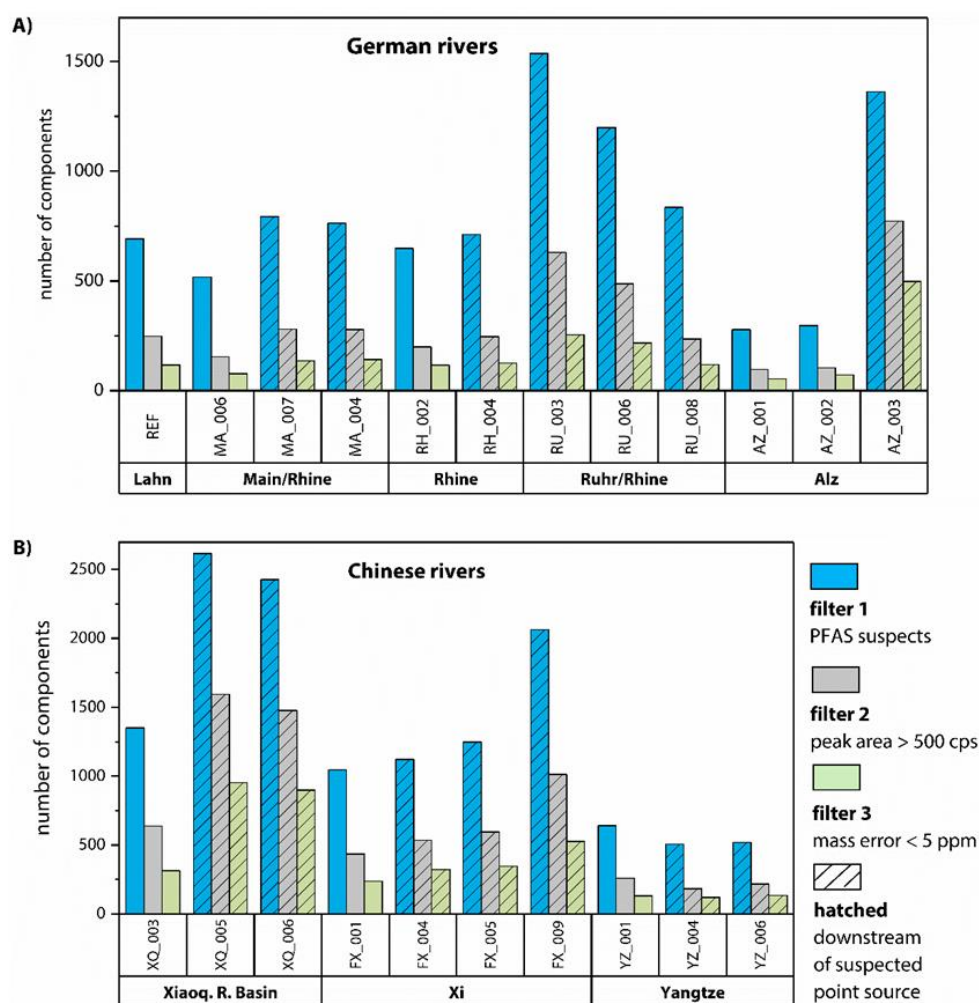


Figure 8.3-3: Filtering of the componentized LC-QTOF-MS^E data in the analysed samples from A) German rivers and B) Chinese rivers. Only the results for the first sample of each triplicate are shown.

8.3.3 Discovery of PFAS homologous series

Evaluating the candidate components, 13 homologous series with ≥ 4 members were discovered. In total, they included 83 PFASs (Figure 8.3-4). Grouped according to the structure categories of the OECD PFAS database [3], the (tentatively) identified PFASs comprised 27 carbonyl compounds, 17 sulfonyl compounds, 16 ether-based substances, 13 fluorotelomer-related compounds and 10 PFASs from other structure categories. Of the discovered PFASs within the 13 homologous series reported here, 14 were included in the spectrum of target analytes (Chapter 7) and 56 have been observed in earlier studies using suspect screening and non-target approaches (reviewed by Liu *et al.* [182]). 13 of the discovered PFASs were novel compounds, which have not been reported in the environment yet. These included four perfluoroalkyl dicarboxylic acids (C_4 , C_5 , C_6 and C_8), one monohydrosubstituted perfluoroalkyl carboxylic acid (C_3), four perfluoroalkyl diether carboxylic acids (C_5 to C_8) and four semifluorinated ketons (C_5 to C_8).

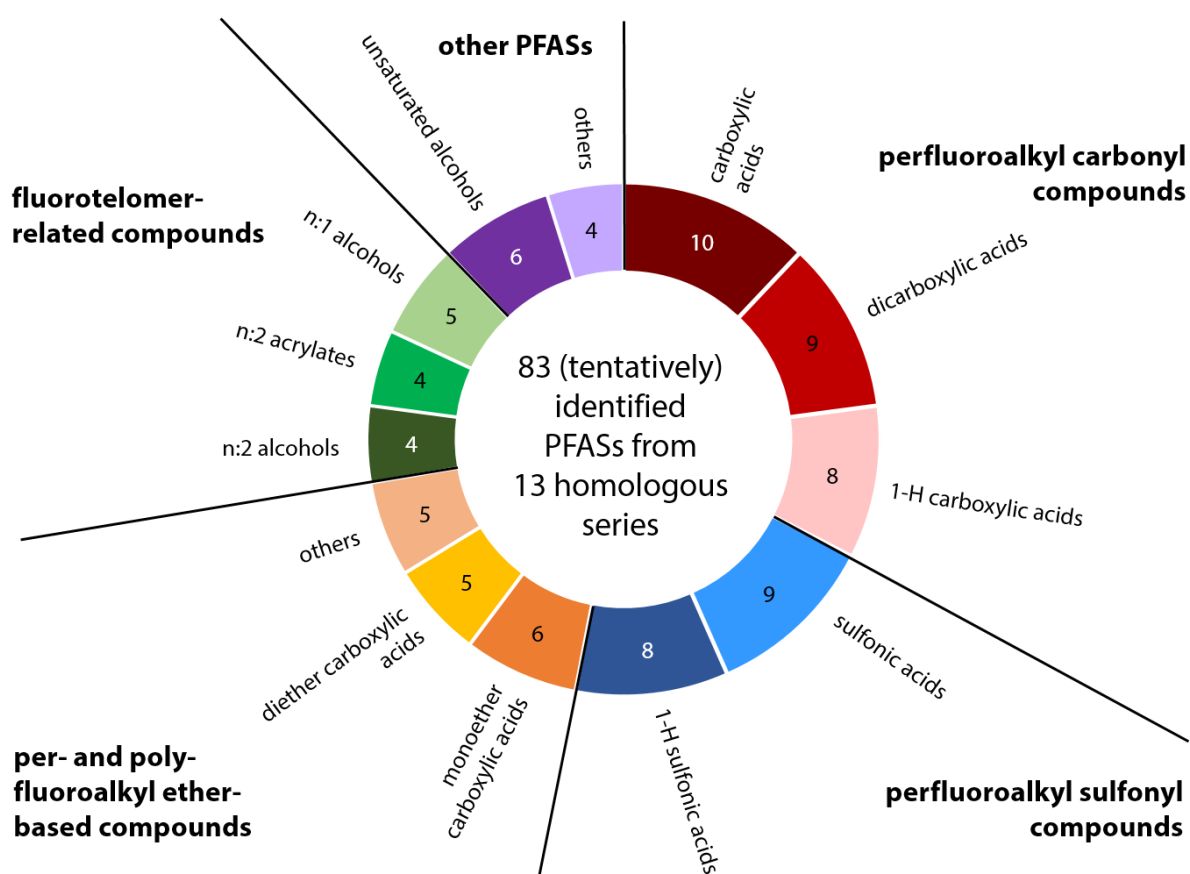


Figure 8.3-4: Overview of PFASs (tentatively) identified in this study, grouped according to their classification in the OECD PFAS database [3].

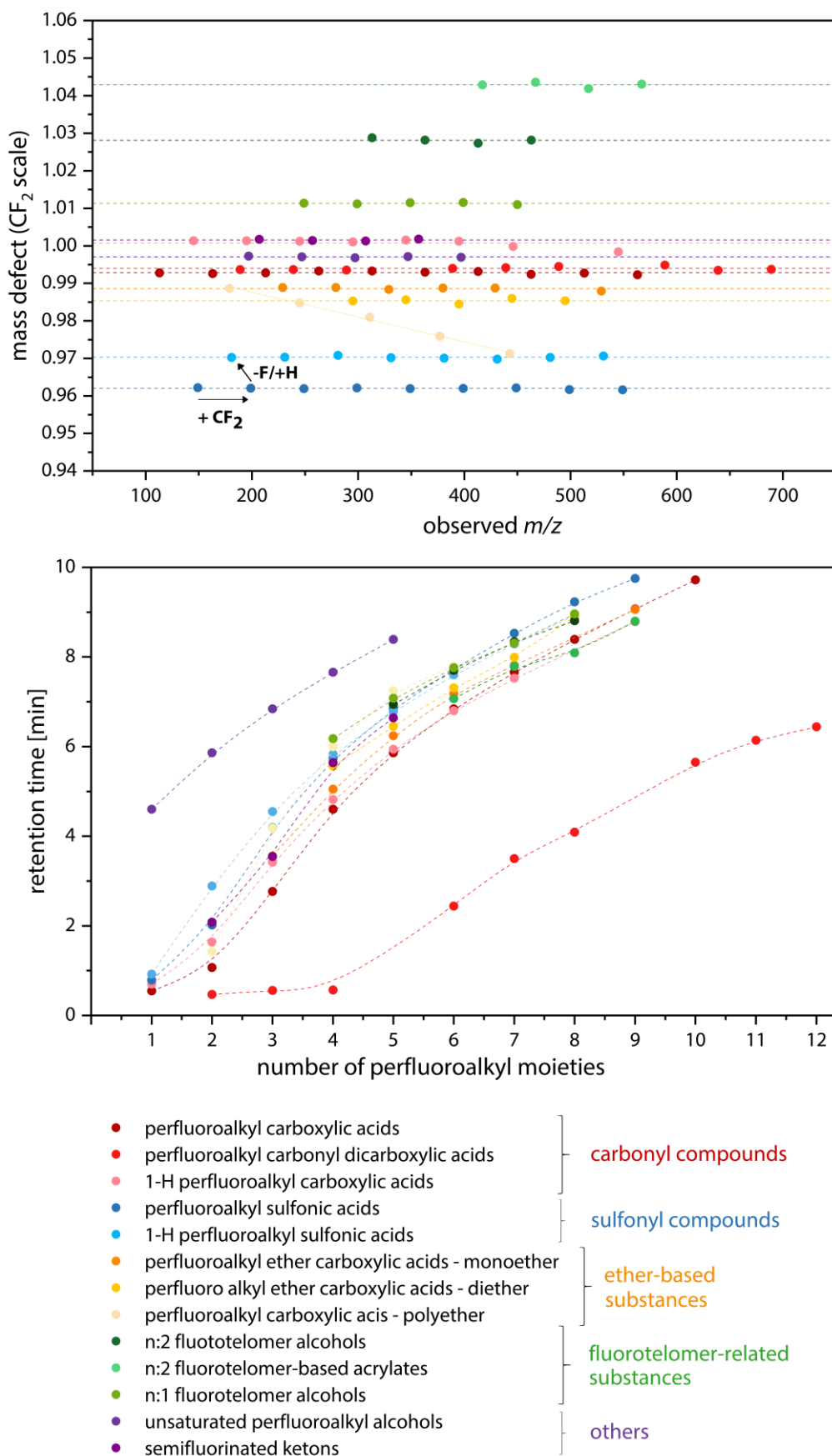


Figure 8.3-5: A) CF₂-adjusted Kendrick mass defect plots and B) retention time versus number of perfluorinated carbon atoms of PFASs (tentatively) identified in this study.

Within all homologous series, the CF_2 normalized Kendrick mass defect of the individual PFASs fell within 0.001 Da of the average mass defect and the retention time increased with increasing chain length of the substances (Figure 8.3-5). In addition, retention time differences between homologous series were plausible regarding the polarity of the functional groups or other structural features. As an example, polarity increases in the order perfluoroalkyl carboxylic acid < hydrosubstituted perfluoroalkyl carboxylic acid < perfluoroalkyl dicarboxylic acid, which is reflected by decreasing retention times on the reversed phase chromatographic column, e.g. 3.42 min > 1.64 min > 0.56 min for members of the respective homologue series having three fluorinated carbon atoms units.

With regard to fragmentation patterns, characteristic neutral losses were observed for the different homologous series. This included loss of CO_2 , indicative of carboxylic acids, loss of SO_3 , indicative of sulfonic acids, and loss of HF, indicative of hydrogen substitution within or immediately neighbouring the fluorinated chain [335]. Typically observed fragments were $\text{C}_m\text{F}_{2m+1}^-$ and $\text{C}_m\text{F}_{2m-1}^-$, suggesting a perfluoroalkyl chain structure. Additionally, $\text{OC}_m\text{F}_{2m+1}^-$ fragments were observed for ether-based compounds, indicating the presence of an ether-bond and providing information on its position. Details on the observed neutral losses and fragments in comparison to MS/MS data in literature are provided in Table 8.3-1 to Table 8.3-4.

For several homologous series, isomer peaks were observed in the chromatograms, which may result from branched isomers or alternative placements of H atoms and/or double bonds, if present. One exact structure of these compounds could not be proposed based on the collected evidences, resulting in assignment of identification confidence level 3. In total, 51 components were classified as tentative candidates at identification confidence level 3, for 18 substances at level 2 probable structures were proposed and 14 compounds were reported at level 1.

The number of sample triplicates in which the identified compounds were detected varied between and within the homologous series. 13 of the 83 compounds were detected in > 80 % of the analysed samples, in particular PFCAs and PFSA. In contrast, 37 compounds were detected in less than 20 % of the samples (Table 8.3-1 to Table 8.3-4).

Mapping the 83 observed molecular formulas and structures back to the original database revealed 200 CAS numbers (Table A.4-1). Particularly, PFCAs and PFSA are related to several CAS numbers in the database, including multiple salts and mixtures. A maximum of 21 CAS numbers is associated with the formula of PFBS, underlining that the substance form observed by the analyst can have its origin in a variety of products available in commerce.

Table 8.3-1: Discovered homologous series of perfluoroalkyl carbonyl compounds. Confidence (conf.) levels were assigned according to the scheme proposed by Schymanski *et al.* [340]. Column “# detects” refers to the number of locations, at which the compound was detected in all 3 samples of the triplicate and the mean response was 5x higher than in the blanks. Column “references” lists previous studies, in which the substance has been reported.

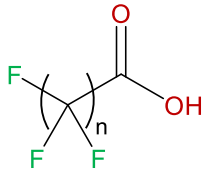
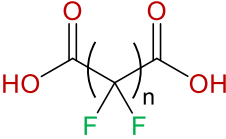
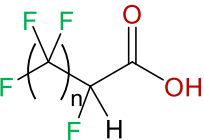
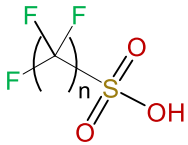
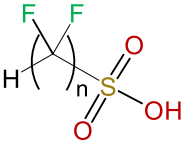
proposed structure	<i>n</i>	neutral formula	observed <i>m/z</i>	additional evidences	conf. level	# detects	references
perfluoroalkyl carboxylic acids (PFCAs), C_nHF_{2n-1}O₂ (OECD category: 102)							
	1	C2HF3O2	112.9856	<ul style="list-style-type: none"> characteristic fragments or neutral losses: <ul style="list-style-type: none"> [M-H-44]⁻, corresponding to neutral loss of CO₂ and suggesting the presence of a carboxyl moiety C_mF_{2m+1}⁻ carbanions of the “9-series” (e.g. <i>m/z</i> 69, 119, 169 corresponding to CF₃⁻, C₂F₅⁻ and C₃F₇⁻), indicative of perfluoroalkyl chain fragmentation pathway described by Arsenault <i>et al.</i> [341] confirmed by internal standards: <i>n</i> = 3, 5, 7, 8, 9, 10 confirmed by target analysis: <i>n</i> = 3-10 	2a	19	numerous, e.g. [338, 342]
	2	C3HF5O2	162.9822		2a	8	
	3	C4HF7O2	212.9792		1	17	
	4	C5HF9O2	262.9765		1	20	
	5	C6HF11O2	312.9733		1	22	
	6	C7HF13O2	362.9698		1	21	
	7	C8HF15O2	412.9668		1	22	
	8	C9HF17O2	462.9629		1	20	
	9	C10HF19O2	512.9600		1	10	
	10	C11HF21O2	562.9564		1	6	
perfluoroalkyl carbonyl dicarboxylic acids (C_nH₂F_{2n-4}O₄) (OECD category: 106)							
	2	C4H2F4O4	188.9816	<ul style="list-style-type: none"> characteristic fragments or neutral losses: <ul style="list-style-type: none"> [M-H-108]⁻, corresponding to [M-H-2CO₂-HF]⁻ ions of series C_mF_{2m-1}⁻ and C_mF_{2m+1}⁻, indicating a perfluoroalkyl chain structure neutral loss and fragment ions were also observed in two other studies, in which perfluorodecane dicarboxylic acid (C₁₀H₂F₁₆O₄) and perfluorododecane dicarboxylic acid (C₁₂H₂F₂₀O₄) were confirmed level 1 by standards [338, 342] 	2b	2	novel
	3	C5H2F6O4	238.9784			3	novel
	4	C6H2F8O4	288.9751			2	novel
	6	C8H2F12O4	388.9692			6	novel
	7	C9H2F14O4	438.9662			7	[338, 342]
	8	C10H2F16O4	488.9633			3	[338, 342]
	10	C12H2F20O4	588.9573			8	[338, 342]
	11	C13H2F22O4	638.9527			4	[338, 342]
	12	C14H2F24O4	688.9498			4	[338, 342]
	1-H perfluoroalkyl carboxylic acids (H-PFCAs) (C_nH₂F_{2n-2}O₂) (OECD category: 108)						
 <p>H position unknown</p>	1	C3H2F4O2	144.9921	<ul style="list-style-type: none"> characteristic fragment: [M-H-64]⁻, corresponding to combined neutral loss of CO₂ (44 Da) and HF (20 Da) and indicating a monohydrosubstituted PFCA losses of HF characteristic for H substitution within or neighbouring the fluorinated chain [14, 335] combined neutral loss of CO₂ and HF has been also observed in other studies, but the exact location of the H substitution could not be confirmed [338, 342-344] 	3a	1	novel
	2	C4H2F6O2	194.9889			12	[338, 344]
	3	C5H2F8O2	244.9856			12	[338, 344]
	4	C6H2F10O2	294.9822			10	[338, 343, 344]
	5	C7H2F12O2	344.9795			10	[338, 343, 344]
	6	C8H2F14O2	394.9760			11	[338, 343]
	7	C9H2F16O2	445.9714			10	[338, 343]
	9	C11H2F20O2	544.9636			9	[338, 343]

Table 8.3-2: Discovered homologous series of perfluoroalkyl sulfonyl compounds. Confidence (conf.) levels were assigned according to the scheme proposed by Schymanski *et al.* [340]. Column “# detects” refers to the number of locations, at which the compound was detected in all 3 samples of the triplicate and the mean response was 5x higher than in the blanks. Column “references” lists previous studies, in which the substances have been observed.

proposed structure	<i>n</i>	neutral formula	observed <i>m/z</i>	additional evidences	conf. level ¹	# detects	references
perfluoroalkyl sulfonic acids (PFSA) (C_nHF_{2n+1}O₃S) (OECD category: 202)							
 multiple isomers	1	CHF ₃ O ₃ S	148.9527	<ul style="list-style-type: none"> characteristic fragments or neutral losses: <ul style="list-style-type: none"> - <i>m/z</i> 79.9573, corresponding to a sulfonate moiety SO₃⁻ - C_{<i>m</i>}F_{2<i>m</i>}SO₃⁻ radical anions of the “0-series” e.g. <i>m/z</i> 130 and 180, corresponding to CF₂SO₃⁻ and C₂F₄SO₃⁻ - ions of the “9-series” (C_{<i>m</i>}F_{2<i>m</i>+1})⁻ (see PFCAs) fragmentation pathway reviewed by Knepper and Lange [14] confirmed by internal standards: <i>n</i> = 4, 6, 8 (linear isomer) confirmed by target analysis: <i>n</i> = 4, 6, 7, 8 (linear isomer) 	2a	12	numerous, e.g. [338, 342]
	2	C ₂ HF ₅ O ₃ S	198.9494		2a	4	
	3	C ₃ HF ₇ O ₃ S	248.9461		2a	9	
	4	C ₄ HF ₉ O ₃ S	298.9431		1	19	
	5	C ₅ HF ₁₁ O ₃ S	348.9397		2a	16	
	6	C ₆ HF ₁₃ O ₃ S	398.9366		1	17	
	7	C ₇ HF ₁₅ O ₃ S	448.9335		1	15	
	8	C ₈ HF ₁₇ O ₃ S	498.9299		1	15	
	9	C ₉ HF ₁₉ O ₃ S	548.9266		2a	2	
1-H perfluoroalkyl sulfonic acids (H-PFSAs) (C_nH₂F_{2n}O₃S) (OECD category: 206)							
 H position unknown	1	C ₂ H ₂ F ₄ O ₃ S	180.9587	<ul style="list-style-type: none"> characteristic fragments or neutral losses: <ul style="list-style-type: none"> - neutral loss of SO₃⁻ (80 Da) and HF (20 Da) - C_{<i>m</i>}F_{2<i>m</i>}SO₃⁻ radical anions of the “0-series” similar fragmentation pattern as reported earlier [335, 345] location of the hydrogen substitution cannot be confirmed 	3a	5	[335]
	2	C ₃ H ₂ F ₆ O ₃ S	230.9556			4	[335, 344]
	3	C ₄ H ₂ F ₈ O ₃ S	280.9529			10	[174, 335, 344]
	4	C ₅ H ₂ F ₁₀ O ₃ S	330.9491			5	[335]
	5	C ₆ H ₂ F ₁₂ O ₃ S	380.9458			7	[174, 335]
	6	C ₇ H ₂ F ₁₄ O ₃ S	430.9423			5	[335]
	7	C ₈ H ₂ F ₁₆ O ₃ S	480.9396			5	[335]
	8	C ₉ H ₂ F ₁₈ O ₃ S	530.9368			1	[335]

¹ Multiple isomer peaks were observed. The assigned confidence level refer to the linear PFSAs.

Table 8.3-3: Discovered homologous series of per- and polyfluoroalkyl ether-based compounds. Confidence (conf.) levels were assigned according to the scheme proposed by Schymanski *et al.* [340]. Column “# detects” refers to the number of locations, at which the compound was detected in all 3 samples of the triplicate and the mean response was 5x higher than in the blanks. Column “references” lists previous studies, in which the substances have been observed.

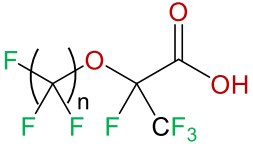
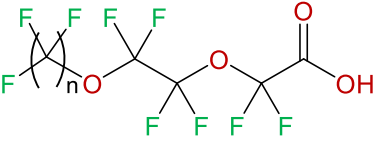
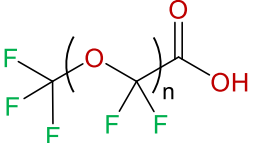
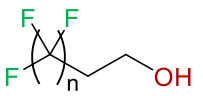
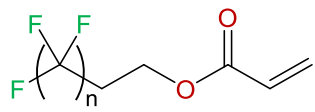
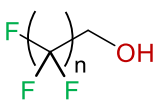
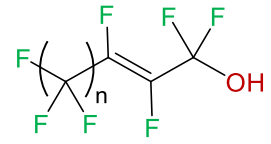
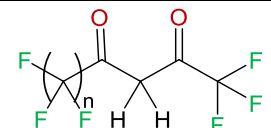
proposed structure	<i>n</i>	neutral formula	observed <i>m/z</i>	additional evidences	conf. level	# detects	references
perfluoroalkyl ether carboxylic acids (PFECAs) – monoethers (C_nHF_{2n-1}O₃) (OECD category 502.01)							
 <p>multiple isomers possible</p>	1	C4HF7O3	228.9743	<ul style="list-style-type: none"> characteristic fragments: ions of series OC_mF_{2m+1}⁻ and C_mF_{2m+1}⁻, indicating that the ether bond is not adjacent to the terminal perfluoromethyl group similar fragmentation pattern observed in previous studies [314, 346] confirmed by target analysis and internal standard: C₆HF₁₁O₃ (HFPO-DA) 	3a	5	[314, 346]
	2	C5HF9O3	278.9711		3a	8	[314, 346]
	3	C6HF11O3	328.9674		1	6	[314, 346]
	4	C7HF13O3	379.9645		3a	7	[314, 346]
	5	C8HF15O3	428.9614		3a	8	[174, 314, 346]
	7	C10HF19O3	528.9542		3a	2	[314]
PFECAs – diethers (C_nHF_{2n-1}O₄) (OECD category 502.02)							
 <p>multiple isomers possible</p>	1	C5HF9O4	294.9665	<ul style="list-style-type: none"> characteristic fragments: ions of series OC_mF_{2m+1}⁻ and C_mF_{2m+1}⁻, indicating that the ether bond is not adjacent to the terminal perfluoromethyl group confirmed by target analysis: C₉HF₁₇O₄ (HFPO-TrA) 	3a	3	novel
	2	C6HF11O4	344.9636		3a	1	novel
	3	C7HF13O4	394.9593		3a	4	novel
	4	C8HF15O4	444.9576		3a	3	novel
	5	C9HF17O4	494.9538		1	9	[134]
PFECAs – polyether (C_nHF_{2n-1}O_n) (OECD category 502.02 to 502.04)							
	1	C3HF5O3	178.9772	<ul style="list-style-type: none"> characteristic fragment: <i>m/z</i> 84.99067, corresponding to OCF₃⁻ and indicating a terminal -OCF₃ group similar fragmentation pattern as reported as reported in previous studies [314, 346] 	3a	2	[346]
	2	C4HF7O4	244.9692		3a	4	[314, 346]
	3	C5HF9O5	310.9611		3a	3	[314, 346]
	4	C6HF11O6	376.9519		3a	2	[314, 346]
	5	C7HF13O7	442.9430		3a	6	[314, 346]

Table 8.3-4: Tentatively identified homologous series of fluorotelomer-related compounds and other PFASs. Confidence (conf.) levels were assigned according to the scheme proposed by Schymanski *et al.* [340]. Column “# detects” refers to the number of locations, at which the compound was detected in all 3 samples of the triplicate and the mean response was 5x higher than in the blanks. Column “references” lists previous studies, in which the substances have been observed.

proposed structure	<i>n</i>	neutral formula	observed <i>m/z</i>	additional evidences	conf. level	# detects	references
<i>n</i>:2 fluorotelomer alcohols (FTOHs) (C_nH₅F_{2<i>n</i>-3}O) (OECD category 402.03)							
	5	C7H5F11O	313.0088	<ul style="list-style-type: none"> characteristic fragments: [M-H-60]⁻, [M-H-40]⁻, [M-H-20]⁻, corresponding to neutral loss of up to 3 HF similar fragmentation pattern observed by Trier <i>et al.</i> [347], who confirmed C₈H₅F₁₃O (6:2 FTOH) and C₁₀H₅F₁₇O (8:2 FTOH) by standards [348] 	3a	1	[347]
	6	C8H5F13O	363.0050		2b	1	[347]
	7	C9H5F15O	413.0010		3a	2	[347]
	8	C10H5F17O	462.9986		2b	1	[347]
<i>n</i>:2 fluorotelomer-based acrylates (C_nH₇F_{2<i>n</i>-9}O₂) (OECD category 402.06)							
	6	C11H7F13O ₂	417.0163	<ul style="list-style-type: none"> characteristic fragments or neutral losses: loss of HF (see FTOHs) similar fragmentation pattern to <i>n</i>:2 FTOHs also observed by Trier <i>et al.</i> [347] 	3a	3	[347]
	7	C12H7F15O ₂	467.0138			1	[347]
	8	C13H7F17O ₂	517.0089			1	[347]
	9	C14H7F19O ₂	567.0069			3	[347]
<i>n</i>:1 fluorotelomer alcohols (FTOHs) (C_nH₃F_{2<i>n</i>-1}O) (OECD category 404.01)							
	4	C5H3F9O	248.9955	<ul style="list-style-type: none"> characteristic fragments or neutral losses: <ul style="list-style-type: none"> [M-H-20]⁻, corresponding to loss of HF 	3b	1	[130]
	5	C6H3F11O	298.9921			1	[130]
	6	C7H3F13O	348.9892			1	[130]
	7	C8H3F15O	398.9861			1	[130]
	8	C9H3F17O	449.9823			1	[130]
unsaturated perfluoroalkyl alcohols (UPFAs) (C_nHF_{2<i>n</i>-1}O) (OECD category 602)							
 <p>position of double bond unknown</p>	1	C4HF7O	196.9847	<ul style="list-style-type: none"> characteristic fragments or neutral losses <ul style="list-style-type: none"> [M-H-66]⁻, corresponding to [M-H-CF₂O]⁻ and indicating a terminal alcohol or ether bond series of C_{<i>m</i>}F_{2<i>m</i>-1}⁻ carbanions, indicative of double bond, carbanions of the of the C_{<i>m</i>}F_{2<i>m</i>+1}⁻ series fragmentation pattern observed in previous studies [338, 342] 	3a	18	[338]
	2	C5HF9O	246.9813			20	[338]
	3	C6HF11O	296.9779			22	[338]
	4	C7HF13O	346.9750			17	[338, 342]
	5	C8HF15O	396.9716			19	[338, 342]
	6	C9HF17O	446.9680			15	[338, 342]
semifluorinated ketons (C_nH₂F_{2<i>n</i>-4}O₂) (OECD category 704)							
	1	C5H2F6O ₂	206.9885	<ul style="list-style-type: none"> characteristic fragments or neutral losses <ul style="list-style-type: none"> [M-H-20]⁻, corresponding to loss of HF series of C_{<i>m</i>}F_{2<i>m</i>+1}⁻ carbanions 	3b	2	novel
	2	C6H2F8O ₂	256.9850			1	novel
	3	C7H2F10O ₂	306.9817			3	novel
	4	C8H2F12O ₂	356.9790			4	novel

8.3.4 Source-specific fingerprints

Although the concentrations of the detected compounds could not be quantified due to lack of reference standards, the samples allowed comparison of source fingerprints and linkage to manufacturing processes and/or use patterns. Heat maps providing an overview of PFASs detected at the different sites in relation to their peak area counts are given in Figure 8.3-7. Differences in peak areas do not necessarily reflect differences in concentrations, as for example the ionization efficiency or losses during sample preparation vary between PFASs. However, peak area relations of homologous series' members can be compared between samples from different sources.

While the well-known PFCAs and PFSA were observed across all sites, emerging and novel PFASs were particularly detected downstream of the suspected point sources at the Alz River, the Dong Zhulong River and the Xi River (Figure 8.3-7). Comparing the peak area relation of PFCAs (OECD category 102) and the only recently discovered H-PFCAs (OECD category 108) [338, 342-344] revealed distinct differences between the sites (Figure 8.3-6).

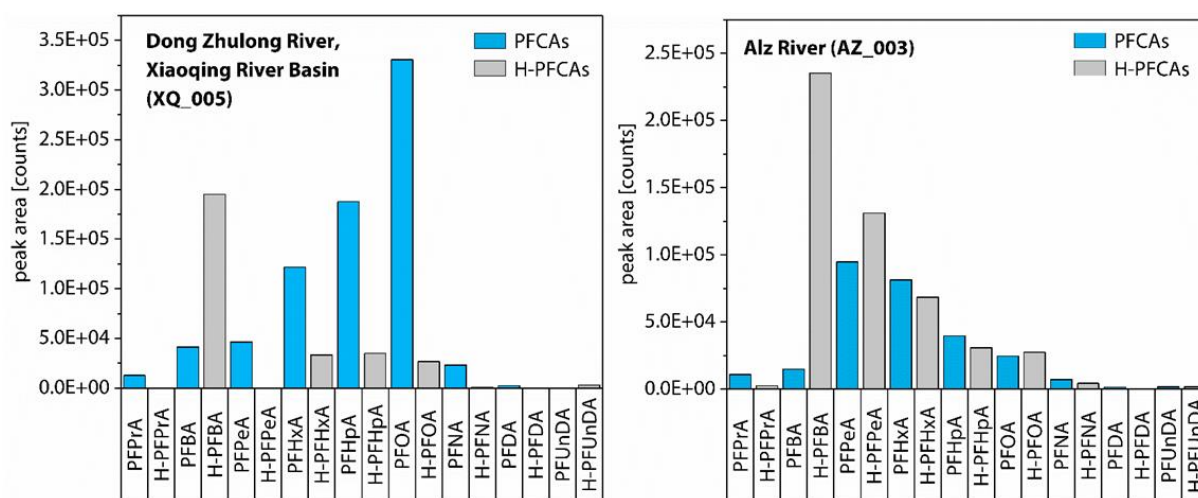


Figure 8.3-6: Peak areas of detected PFCAs and H-PFCAs downstream of the fluorochemical plants located at the Dong Zhulong River and the Alz River.

In sample XQ_005, taken downstream of the fluorochemical park at the Dong Zhulong River, the peak areas of PFCAs increased with increasing chain length up to PFOA as the most abundant peak. This pattern reflects ECF-based production of PFOA at the site (see Chapter 7.4.3). Peak areas of C₅ to C₈ H-PFCAs were a factor 4 to 13 lower than those of PFCAs with the same number of C atoms. In contrast, C₅ to C₈ peak areas of PFCAs and H-PFCAs were comparable in sample AZ_003, collected downstream of the fluorochemical manufacturing plant at the Alz River. They decreased with increasing chain length, underlining the lower relevance of long-chain PFASs at the German manufacturing site compared to the Chinese fluorochemical plant. This can be explained by the phase-out of long-chain PFAAs and their precursors in Europe and a geographical shift of the production to Asian countries [128].

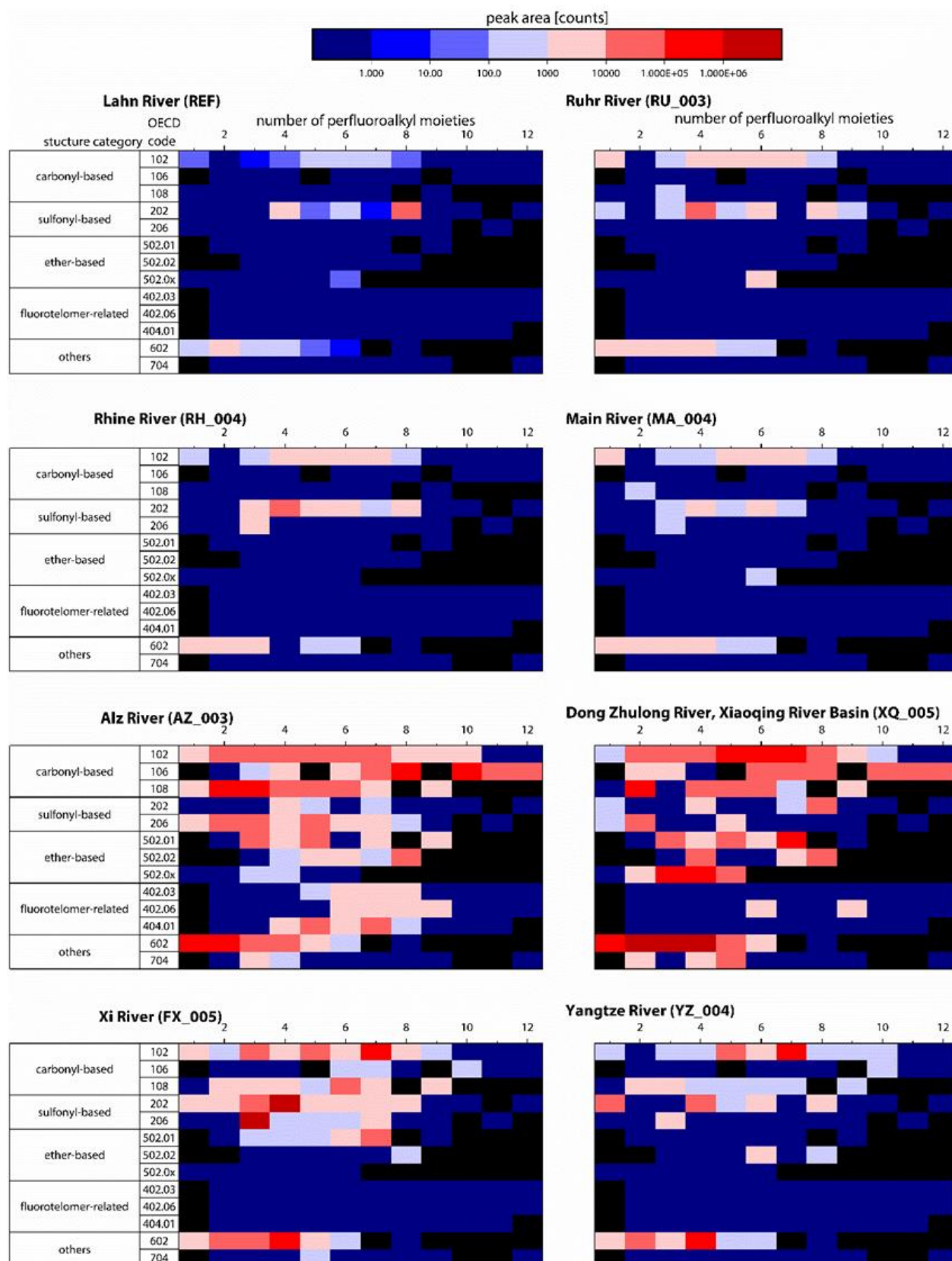


Figure 8.3-7: Source-specific fingerprints of detected PFASs in selected samples. Coloured rectangles represent the peak area of individual PFASs with a defined number of CF₂ units (x-axis) within a particular homologous series (y-axis). Black rectangles represent compounds which were not included in the PFAS suspect list.

Interestingly, peak areas of H-PFBA were higher than those of PFBA at both sites (factor 5 in sample XQ_005 and factor 16 in sample AZ_003). In general, H-PFCAs can be present as impurities or they can be intentionally produced or used as processing aids [314]. Based on the observed patterns, it can be hypothesized that H-PFBA is intentionally used or a by-product of compounds other than PFCAs and H-PFCAs, which are used in high intensities at the two sites. C₅ to C₈ H-PFCAs are more likely by-products due to their lower abundance. However, the two pathways of release are not exclusive and may occur in parallel.

Differences between the sites were also obvious for the homologous series of PFECAs (OECD category 502.01). A member of this series is HFPO-DA (C₆HF₁₁O₃), which is used as replacement for PFOA in fluoropolymer manufacture [132]. While this compound has been increasingly studied over the last years and was shown to be ubiquitously present (Chapters 5 to 7), reports on the other detected homologues of this series are limited so far [338, 343, 344]. A comparison of the homologues' peak areas shows that also for ether-based substances, the long-chain C₈ homologue is the most prevalent compound in river water taken downstream of the Chinese manufacturing sites located at Dong Zhulong River (XQ_005) and Xi River (FX_005) (Figure 8.3-8). In contrast, the short-chain C₄ and C₆ (HFPO-DA) homologues are dominant in the German Alz River, contributing 52 % and 39 % to the sum of the peak areas of the homologous series.

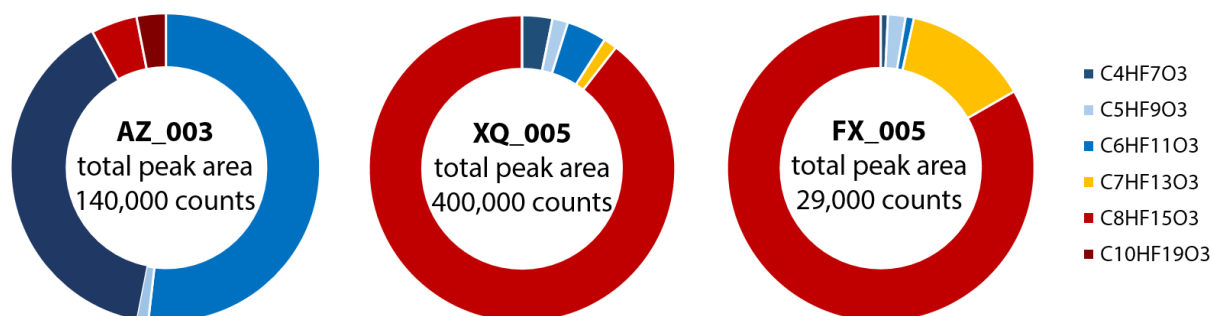


Figure 8.3-8: Contribution of individual PFECAs to the total peak area of PFECAs downstream of the fluorochemical plants located at the German Alz River (AZ_003) and the Chinese Dong Zhulong River (XQ_005) and Xi River (FX_005).

Additionally, the PFBS/H-PFBS peak area ratio varied between the point sources. PFBS is typically included in target analysis of PFASs, whereas H-PFBS has been reported only in three other HRMS-based studies - downstream of a fluorochemical manufacturer near Decatur in the United States [344], in Chinese wastewater of a fluorochemical plant [343] and in 3M AFFFs [335]. In our study, the peak area of H-PFBS was higher or as high as the peak area of PFBS downstream of the manufacturing sites located at the Alz River (AZ_003, ratio H-PFBS/PFBS 5:1) and Xi River (FX_005, ratio H-PFBS/PFBS 1:1) (Figure 8.3-9). In contrast, the contribution of H-PFBS was below 10 % in the samples from the Rhine River (RH_002), the Main River (MA_004) and the

Yangtze River (YZ_004) and the compound was not detected at the other sites. In a 2011 patent, H-PFBS was reported as impurity in the manufacture of PFBS [344]. However, its higher or equal abundance compared to PFBS downstream of the fluorochemical parks at the Alz and Xi Rivers suggests that H-PFBS has to be an impurity in additional products or is intentionally produced and used at these sites. A higher abundance for H-PFBS compared to PFBS was also observed downstream a the manufacturer in the United States [344].

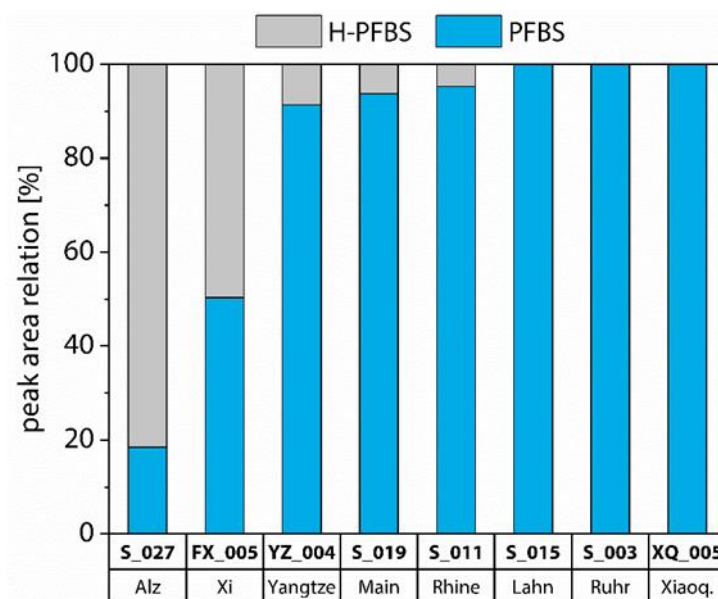


Figure 8.3-9: PFBS/H-PFBS peak area ratio in the investigated rivers.

8.4 Summary and conclusion

Based on the developed PFAS suspect screening workflow, 83 PFASs from 13 homologous series were discovered in German and Chinese river water samples impacted by point sources. 13 of them have not been reported in the environment before, underlining the potential of HRMS-based suspect screening approaches. Due to time constraints, only homologous series with at least four members have been included in the evaluation so far. Componentized and filtered raw data indicate the presence of additional PFASs within homologous series having less than four members or as single compounds. The results also revealed the limitations of HRMS-based approaches. For 51 of the compounds, complete structure elucidation could not be achieved, resulting in assignment of identification confidence level 3. For the majority of these compounds, reference standards needed for unambiguous identification of the compounds are not available. Nevertheless, even without authentic standards, the samples analysed in this study and other studies using HRMS-based approaches can be used as reference to develop LC-MS/MS methods for environmental monitoring to determine the wider environmental relevance of the identified compounds.

Even though the suspect list used in this study was created based on a database with more than 5000 PFASs, it included only a fraction of the whole group of PFASs. Consequently, filtering the processed raw data based on the suspect list, has led to false negative results. As an example, the C7 compound within the series of perfluoroalkyl dicarboxylic acids was not included in the suspect list, but a look into the unfiltered data showed that it was present in the samples. This was also the case for a homologous series of α H-PFCAs ($C_{2n}F_{2n}H_{2n}O_2$), which was reported in previous non target-studies [314, 343] but was lost during post-acquisition data treatment in this study. False negative results may particularly concern by- and reaction products as these are typically less covered in PFAS databases than final commercial products.

The source-related PFAS fingerprints observed in this study can help to understand the PFAS contamination pattern at the investigated sites, which is relevant to estimate, prioritize and abate contributions of specific sources. A comprehensive assessment is challenging because little is known on the toxicity, persistence and transport of the identified emerging and novel series of PFASs, such as monohydrogensubstituted PFCAs and PFSA and per- and polyfluoroether-based substances other than HFPO-DA. Nevertheless, the large number of discovered PFASs having similar structures and comparable peak areas to the well-known legacy PFASs indicates that only based on conventional target analysis, environmental and human health risks can be considerably underestimated.

9. Overall Conclusions and Future Perspectives

The main conclusions drawn from the findings in this PhD project can be summarized as follows:

- i) The developed and validated analytical method is suitable for the determination of 29 legacy and emerging PFASs in seawater, river water and sediment in the pg/L and pg/g range, respectively.
- ii) The replacement compound HFPO-DA is ubiquitously present in surface water and its detection in the Greenland Sea and Fram Strait provides evidence that the compound undergoes long-range transport to remote areas, similar to the legacy compound PFOA.
- iii) In coastal waters of the North Sea, a downward trend of legacy long-chain PFASs in combination with a shift to emerging PFASs as most prevalent compounds show an effect of the phase-out and regulation of long-chain compounds. In surface water from the Baltic Sea and sediments from both the North and Baltic Seas, legacy long-chain compounds still play a major role. This points to ongoing emissions from diffuse sources and underlines the relevance of sediments as sink of legacy long-chain PFASs in the marine environment.
- iv) For long-chain PFASs with ≥ 8 perfluoroalkyl moieties, mass transport estimates indicate a net transport into the Arctic Ocean from the Atlantic Ocean. In contrast, shorter-chain homologues showed a net transport out of the Arctic. This may be attributed to a higher contribution from atmospheric sources to the Arctic outflow compared to ocean circulation and a higher retention of the long-chain compounds in melting snow and ice.
- v) Conventionally analysed PFASs only represent a fraction of the PFASs present in German and Chinese river water impacted by point sources, indicating that environmental and human exposure to PFASs may be considerably underestimated.

More specifically, the developed LC-MS/MS method for instrumental analysis of the target analytes was improved by optimization of the mobile phase composition. Compared to the tested commonly used eluents, the use of 2 mM NH_4OAc in water as eluent A and 0.05 % CH_3COOH in methanol as eluent B resulted in signal enhancement for all analytes. In combination with the adjustment of the injection solvent, this also resulted in improved peak shapes for the early eluting compound PFBA. Regarding the sample preparation of aqueous matrices, absolute recoveries of long-chain PFASs in seawater were improved by using a comparatively large washing volume of 15 mL water:methanol 80:20 (v/v) during SPE. For both the aqueous matrices and sediments, the sample transfer from the glass vessel used for volume reduction after SPE to the LC vial for the measurement was identified to cause losses of all analytes, probably due to adsorption of the

analytes to the vessel walls. An improvement was achieved by the inclusion of an ultrasonication step and a rinsing step, respectively. Validation proved that the selectivity, precision, accuracy and robustness of the developed method is acceptable based on criteria for ultratrace analysis in complex matrices. MDLs for most of the target analytes ranged from 0.0019 ng/g dw to 0.067 ng/g dw in sediment and 0.0022 ng/L to 0.050 ng/L in 1 L aqueous samples. This shows that the method is generally capable of detecting PFASs in marine sediment, seawater and river water with expected concentrations in the pg/g range and pg/L range, respectively. For single PFASs, MDLs were higher for samples from particular sampling campaigns due to comparatively high concentrations of the compound in the blank samples. This underlines the importance of campaign- and batch-specific blank samples in addition to the measures which have to be taken to avoid PFAS contamination throughout the process.

Based on the developed method, the emerging ether-based compound HFPO-DA, used to replace the legacy substance PFOA in fluoropolymer manufacture, was detected in 191 of the 202 surface water samples analysed for this PhD project. Study areas included coastal areas of the North and Baltic Seas, open waters in the Norwegian Sea, the Greenland Sea and Fram Strait, located between Greenland and Svalbard, as well as German and Chinese rivers. These findings add to a growing body of literature indicating the ubiquitous presence of HFPO-DA. In addition, HFPO-DA was detected in Arctic surface water for the first time, adding empirical evidence to modelling assessments predicting that the compound undergoes long-range transport toward remote regions. Thus, the findings suggest that HFPO-DA is a compound of global environmental concern, fulfilling the criterion of long-range transport potential to be classified as POP under the Stockholm Convention, similar to the legacy compound PFOA.

Of the other investigated replacement compounds and/or overlooked PFASs, the cyclic compound PFECHS was detected in 86 % of the Baltic Sea surface water samples and in the German Ruhr, Rhine and Main rivers. 6:6 and 6:8 PFPiAs were primarily identified in sediment samples taken close to potential industrial inputs and in sedimentation areas in the North and Baltic Seas and the Rhine River. DONA, another replacement compound for PFOA in fluoropolymer manufacture, contributed to Σ PFASs with about 40 % in the German Alz River, taken downstream of a fluorochemical park. While DONA was only detected in German rivers, 6:2 Cl-PFESA, used as PFOS alternative in the Chinese plating industry, was only identified in Chinese river water. Hence, the occurrence of investigated replacement and/or overlooked compounds other than HFPO-DA was limited to particular study areas, country-specific or source-specific. With exception of DONA in the samples from the German Alz River, concentrations of these emerging PFASs were generally approximately an order of magnitude lower than that of legacy PFCAs and

PFASs. This may be attributed to lower production volumes and a different environmental behaviour, including degradation, biotransformation and partitioning. As an example, the results from the TOP assay indicate that DONA is less stable compared to HFPO-DA and PFOA upon oxidation. PFPiAs may undergo biotransformation to PFPAs and preferentially be retained by sediments and other solid phases. In contrast to HFPO-DA, none of these compounds was detected in open and remote surface water.

HFPO-DA concentrations were approximately three times higher than those of its predecessor PFOA in surface water from the European North Sea, reflecting the shift of production from regulated long-chain compounds to replacements in Europe. In contrast, analysis of Chinese river water samples and estimation of annual riverine mass flows underlined the ongoing high emissions of the legacy compound PFOA in China from point sources in the Xiaoqing River Basin and along the Yangtze River. One explanation for this difference is the geographical shift of the production of long-chain PFASs from Europe, North America and Japan to countries with less stringent regulations, such as China. As PFOA has been recently added to the Stockholm Convention [122], also ratified by China, it can be expected that major producers in continental Asia will reduce emissions of PFOA and its precursors in the foreseeable future [4]. Hence, the evaluation and regulation of HFPO-DA and other replacement compounds on an international level is essential. It could help to avoid repeating the industrial transition from the legacy compound PFOA to HFPO-DA and other ether-based replacements as potential “regrettable substitutes”, which has taken place in the Europe, North America and Japan since the 2000s, in continental Asia. On European level, HFPO-DA was classified as Substance of Very High Concern in 2019 [302], which may stimulate the global debate on the compound, for example for listing under the Stockholm Convention.

In addition to the need for safe alternatives, the findings of this PhD project underline the ongoing relevance of regulated long-chain PFASs in the aquatic environment. Even though their emissions have been reduced in Europe starting in the 2000s, long-chain PFCAs and PFASs still significantly contributed to the sum of PFASs in the analysed surface water samples from the Baltic Sea with a limited water exchange and dominance of diffuse sources. In addition, the long-chain legacy substance PFOS was the predominant compound in sediments from both North and Baltic Sea. The field-based sediment-water partitioning coefficients $\log K_{OC}$ increased with an increasing number of perfluoroalkyl moieties. This underlines the importance of marine sediments as sink particularly for legacy long-chain PFASs. In general, the findings stress that environmental exposure is only slowly reversed and depends on geographical conditions and the dominating type of sources. Emissions from point sources, such as fluorochemical production plants, can be quickly

reduced by phase-out of compounds. But emissions from diffuse sources, such as release of PFAS residuals from consumer products in use and waste phases of their lifecycle (partly imported from countries with less stringent regulations), can be expected to continue for decades. Thus, for legacy PFASs, future research should focus on viable remediation technologies and end-of life product treatment to minimize the compounds' transport from terrestrial ecosystems via rivers to the marine environment.

Moreover, understanding the global dynamics and ultimate sinks of the compounds is essential to assess their environmental impact and fate in the upcoming decades. Prior studies had investigated the distribution of PFASs in oceanic surface waters, whereas data on deeper ocean waters was still limited when starting this PhD project. The analysis of seven depth profiles from Fram Strait, the Atlantic gateway to the Arctic Ocean, revealed higher PFAS concentrations in the surface water layer than in intermediate waters and a negligible intrusion into deep waters (> 1,000 m). Based on the combination of the measured PFAS concentrations with water volume transport data from an ocean circulation model, mass transport estimates indicated a net inflow into the Arctic Ocean of PFASs with ≥ 8 perfluorinated carbons and a net outflow of shorter-chain homologues. Based on the PFAS composition profile, it can be hypothesized that this reflects higher contributions from atmospheric sources to the Arctic outflow. The higher retention of the long-chain compounds in melting snow and ice can be an additional explanation. The chain-length dependency of Arctic in- and outflow is a novel finding added to discussion on the contribution of atmospheric sources versus ocean transport to PFASs in remote areas, which is ongoing in the scientific community since the 2000s.

Additionally, the outcome highlights the potential role of the Arctic as a secondary source, which may be reinforced by the loss of perennial glacial mass and snow due to climate change. The results can be used to reduce uncertainties in global PFAS mass balances and feed and/or validate environmental fate models. Future PFAS depth profiles in Fram Strait and other key regions of the global oceanic circulation, as well as mechanistic studies on the post-deposition characteristics of PFASs in snow and ice interacting with ocean surface water, can help to elucidate how PFAS cycling is linked to climate change. Moreover, future research could link the findings resulting from analysis of ocean water to bioaccumulation- and -magnification in marine food webs.

An additional aspect of this PhD project was the question if the PFASs commonly monitored by conventional target analysis are representative. Reanalysis of North Sea water sample extracts from the last decade showed that HFPO-DA had already been present in 2011, when it had not yet been in focus and analytical standards had not been available yet. In addition, PFECHS and PFPiAs as

“overlooked” PFASs were detected in the European coastal environment for the first time. These compounds have already been in use for decades, but are typically not included in the analytical scope of conventional target analysis. These findings underline the limitations of target analysis focussing on a predefined spectrum of well-known PFASs. As an upcoming analytical approach, the TOP assay was applied to estimate the sum of PFAS precursors in a sample that oxidize to targeted PFASs. Upon oxidative conversion, the sum of PFCAs significantly increased in German and Chinese river water samples impacted by point sources, indicating the presence of unknown precursors. While the original TOP assay protocol focuses on PFCAs, its scope was extended by the inclusion of ether-based PFASs in this PhD project. The increase of HFPO-DA upon oxidation at particular sites underlines that expanding the original TOP assay protocol can result in capturing a larger amount of the unknown PFAS fraction. This implies that even though the TOP assay is a more inclusive method than target analysis by LC-MS/MS, it still depends on targeted PFASs and only gives a minimum estimate of the unknown oxidizable precursors present in an environmental sample. To obtain a more comprehensive view, target analysis and TOP assay were complemented with a suspect screening approach by means of LC-QToF-MS^E. Based on the developed PFAS suspect screening workflow, 83 PFASs from 13 homologous series were identified in German and/or Chinese river water samples on different levels of confidence. 13 of them have not been reported in the environment before, underlining the potential of HRMS-based suspect screening approaches. These findings suggest that dependent on the type of point source and the spectrum of target analytes, environmental and human exposure to PFASs can be considerably underestimated when analysing only on a small proportion of the PFASs on the worldwide market.

The combination of target analysis with an extended spectrum of target analytes, further improved sum parameters and more harmonized and automated suspect and non-target analysis workflows will help environmental chemists to draw a more and more comprehensive picture of environmental and human exposure to PFASs in the future. However, challenges will continue in how to prioritize and assess these compounds. Facing a group of more than 4,700 PFAS-related CAS numbers, it is unlikely that money and time will be spent to assess the risk related to each of them. As recently recommended by a group of more than 50 international scientists and regulators, further actions on PFASs require a grouping approach [153]. If a grouping approach is implemented on a regulatory level, this will also help to avoid regrettable substitution of regulated PFASs by similar, but not yet regulated PFASs. This is outlined in a plan on the “Elements for an EU-strategy for PFASs”, announced by the national authorities of Sweden, the Netherlands, Germany, Norway and Denmark in December 2019 [349]. The authorities call for minimization of environmental and human exposure to PFASs, at all stages of their life cycle, under Europe’s

chemicals regulation REACH as a key legislation. In line with the timeframe of the United Nations Global Goals for Sustainable Development, they propose that actions on EU level should be taken at the latest by 2025, to be in effect by 2030 [349].

Beyond the prioritization and assessment of replacements in use, future research should focus on non-chemical solutions and on alternatives that are truly “benign by design”, for instance according to the 12 principles of Green Chemistry [350]. Although it is challenging to design environmentally and economically acceptable alternatives for PFASs as compounds that are used because of their extraordinary stability, market demand for sustainable products is growing and can support this development. In this context, raising public awareness of PFAS-related issues will play an important role, with the aim to enable consumers, retailers and product manufacturers to take their own informed decisions. As an example, in the course of its Detox campaign on chemicals in textiles, Greenpeace has started to put the spotlight on the use of PFASs in the outdoor industry in 2012. Responding to growing consumer demands for alternatives, PFAS-free technologies and products have been developed in a relatively short time and several outdoor brands have set PFAS elimination timelines [351]. To transfer this example to other industrial sectors and guide and structure a PFAS phase-out, the concept of essential uses, as recently proposed by Cousins and co-authors [18], can be a way forward. PFASs have unique properties and as the FluoroCouncil, an organization representing the world’s leading fluorotechnology companies, states, they are “integral to modern life” [352]. Specific applications certainly are essential for health and safety, such as protective clothing for fire fighters and specific medical devices. However, for other uses, suitable alternatives have already been developed, such as for most fire fighting foams. Further PFAS applications can be considered as “nice to have” but not essential, for example their use in non-stick kitchenware, fast food wrappers, cosmetics, ski waxes and consumer outdoor gear [18]. In parallel to developing safe alternatives and processes to substitute still essential applications, the definition of non-essential uses can inform and encourage product manufacturers, retailers and consumers to reduce and eventually phase-out those uses of PFASs as a starting point.

10. Experimental

10.1 Chemicals

10.1.1 Solvents and other chemicals

Information on chemicals other than PFASs used for sample preparation, measurement and cleaning is provided in Table 10.1-1.

Table 10.1-1: Solvents, other chemicals and gases used for sample preparation (P), measurement (M) and cleaning (C). Safety data information according to the Globally Harmonized System of Classification and Labelling of Chemicals (GHS) is provided in Table A.5-1.

chemical	specification by supplier	supplier	use
acetic acid	glacial, 100 %	Merck, Germany	P
acetic acid	≥ 99.8 % eluent additive, for LC-MS	Honeywell Fluka, USA	M
acetone	for residue analysis, picograde	LGC Standards, Germany	C
acetonitrile	hypergrade for LC-MS, LiChrosolv	Merck, Germany	M
ammonia solution	25 %, suprapur	Merck, Germany	P
ammonium acetate	for mass spectrometry, eluent additive for LC-MS	Merck, Germany	M
ethyl acetate	hypergrade for LC-MS, LiChrosolv	Merck, Germany	P
formic acid	98–100 %, suprapur	Merck, Germany	P
hydrochloric acid	30 %, suprapur	Merck, Germany	P
methanol	hypergrade for LC-MS, LiChrosolv	Merck, Germany	P, M, C
methanol	for residue analysis, picograde	LGC Standards, Germany	C
nitrogen	liquid, 99.9 %	Air Liquide, France	P, M
2-propanol	hypergrade for LC-MS, LiChrosolv	Merck, Germany	C
potassium peroxide	≥ 99.9 %	Honeywell Fluka, USA	P
silicium dioxide	seasand, purified by acid and calcined for analysis	Merck, Germany	P
sodium hydroxide	30 %, suprapur	Merck, Germany	P
ultrapure water	supplied by Milli-Q Integral 5 system	Merck, Germany	P, M, C

10.1.2 Analytical standards

An overview of the analytical standards used for qualification and quantification of PFASs is provided in Table 10.1-2 to Table 10.1-4. All standards had chemical purities of > 98 % except for HFPO-TrA with a purity > 95 %. They contained the linear isomers of the target analytes, unless stated otherwise. The suppliers prepared the standards from salts of the substances or the free acid (see column 2). The acronyms given in column 1 are used for both forms. If standards were provided as dissolved salts, the CAS registry number of the salt and the free acid counterpart is given in column 3 of the table, if available. The concentrations of the purchased standard solutions in column 4 refer to the salt, or respectively the free acid, given in column 2.

Table 10.1-2: Overview of analytical standards for PFCAs and PFSAs, their CAS registry number and IUPAC names, the standards' suppliers, purity and concentration.

acronym	IUPAC name	CAS number	supplier, purity and concentration
PFBA	butanoic acid, 2,2,3,3,4,4,4-heptafluoro-	375-22-4 (acid)	PFC-MXA (mixture) Wellington Laboratories, 2.0 µg/mL±5 % of the single compounds in methanol
PFPeA	pentanoic acid, 2,2,3,3,4,4,5,5,5-nonafluoro-	2706-90-3 (acid)	
PFHxA	hexanoic acid, 2,2,3,3,4,4,5,5,6,6,6-undecafluoro-	307-24-4 (acid)	
PFHpA	heptanoic acid, 2,2,3,3,4,4,5,5,6,6,7,7,7-tridecafluoro-	375-85-9 (acid)	
PFOA	octanoic acid, 2,2,3,3,4,4,5,5,6,6,7,7,8,8,8-pentadecafluoro-	335-67-1 (acid)	
PFNA	nonanoic acid, 2,2,3,3,4,4,5,5,6,6,7,7,8,8,9,9,9-heptadecafluoro-	375-95-1 (acid)	
PFDA	decanoic acid, 2,2,3,3,4,4,5,5,6,6,7,7,8,8,9,9,10,10,10-nonadecafluoro	335-76-2 (acid)	
PFUnDA	undecanoic acid, 2,2,3,3,4,4,5,5,6,6,7,7,8,8,9,9,10,10,11,11,11-heneicosafuoro-	2058-94-8 (acid)	
PFDoDA	dodecanoic acid, 2,2,3,3,4,4,5,5,6,6,7,7,8,8,9,9,10,10,11,11,12,12,12-tricosafuoro-	307-55-1 (acid)	
PFTriDA	tridecanoic acid, 2,2,3,3,4,4,5,5,6,6,7,7,8,8,9,9,10,10,11,11,12,12,13,13,13-pentacosafuoro-	72629-94-8 (acid)	
PFTeDA	tetradecanoic acid, 2,2,3,3,4,4,5,5,6,6,7,7,8,8,9,9,10,10,11,11,12,12,13,13,14,14,14-heptacosafuoro-	376-06-7 (acid)	
PFBS	1-butanefluoronic acid, 1,1,2,2,3,3,4,4,4-nonafluoro-, potassium salt (1:1)	29420-49-3 (K ⁺ salt) 375-73-5 (acid)	PFS-MXA (mixture) Wellington Laboratories, 2.0 µg/mL±5 % of the single compounds in methanol
PFHxS	1-hexanesulfonic acid, 1,1,2,2,3,3,4,4,5,5,6,6,6-tridecafluoro-, sodium salt (1:1)	82382-12-5 (Na ⁺ salt) 355-46-4 (acid)	
PFHpS	1-heptanesulfonic acid, 1,1,2,2,3,3,4,4,5,5,6,6,7,7,7-pentadecafluoro-, sodium salt (1:1)	22767-50-6 (Na ⁺ salt) 375-92-8 (acid)	
PFOS	1-octanesulfonic acid, 1,1,2,2,3,3,4,4,5,5,6,6,7,7,8,8,8-heptadecafluoro-, sodium salt (1:1)	4021-47-0 (Na ⁺ salt) 1763-23-1 (acid)	
PFDS	1-decanesulfonic acid, 1,1,2,2,3,3,4,4,5,5,6,6,7,7,8,8,9,9,10,10,10-heneicosafuoro-, sodium salt (1:1)	2806-15-7 (Na ⁺ salt)	
		335-77-3 (acid)	

Table 10.1-3: Overview of analytical standards for replacement compounds and/or overlooked PFASs, as well as precursors to PFAAs, their CAS number and IUPAC names, the standards' suppliers, purity and concentration, or respectively amount. All standards were solved in methanol with exception of FOSA, which was solved in isopropanol.

acronym	IUPAC name	CAS number	supplier, purity and conc./amount
DONA	propanoic acid, 2,2,3-trifluoro-3-[1,1,2,2,3,3-hexafluoro-3-(trifluoromethoxy)propoxy]-, sodium salt (1:1)	958445-44-8 (NH ₄ ⁺) 919005-14-4 (acid)	Wellington Laboratories, (50±2.5) µg/mL
HFPO-DA	propanoic acid, 2,3,3,3-tetrafluoro-2-(1,1,2,2,3,3,3-heptafluoropropoxy)-	13252-13-6 (acid) 62037-80-3 (NH ₄ ⁺ salt)	Wellington Laboratories, (50±2.5) µg/mL
HFPO-TrA	propanoic acid, 2,3,3,3-tetrafluoro-2-[1,1,2,3,3,3-hexafluoro-2-(1,1,2,2,3,3,3-heptafluoropropoxy)propoxy]-	13252-14-7 (acid)	ABCR, 5 g
HFPO-TeA	propanoic acid, 2,3,3,3-tetrafluoro-2-[1,1,2,3,3,3-hexafluoro-2-[1,1,2,3,3,3-hexafluoro-2-(1,1,2,2,3,3,3-heptafluoropropoxy)propoxy]propoxy]-	65294-16-8 (acid)	Apollo Scientific, 5 g
6:2 Cl-PFESA	ethanesulfonic acid, 2-[(6-chloro-1,1,2,2,3,3,4,4,5,5,6,6-dodecafluorohexyl)oxy]-1,1,2,2-tetrafluoro-, potassium salt (1:1)	73606-19-6 (K ⁺ salt) 756426-58-1 (acid)	Wellington Laboratories, > 98 %, (50±2.5) µg/mL
8:2 Cl-PFESA	ethanesulfonic acid, 2-[(8-Chloro-1,1,2,2,3,3,4,4,5,5,6,6,-6,7,7,8,8-hexadecafluorooctyl)oxy]-1,1,2,2-tetrafluoro-, potassium salt (1:1)	83329-89-9 (K ⁺ salt)	
6:6 PFPiA	phosphinic acid, bis(tridecafluorohexyl)-, sodium salt (9Cl)	70609-44-8 (Na ⁺ salt) 40143-77-9 (acid)	Wellington Laboratories, > 98 %, (50±2.5) µg/mL
6:8 PFPiA	phosphinic acid, P-(1,1,2,2,3,3,4,4,5,5,6,6,7,7,8,8,8-heptadecafluorooctyl)-P-(1,1,2,2,3,3,4,4,5,5,6,6,6-tridecafluorohexyl)-, sodium salt	610800-34-5 (acid)	
PFECHS	cyclohexanesulfonic acid, 1,2,2,3,3,4,4,5,5,6,6-decafluoro-4-(1,1,2,2,2-pentafluoroethyl)-, potassium salt (1:1)	335-24-0 (K ⁺ salt) 646-83-3 (acid)	Chiron AS, 99.9 %, 50 µg/mL±5 %
FOSA	1-octanesulfonamide, 1,1,2,2,3,3,4,4,5,5,6,6,7,7,8,8,8-heptadecafluoro-	754-91-6 (amide)	
N-EtFOSA ¹	1-octanesulfonamide, N-ethyl-1,1,2,2,3,3,4,4,5,5,6,6,7,7,8,8,8-heptadecafluoro-	4151-50-2 (amide)	
N-EtFOSE ¹	1-octanesulfonamide, N-ethyl-1,1,2,2,3,3,4,4,5,5,6,6,7,7,8,8,8-heptadecafluoro-N-(2-hydroxyethyl)-	1691-99-2 (amide)	Wellington Laboratories, > 98 %, (50±2.5) µg/mL
N-EtFOSAA ¹	glycine, N-ethyl-N-[(1,1,2,2,3,3,4,4,5,5,6,6,7,7,8,8,8-heptadecafluorooctyl)sulfonyl]-	2991-50-6 (acid)	
4:2 FTSA	1-hexanesulfonic acid, 3,3,4,4,5,5,6,6,6-nonafluoro-, sodium salt (1:1)	757124-72-4 (acid)	
6:2 FTSA	1-octanesulfonic acid, 3,3,4,4,5,5,6,6,7,7,8,8,8-tridecafluoro-, sodium salt (1:1)	27619-94-9 (Na ⁺ salt) 27619-97-2 (acid)	
8:2 FTSA	1-decanesulfonic acid, 3,3,4,4,5,5,6,6,7,7,8,8,9,9,10,10,10-heptadecafluoro-, sodium salt (1:1)	39108-34-4 (acid)	

¹ These standards were not included in the initial method development and validation (Chapter 4). They became available at a later point in time and were used solely for the point source study (Chapter 7).

Table 10.1-4: Overview of isotopically-labelled internal standards, their IUPAC names, the standards' suppliers, purity and concentration. Isotopic purities were $\geq 99\%$ per ^{13}C or $> 94\%$ per ^{18}O . The standards were solved in methanol with exception of $^{13}\text{C}_8$ -FOSA, which was solved in isopropanol.

acronym	IUPAC name	supplier, purity and concentration
$^{13}\text{C}_4$ -PFBA	[$^{13}\text{C}_4$]-butanoic acid, 2,2,3,3,4,4,4-heptafluoro-	MPFAC-MXA (mixture) Wellington Laboratories, > 98 %, 2.0 $\mu\text{g}/\text{mL} \pm 5\%$
$^{13}\text{C}_2$ -PFHxA	[1,2- $^{13}\text{C}_2$]-hexanoic acid, 2,2,3,3,4,4,5,5,5-nonafluoro-	
$^{13}\text{C}_4$ -PFOA	[1,2,3,4- $^{13}\text{C}_4$]-octanoic acid, 2,2,3,3,4,4,5,5,6,6,7,7,8,8,8-pentadecafluoro-	
$^{13}\text{C}_5$ -PFNA	[1,2,3,4,5- $^{13}\text{C}_5$]-nonanoic acid, 2,2,3,3,4,4,5,5,6,6,7,7,8,8,9,9,9-heptadecafluoro-	
$^{13}\text{C}_2$ -PFDA	[1,2- $^{13}\text{C}_2$]-decanoic acid, 2,2,3,3,4,4,5,5,6,6,7,7,8,8,9,9,10,10,10-nonadecafluoro	
$^{13}\text{C}_2$ -PFUnDA	[1,2- $^{13}\text{C}_2$]-undecanoic acid, 2,2,3,3,4,4,5,5,6,6,7,7,8,8,9,9,10,10,11,11,11-heneicosfluoro-	
$^{13}\text{C}_2$ -PFDoDA	[1,2- $^{13}\text{C}_2$]-dodecanoic acid, 2,2,3,3,4,4,5,5,6,6,7,7,8,8,9,9,10,10,11,11,12,12,12-tricosfluoro-	
$^{18}\text{O}_2$ -PFHxS	[$^{18}\text{O}_2$]-1-hexanesulfonic acid, 1,1,2,2,3,3,4,4,5,5,6,6,6-tridecafluoro-, sodium salt (1:1)	
$^{13}\text{C}_4$ -PFOS	[1,2,3,4- $^{13}\text{C}_4$]-1-octanesulfonic acid, 1,1,2,2,3,3,4,4,5,5,6,6,7,7,8,8,8-heptadecafluoro-, sodium salt (1:1)	
$^{13}\text{C}_3$ -PFBS	[2,3,4- $^{13}\text{C}_3$]-1-butanesulfonic acid, 1,1,2,2,3,3,4,4,4-nonafluoro-, potassium salt (1:1)	
$^{13}\text{C}_3$ -HFPO-DA	[$^{13}\text{C}_3$]-propanoic acid, 2,3,3,3-tetrafluoro-2-(1,1,2,2,3,3,3-heptafluoropropoxy)-	Wellington Laboratories, > 98 %, (50 \pm 2.5) $\mu\text{g}/\text{mL}$
$^{13}\text{C}_8$ -FOSA	[$^{13}\text{C}_8$]-1-octanesulfonamide, 1,1,2,2,3,3,4,4,5,5,6,6,7,7,8,8,8-heptadecafluoro-	
<i>N</i> -EtFOSE-d ₉ ¹	1-octanesulfonamide-d ₅ , <i>N</i> -ethyl-d ₂ -1,2,2,3,3,4,4,5,5,6,6,7,7,8,8,8-heptadecafluoro- <i>N</i> -(2-hydroxyethyl)-d ₂	
$^{13}\text{C}_2$ -4:2 FTSA ¹	[1,2- $^{13}\text{C}_2$]-1-hexanesulfonic acid, 3,3,4,4,5,5,6,6,6-nonafluoro-, sodium salt (1:1)	
$^{13}\text{C}_2$ -6:2 FTSA	[1,2- $^{13}\text{C}_2$]-1-octanesulfonic acid, 3,3,4,4,5,5,6,6,7,7,8,8,8-tridecafluoro-, sodium salt (1:1)	
$^{13}\text{C}_2$ -8:2 FTSA ¹	[1,2- $^{13}\text{C}_2$]-1-decanesulfonic acid, 3,3,4,4,5,5,6,6,7,7,8,8,9,9,10,10,10-heptadecafluoro-, sodium salt (1:1)	
$^{13}\text{C}_8$ -PFOA	[$^{13}\text{C}_8$]-octanoic acid, 2,2,3,3,4,4,5,5,6,6,7,7,8,8,8-pentadecafluoro- (injection standard)	

¹These standards were not included in the initial method development and validation (Chapter 4). They became available at a later point in time and were used solely for the point source study (Chapter 7).

10.2 Instrumental methods

10.2.1 LC-MS/MS

Table 10.2-1 and Table 10.2-2 provide an overview of the hardware components and the compound-independent parameter settings for the LC-MS/MS analysis of PFASs.

Table 10.2-1: Overview of hardware components and parameter settings for the chromatographic separation of the target analytes.

component	type (manufacturer, country)																												
binary pump	HP 1100 LC binary pump G1312 (Agilent, USA)																												
autosampler	HP 1100 LC autosampler G1313 (Agilent, USA)																												
analytical column	Synergi Fusion-RP: polar embedded C ₁₈ phase with trimethylsilyl endcapping, 150 mm x 2 mm, particle size 4 μm, pore size 80 Å (Phenomenex, USA)																												
guard column	SecurityGuard cartridge for Fusion-RP HPLC columns, 4 mm x 2 mm (Phenomenex, USA)																												
software	Analyst 1.5 (AB Sciex, USA)																												
parameter	setting																												
injection volume	10 μL (needle rinsed twice with methanol before injection)																												
column temperature	30 °C																												
flow rate	0.2 mL/min																												
mobile phases	A: 2 mM ammonium acetate aqueous solution B: 0.05 % acetic acid in methanol																												
sample/standard solvent	methanol:water 80:20 (v/v)																												
gradient	<table border="1"> <thead> <tr> <th>time [min]</th> <th>A [%]</th> <th>B [%]</th> <th>note</th> </tr> </thead> <tbody> <tr> <td>-8</td> <td>70</td> <td>30</td> <td>equilibration</td> </tr> <tr> <td>0</td> <td>70</td> <td>30</td> <td></td> </tr> <tr> <td>3</td> <td>30</td> <td>70</td> <td></td> </tr> <tr> <td>29</td> <td>10</td> <td>90</td> <td></td> </tr> <tr> <td>31</td> <td>0</td> <td>100</td> <td></td> </tr> <tr> <td>45</td> <td>0</td> <td>100</td> <td>purging</td> </tr> </tbody> </table>	time [min]	A [%]	B [%]	note	-8	70	30	equilibration	0	70	30		3	30	70		29	10	90		31	0	100		45	0	100	purging
time [min]	A [%]	B [%]	note																										
-8	70	30	equilibration																										
0	70	30																											
3	30	70																											
29	10	90																											
31	0	100																											
45	0	100	purging																										

Table 10.2-2: Overview of hardware components and parameter settings for the mass-spectrometric detection of the target analytes.

component	type (manufacturer, country)
instrument	API 4000 triple quadrupole mass spectrometer (AB Sciex, USA)
ion source	Turbo V Ion Source (AB Sciex, USA)
roughing pump 1 (interface)	rotary vane vacuum pump D16B (Leybold, Germany)
roughing pump 2 (backing turbo pump)	rotary vane vacuum pump HS602 (Agilent Varian, USA)
software	Analyst 1.5 (AB Sciex, USA)
parameter	settings
ionization	electrospray ionization (ESI) in negative mode
ion spray voltage	-4500 V
source temperature	400 °C
gas 1 (nebulizer gas)	N ₂ , 4.2 bar
gas 2 (heater gas)	N ₂ , 2.8 bar
curtain gas	N ₂ , 1.0 bar
collision gas	N ₂ , 0.6 bar
scan type	<i>Scheduled</i> Multiple Reaction Monitoring (MRM) retention time window: 180 s, target scan time: 2 s

Table 10.2-3 to Table 10.2-5 give an overview of the compound-specific settings for the LC-MS/MS analysis of the target analytes and internal standards. Exemplary retention times (t_R) are given in column 1. They changed in dependence of the age of the column and were determined before each measurement sequence in a non-scheduled MRM run. Column 2 shows the molecular formula of the precursor ion, which is the $[M-H]^-$ ion of the target analytes. Monitored mass transitions are given in column 4. Asterisks mark the product ion which was used as quantifier, whereas the second product ion was used as qualifier. Column 5 lists the optimized transition-specific mass spectrometric parameters, including the declustering potential (DP), the entrance potential (EP), the collision energy (CE) and the cell exit potential (CXP).

Table 10.2-3: Compound-specific parameter settings for the LC-MS/MS analysis of PFCAs and PFSA.

acronym analyte	t_R [min] ¹	molecular formula precursor ion	mass transition [m/z]	transition-specific parameters [V]			
				DP	EP	CE	CXP
PFBA	6.1	$[C_4F_7O_2]^-$	213>169*	-30	-5	-13	-9
PFPeA	9.6	$[C_5F_9O_2]^-$	263>219*	-26	-4	-12	-13
PFHxA	10.4	$[C_6F_{11}O_2]^-$	313>269*	-28	-4	-13	-16
			313>119	-28	-4	-30	-5
PFHpA	11.1	$[C_7F_{13}O_2]^-$	363>319*	-29	-4	-14	-19
			363>169	-29	-4	-25	-8
PFOA	11.9	$[C_8F_{15}O_2]^-$	413>369*	-24	-4	-15	-8
			413>169	-24	-4	-28	-8
PFNA	12.9	$[C_9F_{17}O_2]^-$	463>419*	-34	-4	-15	-9
			463>219	-34	-4	-24	-12
PFDA	14.2	$[C_{10}F_{19}O_2]^-$	513>469*	-35	-6	-15	-11
			513>219	-35	-6	-29	-12
PFUnDA	15.9	$[C_{11}F_{21}O_2]^-$	563>519*	-35	-5	-17	-13
			563>169	-35	-5	-37	-8
PFDoDA	18.0	$[C_{12}F_{23}O_2]^-$	613>569*	-38	-9	-17	-15
			613>169	-38	-9	-38	-8
PFTrDA	20.3	$[C_{13}F_{25}O_2]^-$	663>619*	-39	-8	-18	-14
			663>169	-39	-8	-41	-8
PFTeDA	22.7	$[C_{14}F_{27}O_2]^-$	713>669*	-36	-9	-22	-15
			713>169	-36	-9	-40	-8
PFBS	9.7	$[C_4F_9O_3S]^-$	299>99*	-66	-12	-42	-16
			299>80	-66	-12	-60	-2
PFHxS	11.1	$[C_6F_{13}O_3S]^-$	399>99	-70	-14	-50	-15
			399>80*	-70	-14	-66	-2
PFHpS	11.8	$[C_7F_{15}O_3S]^-$	449>99	-80	-12	-61	-16
			449>80*	-80	-12	-85	-2
PFOS	12.8	$[C_8F_{17}O_3S]^-$	499>99	-73	-12	-74	-17
			499>80*	-73	-12	-90	-2
PFDS	15.8	$[C_{10}F_{21}O_3S]^-$	599>99	-80	-14	-62	-3
			599>80*	-80	-14	-90	-2

¹ The retention time given in the table refers to the linear isomers of the compounds.

Table 10.2-4: Compound-specific parameter settings for the LC-MS/MS analysis of replacement compounds, overlooked PFASs and precursors.

acronym analyte	t _R [min] ¹	molecular formula precursor ion	mass transition [m/z]	transition-specific parameters [V]			
				DP	EP	CE	CXP
DONA	11.2	[C ₇ HF ₁₂ O ₄] ⁻	377>251* 377>85	-33 -33	-6 -6	-22 -50	-16 -14
HFPO-DA	10.6	[C ₆ F ₁₁ O ₃] ⁻	329>285 329>169*	-22 -22	-4 -4	-7 -18	-18 -8
HFPO-TrA	13.3	[C ₉ F ₁₇ O ₄] ⁻	495>185*	-15	-4	-9	-12
HFPO-TcA	18.0	[C ₁₂ F ₂₃ O ₅] ⁻	661>351* 661>185	-8 -30	-8 -4	-8 -45	-2 -14
6:2 Cl-PFESA	13.5	[C ₈ ClF ₁₆ O ₄ S] ⁻	531>351* 531>83	-60 -60	-14 -14	-39 -61	-20 -14
8:2 Cl-PFESA	16.9	[C ₁₀ ClF ₂₀ O ₄ S] ⁻	631>451* 631>83	-75 -75	-13 -13	-44 -82	-20 -2
6:6 PFPiA	18.9	[C ₁₂ F ₂₆ O ₂ P] ⁻	701>401* 701>63	-75 -75	-8 -8	-77 -89	-16 -10
6:8 PFPiA	22.8	[C ₁₄ F ₃₀ O ₂ P] ⁻	801>501* 801>401	-57 -57	-11 -11	-83 -82	-20 -18
PFECHS	11.7	[C ₈ F ₁₅ O ₃ S] ⁻	461>381* 461>99	-60 -60	-10 -10	-40 -55	-20 -4
FOSA	20.5	[C ₈ HF ₁₇ NO ₂ S] ⁻	498>78*	-84	-10	-69	-2
N-EtFOSA ²	22.7	[C ₁₀ H ₅ F ₁₇ NO ₂ S] ⁻	526>219 526>169*	-70 -70	-11 -11	-38 -40	-11 -8
N-EtFOSE ²	22.4	[C ₁₂ H ₁₀ F ₁₇ NO ₃ S] [CH ₃ COO] ⁻	630>59*	-40	-8	-65	-10
N-EtFOSAA ²	23.1	[C ₁₂ H ₇ F ₁₇ NO ₄ S] ⁻	584>526 584>419	-50 -40	-8 -8	-30 -30	-20 -20
4:2 FTSA	10.3	[C ₆ H ₄ F ₉ O ₃ S] ⁻	327>307 327>81*	-60 -60	-10 -10	-28 -48	-18 -2
6:2 FTSA	11.7	[C ₈ H ₄ F ₁₃ O ₃ S] ⁻	427>407 427>81*	-70 -70	-13 -13	-34 -68	-20 -2
8:2 FTSA	14.1	[C ₁₀ H ₄ F ₁₇ O ₃ S] ⁻	527>507 527>81*	-80 -80	-14 -14	-40 -76	-20 -2

¹ The retention time given in the table refers to the linear isomers of the compounds.

² These compounds were not included in the initial method development and validation (Chapter 4). They became available at a later point in time and were used solely for the point source study (Chapter 7).

Table 10.2-5: Compound-specific parameter settings for the LC-MS/MS analysis of the internal standards used for quantification of PFASs. $^{13}\text{C}_8$ -PFOA was added as injection standard.

acronym analyte	t_{R} [min]	molecular formula precursor ion	mass transition s [m/z]	transition-specific parameters [V]			
				DP	EP	CE	CXP
$^{13}\text{C}_4$ -PFBA	6.1	$[^{13}\text{C}_4\text{F}_7\text{O}_2]^-$	217>172*	-22	-4	-13	-9
$^{13}\text{C}_2$ -PFHxA	10.4	$[^{13}\text{C}_2^{12}\text{C}_4\text{F}_{11}\text{O}_2]^-$	315>270*	-23	-6	-12	-16
			315>120	-23	-6	-31	-4
$^{13}\text{C}_4$ -PFOA	11.9	$[^{13}\text{C}_4^{12}\text{C}_4\text{F}_{15}\text{O}_2]^-$	417>372*	-32	-4	-13	-8
			417>169	-32	-4	-27	-8
$^{13}\text{C}_8$ -PFOA	11.9	$[^{13}\text{C}_8\text{F}_{15}\text{O}_2]^-$	421>376*	-25	-6	-14	-8
			421>172	-25	-6	-26	-8
$^{13}\text{C}_5$ -PFNA	12.9	$[^{13}\text{C}_5^{12}\text{C}_4\text{F}_{17}\text{O}_2]^-$	468>423*	-30	-7	-14	-10
			468>223	-30	-7	-24	-12
$^{13}\text{C}_2$ -PFDA	14.2	$[^{13}\text{C}_2^{12}\text{C}_8\text{F}_{19}\text{O}_2]^-$	515>470*	-39	-6	-16	-10
			515>220	-39	-6	-26	-12
$^{13}\text{C}_2$ -PFUnDA	15.9	$[^{13}\text{C}_2^{12}\text{C}_9\text{F}_{21}\text{O}_2]^-$	565>520*	-33	-6	-16	-13
			565>169	-33	-6	-34	-8
$^{13}\text{C}_2$ -PFDoDA	18.0	$[^{13}\text{C}_2^{12}\text{C}_{10}\text{F}_{23}\text{O}_2]^-$	615>570*	-38	-9	-17	-15
			615>169	-38	-9	-41	-8
$^{13}\text{C}_3$ -PFBS	9.7	$[^{13}\text{C}_3^{12}\text{CF}_9\text{O}_3\text{S}]^-$	302>99*	-67	-10	-42	-16
			302>80	-67	-10	-60	-2
$^{18}\text{O}_2$ -PFHxS	11.1	$[\text{C}_6\text{F}_{13}^{18}\text{O}_2^{16}\text{OS}]^-$	403>103	-82	-10	-55	-4
			403>84*	-82	-10	-79	-2
$^{13}\text{C}_4$ -PFOS	12.8	$[^{13}\text{C}_4^{12}\text{C}_4\text{F}_{17}\text{O}_3\text{S}]^-$	503>99	-65	-12	-64	-4
			503>80*	-65	-12	-92	-2
$^{13}\text{C}_3$ -HFPO-DA	10.6	$[^{13}\text{C}_3^{12}\text{C}_3\text{F}_{11}\text{O}_3]^-$	332>287	-21	-3	-7	-14
			332>169*	-21	-3	-23	-8
$^{13}\text{C}_8$ -FOSA	20.5	$[^{13}\text{C}_8\text{HF}_{17}\text{NO}_2\text{S}]^-$	506>78*	-70	-15	-64	-12
N-EtFOSE-d ₉ ¹	22.4	$[\text{C}_{12}\text{D}_9\text{HF}_{17}\text{NO}_3\text{S}]^-$ $[\text{CH}_3\text{COO}]^-$	639>59*	-80	-14	-46	-20
$^{13}\text{C}_2$ -4:2 FTSA ¹	10.3	$[^{13}\text{C}_2^{12}\text{C}_4\text{H}_4\text{F}_9\text{O}_3\text{S}]^-$	329>309	-60	-10	-28	-18
			329>81*	-60	-10	-48	-2
$^{13}\text{C}_2$ -6:2 FTSA	11.7	$[^{13}\text{C}_2^{12}\text{C}_6\text{H}_4\text{F}_{13}\text{O}_3\text{S}]^-$	429>409	-70	-14	-33	-8
			429>81*	-70	-14	-68	-2
$^{13}\text{C}_2$ -8:2 FTSA ¹	14.1	$[^{13}\text{C}_2^{12}\text{C}_8\text{H}_4\text{F}_{17}\text{O}_3\text{S}]^-$	529>509	-80	-14	-46	-20
			529>81*	-80	-14	-76	-2

¹ These internal standards were not included in the initial method development and validation (Chapter 4). They became available at a later point in time and were used solely for the point source study (Chapter 7).

10.2.2 LC-QToF-MS^E

LC-QToF-MS^E analysis was conducted at the Department of Aquatic Sciences and Assessment, Swedish University of Agricultural Sciences, Uppsala, Sweden.

Table 10.2-6: Overview of hardware components and parameter settings for the chromatographic separation as first step of the LC-QToF-MS^E analysis.

component	type																								
system	Acquity H-Class with flow-through needle (FTN) injector, Waters, USA																								
analytical column	Acquity bridged ethylsiloxane/silica hybrid (BEH) UPLC C ₁₈ column, 100 mm x 2.1 mm, particle size 1.7 μm, pore size 130 Å (Waters, USA)																								
software	Unifi Scientific Information System, version 1.9.4 (Waters, USA)																								
parameter	setting																								
injection volume	5 μL																								
column temperature	40 °C																								
flow rate	0.5 mL/min																								
mobile phases	A: 5 mM ammonium acetate buffer with 0.01 % ammonia B: acetonitrile with 0.01 % ammonia																								
sample solvent	methanol:water ~80:20 (v/v)																								
gradient	<table border="1"> <thead> <tr> <th>time [min]</th> <th>A [%]</th> <th>B [%]</th> </tr> </thead> <tbody> <tr> <td>0.0</td> <td>95</td> <td>5</td> </tr> <tr> <td>0.5</td> <td>95</td> <td>5</td> </tr> <tr> <td>16.0</td> <td>5</td> <td>95</td> </tr> <tr> <td>16.1</td> <td>1</td> <td>99</td> </tr> <tr> <td>19.0</td> <td>1</td> <td>99</td> </tr> <tr> <td>19.1</td> <td>95</td> <td>5</td> </tr> <tr> <td>21.0</td> <td>95</td> <td>5</td> </tr> </tbody> </table>	time [min]	A [%]	B [%]	0.0	95	5	0.5	95	5	16.0	5	95	16.1	1	99	19.0	1	99	19.1	95	5	21.0	95	5
time [min]	A [%]	B [%]																							
0.0	95	5																							
0.5	95	5																							
16.0	5	95																							
16.1	1	99																							
19.0	1	99																							
19.1	95	5																							
21.0	95	5																							

Table 10.2-7: Overview of hardware components and parameter settings for the mass spectrometric measurement as the second step of the LC-QToF-MS^E analysis.

component	type (manufacturer, country)
instrument	Xevo G2-S, quadrupole time-of-flight mass spectrometer (Waters, USA)
software	Unifi Scientific Information System, version 1.9.4 (Waters, USA)
ion source settings	
ionization	electrospray ionization (ESI) in negative mode
capillary voltage	0.4 kV
cone voltage	30 V
source temperature	120 °C
cone gas flow	25 L/h
desolvation temperature	450 °C
desolvation gas flow	700 L/h
mass spectrometric analysis settings	
mode	MS ^E ; resolution
mass range	m/z 50–1200
scan time	0.25 s
scan function 1	Q1 scanning mass range, q2 (collision cell) uses “low” collision energy (CE)
low CE	4 eV
scan function 2	Q1 scanning mass range, q2 uses a “high” collision energy ramp
high CE ramp start	10 eV
high CE ramp end	45 eV

lock spray infusion	
reference compound	leucine enkephalin, 2 µg/mL in ACN/water (50:50) with 0.1 % formic acid
lock mass	m/z 236.1041; 554.262
flow	10 µL/min
interval	10 s
scan time	0.25 s
capillary voltage	3.0 kV
cone voltage	30 V

10.3 Sampling

A stainless steel frame was used to collect water samples from the research vessel *Ludwig Prandtl* and from pontoons, moles and bridges during land-based sampling campaigns. A 1 L polypropylene bottle was mounted on it and samples were taken 0.5 m below the surface (Figure 10.3-1A). Samples were stored at 4 °C and processed in the lab within four weeks after sampling.

During the *Polarstern* expedition, surface water samples were taken at approximately 11 m depth using the ship's seawater intake system (stainless steel pipe) (Figure 10.3-1B). The stainless steel pipe was flushed for at least ten minutes before sampling to ensure that the sampled water is from the respective sampling site and does not contain remainders from an earlier station. To take water from different depths, a CTD/rosette sampler was deployed from deck to the ocean bottom (Figure 10.3-1C). On its way back to the surface, 12 L Niskin bottles mounted on the steel frame of the sampler were closed at predefined depths. After the sampler was lifted to the filling room, 1 L samples for PFAS analysis were taken from the Niskin bottles. The samples were stored at 5 °C and extracted on board within one week after sampling.

Before the sampling campaigns, the sampling bottles were cleaned twice in a laboratory dishwasher and rinsed with 10 mL methanol three times. At the respective sampling location, the bottles were rinsed with water from the sampling site.

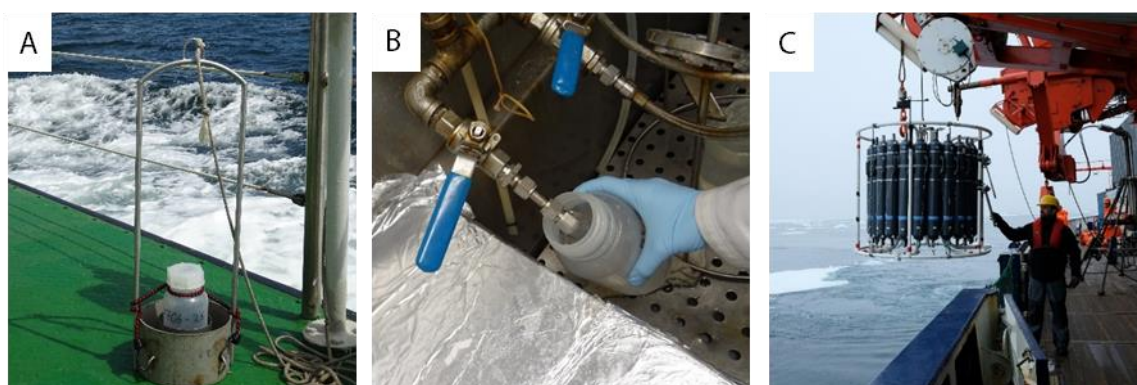


Figure 10.3-1: Different techniques for the collection of water samples, including A) a stainless steel frame with a mounted PP bottle, B) the ship's seawater intake system (stainless steel pipe), and C) a CTD/rosette sampler.

Surface sediment samples were collected by a stainless steel box corer or van Veen grabs. After homogenization and removal of large pieces, such as sea shells and stones, sediment samples were

transferred to aluminium shells and stored at $-20\text{ }^{\circ}\text{C}$ until sample preparation. Aluminium shells were cleaned with acetone and baked at $250\text{ }^{\circ}\text{C}$ before usage.

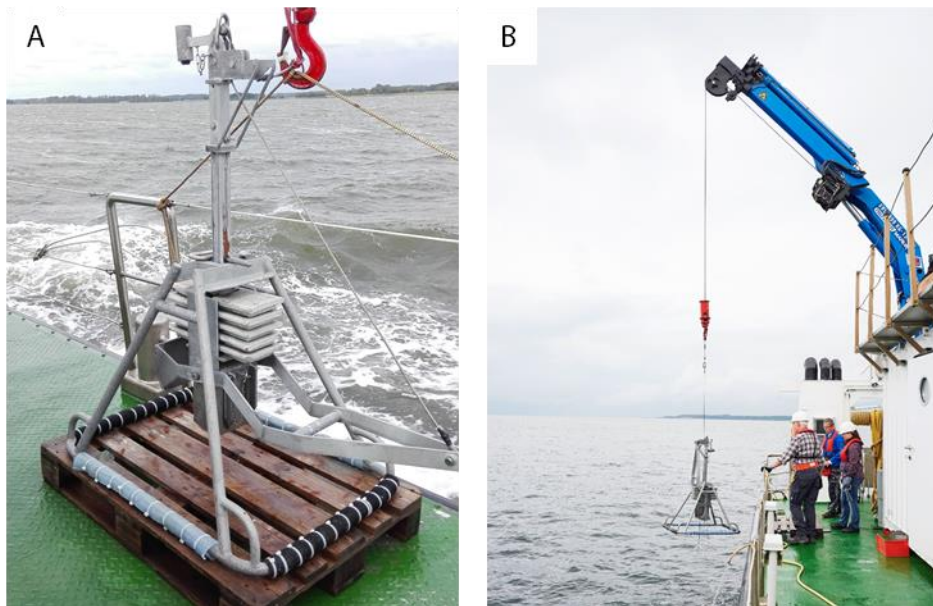


Figure 10.3-2: Sample collection of sediment samples using a stainless steel box corer (picture A: Christina Apel\HZG, picture B: Christian Schmid\HZG).

Table 10.3-1 gives an overview of the samples collected for this PhD project and the sampling techniques used during the different campaigns.

Table 10.3-1: Overview of samples collected and analysed for this PhD project.

region/transect	research vessel campaign code	date	number of samples ⁴	sampling technique	chapter
North Sea, German Bight	<i>Ludwig Prandtl</i> ¹ LP20170606	06/2017	water: 45 sediment: 8	stainless steel frame with PP bottle box corer	5
Baltic Sea, German coastal areas	<i>Ludwig Prandtl</i> ¹ LP20170904	09/2017	water: 47 sediment: 7	stainless steel frame with PP bottle box corer	5
North Sea – Skagerrak/ Kattegat – Baltic Sea	<i>Maria S. Merian</i> ³ MSM50	01/2016	sediment: 9	box corer or van Veen grabs	5
North Sea – Norwegian Sea – Greenland Sea – Fram Strait – Norwegian Sea	<i>Polarstern</i> ² PS114 (ARK-XXXII/1)	07/2018 – 08/2018	surface water: 40 different depths: 58	seawater intake system (stainless steel pipe) CTD/rosette sampler	6
River Rhine and tributaries (pre-study)	<i>Tümmeler</i> ³ Rhine2017	08/2017	water: 12 sediment: 11	stainless steel frame with PP bottle	7
River Rhine and tributaries, River Alz	land-based ¹ RhineAlz20180910	09/2018	water: - target analysis: 30 - TOP assay: 24 - suspect screening: 12	stainless steel frame with PP bottle	7, 8
Rivers Xiaoqing, Xi and Yangtze	land-based ¹ ChineseRivers20181111	11/2018	water: - target analysis: 28 - TOP assay: 11 - suspect screening: 10	stainless steel bucket	7, 8

¹ The land-based sampling campaigns and the *Ludwig Prandtl* campaigns were organized and performed together with colleagues from the department of environmental chemistry (RhineAlz20180910, LP20170606, LP20170904), or respectively from the Yantai Institute of Coastal Zone Research in China (ChineseRivers20181111).

² In the beginning of the PhD, the research objectives of study 3 were included in a proposal for supplemental use of the research vessel *Polarstern* (Dr. Zhiyong Xie, N-2016-N-53). Supplemental use was approved for expedition PS114, during which the samples could be taken.

³ The department of marine bioanalytical chemistry organized the campaigns and took the samples on the *Maria S. Merian* cruise MSM50 and for the Rhine River pre-study in 2017.

⁴ The number of samples given refer to the number of different sampling locations and do not include QA/QC samples, such as triplicates or blank samples.

10.4 Analysis of physicochemical parameters

10.4.1 Water temperature, pH value and salinity

During the ship-based sampling campaigns, water temperature, pH value and salinity and were measured continuously by the *in situ* FerryBox system [249]. During the land-based sampling campaigns, physicochemical parameters were analysed using a portable multiparameter measuring device (Multi 3430 SET G, WTW Wissenschaftlich Technische Werkstätten, Germany). It was equipped with a pH electrode with built-in temperature sensor (SenTix 940-3) and a conductivity measuring cell (TetraCon 925-3). The measurement was performed onsite, directly after sampling.

10.4.2 Total organic carbon

For the analysis of total organic carbon (TOC) in sediment samples, separate sub-samples were dried to constant weight at 40 °C. TOC₄₀₀-values were determined in duplicates using a RC612 multiphase carbon/hydrogen/moisture determinator (LECO, USA). The method was based on dry combustion, applying a temperature ramp from 150 °C to 400 °C at 70 °C/min in an oxygen flow. The generated carbon dioxide was infrared-detected. The quantification limit was 0.03 mg carbon (absolute), corresponding to a TOC content of 0.006 % in a 500 mg sample aliquot.

10.5 Sample preparation of aqueous samples

10.5.1 Target analysis

Samples with a high load of particulate matter (river water, coastal seawater) were filtered through glass microfiber filters before analysis (Whatman, grade GF/F, pore size 0.7 µm, diameter 47 mm, GE Healthcare, USA). For PFAS analysis in 1 L water samples, weak anion exchange cartridges (Oasis WAX, 6 cc, 500 mg sorbent, 60 µm particle size, Waters, USA) were preconditioned by 6 mL 0.1 % ammonium hydroxide in methanol, 6 mL methanol and 6 mL water. Samples were spiked with internal standards (3 ng each) and loaded onto the cartridges at a flow rate of 2–3 drops/s (3–4 mL/min). A washing step with 15 mL of an 80:20 (v/v) water:methanol solution followed. After vacuum drying of the cartridges, the target compounds were eluted using 6 mL methanol and 6 mL 0.1 % ammonium hydroxide in methanol. The eluates were reduced to 150 µL under nitrogen (Flowtherm Optocontrol evaporator, Barkey, Germany) and the glass vessels with the concentrated samples were ultrasonicated for 20 min (Sonorex Digiplus DL510H, Bandelin, Germany; nominal power 24 W/L, ultrasonic frequency 35 kHz). Finally, the samples were transferred to polypropylene vials and 1 ng of the injection standard ¹³C₈-PFOA (10 µL of a 100 pg/µL solution) and 40 µL water (20 % v/v) were added. A schematic overview of the method is given in Figure 10.5-1.

Developed on the basis of coastal seawater and river water impacted by diffuse sources, this procedure was adapted to open seawater and river water impacted by point sources with expected lower or higher PFAS concentrations. Open seawater samples were spiked with 400 pg of each internal standard and 400 pg of the injection standard only (Chapter 6.2). For river water samples taken close to particular point sources in China and Germany, the initial sample volume was decreased to 500 mL, 100 mL or 1 mL (Chapter 7.3).

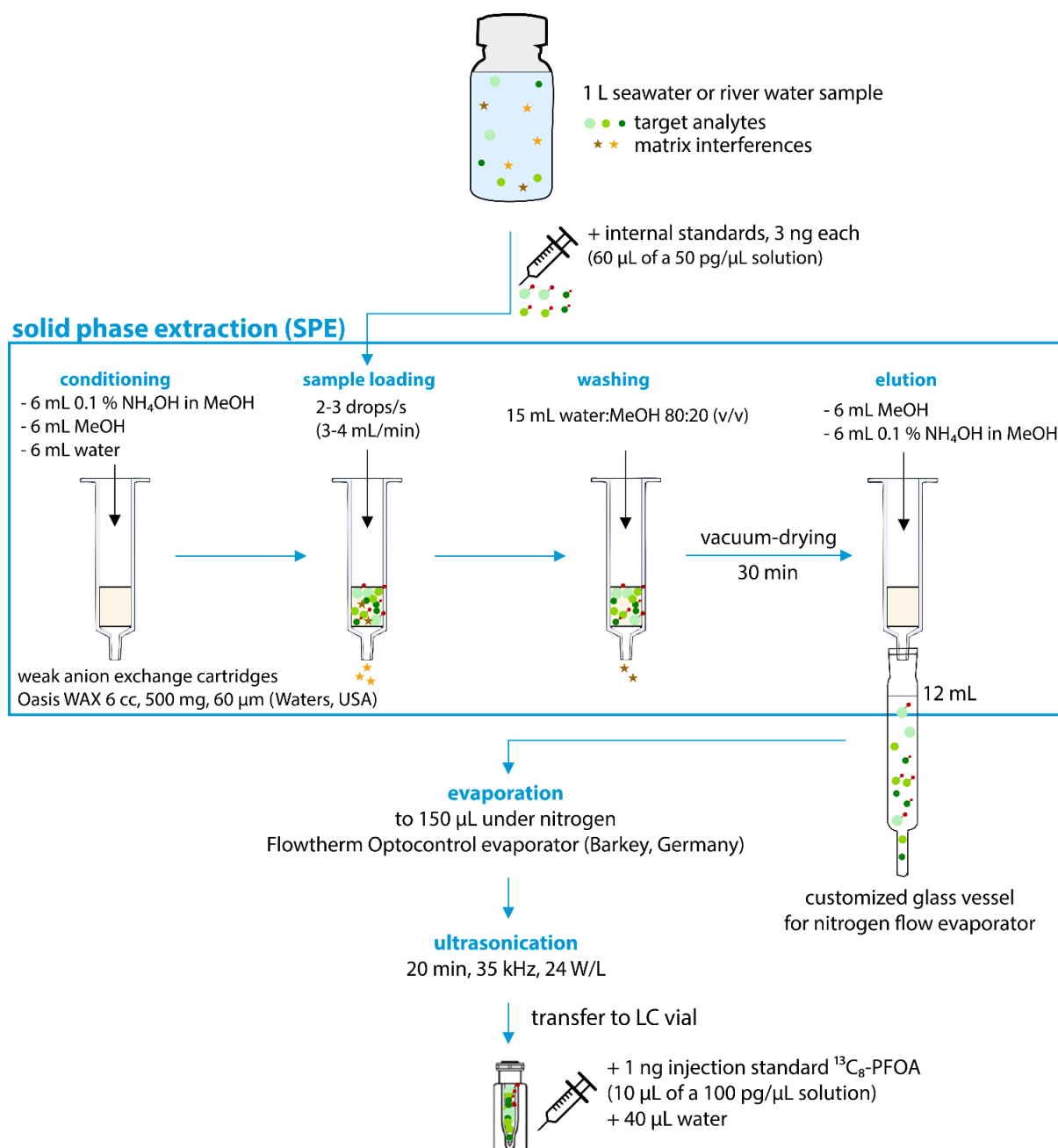


Figure 10.5-1: Schematic overview of the sample preparation of aqueous samples.

10.5.2 TOP assay

The TOP assay was performed according to Houtz and Sedlak [192]. One of the two 125 mL sample aliquots was amended with 2 g potassium persulfate (60 mM) and 1.9 mL of 10 N sodium hydroxide solution (150 mM). The samples were placed in a temperature-controlled water bath at 85 °C for 6 h (20 L Circulation Bath, PolyScience, USA). After cooling them down in an ice bath, the pH of the samples was adjusted to a value between 6 and 8. The oxidized aliquot and a second untreated aliquot were spiked with internal standards (1.5 ng each) and processed using the target analysis method.

10.5.3 Suspect screening

The samples were filtered through glass microfiber filters before analysis of the dissolved phase (Whatman, grade GF/F, pore size 0.7 μm, diameter 47 mm, GE Healthcare, USA). Samples triplicates of 500 mL were prepared, adjusted to pH 6.5 with formic acid and spiked with a mixture of internal standards (2.5 ng each).

To achieve enrichment for a broad range of PFASs, mixed-bed cartridges with four different sorbents were used. For this, empty cartridges with a volume of 6 cm³ (Phenomenex, USA) were filled manually with a mixture of 150 mg Isolute ENV+ (Biotage, Sweden), 100 mg Strata-X-AW and 100 mg Strata-X-CW (both Phenomenex, USA) in the first compartment and 200 mg Strata-X (Phenomenex, USA) in the second compartment. As schematically shown in Figure 10.5-2, the compartments were separated by a polyethylene frit (pore size: 20 μm, diameter: 13 mm; Biotage, Sweden). According to the manufacturers' specifications, Isolute ENV+ is a hydroxylated polystyrene-divinylbenzene copolymer for extracting polar analytes, whereas Strata-X is a reversed-phase sorbent for extracting neutral compounds and aromatics, Strata-X-AW a weak anion-exchange resin for retention of acidic compounds and Strata-X-CW a weak-cation exchange resin for retention of basic compounds.

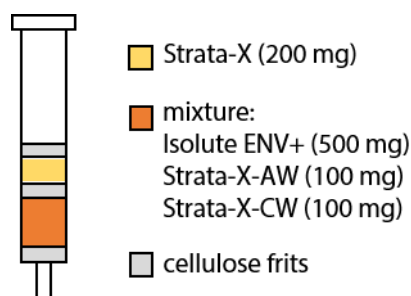


Figure 10.5-2: Scheme of in-house prepared solid-phase extraction cartridges.

The sorbent mixture was preconditioned using 6 mL and 6 mL water, before 500 mL aliquots of the samples were passed through the cartridges at a flow rate of 2–3 drops/s (3–4 mL/min). After the cartridges were dried under vacuum for 30 min, they were stored at –20 °C. Up to here,

extraction of the German samples took place at HZG, whereas Chinese samples were processed at the Yantai Institute of Coastal Zone Research. The dried cartridges were shipped from China to Germany and further steps were performed at HZG. The target compounds were eluted using 4 mL methanol/ethyl acetate (v/v 50:50), containing 0.5 % ammonia, followed by 2 mL of methanol/ethyl acetate (v/v 50:50), containing 1.7 % formic acid. The eluates were reduced to 200 μ L under nitrogen (Flowtherm Optocontrol evaporator, Barkey, Germany) and transferred to polypropylene vials. Methanol was added to a final volume of a 0.5 mL.

10.6 Sample preparation of sediment samples

Wet sediment was freeze-dried prior to sample extraction (Gamma 1-16 LSCplus, Christ, Germany). Afterwards, small stones and sticks were removed with forceps and the samples were homogenized using an agate mortar and pestle. 5 g of the freeze-dried, homogenized sediment samples was transferred to 50 mL polypropylene tubes and spiked with internal standards (3 ng each). 30 mL of a 1 % acetic acid in water solution was added before the samples were vortexed, ultrasonicated (60 °C, 15 min) and centrifuged (3,000 rpm, 5 min). The supernatant was transferred to a 125 mL high-density polyethylene bottle. Subsequently, 7.5 mL of a mixture of methanol and 1 % acetic acid in water (90:10, v/v) was added to the original polypropylene tube and the process of vortexing, ultrasonication, centrifugation and transferring the supernatant to the 125 mL high-density polyethylene bottle was repeated. This combination of acetic acid wash and methanol extraction was repeated twice for each sample. To clean and concentrate the sample extracts, an SPE extraction was performed for the pooled supernatants in the same way as for the water samples. The eluate was reduced in volume under nitrogen to 1 mL (Flowtherm Optocontrol evaporator, Barkey, Germany) and passed through a syringe filter (Spartan Whatman, pore size 0.2 μ m, diameter 13 mm, GE Healthcare, USA). Afterwards, the filtered eluate was concentrated to 150 μ L and transferred to a polypropylene vial. The walls of the glass vessel, in which the sample had been concentrated, were rinsed with 3 mL methanol. The rinse was also reduced in volume under nitrogen to 150 μ L and transferred to the same polypropylene vial as the sample. 2 ng of the injection standard $^{13}\text{C}_8$ -PFOA (20 μ L of a 100 pg/ μ L solution) and 80 μ L water were added. A schematic overview of the preparation of sediment samples is given in Figure 10.6-1.

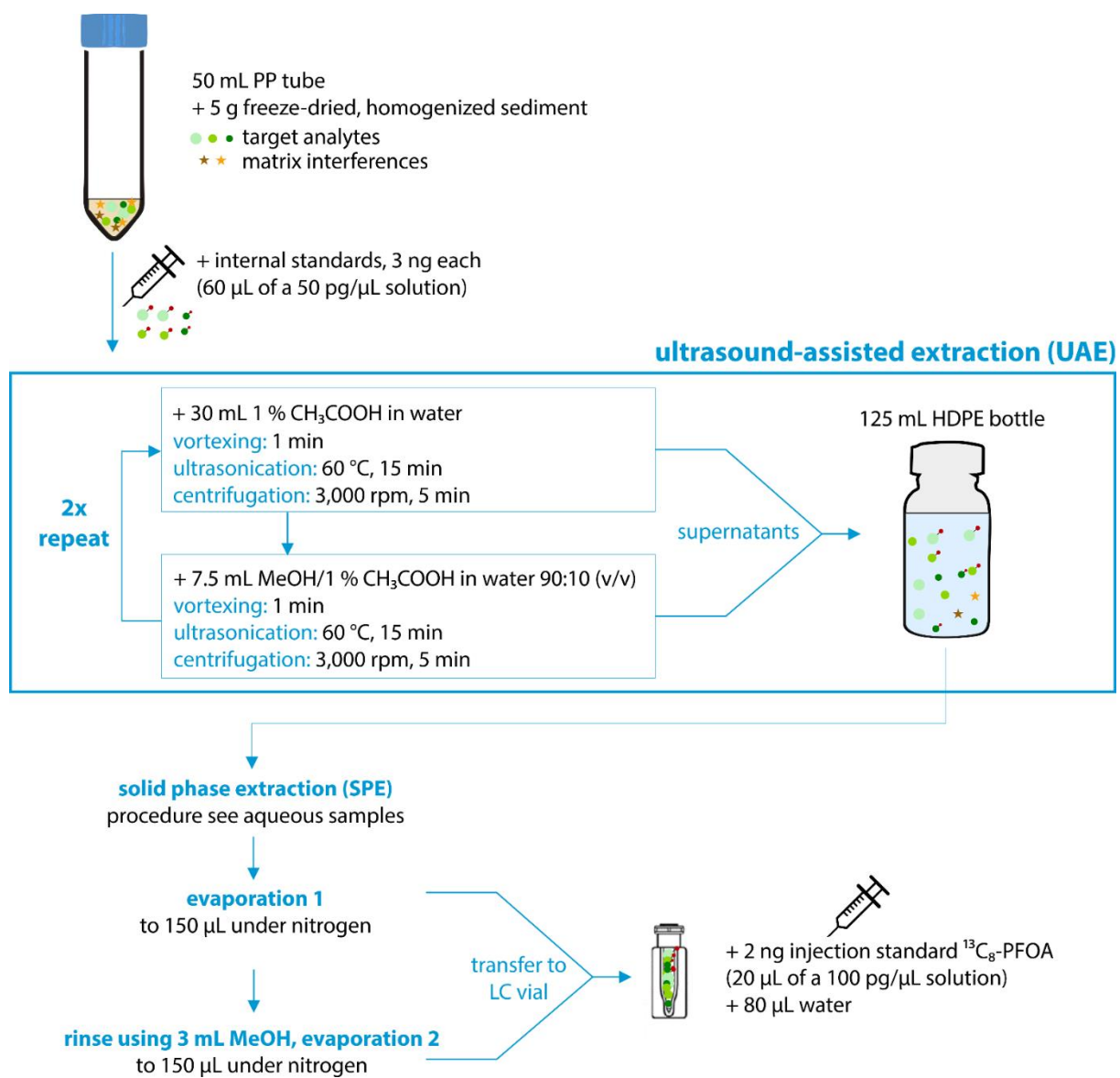


Figure 10.6-1: Schematic overview of the sample preparation of sediment samples.

10.7 Quantification of PFASs

10.7.1 Calculation of PFAS concentrations

To determine the calibration function for each target substance, the peak area ratio of the target analyte and the internal standard was plotted as the ordinate and the associated ratio of the concentrations as the abscissa by the Analyst 1.5 software. The linear regression function was in accordance with Equation 10.7.1.

$$\frac{\text{area (analyte cal)}}{\text{area (IS cal)}} = m \cdot \frac{c \text{ (analyte cal)}}{c \text{ (IS cal)}} + b \quad (10.7.1)$$

<i>area (analyte cal)</i>	peak area of the target analyte in the calibration [cps]
<i>area (IS cal)</i>	peak area of the internal standard in the calibration [cps]
<i>m</i>	slope of the calibration curve
<i>c (analyte cal)</i>	concentration of the target analyte [pg/μL]
<i>c (IS cal)</i>	concentration of the internal standard in the calibration [pg/μL]
<i>b</i>	ordinate intercept of the calibration curve

Using the Analyst 1.5 software, a weighting factor of 1/x was applied to this calibration curve, as discussed in Chapter 4.3.3. Based on the weighted calibration function, the concentration of the target analyte in the measured sample extract was calculated according to Equation 10.7.2.

$$c \text{ (analyte sample extr.)} = \left(\frac{\text{area (analyte sample extr.)}}{\text{area (IS sample extr.)}} - b \right) \cdot \frac{c \text{ (IS sample extr.)}}{m} \quad (10.7.2)$$

<i>c (analyte sample extract)</i>	concentration of the target analyte in the measured sample extract [pg/μL]
<i>area (analyte sample extract)</i>	peak area of the target analyte in the sample extract [cps]
<i>area (IS sample extract)</i>	peak area of the internal standard in the sample extract [cps]
<i>b</i>	ordinate intercept of the calibration curve, derived from Equation 10.7.1
<i>c (IS sample extract)</i>	concentration of the internal standard in the sample extract [pg/μL]
<i>m</i>	slope of the calibration curve, derived from Equation 10.7.1

The volume of the measured sample extract and the volume, or respectively weight, of the initial sample had to be considered to calculate the concentration in the analysed sample, as shown for water samples in Equation 10.7.3 and for sediment samples in Equation 10.7.4.

$$c \text{ (analyte water sample)} = \frac{c \text{ (analyte sample extract)} \cdot V \text{ (sample extract)}}{V \text{ (water sample)} \cdot 1000} \quad (10.7.3)$$

<i>c (analyte sample)</i>	concentration of the target analyte in the sample [ng/L]
<i>c (analyte sample extract)</i>	concentration of the target analyte in the measured sample extract [pg/μL], derived from Equation 10.7.2
<i>V (sample extract)</i>	volume of the measured sample extract of the water sample [μL], typically 200 μL
<i>V (sample)</i>	analysed sample volume [L], typically 1 L
1000	conversion factor from pg to ng

$$c(\text{analyte sediment sample}) = \frac{c(\text{analyte sample extract}) \cdot V(\text{sample extract})}{m(\text{sample}) \cdot 1000} \quad (10.7.4)$$

$c(\text{analyte sediment sample})$	concentration of the target analyte in the sediment sample [ng/g dw]
$c(\text{analyte sample extract})$	concentration of the target analyte in the measured sample extract [pg/ μ L], derived from Equation 10.7.2
$V(\text{sample extract})$	volume of the measured sample extract of the water sample [μ L], typically 400 μ L
$m(\text{sample})$	analysed sample amount [g dw], typically 5 g dw
1000	conversion factor from pg to ng

Afterwards, results were blank-corrected by subtracting the mean PFAS concentration in the blank samples from the concentrations in the samples (Equation 10.7.5).

$$c(\text{analyte sample, blank-c.}) = c(\text{analyte sample}) - c_{\text{mean}}(\text{blank samples}) \quad (10.7.5)$$

$c(\text{analyte sample, blank-c.})$	blank-corrected concentration of the target analyte in the water sample [ng/L] or in the sediment sample [ng/g dw]
$c(\text{analyte sample})$	concentration of the target analyte in the sample [ng/L] or [ng/g], derived from Equation 10.7.3, or respectively Equation 10.7.4
$c(\text{mean blank samples})$	mean concentration of the target analyte in the blank samples in [ng/L], or [ng/g dw]

The standards used for the calibration curve were prepared from salts or the free acid of the target analytes (Table 10.1-2 to Table 10.1-4). To report the results for all target analytes as the free acid, the calculated concentration of the compounds whose standards were prepared from salts were corrected for the mass of the counter ion according to Equation 10.7.6.

$$c(\text{analyte sample}_{\text{free acids}} \text{ blank-c.}) = c(\text{analyte sample, blank-corr.}) \cdot \frac{MW(\text{free acid})}{MW(\text{salt})} \quad (10.7.6)$$

$c(\text{analyte sample}_{\text{free acids}} \text{ blank-c.})$	blank-corrected concentration of the target analyte in the water sample [ng/L] or in the sediment sample [ng/g], calculated as the free acid
$c(\text{analyte sample, blank-c.})$	blank-corrected concentration of the target analyte in the water sample [ng/L] or in the sediment sample [ng/g], derived from Equation 10.7.5
$MW(\text{free acid})$	molecular weight of the target analyte as free acid [g/mol]
$MW(\text{salt})$	molecular weight of the target analyte as the purchased salt (typically Na ⁺ or K ⁺ salt) [g/mol]

10.7.2 Calculation of recovery rates

Absolute recoveries for the internal standards were calculated according to Equation 10.7.7 and Equation 10.7.8 and explained for recovery tests during method optimization in Chapter 4.4.

$$RF = \frac{\text{area (InjS cal)}}{\text{area (IS cal)}} \cdot \frac{c (IS cal)}{c (InjS cal)} \quad (10.7.7)$$

RF	response factor
<i>area (InjS cal)</i>	peak area of the injection standard ¹³ C ₈ -PFOA in the calibration standard [cps]
<i>area (IS cal)</i>	peak area of the internal standard in the calibration standard [cps]
<i>c (IS cal)</i>	concentration of the internal standard in the calibration standard [pg/μL]
<i>c (InjS cal)</i>	concentration of the injection standard ¹³ C ₈ -PFOA in the calibration standard [pg/μL]

$$\text{absolute IS recovery rate [\%]} = RF (mean) \cdot \frac{\text{area (IS sample)}}{\text{area (InjS sample)}} \cdot \frac{c (InjS sample)}{c (IS sample)} \cdot 100 \% \quad (10.7.8)$$

RF (mean)	mean response factor of all calibration standards
<i>area (IS sample)</i>	peak area of the internal standard in the sample [cps]
<i>area (InjS sample)</i>	peak area of the injection standard ¹³ C ₈ -PFOA in the sample [cps]
<i>c (InjS sample)</i>	concentration of the injection standard ¹³ C ₈ -PFOA in the sample [pg/μL]
<i>c (IS sample)</i>	concentration of the internal standard in the sample [pg/μL]

10.8 Data analysis

Calculation of arithmetic means and further statistical analysis was performed only for PFASs with a detection frequency > 50 %, if not stated otherwise. Results < MDL were considered as zero and the calculated values between MDL and MQL were used unaltered for calculations.

Statistical analysis was performed with OriginPro 2018 (version 9.5), setting the significance level at $\alpha = 0.05$. Normality was tested by the Kolmogorov-Smirnov test, before further statistical analysis followed. If data was normally distributed, a Pearson correlation analysis was conducted to investigate the relationship among individual PFASs and between PFASs and physicochemical parameters. Otherwise, Spearman's correlation analysis was used. To test for significant differences in PFAS patterns, two-sample t-tests were conducted. If data sets did not show homogeneity of variance according to Leuvene's test, the Welch correction was applied.

As other types of data analysis were study-specific, details are given in the respective chapters, for example for the calculation of sediment-water partitioning coefficients (Chapter 5.2.3), PFAS mass transport estimates through Fram Strait (Chapter 6.2.3), principal component analysis and PFAS mass flow estimates in German and Chinese rivers (Chapter 7.3.4).

11. List of Publications

Part of this thesis have been published, are submitted or in preparation for publication in peer-reviewed journals. The status of the publications and declarations to the contributions of the co-authors are given in the following. Moreover, presentations on conferences and popular science contributions are listed.

Emerging per- and polyfluoroalkyl substances (PFASs) in surface water and sediment of the North and Baltic Seas

Hanna Joerss,^{1,2} Christina Apel,^{1,2} Ralf Ebinghaus¹

¹ Helmholtz-Zentrum Geesthacht, Institute of Coastal Research, Max-Planck-Str. 1, 21502 Geesthacht, Germany

² Universität Hamburg, Institute of Inorganic and Applied Chemistry, Martin-Luther-King-Platz 6, 20146 Hamburg, Germany

contribution	<ul style="list-style-type: none"> • Hanna Joerss (90 %): concept, sampling, method development, laboratory work, data evaluation and analysis, discussion, manuscript preparation • Christina Apel (5 %): sampling, comments on the manuscript • Ralf Ebinghaus (5 %): concept, comments on the manuscript
status	published (https://doi.org/10.1016/j.scitotenv.2019.05.363), copyright (2019) Elsevier
journal	Science of the Total Environment 2019 , 686, 360-369
impact factor	5.589 (2018)
presentations	<ul style="list-style-type: none"> • SETAC Europe 28th Annual Meeting, Rome, Italy, 13-17 May 2018 (poster presentation) The poster was awarded with the “Young Scientist Award” for the best poster presentation on the conference. • DIOXIN Conference, 38th International Symposium on Halogenated Persistent Organic Pollutants, Kraków, Poland, 26-31 August 2018 (oral presentation)
popular science	<ul style="list-style-type: none"> • spotlight on HZG website (“science in a nutshell” – scientific information for the interested public): https://coastmap.hzg.de/schlaglichter/schadstoffe/ • photo feature about sampling and analysis in 2science magazine #5: https://www.hzg.de/public_relations_media/media/index.php.en?ref=74778 • blog post during the North Sea sampling campaign: https://blogs.helmholtz.de/kuestenforschung

**Transport of legacy perfluoroalkyl substances and the replacement compound HFPO-DA through the Atlantic gateway to the Arctic Ocean –
Is the Arctic a sink or a source?**

Hanna Joerss,^{1,2} Zhiyong Xie,¹ Charlotte C. Wagner,³ Wilken-Jon von Appen,⁴
Elsie M. Sunderland³, Ralf Ebinghaus¹

¹ Department for Environmental Chemistry, Helmholtz-Zentrum Geesthacht, Centre for Materials and Coastal Research, 21502 Geesthacht, Germany

² Institute of Inorganic and Applied Chemistry, Universität Hamburg, 20146 Hamburg, Germany

³ Harvard John A. Paulson School of Engineering and Applied Sciences, Harvard University, Cambridge, Massachusetts 02138, United States

⁴ Section Physical Oceanography of Polar Seas, Alfred Wegener Institute, Helmholtz Centre for Polar and Marine Research, 27570 Bremerhaven, Germany

contribution	<ul style="list-style-type: none"> • Hanna Joerss (75 %): concept, sampling, method development, laboratory work, data evaluation and analysis, discussion, manuscript preparation • Zhiyong Xie (5 %): concept, sampling • Charlotte C. Wagner (5 %): data evaluation and analysis, comments on the manuscript • Wilken-Jon von Appen (5 %): discussion, comments on the manuscript • Elsie M. Sunderland (5 %): comments on the manuscript • Ralf Ebinghaus (5 %): concept, comments on the manuscript
status	in press (http://dx.doi.org/10.1021/acs.est.0c00228), copyright (2020) American Chemical Society
journal	Environmental Science and Technology
impact factor	7.149 (2018)
note	The publication was selected to be highlighted by a press release of the American Chemical Society (ACS).
presentations	<ul style="list-style-type: none"> • SETAC Europe 29th Annual Meeting, Helsinki, Finland, 13-17 May 2018 (oral presentation)
popular science	<ul style="list-style-type: none"> • <i>Polarstern</i>, PS114, Weekly Report No. 2, 16-22 July 2018, published by the Alfred-Wegener-Institute: https://www.awi.de/en/about-us/service/press/press-release/chemistry-on-board.html • expedition report on HZG website: https://www.hzg.de/public_relations_media/magazine/what_motivates_us/078941/index.php.en

Per- and polyfluoroalkyl substances in Chinese and German river water – Point source- and country-specific fingerprints including unknown precursors

Hanna Joerss,^{1,2} Thekla-Regine Schramm,¹ Linting Sun,^{3,4} Chao Guo,^{3,4}

Jianhui Tang,^{3,5} Ralf Ebinghaus¹

¹ Helmholtz-Zentrum Geesthacht, Institute of Coastal Research, 21502 Geesthacht, Germany

² Universität Hamburg, Institute of Inorganic and Applied Chemistry, 20146 Hamburg, Germany

³ CAS Key Laboratory of Coastal Environmental Processes and Ecological Remediation; Shandong Key Laboratory of Coastal Environmental Processes, Yantai Institute of Coastal Zone Research, Chinese Academy of Sciences (CAS), Yantai 264003, China

⁴ University of Chinese Academy of Sciences, Beijing 100049, China

⁵ Center for Ocean Mega-Science, Chinese Academy of Sciences, Qingdao 266071, China

contribution	<ul style="list-style-type: none"> • Hanna Joerss (70 %): concept, sampling, method development, laboratory work, data evaluation and analysis, discussion, manuscript preparation • Thekla-Regine Schramm (10 %): sampling, laboratory work, data evaluation and analysis, comments on the manuscript • Linting Sun (5 %): sampling, laboratory work • Chao Guo (5 %): sampling, comments on the manuscript • Jianhui Tang (5 %): concept, sampling, comments on the manuscript • Ralf Ebinghaus (5 %): concept, comments on the manuscript
status	under review, copyright (2020) Elsevier
journal	Environmental Pollution
impact factor	5.714 (2018)
presentations	<ul style="list-style-type: none"> • PFAS-Erfahrungsaustausch Arcadis/SGS Institut Fresenius, 5 November 2019 (invited oral presentation) • The DIOXIN Conference 2020, on which the results of this study were intended to be presented, was cancelled due to the Covid-19 pandemic.
popular science	<ul style="list-style-type: none"> • blogpost during the research stay in China: https://blogs.helmholtz.de/kuestenforschung/2018/11/26/from-pesticides-to-frogs-legs-research-stay-in-china/
note	<ul style="list-style-type: none"> • A second manuscript on the River Rhine pre-study is in preparation for submission to the journal <i>Chemosphere</i>.

Discovery of Emerging and Novel Per- and Polyfluoroalkyl Substances in Chinese and German River Water Using a Suspect Screening Approach

Hanna Joerss,^{1,2} Frank Menger³, Jianhui Tang^{4,5}, Lutz Ahrens³, Ralf Ebinghaus¹

¹ Helmholtz-Zentrum Geesthacht, Institute of Coastal Research, 21502 Geesthacht, Germany

² Universität Hamburg, Institute of Inorganic and Applied Chemistry, 20146 Hamburg, Germany

³ Department of Aquatic Sciences and Assessment, Swedish University of Agricultural Sciences, Uppsala, Sweden

⁴ CAS Key Laboratory of Coastal Environmental Processes and Ecological Remediation; Shandong Key Laboratory of Coastal Environmental Processes, Yantai Institute of Coastal Zone Research, Chinese Academy of Sciences (CAS), Yantai 264003, China

⁵ Center for Ocean Mega-Science, Chinese Academy of Sciences, Qingdao 266071, China

contribution	<ul style="list-style-type: none"> • Hanna Joerss (70 %): concept, sampling, laboratory work, data evaluation and analysis, discussion, manuscript preparation • Frank Menger (15 %): concept, data evaluation and analysis, discussion, comments on the manuscript • Jianhui Tang (5 %): concept, sampling • Lutz Ahrens (5 %): concept, comments on the manuscript • Ralf Ebinghaus (5 %): concept
status	in preparation for submission to <i>Environmental Science and Technology</i>
presentations	<ul style="list-style-type: none"> • PFAS-Erfahrungsaustausch Arcadis/SGS Institut Fresenius, 5 November 2019 (invited oral presentation)

12. References

- [1] Buck, R.C., Franklin, J., Berger, U., Conder, J.M., Cousins, I.T., de Voogt, P., van Leeuwen, S.P., **2011**. Perfluoroalkyl and polyfluoroalkyl substances in the environment: terminology, classification, and origins. *Integrated Environmental Assessment and Management* 7(4), 513-541.
- [2] OECD; Organisation for Economic Co-operation and Development, **2018**. Classification of per- and polyfluoroalkyl substances (PFASs) based on a commonly agreed terminology for nomenclature of PFASs. <https://www.oecd.org/chemicalsafety/portal-perfluorinated-chemicals/aboutpfass/Figure1-classification-of-per-and-polyfluoroalkyl-substances%20-PFASs.pdf> (accessed: 9 January 2020).
- [3] OECD; Organisation for Economic Co-operation and Development, **2018**. Toward a new comprehensive global database of per- and polyfluoroalkyl substances (PFASs): Summary report on updating the OECD 2007 list of per- and polyfluoroalkyl substances (PFASs). *Series on Risk Management* 39, 1-24.
- [4] Wang, Z., DeWitt, J.C., Higgins, C.P., Cousins, I.T., **2017**. A Never-Ending Story of Per- and Polyfluoroalkyl Substances (PFASs)? *Environmental Science & Technology* 51 (5), 2508-2518.
- [5] Kissa, E., **2001**. Fluorinated Surfactants and Repellents. 2nd edition, Marcel Dekker, New York.
- [6] Pauling, L., **1941**. The nature of the chemical bond and the structure of molecules and crystals. *Nature* 148, 677.
- [7] O'Hagan, D., **2008**. Understanding organofluorine chemistry. An introduction to the C-F bond. *Chemical Society Reviews* 37(2), 308-319.
- [8] Kirsch, P., **2004**. Modern Fluoroorganic Chemistry. 1st edition, Wiley-VCH, Weinheim, 171-202.
- [9] Bondi, A., **1964**. van der Waals Volumes and Radii. *The Journal of Physical Chemistry* 68(3), 441-451.
- [10] Banks, R.E., Tatlow, E.C., **1994**. Organofluorine Chemistry: Nomenclature and Historical Landmarks. In *Organofluorine Chemistry: Principles and Commercial Applications*, Springer, New York, 1-24.
- [11] Vierke, L., Berger, U., Cousins, I.T., **2013**. Estimation of the acid dissociation constant of perfluoroalkyl carboxylic acids through an experimental investigation of their water-to-air transport. *Environmental Science & Technology* 47(19), 11032-11039.
- [12] Simons, J.H., **1950**. Electrochemical process of making fluorine-containing carbon compounds. *United States Patent* US 2519983.
- [13] Simons, J.H., **1949**. Production of Fluorocarbons: I. The Generalized Procedure and its Use with Nitrogen Compounds. *Journal of The Electrochemical Society* 95(2), 47-52.
- [14] Knepper, T.P., Lange, F.T., **2011**. Polyfluorinated Chemicals and Transformation Products. Springer, Berlin.
- [15] Alsmeyer, Y.W., Childs, W.V., Flynn, R.M., Moore, G.G.I., Smeltzer, C., **1994**. Electrochemical Fluorination and Its Applications. In *Organofluorine Chemistry: Principles and Commercial Applications*, Springer, New York, 57-88.

- [16] Millauer, H., Schwertfeger, W., Siegemund, G., **1985**. Hexafluoropropene Oxide - A Key Compound in Organofluorine Chemistry. *Angewandte Chemie International Edition* 24(3), 161-179.
- [17] Flynn, R.M., Mahtomedi, M.N., Vitcak, D.R., Buckanin, R.S.; Cheryl, L.S., **2003**. Fluorinated polyether compositions. *United States Patent* US2004/0124396A1.
- [18] Cousins, I.T., Goldenman, G., Herzke, D., Lohmann, R., Miller, M., Ng, Carla, Patton, S., Scheringer, M., Trier, X., Vierke, L., Wang, Z., deWitt, J., **2019**. The concept of essential use for determining when uses of PFASs can be phased out. *Environmental Science: Processes & Impacts* 21(11), 1803-1815.
- [19] OECD; Organisation for Economic Co-operation and Development, **2013**. Synthesis paper on per- and polyfluorinated chemicals (PFCs). https://www.oecd.org/env/ehs/risk-management/PFC_FINAL-Web.pdf (accessed: 09 January 2020).
- [20] Zhou, Y., Jiang, W., Zhanni, G., Wang, S., Zhu, W., Acena, L., Soloshonok, V., Izawa, K., Liu, H., **2016**. Next Generation of Fluorine-Containing Pharmaceuticals, Compounds Currently in Phase II–III Clinical Trials of Major Pharmaceutical Companies: New Structural Trends and Therapeutic Areas. *Chemical Reviews* 116(2), 422-518.
- [21] Ahrens, L., **2011**. Polyfluoroalkyl compounds in the aquatic environment: a review of their occurrence and fate. *Journal of Environmental Monitoring* 13(1), 20-31.
- [22] Liu, J., Mejia Avendaño, S., **2013**. Microbial degradation of polyfluoroalkyl chemicals in the environment: A review. *Environment International* 61, 98-114.
- [23] Young, C. J.; Mabury, S. A., **2010**. Atmospheric Perfluorinated Acid Precursors: Chemistry, Occurrence, and Impacts. In *Reviews of Environmental Contamination and Toxicology* Volume 208: Perfluorinated alkylated substances, Springer, New York, 109.
- [24] Frömel, T., Knepper, T.P., **2010**. Biodegradation of Fluorinated Alkyl Substances. In *Reviews of Environmental Contamination and Toxicology* Volume 208: Perfluorinated alkylated substances, Springer, New York, 109.
- [25] Hurley, M.D., Sulbaek Andersen, M.P., Wallington, T.J., Ellis, D.A., Martin, J.W., Mabury, S.A., **2004**. Atmospheric Chemistry of Perfluorinated Carboxylic Acids: Reaction with OH Radicals and Atmospheric Lifetimes. *Journal of Physical Chemistry A* 108(4), 615-620.
- [26] Liou, J.S.C., Szostek, B., Madsen, E.L., **2010**. Investigating the biodegradability of perfluorooctanoic acid. *Chemosphere* 80(2), 176-183.
- [27] Liu, D., Xiu, Z., Liu, F., Wu, G., Adamson, D., Newell, C., Vikesland, P., Tsai, A., Alvarez, P., **2013**. Perfluorooctanoic acid degradation in the presence of Fe(III) under natural sunlight. *Journal of Hazardous Materials* 262, 456-463.
- [28] Vaalgamaa, S., Vähätalo, A., Perkola, N., Huhtala, S., **2011**. Photochemical reactivity of perfluorooctanoic acid (PFOA) in conditions representing surface water. *Science of The Total Environment* 409(16), 3043-3048.
- [29] Prevedouros, K., Cousins, I.T., Buck, R.C., Korzeniowski, S.H., **2006**. Sources, fate and transport of perfluorocarboxylates. *Environmental Science & Technology* 40(1), 32-44.
- [30] Conder, J.M., Hoke, R.A., de Wolf, W., Russell, M.H., Buck, R.C., **2008**. Are PFCA's Bioaccumulative? A Critical Review and Comparison with Regulatory Criteria and Persistent Lipophilic Compounds. *Environmental Science & Technology* 42(4), 995-1003.
- [31] Martin, J.W., Mabury, S.A., Solomon, K., Muir, D.C.G., **2013**. Progress toward understanding the bioaccumulation of perfluorinated alkyl acids. *Environmental Toxicology and Chemistry* 32(11), 2421-2423.

- [32] Loi, E.I., Yeung, L.W.Y., Taniyasu, S., Lam, P.K.S., Kannan, K., Yamashita, N., **2011**. Trophic magnification of poly- and perfluorinated compounds in a subtropical food web. *Environmental Science & Technology* 45(22), 5506-5513.
- [33] Müller, C.E., de Silva, A.O., Small, J., Williamson, M., Wang, X., Morris, A., Katz, S., Gamberg, M., Muir, D.C.G., **2011**. Biomagnification of Perfluorinated Compounds in a Remote Terrestrial Food Chain: Lichen–Caribou–Wolf. *Environmental Science & Technology* 45(20), 8665-8673.
- [34] Houde, M., Bujas, T.A.D., Small, J., Wells, R., Fair, P., Bossart, G.D., Solomon, K., Muir, D.C.G., **2006**. Biomagnification of Perfluoroalkyl Compounds in the Bottlenose Dolphin (*Tursiops truncatus*) Food Web. *Environmental Science & Technology* 40(13), 4138-4144.
- [35] Chang, S.-C., Noker, P.E., Gorman, G.S., Gibson, S., Hart, J.A., Ehresman, D.J., Butenhoff, J.L., **2012**. Comparative pharmacokinetics of perfluorooctanesulfonate (PFOS) in rats, mice, and monkeys. *Reproductive Toxicology* 33(4), 428-440.
- [36] Olsen, G.W., Burris, J.M., Ehresman, D.J., Froehlich, J.W., Seacat, A.M., Butenhoff, J.L., Zobel, L.R., **2007**. Half-Life of Serum Elimination of Perfluorooctanesulfonate, Perfluorohexanesulfonate, and Perfluorooctanoate in Retired Fluorochemical Production Workers. *Environmental Health Perspectives* 115(9), 1298-1305.
- [37] Ahrens, L., Siebert, U., Ebinghaus, R., **2009**. Total body burden and tissue distribution of polyfluorinated compounds in harbor seals (*Phoca vitulina*) from the German Bight. *Marine Pollution Bulletin* 58(4), 520-525.
- [38] Vestergren, R., Cousins, I.T., **2009**. Tracking the Pathways of Human Exposure to Perfluorocarboxylates. *Environmental Science & Technology* 43(15), 5565-5575.
- [39] Verreault, J., Houde, M., Gabrielsen, G.W., Berger, U., Haukas, M., Letcher, R., Muir, D.C.G., **2005**. Perfluorinated Alkyl Substances in Plasma, Liver, Brain, and Eggs of Glaucous Gulls (*Larus hyperboreus*) from the Norwegian Arctic. *Environmental Science & Technology* 39(19), 7439-7445.
- [40] MacManus-Spencer, L.A., Tse, M.L., Hebert, P.C., Bischel, H.N., Luthy, R.G., **2010**. Binding of Perfluorocarboxylates to Serum Albumin: A Comparison of Analytical Methods. *Analytical Chemistry* 82(3), 974-981.
- [41] Chen, Y.-M, Guo, L.-H., **2008**. Fluorescence study on site-specific binding of perfluoroalkyl acids to human serum albumin. *Archives of Toxicology* 83(3), 255.
- [42] Yang, C.-H., Glover, K.P., Han, X., **2010**. Characterization of Cellular Uptake of Perfluorooctanoate via Organic Anion-Transporting Polypeptide 1A2, Organic Anion Transporter 4, and Urate Transporter 1 for Their Potential Roles in Mediating Human Renal Reabsorption of Perfluorocarboxylates. *Toxicological Sciences* 117(2), 294-302.
- [43] Luebker, D.J., Hansen, K.J., Bass, N.M., Butenhoff, J.L., Seacat, A.M., **2002**. Interactions of fluorochemicals with rat liver fatty acid-binding protein. *Toxicology* 176(3), 175-185.
- [44] Hickey, N.J., Crump, D., Jones, S., Kennedy, S., **2009**. Effects of 18 Perfluoroalkyl Compounds on mRNA Expression in Chicken Embryo Hepatocyte Cultures. *Toxicological Sciences* 111(2), 311-320.
- [45] Weisiger, R.A., **2007**. Mechanisms of Intracellular Fatty Acid Transport: Role of Cytoplasmic-Binding Proteins. *Journal of Molecular Neuroscience* 33(1), 42-44.
- [46] Fromme, H., Mosch, C., Morovitz, M., Alba-Alejandre, I., Boehmer, S., Kiranoglu, M., Faber, F., Hannibal, I., Genzel, O., Koletzko, B., Völkel, W., **2010**. Pre- and Postnatal Exposure to Perfluorinated Compounds (PFCs). *Environmental Science & Technology* 44(18), 7123-7129.

- [47] Glynn, A., Berger, U., Bignert, A., Ullah, S., Aune, M., Lignell, S., Darnerud, P.O., **2012**. Perfluorinated alkyl acids in blood serum from primiparous women in Sweden: serial sampling during pregnancy and nursing, and temporal trends 1996–2010. *Environmental Science & Technology* 46, 9071-9079.
- [48] Ng, C.A., Hungerbühler, K., **2013**. Bioconcentration of Perfluorinated Alkyl Acids: How Important Is Specific Binding? *Environmental Science & Technology* 47(13), 7214-7223.
- [49] EFSA, European Food Safety Authority, **2018**. Risk to human health related to the presence of perfluorooctane sulfonic acid and perfluorooctanoic acid in food. *EFSA Journal* 16(12), 5194.
- [50] Lau, C., **2015**. Perfluorinated Compounds: An Overview. In *Toxicological Effects of Perfluoroalkyl and Polyfluoroalkyl Substances*, Springer, New York, 1-21.
- [51] Luebker, D.J., Hansen, K., Bass, N., Butenhoff, J., Seacat, A.M., **2005**. Neonatal mortality from in utero exposure to perfluorooctanesulfonate (PFOS) in Sprague–Dawley rats: Dose–response, and biochemical and pharmacokinetic parameters. *Toxicology* 215(1), 149-169.
- [52] Abbott, B.D., **2015**. Developmental Toxicity. In *Toxicological Effects of Perfluoroalkyl and Polyfluoroalkyl Substances*, Springer, New York, 203-218.
- [53] Lau, C., Thibodeau, J., Hanson, R.G., Rogers, J.M., Grey, B., Stanton, M.E., butenhoff, J.L., Stevenson, L.A., **2003**. Exposure to Perfluorooctane Sulfonate during Pregnancy in Rat and Mouse. II: Postnatal Evaluation. *Toxicological Sciences* 74(2), 382-392.
- [54] Wan, H.T., Zhao, Y.G., Leung, P.Y., Wong, C.K.C., **2014**. Perinatal Exposure to Perfluorooctane Sulfonate Affects Glucose Metabolism in Adult Offspring. *PLOS ONE* 9(1), 87137.
- [55] Abbott, B.D., Wolf, C., Schmid, J., Das, K., Zehr, R., Helfant, L., Nakayama, S., Lindstrom, A.B., Strynar, M., Lau, C., **2007**. Perfluorooctanoic Acid–Induced Developmental Toxicity in the Mouse is Dependent on Expression of Peroxisome Proliferator–Activated Receptor–alpha. *Toxicological Sciences* 98(2), 571-581.
- [56] Regulation (EC) No 1272/2008 of the European Parliament and of the Council of 16 December 2008 on classification, labelling and packaging of substances and mixtures, amending and repealing Directives 67/548/EEC and 1999/45/EC, and amending Regulation (EC) No 1907/2006.
- [57] Peden-Adams, M.M., Keller, J.M., EuDaly, J., Berger, J., Gilkeson, G.S., Keil, D.E., **2008**. Suppression of Humoral Immunity in Mice following Exposure to Perfluorooctane Sulfonate. *Toxicological Sciences* 104(1), 144-154.
- [58] Loveless, S.E., Hoban, D., Sykes, G., Frame, S.R., Evers, N.E., **2008**. Evaluation of the Immune System in Rats and Mice Administered Linear Ammonium Perfluorooctanoate. *Toxicological Sciences* 105(1), 86-96.
- [59] Butenhoff, J.L., Chang, S., Olsen, G., Thomford, P., **2012**. Chronic dietary toxicity and carcinogenicity study with potassium perfluorooctanesulfonate in Sprague Dawley rats. *Toxicology* 293(1), 1-15.
- [60] Butenhoff, J.L., Chang, S., Olsen, G., Thomford, P., **2012**. Chronic dietary toxicity and carcinogenicity study with potassium perfluorooctanesulfonate in Sprague Dawley rats. *Toxicology* 293(1), 1-15.
- [61] IARC, International Agency for Research on Cancer, **2016**. Monographs on the Evaluation of Carcinogenic Risks to Humans: Perfluorooctanoic acid. <https://monographs.iarc.fr/wp-content/uploads/2018/06/mono110-01.pdf> (accessed: 30 January 2020).

- [62] Corton, J.C., Cunningham, M.L., Hummer, T., Lau, C., Meek, B., Peters, J., Popp, J.A., Rhonberg, L., Seed, J., Klaunig, J.E., **2014**. Mode of action framework analysis for receptor-mediated toxicity: The peroxisome proliferator-activated receptor alpha (PPAR α) as a case study. *Critical Reviews in Toxicology* 44(11), 1-49.
- [63] DeWitt, J.C., Peden-Adams, M.M., Keller, J., Germolec, D., **2012**. Immunotoxicity of Perfluorinated Compounds: Recent Developments. *Toxicologic Pathology* 40(2), 300-311.
- [64] Vanden Heuvel, J.P., **2007**. The PPAR resource page. *Biochimica et Biophysica Acta (BBA) - Molecular and Cell Biology of Lipids* 1771(8), 1108-1112.
- [65] Wolf, C.J., **2008**. Activation of Mouse and Human Peroxisome Proliferator-Activated Receptor Alpha by Perfluoroalkyl Acids of Different Functional Groups and Chain Lengths. *Toxicological Sciences* 106(1), 162-171.
- [66] Wolf, C.J., Schmid, J., Lau, C., Abbott, B.D., **2012**. Activation of mouse and human peroxisome proliferator-activated receptor-alpha (PPAR α) by perfluoroalkyl acids (PFAAs): Further investigation of C4-C12 compounds. *Reproductive Toxicology* 33(4), 546-551.
- [67] Bjork, J.A., Wallace, K.B., **2009**. Structure-Activity Relationships and Human Relevance for Perfluoroalkyl Acid-Induced Transcriptional Activation of Peroxisome Proliferation in Liver Cell Cultures. *Toxicological Sciences* 111(1), 89-99.
- [68] The C8 Science Panel, <http://www.c8sciencepanel.org/index.html>. (accessed: 1 February 2020).
- [69] Lopez-Espinosa, M.-J., Mondal, D., Armstrong, B., Bloom, M., Fletcher, T., **2012**. Thyroid function and perfluoroalkyl acids in children living near a chemical plant. *Environmental Health Perspectives* 120(7), 1036-1041.
- [70] Darrow, L.A., Stein, C.R., Steenland, K., **2013**. Serum perfluorooctanoic acid and perfluorooctane sulfonate concentrations in relation to birth outcomes in the Mid-Ohio Valley, 2005-2010. *Environmental Health Perspectives* 121(10), 1207-1213.
- [71] Steenland, K., Zhao, L., Winqvist, A., Parks, C., **2013**. Ulcerative Colitis and Perfluorooctanoic Acid (PFOA) in a Highly Exposed Population of Community Residents and Workers in the Mid-Ohio Valley. *Environmental Health Perspectives* 121(8), 900-905.
- [72] Barry, V., Winqvist, A., Steenland, K., **2013**. Perfluorooctanoic Acid (PFOA) Exposures and Incident Cancers among Adults Living Near a Chemical Plant. *Environmental Health Perspectives* 121(11-12), 1313-1318.
- [73] Grandjean, P., Andersen, E.W., Budtz, E., Nielsen, F., Molbak, K., Weihe, P., Heilmann, C., **2012**. Serum Vaccine Antibody Concentrations in Children Exposed to Perfluorinated Compounds. *Journal of the American Medical Association* 307(4), 391-397.
- [74] EFSA, European Food Safety Authority. Glossary - Critical Effect. <https://www.efsa.europa.eu/en/glossary-taxonomy-terms> (accessed: 1 February 2020).
- [75] BfR, Bundesinstitut für Risikobewertung, **2019**. New health-based guidance values for the industrial chemicals PFOS and PFOA: BfR Opinion No 032/2019 of 21 August 2019. <https://www.bfr.bund.de/cm/349/new-health-based-guidance-values-for-the-industrial-chemicals-pfos-and-pfoa.pdf> (accessed: 1 February 2020).
- [76] Giesy, J.P., Kannan, K., **2001**. Global distribution of perfluorooctane sulfonate in wildlife. *Environmental Science & Technology* 35, 1339-1342.
- [77] McLachlan, M.S., Holmstrom, K.E., Reth, M., Berger, U., **2007**. Riverine discharge of perfluorinated carboxylates from the European continent. *Environmental Science and Technology* 41 (21), 7260-7265.

- [78] Giesy, J.P., Kannan, K., **2002**. Perfluorochemical Surfactants in the Environment. *Environmental Science & Technology* 36(7), 146-152.
- [79] Houde, M., de Silva, A.O., Muir, D.C.G., Letcher, R., **2011**. Monitoring of perfluorinated compounds in aquatic biota: an updated review. *Environmental Science & Technology* 45, 7962-7973.
- [80] Reiner, J.L., Place, B.J., **2015**. Perfluorinated Alkyl Acids in Wildlife, in *Toxicological Effects of Perfluoroalkyl and Polyfluoroalkyl Substances*, Springer, New York, 127-150.
- [81] Fromme, H., Tittlemeier, S., Völker, W., Wilhelm, M., Twardella, D., **2009**. Perfluorinated compounds--exposure assessment for the general population in Western countries. *International Journal of Hygiene and Environmental Health* 212(3), 239-270.
- [82] Kato, K., **2011**. Trends in exposure to polyfluoroalkyl chemicals in the U.S. Population: 1999-2008. *Environmental Science & Technology* 45(19), 8037-45.
- [83] Olsen, G.W., Lange, C., Ellefson, M., Mair, D., Church, T., Goldberg, C., Herron, R., Nobilett, J., Rios, J., Reagen, W., Zobel, L., **2012**. Temporal Trends of Perfluoroalkyl Concentrations in American Red Cross Adult Blood Donors, 2000–2010. *Environmental Science & Technology* 46(11), 6330-6338.
- [84] Toms, L.M.L., Thompson, J., Rotander, A., Hobson, P., Calafat, A.M., Kato, K., Ye, X., Broomhall, S., Harden, F., Müller, J.F., **2014**. Decline in perfluorooctane sulfonate and perfluorooctanoate serum concentrations in an Australian population from 2002 to 2011. *Environment International* 71, 74-80.
- [85] Butt, C.M., Berger, U., Bossi, R., Tomy, G.T., **2010**. Levels and trends of poly- and perfluorinated compounds in the arctic environment. *Science of the Total Environment* 408, 2936-2965.
- [86] Muir, D., Bossi, R., Carlsson, P., Evans, M., de Silva, A.O., Halsall, C., Rauert, .C., Herzke, D., Hung, H., Letcher, R., Rigét, F., Roos, A., **2019**. Levels and trends of poly- and perfluoroalkyl substances in the Arctic environment – An update. *Emerging Contaminants* 5, 240-271.
- [87] Zhao, Z., Xie, Z., Tang, J., Zhang, G., Ebinghaus, R., **2015**. Spatial distribution of perfluoroalkyl acids in surface sediments of the German Bight, North Sea. *Science of the Total Environment* 511, 145-152.
- [88] Busch, J., Ahrens, L., Xie, Z., Sturm, R., Ebinghaus, R., **2010**. Polyfluoroalkyl compounds in the East Greenland Arctic Ocean. *Journal of Environmental Monitoring* 12 (6), 1242-1246.
- [89] Vento, S.D., Halsall, C., Gioia, R., Jones, K., Dachs, J., **2012**. Volatile per- and polyfluoroalkyl compounds in the remote atmosphere of the western Antarctic Peninsula: an indirect source of perfluoroalkyl acids to Antarctic waters? *Atmospheric Pollution Research* 3(4), 450-455.
- [90] Routti, H., Krafft, B., Herzke, D., Eisert, R., Oftedal, O., **2015**. Perfluoroalkyl substances detected in the world's southernmost marine mammal, the Weddell seal (*Leptonychotes weddellii*). *Environmental Pollution* 197, 62-67.
- [91] Dreyer, A., Weinberg, I., Temme, C., Ebinghaus, R., **2009**. Polyfluorinated Compounds in the Atmosphere of the Atlantic and Southern Oceans: Evidence for a Global Distribution. *Environmental Science & Technology* 43(17), 6507-6514.
- [92] Zhao, Z., Tang, J., Mi, L., Tian, C., Zhong, G., Zhang, G., Wang, S., Li, Q., Ebinhaus, R., Xie, Z., Sun, H., **2017**. Perfluoroalkyl and polyfluoroalkyl substances in the lower atmosphere and surface waters of the Chinese Bohai Sea, Yellow Sea, and Yangtze River estuary. *Science of The Total Environment* 599, 114-123.

- [93] Habibullah-Al-Mamun, M., Ahmed, M.K., Raknuzzaman, M., Islam, M.S., Negishi, J., Nakamichi, S., Masunaga, S., **2016**. Occurrence and distribution of perfluoroalkyl acids (PFAAs) in surface water and sediment of a tropical coastal area (Bay of Bengal coast, Bangladesh). *Science of The Total Environment* 571, 1089-1104.
- [94] Ahrens, L., Barber, J. L., Xie, Z., Ebinghaus, R., **2009**. Longitudinal and latitudinal distribution of perfluoroalkyl compounds in the surface water of the Atlantic Ocean. *Environmental Science & Technology* 43 (9), 3122-7.
- [95] Benskin, J. P., Muir, D. C. G., Scott, B. F., Spencer, C., De Silva, A. O., Kylin, H., **2012**. Perfluoroalkyl acids in the Atlantic and Canadian Arctic Oceans. *Environmental Science & Technology* 46, 5815-5823.
- [96] González-Gaya, B., Dachs, J., Roscales, G., Jimenez, B., **2014**. Perfluoroalkylated Substances in the Global Tropical and Subtropical Surface Oceans. *Environmental Science & Technology* 48(22), 13076-13084.
- [97] Armitage, J.M., Schenker, U., Scheringer, M., Martin, J.W., Macleod, M., Cousins, I.T., **2009**. Modeling the Global Fate and Transport of Perfluorooctane Sulfonate (PFOS) and Precursor Compounds in Relation to Temporal Trends in Wildlife Exposure. *Environmental Science & Technology* 43(24), 9274-9280.
- [98] Ellis, D.A., Martin, J.W., de Silva, A.O., Mabury, S., Hurley, M., Andersen, M., Wallington, T., **2004**. Degradation of Fluorotelomer Alcohols: A Likely Atmospheric Source of Perfluorinated Carboxylic Acids. *Environmental Science & Technology* 38(12), 3316-3321.
- [99] Ahrens, L., Felizeter, S., Ebinghaus, R., **2009**. Spatial distribution of polyfluoroalkyl compounds in seawater of the German Bight. *Chemosphere* 76(2), 179-184.
- [100] Heydebreck, F., Tang, J., Xie, Z., Ebinghaus, R., **2015**. Alternative and legacy perfluoroalkyl substances: Differences between European and Chinese river/estuary systems. *Environmental Science & Technology* 49(14), 8386-8395.
- [101] Ahrens, L., Gerwinski, W., Theobald, N., Ebinghaus, R., **2010**. Sources of polyfluoroalkyl compounds in the North Sea, Baltic Sea and Norwegian Sea: Evidence from their spatial distribution in surface water. *Marine Pollution Bulletin* 60(2), 255-260.
- [102] Heydebreck, F., **2017**. Per- and polyfluoroalkyl substances in the environment - Shifting toward fluorinated alternatives? Dissertation. University of Hamburg.
- [103] Brumovský, M., Karaskova, P., Borghini, M., Nizzetto, L., **2016**. Per- and polyfluoroalkyl substances in the Western Mediterranean Sea waters. *Chemosphere* 159, 308-316.
- [104] Theobald, N., Gerwinski, W., Caliebe, C., Haarich, M., **2007**. Entwicklung und Validierung einer Methode zur Bestimmung von polyfluorierten organischen Substanzen in Meerwasser, Sedimenten und Biota; Untersuchungen zum Vorkommen dieser Schadstoffe in der Nord- und Ostsee. Umweltbundesamt, Report 20222213.
- [105] Cai, M., Zhao, Z., Yin, Z., Ahrens, L., Huang, P., Cai, M., Yang, H., He, J., Sturm, R., Ebinghaus, R., Xie, Z., **2012**. Occurrence of perfluoroalkyl compounds in surface waters from the North Pacific to the Arctic Ocean. *Environmental Science & Technology* 46(2), 661-668.
- [106] Yamashita, N., Kannan, K., Taniyasu, S., Horii, Y., Petrick, G., Gamo, T., **2005**. A global survey of perfluorinated acids in oceans. *Marine Pollution Bulletin* 51, 658-668.
- [107] Wei, S., Chen, L.Q., Taniyasu, S., So, M.K., Murphy, M.B., Yamashita, N., Yeung, L.W.Y., Lam, P.K.S., **2007**. Distribution of perfluorinated compounds in surface seawaters between Asia and Antarctica. *Marine Pollution Bulletin* 54(11), 1813-1818.

- [108] Yeung, L. W. Y., Dassuncao, C., Mabury, S., Sunderland, E. M., Zhang, X., Lohmann, R., **2017**. Vertical Profiles, Sources, and Transport of PFASs in the Arctic Ocean. *Environmental Science and Technology* 51 (12), 6735-6744.
- [109] Busch, J., Ahrens, L., Xie, Z., Sturm, R., Ebinghaus, R., **2010**. Polyfluoroalkyl compounds in the East Greenland Arctic Ocean. *Journal of Environmental Monitoring* 12 (6), 1242-1246.
- [110] Zhang, X., Zhang, Y., Dassuncao, C., Lohmann, R., Sunderland, E. M., **2017**. North Atlantic Deep Water formation inhibits high Arctic contamination by continental perfluorooctane sulfonate discharges. *Global Biogeochemical Cycles* 31 (8), 1332-1343.
- [111] Rhein, M., Kieke, D., Steinfeldt, R., **2015**. Advection of North Atlantic Deep Water from the Labrador Sea to the southern hemisphere. *Journal of Geophysical Research: Oceans* 120 (4), 2471-2487.
- [112] Yamashita, N.; Taniyasu, S.; Petrick, G.; Wei, S.; Gamo, T.; Lam, P. K. S., **2008**, Perfluorinated acids as novel chemical tracers of global circulation of ocean waters. *Chemosphere* 70, 1247-1255.
- [113] Schlosser, P.; Bayer, R.; Bönisch, G.; Cooper, L. W.; Ekwurzel, B.; Jenkins, W. J.; Khatiwala, S.; Pfirman, S.; Smethie, W. M., **1999**. Pathways and mean residence times of dissolved pollutants in the ocean derived from transient tracers and stable isotopes. *Science of the Total Environment* 237-238, 15-30.
- [114] Zhao, Z., Xie, Z., Tang, J., Zhang, G., Ebinghaus, R., **2015**. Spatial distribution of perfluoroalkyl acids in surface sediments of the German Bight, North Sea. *Science of the Total Environment* 511, 145-152.
- [115] Theobald, N., Caliebe, C., Gerwinski, W., Hühnerfuss, H., Lepom, P., **2012**. Occurrence of perfluorinated organic acids in the North and Baltic Seas. Part 2: distribution in sediments. *Environmental Science and Pollution Research* 19(2), 313-324.
- [116] Zhao, Z., Tang, J., Xie, Z., Chen, Y., Pan, X., Zhong, G., Sturm, R., Zhang, G., Ebinghaus, R., **2013**. Perfluoroalkyl acids (PFAAs) in riverine and coastal sediments of Laizhou Bay, North China. *Science of The Total Environment* 447, 415-423.
- [117] Ahrens, L., Taniyasu, S., Yeung, L.W.Y., Yamashita, N., Lam, P.K.S., Ebinghaus, R., **2010**. Distribution of polyfluoroalkyl compounds in water, suspended particulate matter and sediment from Tokyo Bay, Japan. *Chemosphere* 79(3), 266-272.
- [118] Zhu, Z., Wang, T., Wang, P., Lu, Y., Giesy, J.P., **2014**. Perfluoroalkyl and polyfluoroalkyl substances in sediments from South Bohai coastal watersheds, China. *Marine Pollution Bulletin* 85(2), 619-627.
- [119] Ahrens, L., Yamashita, N., Yeung, L.W.Y., Taniyasu, S., Horii, Y., Lam, P.K.S., Ebinghaus, R., **2009**. Partitioning behavior of per- and polyfluoroalkyl compounds between pore water and sediment in two sediment cores from Tokyo Bay, Japan. *Environmental Science & Technology* 43(18), 6969-6975.
- [120] US EPA; United States Environmental Protection Agency, **2006**. 2010/15 PFOA Stewardship Program. <https://www.epa.gov/assessing-and-managing-chemicals-under-tsca/and-polyfluoroalkyl-substances-pfass-under-tsca#tab-3> (accessed: 4 February 2019).
- [121] BRS Secretariat; Secretariat of the Basel, Rotterdam and Stockholm Conventions, **2009**. Listing of perfluorooctane sulfonic acid, its salts and perfluorooctane sulfonyl fluoride. UNEP/POPS/COP.4-SC-4/17. <http://chm.pops.int/TheConvention/ConferenceoftheParties/Meetings/COP4/COP4Documents/tabid/531/Default.aspx> (accessed 01 November 2019).

- [122] BRS Secretariat; Secretariat of the Basel, Rotterdam and Stockholm Conventions, **2019**. Listing of perfluorooctanoic acid (PFOA), its salts and PFOA-related compounds. UNEP/POPS/COP.9-SC-9/12.
- [123] BRS Secretariat; Secretariat of the Basel, Rotterdam and Stockholm Conventions, **2019**. POPRC Recommendations for listing chemicals – Chemicals under review. <http://chm.pops.int/Convention/POPsReviewCommittee/Chemicals/tabid/243/Default.aspx> (accessed 03 February 2019).
- [124] Directive 2013/39/EU of the European Parliament and of the Council of 12 August 2013 amending Directives 2000/60/EC and 2008/105/EC as regards priority substances in the field of water policy.
- [125] Bundesministerium für Umwelt, Naturschutz, Bau und Reaktorsicherheit, **2017**. Bericht zu perfluorierten Verbindungen; Reduzierung/Vermeidung, Regulierung und Grenzwerte, einheitliche Analyse- und Messverfahren für fluororganische Verbindungen. https://www.umweltministerkonferenz.de/umlbeschluesse/umlaufBericht2017_19.pdf (accessed: 01 February 2020).
- [126] German Fertiliser Ordinance – Düngemittelverordnung(DüMV) vom 5. Dezember 2012 (BGBl. I S. 2482), die zuletzt durch Artikel 1 der Verordnung vom 2. Oktober 2019 (BGBl. I S. 1414) geändert worden ist.
- [127] Wang, Z., Boucher, J., Scheringer, M., Cousins, I.T., Hungerbühler, K., **2017**. Toward a Comprehensive Global Emission Inventory of C4–C10 Perfluoroalkanesulfonic Acids (PFSAs) and Related Precursors: Focus on the Life Cycle of C8-Based Products and Ongoing Industrial Transition. *Environmental Science & Technology* 51(8), 4482-4493.
- [128] Wang, Z., Cousins, I.T., Scheringer, M., Buck, R.C., Hungerbühler, K., **2014**. Global emission inventories for C4–C14 perfluoroalkyl carboxylic acid (PFCA) homologues from 1951 to 2030, Part I: production and emissions from quantifiable sources. *Environment International* 70, 62-75.
- [129] OECD, Organisation for Economic Co-operation and Development, **2016**. Consolidated guidance on alternatives to perfluorooctane sulfonic acid and its related chemicals (PFOS). <https://www.informea.org/en/consolidated-guidance-alternatives-perfluorooctane-sulfonic-acid-and-its-related-chemicals> (accessed: 14 February 2020).
- [130] Wang, Z., Cousins, I.T., Scheringer, M., Buck, R.C., Hungerbühler, K., **2014**. Global emission inventories for C4–C14 perfluoroalkyl carboxylic acid (PFCA) homologues from 1951 to 2030, part II: the remaining pieces of the puzzle. *Environment International* 69, 166-176.
- [131] GEF, Global Environment Facility, **2015**. Reduction and Phase-out of PFOS in Priority Sectors. <https://www.thegef.org/project/reduction-and-phase-out-pfos-priority-sectors> (accessed: 20 February 2020).
- [132] Wang, Z., Cousins, I.T., Scheringer, M., Hungerbühler, K., **2013**. Fluorinated alternatives to long-chain perfluoroalkyl carboxylic acids (PFCAs), perfluoroalkane sulfonic acids (PFSAs) and their potential precursors. *Environment International* 60, 242-248.
- [133] ECHA; European Chemicals Agency, **2014**. Annex XV proposal for a restriction - Perfluorooctanoic acid (PFOA), PFOA salts and PFOA-related substances. <https://echa.europa.eu/documents/10162/e9cddee6-3164-473d-b590-8fcf9caa50e7> (accessed: 15 February 2020).
- [134] Pan, Y., Zhang, H., Cui, Q., Sheng, N., Yeung, L.W.Y., Sun, Y., Dai, J., **2018**. Worldwide distribution of novel perfluoroether carboxylic and sulfonic acids in surface water. *Environmental Science & Technology* 52(14), 7621-7629.

- [135] OECD, Organisation for Economic Co-operation and Development, **2019**. Report on the assessment of alternatives to perfluorooctane sulfonic acid, its salts and perfluorooctane sulfonyl fluoride. <https://www.informea.org/en/report-assessment-alternatives-perfluorooctane-sulfonic-acid-its-salts-and-perfluorooctane-sulfonyl> (accessed: 15 February 2020).
- [136] Sun, M., Arevalo, E., Strynar, M.J., Lindstrom, A.B., Richardson, M., Kearns, B., Knappe, D.R.U., **2016**. Legacy and emerging perfluoroalkyl substances are important drinking water contaminants in the Cape Fear River watershed of North Carolina. *Environmental Science & Technology Letters* 3(12), 415-419.
- [137] EFSA, European Food Safety Authority, **2011**. Scientific opinion on the safety evaluation of the substance *(ADONA)*, 3H-perfluoro-3-[(3-methoxy-propoxy)propanoic acid], ammonium salt, CAS No. 958445-44-8, for use in food contact materials, *EFSA Journal* 9(6), 2182-2193.
- [138] EFSA, European Food Safety Authority, **2011**. Scientific Opinion on the safety evaluation of the substance, Perfluoro[(2-ethyloxy-ethoxy)acetic acid], ammonium salt, CAS No. 908020-52-0, for use in food contact materials. *EFSA Journal* 9(6) 2183-2194.
- [139] OECD, Organisation for Economic Co-operation and Development, **2016**. Second Draft - Consolidated guidance on alternatives to perfluorooctane sulfonic acid and its related chemicals. <http://chm.pops.int/TheConvention/POPsReviewCommittee/Meetings/POPRC11/POPRC11Followup/tabid/4723/Default.aspx> (accessed: 15 February 2020)
- [140] Danish Ministry of the Environment, Environmental Protection Agency, **2011**. Substitution of PFOS for use in nondecorative hard chrome plating. <https://www2.mst.dk/udgiv/publications/2011/06/978-87-92779-10-6.pdf> (accessed: 22 February 2020).
- [141] ECHA; European Chemicals Agency, **2016**. Registration Dossier - Carboxymethyldimethyl-3-[[[3,3,4,4,5,5,6,6,7,7,8,8,8-tridecafluorooctyl]sulphonyl]amino]propylammonium hydroxide. <https://echa.europa.eu/de/registration-dossier/-/registered-dossier/17549> (accessed: 22 February 2020).
- [142] Trier, X., Taxvig, C., Rosenmai, A.K.; Pedersen, G.A., **2017**. PFAS in paper and board for food contact : Options for risk management of poly- and perfluorinated substances. Nordic Council of Ministers. *TemalNord* 573.
- [143] Holmquist, H., Schellenberger, S., van der Veen, I., Peters, G.M., Leonards, P.E.G., Cousins, I.T., **2016**. Properties, performance and associated hazards of state-of-the-art durable water repellent (DWR) chemistry for textile finishing. *Environment International* 91, 251-264.
- [144] Archroma, **2013**. Regulatory affairs - The challenge PFOA free. <https://www.performance-days.com/the-fair/program/expert-talks/details/regulatory-affairs-the-challenge-pfoa-free.html> (accessed: 01 March 2020).
- [145] Umweltbundesamt, **2017**. Use of PFOS in chromium plating – Characterisation of closed-loop systems, use of alternative substances. Report No. (UBA-FB) 002369/ENG.
- [146] Wang, Z., Cousins, I.T., Berger, U., Hungerbühler, K., Scheringer, M., **2016**. Comparative assessment of the environmental hazards of and exposure to perfluoroalkyl phosphonic and phosphinic acids (PFPA and PFPiA): Current knowledge, gaps, challenges and research needs. *Environment International* 89–90, 235-247.
- [147] de Silva, A.O., Spencer, C., Scott, B.F., Backus, S., Muir, D.C.G., **2011**. Detection of a cyclic perfluorinated acid, perfluoroethylcyclohexane sulfonate, in the Great Lakes of North America. *Environmental Science and Technology* 45(19), 8060-8066.

- [148] Yeung, L.W.Y., Mabury, S.A., **2016**. Are humans exposed to increasing amounts of unidentified organofluorine? *Environmental Chemistry* 13(1), 102-110.
- [149] Bergman, Å., Ryden, A., Law, R., de Boer, J., Covaci, A., Alace, M., Birnbaum, L., Petreas, M., Rose, M., Sakai, S. van den Eede, N., van der Veen, I., **2012**. A novel abbreviation standard for organobromine, organochlorine and organophosphorus flame retardants and some characteristics of the chemicals. *Environment International* 49, 57-82.
- [150] Hutchinson, T.H., Lyons, B.P., Thain, J.E., Law, R.J., **2013**. Evaluating legacy contaminants and emerging chemicals in marine environments using adverse outcome pathways and biological effects-directed analysis. *Marine Pollution Bulletin* 74, 517-525.
- [151] Coggan, T.L., Anumol, T., Pyke, J., Shimeta, J., Clarke, B.O., **2019**. A single analytical method for the determination of 53 legacy and emerging per- and polyfluoroalkyl substances (PFAS) in aqueous matrices. *Analytical and Bioanalytical Chemistry* 411(16), 3507-3520.
- [152] Chen, X., Zhu, L., Pan, X., Fang, S., Zhang, Y., Yang, L., **2015**. Isomeric specific partitioning behaviors of perfluoroalkyl substances in water dissolved phase, suspended particulate matters and sediments in Liao River Basin and Taihu Lake, China. *Water Research* 80, 235-244.
- [153] Ritscher, A., Wang, Z., Scheringer, M., Boucher, J., Ahrens, L., Berger, U., Bintein, S., Bopp, S., Borg, D., Buser, A., Cousins, I., deWitt, J., Fletcher, T., Green, C., Herzke, D., Higgins, C., Huang, J., Hung, H., Knepper, T., Lau, C., Leinala, E., Lindstrom, A., Liu, J., Miller, M., Ohno, K., Perkola, N., Shi, Y., Haug, L., Trier, X., Valsecchi, S., van der Jagt, K., Vierke, L., **2018**. Zürich Statement on Future Actions on Per- and Polyfluoroalkyl Substances (PFASs). *Environmental Health Perspectives* 126(8), 084502.
- [154] Scheringer, M., Trier, X., Cousins, I.T., de Voogt, P., Fletcher, T., Wang, Z., Webster, T.F., **2014**. Helsingor statement on poly- and perfluorinated alkyl substances (PFASs). *Chemosphere* 114, 337-339.
- [155] Blum, A., Balan, S.A., Scheringer, M., Trier, X., Goldenman, G., Cousins, I.T., Diamond, M., Fletcher, T., Higgins, C., Lindeman, A.E., Peaslee, G., de Voogt, P., Wang, Z., Weber, R., **2015**. The Madrid Statement on Poly- and Perfluoroalkyl Substances (PFASs). *Environmental Health Perspectives* 123(5), A107-111.
- [156] Martin, J.W., Mabury, S.A., Solomon, K., Muir, D.C.G., **2003**. Bioconcentration and tissue distribution of perfluorinated acids in rainbow trout (*Oncorhynchus mykiss*). *Environmental Toxicology and Chemistry* 22(1), 196-204.
- [157] Martin, J.W., Mabury, S.A., Solomon, K.R., Muir, D.C.G., **2003**. Dietary accumulation of perfluorinated acids in juvenile rainbow trout (*Oncorhynchus mykiss*). *Environmental Toxicology and Chemistry* 22(1), 189-195.
- [158] Brendel, S., Fetter, E., Staude, C., Vierke L., Biegel-Engler, A., **2018**. Short-chain perfluoroalkyl acids: environmental concerns and a regulatory strategy under REACH. *Environmental Sciences Europe* 30(1), 9.
- [159] D'Agostino, L.A., Mabury, S.A., **2017**. Aerobic biodegradation of 2 fluorotelomer sulfonamide-based aqueous film-forming foam components produces perfluoroalkyl carboxylates. *Environmental Toxicology and Chemistry* 36(8), 2012-2021.
- [160] Vierke, L., **2014**. Environmental Mobility of Short Chain Perfluoroalkyl Carboxylic Acids – Partition Behaviour and Resulting Environmental Concern. Dissertation. Leuphana Universität Lüneburg.

- [161] Möller, A., Ahrens, L., Sturm, R., Westerveld, J., van der Wielen, F., Ebinghaus, R., de Voogt, P., **2010**. Distribution and sources of polyfluoroalkyl substances (PFAS) in the River Rhine watershed. *Environmental Pollution* 158 (10), 3243-3250.
- [162] Lorenzo, M., Campo, J., Farré, M., Pérez, F., Picó, Y., Barceló, D., **2016**. Perfluoroalkyl substances in the Ebro and Guadalquivir river basins (Spain). *Science of The Total Environment* 540, 191-199.
- [163] Gebbink, W.A., Bignert, A., Berger, U., **2016**. Perfluoroalkyl Acids (PFAAs) and Selected Precursors in the Baltic Sea Environment: Do Precursors Play a Role in Food Web Accumulation of PFAAs? *Environmental Science & Technology* 50(12), 6354-6362.
- [164] Glynn, A., Berger, U., Bignert, A., Ullah, S., Aune, M., Lignell, S., Darnerud, P.O., **2012**. Perfluorinated alkyl acids in blood serum from primiparous women in Sweden: serial sampling during pregnancy and nursing, and temporal trends 1996-2010. *Environmental Science & Technology* 46(16), 9071-9079.
- [165] Kirchgeorg, T., Dreyer, A., Gabrielli, P., Gabrieli, J., Thomson, L.G., Barbante, C., Ebinghaus, R., **2016**. Seasonal accumulation of persistent organic pollutants on a high altitude glacier in the Eastern Alps. *Environmental Pollution* 218, 804-812.
- [166] Skaar, J.S., Raeder, E.M., Lyche, J.L., Ahrens, L., Kallenborn, R., **2019**. Elucidation of contamination sources for poly- and perfluoroalkyl substances (PFASs) on Svalbard (Norwegian Arctic). *Environmental Science and Pollution Research* 26(8), 7356-7363.
- [167] Llorca, M., Farré, M., Tavano, S., Alonso, B., Koremblit, G., Barceló, D., **2012**. Fate of a broad spectrum of perfluorinated compounds in soils and biota from Tierra del Fuego and Antarctica. *Environmental Pollution* 163, 158-166.
- [168] Krafft, M.P., Riess, J.G., **2015**. Per- and polyfluorinated substances (PFASs): Environmental challenges. *Current Opinion in Colloid & Interface Science* 20(3), 192-212.
- [169] Gomis, M.I., Wang, Z., Scheringer, M., Cousins, I.T., **2015**. A modeling assessment of the physicochemical properties and environmental fate of emerging and novel per- and polyfluoroalkyl substances. *Science of the Total Environment* 505, 981-991.
- [170] Wang, Z., Cousins, I.T., Scheringer, M., Hungerbühler, K., **2015**. Hazard assessment of fluorinated alternatives to long-chain perfluoroalkyl acids (PFAAs) and their precursors: status quo, ongoing challenges and possible solutions. *Environment International* 75, 172-179.
- [171] Gomis, M.I., Vestergren, R., Borg, D., Cousins, I.T., **2018**. Comparing the toxic potency in vivo of long-chain perfluoroalkyl acids and fluorinated alternatives. *Environment International* 113, 1-9.
- [172] LfU, Bayerisches Landesamt für Umwelt, Bavarian Environment Agency, **2019**. Per- und polyfluorierte Chemikalien in Bayern – Untersuchungen 2006-2018 (in German).
- [173] Pan, Y.; Zhang, H.; Cui, Q.; Sheng, N.; Yeung, L. W. Y.; Sun, Y.; Guo, Y.; Dai, J., **2018**. Worldwide distribution of novel perfluoroether carboxylic and sulfonic acids in surface water. *Environmental Science & Technology* 52 (14), 7621-7629.
- [174] Gebbink, W.A., van Asseldonk, L., van Leeuwen, S.P.J., **2017**. Presence of emerging per- and polyfluoroalkyl substances (PFASs) in river and drinking water near a fluorochemical production plant in the Netherlands. *Environmental Science & Technology* 51(19), 11057-11065.
- [175] Wang, S., Huang, J., Yang, Y., Hui, Y., Ge, Y., Larssen, T., Harman, C., **2013**. First report of a Chinese PFOS alternative overlooked for 30 years: Its toxicity, persistence, and presence in the environment. *Environmental Science & Technology* 47(18), 10163-10170.

- [176] Ruan, T., Lin, Y., Wang, T., Liu, R., Jiang, G., **2015**. Identification of novel polyfluorinated ether sulfonates as PFOS alternatives in municipal sewage sludge in China. *Environmental Science & Technology* 49(11), 6519-6527.
- [177] Shi, Y., Vestergren, R., Zhou, Z., Song, X. Xu, L., Liang, Y., Cai, Y., **2015**. Tissue Distribution and Whole Body Burden of the Chlorinated Polyfluoroalkyl Ether Sulfonic Acid F-53B in Crucian Carp (*Carassius carassius*): Evidence for a Highly Bioaccumulative Contaminant of Emerging Concern. *Environmental Science & Technology* 49(24), 14156-14165.
- [178] Shi, Y., Vestergren, R., Xu, L., Zhou, Z., Li, C., Liang, Y., Cai, Y., **2016**. Human Exposure and Elimination Kinetics of Chlorinated Polyfluoroalkyl Ether Sulfonic Acids (Cl-PFESAs). *Environmental Science & Technology* 50(5), 2396-2404.
- [179] Gebbink, W.A., Bossi, R., Rigét, F.F., Rosing-Asvid, A., Sonne, C., and Dietz, R., **2016**. Observation of emerging per- and polyfluoroalkyl substances (PFASs) in Greenland marine mammals. *Chemosphere* 144, 2384-2391.
- [180] Anna Kärrman, Wang, T., Kallenborn, R., **2019**. PFASs in the Nordic environment – Screening of Poly- and Perfluoroalkyl Substances (PFASs) and Extractable Organic Fluorine (EOF) in the Nordic Environment. *TemaNord* 2019:515.
- [181] McDonough, C.A., Guelfo, J.L., Higgins, C.P., **2019**. Measuring total PFASs in water: The tradeoff between selectivity and inclusivity. *Current Opinion in Environmental Science & Health* 7, 13-18.
- [182] Liu, Y., D'Agostino, L., Qu, G., Jiang, G., Martin, J.W., **2019**. High-resolution mass spectrometry (HRMS) methods for nontarget discovery and characterization of poly- and perfluoroalkyl substances (PFASs) in environmental and human samples. *Trends in Analytical Chemistry* 121, 115420.
- [183] Ahrens, L., Vorkamp, K., Lepom, P., Bersuder, P., Theobald, N., Ebinghaus, R., Bossi, B.R., McGovern, E., **2010**. Determination of perfluoroalkyl compounds in water, sediment, and biota. *ICES Techniques in Marine Environmental Sciences* 48, 1-16.
- [184] Umweltbundesamt, German Environment Agency, **2016**. Investigations on the presence and behavior of precursors to perfluoroalkyl substances in the environment as a preparation of regulatory measures. Report No. (UBA-FB) 002223/ENG.
- [185] Berger, U., Kasier, M.A., Kärrman, A., Barber, J.L., van Leeuwen, S.P.J., **2011**. Recent developments in trace analysis of poly- and perfluoroalkyl substances. *Analytical and Bioanalytical Chemistry* 400(6), 1625-1635.
- [186] Wellington Laboratories, **2016**. Product updates from Wellington Laboratories - Reference Standards for Replacement PFCs: Components of ADONA and F-53B. https://well-labs.com/docs/adona_and_f53b_15aug2016_wellington_reporter.pdf (accessed: 01 April 2020).
- [187] Ritter, E.E., Dickinson, M.D., Harron, J.P., Lunderberg, D.M., DeYoung, P.A., Robel, A.E., Field, J.A., Peaslee, G.F., **2017**. PIGE as a screening tool for per- and polyfluorinated substances in papers and textiles. *Nuclear Instruments and Methods in Physics Research Section B: Beam Interactions with Materials and Atoms* 407, 47-54.
- [188] Peaslee, G., **2019**. Developing PIGE into a Rapid Field-Screening Test for PFAS. <https://www.serdp-estcp.org/Program-Areas/Environmental-Restoration/Risk-Assessment/ER19-1142> (accessed: 02 April 2020).
- [189] Moody, C.A., Kwan, W.C., Martin, J.W., Muir, D.C.G., Mabury, S.A., **2001**. Determination of Perfluorinated Surfactants in Surface Water Samples by Two Independent Analytical Techniques: Liquid Chromatography/Tandem Mass Spectrometry and ^{19}F NMR. *Analytical Chemistry* 73(10), 2200-2206.

- [190] Miyake, Y., Yamashita, N., Rostowski, P., So, M.K., Taniyasu, S., Lam, P.K.S., Kannan, K., **2007**. Determination of trace levels of total fluorine in water using combustion ion chromatography for fluorine: A mass balance approach to determine individual perfluorinated chemicals in water. *Journal of Chromatography A* 1143(1), 98-104.
- [191] Wagner, A., Raue, B., Brauch, H.-J., Worch, E., Lange, F.T., **2013**. Determination of adsorbable organic fluorine from aqueous environmental samples by adsorption to polystyrene-divinylbenzene based activated carbon and combustion ion chromatography. *Journal of Chromatography A* 1295, 82-89.
- [192] Houtz, E.F., Sedlak, D.L., **2012**. Oxidative Conversion as a Means of Detecting Precursors to Perfluoroalkyl Acids in Urban Runoff. *Environmental Science & Technology* 46(17), 9342-9349.
- [193] Krauss, M., Singer, H., Hollender, J., **2010**. LC-high resolution MS in environmental analysis: from target screening to the identification of unknowns. *Analytical and Bioanalytical Chemistry* 397(3), 943-951.
- [194] Hollender, J., van Bavel, B., Dulio, V., Farmen, E., Furtmann, K., Koschorreck, J., Kunkel, U., Krauss, M., Munthe, J., Schlabach, M., Slobodnik, J., Stroomberg, G., Ternes, T., Thomaidis, N., Togola, A., Tornero, V., **2019**. High resolution mass spectrometry-based non-target screening can support regulatory environmental monitoring and chemicals management. *Environmental Sciences Europe* 31(1), 42.
- [195] Alygizakis, N.A., Oswald, P., Thomaidis, N.S., Schymanski, E.L., Aalizadeh, R., Schulze, T., Oswaldova, M., Slobodnik, J., **2019**. NORMAN digital sample freezing platform: A European virtual platform to exchange liquid chromatography high resolution-mass spectrometry data and screen suspects in "digitally frozen" environmental samples. *Trends in Analytical Chemistry* 115, 129-137.
- [196] Hollender, J., Schymanski, E.L., Singer, H.P., Ferguson, P.L., **2017**. Nontarget Screening with High Resolution Mass Spectrometry in the Environment: Ready to Go? *Environmental Science & Technology* 51(20), 11505-11512.
- [197] Brack, W., Hollender, J., López de Alda, M., Müller, C., Schulze, T., Schymanski, E., Slobodnik, J., Krauss, M., **2019**. High-resolution mass spectrometry to complement monitoring and track emerging chemicals and pollution trends in European water resources. *Environmental Sciences Europe* 31(1), 62.
- [198] Villaverde-de-Sáa, E., Fernandez-Lopez, M., Rodil, R., Quintana, J., Racamonde, I., Cela, R., **2015**. Solid-phase extraction of perfluoroalkylated compounds from sea water. *Journal of Separation Science* 38(11), 1942-1950.
- [199] Janda, J., **2019**. Polare Perfluoralkylcarbonsäuren - Bestimmung in aquatischen Proben und Untersuchungen zu ihren Präkursoren in Wasser und Feststoffen (in German). Dissertation. Springer Spektrum, Heidelberg.
- [200] Trojanowicz, M., Koc, M., **2013**. Recent developments in methods for analysis of perfluorinated persistent pollutants. *Microchimica Acta* 180(11), 957-971.
- [201] Nakayama, S.F., Yoshikane, M., Onoda, Y., Nishihama, Y., Iwai-Shimada, M., Takagi, M., Kobayashi, Y., Isobe, T., **2019**. Worldwide trends in tracing poly- and perfluoroalkyl substances (PFAS) in the environment. *Trends in Analytical Chemistry* 121, 115410.
- [202] ISO, International Organization for Standardization, **2009**. ISO 25101:2009-03: Water quality - Determination of perfluorooctanesulfonate (PFOS) and perfluorooctanoate (PFOA) - Method for unfiltered samples using solid phase extraction and liquid chromatography/mass spectrometry.

- [203] DIN, Deutsches Institut für Normung, German Institute for Standardization, **2011**. DIN 38407-42:2011-03: German standard methods for the examination of water, waste water and sludge - Jointly determinable substances (group F) - Part 42: Determination of selected polyfluorinated compounds (PFC) in water - Method using high performance liquid chromatography and mass spectrometric detection (HPLC/MS-MS) after solid-liquid extraction (F 42).
- [204] DIN, Deutsches Institut für Normung, German Institute for Standardization, **2011**. DIN 38414-14:2011-08: German standard methods for the examination of water, waste water and sludge - sludge and sediments (group S) - Part 14: Determination of selected polyfluorinated compounds (PFC) in sludge, compost and soil - Method using high performance liquid chromatography and mass spectrometric detection (HPLC-MS/MS) (S 14).
- [205] Lange, V., Picotti, P., Domon, B., Aebersold, R., **2008**. Selected reaction monitoring for quantitative proteomics: a tutorial. *Molecular Systems Biology* 4(1), 222.
- [206] European Commission, **2002**. European Commission Decision 2002/657/EC implementing Council Directive 96/23/EC concerning the performance of analytical methods and the interpretation of results.
- [207] Gremmel, C., Frömel, T., Knepper, T.P., **2017**. HPLC-MS/MS methods for the determination of 52 perfluoroalkyl and polyfluoroalkyl substances in aqueous samples. *Analytical and Bioanalytical Chemistry* 409(6), 1643-1655.
- [208] Munoz, G., Budzinski, H., Labadie, P., **2017**. Influence of environmental factors on the fate of legacy and emerging per- and polyfluoroalkyl substances along the salinity/turbidity gradient of a macrotidal estuary. *Environmental Science & Technology* 51(21) 12347-12357.
- [209] AB Sciex, **2008**. Analyst 1.5 Software - Manual Optimization Tutorial. *Applied Biosystems/MDS Sciex*, Canada.
- [210] Munoz, G., Liu, J., Vo Duy, S., Sauvé, S., **2019**. Analysis of F-53B, Gen-X, ADONA, and emerging fluoroalkylether substances in environmental and biomonitoring samples: A review. *Trends in Environmental Analytical Chemistry* 23, e00066.
- [211] Mullin, L., Katz, D., Riddell, N., Plumb, R., Burgess, J.A., Yeung, L.W.Y., Jogsten, I.E., **2019**. Analysis of hexafluoropropylene oxide-dimer acid (HFPO-DA) by liquid chromatography-mass spectrometry (LC-MS): Review of current approaches and environmental levels. *Trends in Analytical Chemistry* 118, 828-839.
- [212] Ahrens, L., **2009**. Polyfluoroalkyl compounds in the marine environment – Investigations on their distribution in surface water and temporal trends in harbor seals (*Phoca vitulina*). Dissertation. Leuphana Universität Lüneburg.
- [213] Kromidas, S., **2003**. More practical problem solving in HPLC. 1st edition, Wiley-VCH, Weinheim.
- [214] Normenausschuss Wasserwesen, Arbeitskreis 19, **2011**. Validation document for DIN 38407-42:2011-03: German standard methods for the examination of water, waste water and sludge - Jointly determinable substances (group F) - Part 42: Determination of selected polyfluorinated compounds (PFC) in water - Method using high performance liquid chromatography and mass spectrometric detection (HPLC/MS-MS) after solid-liquid extraction (F 42).
- [215] Mansoori, B.A., Volmer, D.A., Boyd, R.K., **1997**. 'Wrong-way-round' Electrospray Ionization of Amino Acids. *Rapid Communications in Mass Spectrometry* 11(10), 1120-1130.

- [216] Monnin, C., Ramrup, P., Daigle-Young, C., Vuckovic, D., **2018**. Improving negative liquid chromatography/electrospray ionization mass spectrometry lipidomic analysis of human plasma using acetic acid as a mobile-phase additive. *Rapid Communications in Mass Spectrometry* 32(3), 201-211.
- [217] Wu, Z., Gao, W., Phelps, M., Wu, D., Miller, D., Dalton, J., **2004**. Favorable Effects of Weak Acids on Negative-Ion Electrospray Ionization Mass Spectrometry. *Analytical Chemistry* 76(3), 839-847.
- [218] Bader, T., **2018**. Mining of LC-HRMS data for the assessment of water treatment processes. Dissertation, Leuphana Universität Lüneburg.
- [219] Keunchkarian, S., Reta, M., Romero, L., Castells, C., **2006**. Effect of sample solvent on the chromatographic peak shape of analytes eluted under reversed-phase liquid chromatographic conditions. *Journal of Chromatography A* 1119(1), 20-28.
- [220] Filipovic, M., Berger, U., **2015**. Are perfluoroalkyl acids in waste water treatment plant effluents the result of primary emissions from the technosphere or of environmental recirculation? *Chemosphere* 129, 74-80.
- [221] Riddell, N., Arsenault, G., Benskin, J.P., Chittim, B., Martin, J.W., Mcalees, A., Mccrindel, R., **2009**. Branched Perfluorooctane Sulfonate Isomer Quantification and Characterization in Blood Serum Samples by HPLC/ESI-MS(/MS). *Environmental Science & Technology* 43(20), 7902-7908.
- [222] AB Sciex, **2001**. API 4000 Hardware Manual. 2001. *Applied Biosystems/MDS Sciex*, Canada.
- [223] Ahrens, L., Plassmann, M., Xie, Z., Ebinghaus, R., **2009**. Determination of polyfluoroalkyl compounds in water and suspended particulate matter in the river Elbe and North Sea, Germany. *Frontiers of Environmental Science & Engineering in China* 3(2), 152-170.
- [224] Reichenbacher, M., Einax, J.W., **2011**. Validation of Method Performance. In *Challenges in Analytical Quality Assurance*, Springer, Berlin, 117-239.
- [225] Krueve, A., Rebane, R., Kipper, K., Oldekop, M.-L., Evard, H., Herodes, K., Ravio, P., Leito, I., **2015**. Tutorial review on validation of liquid chromatography–mass spectrometry methods: Part II. *Analytica Chimica Acta* 870, 8-28.
- [226] Funk, W., Dammann, V., Donnevert, G., **2005**. Qualitätssicherung in der Analytischen Chemie. 2nd edition, Wiley-VCH, Weinheim.
- [227] Gu, H., Liu, G., Wang, J., Aubry, A.-F., Arnold, M.E., **2014**. Selecting the Correct Weighting Factors for Linear and Quadratic Calibration Curves with Least-Squares Regression Algorithm in Bioanalytical LC-MS/MS Assays and Impacts of Using Incorrect Weighting Factors on Curve Stability, Data Quality, and Assay Performance. *Analytical Chemistry* 86(18), 8959-8966.
- [228] Krueve, A., Rebane, R., Kipper, K., Oldekop, M.-L., Evard, H., Herodes, K., Ravio, P., Leito, I., **2015**. Tutorial review on validation of liquid chromatography–mass spectrometry methods: Part I. *Analytica Chimica Acta* 870, 29-44.
- [229] Wells, G., Prest, H., Russ, C.W., **2011**. Why use signal-to-noise as a measure of MS performance when it is often meaningless? Technical Overview, *Agilent Technologies*, Santa Clara, United States.
- [230] Smith, S., **2015**. Solid Phase Extraction (SPE): An introduction to basic theory, method development, and applications. Technical Note, *Waters Corporation*, Manchester, United Kingdom.
- [231] Fontanals, N., Borrull, F., Marcé, R.M., **2020**. Mixed-mode ion-exchange polymeric sorbents in environmental analysis. *Journal of Chromatography A* 1609, 460531.

- [232] Gale, T., **2020**. Ocean Chemical Processes. <http://www.waterencyclopedia.com/Mi-Oc/Ocean-Chemical-Processes.html> (accessed: 28 February 2020).
- [233] Kromidas, S., **2011**. Validierung in der Analytik. 2nd edition, *Wiley VCH*, Weinheim.
- [234] Ricci, M., Kourtchev, I., Emons, H., **2012**. Chemical water monitoring under the Water Framework Directive with Certified Reference Materials. *Trends in Analytical Chemistry* 36, 47-57.
- [235] Ricci, M., Lava, R., Koleva, B., **2016**. Matrix Certified Reference Materials for environmental monitoring under the EU Water Framework Directive: An update. *Trends in Analytical Chemistry* 76, 194-202.
- [236] Ramos, M., van der Veen, I., Charoud-Got, J., Emteborg, H., Weiss, J., Schimmel, H., **2015**. The certification of the mass concentration of perfluoroalkyl substances (PFASs) in water: IRMM-428. *European Commission, Joint Research Centre, Institute for Reference Materials and Measurements (IRMM)*.
- [237] European Federation of National Associations of Measurement, Testing and Analytical Laboratories, **2018**. The assessment of the trueness of a measurement procedure by use of a reference material. <https://www.eurolab.org/CookBooks/15> (accessed: 01 March 2020).
- [238] Cunningham, W.C., Capar, S.G., **2014**. Reference Materials. United States Food and Drug Administration. <https://www.fda.gov/media/89941/download> (accessed: 01 March 2020).
- [239] Beškoski, V.P., Takemine, S., Nakeno, T., Beškoski, L., Cviković, G., Ilic, M., Miletic, S., Vrvic, M., **2013**. Perfluorinated compounds in sediment samples from the wastewater canal of Pančevo (Serbia) industrial area. *Chemosphere* 91(10), 1408-1415.
- [240] Higgins, C.P., Field, J.A., Criddle, C.S., Luthy, R.G., **2005**. Quantitative determination of perfluorochemicals in sediments and domestic sludge. *Environmental Science & Technology* 39(11), 3946-3956.
- [241] Yeung, L.W.Y., de Silva, A.O., Loi, E., Marvin, C., Taniysu, S., Yamashita, N., Mabury, S., Muir, D.C.G., Lam, P.K.S., **2013**. Perfluoroalkyl substances and extractable organic fluorine in surface sediments and cores from Lake Ontario. *Environment International* 59, 389-397.
- [242] Zhang, T., Sun, H., Gereck, A., Kannan, K., Müller, C., Alder, A., **2010**. Comparison of two extraction methods for the analysis of per- and polyfluorinated chemicals in digested sewage sludge. *Journal of Chromatography A* 1217(31), 5026-5034.
- [243] Llorca, M., Ferré, M., Pico, Y., Barceló, D., **2009**. Development and validation of a pressurized liquid extraction liquid chromatography–tandem mass spectrometry method for perfluorinated compounds determination in fish. *Journal of Chromatography A* 1216(43), 7195-7204.
- [244] Siegmund, A.-K., **2016**. Entwicklung einer Methode zur Bestimmung von per- und polyfluorierten Alkylsubstanzen (PFASs) einschließlich der polyfluorierten Phosphorsäure-ester (PAPs) in Sedimenten (in German). Masterarbeit. Hochschule Emden-Leer.
- [245] Lorenzo, M., Campo, J., Picó, Y., **2015**. Optimization and comparison of several extraction methods for determining perfluoroalkyl substances in abiotic environmental solid matrices using liquid chromatography-mass spectrometry. *Analytical and Bioanalytical Chemistry* 407(19), 5767-5781.
- [246] Yan, H., Zhang, C., Zhou, Q., Yang, S., **2015**. Occurrence of perfluorinated alkyl substances in sediment from estuarine and coastal areas of the East China Sea. *Environmental Science and Pollution Research* 22(3), 1662-1669.
- [247] OSPAR Commission, **2010**. Quality Status Report 2010. *OSPAR Commission*. London.

- [248] HELCOM; Baltic Marine Environment Protection Commission, **2018**. State of the Baltic Sea – Second HELCOM holistic assessment 2011-2016. *Baltic Sea Environment Proceedings* 155.
- [249] Petersen, W., Schroeder, F., Bockelmann, F.D., **2011**. FerryBox - Application of continuous water quality observations along transects in the North Sea. *Ocean Dynamics* 61(10), 1541-1554.
- [250] RIVM; Netherlands National Institute for Public Health and the Environment, **2016**. Evaluation of substances used in the GenX technology by Chemours, Dordrecht. *RIVM Letter report* 2016-0174.
- [251] de Solla, S.R., De Silva, A.O., Letcher, R.J., **2012**. Highly elevated levels of perfluorooctane sulfonate and other perfluorinated acids found in biota and surface water downstream of an international airport, Hamilton, Ontario, Canada. *Environment International* 39(1), 19-26.
- [252] Wang, Y., Vestergren, R., Shi, Y., Cao, D., Xu, L., Cai, Y., Wu, F., **2016**. Identification, tissue distribution, and bioaccumulation potential of cyclic perfluorinated sulfonic acids isomers in an airport impacted ecosystem. *Environmental Science & Technology* 50(20), 10923-10932.
- [253] Liu, Y., Zhang, Y., Li, J., Wu, N., Li, W., Niu, Z., **2019**. Distribution, partitioning behavior and positive matrix factorization-based source analysis of legacy and emerging polyfluorinated alkyl substances in the dissolved phase, surface sediment and suspended particulate matter around coastal areas of Bohai Bay, China. *Environmental Pollution* 246, 34-44.
- [254] MacInnis, J.J., French, K., Muir, D.C.G., Spencer, C., Criscitiello, A., De Silva, A.O., Young, C.J., **2017**. Emerging investigator series: a 14-year depositional ice record of perfluoroalkyl substances in the High Arctic. *Environmental Sciences Processes Impacts* 19(1), 22-30.
- [255] Nguyen, M.A., Wiberg, K., Ribeli, E., Josefsson, S., Futter, M., Gustavsson, J., Ahrens, L., **2017**. Spatial distribution and source tracing of per- and polyfluoroalkyl substances (PFASs) in surface water in Northern Europe. *Environmental Pollution* 220, Part B, 1438-1446.
- [256] Filipovic, M., Berger, U., McLachlan, M.S., **2013**. Mass balance of perfluoroalkyl acids in the Baltic Sea. *Environmental Science & Technology* 47(9), 4088-4095.
- [257] BVL; German Federal Office of Consumer Protection and Food Safety, **2018**. Beistoffe in zugelassenen Pflanzenschutzmitteln. https://www.bvl.bund.de/SharedDocs/Downloads-/04_Pflanzenschutzmittel/zul_info_liste_beistoffe.html?nn=1489180 (accessed 06 March 2019) (in German).
- [258] US EPA; United States Environmental Protection Agency, **2006**. Inert ingredient; Revocation of the tolerance exemption of mono- and bis-(1H, 1H, 2H, 2H-perfluoroalkyl)-phosphates where the alkyl group is even numbered and in the C6-C12 range; final rule. *Fed. Regist.* 71 (153), 45408-45411.
- [259] Higgins, C.P., Field, J.A., Criddle, C.S., Luthy, R.G., **2005**. Quantitative determination of perfluorochemicals in sediments and domestic sludge. *Environmental Science & Technology* 39(11), 3946-3956.
- [260] Ahrens, L., Yeung, L.W., Taniyasu, S., Lam, P.K., Yamashita, N., **2011**. Partitioning of perfluorooctanoate (PFOA), perfluorooctane sulfonate (PFOS) and perfluorooctane sulfonamide (PFOSA) between water and sediment. *Chemosphere* 85(5) 731-737.
- [261] Munoz, G., Budzinski, H., Labadie, P., **2017**. Influence of environmental factors on the fate of legacy and emerging per- and polyfluoroalkyl substances along the salinity/turbidity gradient of a macrotidal estuary. *Environmental Science & Technology* 51(21) 12347-12357.

- [262] Hebbeln, D., Scheurle, C., Lamy, F., **2003**. Depositional history of the Helgoland mud area, German Bight, North Sea. *Geo-Marine Letters* 23(2), 81-90.
- [263] Lee, H. and Mabury, S.A., **2017**. Sorption of perfluoroalkyl phosphonates and perfluoroalkyl phosphinates in soils. *Environmental Science & Technology* 51(6), 3197-3205.
- [264] Guelfo, J.L. and Higgins, C.P., **2013**. Subsurface transport potential of perfluoroalkyl acids at aqueous film-forming foam (AFFF)-impacted sites. *Environmental Science & Technology* 47(9), 4164-4171.
- [265] Chen, X., Zhu, L., Pan, X., Fang, S., Zhang, Y., Yang, L., **2015**. Isomeric specific partitioning behaviors of perfluoroalkyl substances in water dissolved phase, suspended particulate matters and sediments in Liao River Basin and Taihu Lake, China. *Water Research* 80, 235-244.
- [266] Benskin, J. P., Yeung, L.W.Y., Yamashita, N., Taniyasu, S., Lam, P.K.S., Martin, J. W., **2010**. Perfluorinated acid isomer profiling in water and quantitative assessment of manufacturing source. *Environmental Science & Technology* 44(23), 9049-9054.
- [267] Beszczynska-Möller, A., Fahrbach, E., Schauer, U., Hansen, E., **2012**. Variability in Atlantic water temperature and transport at the entrance to the Arctic Ocean, 1997–2010. *ICES Journal of Marine Science* 69 (5), 852-863.
- [268] von Appen, W.-J., **2018**. The Expedition PS114 of the Research Vessel POLARSTERN to the Fram Strait in 2018. Reports on Polar and Marine Research, Bremerhaven, *Alfred Wegener Institute for Polar and Marine Research* 723, 84.
- [269] Forget, G., Campin, J. M., Heimbach, P., Hill, C. N., Ponte, R. M., Wunsch, C., **2015**. ECCO version 4: an integrated framework for non-linear inverse modeling and global ocean state estimation. *Geoscientific Model Development* 8 (10), 3071-3104.
- [270] Forget, G., Ferreira, D., Liang, X., **2015**. On the observability of turbulent transport rates by Argo: supporting evidence from an inversion experiment. *Ocean Science* 11 (5), 839-853.
- [271] Forget, G., Ponte, R. M., **2015**. The partition of regional sea level variability. *Progress in Oceanography* 137, 173-195.
- [272] Stöven, T., Tanhua, T., Hoppema, M., von Appen, W.J., **2016**. Transient tracer distributions in the Fram Strait in 2012 and inferred anthropogenic carbon content and transport. *Ocean Science* 12 (1), 319-333.
- [273] Winther, N.G., Johannessen, J.A., **2006**. North Sea circulation: Atlantic inflow and its destination. *Journal of Geophysical Research (Oceans)* 111.
- [274] Joerss, H., Apel, C., Ebinghaus, R., **2019**. Emerging per- and polyfluoroalkyl substances (PFASs) in surface water and sediment of the North and Baltic Seas. *Science of the Total Environment* 686, 360-369.
- [275] Mork, K. A.; Skagseth, Ø., **2010**. A quantitative description of the Norwegian Atlantic Current by combining altimetry and hydrography. *Ocean Science* 6 (4), 901-911.
- [276] Smith, J. N., McLaughlin, F. A., Smethie Jr., W. M., Moran, S. B., Lepore, K., **2011**. Iodine-129, 137Cs, and CFC-11 tracer transit time distributions in the Arctic Ocean. *Journal of Geophysical Research: Oceans* 116 (C4).
- [277] United Nations, **2009**. Stockholm Convention on Persistent Organic Pollutants. New York.
- [278] Scheringer, M., **2009**. Long-range transport of organic chemicals in the environment. *Environmental Toxicology and Chemistry* 28(4), 677-690.
- [279] Walczowski, W., **2013**. Frontal structures in the West Spitsbergen Current margins. *Ocean Science* 9 (6), 957-975.

- [280] Grosfeld, K. T., R., Asseng, J., Bartsch, A., Bräuer, B., Fritzsche, B., Gerdes, R., Hendricks, S., Hiller, W., Heygster, G., Krumpfen, T., Lemke, P., Melsheimer, C., Nicolaus, M., Ricker, R. and Weigelt, M., **2016**. Online sea-ice knowledge and data platform www.meereisportal.de. Polarforschung, Bremerhaven, *Alfred Wegener Institute for Polar and Marine Research & German Society of Polar Research* 85 (2), 143-155.
- [281] Dahlgard, H., **1995**. Transfer of European coastal pollution to the arctic: Radioactive tracers. *Marine Pollution Bulletin* 31 (1), 3-7.
- [282] de Steur, L., Peralta-Ferriz, C., Pavlova, O., **2018**. Freshwater Export in the East Greenland Current Freshens the North Atlantic. *Geophysical Research Letters* 45 (24), 13,359-13,366.
- [283] Pickard, H. M., Criscitiello, A. S., Spencer, C., Sharp, M. J., Muir, D. C. G., De Silva, A. O., Young, C. J., **2018**. Continuous non-marine inputs of per- and polyfluoroalkyl substances to the High Arctic: a multi-decadal temporal record. *Atmospheric Chemistry and Physics* 18 (7), 5045-5058.
- [284] MacInnis, J. J., Lehnerr, I., Muir, D. C. G., St. Pierre, K. A., St. Louis, V. L., Spencer, C., De Silva, A. O., **2019**. Fate and Transport of Perfluoroalkyl Substances from Snowpacks into a Lake in the High Arctic of Canada. *Environmental Science & Technology* 53 (18), 10753-10762.
- [285] Kwok, K. Y., Yamazaki, E., Yamashita, N., Taniyasu, S., Murphy, M. B., Horii, Y., **2013**. Transport of Perfluoroalkyl substances (PFAS) from an arctic glacier to downstream locations: implications for sources. *Science of the Total Environment* 447, 46-55.
- [286] von Appen, W.-J., Rohardt, G., **2019**. Continuous thermosalinograph oceanography along POLARSTERN cruise track PS114. *Alfred Wegener Institute, Helmholtz Centre for Polar and Marine Research, Bremerhaven, PANGAEA*. doi: 10.1594/PANGAEA.898225.
- [287] Rudels, B., Björk, G., Nilsson, J., Winsor, P., Lake, I., Nohr, C., **2005**. The interaction between waters from the Arctic Ocean and the Nordic Seas north of Fram Strait and along the East Greenland Current: results from the Arctic Ocean-02 Oden expedition. *Journal of Marine Systems* 55 (1), 1-30.
- [288] Ma, Y., Adelman, D. A., Bauerfeind, E., Cabrerizo, A., McDonough, C. A., Muir, D., Soltwedel, T., Sun, C., Wagner, C. C., Sunderland, E. M., Lohmann, R., **2018**. Concentrations and Water Mass Transport of Legacy POPs in the Arctic Ocean. *Geophysical Research Letters* 45 (23), 12,972-12,981.
- [289] Lohmann, R., Jurado, E., Dijkstra, H. A., Dachs, J., **2013**. Vertical eddy diffusion as a key mechanism for removing perfluorooctanoic acid (PFOA) from the global surface oceans. *Environmental Pollution* 179, 88-94.
- [290] von Appen, W.-J., Schaffer, J., Rohardt, G., Wisotzki, A., **2019**. Physical oceanography measured on water bottle samples during POLARSTERN cruise PS114. *Alfred Wegener Institute, Helmholtz Centre for Polar and Marine Research, Bremerhaven, PANGAEA*. doi: 10.1594/PANGAEA.898695
- [291] Schlitzer, R. Ocean Data View. <https://odv.awi.de>, **2018**.
- [292] Stemmler, I., Lammel, G., **2010**. Pathways of PFOA to the Arctic: variabilities and contributions of oceanic currents and atmospheric transport and chemistry sources. *Atmospheric Chemistry and Physics* 10 (20), 9965-9980.
- [293] Wania, F., **2007**. A Global Mass Balance Analysis of the Source of Perfluorocarboxylic Acids in the Arctic Ocean. *Environmental Science & Technology* 41 (13), 4529-4535.

- [294] Armitage, J., Cousins, I. T., Buck, R. C., Prevedouros, K., Russell, M. H., MacLeod, M., Korzeniowski, S. H., **2006**. Modeling global-scale fate and transport of perfluorooctanoate emitted from direct sources. *Environmental Science & Technology* 43 (24), 9274-9280.
- [295] Young, C. J., Furdui, V. I., Franklin, J., Koerner, R. M., Muir, D. C. G., Mabury, S. A., **2007**. Perfluorinated Acids in Arctic Snow: New Evidence for Atmospheric Formation. *Environmental Science & Technology* 41 (10), 3455-3461.
- [296] Dassuncao, C., Hu, X. C., Zhang, X., Bossi, R., Dam, M., Mikkelsen, B., Sunderland, E. M., **2017**. Temporal shifts in poly- and perfluoroalkyl substances (PFASs) in North Atlantic pilot whales indicate large contribution of atmospheric precursors. *Environmental Science & Technology* 51 (8), 4512-4521.
- [297] Plassmann, M. M., Meyer, T., Lei, Y. D., Wania, F., McLachlan, M. S., Berger, U., **2011**. Laboratory studies on the fate of perfluoroalkyl carboxylates and sulfonates during snowmelt. *Environmental Science & Technology* 45 (16), 6872-6878.
- [298] Higgins, C. P., Luthy, R. G., **2006**. Sorption of perfluorinated surfactants on sediments. *Environmental Science & Technology* 40 (23), 7251-7256.
- [299] Pućko, M., Stern, G. A., Macdonald, R. W., Jantunen, L. M., Bidleman, T. F., Wong, F., Barber, D. G., Rysgaard, S., **2015**. The delivery of organic contaminants to the Arctic food web: Why sea ice matters. *Science of the Total Environment* 506-507, 444-452.
- [300] Chen, M., Wang, C., Wang, X., Fu, J., Gong, P., Yan, J., Yu, Z., Yan, F., Nawab, J., **2019**. Release of perfluoroalkyl substances from melting glacier of the Tibetan Plateau: Insights into the impact of global warming on the cycling of emerging pollutants. *Journal of Geophysical Research: Atmospheres* 124 (13), 7442-7456.
- [301] Muir, D.; Zhang, X.; de Wit, C. A.; Vorkamp, K.; Wilson, S., **2019**. Identifying further chemicals of emerging arctic concern based on 'in silico' screening of chemical inventories. *Emerging Contaminants* 5, 201-210.
- [302] ECHA, European Chemicals Agency, **2019**. MSC unanimously agrees that HFPO-DA is a substance of very high concern. <https://echa.europa.eu/de/-/msc-unanimously-agrees-that-hfpo-da-is-a-substance-of-very-high-concern> (accessed: 05 September 2019).
- [303] Ye, F., Tokumura, M., Islam, M.S., Zushi, Y., Oh, J., Masunaga, S., **2014**. Spatial distribution and importance of potential perfluoroalkyl acid precursors in urban rivers and sewage treatment plant effluent – Case study of Tama River, Japan. *Water Research* 67, 77-85.
- [304] Boiteux, V., Dauchy, X., Bach, C., Colin, A., Hemard, J., Sagres, V., Rosin, C., Munoz, J.F., **2017**. Concentrations and patterns of perfluoroalkyl and polyfluoroalkyl substances in a river and three drinking water treatment plants near and far from a major production source. *Science of The Total Environment* 583, 393-400.
- [305] Zhang, C., Hopkins, Z.R., McCord, J., Strynar, M.J., Knappe, D.R.U., **2019**. Fate of Per- and Polyfluoroalkyl Ether Acids in the Total Oxidizable Precursor Assay and Implications for the Analysis of Impacted Water. *Environmental Science & Technology Letters* 6 (11), 662-668.
- [306] Jin, H., Zhang, Y., Zhu, L., Martin, J.W., **2015**. Isomer Profiles of Perfluoroalkyl Substances in Water and Soil Surrounding a Chinese Fluorochemical Manufacturing Park. *Environmental Science & Technology* 49 (8), 4946-4954.
- [307] Shi, Y., Vestergren, R., Xu, L., Song, X., Niu, X., Zhang, C., Cai, Y., **2015**. Characterizing direct emissions of perfluoroalkyl substances from ongoing fluoropolymer production sources: A spatial trend study of Xiaoqing River, China. *Environmental Pollution* 206, 104-112.

- [308] Chen, H., Yao, Y., Zhao, Z., Wang, Y., Wang, Q., Ren, C., Wang, B., Sun, H., Alder, A.C., Kannan, K., **2018**. Multimedia Distribution and Transfer of Per- and Polyfluoroalkyl Substances (PFASs) Surrounding Two Fluorochemical Manufacturing Facilities in Fuxin, China. *Environmental Science & Technology* 52 (15), 8263-8271.
- [309] Schymanski, E., *et al.* **2015**. Non-target screening with high-resolution mass spectrometry: critical review using a collaborative trial on water analysis. *Analytical and Bioanalytical Chemistry* 407(21), 6237-6255.
- [310] Lindim, C., van Gils, J., Cousins, I.T., **2016**. Europe-wide estuarine export and surface water concentrations of PFOS and PFOA. *Water Research* 103, 124-132.
- [311] Bode, H., **1998**. Control of heavy metal emission from metal plating industry in a German river basin. *Water Science and Technology* 38 (4), 121-129.
- [312] Skutlarek, D., Exner M., Farber, H., **2006**. Perfluorinated surfactants in surface and drinking waters. *Environmental Science and Pollution Research Int.* 13 (5), 299-307.
- [313] Fromme, H., Wöckner, M., Roscher, E., Völkel, W., **2017**. ADONA and perfluoroalkylated substances in plasma samples of German blood donors living in South Germany. *International Journal of Hygiene and Environmental Health* 220 (2, Part B), 455-460.
- [314] Song, X., Vestergren, R., Shi, Y., Huang, J., Cai, Y., **2018**. Emissions, Transport, and Fate of Emerging Per- and Polyfluoroalkyl Substances from One of the Major Fluoropolymer Manufacturing Facilities in China. *Environmental Science & Technology* 52 (17), 9694-9703.
- [315] Bao, J., Liu, W., Liu, L., Jin, Y., Dai, J., Ran, X., Zhang, Z., Tsuda, S., **2011**. Perfluorinated Compounds in the Environment and the Blood of Residents Living near Fluorochemical Plants in Fuxin, China. *Environmental Science & Technology* 45(19), 8075-8080.
- [316] Martin, D., Munoz, G., Mejia-Avendaño, S., Duy, S.V., Yao, Y., Volchek, K., Brown, C.E., Liu, J., Sauv e, S., **2019**. Zwitterionic, cationic, and anionic perfluoroalkyl and polyfluoroalkyl substances integrated into total oxidizable precursor assay of contaminated groundwater. *Talanta* 195, 533-542.
- [317] Zhang, K., Cao, Z., Huang, J., Deng, S., Wang, B., Yu, G., **2016**. Mechanochemical destruction of Chinese PFOS alternative F-53B. *Chemical Engineering Journal* 286: 387-393.
- [318] Norwegian Environment Agency, **2017**. Sources of perfluorobutane sulfonic acid (PFBS) in the environment. Report M-759/2017. <https://www.miljodirektoratet.no/globalassets/publikasjoner/M759/M759.pdf> (accessed 19 April 2020).
- [319] Gobelius, L., Hedlund, J., D urig, W., Tr oger, R., Lilja, K., Wiberg, K., Ahrens, L., **2018**. Per- and Polyfluoroalkyl Substances in Swedish Groundwater and Surface Water: Implications for Environmental Quality Standards and Drinking Water Guidelines. *Environmental Science & Technology* 52 (7), 4340-4349.
- [320] Benskin, J. P., de Silva, A.O., Martin, J.W., **2010**. Isomer Profiling of Perfluorinated Substances as a Tool for Source Tracking: A Review of Early Findings and Future Applications. In: *Reviews of Environmental Contamination and Toxicology, Volume 208: Perfluorinated alkylated substances*. Springer, New York, 111-160.
- [321] Jiang, W., Zhang, Y., Yang, L., Chu, X., Zhu, L., **2015**. Perfluoroalkyl acids (PFAAs) with isomer analysis in the commercial PFOS and PFOA products in China. *Chemosphere* 127, 180-187.
- [322] Fang, S., Sha, B., Yin, H., Bian, Y., Yuan, B., Cousins, I.T., **2020**. Environment occurrence of perfluoroalkyl acids and associated human health risks near a major fluorochemical manufacturing park in southwest of China. *Journal of Hazardous Materials* 396, 122617.

- [323] Wang, T., Vestergren, R., Herzke, D., Yu, J., Cousins, I.T., **2016**. Levels, Isomer Profiles, and Estimated Riverine Mass Discharges of Perfluoroalkyl Acids and Fluorinated Alternatives at the Mouths of Chinese Rivers. *Environmental Science & Technology* 50 (21), 11584-11592.
- [324] Gago-Ferrero, P., Krettek, A., Fischer, S., Wiberg, K., Ahrens, L., **2018**. Suspect Screening and Regulatory Databases: A Powerful Combination To Identify Emerging Micropollutants. *Environmental Science & Technology* 52(12), 6881-6894.
- [325] Wrona, M., Mauriala, T., Bateman, K., Mrtishire-Smith, R., O'Connor, D., **2005**. 'All-in-One' analysis for metabolite identification using liquid chromatography/hybrid quadrupole time-of-flight mass spectrometry with collision energy switching. *Rapid Communications in Mass Spectrometry* 19(18), 2597-2602.
- [326] Sage, A., **2005**. Lockspray™: Automated Exact Mass Measurement for electrospray applications. Technical Note, *Waters Corporation*, Manchester, UK.
- [327] Holman, J.D., Tabb, D.L., Mallick, P., **2014**. Employing ProteoWizard to Convert Raw Mass Spectrometry Data. *Current Protocols in Bioinformatics* 46, 13.24.1-13.24.9.
- [328] Goshawk, J., Eatough, D., Wood, M., **2015**. Componentization Following 3D-Peak Detection in the Unifi Scientific Information System. *Waters Corporation*, Manchester, UK.
- [329] KEMI, Swedish Chemicals Agency, **2015**. Occurrence and use of highly fluorinated substances and alternatives. *Report from a government assignment 7/15 2015*, Stockholm.
- [330] Trier, X.; Sunderberg, D., **2015**. PFAS Suspect List: fluorinated substances. 2015. URL: <https://www.norman-network.com/?q=suspect-list-exchange> (accessed: 02 April 2020).
- [331] US EPA; United States Environmental Protection Agency, **2019**. PFAS Master List of PFAS Substances. 2019, URL: https://comptox.epa.gov/dashboard/chemical_lists/pfasmaster (accessed: 29 April 2019).
- [332] Sams, R., 2018. PFAS Tiered Testing Strategy. **2018**. URL: https://epa.figshare.com/articles/PFAS_Tiered_Testing_Strategy/7800800/1 (accessed: 30 April 2019).
- [333] McEachran, A.D., Mansouri, K., Grulke, C., Schymanski, E., Ruttkies, C., Williams, A.L., **2018**. "MS-Ready" structures for non-targeted high-resolution mass spectrometry screening studies. *Journal of Cheminformatics* 10 (1), 45.
- [334] Rosnack, K.J., Reid, M.J., Ladak, A., Cleland, G., **2016**. Screening Solution Using the Software Platform UNIFI: An Integrated Workflow by Waters. In: Assessing Transformation Products of Chemicals by Non-Target and Suspect Screening – Strategies and Workflows Volume 2, *ACS Symposium Series*, American Chemical Society: Washington DC, 155-172.
- [335] Barzen-Hanson, K.A., Roberts, S.C., Choyke, S., Oetjen, K., McAlees, A., Riddell, N., McCrindle, R., Ferguson, P.L., Higgins, C.P., Field, J., **2017**. Discovery of 40 Classes of Per- and Polyfluoroalkyl Substances in Historical Aqueous Film-Forming Foams (AFFFs) and AFFF-Impacted Groundwater. *Environmental Science & Technology* 51 (4), 2047-2057.
- [336] Kendrick, E., **1963**. A Mass Scale Based on CH₂ = 14.0000 for High Resolution Mass Spectrometry of Organic Compounds. *Analytical Chemistry* 35 (13), 2146-2154.
- [337] Myers, A.L., Jobst, K.J., Mabury, S.A., Reiner, E.J., **2014**. Using mass defect plots as a discovery tool to identify novel fluoropolymer thermal decomposition products. *Journal of Mass Spectrometry* 49 (4), 291-296.

- [338] Wang, Y., Yu, N., Zhu, X., Guo, H., Jiang, J., Wang, X., Shi, W., Wu, J., Yu, H., Wei, S., **2018**. Suspect and Nontarget Screening of Per- and Polyfluoroalkyl Substances in Wastewater from a Fluorochemical Manufacturing Park. *Environmental Science & Technology* 52 (19), 11007-11016.
- [339] Kaufmann, A., Butcher, P., Maden, K., Walker, S., Widmer, M., **2017**. Using In Silico Fragmentation to Improve Routine Residue Screening in Complex Matrices. *Journal of the American Society for Mass Spectrometry* 28 (12), 2705-2715.
- [340] Schymanski, E.L., Jeon, J., Gulde, R., Fenner, K., Ruff, M., Singer H., Hollender, J., **2014**. Identifying Small Molecules via High Resolution Mass Spectrometry: Communicating Confidence. *Environmental Science & Technology* 48 (4), 2097-2098.
- [341] Arsenault, G., McAlees, A., McCrindle, R., Riddell, N., **2007**. Analysis of perfluoroalkyl anion fragmentation pathways for perfluoroalkyl carboxylates and sulfonates during liquid chromatography/tandem mass spectrometry: evidence for fluorine migration prior to secondary and tertiary fragmentation. *Rapid Communications in Mass Spectrometry* 21 (23), 3803-3814.
- [342] Yu, N., Guo, H., Yang, J., Jin, L., Wang, X., Shi, W., Zhang, X., Yu, H., Si, W., **2018**. Non-Target and Suspect Screening of Per- and Polyfluoroalkyl Substances in Airborne Particulate Matter in China. *Environmental Science & Technology* 52 (15), 8205-8214.
- [343] Liu, Y., Pereira, A.D.S., Martin, J.W., **2015**. Discovery of C5–C17 Poly- and Perfluoroalkyl Substances in Water by In-Line SPE-HPLC-Orbitrap with In-Source Fragmentation Flagging. *Analytical Chemistry* 87 (8), 4260-4268.
- [344] Newton, S., McMahan, R., Stoeckel, J.A., Chislock, M., Lindstrom, A., Strynar, M., **2017**. Novel Polyfluorinated Compounds Identified Using High Resolution Mass Spectrometry Downstream of Manufacturing Facilities near Decatur, Alabama. *Environmental Science & Technology* 51 (3), 1544-1552.
- [345] Lyon, P.A., Tomer, K.B., Gross, M.L., **1985**. Fast atom bombardment and tandem mass spectrometry for characterizing fluoroalkanesulfonates. *Analytical Chemistry*, 57 (14), 2984-2989.
- [346] Strynar, M., Dagnino, S., McMahan, R., Liang, S., Lindstrom, A., Andersen, E., McMillan, L., Thurman, M., Ferrer, I., Ball, C., **2015**. Identification of Novel Perfluoroalkyl Ether Carboxylic Acids (PFECAs) and Sulfonic Acids (PFESAs) in Natural Waters Using Accurate Mass Time-of-Flight Mass Spectrometry (TOFMS). *Environmental Science & Technology* 49(19), 11622-11630.
- [347] Trier, X., Granby, K., Christensen, J.H., **2011**. Polyfluorinated surfactants (PFS) in paper and board coatings for food packaging. *Environmental Science and Pollution Research Int.* 18 (7), 1108-1120.
- [348] Trier, X., Christensen, J.H., Niessen, W.M.A., **2013**. Negative electrospray ionisation of fluorotelomer alcohols (FTOH) and FTOH-derived acrylate surfactants by liquid chromatography coupled to accurate (tandem) mass spectrometry. Poster presented at 39th *International Symposium on High-Performance-Liquid-Phase Separations and Related Techniques (HPLC2013)*, Amsterdam, Netherlands.
- [349] Elements for an EU-strategy for PFASs, **2019**. <https://www.regjeringen.no/contentassets-/1439a5cc9e82467385ea9f090f3c7bd7/fluor---eu-strategy-for-pfass---december-19.pdf> (accessed: 01 June 2020).
- [350] Anastas, P.T., Warner, J.C., **1998**. Green Chemistry, Theory and Practice. Oxford University Press, New York.

- [351] Greenpeace, **2017**. PFC Revolution in the Outdoor Sector. <https://www.greenpeace.org/international/publication/7150/pfc-revolution-in-outdoor-sector/> (accessed: 01 June 2020).
- [352] FluoroCouncil, **2020**. Fluorinated Chemistries are Integral to Modern Life. <https://fluoro-council.com/> (accessed: 01 June 2020).
- [353] von Appen, W.-J., Schaffer, J., Rohardt, G., Wisotzki, A., **2019**. Physical oceanography during POLARSTERN cruise PS114. *Alfred Wegener Institute, Helmholtz Centre for Polar and Marine Research*, Bremerhaven, PANGAEA, doi: 10.1594/PANGAEA.898694.
- [354] Fieg, K., Gerdes, R., Fahrbach, E., Beszczynska-Möller, A., Schauer, U., **2010**. Simulation of oceanic volume transports through Fram Strait 1995–2005. *Ocean Dynamics* 60 (3), 491–502.
- [355] de Steur, L., Hansen, E., Mauritzen, C., Beszczynska-Möller, A., Fahrbach, E., **2014**. Impact of recirculation on the East Greenland Current in Fram Strait: Results from moored current meter measurements between 1997 and 2009. *Deep Sea Research Part I: Oceanographic Research Papers* 92, 26–40.
- [356] Marnela, M., Rudels, B., Goszczko, I., Beszczynska-Möller, A., Schauer, U., **2016**. Fram Strait and Greenland Sea transports, water masses, and water mass transformations 1999–2010 (and beyond). *Journal of Geophysical Research: Oceans* 121 (4), 2314–2346.
- [357] von Appen, W.-J., Schauer, U., Somavilla, R., Bauerfeind, E., Beszczynska-Möller, A., **2015**. Exchange of warming deep waters across Fram Strait. *Deep Sea Research Part I: Oceanographic Research Papers* 103, 86–100.
- [358] Brandsma, S.H., Koekkoek, J.C., van Velzen, M.J.M., de Boer, J., **2019**. The PFOA substitute GenX detected in the environment near a fluoropolymer manufacturing plant in the Netherlands. *Chemosphere* 220, 493–500.
- [359] GESTIS-Stoffdatenbank. <http://gestis.itrust.de> (accessed: 12 June 2020).
- [360] ECHA, European Chemicals Agency. Classification and Labelling Inventory. <https://echa.europa.eu/de/information-on-chemicals/cl-inventory-database> (accessed: 12 June 2020).

A. Appendix A

A.1 Supplementary to Chapter 5

Table A.1-1: Sampling locations of water and sediment samples analysed in this study and physicochemical parameters measured in the water phase.

station ID	latitude °N	longitude °E	date time of sampling	sample type ¹	water depth [m]	temperature [°C]	pH	salinity [PSU]	
German Bight (<i>Ludwig Prandtl</i> cruise LP1706 (GB1–GB30) and <i>Maria S. Merian</i> cruise MSM50 (GB31–GB34))									
GB1	53.957	8.560	09.06.2017 04:22	w	6	15.8	8.2	26.9	
GB2	53.967	8.491	09.06.2017 04:45	w	-	15.8	8.1	27.8	
GB3	53.987	8.306	09.06.2017 05:21	w	4	15.5	8.2	30.3	
GB4	53.886	7.980	09.06.2017 06:53	w	-	14.9	8.3	32.2	
GB5	53.840	7.723	09.06.2017 08:13	w, s	14	15.6	8.1	31.6	
GB6	53.812	7.489	09.06.2017 09:25	w	-	17.9	8.1	31.6	
GB7	53.745	7.126	09.06.2017 10:53	w, s	12	16.2	8.1	32.2	
GB8	53.745	7.204	10.06.2017 08:10	w	7	16.0	8.1	31.3	
GB9	53.833	7.213	10.06.2017 08:48	w	22	15.7	8.2	32.1	
GB10	53.974	7.141	10.06.2017 10:18	w	30	14.8	8.2	33.0	
GB11	54.053	7.151	10.06.2017 10:56	w, s	34	14.6	8.2	33.2	
GB12	54.102	7.405	10.06.2017 11:59	w	-	14.4	8.2	33.2	
GB13	54.158	7.643	10.06.2017 12:56	w	-	13.5	8.2	33.1	
GB14	54.222	7.806	10.06.2017 13:39	w, s	28	14.0	8.2	32.3	
GB15	54.207	7.856	10.06.2017 14:05	w	20	13.6	8.2	32.4	
GB16	54.194	7.882	10.06.2017 14:17	w	10	13.5	8.2	32.4	
GB17	54.159	7.918	11.06.2017 07:21	w	15	13.8	8.2	32.1	
GB18	54.162	8.115	11.06.2017 08:13	w	20	14.4	8.2	32.2	
GB19	54.173	8.303	11.06.2017 08:58	w	16	15.4	8.3	30.5	
GB20	54.179	8.497	11.06.2017 09:43	w	9	15.9	8.2	29.3	
GB21	54.149	8.710	11.06.2017 10:34	w	-	16.9	8.3	27.4	
GB22	54.138	8.733	11.06.2017 10:44	w	7	16.9	8.2	27.1	
GB23	54.127	8.799	11.06.2017 11:03	w	-	17.1	8.2	26.4	
GB24	54.116	8.850	11.06.2017 11:14	w	5	16.9	8.2	26.3	
GB25	54.115	8.684	12.06.2017 06:50	w	5	17.1	8.2	27.0	
GB26	54.096	8.591	12.06.2017 07:18	w	8	16.9	8.2	27.3	
GB27	54.094	8.536	12.06.2017 07:40	w	10	16.4	8.2	28.2	
GB28	54.011	8.532	12.06.2017 08:55	w	9	16.5	8.2	27.4	
GB29	53.956	8.663	12.06.2017 09:34	s	7	17.2	8.1	21.1	
GB30	54.063	8.015	06.01.2016 20:44	s	23	-	-	33.6	
GB31	54.462	6.275	07.01.2016 07:47	s	34	-	-	35.2	
GB32	54.885	5.644	08.01.2016 06:05	s	37	-	-	34.7	
GB33	55.532	4.166	09.01.2016 05:42	s	33	-	-	34.6	
Elbe estuary (<i>Ludwig Prandtl</i> cruise LP1706)									
E1	53.448	10.089	06.06.2017 06:06	w	-	-	-	-	
E2	53.538	10.003	06.06.2017 08:28	w	-	21.0	8.2	-	
E3	53.544	9.948	06.06.2017 08:59	s	-	21.1	7.8	-	
E4	53.547	9.877	06.06.2017 09:26	w	-	21.2	7.4	-	
E5	53.554	9.813	06.06.2017 09:51	w	-	21.2	7.3	0.5	
E6	53.564	9.731	06.06.2017 10:20	w	-	20.9	7.4	0.5	
E7	53.590	9.600	06.06.2017 11:00	w	-	21.0	7.5	-	
E8	53.737	9.439	06.06.2017 12:17	w	-	19.8	7.8	0.6	
E9	53.815	9.374	06.06.2017 13:00	w	-	20.0	7.7	1.6	
E10	53.820	9.378	12.06.2017 12:34	w, s	6	19.1	7.8	1.1	
E11	53.874	9.270	06.06.2017 13:30	w	-	18.9	7.8	3.2	
E12	53.869	9.250	12.06.2017 12:05	w	8	18.5	7.8	3.0	
E13	53.882	9.077	06.06.2017 14:08	w	-	18.6	7.8	5.3	
E14	53.844	8.970	12.06.2017 11:06	w, s	7	17.9	7.9	7.8	

E15	53.846	8.890	06.06.2017	14:48	w	-	18.8	7.9	9.9
E16	53.844	8.819	06.06.2017	15:02	w	-	18.2	8.0	13.3
E17	53.867	8.736	06.06.2017	15:19	w	-	18.0	8.0	15.6
E18	53.876	8.708	09.06.2017	03:47	w	-	17.6	8.0	17.8
Skagerrak/Kattegat (<i>Maria S. Merian</i> cruise MSM50)									
SK1	57.418	8.452	10.01.2016	04:50	s	53.6	-	-	35
SK2	58.133	9.892	12.01.2016	13:50	s	336.3	-	-	35
SK3	57.967	10.782	13.01.2016	11:37	s	187.0	-	-	35
SK4	57.293	11.491	15.01.2016	05:26	s	77.9	-	-	35
German Baltic Sea (<i>Maria S. Merian</i> cruise MSM50 (BS1) and <i>Ludwig Prandtl</i> cruise LP1709 (BS2–BS45))									
BS1	54.885	13.855	23.01.2016	09:11	s	47.5	-	-	19
BS2	54.156	13.592	04.09.2017	12:00	w	-	18.8	8.1	7.7
BS3	54.180	13.731	04.09.2017	11:06	w	4	18.4	8.1	7.5
BS4	54.200	13.856	04.09.2017	10:26	w	7	18.2	8.1	7.8
BS5	54.133	13.467	04.09.2017	12:49	w	-	18.7	8.2	7.9
BS6	54.226	13.322	04.09.2017	14:01	w	4	19.2	8.2	8.1
BS7	54.282	13.129	04.09.2017	15:08	w, s	5	19.4	8.2	8.5
BS8	54.364	13.106	05.09.2017	08:48	w	6	18.5	8.2	8.8
BS9	54.411	13.073	05.09.2017	09:22	w	5	18.1	8.2	9.1
BS10	54.478	13.057	05.09.2017	10:03	w	4	18.0	8.1	8.9
BS11	54.517	12.795	05.09.2017	11:18	w	-	18.7	8.1	9.1
BS12	54.532	12.530	05.09.2017	12:17	w	-	18.6	8.2	9.0
BS13	54.413	12.379	05.09.2017	13:17	w	11	19.0	8.2	9.8
BS14	54.198	12.117	05.09.2017	15:00	w	-	19.4	8.2	10.5
BS15	54.166	11.769	06.09.2017	11:37	w	11	18.7	8.2	10.8
BS16	54.048	11.482	06.09.2017	13:12	w	4	18.3	8.2	11.0
BS17	54.029	11.277	07.09.2017	09:50	w	11	18.7	8.3	11.6
BS18	53.950	11.363	06.09.2017	15:03	w	4	19.6	8.3	11.7
BS19	53.929	11.425	06.09.2017	15:52	w	4	19.8	8.3	11.3
BS20	53.958	11.430	06.09.2017	15:26	w	4	19.6	8.4	11.3
BS21	53.956	11.283	06.09.2017	14:25	w	10	19.7	8.4	11.7
BS22	54.075	11.140	07.09.2017	10:34	w, s	21	18.5	8.3	12.1
BS23	54.141	11.075	07.09.2017	11:21	w	20	18.2	8.2	12.1
BS24	54.080	10.815	07.09.2017	12:37	w	6	17.8	7.9	14.3
BS25	54.030	10.829	07.09.2017	13:10	w	17	18.5	8.3	12.3
BS26	53.988	10.921	07.09.2017	13:45	w	18	18.5	8.3	11.9
BS27	54.391	11.193	08.09.2017	11:38	w	-	18.1	8.2	12.0
BS28	54.412	10.979	08.09.2017	12:45	w	11	18.4	8.2	13.9
BS29	54.412	10.482	08.09.2017	15:08	w	-	18.2	8.2	14.7
BS30	54.449	10.305	08.09.2017	15:56	w	5	17.9	8.2	15.2
BS31	54.328	10.153	08.09.2017	17:18	w	16	17.9	7.8	16.3
BS32	54.346	10.163	08.09.2017	17:05	w	12	18.1	8.0	16.1
BS33	54.435	10.187	09.09.2017	09:37	w	17	17.7	8.1	15.9
BS34	54.534	10.236	09.09.2017	10:27	w	15	17.9	8.2	14.9
BS35	54.612	10.371	09.09.2017	11:13	w	20	17.9	8.2	15.2
BS36	54.682	10.501	09.09.2017	11:58	w, s	25	18.0	8.2	15.4
BS37	54.519	10.082	09.09.2017	14:00	w	15	17.9	8.2	15.1
BS38	54.465	9.871	09.09.2017	15:00	w	21	17.2	8.1	16.8
BS39	54.637	10.073	10.09.2017	10:26	w	13	17.4	8.2	16.0
BS40	54.830	9.909	10.09.2017	12:30	w	25	17.6	8.2	17.1
BS41	54.823	9.720	10.09.2017	13:20	w	21	17.5	8.2	17.7
BS42	54.887	9.610	10.09.2017	14:05	w, s	10	17.8	8.2	17.8
BS43	54.831	9.452	10.09.2017	15:10	w	16	17.7	8.2	18.0
Oder Lagoon, Peene and Warnow (land-based sampling)									
OL1	53.643	14.544	05.09.2017	16:30	w, s	1	18.4	7.8	0.4
OL2	53.738	14.272	05.09.2017	14:05	w, s	3	17.5	8.7	1.4
OL3	53.847	13.820	05.09.2017	11:25	w, s	2	17.8	8.8	1.1
P1	53.859	13.685	05.09.2017	10:05	w	-	18.2	7.8	0.3
W1	54.102	12.103	05.09.2017	15:55	w	-	20.1	8.9	5.8

¹ “w” stands for a water sample and “s” for a sediment sample taken at the respective locations.

Table A.1-2: Total organic carbon (TOC) content of the sediment samples analysed in this study.

station ID	TOC [%]
GB5	0.01
GB7	2.01
GB11	0.12
GB14	0.43
GB29	0.25
GB30	0.60
GB31	0.10
GB32	0.04
GB33	0.03
E3	1.28
E10	6.00
E14	0.82
SK1	0.03
SK2	1.90
SK3	1.45
SK4	1.72
BS1	4.86
BS7	6.13
BS22	4.57
BS36	2.43
BS42	3.26
OL1	0.52
OL2	0.24
OL3	1.37

Table A.1-3: Mean concentrations of PFASs in procedural blanks \pm standard deviation (SD), method detection limits (MDLs) and method quantification limits (MQLs).

matrix campaign ¹ unit	mean levels in laboratory blanks \pm SD			MDLs and MQLs ³					
	ultrapure water (1 L)		purified seasand (5 g)	water samples (1 L)		sediment samples (5 g)			
	North Sea (<i>n</i> =9)	Baltic Sea (<i>n</i> =7)	North and Baltic Sea (<i>n</i> =6)	North Sea		Baltic Sea		North and Baltic Sea	
	[ng/L]		[ng/g dw]	[ng/L]		[ng/g dw]			
			MDL	MQL	MDL	MQL	MDL	MQL	
PFBA	0.078 \pm 0.027	0.030 \pm 0.015	0.019 \pm 0.004	0.16	0.35	0.077	0.19	0.029	0.054
PFPeA	0.010 \pm 0.011	0.013 \pm 0.013	nd	0.042	0.12	0.051	0.14	0.0064	0.021
PFHxA	0.038 \pm 0.006	nd	0.014 \pm 0.008	0.055	0.095	0.043	0.14	0.037	0.090
PFHpA	nd ²	nd	0.0065 \pm 0.0015	0.024	0.079	0.039	0.13	0.011	0.022
PFOA	0.061 \pm 0.016	0.027 \pm 0.007	0.055 \pm 0.004	0.11	0.22	0.048	0.095	0.067	0.095
PFNA	0.028 \pm 0.012	0.020 \pm 0.004	0.012 \pm 0.001	0.063	0.14	0.033	0.063	0.015	0.023
PFDA	0.021 \pm 0.007	0.015 \pm 0.003	nd	0.041	0.087	0.024	0.046	0.0033	0.011
PFUnDA	0.013 \pm 0.005	0.012 \pm 0.004	nd	0.028	0.063	0.024	0.050	0.0028	0.0094
PFDoDA	nd	nd	nd	0.017	0.057	0.017	0.057	0.0033	0.011
PFTTrDA	nd	nd	nd	0.0046	0.015	0.0046	0.015	0.0028	0.0094
PFTeDA	nd	nd	nd	0.0088	0.029	0.0088	0.029	0.0032	0.011
PFBS	nd	nd	nd	0.045	0.15	0.052	0.17	0.011	0.037
PFHxS	nd	nd	nd	0.073	0.24	0.10	0.34	0.036	0.12
PFHpS	nd	nd	nd	0.027	0.090	0.027	0.090	0.064	0.21
L-PFOS	nd	0.0060 \pm 0.0031	nd	0.0057	0.019	0.015	0.036	0.012	0.040
Br-PFOS	nd	nd	nd	0.0062	0.021	0.0058	0.019	0.0093	0.031
PFDS	nd	nd	nd	0.032	0.093	0.032	0.093	0.056	0.19
PFECHS	nd	nd	nd	0.043	0.14	0.038	0.13	0.042	0.14
HFPO-DA	nd	nd	nd	0.044	0.15	0.018	0.059	0.0049	0.016
HFPO-TrA	nd	nd	nd	0.044	0.15	0.044	0.15	0.10	0.34
HFPO-TeA	nd	nd	nd	0.075	0.25	0.075	0.25	0.15	0.49
DONA	nd	nd	nd	0.0075	0.025	0.0075	0.025	0.0046	0.015

6:2 Cl-PFESA	nd	nd	nd	0.0069	0.023	0.0069	0.023	0.0019	0.0065
8:2 Cl-PFESA	nd	nd	nd	0.0068	0.023	0.0068	0.023	0.0075	0.025
6:6 PFPiA	nd	nd	nd	0.0049	0.016	0.0049	0.016	0.0031	0.010
6:8 PFPiA	nd	nd	nd	0.0087	0.029	0.0087	0.029	0.0039	0.013
L-FOSA	nd	nd	nd	0.0036	0.012	0.0022	0.0074	0.0027	0.0091
Br-FOSA	nd	nd	nd	0.0043	0.014	0.0021	0.0069	0.0026	0.0086
4:2 FTSA	nd	nd	nd	0.030	0.10	0.030	0.10	0.066	0.22
6:2 FTSA	0.025 ± 0.012	0.19 ± 0.03	0.053 ± 0.024	0.061	0.15	0.28	0.48	0.13	0.30
8:2 FTSA	nd	nd	nd	0.036	0.12	0.036	0.12	0.054	0.18

¹ Water samples from the North Sea and Baltic Sea were processed at different points in time, within 4 weeks after each campaign. Consequently, campaign specific blank values, MDLs and MQLs were calculated. All sediment samples were stored at -20°C and processed together after the second sampling campaign.

² nd = not detected

³ For compounds, which were present in blanks, MDLs and MQLs were calculated as the average blank value plus 3 or 10 times the standard deviation, respectively (marked in blue). For PFASs other than these, the MDLs and MQLs were derived from a signal-to-noise ratio of 3 or 10, respectively, observed in low level samples (green) or spiked matrix samples (yellow).

Table A.1-4: Percentage absolute recoveries of internal standards in analysed surface water samples ($n = 92$) and sediment samples ($n = 24$).

internal standard	mean absolute recovery \pm SD	
	[%]	
	water	sediment
$^{13}\text{C}_4$ -PFBA	40 \pm 16	56 \pm 13
$^{13}\text{C}_2$ -PFHxA	52 \pm 14	63 \pm 10
$^{13}\text{C}_4$ -PFOA	62 \pm 13	70 \pm 6
$^{13}\text{C}_5$ -PFNA	64 \pm 10	67 \pm 9
$^{13}\text{C}_2$ -PFDA	49 \pm 15	61 \pm 10
$^{13}\text{C}_2$ -PFUnDA	55 \pm 27	46 \pm 12
$^{13}\text{C}_2$ -PFDoDA	50 \pm 34	42 \pm 13
$^{13}\text{C}_3$ -PFBS	49 \pm 10	75 \pm 9
$^{18}\text{O}_2$ -PFHxS	67 \pm 13	77 \pm 11
$^{13}\text{C}_4$ -PFOS	72 \pm 13	66 \pm 7
$^{13}\text{C}_3$ -HFPO-DA	40 \pm 10	55 \pm 10
$^{13}\text{C}_8$ -FOSA	24 \pm 23	23 \pm 6
$^{13}\text{C}_2$ -6:2 FTSA	133 \pm 30	125 \pm 43

Table A.1-5: Coefficients of variation [%] for quantified PFASs, calculated from triplicate analysis of water samples ($n = 7$) and duplicate analysis of sediment samples ($n = 3$).

analyte	CV [%]										mean
	water							sediment			
	GB6	GB12	GB21	GB29	E4	BS15	BS39	GB7	GB30	SK4	
PFBA	8	5	7	-	7	3	7	12	-	2	7
PFPeA	3	7	8	5	5	-	-	-	-	-	5
PFHxA	17	12	7	5	14	7	3	-	-	-	9
PFHpA	2	2	6	6	10	3	11	8	-	-	6
PFOA	10	14	5	4	7	1	4	2	-	1	5
PFNA	-	-	-	-	13	14	2	4	-	2	7
PFDA	-	-	-	-	12	-	-	3	1	4	5
PFUnDA	-	-	-	-	-	-	-	5	2	2	3
PFDoDA	-	-	-	-	-	-	-	2	4	3	3
PFTTrDA	-	-	-	-	-	-	-	1	11	4	5
PFTeDA	-	-	-	-	-	-	-	-	-	10	10
PFBS	3	2	6	8	6	4	19	-	-	-	7
PFHxS	9	4	3	8	14	-	-	-	-	-	7
L-PFOS	16	8	8	9	3	6	-	2	7	1	7
Br-PFOS	10	2	11	7	8	6	14	-	-	-	8
HFPO-DA	7	4	6	3	-	-	-	-	-	-	5
6:6 PFPiA	-	-	-	-	-	-	-	4	-	-	4
L-FOSA	-	-	-	-	-	-	-	8	3	5	5
Br-FOSA	-	-	-	-	-	-	-	-	4	2	3
6:2 FTS	-	-	-	12	5	-	-	-	-	-	9

Table A.1-6: Detection frequencies, concentration ranges [ng/L], mean concentrations [ng/L] and median values [ng/L] of detected PFASs in surface water from the German Bight, the Elbe River, the German Baltic Sea and the Oder Lagoon. Values in brackets are between MDL and MQL.

compound	German Bight (<i>n</i> = 28)				Elbe River (<i>n</i> = 17)				Baltic Sea (<i>n</i> = 42)				Oder Lagoon (<i>n</i> = 3)			
	DF [%]	range [ng/L]	mean [ng/L]	median [ng/L]	DF [%]	range [ng/L]	mean [ng/L]	median [ng/L]	DF [%]	range [ng/L]	mean [ng/L]	median [ng/L]	DF [%]	range [ng/L]	mean [ng/L]	median [ng/L]
HFPO-DA	100	0.92–2.5	1.6	1.7	100	(0.070)–1.5	0.40	0.18	100	(0.032)–0.082	(0.051)	(0.049)	100	(0.028)–(0.037)	(0.034)	(0.036)
PFECHS	0	<MDL	-	-	6	(0.060)	-	-	86	<MDL–0.14	(0.064)	(0.069)	0	<MDL	-	-
PFBA	100	1.1–2.2	1.5	1.5	100	1.2–1.9	1.5	1.5	100	0.33–0.99	0.49	0.46	100	2.0–3.2	2.5	2.2
PFPeA	100	0.27–0.64	0.40	0.39	100	0.65–1.7	1.1	1.2	100	(0.10)–0.75	0.16	(0.13)	100	0.79–1.1	0.89	0.80
PFHxA	100	0.47–1.3	0.84	0.84	100	1.5–4.6	3.1	2.9	100	0.22–0.84	0.32	0.26	100	1.5–2.6	2.0	1.8
PFHpA	100	0.17–0.45	0.28	0.27	100	0.48–1.2	0.88	0.83	100	(0.13)–0.38	0.20	0.17	100	0.71–0.90	0.81	0.81
PFOA	100	0.27–0.71	0.50	0.51	100	0.87–2.1	1.4	1.4	100	0.20–0.70	0.32	0.27	100	0.79–1.1	1.1	1.0
PFNA	39	<MDL–(0.10)	-	-	100	(0.14)–0.41	0.26	0.25	100	(0.053)–0.21	0.10	0.090	100	0.17–0.30	0.25	0.28
PFDA	4	<MDL–(0.047)	-	-	100	(0.053)–0.27	0.14	0.13	5	<MDL–0.047	-	-	100	(0.034)–0.048	(0.043)	0.048
PFUnDA	0	<MDL	-	-	6	<MDL–0.068	-	-	0	<MDL	-	-	0	-	-	-
PFBS	100	0.44–0.72	0.55	0.53	100	0.43–0.99	0.75	0.73	100	(0.15)–0.43	0.25	0.24	100	0.87–1.1	0.95	0.88
PFHxS	100	(0.12)–0.23	(0.16)	(0.16)	100	(0.22)–0.49	0.32	0.31	95	<MDL–0.48	(0.25)	(0.23)	100	0.42–0.50	0.46	0.47
L-PFOS	100	0.020–0.077	0.044	0.043	100	0.10–0.33	0.20	0.20	100	(0.018)–0.082	0.043	0.040	100	0.10–0.12	0.11	0.12
Br-PFOS	100	0.021–0.080	0.039	0.035	100	0.062–0.28	0.17	0.17	100	0.029–0.098	0.050	0.050	100	0.089–0.14	0.12	0.11
6:2 FTSA	3	<MDL–(0.13)	-	-	100	(0.083)–0.35	0.20	0.19	7	<MDL–0.93	-	-	0	-	-	-
L-FOSA	18	<MDL–0.018	-	-	65	<MDL–0.018	(0.0068)	(0.0072)	17	<MDL–(0.0064)	-	-	67	<MDL–(0.0036)	(0.0020)	-
Br-FOSA	25	<MDL–0.024	-	-	76	<MDL–0.024	(0.0097)	(0.012)	12	<MDL–(0.0064)	-	-	100	(0.0023)–(0.0043)	(0.0034)	-
ΣPFASs	-	4.7–7.4	6.0	6.2	-	8.5–14	10	10	-	1.6–5.2	2.3	2.1	-	7.9–9.8	9.1	9.6

Table A.1-7: Detection frequencies, concentration ranges [ng/g dw], mean concentrations [ng/g dw] and median values [ng/g dw] of detected PFASs in surface sediment from the entire study area, the German Bight, and the Elbe estuary. Values in brackets are between MDL and MQL.

compound	entire study area (<i>n</i> = 24)				German Bight (<i>n</i> = 9)				Elbe estuary (<i>n</i> = 3)			
	DF [%]	range [ng/g dw]	mean [ng/g dw]	median [ng/g dw]	DF [%]	range [ng/g dw]	mean [ng/g dw]	median [ng/g dw]	DF [%]	range [ng/g dw]	mean [ng/g dw]	median [ng/g dw]
6:6 PFPiA	8	<MDL–(0.0054)	-	-	0	<MDL	-	-	33	<MDL–(0.0054)	-	-
6:8 PFPiA	25	<MDL–0.052	-	-	22	<MDL–0.014	-	-	33	<MDL–0.052	-	-
PFBA	67	<MDL–0.54	0.11	0.10	44	<MDL–0.54	-	-	67	<MDL–0.30	0.13	0.079
PFHxA	8	<MDL–(0.057)	-	-	11	<MDL–(0.057)	-	-	33	<MDL–(0.044)	-	-
PFHpA	25	<MDL–0.12	-	-	11	<MDL–0.12	-	-	67	<MDL–(0.018)	(0.011)	(0.011)
PFOA	42	<MDL–0.65	-	-	11	<MDL–0.65	-	-	33	<MDL–(0.084)	-	-
PFNA	71	<MDL–0.28	0.056	(0.021)	67	<MDL–0.21	0.034	(0.016)	67	<MDL–0.051	0.023	(0.018)
PFDA	100	(0.0062)–0.30	0.072	0.049	100	(0.0062)–0.30	0.060	0.038	100	(0.0077)–0.21	0.092	0.060
PFUnDA	100	(0.0052)–0.27	0.074	0.036	100	(0.0060)–0.14	0.037	0.017	100	(0.0076)–0.17	0.070	0.024
PFDoDA	96	<MDL–0.143	0.024	0.013	89	<MDL–0.039	0.012	0.0078	100	(0.0059)–0.14	0.053	0.011
PFTTrDA	100	(0.0051)–0.10	0.027	0.014	100	(0.0059)–0.032	0.013	(0.0083)	100	(0.0058)–0.068	0.027	(0.0084)
PFTeDA	67	<MDL–0.036	(0.0067)	(0.0042)	56	<MDL–(0.0078)	<MDL	(0.0039)	67	<MDL–0.036	0.013	(0.0037)
PFHxS	4	<MDL–0.16	-	-	0	<MDL	-	-	33	<MDL–0.16	-	-
L-PFOS	83	<MDL–0.39	0.13	0.085	78	<MDL–0.39	0.090	(0.029)	67	<MDL–0.37	0.15	0.089
Br-PFOS	17	<MDL–(0.029)	-	-	22	<MDL–(0.017)	-	-	33	<MDL–(0.029)	-	-
6:2 FTSA	4	<MDL–0.40	-	-	0	<MDL	-	-	33	<MDL–0.40	-	-
L-FOSA	75	<MDL–0.045	0.016	0.014	67	<MDL–0.039	0.015	(0.0047)	100	(0.0029)–0.045	0.022	0.018
Br-FOSA	63	<MDL–0.033	0.0094	(0.0060)	44	<MDL–0.018	-	-	67	<MDL–0.012	(0.0066)	(0.0073)
ΣPFASs	-	0.018–2.6	0.64	0.36	-	0.018–2.6	0.43	0.12	-	0.030–2.2	0.85	0.34
TOC	-	0.01–6.1	1.7	1.1	-	0.01–2.0	0.40	0.12	-	0.82–6.0	2.7	1.3

Table A.1-8: Detection frequencies, concentration ranges [ng/g dw], mean concentrations [ng/g dw] and median values [ng/g dw] of detected PFASs in surface sediment from the Kattegat/Skagerrak, the Baltic Sea and the Oder Lagoon. Values in brackets are between MDL and MQL.

compound	Skagerrak/Kattegat (<i>n</i> = 4)				Baltic Sea (<i>n</i> = 5)				Oder Lagoon (<i>n</i> = 3)			
	DF [%]	range [ng/g dw]	mean [ng/g dw]	median [ng/g dw]	DF [%]	range [ng/g dw]	mean [ng/g dw]	median [ng/g dw]	DF [%]	range [ng/g dw]	mean [ng/g dw]	median [ng/g dw]
6:6 PFPiA	0	<MDL	-	-	20	<MDL–0.050	-	-	0	<MDL	-	-
6:8 PFPiA	25	<MDL–(0.012)	-	-	40	<MDL–0.049	-	-	0	<MDL	-	-
PFBA	75	<MDL–0.12	0.078	0.099	100	0.13–0.22	0.16	0.14	67	<MDL–0.23	0.12	0.14
PFHxA	0	<MDL	-	-	0	<MDL	-	-	0	<MDL	-	-
PFHpA	50	<MDL–(0.016)	-	-	20	<MDL–0.050	-	-	0	<MDL	-	-
PFOA	75	<MDL–0.15	(0.084)	(0.092)	100	(0.067)–0.39	0.13	(0.073)	0	<MDL	-	-
PFNA	75	<MDL–0.16	0.084	0.088	100	0.034–0.28	0.12	0.048	33	<MDL–0.048	-	-
PFDA	100	(0.0063)–0.17	0.10	0.11	100	0.021–0.20	0.076	0.050	100	0.016–0.083	0.040	0.020
PFUnDA	100	(0.0052)–0.25	0.16	0.18	100	0.030–0.27	0.10	0.069	100	0.013–0.063	0.036	0.032
PFDoDA	100	(0.0035)–0.043	0.029	0.035	100	(0.0083)–0.063	0.029	0.019	100	(0.0046)–0.020	0.012	0.011
PFTrDA	100	(0.0051)–0.071	0.047	0.056	100	0.014–0.10	0.043	0.030	100	(0.0059)–0.022	0.013	0.011
PFTeDA	75	<MDL–0.12	(0.0077)	(0.0092)	80	<MDL–0.022	0.011	(0.0063)	67	<MDL–0.0064	(0.0033)	(0.0035)
PFHxS	0	<MDL	-	-	0	<MDL	-	-	0	<MDL	-	-
L-PFOS	75	<MDL–0.38	0.21	0.23	100	0.074–0.38	0.17	0.15	100	0.014–0.16	0.066	0.024
Br-PFOS	0	<MDL	-	-	20	<MDL–(0.014)	-	-	0	<MDL	-	-
6:2 FTSA	0	<MDL	-	-	0	<MDL	-	-	0	<MDL	-	-
L-FOSA	75	<MDL–0.031	0.018	0.020	80	<MDL–0.035	0.023	0.025	67	<MDL–(0.0056)	(0.0031)	(0.0036)
Br-FOSA	75	<MDL–0.033	0.017	0.017	100	(0.0031)–0.032	0.019	0.017	33	<MDL–(0.0029)	-	-
ΣPFASs	-	0.020–1.3	0.84	1.0	-	0.36–1.6	0.90	0.72	-	0.095–0.64	0.31	0.20
TOC	-	0.03–1.9	1.3	1.6	-	2.4–6.1	4.3	4.6	-	0.2–1.4	0.71	0.52

Table A.1-9: Concentrations [ng/L] of detected PFASs in surface seawater samples from the German Bight (GB1-GB14). Values in brackets are between MDL and MQL.

station ID	GB1	GB2	GB3	GB4	GB5	GB6	GB7	GB8	GB9	GB10	GB11	GB12	GB13	GB14
HFPO-DA	2.5	1.8	1.8	1.7	2.0	1.7±0.12	1.3	1.3	1.4	0.94	0.92	1.2±0.0	1.5	1.6
PFECHS	<MDL	<MDL	<MDL	<MDL	<MDL	<MDL	<MDL	<MDL	<MDL	<MDL	<MDL	<MDL	<MDL	<MDL
PFBA	1.2	1.1	1.1	1.5	1.5	1.8±0.2	1.5	1.6	1.8	1.6	1.6	1.7±0.1	1.6	1.2
PFPeA	0.50	0.53	0.35	0.28	0.35	0.39±0.01	0.39	0.45	0.43	0.30	0.29	0.28±0.02	0.28	0.31
PFHxA	1.2	1.0	1.2	0.99	0.81	0.89±0.15	0.84	0.76	0.68	0.63	0.61	0.61±0.08	0.65	0.52
PFHpA	0.34	0.33	0.30	0.22	0.26	0.24±0.01	0.23	0.30	0.20	0.22	0.18	0.18±0.00	0.17	0.17
PFOA	0.68	0.66	0.64	0.41	0.50	0.50±0.05	0.45	0.52	0.39	0.35	0.32	0.27±0.04	0.28	0.34
PFNA	(0.078)	(0.078)	(0.077)	<MDL	<MDL	<MDL	<MDL	<MDL	<MDL	<MDL	<MDL	<MDL	<MDL	<MDL
PFDA	<MDL	<MDL	<MDL	<MDL	<MDL	<MDL	<MDL	<MDL	<MDL	<MDL	<MDL	<MDL	<MDL	<MDL
PFUnDA	<MDL	<MDL	<MDL	<MDL	<MDL	<MDL	<MDL	<MDL	<MDL	<MDL	<MDL	<MDL	<MDL	<MDL
PFBS	0.62	0.59	0.55	0.53	0.65	0.72±0.02	0.63	0.69	0.66	0.54	0.48	0.53±0.01	0.44	0.45
PFHxS	(0.19)	(0.23)	(0.18)	(0.14)	(0.15)	(0.19±0.02)	(0.16)	(0.21)	(0.13)	(0.14)	(0.13)	(0.11±0.00)	(0.12)	(0.13)
L-PFOS	0.067	0.062	0.053	0.026	0.038	0.040±0.006	0.054	0.047	0.036	0.030	0.031	0.025±0.002	0.020	0.023
Br-PFOS	0.034	0.040	0.034	0.023	0.027	0.028±0.003	0.033	0.036	0.026	0.024	0.021	0.022±0.001	0.021	0.024
6:2 FTSA	(0.11)	(0.13)	(0.063)	<MDL	<MDL	<MDL	<MDL	<MDL	<MDL	(0.063)	(0.080)	(0.067±0.009)	(0.069)	<MDL
L-FOSA	(0.011)	(0.011)	(0.011)	(0.010)	(0.0079)	<MDL	<MDL	<MDL	<MDL	<MDL	<MDL	<MDL	<MDL	<MDL
Br-FOSA	(0.013)	(0.011)	(0.012)	(0.010)	(0.012)	<MDL	<MDL	<MDL	<MDL	<MDL	<MDL	<MDL	<MDL	<MDL

Table A.1-10: Concentrations [ng/L] of detected PFASs in surface seawater samples from the German Bight (GB15–GB29). Values in brackets are between MDL and MQL.

station ID	GB15	GB17	GB18	GB19	GB20	GB21	GB22	GB23	GB24	GB25	GB26	GB27	GB28	GB29
HFPO-DA	1.7	1.6	2.0	1.7	2.1	1.8±0.1	1.4	1.6	1.8	1.8	1.9	1.7	1.9	1.4±0.04
PFECHS	<MDL	<MDL	<MDL	<MDL	<MDL	< MDL	<MDL	<MDL	<MDL	<MDL	<MDL	<MDL	<MDL	< MDL
PFBA	1.3	1.3	1.1	1.4	2.2	1.9±0.1	1.6	1.4	1.5	1.6	1.5	1.6	1.5	1.2±0.1
PFPeA	0.29	0.32	0.27	0.33	0.40	0.48±0.04	0.48	0.48	0.50	0.46	0.48	0.39	0.47	0.64±0.03
PFHxA	0.47	0.65	0.59	0.83	0.83	0.91±0.06	0.99	0.94	0.96	1.0	0.98	0.77	0.96	1.3±0.1
PFHpA	0.19	0.22	0.19	0.25	0.30	0.35±0.02	0.35	0.39	0.39	0.34	0.33	0.29	0.34	0.45±0.03
PFOA	0.30	0.45	0.35	0.47	0.59	0.57±0.03	0.65	0.64	0.63	0.62	0.57	0.51	0.58	0.71±0.03
PFNA	<MDL	<MDL	<MDL	<MDL	(0.068)	(0.069±0.008)	(0.065)	(0.066)	(0.077)	(0.072)	(0.085)	<MDL	<MDL	(0.10±0.01)
PFDA	<MDL	(0.047)	<MDL	<MDL	<MDL	< MDL	<MDL	<MDL	<MDL	<MDL	<MDL	<MDL	<MDL	<MDL
PFUnDA	<MDL	<MDL	<MDL	<MDL	<MDL	< MDL	<MDL	<MDL	<MDL	<MDL	<MDL	<MDL	<MDL	<MDL
PFBS	0.47	0.47	0.50	0.57	0.53	0.52±0.03	0.53	0.47	0.48	0.51	0.56	0.52	0.65	0.58±0.04
PFHxS	(0.13)	(0.13)	(0.12)	(0.17)	(0.14)	(0.16±0.01)	(0.18)	(0.19)	(0.18)	(0.17)	(0.19)	(0.16)	(0.16)	(0.21±0.02)
L-PFOS	0.032	0.028	0.026	0.038	0.040	0.048±0.004	0.054	0.064	0.062	0.056	0.063	0.046	0.056	0.077±0.010
Br-PFOS	0.031	0.035	0.030	0.040	0.048	0.046±0.005	0.058	0.062	0.060	0.056	0.051	0.042	0.057	0.080±0.010
6:2 FTSA	<MDL	<MDL	<MDL	<MDL	(0.098)	<MDL	<MDL	(0.082)	<MDL	(0.088)	<MDL	(0.066)	<MDL	(0.11±0.01)
L-FOSA	<MDL	<MDL	<MDL	<MDL	<MDL	<MDL	<MDL	<MDL	<MDL	<MDL	<MDL	<MDL	<MDL	<MDL
Br-FOSA	<MDL	<MDL	(0.0069)	(0.0054)	<MDL	<MDL	<MDL	<MDL	<MDL	<MDL	<MDL	<MDL	<MDL	<MDL

Table A.1-11: Concentrations [ng/L] of detected PFASs in surface seawater samples from the Elbe River (E1–E18). Values in brackets are between MDL and MQL.

station ID	E1	E2	E4	E5	E6	E7	E8	E9	E10	E11	E12	E13	E14	E15	E16	E17	E18
HFPO-DA	(0.070)	(0.13)	(0.13±0.02)	(0.12)	(0.12)	(0.14)	(0.095)	0.18	(0.11)	0.30	0.34	0.39	0.52	0.67	1.0	1.0	1.5
PFECHS	<MDL	<MDL	(0.060±0.020)	<MDL	<MDL	<MDL	<MDL	<MDL	<MDL	<MDL	<MDL	<MDL	<MDL	<MDL	<MDL	<MDL	<MDL
PFBA	1.6	1.8	1.6±0.1	1.8	1.6	1.7	1.2	1.2	1.5	1.5	1.4	1.3	1.4	1.9	1.2	1.3	1.5
PFPeA	0.65	1.7	1.2±0.1	1.2	1.2	1.3	1.3	1.2	1.4	1.2	1.5	1.1	1.2	0.86	0.81	0.76	0.75
PFHxA	2.7	4.5	4.1±0.6	2.9	3.5	3.0	4.1	3.3	4.6	2.5	4.3	2.5	2.3	2.5	2.0	2.2	1.5
PFHpA	0.75	1.2	1.2±0.1	1.2	1.2	1.1	0.95	0.82	0.96	0.83	0.92	0.76	0.68	0.66	0.60	0.60	0.48
PFOA	1.3	1.6	1.9±0.1	1.8	2.1	1.6	1.7	1.4	1.6	1.3	1.4	1.2	1.1	1.1	1.0	0.94	0.87
PFNA	0.39	0.26	0.41±0.05	0.39	0.40	0.33	0.33	0.24	0.28	0.22	0.23	0.19	0.17	(0.14)	(0.14)	(0.14)	(0.14)
PFDA	0.27	0.18	0.20±0.02	0.22	0.24	0.16	0.18	0.11	0.17	0.13	0.094	(0.060)	(0.072)	(0.062)	(0.053)	(0.065)	(0.063)
PFUnDA	0.068	<MDL	<MDL	<MDL	<MDL	<MDL	<MDL	<MDL	<MDL	<MDL	<MDL	<MDL	<MDL	<MDL	<MDL	<MDL	<MDL
PFBS	0.43	0.98	0.99±0.06	0.90	0.97	0.88	0.77	0.76	0.79	0.71	0.72	0.67	0.61	0.67	0.73	0.66	0.55
PFHxS	(0.22)	0.31	0.47±0.06	0.37	0.49	0.45	0.27	0.37	0.37	0.27	0.32	0.29	0.32	0.28	(0.23)	(0.24)	0.22
L-PFOS	0.33	0.22	0.27±0.01	0.26	0.29	0.22	0.26	0.20	0.19	0.19	0.15	0.11	0.15	0.13	0.13	0.12	0.099
Br-PFOS	0.21	0.21	0.26±0.02	0.26	0.28	0.21	0.19	0.17	0.17	0.14	0.14	0.12	0.14	0.12	0.12	0.093	0.062
6:2 FTSA	0.31	0.21	0.17±0.01	(0.094)	0.19	(0.083)	0.18	0.19	(0.11)	0.23	0.18	0.35	0.28	0.26	0.19	0.23	(0.13)
L-FOSA	(0.010)	<MDL	<MDL	(0.0092)	(0.011)	(0.012)	0.016	0.013	(0.0072)	(0.0085)	(0.0049)	(0.0064)	<MDL	<MDL	<MDL	<MDL	0.018
Br-FOSA	<MDL	<MDL	<MDL	(0.011)	(0.010)	(0.012)	0.016	0.015	(0.012)	0.016	(0.012)	(0.012)	<MDL	(0.0066)	0.015	(0.0044)	0.024

Table A.1-12: Concentrations [ng/L] of detected PFASs in surface seawater samples from the Baltic Sea (BS2–BS17). Values in brackets are between MDL and MQL.

station ID	BS2	BS3	BS4	BS5	BS6	BS7	BS8	BS9	BS10	BS11	BS12	BS13	BS14	BS15	BS16	BS17
HFPO-DA	(0.051)	(0.040)	(0.034)	(0.046)	(0.043)	(0.047)	(0.048)	(0.039)	(0.043)	(0.032)	(0.035)	(0.047)	(0.043)	(0.040±0.002)	(0.037)	(0.034)
PFECHS	(0.091)	(0.055)	(0.099)	(0.071)	(0.076)	(0.048)	(0.073)	(0.11)	(0.079)	(0.051)	0.14	(0.10)	(0.092)	(0.097±0.021)	(0.086)	(0.086)
PFBA	0.41	0.53	0.55	0.51	0.66	0.62	0.57	0.46	0.44	0.34	0.44	0.42	0.46	0.42±0.01	0.40	0.50
PFPeA	0.15	0.17	0.16	0.17	0.20	(0.13)	(0.13)	0.18	0.16	(0.12)	0.16	(0.13)	(0.11)	(0.12±0.01)	(0.13)	0.15
PFHxA	0.28	0.41	0.43	0.49	0.52	0.49	0.29	0.24	0.24	0.42	0.24	0.26	0.24	0.25±0.02	0.24	0.26
PFHpA	0.19	0.24	0.31	0.33	0.37	0.37	0.28	0.17	0.18	0.15	0.15	0.14	0.18	0.18±0.01	0.16	0.17
PFOA	0.26	0.39	0.50	0.55	0.70	0.60	0.44	0.20	0.25	0.25	0.29	0.23	0.30	0.26±0.00	0.27	0.26
PFNA	0.11	0.18	0.17	0.21	0.19	0.16	0.16	0.10	(0.061)	0.086	0.067	0.078	0.11	0.10±0.01	0.086	0.10
PFDA	<MDL	<MDL	0.047	(0.033)	<MDL	<MDL	<MDL	<MDL	<MDL	<MDL	<MDL	<MDL	<MDL	<MDL	<MDL	<MDL
PFBS	0.25	0.30	0.32	0.43	0.32	0.34	0.26	0.19	0.20	(0.17)	0.29	0.30	0.32	0.22±0.01	0.21	0.20
PFHxS	(0.28)	0.43	0.48	(0.34)	0.37	0.44	(0.29)	0.36	(0.27)	(0.19)	(0.29)	(0.30)	(0.19)	(0.18±0.06)	(0.20)	(0.19)
L-PFOS	0.053	0.056	0.07	0.082	0.06	0.065	(0.032)	0.047	0.04	0.056	(0.033)	(0.030)	0.036	0.047±0.003	0.043	0.05
Br-PFOS	0.056	0.055	0.079	0.054	0.052	0.07	0.061	0.05	0.051	0.047	0.053	0.057	0.061	0.058±0.003	0.058	0.056
6:2 FTSA	<MDL	<MDL	<MDL	<MDL	<MDL	<MDL	<MDL	<MDL	<MDL	<MDL	<MDL	<MDL	<MDL	<MDL	<MDL	<MDL
L-FOSA	<MDL	<MDL	<MDL	<MDL	<MDL	<MDL	<MDL	<MDL	<MDL	<MDL	<MDL	<MDL	<MDL	<MDL	<MDL	<MDL
Br-FOSA	<MDL	<MDL	(0.0022)	<MDL	<MDL	<MDL	<MDL	<MDL	<MDL	<MDL	<MDL	<MDL	<MDL	<MDL	<MDL	<MDL

Table A.1-13: Concentrations [ng/L] of detected PFASs in surface seawater samples from the Baltic Sea (BS18–BS33). Values in brackets are between MDL and MQL.

station ID	BS18	BS19	BS20	BS21	BS22	BS23	BS24	BS25	BS26	BS27	BS28	BS29	BS30	BS31	BS32	BS33
HFPO-DA	(0.054)	0.067	(0.043)	(0.048)	(0.052)	0.076	(0.047)	(0.058)	0.063	(0.046)	(0.041)	(0.039)	0.059	(0.052)	0.082	0.061
PFECHS	(0.040)	(0.053)	(0.075)	(0.067)	(0.082)	(0.12)	(0.058)	(0.10)	(0.056)	(0.086)	(0.062)	(0.076)	(0.043)	(0.057)	(0.091)	<MDL
PFBA	0.99	0.88	0.52	0.54	0.40	0.72	0.41	0.54	0.50	0.42	0.42	0.48	0.63	0.50	0.49	0.46
PFPeA	0.53	0.75	0.15	(0.13)	0.16	0.22	(0.12)	0.15	(0.13)	(0.14)	(0.10)	(0.13)	(0.13)	0.15	(0.11)	(0.13)
PFHxA	0.66	0.84	0.28	0.26	0.38	0.40	0.30	0.27	0.28	0.23	0.25	0.23	0.24	0.31	0.23	0.25
PFHpA	0.34	0.28	0.18	0.19	0.14	0.28	0.14	0.18	0.26	0.19	0.16	0.15	0.19	0.17	0.15	0.17
PFOA	0.50	0.41	0.29	0.28	0.26	0.48	0.27	0.33	0.23	0.26	0.27	0.23	0.31	0.32	0.31	0.26
PFNA	0.15	0.12	0.093	0.079	(0.062)	0.15	0.071	0.089	(0.063)	0.068	0.10	0.066	0.084	0.093	0.091	0.064
PFDA	<MDL	<MDL	<MDL	<MDL	<MDL	<MDL	<MDL	<MDL	<MDL	<MDL	<MDL	<MDL	<MDL	<MDL	<MDL	<MDL
PFBS	0.23	0.32	(0.16)	0.24	0.22	0.33	0.18	(0.17)	0.22	0.24	0.19	0.21	0.31	0.26	0.28	0.29
PFHxS	0.47	0.40	(0.26)	(0.21)	<MDL	(0.28)	(0.16)	(0.26)	(0.28)	(0.19)	(0.20)	(0.26)	(0.30)	(0.18)	(0.14)	0.36
L-PFOS	0.056	0.038	0.042	0.036	0.063	0.072	0.047	(0.030)	(0.035)	(0.022)	0.037	(0.030)	0.037	0.051	0.04	0.039
Br-PFOS	0.056	0.05	0.056	0.045	0.044	0.098	0.043	0.041	0.058	0.038	0.04	0.038	0.047	0.049	0.046	0.052
6:2 FTSA	0.56	0.93	<MDL	<MDL	<MDL	(0.33)	<MDL	<MDL	<MDL	<MDL	<MDL	<MDL	<MDL	<MDL	<MDL	<MDL
L-FOSA	(0.0030)	<MDL	<MDL	<MDL	<MDL	(0.0028)	<MDL	(0.0036)	(0.0041)	<MDL	<MDL	<MDL	<MDL	<MDL	<MDL	<MDL
Br-FOSA	(0.0024)	<MDL	<MDL	<MDL	<MDL	(0.0037)	<MDL	<MDL	<MDL	<MDL	<MDL	<MDL	<MDL	<MDL	<MDL	<MDL

Table A.1-14: Concentrations [ng/L] of detected PFASs in surface seawater samples from the Baltic Sea (BS34–BS43), the Oder Lagoon (OL1–OL3) and the Peene and Warnow Rivers (P1 and W1). Values in brackets are between MDL and MQL.

station ID	BS34	BS35	BS36	BS37	BS38	BS39	BS40	BS41	BS42	BS43	OL1	OL2	OL3	P1	W1
HFPO-DA	(0.056)	0.063	0.059	0.063	0.077	(0.055±0.005)	(0.054)	0.064	(0.051)	(0.051)	(0.036)	(0.037)	(0.028)	(0.031)	(0.028)
PFECHS	<MDL	(0.042)	<MDL	(0.041)	(0.045)	<MDL	<MDL	(0.056)	<MDL	(0.070)	<MDL	<MDL	<MDL	<MDL	<MDL
PFBA	0.34	0.47	0.33	0.42	0.34	0.51±0.04	0.49	0.46	0.42	0.36	2.2	2.0	3.2	2.1	2.6
PFPeA	(0.11)	(0.12)	(0.12)	(0.12)	(0.10)	(0.13±0.00)	(0.12)	(0.13)	(0.13)	(0.13)	0.80	2.0	0.79	0.25	0.17
PFHxA	0.24	0.25	0.34	0.22	0.22	0.26±0.01	0.26	0.27	0.26	0.31	1.5	2.6	1.7	0.71	0.65
PFHpA	0.15	0.14	0.14	0.14	(0.13)	0.18±0.02	0.16	0.16	0.16	0.17	0.71	0.89	0.81	0.29	0.23
PFOA	0.20	0.28	0.22	0.26	0.22	0.28±0.01	0.25	0.28	0.26	0.30	0.79	1.0	1.1	0.49	0.49
PFNA	(0.053)	0.064	0.071	0.099	0.074	0.10±0.00	0.07	0.091	0.079	0.089	0.17	0.30	0.28	<MDL	0.10
PFDA	<MDL	<MDL	<MDL	<MDL	<MDL	<MDL	<MDL	<MDL	<MDL	<MDL	0.048	0.048	(0.034)	<MDL	(0.033)
PFBS	0.35	0.19	0.26	(0.15)	0.19	0.21±0.04	0.19	0.31	0.19	0.28	0.87	1.1	0.87	0.42	0.43
PFHxS	<MDL	(0.18)	(0.17)	(0.15)	(0.14)	(0.22±0.06)	(0.16)	(0.21)	(0.11)	(0.24)	0.50	0.42	0.47	(0.21)	(0.26)
L-PFOS	(0.018)	(0.024)	(0.024)	0.042	(0.035)	0.046±0.002	0.038	0.039	0.04	0.037	0.10	0.12	0.12	0.054	0.04
Br-PFOS	0.032	0.037	0.029	0.038	0.043	0.048±0.007	0.036	0.037	0.048	0.049	0.089	0.11	0.14	0.067	0.041
6:2 FTSA	<MDL	<MDL	<MDL	<MDL	<MDL	<MDL	<MDL	<MDL	<MDL	<MDL	<MDL	<MDL	<MDL	<MDL	<MDL
L-FOSA	<MDL	<MDL	<MDL	<MDL	<MDL	(0.0050±0.007)	(0.0024)	<MDL	<MDL	(0.0064)	<MDL	(0.0036)	(0.0023)	<MDL	<MDL
Br-FOSA	<MDL	<MDL	<MDL	<MDL	<MDL	<MDL	(0.0024)	<MDL	<MDL	(0.0064)	(0.0023)	(0.0043)	(0.0033)	(0.0021)	(0.0022)

Table A.1-15: Concentrations [ng/g dw] of detected PFASs in sediment samples from the German Bight and the Elbe River. Values in brackets are between MDL and MQL.

station ID	GB5	GB7	GB11	GB14	GB29	GB30	GB31	GB32	GB33	E3	E10	E14
6:6 PFPiA	<MDL	<MDL	<MDL	<MDL	<MDL	<MDL	<MDL	<MDL	<MDL	(0.0054)	<MDL	<MDL
6:8 PFPiA	<MDL	0.013±0.001	<MDL	<MDL	<MDL	(0.0091±0.0019)	<MDL	<MDL	<MDL	0.052	<MDL	<MDL
PFBA	<MDL	0.54±0.07	(0.033)	<MDL	<MDL	(0.038±0.002)	<MDL	<MDL	<MDL	0.30	0.079	<MDL
PFHxA	<MDL	(0.057±0.007)	<MDL	<MDL	<MDL	<MDL	<MDL	<MDL	<MDL	(0.044)	<MDL	<MDL
PFHpA	<MDL	0.12±0.01	<MDL	<MDL	<MDL	<MDL	<MDL	<MDL	<MDL	(0.011)	(0.018)	<MDL
PFOA	<MDL	0.65±0.01	<MDL	<MDL	<MDL	<MDL	<MDL	<MDL	<MDL	(0.084)	<MDL	<MDL
PFNA	(0.017)	0.21±0.01	<MDL	(0.016)	(0.016)	(0.019±0.001)	<MDL	<MDL	0.024	0.051	(0.018)	<MDL
PFDA	0.038	0.30±0.01	0.020	0.062	0.048	0.051±0.001	(0.010)	(0.0062)	(0.0090)	0.21	0.060	(0.0077)
PFUnDA	0.017	0.14±0.01	0.017	0.060	0.025	0.050±0.001	(0.0094)	(0.0060)	0.016	0.17	0.024	(0.0076)
PFDoDA	(0.0076)	0.039±0.00	(0.0078)	0.019	0.014	0.015±0.001	(0.0049)	<MDL	(0.0034)	0.14	0.011	(0.0059)
PFTTrDA	(0.0083)	0.032±0.00	(0.0094)	0.023	(0.0073)	0.017±0.002	(0.0059)	(0.0061)	(0.0073)	0.068	(0.0084)	(0.0058)
PFTeDA	(0.0039)	(0.0078±0.0004)	<MDL	(0.0060)	(0.0044)	(0.0043±0.0002)	<MDL	<MDL	<MDL	0.036	(0.0037)	<MDL
PFHxS	<MDL	<MDL	<MDL	<MDL	<MDL	<MDL	<MDL	<MDL	<MDL	0.16	<MDL	<MDL
L-PFOS	(0.026)	0.39±0.01	(0.029)	0.10	0.069	0.17±0.01	(0.022)	<MDL	<MDL	0.37	0.089	<MDL
Br-PFOS	<MDL	(0.017±0.006)	<MDL	<MDL	<MDL	(0.012±0.003)	<MDL	<MDL	<MDL	<MDL	(0.029)	<MDL
6:2 FTSA	<MDL	<MDL	<MDL	<MDL	<MDL	<MDL	<MDL	<MDL	<MDL	0.40	<MDL	<MDL
L-FOSA	(0.0047)	0.039±0.003	(0.0046)	0.011	0.028	0.039±0.001	<MDL	<MDL	<MDL	0.045	0.018	(0.0029)
Br-FOSA	<MDL	0.0095±0.0012	<MDL	(0.0047)	0.010	0.018±0.001	<MDL	<MDL	<MDL	0.012	(0.0073)	<MDL

Table A.1-16: Concentrations [ng/g dw] of detected PFASs in surface sediment samples from the Kattegat/Skagerrak, the Baltic Sea and the Oder Lagoon. Values in brackets are between MDL and MQL.

station ID	SK1	SK2	SK3	SK4	BS1	BS7	BS22	BS36	BS42	OL1	OL2	OL3
6:6 PFPiA	<MDL	<MDL	<MDL	<MDL	(0.0049)	<MDL	<MDL	<MDL	<MDL	<MDL	<MDL	<MDL
6:8 PFPiA	<MDL	<MDL	<MDL	(0.012±0.001)	(0.048)	<MDL	<MDL	<MDL	0.021	<MDL	<MDL	<MDL
PFBA	<MDL	0.12	0.10	0.096±0.002	0.16	0.22	0.13	0.14	0.13	<MDL	0.14	0.23
PFHxA	<MDL	<MDL	<MDL	<MDL	<MDL	<MDL	<MDL	<MDL	<MDL	<MDL	<MDL	<MDL
PFHpA	<MDL	(0.016)	<MDL	(0.015±0.001)	<MDL	0.050	<MDL	<MDL	<MDL	<MDL	<MDL	<MDL
PFOA	<MDL	0.10	(0.079)	0.15±0.00	(0.073)	0.39	(0.067)	0.19	(0.073)	<MDL	<MDL	<MDL
PFNA	<MDL	0.16	0.73	0.10±0.00	0.048	0.28	0.034	0.20	0.038	<MDL	<MDL	0.048
PFDA	(0.0063)	0.14	0.091	0.17±0.01	0.042	0.071	0.021	0.20	0.050	0.019	0.016	0.083
PFUnDA	(0.0052)	0.25	0.16	0.21±0.00	0.068	0.039	0.030	0.27	0.11	0.032	0.013	0.063
PFDoDA	(0.0035)	0.040	0.030	0.043±0.001	0.019	0.012	(0.0083)	0.062	0.044	(0.011)	(0.0046)	0.020
PFTTrDA	(0.0051)	0.066	0.047	0.071±0.003	0.030	0.015	0.014	0.10	0.057	0.011	(0.0059)	0.022
PFTeDA	<MDL	(0.010)	(0.0081)	0.012±0.001	(0.0063)	(0.0042)	<MDL	0.022	0.020	(0.0035)	<MDL	(0.0064)
PFHxS	<MDL	<MDL	<MDL	<MDL	<MDL	<MDL	<MDL	<MDL	<MDL	<MDL	<MDL	<MDL
L-PFOS	<MDL	0.22	0.23	0.38±0.00	0.15	0.074	0.080	0.38	0.16	(0.014)	(0.024)	0.16
Br-PFOS	<MDL	<MDL	<MDL	<MDL	(0.014)	<MDL	<MDL	<MDL	<MDL	<MDL	<MDL	<MDL
6:2 FTSA	<MDL	<MDL	<MDL	<MDL	<MDL	<MDL	<MDL	<MDL	<MDL	<MDL	<MDL	<MDL
L-FOSA	<MDL	0.022	0.019	0.031±0.002	0.035	<MDL	0.023	0.034	0.025	(0.0036)	<MDL	(0.0056)
Br-FOSA	<MDL	0.013	0.020	0.033±0.001	0.027	(0.0031)	0.017	0.032	0.015	<MDL	<MDL	(0.0029)

Table A.1-17: Pearson correlation coefficients r between salinity and PFASs as well as among individual PFASs in surface water samples from the Elbe River. Statistically significant values are marked with * ($p < 0.05$). For correlation analysis between salinity and PFASs, samples E1-E4 and E7, for which salinity was not measured, were excluded.

	salinity	PFBA	PFPeA	PFHxA	PFHpA	PFOA	PFNA	PFDA	PFBS	PFHxS	L-PFOS	Br-PFOS	HFPO-DA	6:2 FTSA	L-FOSA	Br-FOSA	ΣPFASs
salinity	1																
PFBA	-0.19	1															
PFPeA	-0.87*	0.2	1														
PFHxA	-0.71*	0.2	0.75*	1													
PFHpA	-0.85*	0.5	0.68*	0.67*	1												
PFOA	-0.86*	0.35	0.56*	0.66*	0.94*	1											
PFNA	-0.84*	0.35	0.25	0.48	0.80*	0.88*	1										
PFDA	-0.77*	0.43	0.17	0.46	0.71*	0.79*	0.94*	1									
PFBS	-0.63*	0.34	0.66*	0.54*	0.84*	0.74*	0.43	0.32	1								
PFHxS	-0.68*	0.31	0.52*	0.44	0.78*	0.78*	0.60*	0.41	0.76*	1							
L-PFOS	-0.75*	0.32	0.11	0.38	0.65*	0.76*	0.94*	0.97*	0.28	0.4	1						
Br-PFOS	-0.73*	0.45	0.34	0.47	0.87*	0.93*	0.94*	0.89*	0.63*	0.71*	0.89*	1					
HFPO-DA	0.99*	-0.34	-0.57*	-0.65*	-0.76*	-	-	-	-0.37	-0.53*	-0.76*	-0.75*	1				
6:2 FTSA	0.42	-0.24	-0.44	-0.45	-0.6*	-	-	-	0.66*	-0.56*	-0.28	-0.44	0.29	1			
L-FOSA	-0.85*	-0.16	0.17	0.21	0.29	0.48	0.53*	0.47	0.04	0.22	0.53*	0.38	-0.63*	-0.28	1		
Br-FOSA	-0.46	-0.4	0.12	-0.02	-0.08	0.03	-0.15	-0.24	0.06	-0.01	-0.20	-0.20	0.01	-0.34	0.57*	1	
ΣPFASs	-0.84*	0.44	0.77*	0.89*	0.92*	0.88*	0.69*	0.63*	0.79*	0.7*	0.56*	0.75*	-0.74*	-0.57*	0.22	-0.09	1

Table A.1-18: Pearson correlation coefficients r and Spearman correlation coefficients r_{SP} (values in bold) between salinity and PFASs as well as among individual PFASs in surface water samples from the Baltic Sea. Statistically significant values are marked with * ($p < 0.05$).

	salinity	PFBA	PFPeA	PFHxA	PFHpA	PFOA	PFNA	PFBS	PFHxS	L-PFOS	Br-PFOS	HFPO-DA	PFECHS	ΣPFASs
salinity	1													
PFBA	-0.24	1												
PFPeA	-0.50*	0.51*	1											
PFHxA	-0.35*	0.43*	0.50*	1										
PFHpA	-0.56*	0.71*	0.59*	0.50*	1									
PFOA	-0.27	0.73*	0.42*	0.57*	0.65*	1								
PFNA	-0.56*	0.54*	0.37*	0.52*	0.62*	0.67*	1							
PFBS	-0.27	0.29	0.26	0.32*	0.50*	0.49*	0.53*	1						
PFHxS	-0.56*	0.64*	0.70*	0.46*	0.73*	0.52*	0.66*	0.38*	1					
L-PFOS	-0.49*	0.29	0.44*	0.55*	0.39*	0.40*	0.64*	0.33*	0.39*	1				
Br-PFOS	-0.52*	0.42*	0.45*	0.36*	0.63*	0.42*	0.57*	0.37*	0.54*	0.57*	1			
HFPO-DA	0.57*	0.18	-0.20	-0.06	-0.14	0.04	-0.16	0.09	-0.22	-0.19	-0.11	1		
PFECHS	-0.57*	0.06	0.34*	-0.06	0.15	0.12	0.20	0.10	0.23	0.35*	0.49*	-0.29	1	
ΣPFASs	-0.43*	0.90*	0.71*	0.59*	0.82*	0.75*	0.71*	0.50*	0.74*	0.48*	0.51*	0.08	0.14	1

Table A.1-19: Pearson correlation coefficients r between salinity and PFASs as well as among individual PFASs in surface water samples from the German Bight. Statistically significant values are marked with * ($p < 0.05$).

	salinity	PFBA	PFPeA	PFHxA	PFHpA	PFOA	PFBS	PFHxS	L-PFOS	Br-PFOS	HFPO-DA	Σ PFASs
salinity	1											
PFBA	0.1	1										
PFPeA	-0.89*	-0.03	1									
PFHxA	-0.80*	-0.17	0.82*	1								
PFHpA	-0.89*	-0.05	0.92*	0.86*	1							
PFOA	-0.87*	-0.11	0.90*	0.91*	0.95*	1						
PFBS	-0.03	0.14	0.28	0.28	0.15	0.25	1					
PFHxS	-0.75*	-0.18	0.85*	0.79*	0.85*	0.88*	0.39*	1				
L-PFOS	-0.90*	-0.16	0.94*	0.87*	0.93*	0.92*	0.25	0.87*	1			
Br-PFOS	-0.76*	-0.01	0.80*	0.68*	0.91*	0.80*	-0.01	0.68*	0.80*	1		
HFPO-DA	-0.26	-0.24	0.14	0.27	0.26	0.37*	0.09	0.19	0.19	0.18	1	
Σ PFASs	-0.80*	0.1	0.83*	0.86*	0.87*	0.92*	0.34	0.76*	0.82*	0.71*	0.54*	1

Table A.1-20: Pearson correlation coefficients r between TOC and PFASs as well as among individual PFASs in sediment samples over the entire study area, disregarding the four samples with the highest TOC values (BS22, BS7, BS1, E10). Statistically significant values are marked with * ($p < 0.05$).

	TOC	PFBA	PFOA	PFNA	PFDA	PFUnDA	PFDoDA	PFTTrDA	PFTeDA	L-PFOS	L-FOSA	Br-FOSA	ΣPFASs
TOC	1												
PFBA	0.57*	1											
PFOA	0.54*	0.84*	1										
PFNA	0.71*	0.69*	0.82*	1									
PFDA	0.65*	0.85*	0.84*	0.88*	1								
PFUnDA	0.78*	0.49*	0.50*	0.85*	0.80*	1							
PFDoDA	0.56*	0.57*	0.33	0.46*	0.72*	0.70*	1						
PFTTrDA	0.82*	0.43	0.40	0.75*	0.73*	0.96*	0.76*	1					
PFTeDA	0.69*	0.50*	0.29	0.48*	0.67*	0.73*	0.96*	0.84*	1				
L-PFOS	0.75*	0.73*	0.69*	0.83*	0.94*	0.89*	0.77*	0.86*	0.76*	1			
L-FOSA	0.62*	0.58*	0.56*	0.63*	0.80*	0.70*	0.75*	0.70*	0.75*	0.87*	1		
Br-FOSA	0.69*	0.26	0.37	0.65*	0.63*	0.84*	0.52*	0.85*	0.62*	0.82*	0.77*	1	
ΣPFASs	0.70*	0.87*	0.81*	0.84*	0.98*	0.80*	0.79*	0.75*	0.74*	0.94*	0.82*	0.61*	1

A.2 Supplementary to Chapter 6

Table A.2-1: Sampling locations of surface seawater samples analysed in this study and physicochemical parameters measured in the water phase.

sample name	latitude °N	longitude °E	date time of sampling (UTC)	water depth [m]	temperature [°C] ¹	pH ¹	salinity [PSU] ¹
Latitudinal transect from the European continent to the Arctic (57 °N to 79 °N at ~5 °E) distance between N1 and N21: 2,432 km							
N1	57.137	5.409	11.07.2018 09:29	51	na ²	na ²	na ²
N2	57.735	5.023	11.07.2018 12:53	96	14.52	na ²	32.22
N3	58.539	4.488	11.07.2018 17:17	277	11.14	na ²	33.73
N4	60.618	4.169	12.07.2018 04:12	300	14.08	na ²	31.78
N5	62.007	4.203	12.07.2018 11:16	148	13.08	8.19	32.59
N6	63.109	4.256	12.07.2018 16:50	978	13.04	8.28	34.69
N7	64.035	4.305	12.07.2018 21:40	1410	12.93	8.27	34.87
N8	65.301	4.374	13.07.2018 04:18	976	12.20	8.24	35.02
N9	66.139	4.423	13.07.2018 08:32	1219	11.36	8.27	34.86
N10	67.042	4.474	13.07.2018 13:11	1331	10.36	8.22	35.05
N11	68.140	4.540	13.07.2018 18:47	1765	9.91	8.23	34.92
N12	68.937	4.590	13.07.2018 22:45	3159	8.87	8.24	35.02
N13	70.126	4.672	14.07.2018 04:51	3153	8.79	8.24	35.01
N14	71.087	4.739	14.07.2018 09:40	3048	8.26	8.25	35.06
N15	72.240	4.824	14.07.2018 15:31	2450	8.24	8.27	35.05
N16	73.334	4.917	14.07.2018 21:02	2558	7.10	8.26	35.03
N17	74.803	5.025	15.07.2018 04:20	3203	5.45	8.30	35.02
N18	75.755	4.887	15.07.2018 09:10	2657	5.94	8.28	35.04
N19	76.606	4.753	15.07.2018 13:27	2806	5.61	8.34	35.04
N20	77.722	4.568	15.07.2018 19:15	2890	5.36	8.37	35.02
N21	79.021	4.335	16.07.2018 14:36	2476	5.48	8.38	34.86
Longitudinal transect across Fram Strait (9 °E to 18 °W at ~79 °N) distance between F1 and F15: 558 km							
F1	79.000	9.300	19.07.2018 00:10	218.0	6.12	8.37	34.92
F2	79.001	8.901	18.07.2018 23:41	216.7	5.83	8.36	34.93
F3	79.018	8.459	18.07.2018 22:02	476.0	6.28	8.36	34.99
F4	79.002	7.758	18.07.2018 17:20	1194.1	6.31	8.29	35.03
F5 ³	79.021	4.335	16.07.2018 14:36	2476.0	5.48	8.38	34.86
F6	79.259	-1.371	26.07.2018 04:43	2639.4	-0.52	8.24	31.50
F7	78.968	-5.089	27.07.2018 05:36	1216.2	-0.93	8.28	30.00
F8	79.402	-9.004	29.07.2018 13:38	77.8	-0.36	8.17	30.13
F9	79.440	-10.623	28.07.2018 04:20	104.0	0.45	8.09	30.37
F10	79.819	-12.273	27.07.2018 22:13	195.5	-0.36	8.13	30.46
F11	79.676	-13.606	29.07.2018 06:42	140.0	-0.14	8.13	30.77
F12	80.038	-14.643	28.07.2018 01:34	171.1	0.07	8.11	31.42
F13	79.618	-16.591	28.07.2018 19:07	274.0	-1.43	8.14	30.61
F14	80.125	-16.642	28.07.2018 07:18	327.0	-1.41	8.18	30.24
F15	79.619	-17.840	28.07.2018 15:14	439.0	-1.38	8.16	30.00
Latitudinal transect in Fram Strait (78 °N to 81 °N at ~0 °EW) distance between P1 and P5: 284 km							
P1	78.240	0.001	20.07.2018 09:16	3031.3	4.41	8.35	34.44
P2	78.819	0.000	20.07.2018 13:02	2630.1	2.40	8.35	33.25
P3	79.455	0.073	21.07.2018 14:09	2817.3	-1.25	8.30	32.41
P4	80.170	0.125	25.07.2018 06:04	3095.4	-1.26	8.13	32.09
P5	80.792	0.057	24.07.2018 20:30	3168.8	-0.87	8.19	31.74

¹ Data was taken from von Appen and Rohardt [286].

² Because systems measuring the physicochemical parameters had to be set up and calibrated on the first day of the cruise, continuous measurements for those only started on the second day.

³ At sampling location N21/F5, the latitudinal transect from the European continent to the Arctic and the longitudinal transect across Fram Strait crossed. Consequently, this sample was used for evaluation of both sampling transects.

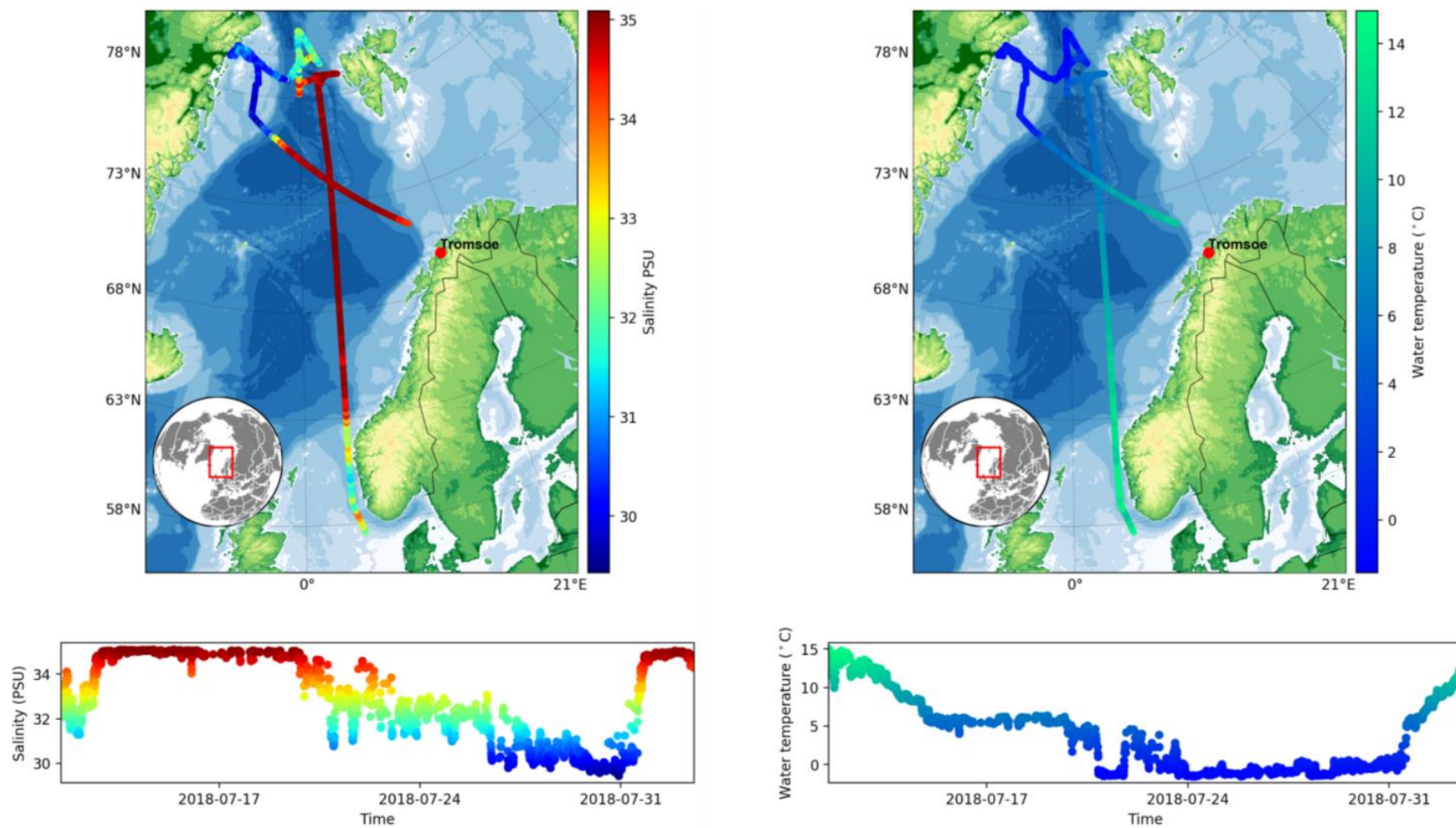


Figure A.2-1: A) Salinity data and B) water temperature data from *Polarstern* cruise PS114, measured by sensor TSG1 (SBE21-3189, SBE38-118). The figure was taken from von Appen and Rohardt [286]. General information on the cruise can be found in the expedition report [268].

Table A.2-2: Sampling information for depth profiles analysed in this study and physicochemical parameters measured in samples from the respective sampling depths.¹

event name ²	sample name	latitude °N	longitude °E	date time (UTC, profile start)	water depth [m]	sampling depth [m] ²	salinity [PSU] ²	temperature [°C] ²	θ [°C] ³	σ_0 [kg/m ³] ⁴	water mass ⁵
vertical profile 1 (V1)											
PS114_12-4	V1/1	79.012	7.033	2018-07-18 15:35	1277	1239	34.91	-0.80	-0.85	28.08	DW
PS114_12-4	V1/2	79.012	7.033	2018-07-18 15:35	1277	1000	34.91	-0.71	-0.75	28.06	DW
PS114_12-1	V1/3	79.012	7.035	2018-07-18 10:41	1277	500	34.99	2.02	1.99	28.01	AW
PS114_12-1	V1/4	79.012	7.035	2018-07-18 10:41	1277	250	35.05	3.52	3.50	27.94	AW
PS114_12-1	V1/5	79.012	7.035	2018-07-18 10:41	1277	100	35.06	4.37	4.36	27.88	AW
PS114_12-1	V1/6	79.012	7.035	2018-07-18 10:41	1277	75	35.05	4.76	4.76	27.85	AW
PS114_12-1	V1/7	79.012	7.035	2018-07-18 10:41	1277	50	35.04	5.35	5.35	27.74	AW
PS114_12-1	V1/8	79.012	7.035	2018-07-18 10:41	1277	10	34.97	6.02	6.01	27.59	AW
vertical profile 2 (V2)											
PS114_9-4	V2/1	78.607	5.047	2018-07-18 00:37	2344	2286	34.92	-0.74	-0.86	28.07	DW
PS114_9-4	V2/2	78.607	5.047	2018-07-18 00:37	2344	1000	34.91	-0.41	-0.45	28.07	IW
PS114_9-1	V2/3	78.607	5.041	2018-07-17 18:53	2347	500	34.93	0.72	0.70	27.96	AW
PS114_9-1	V2/4	78.607	5.041	2018-07-17 18:53	2347	250	35.01	2.52	2.50	27.88	AW
PS114_9-1	V2/5	78.607	5.041	2018-07-17 18:53	2347	100	35.04	3.45	3.44	27.79	AW
PS114_9-1	V2/6	78.607	5.041	2018-07-17 18:53	2347	75	35.03	3.64	3.64	27.74	AW
PS114_9-1	V2/7	78.607	5.041	2018-07-17 18:53	2347	40	35.01	4.57	4.56	27.67	AW
PS114_9-1	V2/8	78.607	5.041	2018-07-17 18:53	2347	10	34.96	5.46	5.46	27.53	AW
vertical profile 3 (V3)											
PS114_25-2	V3/1	78.830	-0.025	2018-07-20 15:53	2636	2573	34.92	-0.72	-0.86	28.08	DW
PS114_25-2	V3/2	78.830	-0.025	2018-07-20 15:53	2636	1001	34.91	-0.23	-0.27	28.05	IW
PS114_25-2	V3/3	78.830	-0.025	2018-07-20 15:53	2636	501	34.92	1.09	1.06	27.98	AW
PS114_25-2	V3/4	78.830	-0.025	2018-07-20 15:53	2636	250	35.00	2.75	2.73	27.91	AW
PS114_25-2	V3/5	78.830	-0.025	2018-07-20 15:53	2636	100	34.93	2.59	2.58	27.87	AW
PS114_25-2	V3/6	78.830	-0.025	2018-07-20 15:53	2636	75	34.89	2.58	2.57	27.84	AW
PS114_25-2	V3/7	78.830	-0.025	2018-07-20 15:53	2636	50	34.72	1.49	1.48	27.78	AW
PS114_25-2	V3/8	78.830	-0.025	2018-07-20 15:53	2636	10	34.51	4.62	4.62	27.33	AW
vertical profile 4 (V4)											
PS114_43-2	V4/1	78.820	-2.779	2018-07-26 14:32	2595	2600	34.93	-0.73	-0.86	28.09	DW
PS114_43-2	V4/2	78.820	-2.779	2018-07-26 14:32	2595	2000	34.92	-0.62	-0.72	28.08	DW
PS114_43-2	V4/3	78.820	-2.779	2018-07-26 14:32	2595	1200	34.91	-0.26	-0.32	28.05	IW
PS114_43-2	V4/4	78.820	-2.779	2018-07-26 14:32	2595	1000	34.90	-0.10	-0.15	28.03	IW
PS114_43-2	V4/5	78.820	-2.779	2018-07-26 14:32	2595	700	34.88	0.21	0.18	28.00	RAW/AAW

PS114_43-2	V4/6	78.820	-2.779	2018-07-26 14:32	2595	500	34.87	0.57	0.54	27.97	RAW/AAW
PS114_43-4	V4/7	78.818	-2.769	2018-07-26 18:32	2598	250	34.91	1.77	1.75	27.92	RAW/AAW
PS114_43-4	V4/8	78.818	-2.769	2018-07-26 18:32	2598	100	34.50	0.02	0.02	27.70	PW
PS114_43-4	V4/9	78.818	-2.769	2018-07-26 18:32	2598	75	34.23	-1.01	-1.02	27.53	PW
PS114_43-4	V4/10	78.818	-2.769	2018-07-26 18:32	2598	60	34.06	-1.57	-1.57	27.41	PW
PS114_43-4	V4/11	78.818	-2.769	2018-07-26 18:32	2598	40	33.92	-1.40	-1.40	27.30	PW
PS114_43-4	V4/12	78.818	-2.769	2018-07-26 18:32	2598	15	33.06	-1.51	-1.51	26.60	PW
PS114_43-4	V4/13	78.818	-2.769	2018-07-26 18:32	2598	5	30.24	-0.69	-0.69	24.29	PW
vertical profile 5 (V5)											
PS114_46-1	V5/1	78.993	-5.436	2018-07-27 07:16	997	959	34.89	-0.02	-0.06	28.02	IW
PS114_46-1	V5/2	78.993	-5.436	2018-07-27 07:16	997	500	34.87	0.54	0.52	27.97	RAW/AAW
PS114_46-1	V5/3	78.993	-5.436	2018-07-27 07:16	997	250	34.84	1.00	0.99	27.92	RAW/AAW
PS114_46-8	V5/4	79.012	-5.285	2018-07-27 15:45	1139	100	34.32	-0.76	-0.76	27.60	PW
PS114_46-8	V5/5	79.012	-5.285	2018-07-27 15:45	1139	75	33.98	-1.33	-1.33	27.34	PW
PS114_46-8	V5/6	79.012	-5.285	2018-07-27 15:45	1139	50	33.61	-1.50	-1.50	27.05	PW
PS114_46-8	V5/7	79.012	-5.285	2018-07-27 15:45	1139	26	33.17	-1.59	-1.59	26.69	PW
PS114_46-8	V5/8	79.012	-5.285	2018-07-27 15:45	1139	5	31.32	-1.01	-1.01	25.17	PW
vertical profile 6 (V6)											
PS114_49-2	V6/1	79.615	-16.525	2018-07-28 20:34	281	271	34.81	0.96	0.95	27.89	RAW/AAW
PS114_49-2	V6/2	79.615	-16.525	2018-07-28 20:34	281	150	34.42	0.44	0.43	27.61	RAW/AAW
PS114_49-2	V6/3	79.615	-16.525	2018-07-28 20:34	281	100	33.68	-0.89	-0.89	27.08	PW
PS114_49-2	V6/4	79.615	-16.525	2018-07-28 20:34	281	50	31.70	-1.68	-1.68	25.50	PW
PS114_49-2	V6/5	79.615	-16.525	2018-07-28 20:34	281	10	31.25	-1.53	-1.53	25.12	PW
vertical profile 7 (V7)											
PS114_36-2	V7/1	80.855	-0.140	2018-07-24 12:48	3181	3117	34.93	-0.70	-0.88	28.09	DW
PS114_36-2	V7/2	80.855	-0.140	2018-07-24 12:48	3181	2000	34.92	-0.67	-0.77	28.08	DW
PS114_36-2	V7/3	80.855	-0.140	2018-07-24 12:48	3181	1000	34.90	-0.23	-0.27	28.04	IW
PS114_36-2	V7/4	80.855	-0.140	2018-07-24 12:48	3181	500	34.90	0.99	0.97	27.97	RAW/AAW
PS114_36-2	V7/5	80.855	-0.140	2018-07-24 12:48	3181	250	34.99	2.76	2.75	27.90	RAW/AAW
PS114_36-2	V7/6	80.855	-0.140	2018-07-24 12:48	3181	100	34.73	1.13	1.13	27.82	RAW/AAW
PS114_36-2	V7/7	80.855	-0.140	2018-07-24 12:48	3181	50	34.22	-1.43	-1.43	27.54	PW
PS114_36-2	V7/8	80.855	-0.140	2018-07-24 12:48	3181	10	33.28	-1.51	-1.51	26.77	PW

¹ At the CTD/rosette stations, physicochemical data was recorded during the casts [353] and measured in water samples taken from the Niskin bottles mounted on the CTD rosette. [290]

Data shown here was taken from von Appen *et al.* [290]

² Event names were taken from the expedition report [268] and are structured as follows: cruise_station_cast. ³ θ : potential temperature; ⁴ σ_0 : potential density referenced to sea surface

⁵ Water masses were classified according to Rudels *et al.* [287], based on measured physicochemical parameters (see Table A.2-15 for further explanation).

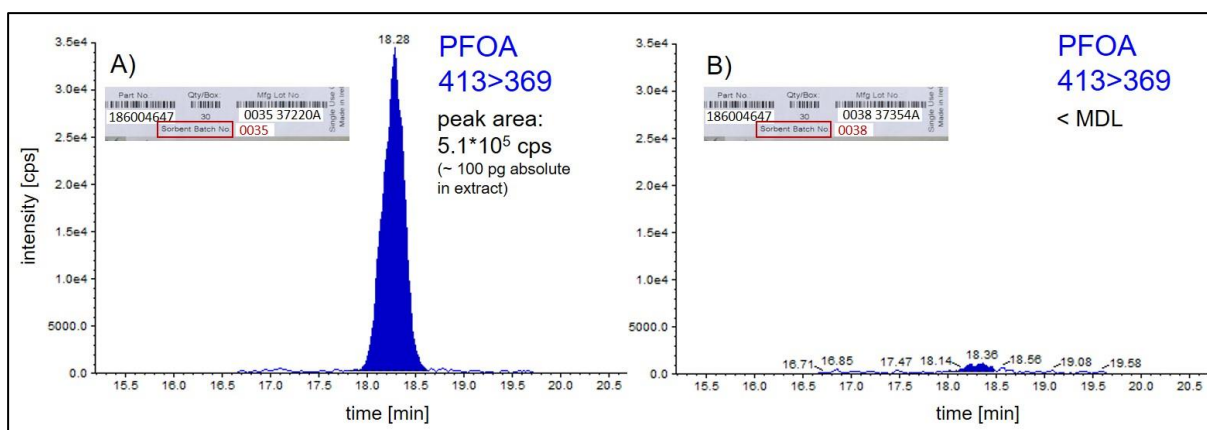


Figure A.2-2: LC-MS/MS chromatograms of PFOA showing differences in contamination between cartridges of the same manufacturer and part number, packed with different WAX resin sorbent batches, 0035 (A) and 0038 (B). Cartridges were preconditioned with 6 mL 0.1 % NH_4OH in methanol and 6 mL methanol. Then, 6 mL methanol and 6 mL 0.1 % NH_4OH in methanol were added as for the elution of the target compounds and the eluates were collected. They were reduced to 200 μL and analysed by LC-MS/MS. The peak area of PFOA in A) was comparable to a 0.5 $\text{pg}/\mu\text{L}$ calibration standard, which contains 100 pg PFOA absolute. The different WAX resin sorbent batches were tested before the cruise and only cartridges packed with sorbent lots for which tests showed no contamination with PFOA were used for extraction.

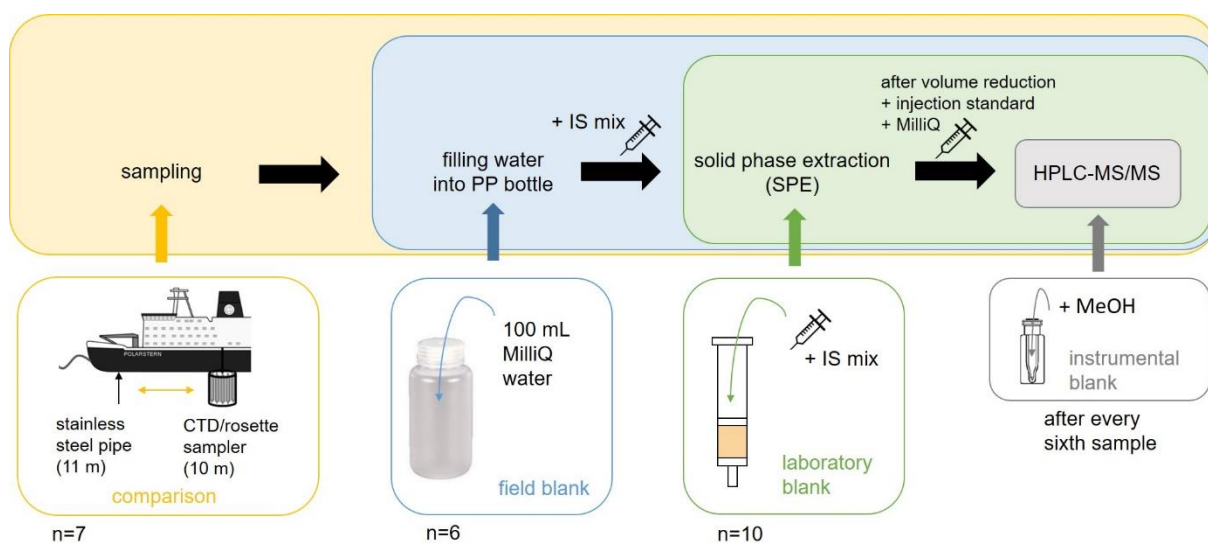


Figure A.2-3: Preparation and analysis of blank samples. Methanol was injected as instrumental blank after every sixth sample in a measurement sequence. On board, one laboratory blank was prepared with every SPE batch by adding the IS mix to a preconditioned cartridge, leaving the cartridge on the vacuum manifold during the extraction and treating it as if it was a sample from the washing step on ($n = 10$). In addition, six field blanks were prepared on different sampling days by filling a sampling bottle with 100 mL of pretested MilliQ water and analyzing it like a field sample. When surface water samples were taken with the CTD/rosette sampler (10 m depth), a sample was taken with the stainless steel pipe (11 m depth) at the same time to compare the two sampling techniques ($n = 7$).

Table A.2-3: Mean concentrations of PFASs in procedural blanks \pm standard deviation (SD), method detection limits (MDLs) and method quantification limits (MQLs).

analyte	laboratory blanks (<i>n</i> = 10)	field blanks (<i>n</i> = 6)	MDL ²	MQL ²
	[pg/L]		[pg/L]	
PFPeA	0.46 \pm 0.53	9.7 \pm 4.4	23	53
PFHxA	5.2 \pm 2.1	5.6 \pm 2.1	12	27
PFHpA	4.8 \pm 1.8	7.9 \pm 1.3	12	21
PFOA	16 \pm 4	11 \pm 2	16	29
PFNA	nd ¹	nd	6.3	21
PFDA	nd	nd	6.4	21
PFUnDA	nd	nd	3.7	12
PFDoDA	nd	nd	3.3	11
PFTTrDA	nd	nd	4.6	15
PFTeDA	nd	nd	8.8	29
PFBS	nd	nd	13	45
PFHxS	nd	nd	18	61
PFHpS	nd	nd	27	90
L-PFOS	11 \pm 3	11 \pm 3	21	44
Br-PFOS	4.2 \pm 2.1	5.2 \pm 2.2	12	28
PFDS	nd	nd	32	93
PFECHS	nd	nd	43	140
HFPO-DA	nd	nd	6.0	20
HFPO-TrA	nd	nd	44	150
HFPO-TeA	nd	nd	75	250
DONA	nd	nd	7.5	25
6:2 Cl-PFESA	nd	nd	6.9	23
8:2 Cl-PFESA	nd	nd	6.8	23
6:6 PFPiA	nd	nd	4.9	16
6:8 PFPiA	nd	nd	8.7	29
L-FOSA	nd	nd	8.0	27
Br-FOSA	nd	nd	11	33
4:2 FTSA	nd	nd	30	100
6:2 FTSA	20 \pm 7	25 \pm 12	61	150
8:2 FTSA	nd	nd	36	120
PFBA ³	390 \pm 580	330 \pm 510	-	-

¹ nd = not detected

² For compounds present in blanks, MDLs and MQLs were calculated as the average blank value plus 3 or 10 times the standard deviation, respectively (blue). For PFASs other than these, the MDLs and MQLs were derived from a signal-to-noise ratio of 3 or 10, respectively, observed in low-level samples (green) or spiked matrix samples (yellow).

³ In blank samples processed on board, comparatively high concentrations of PFBA were found, strongly varying between the different SPE batches (red). Consequently, no results are reported for PFBA

Table A.2-4: Coefficients of variation [%] for quantified PFASs, calculated from triplicate analysis of surface water samples taken by seawater intake system ($n = 2$) and samples taken by CTD/rosette sampler and seawater intake system at the same time ($n = 7$).

compound	coefficient of variation [%]										
	triplicates seawater intake system			comparison between sampling techniques							
	N5	N22	mean	CTD_049	CTD_009	CTD_025	CTD_036	CTD_012	CTD_043	CTD_046	mean
PFHxA	6	6	6	6	22	3	4	12	1	10	8
PFHpA	2	9	5	4	3	19	14	3	11	3	8
PFOA	5	2	5	11	16	13	13	-	-	-	13
PFNA	5	7	6	8	15	9	1	24	3	4	9
PFDA	-	-	-	-	-	-	-	-	-	18	18
PFUnDA	-	1	1	-	19	-	-	-	21	3	14
PFBS	11	12	11	-	-	-	3	-	-	-	3
PFHxS	5	-	5	-	-	-	-	-	-	-	-
L-PFOS	18	16	17	-	20	-	-	-	-	-	20
Br-PFOS	3	11	7	-	-	-	3	-	-	-	3
HFPO-DA	7	-	7	1	-	-	-	1	-	-	1

Table A.2-5: Percent absolute recoveries of internal standards¹ in analysed seawater samples ($n = 109$).

internal standard	mean absolute recovery \pm SD [%]
¹³ C ₄ -PFBA	24 \pm 12
¹³ C ₂ -PFHxA	46 \pm 7
¹³ C ₄ -PFOA	51 \pm 9
¹³ C ₅ -PFNA	48 \pm 9
¹³ C ₂ -PFDA	49 \pm 10
¹³ C ₂ -PFUnDA	53 \pm 11
¹³ C ₂ -PFDoDA	50 \pm 12
¹⁸ O ₂ -PFHxS	51 \pm 8
¹³ C ₄ -PFOS	47 \pm 9
¹³ C ₃ -HFPO-DA	43 \pm 6

Section A.2-1: Water transport data used for calculation of PFAS mass transport estimates through Fram Strait

Reported estimates of water transport budgets in and out of Fram Strait vary significantly due to complex recirculation patterns and strong mesoscale activity that complicate data interpretation [267, 354-356]. Here, we focused on the boundary currents defined in accordance with Stöven *et al.* [272]:

- Atlantic Water (AW) advected in the West Spitsbergen Current (WSC): longitude 5–9 °E and depth \leq 840 m
- Polar Water (PW) flowing southward in the EGC, defined as mean temperature \leq 1 °C and depth \leq 400 m
- Recirculating and Arctic Atlantic Water (RAW/AAW), transported through Fram Strait both due to recirculation of Atlantic Water and the long loop of Atlantic Water through the Arctic Ocean: longitude 7°W to 1°E, depth \leq 840 m, not defined as Polar Water

Stöven *et al.* assumed the exchange flow across Fram Strait below 840 m to be 0 Sv as there are no connections between the Nordic Seas and the Arctic Ocean below the sill depth of the Greenland-Scotland-Ridge (840 m) other than Fram Strait [272]. No vertical displacements of isopycnals in these two basins are observed indicating a non-zero net transport through Fram Strait below 840 m [357].

Water mass transport estimates with the AW, PW and RAW/AAW were based on the MIT general circulation model (MITgcm) ECCO v4. The MITgcm has a global resolution of 1° x 1°, with a finer resolution in the Arctic and near the equator and 50 vertical layers spanning 10 m intervals near the surface and 500 m at the bottom of the ocean. Ocean state estimates are derived from the Estimating the Circulation & Climate of the Ocean (ECCO v4) climatology [269].

The water transport masses reported here are averages over the years 2011-2015. While transport velocities change strongly between seasons and on shorter time scales, there is no strong interannual trend in Fram Strait [267]. Therefore, modeled average volume transport over the period 2011-2015 is assumed representative of the volume transport through Fram Strait in 2018, when the samples for PFAS analysis were taken.

Modeled net transport through Fram Strait with the boundary currents is southward. It is in the same range as estimated from an array of 17 moorings at 78°50' N between 2002 and 2010 [272] (see table below).

water mass	volume (Sv)	
	MITgcm (2011–2015)	observations[272] (mooring array, 2002–2010)
AW	3.7	4.4(±3.2)
PW	–0.6	–1.4(±0.8)
RAW/AAW	–3.8	–3.5(±1.9)
Σ	–0.7	–0.5

Table A.2-6: Detection frequencies [%], concentration ranges [pg/L], mean concentrations [pg/L] and median values [pg/L] of detected PFASs in surface water samples of the entire study area and along a latitudinal transect from the European continent to the Arctic. Values in brackets are between MDL and MQL. Of the physicochemical parameters, temperature [°C], salinity [PSU] and water depth [m] are given for the different sampling areas.

PFASs ¹	entire study area (<i>n</i> = 40)				latitudinal transect from the European continent to the Arctic Ocean (57 °N to 79 °N at ~5 °E)											
					North Sea/continental shelf <i>Norwegian Coastal Current (NCC)</i> (<i>n</i> = 5)				Norwegian Sea/continental slope <i>Norwegian Atlantic Current (NwAC)</i> (<i>n</i> = 6)				Greenland and Norwegian Sea/deep waters (<i>n</i> = 10)			
	DF [%]	range [pg/L]	mean [pg/L]	median [pg/L]	DF [%]	range [pg/L]	mean [pg/L]	median [pg/L]	DF [%]	range [pg/L]	mean [pg/L]	median [pg/L]	DF [%]	range [pg/L]	mean [pg/L]	median [pg/L]
HFPO-DA	90	<MDL–120	30	21	100	52–120	92	94	100	(19)–33	25	25	80	<MDL–26	(16)	(17)
PFHxA	100	(17)–110	56	53	100	74–110	96	100	100	33–70	51	51	100	(17)–66	35	30
PFHpA	100	(20)–100	40	32	100	67–100	86	88	100	25–44	33	30	100	(20)–30	23	22
PFOA	100	38–170	66	56	100	120–170	140	140	100	41–76	59	59	100	38–56	47	45
PFNA	100	22–55	34	33	100	45–55	49	49	100	35–44	38	38	100	22–45	31	31
PFDA	68	<MDL–(20)	(8.1)	(8.2)	100	13–(20)	(16)	(16)	100	(11)–(19)	(14)	(14)	100	(7.0)–(16)	(11)	(11)
PFUnDA	83	<MDL–17	(7.5)	(6.8)	100	(9.3)–(13)	(11)	(11)	100	(10)–17	13	13	100	(6.4)–16	(10)	(9.3)
PFDoDA	42	<MDL–(10)	-	-	80	<MDL–6.5	(4.1)	(5.0)	67	<MDL–(10)	(4.9)	(5.8)	60	MDL–(10)	(3.4)	(4.0)
PFBS	100	(15)–93	(39)	(38)	100	57–93	75	69	67	(19)–(39)	(31)	(32)	100	(15)–(28)	(23)	(25)
PFHxS	39	<MDL–54	-	-	100	(38)–(54)	(49)	(52)	100	(19)–(24)	(21)	(22)	0	<MDL	-	-
L-PFOS	2	<MDL–110	(42)	(32)	100	60–110	91	100	100	(35)–83	56	58	80	<MDL–(32)	(23)	(27)
Br-PFOS	2	<MDL–68	(24)	(19)	100	46–68	57	58	100	(19)–35	(28)	(27)	80	<MDL–(19)	(13)	(15)
ΣPFASs	-	140–850	340	280	-	680–850	770	780	-	270–430	370	390	-	140–290	230	240
		range	mean	median		range	mean	median		range	mean	median		range	mean	median
temperature [°C]	-	-1.43–14.52	5.48	5.72	-	11.14–14.52	13.21	13.58	-	9.91–13.14	11.63	11.78	-	5.36–8.87	6.91	6.52
salinity [psu]	-	30.00–35.06	33.35	34.78	-	31.78–33.73	32.58	32.41	-	34.69–35.05	34.90	34.90	-	34.86–35.06	35.02	35.03
water depth [m]	-	51–3200	1630	1770	-	51–300	170	150	-	976–1765	1280	1280	-	2450–3200	2840	2850

¹ Due to high blanks, no values can be reported for PFBA. In addition, PFPeA could not be evaluated because of matrix interferences.

² PFOS could not be evaluated in 10 of the 40 samples because of matrix interferences. The given values refer to only the samples in which no interferences occurred.

Table A.2-7: Detection frequencies [%], concentration ranges [pg/L], mean concentrations [pg/L] and median values [pg/L] of detected PFASs in surface water samples along a longitudinal and a latitudinal sampling transect in Fram Strait. Values in brackets are between MDL and MQL. Of the physicochemical parameters, temperature [°C], salinity [PSU] and water depth [m] are given for the different sampling areas.

	longitudinal transect across Fram Strait (9 °E to 18 °W at ~ 79 °N)								latitudinal transect along the prime meridian (78 °N to 81 °N at ~ 0 °EW) (n = 5)			
	east of 0 °EW, ice-free (n = 4+1 ¹)				west of 0 °EW, ice-covered (n = 10)							
PFASs ²	DF [%]	range [pg/L]	mean [pg/L]	median [pg/L]	DF [%]	range [pg/L]	mean [pg/L]	median [pg/L]	DF [%]	range [pg/L]	mean [pg/L]	median [pg/L]
HFPO-DA	100	(14)–45	29	29	80	<MDL	(14)	(12)	100	(15)–70	33	28
PFHxA	100	39–51	44	43	100	52–78	64	63	100	39–75	58	57
PFHpA	100	21–28	24	24	100	36–58	46	46	100	26–54	39	41
PFOA	100	38–48	43	42	100	49–66	57	57	100	61–95	73	71
PFNA	100	22–29	25	24	100	31–38	33	32	100	29–36	32	31
PFDA	60	<MDL–(8.2)	<MDL	(7.0)	0	<MDL	-	-	80	<MDL–8.1	<MDL	(6.9)
PFUnDA	100	(4.9)–(7.1)	(6.1)	(6.4)	30	<MDL–(5.7)	-	-	100	5.3–7.4	(6.0)	(5.8)
PFDoDA	40	<MDL–(3.6)	-	-	0	<MDL	-	-	20	<MDL–5.0	-	-
PFBS	100	(21)–(29)	(24)	(23)	100	(38)–56	(43)	(40)	100	23–64	53	59
PFHxS	0	<MDL	-	-	20	<MDL–(24)	-	-	60	<MDL–27	<MDL	(23)
L-PFOS	^{3a}	(24)–(33)	(29)	(29)	^{3b}	<MDL–(37)	(22)	(28)	^{3c}	25–35	(31)	34
Br-PFOS	^{3a}	(12)–(19)	(16)	(17)	^{3b}	<MDL–(13)	<MDL	(13)	^{3c}	15–21	(18)	(17)
ΣPFASs (DF > 50 %) ⁴	-	170–210	190	190	-	230–290	260	260	-	190–310	260	280
physicoch. par.		range	mean	median		range	mean	median		range	mean	median
temperature [°C]	-	5.48–6.31	6.00	6.12	-	-1.43–0.45	-0.6	-0.44	-	-1.26–4.41	0.69	-0.87
salinity [PSU]	-	34.86–35.03	34.95	34.93	-	30.00–31.50	30.55	30.42	-	31.74–34.44	32.79	32.41
water depth [m]	-	220–2500	920	480	-	78–2600	558	235	-	2600–3200	2900	3000

¹ At sampling location N21/F5, the latitudinal transect from the European continent to the Arctic and the longitudinal transect across Fram Strait crossed. Consequently, this sample was used for evaluation of both sampling transects.

² Due to high blanks, no values can be reported for PFBA. In addition, PFPeA could not be evaluated because of matrix interferences.

^{3a-c} PFOS could not be evaluated in (a) two, (b) seven and (c) two of the samples because of matrix interferences. The given values refer to only the samples in which no interferences occurred.

⁴ ΣPFASs only includes the compounds with a detection frequency > 50 % in samples of the longitudinal sampling transect across Fram Strait (C₆–C₉ PFCAs, PFBS and HFPO-DA).

Table A.2-8: Concentrations [pg/L] of detected PFASs in surface seawater samples taken along a latitudinal transect from the European continent to the Arctic (57 °N to 79 °N at ~5 °E). Values in brackets are between MDL and MQL.

station ID	HFPO-DA	PFHxA	PFHpA	PFOA	PFNA	PFDA	PFUnDA	PFDoDA	PFBS	PFHxS	L-PFOS	Br-PFOS	ΣPFASs
N1	86	74	84	150	48	(16)	(12)	(6.0)	69	(52)	66	46	710
N2	94	110	88	140	45	(13)	(9.3)	<MDL	93	(50)	110	68	820
N3	52	110	67	120	49	(18)	13	(6.5)	57	(38)	100	53	680
N4	100	100	100	170	55	(20)	(9.6)	(5.0)	69	(54)	110	60	850
N5 ¹	120±8	93±5	92±2	140±10	49±2	(14±3)	(11±1)	<MDL	88±9	(53±3)	60±11	58±2	780±30
N6	33	70	44	76	39	(13)	(11)	<MDL	(39)	(23)	58	(27)	430
N7	23	53	28	50	37	(11)	14	(6.2)	(38)	(22)	83	35	400
N8	21	40	29	57	37	(13)	15	(7.5)	(38)	(22)	57	(27)	360
N9	26	58	32	30	35	(14)	(11)	(5.4)	(26)	(24)	60	(27)	380
N10	(19)	33	25	41	39	(15)	(10)	<MDL	(19)	(18)	(35)	(19)	270
N11	29	49	39	74	44	(19)	17	(10)	(25)	(19)	(40)	30	390
N12	26	31	22	47	33	(14)	(12)	(5.5)	(15)	<MDL	(32)	(15)	250
N13	21	29	30	55	45	(16)	16	(10)	(25)	<MDL	(28)	(15)	290
N14	(15)	44	26	53	36	(14)	(10)	(6.2)	(27)	<MDL	(29)	(19)	280
N15	(14)	(26)	24	42	31	(12)	(10)	(4.4)	(25)	<MDL	(27)	(15)	230
N16	<MDL	29	21	39	27	(10)	(6.5)	<MDL	(24)	<MDL	<MDL	<MDL	160
N17	<MDL	(17)	(20)	42	23	(8.8)	(8.2)	<MDL	(21)	<MDL	<MDL	<MDL	140
N18	(15)	(25)	(20)	43	26	(9.2)	(8.5)	<MDL	(28)	<MDL	(29)	(18)	220
N19	24	33	(20)	53	31	(12)	(11)	(4.4)	(25)	<MDL	(27)	(18)	260
N20	(20)	66	23	56	35	(9.7)	(6.8)	<MDL	(21)	<MDL	(30)	(13)	280
N21	21	51	24	37	22	(7.0)	(6.4)	(3.6)	(22)	<MDL	(24)	(19)	240

¹ Mean±SD is given for this sample, as a triplicate of the sample was analysed.

Table A.2-9: Concentrations [pg/L] of detected PFASs in surface seawater samples taken along a longitudinal transect across Fram Strait (9 °E to 18 °W at ~79 °N). Values in brackets are between MDL and MQL.

station ID	HFPO-DA	PFHxA	PFHpA	PFOA	PFNA	PFDA	PFUnDA	PFDoDA	PFBS	PFHxS	L-PFOS	Br-PFOS	ΣPFASs(DF>50 %) ²
F1	45	41	21	45	24	(7.1)	(6.7)	(3.6)	(29)	<MDL	(31)	(18)	205.8
F2	(14)	43	24	41	24	<MDL	(5.3)	<MDL	(25)	<MDL	(27)	(12)	171.0
F3	35	43	22	41	28	(8.2)	(7.1)	<MDL	(21)	<MDL	(33)	(16)	190.4
F4	29	39	28	48	29	<MDL	(5.0)	<MDL	(23)	<MDL	na ¹	na	196.2
F5(=N21)	21	51	24	37	22	(7.0)	(6.4)	(3.6)	(22)	<MDL	(24)	(19)	177.5
F6	<MDL	71	36	63	31	<MDL	<MDL	<MDL	56	<MDL	na	na	258.4
F7	(12)	67	37	48	32	<MDL	<MDL	<MDL	(38)	<MDL	na	na	234.5
F8	(11)	63	45	50	34	<MDL	<MDL	<MDL	(39)	(19)	na	na	241.6
F9	(11)	55	49	58	32	<MDL	<MDL	<MDL	(39)	<MDL	na	na	243.5
F10	<MDL	58	44	56	32	<MDL	<MDL	<MDL	(39)	<MDL	na	na	228.0
F11	38	62	47	54	33	<MDL	(5.4)	<MDL	(44)	<MDL	na	na	278.5
F12	(13)	78	46	58	35	<MDL	<MDL	<MDL	(40)	<MDL	na	na	269.3
F13	(13)	64	49	57	38	<MDL	(5.7)	<MDL	52	(24)	<MDL	<MDL	272.0
F14	(16)	52	54	65	32	<MDL	(4.8)	<MDL	(38)	<MDL	(37)	(13)	257.5
F15	24	69	58	64	32	<MDL	<MDL	<MDL	45	<MDL	(28)	(13)	291.5

¹na: not analyzable (PFOS could not be evaluated in these samples because of matrix interferences)

²ΣPFASs only includes the compounds with a detection frequency > 50 % in samples of the longitudinal sampling transect across Fram Strait (C₆-C₉ PFCAs, PFBS and HFPO-DA).

Table A.2-10: Concentrations [pg/L] of detected PFASs in surface seawater samples taken along a latitudinal transect along the prime meridian (78 °N to 81 °N at ~ 0 °EW). Values in brackets are between MDL and MQL.

station ID	HFPO-DA	PFHxA	PFHpA	PFOA	PFNA	PFDA	PFUnDA	PFDoDA	PFBS	PFHxS	L-PFOS	Br-PFOS	ΣPFASs(DF > 50 %) ²
P1	(15)	39	26	61	29	<MDL	(5.3)	<MDL	(23)	<MDL	(25)	(15)	193.3
P2	28	50	26	64	31	(8.1)	(7.4)	(5.0)	58	<MDL	(34)	(17)	228.9
P3	22	68	41	71	30	(6.9)	(5.3)	<MDL	64	(27)	na ¹	na	296.0
P4	31	75	54	91	33	(7.5)	(6.1)	<MDL	59	(25)	na	na	314.5
P5	70	57	48	77	36	(6.5)	(5.8)	<MDL	60	(23)	(35)	(21)	277.4

¹na: not analyzable (PFOS could not be evaluated in these samples because of matrix interferences)

²ΣPFASs only includes the compounds with a detection frequency > 50 % in samples of the longitudinal sampling transect across Fram Strait (C₆-C₉ PFCAs, PFBS and HFPO-DA).

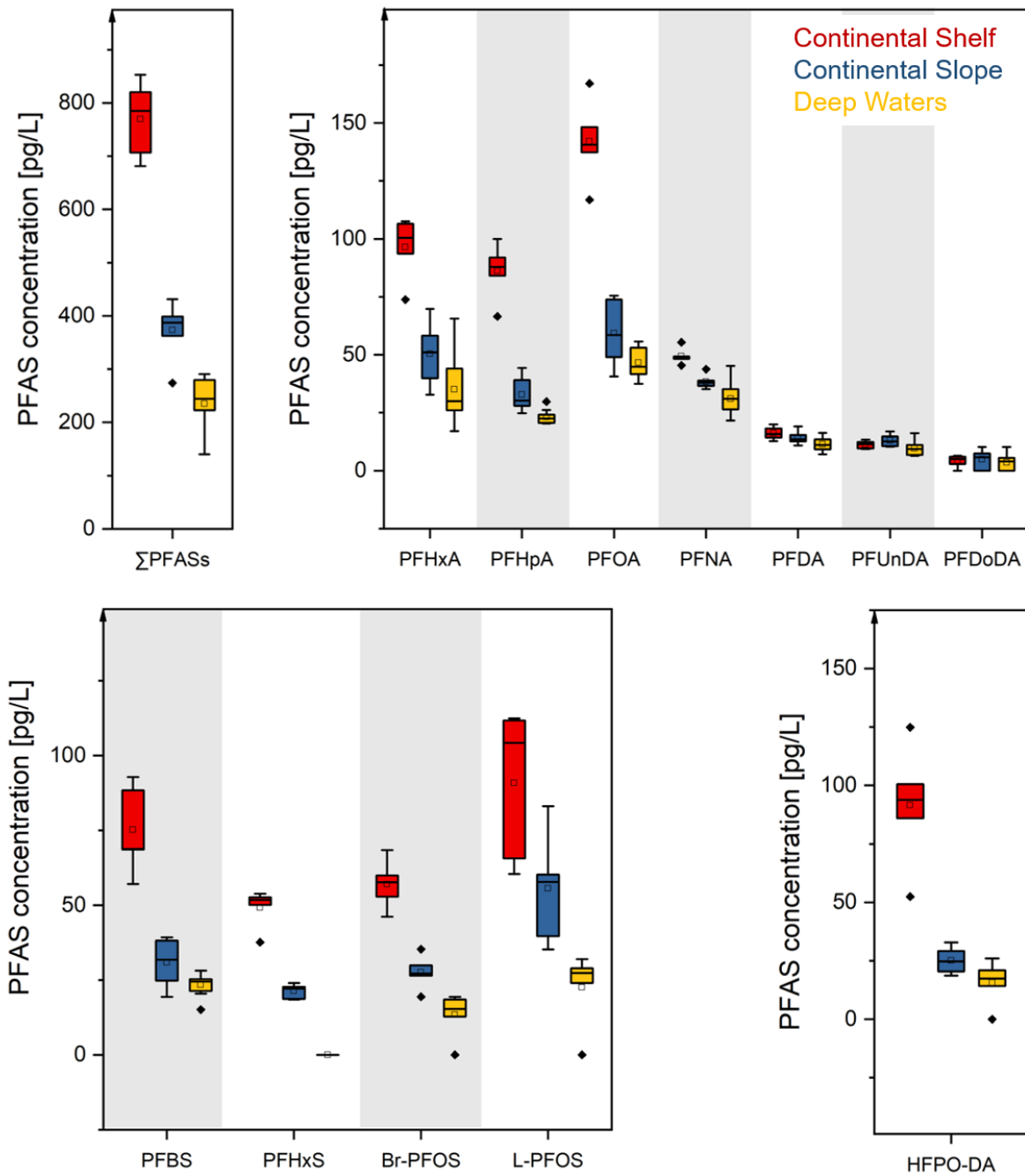


Figure A.2-4: Boxplots showing PFAS concentrations in surface water samples from the North Sea continental shelf (samples N1–N5, red), the continental slope (N6 to N11, blue) and deep water regions of the Norwegian Sea and Greenland Sea (N12 to N21, yellow). The box represents the 25 % to 75 % quartile, the median is plotted by the band inside the box and the mean by the blank square. The ends of the whiskers display the lowest and the highest concentration still within 1.5 IQR of the lower and higher quartile. Outliers are plotted with a black diamond.

Section A.2-2: Potential sources of HFPO-DA to European coastal waters

A fluoropolymer manufacturing plant in the Rhine-Meuse delta is assumed a major source of HFPO-DA in European coastal areas [100, 174, 358]. The manufacturer started to replace PFOA by HFPO-DA in the United States in 2005. No information is available on when HFPO-DA production and use started at the plant in the Rhine-Meuse delta, but PFOA emissions decreased strongly from 2002 on and ceased in 2012 [250]. Reanalysis of water sample extracts from the Rhine-Meuse delta showed that the compound had been present in 2008 already (Figure A.2-5 and Figure A.2-6). This indicates that at least since then, there have been HFPO-DA emissions into the European environment.

The emission permit of the fluoropolymer manufacturer in the Netherlands of HFPO-DA to surface water was 6400 kg/year from 2012 to 2017, before being lowered to 2035 kg/year in 2017 and to 148 kg/year in 2019 [250]. HFPO-DA concentrations up to 812 ng/L were reported for river water samples taken downstream of the chemical park in 2016 [174]. It can be hypothesized that HFPO-DA is transported from the Rhine-Meuse delta to North Sea coastal waters, from where radionuclide tracer studies suggest transit times of 2–3 years to Fram Strait [276].

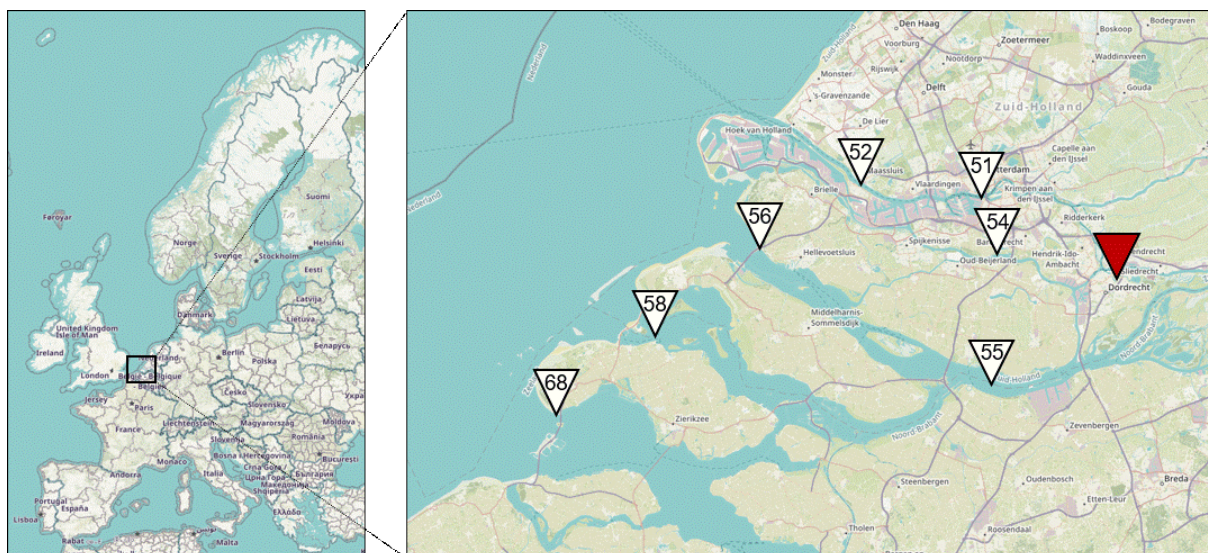


Figure A.2-5: Sampling locations of reanalysed samples, taken in the Rhine-Meuse delta in 2008 by Möller *et al.* [161]. The red triangle shows the fluoropolymer manufacturing plant, which is assumed to be a major source of HFPO-DA in European coastal areas. The replacement compound HFPO-DA has not yet been under discussion in 2008 and was not included in the analytical method. Results for legacy PFASs can be found in reference [161]. The basic map was taken from Openstreetmap (CC-BY-SA 2.0).

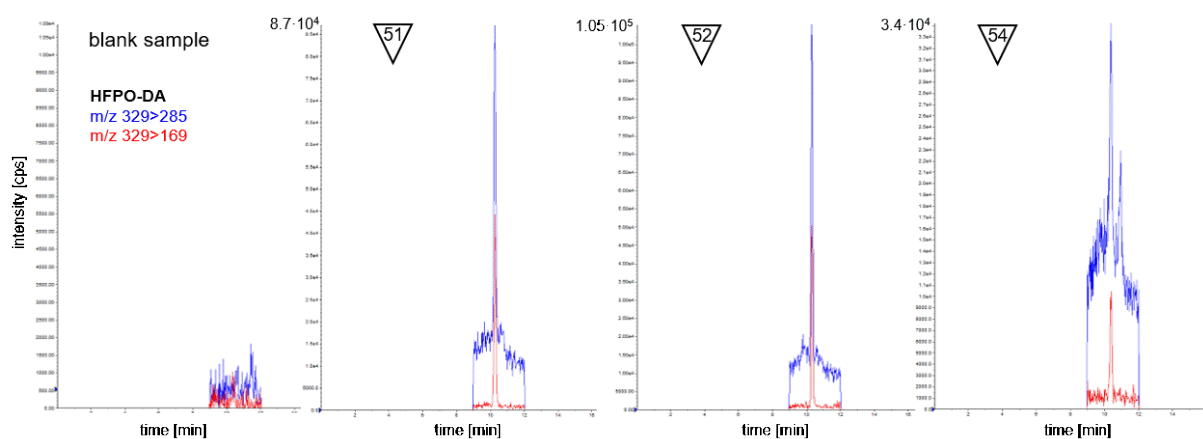


Figure A.2-6: LC-MS/MS chromatograms of the replacement compound HFPO-DA in sample extracts from 2008, reanalysed using the current instrumental method. The extracts had been stored in brown-glass vials at $-20\text{ }^{\circ}\text{C}$ for ten years. Before instrumental analysis, methanol was topped on to a volume of approximately $200\text{ }\mu\text{L}$. The vials were put into an ultrasonic bath for 30 min and vortexed for 5 min. Chromatograms are shown for the blank sample and the samples in which HFPO-DA was detected. In samples 55, 56, 58 and 68, HFPO-DA was not detected.

Table A.2-11: Pearson correlation coefficients r between physicochemical parameters and PFASs as well as among individual PFASs in surface water samples taken along a longitudinal transect across Fram Strait (9 °E to 18 °W at ~79 °N). Statistically significant values are marked with * ($p < 0.05$). Correlation analysis was conducted only for compounds with a detection frequency $> 50\%$ (C₆–C₉ PFCAs, PFBS and HFPO-DA).

	temperature	pH	salinity	PFHxA	PFHpA	PFOA	PFNA	PFBS	HFPO-DA	ΣPFASs (DF > 50 %)	PFHpA/PFNA
temperature	1										
pH	0.82*	1									
salinity	0.98*	0.85*	1								
PFHxA	-0.82*	-0.66*	-0.76*	1							
PFHpA	-0.90*	-0.91*	-0.91*	0.67*	1						
PFOA	-0.82*	-0.79*	-0.78*	0.62*	0.86*	1					
PFNA	-0.83*	-0.85*	-0.82*	0.70*	0.79*	0.71*	1				
PFBS	-0.87*	-0.70*	-0.80*	0.81*	0.73*	0.82*	0.75*	1			
HFPO-DA	0.56	0.42	0.52*	-0.52*	-0.38	-0.40	-0.39	-0.49	1		
ΣPFASs(DF > 50 %)	-0.88*	-0.84*	-0.85*	0.80*	0.89*	0.86*	0.83*	0.87*	-0.21	1	
PFHpA/PFNA	-0.79*	-0.83*	-0.80*	0.54*	0.94*	0.78*	0.52*	0.58*	-0.33	0.79*	1

Table A.2-12: Detection frequencies [%], concentration ranges [pg/L], mean concentrations [pg/L] and median values [pg/L] of detected PFASs in all samples and in different water masses (Atlantic Water (AW), Polar Surface Water (PSW)) of the seven depth profiles taken in Fram Strait. Values in brackets are between MDL and MQL.

PFASs ¹	all samples (<i>n</i> = 58)				Atlantic Water (AW) (<i>n</i> = 18)				Polar Surface Water (PSW) (<i>n</i> = 16)			
	DF [%]	range [pg/L]	mean [pg/L]	median [pg/L]	DF [%]	range [pg/L]	mean [pg/L]	median [pg/L]	DF [%]	range [pg/L]	mean [pg/L]	median [pg/L]
HFPO-DA	21	<MDL–(17)	-	-	39	<MDL–(14)	-	-	19	<MDL–(12)	-	-
PFHxA	91	<MDL–74	37	39	100	(25)–54	41	40	100	41–74	54	53
PFHpA	81	<MDL–56	24	24	100	(14)–32	25	26	100	26–56	42	44
PFOA	^{2a}	<MDL–120	49	50	^{2b}	44–72	55	52	^{2c}	48–120	76	60
PFNA	91	<MDL–51	25	26	100	(19)–39	31	29	100	(21)–51	31	28
PFDA	24	<MDL–(21)	-	-	56	<MDL–(16)	(7.8)	13	25	<MDL–(21)	-	-
PFUnDA	66	<MDL–15	(5.6)	(6.6)	78	<MDL–15	(7.2)	(8.0)	69	<MDL–14	(6.0)	(6.7)
PFBS	57	<MDL–50	16	17	61	<MDL–(34)	(13)	(16)	100	(21)–50	(36)	(37)
PFHxS	34	<MDL–(29)	-	-	17	<MDL–(28)	-	-	75	<MDL–(29)	(17)	(22)
L-PFOS	36	<MDL–44	-	-	83	<MDL–44	(22)	(23)	19	<MDL–(33)	-	-
Br-PFOS	43	<MDL–33	-	-	83	<MDL–27	(13)	(15)	38	<MDL–33	-	-
ΣPFASs(DF>50 %)³	-	<MDL–230	110	110	-	64–140	120	120	-	120–230	170	170

¹ Due to high blanks, no values can be reported for PFBA. In addition, PFPeA could not be evaluated because of matrix interferences.

² PFOA could not be evaluated in a) 29, b) 6, c) 11 of the samples because of matrix interferences. The given values refer to only the samples in which no interferences occurred.

³ ΣPFASs only includes the compounds with a detection frequency > 50 % in all depth profiles samples (C₆, C₇, C₉, C₁₁ PFCAs and PFBS).

Table A.2-13: Detection frequencies [%], concentration ranges [pg/L], mean concentrations [pg/L] and median values [pg/L] of detected PFASs in different water masses (Recirculating Atlantic Water/Arctic Atlantic Water (RAW/AAW), Intermediate Waters (IW) and Deep Waters (DW)) of the seven depth profiles taken in Fram Strait. Values in brackets are between MDL and MQL.

PFASs ¹	Recirculating Atlantic Water/Arctic Atlantic Water (RAW/AAW) (n = 10)				Intermediate Waters (IW) (n = 6)				Deep Waters (DW) (n = 8)			
	DF [%]	range [pg/L]	mean [pg/L]	median [pg/L]	DF [%]	range [pg/L]	mean [pg/L]	median [pg/L]	DF [%]	range [pg/L]	mean [pg/L]	median [pg/L]
HFPO-DA	20	<MDL-(17)	-	-	0	<MDL	-	-	0	<MDL	-	-
PFHxA	100	(22)–66	34	30	100	(14)–43	28	28	38	<MDL-(20)	-	-
PFHpA	90	<MDL–46	(21)	(20)	50	<MDL–19	8.5	8.0	13	<MDL-(20)	-	-
PFOA	2a	36–94	54	48	2b	34–50	40	37	2c	<MDL	-	-
PFNA	100	(14)–34	22	(20)	100	(16)–26	(21)	20	38	<MDL-(19)	-	-
PFDA	0	<MDL	-	-	0	<MDL	-	-	0	<MDL	-	-
PFUnDA	70	<MDL-(10)	(5.1)	(6.1)	67	<MDL–13	(6.1)	(7.1)	25	<MDL-(7.3)	-	-
PFBS	30	<MDL-(33)	-	-	50	<MDL-(25)	(10)	(7.0)	0	<MDL	-	-
PFHxS	40	<MDL-(23)	-	-	17	<MDL-(23)	-	-	0	<MDL	-	-
L-PFOS	10	<MDL-(33)	-	-	33	<MDL-(36)	-	-	0	<MDL	-	-
Br-PFOS	20	<MDL–31	-	-	33	<MDL-(17)	-	-	0	<MDL	-	-
ΣPFASs (DF > 50 %)	-	60–180	90	76	-	40–120	73	73	-	<MDL–40	16	13

¹ Due to high blanks, no values can be reported for PFBA. In addition, PFPeA could not be evaluated because of matrix interferences.

² PFOA could not be evaluated in a) 4, b) 3, c) 4 of the samples because of matrix interferences. The given values refer to only the samples in which no interferences occurred.

³ ΣPFASs only includes the compounds with a detection frequency > 50 % in all depth profiles samples (C₆, C₇, C₉, C₁₁ PFCAs and PFBS).

Table A.2-14: Concentrations [pg/L] of detected PFASs in depth profiles. Values in brackets are between MDL and MQL.

sample name	sampling depth	water mass	HFPO-DA	PFHxA	PFHpA	PFOA	PFNA	PFDA	PFUnD	PFBS	PFHxS	L-PFOS	Br-PFOS	ΣPFASs (DF > 5 0%) ²
V1/1	1239	DW	<MDL	<MDL	<MDL	na ¹	<MDL	<MDL	<MDL	<MDL	<MDL	<MDL	<MDL	0.0
V1/2	1000	DW	<MDL	(20)	(20)	na	<MDL	<MDL	<MDL	<MDL	<MDL	<MDL	<MDL	40.0
V1/3	500	AW	<MDL	(25)	(21)	na	(19)	<MDL	<MDL	<MDL	<MDL	<MDL	<MDL	64.7
V1/4	250	AW	<MDL	33	24	na	24	<MDL	<MDL	<MDL	<MDL	<MDL	<MDL	81.7
V1/5	100	AW	<MDL	28	26	na	23	<MDL	<MDL	(34)	<MDL	<MDL	<MDL	110.5
V1/6	75	AW	<MDL	41	24	na	34	(14)	(8.1)	<MDL	<MDL	(26)	(17)	106.8
V1/7	50	AW	<MDL	36	29	na	28	(13)	(6.4)	<MDL	<MDL	(23)	(16)	99.2
V1/8	10	AW	<MDL	32	26	na	29	(15)	(8.1)	(20)	<MDL	(21)	(13)	114.7
V2/1	2286	DW	<MDL	<MDL	<MDL	<MDL	<MDL	<MDL	(7.1)	<MDL	<MDL	<MDL	<MDL	7.1
V2/2	1000	IW	<MDL	30	<MDL	37	26	<MDL	13	(21)	<MDL	<MDL	<MDL	89.4
V2/3	500	AW	<MDL	35	(14)	44	35	<MDL	(9.2)	(18)	<MDL	(28)	(16)	110.6
V2/4	250	AW	<MDL	53	21	52	34	(13)	(8.0)	(16)	<MDL	(24)	(13)	132.7
V2/5	100	AW	<MDL	43	31	50	39	(16)	14	(15)	<MDL	(21)	(16)	141.9
V2/6	75	AW	<MDL	50	32	67	31	(14)	(11)	<MDL	<MDL	(22)	(13)	124.3
V2/7	40	AW	(11)	39	24	55	34	(14)	(10)	<MDL	<MDL	(27)	(13)	107.4
V2/8	10	AW	(9.9)	54	28	60	38	(15)	(15)	<MDL	<MDL	(44)	(27)	135.6
V3/1	2573	DW	<MDL	<MDL	<MDL	<MDL	<MDL	<MDL	<MDL	<MDL	<MDL	<MDL	<MDL	0.0
V3/2	1001	IW	<MDL	37	(15)	34	(18)	<MDL	(9.8)	<MDL	<MDL	(36)	(17)	80.2
V3/3	501	AW	<MDL	32	(19)	48	28	<MDL	(10)	(19)	<MDL	(21)	(13)	107.6
V3/4	250	AW	(14)	48	29	52	38	(14)	(12)	(15)	<MDL	(21)	(15)	142.5
V3/5	100	AW	(14)	45	27	48	29	<MDL	<MDL	(21)	(21)	(23)	(16)	122.8
V3/6	75	AW	(13)	47	32	72	29	<MDL	(6.6)	(21)	(20)	(22)	(18)	135.2
V3/7	50	AW	(11)	53	23	62	27	<MDL	(6.6)	(28)	(28)	(23)	(16)	138.9
V3/8	10	AW	(8.0)	39	26	46	29	(13)	(5.0)	(30)	<MDL	(40)	(20)	129.6
V4/1	2600	DW	<MDL	<MDL	<MDL	na	(19)	<MDL	<MDL	<MDL	<MDL	<MDL	<MDL	19.2
V4/2	2000	DW	<MDL	(14)	<MDL	na	(12)	<MDL	<MDL	<MDL	<MDL	<MDL	<MDL	26.4
V4/3	1200	IW	<MDL	(14)	<MDL	na	(18)	<MDL	<MDL	(14)	<MDL	<MDL	<MDL	46.2
V4/4	1000	IW	<MDL	(26)	(19)	na	21	<MDL	<MDL	<MDL	<MDL	<MDL	<MDL	65.8
V4/5	700	RAW/AAW	<MDL	(22)	(15)	na	(20)	<MDL	<MDL	<MDL	<MDL	<MDL	<MDL	56.7
V4/6	500	RAW/AAW	<MDL	(23)	(18)	na	25	<MDL	(10)	<MDL	<MDL	<MDL	<MDL	75.5
V4/7	250	RAW/AAW	<MDL	28	(19)	na	22	<MDL	(7.8)	<MDL	<MDL	<MDL	<MDL	76.6
V4/8	100	PW	<MDL	41	26	na	25	<MDL	(7.2)	(23)	(22)	<MDL	<MDL	122.8
V4/9	75	PW	<MDL	48	28	na	27	<MDL	(6.3)	(21)	(24)	(22)	(17)	130.3
V4/10	60	PW	<MDL	51	41	na	26	<MDL	(5.6)	(38)	(25)	<MDL	<MDL	161.8
V4/11	40	PW	<MDL	56	40	na	28	<MDL	(9.0)	(32)	(23)	<MDL	<MDL	165.6

V4/12	15	PW	<MDL	59	45	na	36	<MDL	(6.1)	(24)	(23)	<MDL	<MDL	169.5
V4/13	5	PW	<MDL	42	56	na	44	(14)	13	(31)	<MDL	<MDL	<MDL	186.2
V5/1	959	IW	<MDL	(16)	<MDL	na	(16)	<MDL	(4.9)	<MDL	<MDL	<MDL	<MDL	37.7
V5/2	500	RAW/AAW	<MDL	(25)	(16)	na	(18)	<MDL	(5.7)	<MDL	<MDL	<MDL	<MDL	65.2
V5/3	250	RAW/AAW	<MDL	(24)	22	na	(20)	<MDL	(7.5)	<MDL	(19)	<MDL	<MDL	73.8
V5/4	100	PW	<MDL	48	31	na	26	<MDL	(8.6)	(36)	(19)	<MDL	<MDL	148.8
V5/5	75	PW	<MDL	52	41	na	(21)	<MDL	<MDL	47	(18)	<MDL	<MDL	160.0
V5/6	50	PW	<MDL	46	50	na	24	<MDL	<MDL	(38)	(25)	<MDL	<MDL	157.5
V5/7	26	PW	<MDL	54	51	na	34	<MDL	(7.7)	(35)	(22)	<MDL	<MDL	182.1
V5/8	5	PW	<MDL	44	46	na	51	(21)	(14)	(28)	(25)	<MDL	<MDL	183.8
V6/1	271	RAW/AAW	<MDL	36	<MDL	36	(14)	<MDL	<MDL	(23)	<MDL	<MDL	<MDL	72.8
V6/2	150	RAW/AAW	(8.4)	44	23	39	(19)	<MDL	<MDL	(33)	<MDL	<MDL	(20)	117.6
V6/3	100	PW	(12)	57	32	48	21	<MDL	<MDL	(44)	<MDL	<MDL	(17)	153.8
V6/4	50	PW	(9.2)	61	47	60	27	<MDL	<MDL	(42)	<MDL	<MDL	(17)	177.7
V6/5	10	PW	(9.8)	56	47	51	28	<MDL	<MDL	(43)	<MDL	<MDL	(12)	174.0
V7/1	3117	DW	<MDL	<MDL	<MDL	<MDL	<MDL	<MDL	<MDL	<MDL	<MDL	<MDL	<MDL	0.0
V7/2	2000	DW	<MDL	(15)	<MDL	<MDL	(14)	<MDL	(7.3)	<MDL	<MDL	<MDL	<MDL	36.4
V7/3	1000	IW	<MDL	43	(17)	50	24	<MDL	(9.2)	(25)	(23)	(22)	(13)	118.7
V7/4	500	RAW/AAW	<MDL	33	22	48	(20)	<MDL	(6.5)	<MDL	(20)	<MDL	<MDL	81.6
V7/5	250	RAW/AAW	(17)	36	32	52	31	<MDL	(5.6)	<MDL	(20)	<MDL	<MDL	105.0
V7/6	100	RAW/AAW	<MDL	66	46	94	34	<MDL	(7.7)	(21)	(23)	(33)	31	175.0
V7/7	50	PW	<MDL	74	43	120	39	(12)	(9.4)	45	(29)	(30)	(26)	210.9
V7/8	10	PW	<MDL	73	55	110	41	(11)	(8.2)	50	(19)	(33)	33	226.1

¹na: not analyzable (PFOA could not be evaluated these samples because of matrix interferences)

²ΣPFASs only includes the compounds with a detection frequency > 50 % in all depth profiles samples (C₆, C₇, C₉, C₁₁ PFCAs and PFBS).

Table A.2-15: Water mass definitions used for classification of water samples taken for this study, adapted from Rudels *et al.* [287]. Boundaries of potential temperature Θ [°C] and potential density σ [kg/m³] are given. σ_0 and σ_{500} is potential density at reference pressure 0 m (sea surface) and 500 m. Deviating from the definition by Rudels *et al.* [287], water with a potential density σ lower than 27.70 kg/m³ is included in the definition of Atlantic Water to also classify surface water in the West Spitsbergen Current as Atlantic Water. Moreover, our water mass definitions do not differentiate between Recirculating Atlantic Water and Arctic Atlantic Water and between different classes of Intermediate Water and Deep Water.

Water mass (acronym)	Definition
Atlantic Water (AW)	$0 < \Theta, \sigma_0 \leq 27.97$
Polar Surface Water (PSW)	$\Theta \leq 0, \sigma_0 \leq 27.70$
Recirculating and Arctic Atlantic Water (RAW/AAW)	$0 < \Theta, 27.70 < \sigma_0, \sigma_{500} \leq 30.444$
Intermediate Water (IW)	$\Theta \leq 0, 27.97 < \sigma_0, \sigma_{500} \leq 30.444$
Deep Water (DW)	$\Theta \leq 0, 30.444 \leq \sigma_{500}$

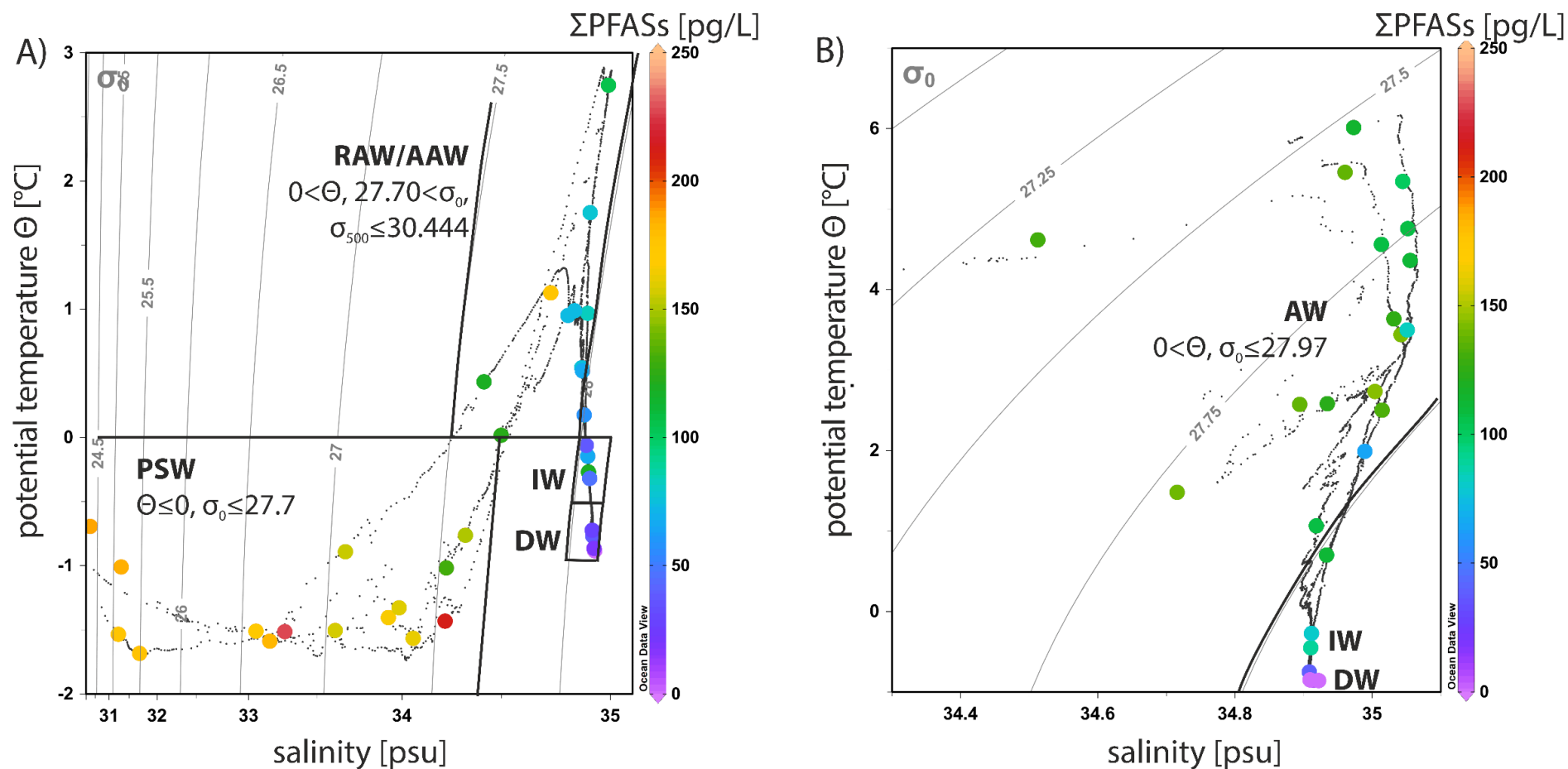


Figure A.2-7: Potential temperature θ [°C] versus salinity [psu] plots for A) CTD/rosette casts taken west of the surface front between inflowing Atlantic Water (AW) and outflowing Polar Surface Water (PSW) ($\sim 79^\circ\text{N}$) and B) CTD/rosette casts taken east of it. Note that in order to show the vast range of salinity values, the x-scale in A) is non-linear and in B) it is a zoom on the Atlantic water masses that is linear. Temperature and salinity data was taken from references [290] and [353]. Samples analysed for PFASs are colour-coded depending on the sum of PFASs with a detection frequency $> 50\%$ (C_6, C_7, C_9, C_{11} PFCAs and PFBS). Thin grey contour lines show potential density isopycnals referenced to 0 dbar (σ_0 [kg/m³]). Solid black lines highlight water mass boundaries. Water mass definitions for AW, PSW, Recirculating/Arctic Atlantic Water (RAW/AAW), Intermediate Water (IW; $\Theta \leq 0, 27.97 < \sigma_0, \sigma_{500} \leq 30.444$) and Deep Water (DW; $\Theta \leq 0, 30.444 \leq \sigma_{500}$) were adapted from reference [287] (Table A.2-15). Data were plotted using Ocean Data View [291].

Table A.2-16: PFAS mass transport estimates through Fram Strait via the boundary currents, based on water transport data derived from MITgcm model (Section A.2-1). All values < MDL were replaced by a) zero (blue), b) $\sqrt{2}/2$ times the MDL (yellow) c) the MDL (green) to calculate the mean value for each water mass. To calculate the PFAS transport, the mean PFAS concentration of AW, PW and RAW/AAW was multiplied by the transported water volume of the particular water mass, derived from the MITgcm. Positive values describe northward fluxes into the Arctic Ocean, whereas negative values describe southward fluxes to the Nordic Seas. Italicized values are derived from datasets with detection frequencies < 50 %. If detection frequency of a compound was 100 % in a specific water mass, only one mass transport estimate is given.

Estimated transport through Fram Strait (mean±SD) [kg/y]												
water mass	Substitution of values <MDL	PFHxA	PFHpA	PFOA	PFNA	PFDA	PUnDA	PFBS	PFHxS	L-PFOS	Br-PFOS	HFPO-DA
AW	0					920±852	850±553	1546±1393	446±1041	2536±1383	1587±827	523±629
	$\sqrt{2}/2$ *MDL	4819±1058	2984±560	6446±1026	3595±656	1159±580	919±446	1980±912	1719±475	2833±886	1753±520	829±450
	MDL					1258±468	947±407	2160±746	2247±267	2956±769	1822±431	956±353
PW	0					-69±130	-116±92		-330±204	-102±224	-148±215	-37±80
	$\sqrt{2}/2$ *MDL	-1043±190	-819±176	-1471±624	-603±166	-136±93	-132±72	-697±170	-393±100	-340±1120	-251±143	-104±47
	MDL					-163±78	-138±64		-419±65	-438±67	-293±117	-131±34
RAW/AAW	0		-			0±0	-	-932±1545	-998±1295	-403±1275	-615±1329	-302±677
	$\sqrt{2}/2$ *MDL	-	2557±1439	-		-	616±453	-1733±1017	-1938±497	-2047±698	-1435±913	-713±479
	MDL	4069±1618	2657±1265	6512±2843	-2705±741	-551±0	712±313	-2065±807	-2328±196	-2728±458	-1774±746	-883±403
Net	0		-392			851	118	-83	-882	2030	824	184
	$\sqrt{2}/2$ *MDL	-292	-492	-1537	287	472	75	-450	-612	445	68	12
	MDL		-534			315	58	-602	-500	-211	-245	-59

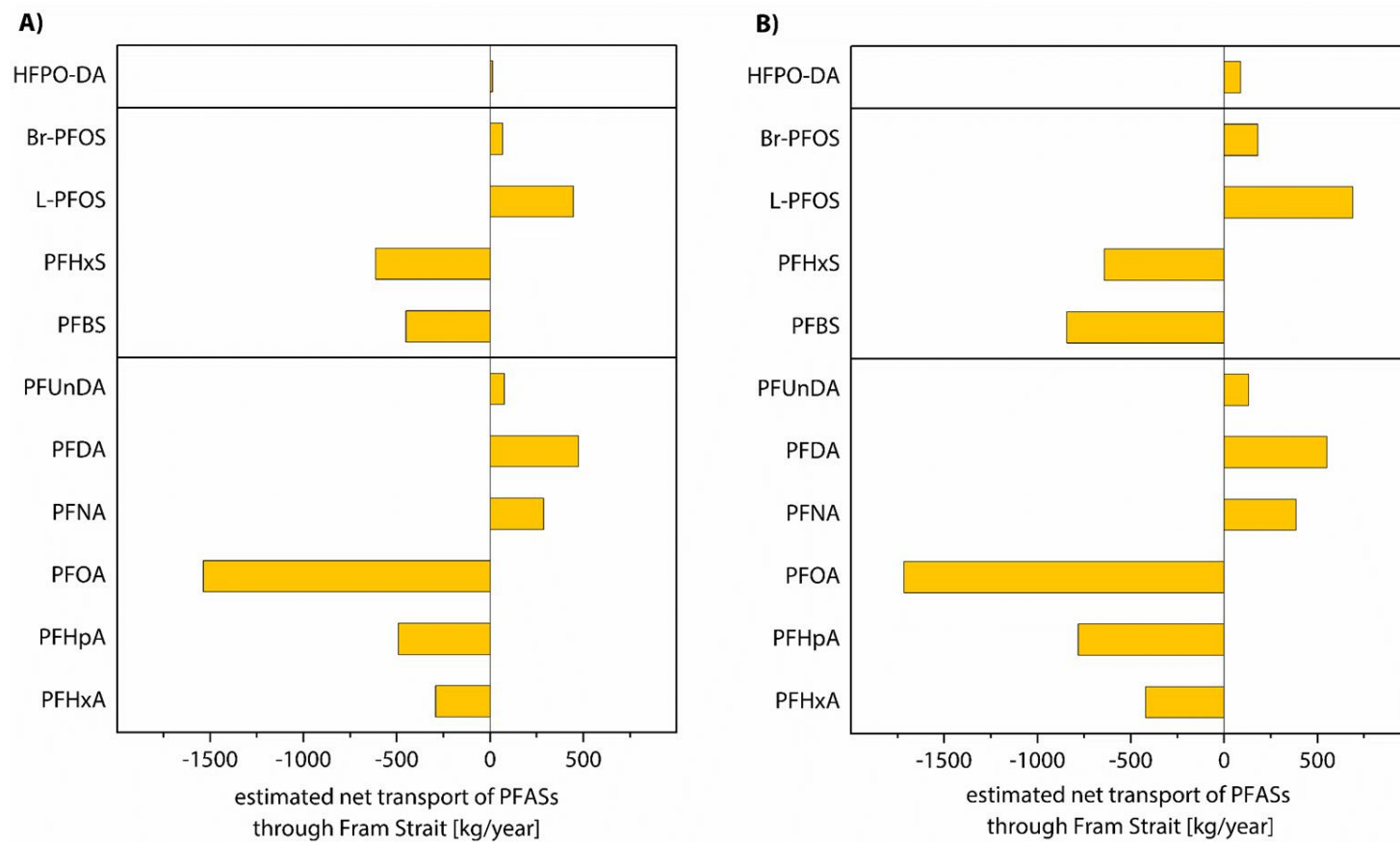


Figure A.2-8: Comparison of estimated net transport of PFASs through Fram Strait via the boundary columns, calculated by combining measured PFAS concentrations in this study with average water volume transport derived from A) the MITgcm ECCO v4 and B) observational data (mooring array) (Section A.2-1).

A.3 Supplementary to Chapter 7

Table A.3-1: Sampling locations and results of physicochemical parameters for surface water samples collected from German rivers.

station ID	river	latitude °N	longitude °E	date time of sampling	TOP ¹	SUS ¹	temp. ² [°C]	pH	sal. ³ [PSU]
AZ_001	Alz	48.152	12.655	13.09.2018 18:38	x	x	19.5	8.5	0.1
AZ_002	Alz	48.171	12.731	13.09.2018 17:58	x	x	19.5	8.2	0.1
AZ_003	Alz	48.179	12.744	13.09.2018 17:14	x	x	22.3	8.3	0.3
AZ_004	Alz	48.194	12.773	13.09.2018 16:31	x		21.5	8.6	0.2
AZ_005	Alz	48.262	12.809	13.09.2018 15:42	x		20.1	8.8	0.2
AZ_006	Inn	48.257	12.763	13.09.2018 12:47	x		16.7	7.8	0.0
AZ_007	Inn	48.249	12.844	13.09.2018 14:37	x		17.1	7.9	0.0
AZ_008	Salzach	48.193	12.862	14.09.2018 09:55	x		19.4	8.3	0.1
RU_001	Ruhr	51.417	7.210	10.09.2018 09:56			18.8	8.0	0.2
RU_002	Ruhr	51.410	7.079	10.09.2018 11:45			20.8	7.8	0.2
RU_003	Ruhr	51.381	6.902	10.09.2018 12:55		x	20.3	7.7	0.2
RU_004	Ruhr	51.408	6.894	10.09.2018 13:42			20.1	7.6	0.2
RU_005	Ruhr	51.449	6.793	10.09.2018 15:24			20.1	7.6	0.2
RU_006	Ruhr	51.443	6.754	10.09.2018 16:13	x	x	20.3	8.3	0.2
RU_007	Rhine	51.470	6.716	10.09.2018 17:15	x		21.9	8.0	0.2
RU_008	Rhine	51.435	6.715	10.09.2018 18:10	x	x	21.6	8.0	0.2
RH_001	Rhine	50.896	7.022	11.09.2018 16:05			22.8	7.7	0.2
RH_002	Rhine	50.984	6.987	11.09.2018 09:30	x	x	20.9	8.0	0.2
RH_003	Rhine	51.031	6.968	11.09.2018 10:22			21.2	7.8	0.2
RH_004	Rhine	51.057	6.916	11.09.2018 11:26	x	x	21.7	7.7	0.2
RH_005	Rhine	51.097	6.880	11.09.2018 13:29			22.1	7.8	0.2
RH_006	Wupper	51.051	6.966	11.09.2018 12:32			17.8	7.7	0.1
REF	Lahn	50.319	7.734	11.09.2018 18:30	x	x	20.4	7.9	0.3
MA_001	Main	50.130	8.837	12.09.2018 16:53	x		23.5	8.3	0.3
MA_002	Main	50.094	8.571	12.09.2018 15:26			23.0	8.4	0.3
MA_003	Main	50.076	8.522	12.09.2018 14:21	x		23.3	8.3	0.4
MA_004	Main	50.018	8.452	12.09.2018 12:42	x	x	22.7	8.3	0.4
MA_005	Main	49.999	8.354	12.09.2018 11:50	x		21.3	8.3	0.4
MA_006	Rhine	49.971	8.328	12.09.2018 10:52	x	x	22.6	7.8	0.1
MA_007	Rhine	50.006	8.280	12.09.2018 09:52	x	x	20.2	8.3	0.3

¹TOP/SUS: An “x” marks sampling locations at which samples for TOP assay analysis and suspect screening were taken. Target analysis was performed for samples from all sampling locations.

²temperature; ³salinity

Table A.3-2: Sampling locations and results of physicochemical parameters for surface water samples collected from Chinese rivers.

station ID	river	latitude °N	longitude °E	date time of sampling	TOP ¹	SUS ²	temp. ² [°C]	pH	sal. ³ [PSU]
XQ_001	Xiaoqing	37.066	117.892	11.11.2018 14:12			13.2	8.3	1.1
XQ_002	Xiaoqing	37.085	117.990	11.11.2018 13:13			14.0	8.3	1.3
XQ_003	D. Zhul. ⁴	36.891	118.038	11.11.2018 08:30	x	x	17.1	7.8	1.5
XQ_004	D. Zhul.	36.973	118.041	11.11.2018 09:33			17.3	8.1	1.5
XQ_005	D. Zhul.	36.998	118.034	11.11.2018 10:32	x	x	17.3	8.1	0.8
XQ_006	D. Zhul.	37.041	118.046	11.11.2018 11:29	x	x	17.1	8.1	1.5
XQ_007	D. Zhul.	37.095	118.048	11.11.2018 12:04			16.4	8.1	1.4
XQ_008	Xiaoqing	37.111	118.111	11.11.2018 15:37			13.8	8.2	1.4
XQ_009	Xiaoqing	37.118	118.190	11.11.2018 16:23			14.7	8.3	1.7
FX_001	Xi	41.990	121.608	15.11.2018 08:21	x	x	4.2	8.8	0.6
FX_002	Xi	41.960	121.586	15.11.2018 09:11			12.1	8.0	0.6
FX_002S	Xi	41.960	121.586	15.11.2018 09:02			6.7	8.0	0.7
FX_003	Xi	41.947	121.579	15.11.2018 10:05			12.6	8.7	0.3
FX_004	Xi	41.940	121.580	15.11.2018 10:44	x	x	12.1	8.7	0.6
FX_005	Xi	41.903	121.561	15.11.2018 11:30	x	x	10.0	8.7	0.6
FX_006	Xi	41.835	121.576	15.11.2018 14:59			8.2	8.7	0.8
FX_007	Yimatu	41.863	121.510	15.11.2018 12:31			3.7	8.8	0.5
FX_008	Yimatu	41.830	121.525	15.11.2018 13:15			4.3	8.5	1.0
FX_009	Xi	41.802	121.537	15.11.2018 13:56	x	x	6.8	8.8	0.7
YZ_001	Yangtze	31.885	120.813	21.11.2018 09:25	x	x	16.5	8.7	0.2
YZ_002	Fushan	31.801	120.816	21.11.2018 10:25			14.7	8.4	0.3
YZ_003	Fushan	31.814	120.829	21.11.2018 11:00	x		15.5	8.3	0.2
YZ_004	Yangtze	31.792	120.806	21.11.2018 14:00	x	x	15.0	8.5	0.2
YZ_005	Yangtze	31.784	120.816	21.11.2018 11:55			16.0	8.5	0.2
YZ_006	Yangtze	31.786	120.814	21.11.2018 14:18	x	x	na ⁴	na	na
YZ_007	Wangyu	31.775	120.813	21.11.2018 12:25			15.8	8.5	0.2
YZ_008	Yangtze	31.765	120.875	21.11.2018 15:36			16.6	8.5	0.2
YZ_009	Yangtze	31.753	120.958	21.11.2018 16:30			18.7	8.5	0.2

¹TOP/SUS: An “x” marks sampling locations at which samples for TOP assay analysis and suspect screening were taken. Target analysis was performed for samples from all sampling locations.

²temperature; ³salinity; ⁴na = not analysable

⁴D. Zhul. = Dong Zhulong River

Table A.3-3: Categorization of samples for target analysis.

expected concentration range ¹	sample volume taken for extraction	samples
< 1 ng/L to ~100 ng/L	1 L	samples from Germany, except for AZ_003, AZ_004, AZ_005
up to 200 ng/L	500 mL	AZ_003, AZ_004, AZ_005 XQ_001 to XQ_004 FX_001, FX_007 YZ_001 to YZ_009
up to 1000 ng/L	100 mL	FX_002 to FX_006, FX_008 and FX_009
up to 100,000 ng/L	1 mL diluted in 250 mL ultrapure water	XQ_005 to XQ_009

¹ Based on concentrations reported in previous studies: German samples: Möller *et al.*, 2010; Heydebreck *et al.*, 2015 and own data, not published; site XQ: Heydebreck *et al.*, 2015; Shi *et al.*, 2015; site FX: Wang *et al.*, 2015; Chen *et al.*, 2018; site YZ: Jin *et al.*, 2015.

Section A.3-1: Implementation of three additional precursors in the analytical method

For validation of the TOP assay, Thekla-Regine Schramm implemented three additional sulfonamide-containing precursors (*N*-EtFOSE, *N*-EtFOSAA, *N*-EtFOSA) and one internal standard (*d9-N*-EtFOSE) in the instrumental method. Information on the analytical standards and the optimized mass-spectrometric parameters is provided in Table 10.1-3 and Table 10.2-4. The analytical method was not fully validated for these compounds, but matrix spike recoveries were (103±3)% and (86±3)% for *N*-EtFOSE and *N*-EtFOSAA, respectively, showing that the method is generally suitable for these compounds. Consequently, they substances were also measured when analysing the river water samples taken up- and downstream of potential point sources.

Table A.3-4: Percentage absolute recoveries of internal standards in river water samples analysed by target analysis ($n = 58$) and TOP assay ($n = 31$).

internal standard	mean absolute recovery \pm SD [%]	
	target analysis and unoxidized aliquots TOP assay	oxidized aliquots TOP assay
$^{13}\text{C}_4$ -PFBA	34 \pm 15	28 \pm 16
$^{13}\text{C}_2$ -PFHxA	49 \pm 15	29 \pm 15
$^{13}\text{C}_4$ -PFOA	56 \pm 14	30 \pm 13
$^{13}\text{C}_5$ -PFNA	58 \pm 15	27 \pm 12
$^{13}\text{C}_2$ -PFDA	57 \pm 17	25 \pm 9
$^{13}\text{C}_2$ -PFUnDA	54 \pm 20	20 \pm 7
$^{13}\text{C}_2$ -PFDoDA	47 \pm 19	17 \pm 5
$^{13}\text{C}_4$ -PFBS	50 \pm 17	63 \pm 19
$^{18}\text{O}_2$ -PFHxS	60 \pm 15	47 \pm 15
$^{13}\text{C}_4$ -PFOS	55 \pm 14	35 \pm 10
$^{13}\text{C}_3$ -HFPO-DA	56 \pm 28	43 \pm 14
$^{13}\text{C}_2$ -4:2 FTSA	79 \pm 30	49 \pm 19
$^{13}\text{C}_2$ -8:2 FTSA	62 \pm 30	29 \pm 10
$^{13}\text{C}_8$ -FOSA	44 \pm 18	20 \pm 7
d9-N-EtFOSE	50 \pm 34	10 \pm 5

Table A.3-5: Method detection limits (MDLs) [ng/L] and method quantification limits (MQLs) [ng/L] for target analysis.¹

campaign sample extraction	German rivers (09/2018) HZG ²		Chinese rivers (11/2018) YIC ³					
	1 L		500 mL		100 mL		1 mL	
compound	MDL	MQL	MDL	MQL	MDL	MQL	MDL	MQL
PFBA	0.14	0.33	0.20	0.52	0.39	1.3	39	130
PFPeA	0.032	0.085	0.25	0.70	0.72	2.4	45	150
PFHxA	0.083	0.28	0.19	0.63	1.0	3.5	93	310
L-PFHpA	0.015	0.050	0.043	0.11	0.20	0.67	31	100
Br-PFHpA	0.015	0.050	0.028	0.094	0.20	0.67	31	100
L-PFOA	0.050	0.17	4.7	13	4.7	13	110	370
Br-PFOA	0.050	0.17	0.53	1.8	0.53	1.8	110	370
PFNA	0.033	0.084	0.13	0.40	0.16	0.53	16	53
PFDA	0.033	0.087	0.12	0.33	0.18	0.59	21	71
PFUnDA	0.023	0.051	0.077	0.21	0.077	0.21	12	41
PFDoDA	0.029	0.073	0.051	0.12	0.083	0.28	23	76
PFTrDA	0.048	0.16	0.10	0.32	0.48	1.6	48	160
PFTeDA	0.0082	0.027	0.016	0.054	0.082	0.27	8	27
PFBS	0.037	0.12	0.12	0.39	0.75	2.5	34	110
L-PFHxS	0.087	0.29	0.048	0.16	0.30	0.99	30	99
Br-PFHxS	0.087	0.29	0.048	0.16	0.30	0.99	30	99
PFHpS	0.049	0.16	0.060	0.20	0.37	1.2	37	120
L-/Br-PFOS	0.074	0.25	0.048	0.16	0.15	0.49	15	49
PFDS	0.032	0.11	0.065	0.22	0.32	1.1	32	110
PFECHS	0.029	0.098	0.059	0.20	0.29	0.98	29	98
HFPO-DA	0.010	0.034	0.031	0.10	0.22	0.73	23	78
DONA	0.013	0.035	0.019	0.061	0.093	0.31	9	31
6:2 Cl-PFESA	0.0070	0.023	0.014	0.047	0.037	0.12	4	12
8:2 Cl-PFESA	0.011	0.033	0.015	0.050	0.075	0.25	8	25
6:6 PFPiA	0.0068	0.023	0.014	0.045	0.068	0.23	7	23
6:8 PFPiA	0.013	0.042	0.026	0.084	0.13	0.42	13	42
4:2 FTSA	0.030	0.10	0.060	0.20	0.30	1.0	30	100
6:2 FTSA	0.063	0.21	0.11	0.35	0.53	1.8	53	180
8:2 FTSA	0.072	0.24	0.14	0.48	0.72	2.4	72	240
L-FOSA	0.012	0.017	0.012	0.040	0.070	0.23	7	23
Br-FOSA	0.003	0.011	0.0068	0.023	0.034	0.11	3	11
N-EtFOSE	0.010	0.033	0.020	0.066	0.10	0.33	10	33
N-EtFOSAA	0.0094	0.031	0.019	0.063	0.094	0.31	9	31

¹ For compounds present in blanks, MDLs and MQLs were calculated as the average blank value plus 3 or 10 times the standard deviation, respectively (blue). For PFASs other than these, the MDLs and MQLs were derived from a signal-to-noise ratio of 3 or 10, respectively, observed in low-level samples (green) or spiked matrix samples (yellow). MDLs and MQLs marked in orange were calculated based on the results for a different sample volume.

² HZG: laboratories at Helmholtz-Zentrum Geesthacht, Germany

³ YIC: laboratories at Yantai Institute of Coastal Zone Research, China

Table A.3-6: Conversion yields of model precursors derived from oxidation tests in this study compared to data from literature.¹

	[persulfate] ₀	[NaOH] ₀	[precursor] ₀	sample volume	PFPrA	PFBA	PFPeA	PFHxA	PFHpA	PFOA
6:2 FTSA										
this study ²	60 mM	150 mM	15 ng/L	125 mL	³	25±4	32±2	31±1	3±1	
Houtz and Sedlak (2012)	5 to 60 mM	150 mM	5 to 10 µg/L	125 mL	³	22±5	27±2	22±2	2±1	
Janda (2019)	60 mM	150 mM	2 µg/L	125 mL	10.1±2.8	33.8±3.5	54.0±4.6	33.2±14. 9	3.84±1.5 8	
Martin et al. (2019)	60 mM	150 mM	100 ng/mL	2 mL	23±2	21±1	24±1	17±1	2±0.1	
4:2 FTSA										
this study ²	60 mM	150 mM	15 ng/L	125 mL	³	54±6				
Janda (2019)	60 mM	150 mM	2 µg/L	125 mL	15.9±2.6	42.1±1.2	5.4±0.3			
Martin et al. (2019)	60 mM	150 mM	100 ng/mL	2 mL	35±5	24±2	3±1			
N-EtFOSAA										
this study ²	60 mM	150 mM	15 ng/L	125 mL	³				3±4	89±3
Houtz and Sedlak (2012)	20 mM	150 mM	25 ng/L, 250 ng/L	125 mL	³					92±4
Martin et al. (2019)	60 mM	150 mM	100 ng/mL	2 mL					1.2±0.1	95±6
N-EtFOSE										
this study ²	60 mM	150 mM	15 ng/L	125 mL	³				4±5	46±6 ⁴

¹ Full disappearance of model precursors was observed in this study, as in the other studies referred to in the table.

² The oxidation tests were conducted by Thekla-Regine Schramm.

³ The ultrashort-chain compound PFPrA was not included in the target list of these studies.

⁴ The low conversion yield of N-EtFOSE can be related to the high volatility of the compound, which may lead to losses during the TOP assay.

Table A.3-7: Method detection limits (MDLs) [ng/L] and method quantification limits (MQLs) [ng/L] for unoxidized and oxidized aliquots from the total oxidizable precursor (TOP) assay.

campaign	German rivers				Chinese rivers			
	unoxidized		oxidized		unoxidized		oxidized	
aliquot	MDL	MQL	MDL	MQL	MDL	MQL	MDL	MQL
compound ¹	MDL	MQL	MDL	MQL	MDL	MQL	MDL	MQL
PFBA	0.98	2.1	2.4	4.6	1.1	3.0	1.8	3.7
PFPeA	0.94	2.3	1.8	3.4	0.45	1.0	1.5	1.9
PFHxA	0.39	0.88	1.4	2.7	1.9	6.3	1.9	6.3
PFHpA	0.32	0.73	1.0	1.8	0.18	0.34	0.67	1.0
PFOA	0.66	1.2	3.4	7.9	0.54	1.1	8.3	21
PFNA	0.15	0.50	0.15	0.50	0.23	0.78	0.23	0.78
PFDA	0.27	0.90	0.27	0.90	0.080	0.28	0.080	0.28
PFUnDA	0.15	0.50	0.15	0.50	nd	nd	nd	nd
PFDoDA	0.16	0.52	0.16	0.52	nd	nd	nd	nd
PFBS	0.83	2.8	0.83	2.8	1.2	3.2	0.73	2.6
PFHxS	0.49	1.6	0.49	1.6	0.04	0.06	0.22	0.64
PFOS	1.0	2.5	1.6	2.9	0.39	1.1	0.18	0.31
PFECHS	0.23	0.78	0.23	0.78	nd	nd	nd	nd
HFPO-DA	1.4	3.5	0.78	1.9	0.12	0.39	0.12	0.39
DONA	0.21	0.58	nd	nd	nd	nd	nd	nd
6:2 Cl-PFESA	nd	nd	nd	nd	0.04	0.12	0.04	0.12
6:2 FTSA	0.20	0.68	0.20	0.68	0.30	1.0	0.30	1.0
FOSA	nd	nd	nd	nd	0.11	0.36	0.11	0.36

¹ The given MDLs and MQLs refer to the linear isomers of the target analytes.

² nd = not detected

³ For compounds, which were present in blanks, MDLs and MQLs were calculated as the average blank value plus 3 or 10 times the standard deviation, respectively (marked in blue). For PFASs other than these, the MDLs and MQLs were derived from a signal-to-noise ratio of 3 or 10, respectively, observed in low-level samples (green).

Table A.3-8: Annual flow rates for the investigated rivers.

river	gauging station	flow rate [m ³ /s]	year	source
Rhine	Cologne (Rhine km 688)	1880	2018 (mean of daily discharge values)	German Federal Waterways and Shipping Administration, data provided by Federal Institute of Hydrology (gauging station number 2730010).
Main	Frankfurt Osthafen	154	2018 (mean of daily discharge values)	German Federal Waterways and Shipping Administration, data provided by Federal Institute of Hydrology (gauging station number 24700404).
Ruhr	Mülheim	51.4	2018 (mean of daily discharge values)	German Federal Institute of Hydrology (2019) Deutsches Gewässerkundliches Jahrbuch (in German), gauging station number 2769990000100. URL: https://www.talsperrenleitzentrale-ruhr.de/daten/internet/onlinedaten/dokumente/dgj/q/dgj_2769990000100_q.pdf (accessed: October 17th 2019)
Lahn	Kalkofen	41.2	2018 (mean of daily discharge values)	German Federal Waterways and Shipping Administration, data provided by Federal Institute of Hydrology (gauging station number 25800600).
Alz	Burgkirchen	5.2	2018 (mean of daily discharge values)	Bavarian Environment Agency. Data base query (raw data) on April 16 th 2020, gauging station number 18408200. URL: https://www.hnd.bayern.de/pegel/inn/burgkirchen-18408200/abfluss?
Yangtze	Datong	27433	2013-2015	Pan <i>et al.</i> (2018)
Xiaoqing		20.6	2013	Pan <i>et al.</i> (2017)
Xi	after confluence with Yimatu River	1.7	2014 (mean of data for the four seasons)	Zhu <i>et al.</i> (2015), site number 5

Table A.3-9: Concentrations [ng/L] of detected PFCAs and PFSAs in surface water samples taken from German rivers. Values in brackets are between MDL and MQL.

station ID	PFBA	PFPeA	PFHxA	L-PFHpA	Br-PFHpA	L-PFOA	Br-PFOA	PFNA	PFDA	PFUnDA	PFTTrDA	PFBS	L-PFHxS	Br-PFHxS	PFHpS	L-PFOS	Br-PFOS
AZ_001	0.65	0.3	0.38	0.25	<MDL	0.77	(0.12)	(0.075)	(0.038)	0.059	<MDL	0.44	(0.14)	<MDL	<MDL	0.45	(0.035)
AZ_002	1.1	1	0.67	0.55	<MDL	2.5	0.35	0.39	0.13	0.19	<MDL	0.44	(0.16)	<MDL	<MDL	0.42	(0.077)
AZ_003	190	280	110	37	2.3	20	3.1	6.0	1.0	1.6	(0.12)	3.7	(0.21)	<MDL	<MDL	0.47	<MDL
AZ_004	140	200	80	26	1.6	20	3.0	4.1	0.84	1.3	(0.11)	3.1	(0.020)	<MDL	<MDL	0.40	<MDL
AZ_005	130	220	75	29	1.5	180	20	3.4	1.2	1.2	(0.073)	3.5	0.32	<MDL	<MDL	0.44	<MDL
AZ_006	1.3	0.24	(0.28)	0.22	<MDL	0.36	<MDL	(0.075)	<MDL	<MDL	<MDL	0.30	(0.15)	<MDL	<MDL	(0.18)	<MDL
AZ_007	0.73	0.21	(0.27)	0.22	<MDL	0.45	<MDL	(0.061)	<MDL	<MDL	<MDL	0.33	(0.14)	<MDL	<MDL	(0.15)	<MDL
AZ_008	1.5	1.8	1.1	0.96	<MDL	4.8	0.76	0.15	(0.042)	<MDL	<MDL	0.44	(0.22)	<MDL	<MDL	0.28	<MDL
RU_001	6.9	5.2	7.7	3.2	(0.048)	5.4	0.87	0.29	0.15	<MDL	<MDL	5.3	0.59	(0.20)	<MDL	2.6	0.5
RU_002	6.5	5.2	7.5	3.6	(0.038)	4.9	0.88	0.27	0.12	<MDL	<MDL	5.2	0.63	(0.18)	<MDL	2.3	0.46
RU_003	6.6	5.0	7.7	3.4	(0.040)	5.3	0.82	0.39	0.23	<MDL	<MDL	4.8	0.59	(0.17)	<MDL	3.1	0.66
RU_004	6.6	4.9	7.3	3.3	(0.039)	5.0	0.76	0.35	0.19	<MDL	<MDL	4.8	0.56	(0.22)	<MDL	2.7	0.55
RU_005	5.8	4.7	7.4	3.6	(0.041)	4.8	0.78	0.35	0.17	<MDL	<MDL	4.8	0.57	(0.15)	<MDL	2.6	0.72
RU_006	6.7	5.4	7.6	5.3	0.055	5.0	1.0	0.43	0.35	(0.026)	<MDL	5.7	0.62	(0.17)	(0.057)	4.7	0.91
RU_007	4.6	3.2	3.3	1.6	(0.018)	2.5	0.24	0.45	0.23	<MDL	<MDL	30	2.0	0.42	(0.11)	2.3	0.59
RU_008	4.9	3.2	3.7	1.7	(0.018)	2.8	0.27	0.48	0.30	<MDL	<MDL	28	1.9	0.34	(0.082)	3.2	0.75
RH_001	3.8	2.8	3.2	1.4	<MDL	2.3	0.22	0.38	0.21	<MDL	<MDL	3.8	1.8	0.35	<MDL	2.1	0.58
RH_002	3.8	3.0	3.3	1.5	<MDL	2.4	0.26	0.44	0.23	<MDL	<MDL	3.1	1.8	0.36	(0.10)	2.2	0.63
RH_003	4.1	2.8	3.3	1.6	(0.016)	2.4	0.26	0.42	0.23	<MDL	<MDL	66	2.0	0.34	(0.14)	2.5	0.73
RH_004	4.0	2.8	3.1	1.4	<MDL	2.3	0.26	0.42	0.22	<MDL	<MDL	35	1.8	0.41	(0.13)	2.3	0.65
RH_005	4.4	2.8	3.3	1.5	(0.017)	2.5	0.25	0.47	0.28	<MDL	<MDL	34	1.9	0.39	(0.14)	2.9	0.86
RH_006	3.8	2.1	3.4	1.3	(0.027)	2.7	0.39	0.58	0.26	<MDL	<MDL	4.6	1.9	0.47	0.22	2.1	1.2
REF	4.5	2.1	3.8	1.3	<MDL	2.7	0.18	0.45	0.26	<MDL	<MDL	3.7	0.83	(0.17)	<MDL	4.5	0.75
MA_001	3.1	1.9	2.8	1.4	<MDL	2.1	0.21	0.45	0.14	<MDL	<MDL	2.9	0.87	(0.20)	<MDL	1.0	0.34
MA_002	4.2	2.2	3.1	1.5	<MDL	2.2	0.21	0.46	0.15	<MDL	<MDL	2.9	0.89	(0.23)	(0.056)	1.0	0.41
MA_003	4.4	2.6	3.6	1.8	<MDL	2.7	0.25	0.58	0.20	<MDL	<MDL	3.7	1.3	(0.26)	<MDL	1.4	0.58
MA_004	3.5	2.3	3.2	1.5	<MDL	2.4	0.21	0.46	0.16	<MDL	<MDL	3.5	1.2	(0.23)	(0.10)	1.3	0.41
MA_005	3.5	2.3	3.3	1.5	<MDL	2.4	0.24	0.47	0.18	<MDL	<MDL	3.7	1.2	(0.24)	<MDL	1.3	0.42
MA_006	5.2	2.3	2.9	1.3	<MDL	1.9	0.20	0.36	0.19	<MDL	<MDL	2.4	1.4	(0.29)	(0.12)	2.0	0.5
MA_007	3.47	2.4	3.3	1.5	<MDL	2.3	0.25	0.45	0.16	<MDL	<MDL	3.6	1.4	0.32	<MDL	1.3	0.55

Table A.3-10: Concentrations [ng/L] of detected PFCAs and PFSAs in surface water samples taken from Chinese rivers. Values in brackets are between MDL and MQL.

station ID	PFBA	PFPeA	PFHxA	L-PFHpA	Br-PFHpA	L-PFOA	Br-PFOA	PFNA	PFDA	PFUnDA	PFDoDA	PFBS	L-PFHxS	Br-PFHxS	PFHpS	L-PFOS	Br-PFOS
XQ_001	12	4.3	4.3	3.2	0.22	41	9.6	0.78	(0.31)	<MDL	<MDL	3.8	2.5	3.3	<MDL	2.7	2.7
XQ_002	47	27	26	9.2	1.2	170*	48	0.92	0.44	<MDL	<MDL	3.4	2.8	5.0	0.31	5.1	5.04
XQ_003	59	21	9.7	3.2	0.28	58	11	0.94	(0.30)	<MDL	<MDL	1.9	0.41	1.2	<MDL	3.1	2.2
XQ_004	230	160	76	18	1.9	250	50	1.2	(0.32)	<MDL	<MDL	1.5	0.76	0.77	<MDL	5.3	2.3
XQ_005	3000	200	2700	5400	780	200000	52000	(30)	<MDL	<MDL	<MDL	(120)	<MDL	<MDL	<MDL	(16)	<MDL
XQ_006	3600	2200	3100	8300	1200	250000	69000	(32)	<MDL	<MDL	<MDL	(47)	<MDL	<MDL	<MDL	<MDL	<MDL
XQ_007	4100	2500	3600	11000	1400	320000	69000	(29)	<MDL	<MDL	<MDL	(59)	<MDL	<MDL	<MDL	<MDL	<MDL
XQ_008	530	470	580	1100	140	42000	11000	(21)	<MDL	<MDL	<MDL	<MDL	(3.6)	<MDL	<MDL	<MDL	<MDL
XQ_009	310	270	320	250	28	6200	1900	<MDL	<MDL	<MDL	<MDL	<MDL	(2.3)	<MDL	<MDL	<MDL	<MDL
FX_001	300*	1.3	3.4	3.22	0.30	88	19	0.80	<MDL	<MDL	<MDL	750	0.51	0.89	0.42	0.7	2.13
FX_002	1500*	5.1	11	6.5	0.99	50	12	0.66	(0.23)	<MDL	<MDL	4800*	2.0	3.0	2.1	1.8	7.2
FX_002S ¹	4100*	19	45	53	7.4	540*	170	0.94	(0.34)	<MDL	<MDL	18000*	11	17	8.8	2.8	29.1
FX_003	1100*	4	7.9	5.2	0.68	49	11	0.74	<MDL	<MDL	<MDL	3100*	1.4	2.1	(0.89)	1.4	4.8
FX_004	1100*	5.4	9.1	6	0.74	67	18	0.87	(0.53)	<MDL	<MDL	2600*	1.1	1.9	(1.1)	0.78	2.98
FX_005	610*	13	21	14	0.74	110	25	1.53	0.90	<MDL	(0.15)	1400*	(0.85)	1.2	<MDL	1.4	2.8
FX_006	770*	7.4	12	5.1	(0.61)	86	20	1.18	0.81	<MDL	<MDL	1700*	1.0	(0.97)	<MDL	2.7	6.1
FX_007	130*	(0.45)	(0.54)	0.64	<MDL	(10)	2.7	<MDL	<MDL	<MDL	<MDL	11	<MDL	<MDL	<MDL	0.26	<MDL
FX_008	590*	5.4	4.1	3	<MDL	43	7.9	0.68	<MDL	<MDL	<MDL	98	<MDL	<MDL	<MDL	(0.27)	<MDL
FX_009	990*	8.2	18	8.2	1.3	110	31	1.0	(0.38)	<MDL	<MDL	2400*	1.1	1.2	<MDL	1.5	4.1
YZ_001	6.5	(0.62)	29	1.3	0.11	32	5.5	(0.40)	<MDL	<MDL	<MDL	6.3	0.81	0.30	<MDL	1.1	1.9
YZ_002	120	56	1300	29	2.0	710	78	3.5	2.1	0.64	0.17	6.8	2.1	0.63	<MDL	2.1	1.9
YZ_004	5.7	1.3	77	1.6	<MDL	58	2.4	0.46	(0.17)	<MDL	<MDL	4.4	0.86	0.22	<MDL	0.69	0.60
YZ_005	5.9	1.2	68	2.2	0.25	80	20	(0.26)	<MDL	<MDL	<MDL	4.9	0.57	0.16	<MDL	0.72	0.46
YZ_006 ¹	24	8.6	120	9.3	0.14	180	9.9	3.0	1.2	0.35	<MDL	3.6	2.8	0.48	<MDL	2.5	1.2
YZ_007	6.0	1.1	90	1	<MDL	18	1.9	(0.29)	<MDL	<MDL	<MDL	5.2	0.74	(0.13)	<MDL	0.72	0.56
YZ_008	4.9	(0.61)	30	0.82	(0.058)	(9.6)	1.3	(0.31)	<MDL	<MDL	<MDL	5.2	0.65	(0.11)	<MDL	1.2	0.68
YZ_009	5.0	(0.64)	15	1.1	(0.091)	25	4.0	(0.39)	(0.20)	<MDL	<MDL	5.2	0.66	(0.14)	(0.094)	0.87	0.57

* Results marked with a star have to be considered semiquantitative, as the concentration was out of the calibration range.

¹ Samples were not taken from flowing river water, but from stagnant water at the riverside.

Table A.3-11: Concentrations [ng/L] of detected PFASs other than PFCAs and PFSA in surface water samples taken from German rivers. Values in brackets are between MDL and MQL.

station ID	PFECHS	HFPO-DA	DONA	6:2 Cl-PFESA	6:6 PFPiA	4:2 FTSA	6:2 FTSA	8:2 FTSA	L-FOSA	Br-FOSA	N-EtFOSAA
AZ_001	<MDL	0.55	1.2	<MDL	<MDL	<MDL	<MDL	<MDL	(0.017)	0.020	<MDL
AZ_002	<MDL	25	37	<MDL	<MDL	<MDL	<MDL	<MDL	<MDL	0.017	<MDL
AZ_003	<MDL	3600*	2500*	<MDL	(0.0049)	<MDL	2.9	<MDL	0.075	0.066	<MDL
AZ_004	<MDL	2300*	1800*	<MDL	(0.0070)	<MDL	2.1	<MDL	0.059	0.050	<MDL
AZ_005	<MDL	1900*	2000*	<MDL	0.018	<MDL	0.91	<MDL	0.039	0.044	<MDL
AZ_006	<MDL	0.043	<MDL	<MDL	<MDL	<MDL	<MDL	<MDL	(0.013)	0.012	(0.021)
AZ_007	<MDL	0.048	(0.025)	<MDL	<MDL	<MDL	<MDL	<MDL	<MDL	0.015	<MDL
AZ_008	<MDL	18	12	<MDL	<MDL	<MDL	(0.11)	<MDL	<MDL	0.016	<MDL
RU_001	0.11	0.085	0.079	<MDL	(0.0029)	<MDL	11	<MDL	0.033	0.035	0.043
RU_002	0.12	0.063	(0.013)	<MDL	<MDL	<MDL	8.8	<MDL	0.032	0.035	0.040
RU_003	0.16	0.073	(0.016)	<MDL	(0.0037)	<MDL	7.4	<MDL	0.042	0.045	0.059
RU_004	0.15	0.065	<MDL	<MDL	(0.0035)	<MDL	6.8	<MDL	0.044	0.038	0.056
RU_005	0.13	0.070	<MDL	<MDL	(0.0039)	<MDL	3.3	<MDL	0.039	0.038	0.039
RU_006	0.16	0.060	<MDL	<MDL	0.011	<MDL	2.2	<MDL	0.10	0.062	0.14
RU_007	(0.038)	0.057	(0.027)	<MDL	(0.0040)	<MDL	0.67	<MDL	0.053	0.055	(0.020)
RU_008	(0.059)	0.066	(0.017)	<MDL	(0.0075)	<MDL	0.8	<MDL	0.080	0.066	0.053
RH_001	(0.031)	0.049	<MDL	<MDL	(0.0043)	<MDL	0.51	<MDL	0.050	0.060	(0.016)
RH_002	(0.036)	0.052	<MDL	<MDL	(0.0046)	<MDL	0.64	<MDL	0.063	0.061	(0.024)
RH_003	<MDL	0.047	(0.035)	<MDL	(0.0040)	<MDL	0.61	<MDL	0.069	0.064	(0.026)
RH_004	(0.043)	0.057	(0.030)	<MDL	(0.0042)	<MDL	0.60	<MDL	0.057	0.070	(0.017)
RH_005	(0.051)	0.043	(0.017)	<MDL	(0.0051)	<MDL	0.76	<MDL	0.072	0.069	0.033
RH_006	0.21	0.108	(0.016)	<MDL	<MDL	<MDL	1.8	<MDL	0.049	0.058	0.035
REF	(0.050)	0.059	<MDL	<MDL	(0.0042)	<MDL	0.28	<MDL	0.040	0.065	(0.023)
MA_001	(0.066)	0.074	(0.026)	<MDL	<MDL	<MDL	0.26	<MDL	0.025	0.050	(0.013)
MA_002	(0.064)	0.082	(0.024)	<MDL	<MDL	<MDL	0.29	<MDL	0.027	0.049	(0.017)
MA_003	(0.071)	0.21	(0.033)	<MDL	(0.0055)	<MDL	0.63	<MDL	0.037	0.064	(0.029)
MA_004	0.10	0.18	(0.030)	<MDL	(0.0046)	<MDL	0.54	<MDL	0.038	0.058	(0.025)
MA_005	0.12	0.19	(0.024)	<MDL	(0.0045)	<MDL	0.57	<MDL	0.037	0.055	(0.025)
MA_006	<MDL	0.030	<MDL	<MDL	(0.0036)	<MDL	0.79	<MDL	0.052	0.057	0.032
MA_007	0.12	0.16	(0.024)	<MDL	(0.0045)	<MDL	0.67	<MDL	0.041	0.058	(0.025)

* Results marked with a star have to be considered as semiquantitative, as the concentration was out of the calibration range.

Table A.3-12: Concentrations [ng/L] of detected PFASs other than PFCAs and PFSAs in surface water samples taken from Chinese rivers. Values in brackets are between MDL and MQL.

station ID	PFECHS	HFPO-DA	DONA	6:2 Cl-PFESA	6:6 PFPIA	4:2 FTSA	6:2 FTSA	8:2 FTSA	L-FOSA	Br-FOSA	N-EtFOSAA
XQ_001	<MDL	1.5	<MDL	3.3	<MDL	<MDL	1.7	<MDL	0.046	0.041	<MDL
XQ_002	<MDL	3.2	<MDL	4.2	<MDL	<MDL	2.0	<MDL	0.067	0.061	<MDL
XQ_003	<MDL	1.6	<MDL	1.2	<MDL	<MDL	0.53	<MDL	0.29	0.21	<MDL
XQ_004	<MDL	95	<MDL	0.88	<MDL	<MDL	0.48	<MDL	0.32	0.40	<MDL
XQ_005	<MDL	1900	<MDL	<MDL	<MDL	<MDL	<MDL	<MDL	<MDL	<MDL	<MDL
XQ_006	<MDL	3300	<MDL	<MDL	<MDL	<MDL	<MDL	<MDL	<MDL	<MDL	<MDL
XQ_007	<MDL	3800	<MDL	<MDL	<MDL	<MDL	<MDL	<MDL	<MDL	<MDL	<MDL
XQ_008	<MDL	560	<MDL	<MDL	<MDL	<MDL	<MDL	<MDL	<MDL	<MDL	<MDL
XQ_009	<MDL	260	<MDL	<MDL	<MDL	<MDL	<MDL	<MDL	(3.7)	(3.7)	<MDL
FX_001	<MDL	0.69	<MDL	0.23	<MDL	<MDL	<MDL	<MDL	0.089	0.11	<MDL
FX_002	<MDL	(0.28)	<MDL	(0.075)	<MDL	<MDL	<MDL	<MDL	<MDL	<MDL	<MDL
FX_002_S ¹	<MDL	0.91	<MDL	(0.10)	<MDL	<MDL	<MDL	<MDL	(0.110)	(0.19)	<MDL
FX_003	<MDL	(0.24)	<MDL	0.14	<MDL	<MDL	<MDL	<MDL	(0.076)	(0.099)	<MDL
FX_004	<MDL	(0.27)	<MDL	0.12	<MDL	<MDL	<MDL	<MDL	<MDL	(0.083)	<MDL
FX_005	<MDL	(0.50)	0.197	0.26	<MDL	<MDL	<MDL	<MDL	<MDL	<MDL	<MDL
FX_006	<MDL	(0.27)	<MDL	0.47	<MDL	<MDL	<MDL	<MDL	(0.110)	(0.23)	<MDL
FX_007	<MDL	<MDL	<MDL	<MDL	<MDL	<MDL	<MDL	<MDL	(0.021)	(0.016)	<MDL
FX_008	<MDL	(0.32)	<MDL	<MDL	<MDL	<MDL	<MDL	<MDL	<MDL	(0.083)	<MDL
FX_009	<MDL	(0.30)	<MDL	0.16	<MDL	<MDL	<MDL	<MDL	(0.092)	<MDL	<MDL
YZ_001	<MDL	0.59	<MDL	0.26	<MDL	<MDL	(0.20)	<MDL	0.10	0.070	<MDL
YZ_002	<MDL	95	<MDL	0.47	<MDL	0.66	210	(0.22)	0.45	0.15	<MDL
YZ_004	<MDL	1.8	<MDL	0.23	<MDL	<MDL	0.74	<MDL	0.072	0.041	<MDL
YZ_005	<MDL	1.5	<MDL	0.15	<MDL	<MDL	1.2	<MDL	0.068	(0.038)	<MDL
YZ_006 ¹	<MDL	6.3	<MDL	1.3	<MDL	<MDL	1.3	<MDL	0.091	0.053	<MDL
YZ_007	<MDL	1.3	<MDL	0.20	<MDL	<MDL	1.4	<MDL	0.075	(0.033)	<MDL
YZ_008	<MDL	0.43	<MDL	0.29	<MDL	<MDL	1.0	<MDL	0.089	0.058	<MDL
YZ_009	<MDL	0.48	<MDL	0.19	<MDL	<MDL	3.0	<MDL	0.086	0.052	<MDL

¹ Samples were not taken from flowing river water, but from stagnant water at the riverside.

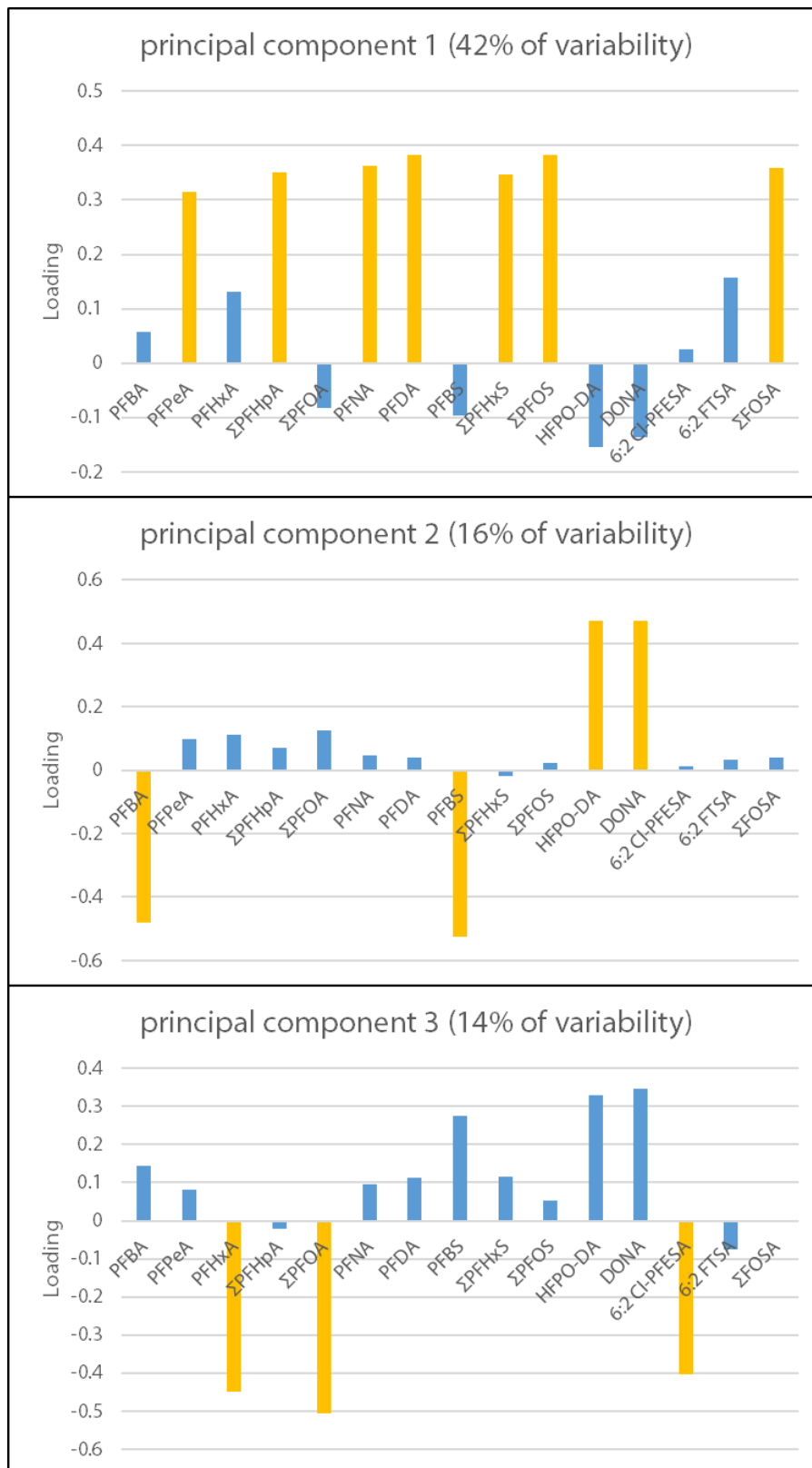


Figure A.3-1: Loadings for each principal component with dominant loadings shaded.

Table A.3-13: Percent contribution of the sum of branched isomers to total PFHpA, PFOA, PFHxS, PFOS and FOSA. The percentage of the linear isomer can be calculated as 100 % minus the percentage for the sum of branched isomers.

river	% sum-branched isomers (mean±SD)				
	PFHpA	PFOA	PFHxS	PFOS	FOSA
Alz	4.5±1.7	12.5±1.3	24.1±5.6	8.9±3.7	53.5±8.8
Ruhr	1.2±0.2	14.5±0.5	23.3±2.6	17.6±2.1	48.2±5.2
Rhine	0.9±0.2	9.4±0.6	16.6±1.4	22.4±0.4	51.2±3.4
Main	0.7±0.1	8.7±0.5	17.8±1.9	26.7±2.6	63.1±2.8
Dong Zhulong	11.1±2.1	18.6±2.6	<MDL ¹	<MDL ¹	<MDL ¹
Xi	10.8±2.8	19.8±2.2	58.5±5.4	76.7±7.6	54.4±17.0
Yangtze	5.8±3.8	12.7±3.6	19.2±5.4	43.6±11.7	36.1±3.6

¹ Both linear and branched isomers were below MDL in more than 50 % of the samples from the Dong Zhulong River. Consequently, no mean value of % sum-branched isomers was calculated for this river. If one of the isomers was <MDL in individual samples (see Table A.3-9 to Table A.3-12), the value was replaced by $\sqrt{2}/2$ *MDL for calculation of % sum-branched isomers.

Table A.3-14: Difference in PFAS concentrations between unoxidized and oxidized aliquots of samples taken from German rivers.¹

station ID	$\Delta c_{\text{pre-post}}^2$	PFBA	PFPeA	PFHxA	PFHpA	PFOA	PFNA	PFDA	PFUnDA	PFBS	PFHxS	PFOS	HFPO-DA	DONA	PFECHS
RU_006	[ng/L]	7.1	7.5	5.8	1.2	-	-	-	-	0.41	0.017	-0.25	-	-	-
	[%]	85	78	44	19	-	-	-	-	8.1	2.9	-3.7	-	-	-
RU_007	[ng/L]	6.0	5.2	3.2	0.03	-	-	-	-	0.82	0.063	-0.46	-	0.03	-
	[%]	110	110	57	1.4	-	-	-	-	2.7	3.4	-11	-	14	-
RU_008	[ng/L]	5.0	5.1	3.6	-0.12	-	-	-	-	-0.06	0.003	-0.46	-	-	-
	[%]	90	93	56	-4.5	-	-	-	-	-0.19	0.15	-12	-	-	-
RH_002	[ng/L]	4.6	4.8	3.0	0.34	-	-	-	-	-0.03	-0.087	-1.15	-	-	-
	[%]	100	96	52	15	-	-	-	-	-1.0	-4.7	-24	-	-	-
RH_003	[ng/L]	5.0	3.4	2.9	-0.09	-	-	-	-	4.99	-0.090	0.49	-	-	-
	[%]	99	70	50	-3.9	-	-	-	-	7.3	-5.0	14	-	-	-
RH_004	[ng/L]	5.6	6.2	3.7	-0.15	-	0.36	-	-	-0.58	-0.22	0.08	-	-	-
	[%]	100	130	62	-6.2	-	60	-	-	-1.4	-11	1.4	-	-	-
REF	[ng/L]	5.3	2.4	4.9	0.03	-	-	-	-	-0.42	0.028	-0.58	-	-	-
	[%]	120	66	70	1.6	-	-	-	-	-12	4.1	-11	-	-	-
MA_001	[ng/L]	2.9	3.5	0.88	0.24	-	-	-	-	-0.41	-0.023	-0.26	-	-	-
	[%]	69	97	18	10	-	-	-	-	-14	-2.7	-14	-	-	-
MA_003	[ng/L]	3.1	3.9	0.82	0.17	-	-	-	-	-0.25	-0.11	-0.44	-	-	-
	[%]	68	110	16	7.2	-	-	-	-	-8.3	-12	-22	-	-	-
MA_004	[ng/L]	4.0	4.7	1.1	0.14	-	-	-	-	-0.26	-0.010	-0.03	-	-	-
	[%]	97	120	20	6.0	-	-	-	-	-8.5	-1.0	-1.5	-	-	-
MA_005	[ng/L]	3.8	4.5	1.3	0.26	-	-	-	-	-0.43	0.013	-0.31	-	-	-
	[%]	100	120	24	11	-	-	-	-	-13	1.3	-14	-	-	-
MA_006	[ng/L]	3.6	4.6	2.0	-0.19	-	-	-	-	0.17	-0.15	-0.45	-	-	-
	[%]	62	110	42	-8.2	-	-	-	-	8.0	-11	-14	-	-	-
MA_007	[ng/L]	4.5	5.0	2.0	0.14	-	-	-	-	-0.53	-0.064	-0.57	-	-	0.023
	[%]	100	110	34	5.5	-	-	-	-	-15	-4.6	-18	-	-	10
AZ_002	[ng/L]	-	-	-	-	-	-	-	-	-	-	-	-	-	-
	[%]	-	-	-	-	-	-	-	-	-	-	-	-	-	-
AZ_003	[ng/L]	100	110	49	-0.87	-3.3	-0.98	-0.01	0.32	0.28	-	-	450	-780	-

	[%]	41	51	31	-1.5	-14	-13	-1.5	13	7.4	-	-	35	-100	-
AZ_004	[ng/L]	37	54	14	-1.6	-0.53	0.50	-	0.59	0.15	-	-	220	-750	-
	[%]	19	26	12	-3.7	-2.8	12	-	45	4.8	-	-	18	-100	-
AZ_005	[ng/L]	42	58	13	-6.1	-12	0.20	0.30	0.39	-0.092	-	-	170	-690	-
	[%]	25	30	11	-15	-6.1	5.3	25	35	-2.6	-	-	17	-100	-
AZ_006	[ng/L]	-	-	-	-	-	-	-	-	-	-	-	-	0.13	-
	[%]	-	-	-	-	-	-	-	-	-	-	-	-	51	-
AZ_007	[ng/L]	-	-	-	-	-	-	-	-	-	-	-	-	-	-
	[%]	-	-	-	-	-	-	-	-	-	-	-	-	-	-
AZ_008	[ng/L]	-	2.3	-	-	-	-	-	-	-	-	-	12	-	-
	[%]	-	81	-	-	-	-	-	-	-	-	-	73	-	-

¹ Due to the different MDLs and MQLs of unoxidized and oxidized samples, the calculation was only performed for compounds, which were > MQL in both sample aliquots. “-” marks compounds for which results of one or both aliquots were <MQL. Only linear isomers were considered. Target analytes, for which no value was calculated due to concentrations <MQL, are not shown.

$$^2 \Delta c_{\text{pre-post}} [\text{ng/L}] = c_{\text{pre-TOP}} [\text{ng/L}] - c_{\text{post-TOP}} [\text{ng/L}]$$

$$\Delta c_{\text{pre-post}} [\%] = \Delta c_{\text{pre-post}} [\text{ng/L}] / c_{\text{pre-TOP}} \cdot 100 \%$$

Table A.3-15: Difference in PFAS concentrations between unoxidized and oxidized aliquots of samples taken from Chinese rivers.¹

station ID	$\Delta c_{\text{pre-post}}^2$	PFBA	PFPeA	PFHxA	PFHpA	PFOA	PFNA	PFDA	PFBS	PFHxS	PFOS	HFPO-DA	6:2 Cl-PFESA
YZ_001	[ng/L]	-0.057	-	1.7	0.34	-3.0	-	-	0.053	0.17	-0.34	0.24	-0.032
	[%]	-1.1	-	5.1	24	-11	-	-	1.1	25	-27	42	-10
YZ_003	[ng/L]	15	36	43	3.9	14	0.14	0.22	0.13	-0.10	0.23	-1.9	-0.033
	[%]	29	180	9.3	43	4.6	9.8	36	3.4	-7.8	18	-5.7	-11
YZ_004	[ng/L]	0.068	0.76	-1.2	0.32	-12	-	0.24	0.32	-0.096	-0.18	-0.045	-0.11
	[%]	1.1	41	-1.3	19	-18	-	68	8.2	-11	-	-2.7	-31
YZ_006	[ng/L]	6.2	7.3	13	23	970	0.22	-0.018	0.45	-0.013	0.13	8.2	-0.59
	[%]	36	73	11	250	460	7.3	-1.1	-	-0.56	4.9	160	-40
FX_001	[ng/L]	51	-0.16	-	0.45	2.0	0.11	-	17	0.15	-0.25	7.1	-0.005
	[%]	14	-7.3	-	13	1.1	13	-	2.4	-	-	1000	-2.4
FX_004	[ng/L]	-	0.78	1.1	1.3	-2.8	0.20	0.069	-6.2	0.34	0.16	-	0.015
	[%]	-	13	11	24	-4.2	17	5.2	-0.25	47	-	-	10
FX_005	[ng/L]	100	4.2	8.1	17	22	0.26	0.13	27	-0.11	-0.10	-	-0.001
	[%]	18	29	30	46	6.7	6.4	9.8	2.0	-	-6.7	-	-0.35
FX_009	[ng/L]	170	1.7	0.94	2.1	-1.0	0.24	0.067	86	-0.22	0.68	-	-0.004
	[%]	21	19	5.0	29	-0.90	24	14	4.2	-18	54	-	-2.5
XQ_003	[ng/L]	-5.3	4.9	0.93	0.28	1.9	0.039	-0.007	-	-	-0.15	-0.13	-0.17
	[%]	-11	21	11	8.9	3.9	4.7	-2.2	-	-	-6.1	-11	-16
XQ_005	[ng/L]	270	2,500	-	160	28,000	-3.7	0.41	-	-	5.0	-340	-
	[%]	7.2	89	-	1.0	19	-8.8	11	-	-	78	-8.3	-
XQ_006	[ng/L]	160	3,900	-240	680	38,000	-6.7	-0.052	-	-	2.9	-420	-
	[%]	3.9	130	-4.3	3.8	25	-15	-1.4	-	-	42	-9.2	-

¹ Due to the different MDLs and MQLs of unoxidized and oxidized samples, the calculation was only performed for compounds, which were > MQL in both sample aliquots. “-“ marks compounds for which results of one or both aliquots were <MQL. Only linear isomers were considered. Target analytes, for which no value was calculated due concentrations <MQL are not shown.

² $\Delta c_{\text{pre-post}} [\text{ng/L}] = c_{\text{pre-TOP}} [\text{ng/L}] - c_{\text{post-TOP}} [\text{ng/L}]$

$\Delta c_{\text{pre-post}} [\%] = \Delta c_{\text{pre-post}} [\text{ng/L}] / c_{\text{pre-TOP}} \cdot 100 \%$

Table A.3-16: Theoretical conversion of the precursor 6:2 FTSA, detected in German and Chinese river samples.¹

station ID	c (6:2 FTSA) _{pre-TOP}		theoretical conversion by oxidation of 6:2 FTSA [pmol]				theoretical conversion by oxidation of 6:2 FTSA [ng]			
	[ng/L]	[pmol]	PFBA	PFPeA	PFHxA	PFHpA	PFBA	PFPeA	PFHxA	PFHpA
RU_006	1.2	2.9	0.70	0.92	0.88	0.007	0.151	0.24	0.28	0.003
RU_007	0.26	0.60	0.15	0.20	0.19	0.002	0.032	0.052	0.058	0.001
RU_008	0.37	0.85	0.21	0.28	0.26	0.002	0.045	0.073	0.082	0.001
RH_002	0.34	0.80	0.20	0.26	0.24	0.002	0.042	0.068	0.077	0.001
RH_003	0.26	0.61	0.15	0.20	0.19	0.002	0.032	0.052	0.059	0.001
RH_004	0.32	0.74	0.18	0.24	0.23	0.002	0.039	0.063	0.071	0.001
MA_006	0.28	0.67	0.16	0.21	0.20	0.002	0.035	0.057	0.064	0.001
MA_007	0.16	0.37	0.09	0.12	0.11	0.001	0.019	0.031	0.035	0.000
AZ_003	2.30	5.4	1.3	1.7	1.6	0.014	0.28	0.46	0.52	0.005
AZ_004	1.4	3.2	0.81	1.1	1.0	0.009	0.17	0.28	0.32	0.003
AZ_005	0.88	2.1	0.50	0.66	0.63	0.005	0.11	0.17	0.20	0.002
YZ_003	150	350	85	110	110	0.90	18	30	33	0.33
YZ_004	0.60	1.4	0.35	0.46	0.43	0.004	0.074	0.120	0.14	0.001

¹ Calculation was based on the molar conversion yield determined in oxidation tests (Table A.3-6).

Table A.3-17: Percentage of measured difference in concentration of C₄ to C₇-PFCAs attributed and unattributed to oxidation of 6:2 FTSA.¹

station ID	measured $\Delta c_{\text{pre-post}}$ [ng/L]					% attributed to conversion of 6:2 FTSA					% unattributed to conversion of 6:2 FTSA				
	PFBA	PFPeA	PFHxA	PFHpA	ΣC_4-C_7 PFCAs	PFBA	PFPeA	PFHxA	PFHpA	ΣC_4-C_7 PFCAs	PFBA	PFPeA	PFHxA	PFHpA	ΣC_4-C_7 PFCAs
RU_006	7.1	7.5	5.8	1.2	21.53	2.1	3.3	4.8	0.2	3.1	97.9	96.7	95.2	99.8	96.9
RU_007	6.0	5.2	3.2	0.03	14.50	0.5	1.0	1.8	1.8	1.0	99.5	99.0	98.2	98.2	99.0
RU_008	5.0	5.1	3.6	-0.12	13.58	0.9	1.4	2.3	-0.7	1.5	99.1	98.6	97.7	100.7	98.5
RH_002	4.6	4.8	3.0	0.34	12.85	0.9	1.4	2.5	0.2	1.5	99.1	98.6	97.5	99.8	98.5
RH_003	5.0	3.4	2.9	-0.09	11.27	0.6	1.5	2.0	-0.7	1.3	99.4	98.5	98.0	100.7	98.7
RH_004	5.6	6.2	3.7	-0.15	15.34	0.7	1.0	1.9	-0.5	1.1	99.3	99.0	98.1	100.5	98.9
MA_006	3.6	4.6	2.0	-0.19	10.03	1.0	1.2	3.2	-0.3	1.6	99.0	98.8	96.8	100.3	98.4
MA_007	4.4	5.0	2.0	0.14	11.61	0.4	0.6	1.8	0.3	0.7	99.6	99.4	98.2	99.7	99.3
AZ_003	100	110	49	-0.87	262.11	0.3	0.4	1.0	-0.6	0.5	99.7	99.6	99.0	100.6	99.5
AZ_004	37	54	15	-1.6	104.10	0.5	0.5	2.2	-0.2	0.7	99.5	99.5	97.8	100.2	99.3
AZ_005	42	58	13	-6.1	106.98	0.3	0.3	1.5	0.0	0.4	99.7	99.7	98.5	100.0	99.6
YZ_003	15	36	43	3.9	98.01	125.8	81.4	76.8	8.4	83.0	-25.8	18.6	23.2	91.6	17.0
YZ_004	0.07	0.76	0.00	0.32	1.15	108.6	15.8	0.0	0.4	28.7	-8.6	84.2	0.0	99.6	71.3

¹ Calculation was based on the molar conversion yield determined in oxidation tests (Table A.3-6).

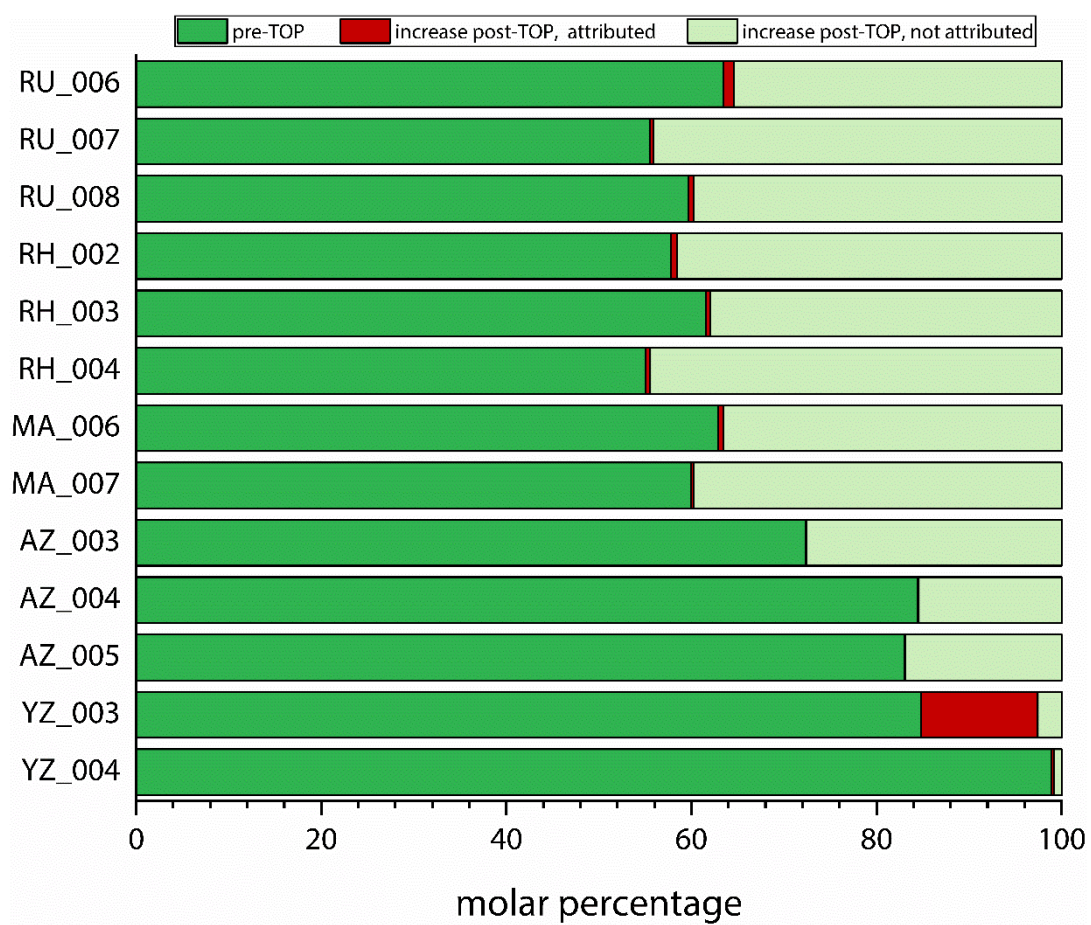


Figure A.3-2: Molar percentage of C₄ to C₇ PFCAs pre-TOP and post-TOP, attributed and unattributed to conversion of the detected precursor 6:2 FTSA.

Table A.3-18: Average PFAS mass flows estimates in river water downstream of point sources investigated in this study. The calculation was based on the river water samples taken after the respective point source (mean±standard deviation). *Italicized rivers are tributaries of the Rhine River.*

river	average PFAS mass flow [kg/yr]						
	PFBA	PFPeA	PFHxA	ΣPFHpA	ΣPFOA	PFNA	PFDA
Rhine River	260±23	180±13	200±12	93±8	160±10	27±2	15±2
<i>Main River</i>	11±1	8.2±0.4	12±0.3	6.1±1.3	9.6±0.4	0.6±0.1	0.3±0.1
<i>Lahn River¹</i>	5.8	2.8	5.0	1.7	3.7	0.6	0.3
<i>Ruhr River</i>	18±3	12±1	16±1	7.7±0.8	13±1	2.4±0.3	0.9±0.1
Alz River	25±6	39±7	14±3	5.3±1.0	13±16	0.7±0.2	0.2±0.1
Yangtze River	4670±420	810±310	41,000 ±26,000	1300 ±600	43,000 ±34,000	310±77	80±93
Xi River	54±16	0.4±0.2	0.7±0.3	0.4±0.2	5.3±1.9	0.2±0.0	0.03±0.02
Xiaoqing River	270±100	240±93	290±120	490 ±430	20,000 ±21,000	6.9±9.7	*

river	PFBS	ΣPFHxS	ΣPFOS	HFPO-DA	DONA	6:2 Cl-PFESA	6:2 FTSA	ΣFOSA
Rhine River	2300 ±930	140±4	200±29	3.2±0.5	1.5±0.5	*	40±4	7.8±0.9
<i>Main River</i>	8.3 ±0.5	1.3±0.1	5.9±1.7	0.1±0.1	*	*	11±6	0.1±0.1
<i>Lahn River</i>	4.8	1.3	6.8	0.1	*	*	0.4	0.1
<i>Ruhr River</i>	18±1	7.2±0.3	8.7±0.8	0.9±0.1	0.1 ±0.0	*	2.8±0.2	0.5±0.0
Alz River	0.6±0.1	0.01 ±0.01	0.1±0.0	430 ±150	350 ±65	*	0.3±0.2	0.02 ±0.00
Yangtze River	4300 ±320	730 ±140	1240 ±240	930 ±620	*	190±51	1270 ±870	110±17
Xi River	140±60	0.16 ±0.06	0.3±0.1	0.02 ±0.01	*	0.01 ±0.01	*	0.01 ±0.01
Xiaoqing River	*	*	*	270 ±140	*	*	*	*

¹ No standard deviation is given for the Lahn River, as only one sample was taken.

* No mass flow was calculated, as the compound was below MDL in the respective rivers.

A.4 Supplementary to Chapter 8

Table A.4-1: Back-mapping of observed structures to the original US EPA PFAS Master List.























results from HRMS observations		database entries matching the observations	
neutral formula	SMILES string	names	CAS numbers
C2HF3O2	<chem>OC(=O)C(F)(F)F</chem>	Trifluoroacetic acid Trifluoroacetate	76-05-1 14477-72-6
C3HF5O2	<chem>OC(=O)C(F)(F)C(F)(F)F</chem>	Pentafluoropropanoic acid Sodium pentafluoropropanoate Pentafluoropropanoate	422-64-0 378-77-8 44864-55-3
C4HF7O2	<chem>OC(=O)C(F)(F)C(F)(F)C(F)(F)F</chem>	Perfluorobutanoic acid Sodium perfluorobutanoate Potassium heptafluorobutanoate Silver perfluorobutanoate Heptafluorobutanoic acid--piperazine (1/1) 4-Chlorobenzenediazonium perfluorobutanoate perfluorobutanoic acid (1:1:1) Rhodium(II) perfluorobutyrate dimer Ammonium perfluorobutanoate	375-22-4 2218-54-4 2966-54-3 3794-64-7 375-04-2 630-31-9 73755-28-9 10495-86-0
C5HF9O2	<chem>OC(=O)C(F)(F)C(F)(F)C(F)(F)C(F)(F)F</chem>	Perfluoropentanoic acid Sodium perfluoropentanoate Potassium nonafluoropentanoate Ammonium perfluoropentanoate	2706-90-3 2706-89-0 336-23-2 68259-11-0
C6HF11O2	<chem>OC(=O)C(F)(F)C(F)(F)C(F)(F)C(F)(F)C(F)(F)F</chem>	Perfluorohexanoic acid Sodium perfluorohexanoate Ammonium perfluorohexanoate Potassium undecafluorohexanoate Undecafluorohexanoic acid--piperazine (1/1)	307-24-4 2923-26-4 21615-47-4 3109-94-2 423-47-2
C7HF13O2	<chem>OC(=O)C(F)(F)C(F)(F)C(F)(F)C(F)(F)C(F)(F)F</chem>	Perfluoroheptanoic acid Ammonium perfluoroheptanoate Sodium perfluoroheptanoate Potassium tridecafluoroheptanoate Caesium perfluoroheptanoate	375-85-9 6130-43-4 20109-59-5 21049-36-5 171198-24-6
C8HF15O2	<chem>OC(=O)C(F)(F)C(F)(F)C(F)(F)C(F)(F)C(F)(F)F</chem>	Perfluorooctanoic acid Sodium perfluorooctanoate Potassium perfluorooctanoate Ammonium perfluorooctanoate Silver perfluorooctanoate N,N,N-Triethylethanaminium pentadecafluorooctanoate Chromium(3+) perfluorooctanoate N,N,N-Trimethyloctan-1-aminium pentadecafluorooctanoate Potassium pentadecafluorooctanoate--water (1/1/2) Perfluorooctanoate N,N,N-trimethylmethanaminium Tetrapropylammonium perfluorooctanoate	335-67-1 335-95-5 2395-00-8 3825-26-1 335-93-3 98241-25-9 68141-02-6 927835-01-6 98065-31-7 32609-65-7 277749-00-5
C9HF17O2	<chem>OC(=O)C(F)(F)C(F)(F)C(F)(F)C(F)(F)C(F)(F)F</chem>	Perfluorononanoic acid Ammonium perfluorononanoate Sodium heptadecafluorononanoate Potassium heptadecafluorononanoate Heptadecafluorononanoic acid--N-ethylethanamine (1/1) Heptadecafluorononanoic acid--N-methylmethanamine (1/1) Methanaminium perfluorononanoate N,N-Diethylethanaminium heptadecafluorononanoate Piperidinium perfluorononanoate Heptadecafluorononanoic acid--aniline (1/1) Cyclohexanaminium perfluorononanoate	375-95-1 4149-60-4 21049-39-8 21049-38-7 77032-27-0 77032-24-7 77032-23-6 327176-80-7 95682-66-9 95682-67-0 328531-06-2
C10HF19O2	<chem>OC(=O)C(F)(F)C(F)(F)C(F)(F)C(F)(F)C(F)(F)F</chem>	Perfluorodecanoic acid Ammonium perfluorodecanoate Sodium perfluorodecanoate	335-76-2 3108-42-7 3830-45-3
C11HF21O2	<chem>OC(=O)C(F)(F)C(F)(F)C(F)(F)C(F)(F)C(F)(F)F</chem>	Perfluoroundecanoic acid Sodium hencosafluoroundecanoate Ammonium perfluoroundecanoate Potassium hencosafluoroundecanoate Perfluoroundecanoic acid calcium salt (2:1)	2058-94-8 60871-96-7 4234-23-5 30377-53-8 97163-17-2
C4H2F4O4	<chem>OC(=O)C(F)(F)C(F)(F)C(O)=O</chem>	Tetrafluorobutanedioic acid	377-38-8
C5H2F6O4	<chem>OC(=O)C(F)(F)C(F)(F)C(O)=O</chem>	Hexafluoroglutaric acid	376-73-8

		Hexyl-1-methyl-1H-Imidazolium perfluorobutanesulfonate N,N-Dimethyl-N-(propan-2-yl)propan-2-aminium nonafluorobutane-1-sulfonate [4-(2-tert-Butoxy-2-oxoethoxy)phenyl](diphenyl)sulfanium nonafluorobutane-1-sulfonate N,N-Dibutyl-N-methylbutan-1-aminium nonafluorobutane-1-sulfonate Magnesium nonafluorobutanesulfonate N,N,N-Tripentylpentan-1-aminium nonafluorobutane-1-sulfonate Bis(2-hydroxyethyl)ammonium perfluorobutanesulfonate Tetrabutylphosphonium perfluorobutanesulfonate	
C5HF11O3S	OS(=O)(=O)C(F)(F)C(F)(F)C(F)(F)C(F)(F)C(F)(F)C(F)(F)F	Perfluoropentanesulfonic acid Potassium perfluoropentanesulfonate Ammonium perfluoropentanesulfonate Bis(2-hydroxyethyl)ammonium perfluoropentanesulfonate	2706-91-4 3872-25-1 68259-09-6 70225-17-1
C6HF13O3S	OS(=O)(=O)C(F)(F)C(F)(F)C(F)(F)C(F)(F)C(F)(F)C(F)(F)C(F)(F)F	Perfluorohexanesulfonic acid Potassium perfluorohexanesulfonate Lithium perfluorohexanesulfonate Ammonium perfluorohexanesulfonate Bis(2-hydroxyethyl)ammonium perfluorohexanesulfonate Sodium perfluorohexanesulfonate	355-46-4 3871-99-6 55120-77-9 68259-08-5 70225-16-0 82382-12-5
C7HF15O3S	OS(=O)(=O)C(F)(F)C(F)(F)C(F)(F)C(F)(F)C(F)(F)C(F)(F)C(F)(F)C(F)(F)F	Perfluoroheptanesulfonic acid Potassium perfluoroheptanesulfonate Ammonium perfluoroheptanesulfonate Bis(2-hydroxyethyl)ammonium perfluoroheptanesulfonate Lithium perfluoroheptanesulfonate	375-92-8 60270-55-5 68259-07-4 70225-15-9 117806-54-9
C8HF17O3S	OS(=O)(=O)C(F)(F)C(F)(F)C(F)(F)C(F)(F)C(F)(F)C(F)(F)C(F)(F)C(F)(F)C(F)(F)C(F)(F)F	Perfluorooctanesulfonic acid Potassium perfluorooctanesulfonate Sodium perfluorooctanesulfonate Ammonium perfluorooctanesulfonate Lithium perfluorooctanesulfonate Tetraethylammonium perfluorooctanesulfonate Tetrabutylammonium perfluorooctanesulfonate N,N-Dibutyl-N-methylbutan-1-aminium heptadecafluorooctane-1-sulfonate Bis(2-hydroxyethyl)ammonium perfluorooctanesulfonic acid N,N,N-Tripentylpentan-1-aminium heptadecafluorooctane-1-sulfonate N,N,N-Triethyldecyl-1-aminium heptadecafluorooctane-1-sulfonate Ammonium perfluorooctanesulfonate Piperidinium perfluorooctanesulfonate N-Decyl-N,N-dimethyl-1-decanaminium perfluorooctanesulfonate Diphenyl(2,4,6-trimethylphenyl)sulfonium perfluoro-1-octanesulfonate	1763-23-1 2795-39-3 4021-47-0 29081-56-9 29457-72-5 56773-42-3 111873-33-7 124472-68-0 70225-14-8 56773-56-9 773895-92-4 1379454-92-8 71463-74-6 251099-16-8 258341-99-0
C9HF19O3S	OS(=O)(=O)C(F)(F)C(F)(F)C(F)(F)C(F)(F)C(F)(F)C(F)(F)C(F)(F)C(F)(F)C(F)(F)C(F)(F)F	Perfluorononanesulfonic acid Ammonium perfluorononanesulfonate Perfluorononanesulfonate potassium Sodium perfluorononanesulfonate	68259-12-1 17202-41-4 29359-39-5 98789-57-2
C2H2F4O3S	OS(=O)(=O)C(F)(F)C(F)F	1,1,2,2-Tetrafluoroethane-1-sulfonic acid	464-14-2
C3H2F6O3S	FC(F)(F)COS(=O)(=O)C(F)(F)F	2,2,2-Trifluoroethyl trifluoromethanesulfonate	6226-25-1
C4H2F8O3S	OS(=O)(C(F)(C(F)(C(F)(C(F)F)F)F)F)=O	Potassium 1,1,2,2,3,3,4,4-octafluorobutane-1-sulphonate 1,1,2,2,3,3,4,4-Octafluorobutane-1-sulphonic acid	70259-85-7 70259-86-8
C5H2F10O3S	FC(F)(F)C(F)(F)C(F)(F)COS(=O)(=O)C(F)(F)F	1H,1H-Heptafluorobutyl triflate	6401-01-0
C6H2F12O3S	FC(F)(F)COS(=O)(=O)C(F)(F)C(F)(F)C(F)(F)C(F)(F)F	2,2,2-Trifluoroethyl perfluorobutanesulfonate	79963-95-4
C7H2F14O3S	FC(F)(F)C(F)(F)COS(=O)(=O)C(F)(F)C(F)(F)C(F)(F)F	2,2,3,3,3-Pentafluoropropyl nonafluorobutane-1-sulfonate	893556-35-9
C8H2F16O3S	FC(F)(F)C(F)(F)C(F)(F)COS(=O)(=O)C(F)(F)C(F)(F)C(F)(F)C(F)(F)F	1H,1H-Perfluorobutyl perfluorobutanesulfonate	883499-32-9
C9H2F18O3S	FC(F)(F)C(F)(F)C(F)(F)C(F)(F)C(F)(F)C(F)(F)C(F)(F)C(F)(F)C(F)(F)F	2,2,3,3,4,4,5,5,6,6,7,7,8,8,8-Pentadecafluorooctyl trifluoromethanesulfonate	17352-09-9

C4HF7O3	OC(=O)C(F)(OC(F)(F)F)C(F)(F)F	Perfluoro-2-(perfluoromethoxy)propanoic acid	13140-29-9
C5HF9O3	OC(=O)C(F)(OC(F)(F)C(F)(F)F)C(F)(F)F	2,3,3,3-Tetrafluoro-2-(pentafluoroethoxy)propanoic acid	267239-61-2
C6HF11O3	OC(=O)C(F)(OC(F)(F)C(F)(F)C(F)(F)F)C(F)(F)F	Perfluoro-2-methyl-3-oxahexanoic acid Ammonium perfluoro-2-methyl-3-oxahexanoate Sodium 2,3,3,3-tetrafluoro-2-(heptafluoropropoxy)propanoate Potassium 2,3,3,3-tetrafluoro-2-(heptafluoropropoxy)propanoate 2,3,3,3-Tetrafluoro-2-(heptafluoropropoxy)propanoic acid--N-propylpropan-1-amine (1/1) Triethylaminium perfluoro-2-propoxypropanoate	13252-13-6 62037-80-3 67963-75-1 67118-55-2 165951-17-7 165951-18-8
C7HF13O3	OC(=O)C(F)(F)C(F)(F)C(F)(F)OC(F)(C(F)(F)F)C(F)(F)F	Perfluoro-4-isopropoxybutanoic acid	801212-59-9
C8HF15O3	OC(=O)C(F)(OC(F)(F)C(F)(F)C(F)(F)C(F)(F)C(F)(F)F)C(F)(F)F	Perfluoro-2-[(perfluoropentyl)oxy]propanoic acid Ammonium 2,3,3,3-tetrafluoro-2-[(undecafluoropentyl)oxy]propanoate	504435-11-4 510774-81-9
C10HF19O3	OC(=O)C(F)(F)C(F)(F)C(F)(F)C(F)(F)C(F)(F)C(F)(F)C(F)(F)OC(F)(C(F)(F)F)C(F)(F)F	2,2,3,3,4,4,5,5,6,6,7,7-Dodecafluoro-7-[(1,1,1,2,3,3,3-heptafluoropropan-2-yl)oxy]heptanoic acid	32347-41-4
C5HF9O4	OC(=O)C(F)(F)OC(F)(F)C(F)(F)OC(F)(F)F	Perfluoro-3,6-dioxahexanoic acid	151772-58-6
C6HF11O4	OC(=O)C(F)(F)OC(F)(F)C(F)(F)OC(F)(F)C(F)(F)F	Perfluoro-3,6-dioxaoctanoic acid Perfluoro(2-ethoxy-2-fluoroethoxy)acetic acid ammonium salt	80153-82-8 908020-52-0
C7HF13O4	OC(C(OC(F)(C(F)(C(F)(OC(F)(F)F)F)F)F)C(F)(F)F)=O	Perfluoro-2-(3-methoxypropoxy)propanoic acid potassium salt	496805-64-2
C8HF15O4	OC(=O)C(F)(F)OC(F)(F)C(F)(F)OC(F)(F)C(F)(F)C(F)(F)C(F)(F)F	Perfluoro-3,6-dioxadecanoic acid	137780-69-9
C9HF17O4	OC(=O)C(F)(OC(F)(F)C(F)(OC(F)(F)C(F)(F)C(F)(F)F)C(F)(F)F)C(F)(F)C(F)(F)F	Perfluoro-2,5-dimethyl-3,6-dioxanonanoic acid Potassium perfluoro(2-(2-propoxypropoxy)propanoate) Triethylaminium perfluoro-2-(2-propoxypropoxy)propanoate Methanaminium perfluoro-2-(2-propoxypropoxy)propanoate 2,3,3,3-Tetrafluoro-2-[1,1,2,3,3,3-hexafluoro-2-(heptafluoropropoxy)propoxy]propanoic acid--N-methylmethanamine (1/1)	13252-14-7 67118-57-4 165951-19-9 328065-29-8 328065-54-9
C3HF5O3	OC(=O)C(F)(F)OC(F)(F)F	Difluoro(trifluoromethoxy)acetic acid Difluoro(trifluoromethoxy)acetic acid--piperazine (1/1)	674-13-5 2266-82-2
C4HF7O4	OC(=O)C(F)(F)OC(F)(F)OC(F)(F)F	[Difluoro(trifluoromethoxy)methoxy](difluoro)acetic acid	39492-88-1
C5HF9O5	OC(=O)C(F)(F)OC(F)(F)OC(F)(F)OC(F)(F)F	[(Difluoro(trifluoromethoxy)methoxy)(difluoro)methoxy(difluoro)acetic acid	39492-89-2
C6HF11O6	OC(=O)C(F)(F)OC(F)(F)OC(F)(F)OC(F)(F)OC(F)(F)F	1,1,1,3,3,5,5,7,7,9,9-Undecafluoro-2,4,6,8-tetraoxadecan-10-oic acid	39492-90-5
C7HF13O7	OC(=O)C(F)(F)OC(F)(F)OC(F)(F)OC(F)(F)OC(F)(F)OC(F)(F)F	1,1,1,3,3,5,5,7,7,9,9,11,11-Tridecafluoro-2,4,6,8,10-pentaoxadodecan-12-oic acid	39492-91-6
C7H5F11O	OCCC(F)(F)C(F)(F)C(F)(F)C(F)(F)C(F)(F)F	5:2 Fluorotelomer alcohol	185689-57-0
C8H5F13O	OCCC(F)(F)C(F)(F)C(F)(F)C(F)(F)C(F)(F)C(F)(F)F	6:2 Fluorotelomer alcohol	647-42-7
C9H5F15O	OCCC(F)(F)C(F)(F)C(F)(F)C(F)(F)C(F)(F)C(F)(F)C(F)(F)F	3,3,4,4,5,5,6,6,7,7,8,8,9,9,9-Pentadecafluorononan-1-ol	755-02-2
C10H5F17O	OCCC(F)(F)C(F)(F)C(F)(F)C(F)(F)C(F)(F)C(F)(F)C(F)(F)F	8:2 Fluorotelomer alcohol	678-39-7

A.5 Safety data information

Table A.5-1: Safety data information for used chemicals other than PFASs according to the *Globally Harmonized System of Classification and Labelling of Chemicals* (GHS) [359].

chemical	signal	pictograms	H statements	P statements
acetic acid C ₂ H ₄ O ₂ CAS: 64-19-7	danger	 	H226, H314	P210, P280, P301+P330+P331, P303+P361+P353, P305+P351+P338
acetone C ₃ H ₆ O CAS: 67-64-1	danger	 	H225, H319, H336	P210, P240, P305+P351+P338, P403+P233
acetonitrile C ₂ H ₃ N CAS: 75-05-8	danger	 	H225, H302+H312+H332, H319	P210, P240, P302+P352, P305+P351+P338, P403+P233
ammonia solution 25% H ₅ NO CAS: 1336-21-6	danger	  	H290, H314, H335, H400	P260, P273, P280, P301+P330+P331, P303+P361+P353, P305+P351+P338
ammonium acetate C ₂ H ₇ NO ₂ CAS: 631-61-8	-	-	-	-
ethyl acetate C ₄ H ₈ O ₂ CAS: 141-78-6	danger	 	H225, H319, H336; EUH066	P210, P233, P240, P305+P351+P338, P403+P235
formic acid CH ₂ O ₂ CAS: 64-18-6	danger	  	H226, H302, H314, H331; EUH071	P210, P280, P303+P361+P353, P304+P340+P310, P305+P351+P338, P403+P233
hydrochloric acid HCl CAS: 7647-01-0	danger	 	H290, H314, H335	P260, P280, P303+P361+P353, P304+P340+P310, P305+P351+P338
methanol¹ CH ₄ O CAS: 67-56-1	danger	  	H225, H331, H311, H301, H370	P210, P233, P280, P302+P352, P304+P340, P308+P310, P403+P235
nitrogen, liquid N ₂ CAS: 7727-37-9	warning		H281	P282, P336+P315, P403
2-propanol C ₃ H ₈ O CAS: 67-63-0	danger	 	H225, H319, H336	P210, P240, P305+P351+P338, P403+P233



chemical	signal	pictograms	H statements	P statements
potassium peroxide $K_2S_2O_8$ CAS: 7727-21-1	danger		H272, H302, H315, H317, H319, H334, H335	P220, P261, P280, P305+P351+P338, P342+P311
silicium dioxide SiO_2 CAS: 14808-60-7	-	-	-	-
sodium hydroxide NaOH CAS: 1310-73-2	danger		H290, H314	P280, P301+P330+P331, P305+P351+P338,
ultrapure water H_2O CAS: 7732-18-5	-	-	-	-

Table A.5-2: Safety data information on PFCAs according to the *Globally Harmonized System of Classification and Labelling of Chemicals* (GHS) [360]. For most PFASs, classification is incomplete due to lacking data or conclusive but not sufficient data on hazards. For PFCAs not included in the table, no GHS classification is available at all.

acronym	IUPAC name CAS number	pictograms	H statements	P statements
PFBA	butanoic acid, 2,2,3,3,4,4,4-heptafluoro- CAS: 375-22-4	danger	H314, H318	P280, P305+P351+P338 P310
PFPeA	pentanoic acid, 2,2,3,3,4,4,5,5,5-nonafluoro- CAS: 2706-90-3	danger	H314	P280, P305+P351+P338 P310
PFHxA	hexanoic acid, 2,2,3,3,4,4,5,5,6,6,6-undecafluoro- CAS: 307-24-4	danger	H314	P280, P305+P351+P338 P310
PFHpA	heptanoic acid, 2,2,3,3,4,4,5,5,6,6,7,7,7-tridecafluoro- CAS: 375-85-9	danger	H302, H314	P280, P305 +P351+P338, P310
PFOA	octanoic acid, 2,2,3,3,4,4,5,5,6,6,7,7,8,8,8-pentadecafluoro- CAS: 335-67-1	danger	H302+H332, H318, H351, H360D, H362, H372	P201, P260, P263, P280, P305+P351 +P338+P310, P308+P313
PFNA	nonanoic acid, 2,2,3,3,4,4,5,5,6,6,7,7,8,8,9,9,9-heptadecafluoro- CAS: 375-95-1	danger	H302, H332, H318, H351, H360Df, H362, H372	P260, P280, P302+P352, P305+P351+P338
PFDA	decanoic acid, 2,2,3,3,4,4,5,5,6,6,7,7,8,8,9,9,10,10,10-nonadecafluoro- CAS: 335-76-2	danger	H301, H315, H319, H335, H351, H360Df, H362	P301+P330+P331 +P310, P305+P351+P338
PFUnDA	undecanoic acid, 2,2,3,3,4,4,5,5,6,6,7,7,8,8,9,9,10,10,11,11,11-heneicosafuoro- CAS: 2058-94-8	danger	H302, H312, H315, H319, H332	P301+P330+P331 +P310, P305+P351+P338
PFDoDA	dodecanoic acid, 2,2,3,3,4,4,5,5,6,6,7,7,8,8,9,9,10,10,11,11,12,12,12-tricosafuoro- CAS: 307-55-1	danger	H315, H319, H335	P280, P305+P351+P338 P310
PFTeDA	tetradecanoic acid, 2,2,3,3,4,4,5,5,6,6,7,7,8,8,9,9,10,10,11,11,12,12,13,13,14,14,14-heptacosafuoro- CAS: 376-06-7	danger	H314	P280, P305+P351+P338 P310

Table A.5-3: Safety data information on PFSA and precursors according to the *Globally Harmonized System of Classification and Labelling of Chemicals* (GHS) [360]. For most PFASs, classification is incomplete due to lacking data or conclusive but not sufficient data on hazards. For PFSA and precursors not included in the table, no GHS classification is available at all.






















acronym	IUPAC name CAS number	pictograms	H statements	P statements
PFBS	1-butanefluorosulfonic acid, 1,1,2,2,3,3,4,4,4-nonafluoro-, potassium salt (1:1) CAS: 375-73-5	  danger	H302, H314	P280, P305+P351+P338 P310
PFHxS	1-hexanesulfonic acid, 1,1,2,2,3,3,4,4,5,5,6,6,6- tridecafluoro-, sodium salt (1:1) CAS: 355-46-4	  danger	H302, H314	P280, P305+P351+P338 P310
PFHpS	1-heptanesulfonic acid, 1,1,2,2,3,3,4,4,5,5,6,6,7,7,7- pentadecafluoro-, sodium salt (1:1), CAS: 375-92-8	  danger	H302, H312, H314, H332	P210, P260, P270
PFOS	1-octanesulfonic acid, 1,1,2,2,3,3,4,4,5,5,6,6,7,7,8,8,8- heptadecafluoro-, sodium salt (1:1), CAS: 1763-23-1	    danger	H302+H332, H314, H351, H360D, H362, H372, H411	P201, P263, P273, P280, P305+P351+P338, P310
FOSA	1-octanesulfonamide, 1,1,2,2,3,3,4,4,5,5,6,6,7,7,8,8,8- heptadecafluoro- CAS: 754-91-6	   danger	H301, H400, H410	P280, P305+P351+P338
N-EtFOSA	1-octanesulfonamide, N-ethyl- 1,1,2,2,3,3,4,4,5,5,6,6,7,7,8,8,8- heptadecafluoro- CAS: 4151-50-2	  danger	H302, H302+H312, H312, H411	P261, P280, P312
4:2 FTSA	1-hexanesulfonic acid, 3,3,4,4,5,5,6,6,6-nonafluoro-, sodium salt (1:1) CAS: 757124-72-4	  danger	H302, H312, H314, H332	P210, P260, P270
6:2 FTSA	1-octanesulfonic acid, 3,3,4,4,5,5,6,6,7,7,8,8,8- tridecafluoro-, sodium salt (1:1) CAS: 27619-97-2	   danger	H302, H314, H318, H373	P270, P280, P302+P330+P331 +P310, P305+P351+P338, P303+P361+P353, P314
8:2 FTSA	1-decanesulfonic acid, 3,3,4,4,5,5,6,6,7,7,8,8,9,9,10,10, 10-heptadecafluoro-, sodium salt (1:1) CAS: 39108-34-4	 danger	H302, H318, H373	P210, P260, P270

Table A.5-4: Safety data information on PFAS standards other than PFCAs, PFSAs and precursors according to the *Globally Harmonized System of Classification and Labelling of Chemicals* (GHS) [360]. For most PFASs, classification is incomplete due to lacking data or conclusive but not sufficient data on hazards. For replacements not included in the table, no GHS classification is available at all.

acronym	IUPAC name CAS number	pictograms	H ¹	P statements
DONA	propanoic acid, 2,2,3-trifluoro-3-[1,1,2,2,3,3-hexafluoro-3-(trifluoromethoxy)propoxy]-, sodium salt (1:1) CAS: 919005-14-4	danger	H290 H314 H318	P260, P310, P280, P305+P351+P338, P303+P361+P353
HFPO-DA	propanoic acid, 2,3,3,3-tetrafluoro-2-(1,1,2,2,3,3,3-heptafluoropropoxy)- CAS: 62037-80-3	danger	H302 H318 H373	P261, P264, P280, P301+P312, P305+P351+P338, P310
HFPO-TrA	propanoic acid, 2,3,3,3-tetrafluoro-2-[1,1,2,3,3,3-hexafluoro-2-(1,1,2,2,3,3,3-heptafluoropropoxy)propoxy]- CAS: 13252-14-7	danger	H314 H335	P260, P280, P301+P330+P331
HFPO-TeA	propanoic acid, 2,3,3,3-tetrafluoro-2-[1,1,2,3,3,3-hexafluoro-2-[1,1,2,3,3,3-hexafluoro-2-(1,1,2,2,3,3,3-heptafluoropropoxy)propoxy]propoxy]- CAS: 65294-16-8	danger	H314 H335	P260, P280, P301+P330+P331

¹ H statements

Eidesstattliche Versicherung

Hiermit versichere ich an Eides statt, die vorliegende Dissertation selbst verfasst und keine anderen als die angegebenen Hilfsmittel benutzt zu haben. Die eingereichte schriftliche Fassung entspricht der auf dem elektronischen Speichermedium. Ich versichere, dass diese Dissertation nicht in einem früheren Promotionsverfahren eingereicht wurde.

Hamburg, 25.06.2020